Drought indices validation: Improving monitoring knowledge on different systems in Spain and the United States

PhD dissertation

Marina Peña Gallardo

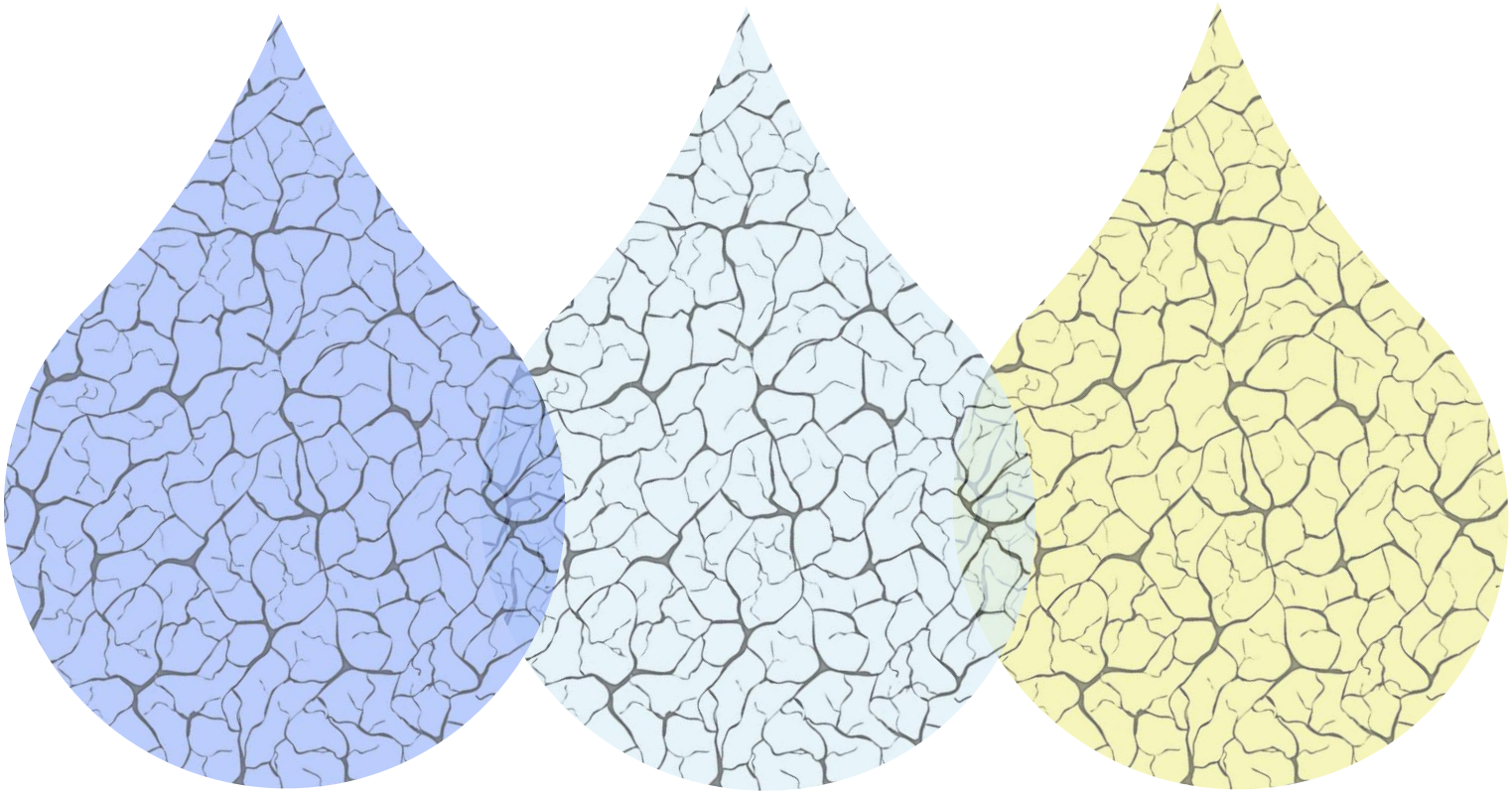

Universidad de Sevilla

Tesis Doctoral

Drought indices validation: Improving monitoring knowledge on different systems in Spain and the United States.

Autora: Marina Peña Gallardo

Directores:

Dr. Sergio Martín Vicente Serrano (Instituto Pirenaico de Ecología)

Dr. Santiago Beguería Portugués (Estación Experimental Aula Dei)

Tutor:

Dr. José Ojeda Zújar (Universidad de Sevilla)

Zaragoza, abril de 2019

The present PhD dissertation is submitted to the department of Physical Geography and Regional Geography Analysis of the University of Seville in partial fulfillment of the requirements for the degree of Doctor in Geography. The dissertation is presented in the modality of published scientific articles and includes the following referenced papers:

La presente tesis doctoral es presentada ante el departamento de Geografía Física y Análisis Geográfico Regional de la Universidad de Sevilla en cumplimiento parcial de los requerimientos para la obtención del título de Doctor en Geografía. La disertación se presenta en la modalidad de compendio de artículos científicos incluyendo los siguientes trabajos referenciados:

Research article 1

Peña-Gallardo, M., Vicente-Serrano, S.M, Domínguez-Castro, F., Quiring, S., Svoboda, M., Beguería, S., Hannaford, J., 2018. *Effectiveness of drought indices in identifying impacts on major crops across the USA*. Climate Research 75, 221–240. **DOI:** 10.3354/cr01519

Research article 2

Peña-Gallardo, M., Vicente-Serrano, S.M., Quiring, S., Svoboda, M., Hannaford, J., Tomas-Burguera, M., Martín-Hernández, N., Domínguez-Castro, F., El Kenawy, A., 2018b. *Response of crop yield to different time-scales of drought in the United States: Spatio-temporal patterns and climatic and environmental drivers*. Agricultural and Forest Meteorology 264, 40–55. **DOI:** 10.1016/j.agrformet.2018.09.019

Research article 3

Peña-Gallardo, M., Vicente-Serrano, S.M., Camarero, J., Gazol, A., Sánchez-Salguero, R., Domínguez-Castro, F., El Kenawy, A., Beguería-Portugés, S., Gutiérrez, E., de Luis, M., Sangüesa-Barreda, G., Novak, K., Rozas, V., Tíscar, P., Linares, J., Martínez del Castillo, E., Ribas Matamoros, M., García-González, I., Silla, F., Camisón, Á., Génova, M., Olano, J., Longares, L., Hevia, A., Galván, J., 2018a. *Drought Sensitiveness on Forest Growth in Peninsular Spain and the Balearic Islands*. Forests 9, 524. **DOI:** 10.3390/f9090524

Research article 4

Peña-Gallardo, M., Vicente-Serrano, S.M., Hannaford, J., Lorenzo-Lacruz, J., Svoboda, M., Domínguez-Castro, F., Maneta, M., Tomas-Burguera, M., Kenawy, A. El, 2019. *Complex influences of meteorological drought time-scales on hydrological droughts in natural basins of the contiguous Unites States*. Journal of Hydrology 568, 611–625. **DOI:** 10.1016/J.JHYDROL.2018.11.026

Additionally, two unpublished studies complete the work presented in this dissertation. First unpublished research has finished the peer revision by the time of this Thesis submission. The second unpublished research has recently sent to an indexed international journal.

Dos estudios no publicados completan el trabajo que se presenta en esta tesis. El primer manuscrito no publicado ha finalizado recientemente el periodo de revisión. El segundo manuscrito ha sido recientemente enviado a una revista internacional.

Unpublished research article 1:

Peña-Gallardo, M., Vicente-Serrano, S.M., Domínguez-Castro, F., Beguería, S., 2019. *The impact of drought on the productivity of two rainfed crops in Spain*. Natural Hazards Earth System Sciences Discuss. 1–30. DOI: https://doi.org/10.5194/nhess-2019-1

Unpublished research article 2:

Peña-Gallardo, M., Vicente-Serrano, S.M., Domínguez-Castro, F., Beguería, S., Van Loon, A., 2019 submitted. *Response of natural river basins to drought in Spain: Evaluation of different climatic drought indices. Water Resources Management. Submitted.*

Dr. Sergio Martín Vicente Serrano, Investigador científico del Instituto Pirenaico de Ecología (IPE-CSIC) y el Dr. Santiago Beguería Portugués, Investigador científico de la Estación Experimental Aula Dei (EEAD-CSIC)

Certifican:

Que Marina Peña Gallardo ha realizado bajo su dirección la tesis doctoral que lleva por título:

'Drought indices validation: Improving monitoring knowledge on different systems in Spain and United States'

Y que a su criterio, el trabajo cumple con los objetivos y estándares de calidad para la obtención del título de Doctor en Geografía en el marco del programa doctoral 'Medio litoral y marino: políticas, ordenación y tecnología de la información geográfica'.

En reconocimiento de ello y para que así conste en base a los requerimientos legales, firman el presente certificado en Zaragoza, a 2 de abril de 2019.

Dr. Sergio Martín Vicente Serrano
(Director 1)

Dr. Santiago Beguería Portugués
(Director 2)

Acknowledgements / Agradecimientos

Realizar una tesis doctoral se asemeja a una película multigénero. El inicio es muy fantástico, vamos a por el Nobel como mi buen compañero *Javi* diría. Al poco la cosa torna al género de suspense, ¡ui! que no es todo tan bonito y maravilloso como parece. *¡Ay! Que esto no es tan lineal como pensaba, SOS*. En este momento la película se vuelve un clásico de terror que enlaza al drama absoluto: ¡*A R pongo por testigo, que jamás conseguiré publicar nada!*. Pero como buena película, los giros provocan una vuelta de tuerca y las aventuras se abren paso a través de experiencias que devuelven la comedia, la risa y la ilusión a escena.

Esta tesis no ha sido realmente una película, sino un trabajo que ha requerido esfuerzo y sacrificio, pero también ha supuesto satisfacción y crecimiento personal y profesional. Me dejo a muchas personas en el tintero seguramente, pero por lo pronto:

A la profesora *María Fernanda Pita* debo agradecerle haber sido la responsable de despertar en mi el interés por la investigación - ya desde los inicios con las sequías- , siendo una maravillosa maestra.

Al profesor *José Ojeda* le agradezco su amabilidad por tomar el relevo de la tutorización de esta tesis y facilitarme todos los trámites.

A mi principal director *Sergio M. Vicente Serrano* le doy las gracias por haberme dado la oportunidad de trabajar con él y aprender de él. Por las múltiples oportunidades de viajar y vivir experiencias a lo largo de este tiempo. Por haberme dejado hacer a mi manera, aunque no siempre acertara. Por sacar de mi aptitudes con las que ni yo pensaba que contaba. Le agradezco el compromiso tan firme que ha mantenido constantemente. Gracias por todo el cuidado, la calidad humana transmitida y por haber sido un verdadero maestro.

A *Santiago Beguería* debo agradecerle muy sinceramente por las numerosas ideas que me ha aportado y el conocimiento transmitido. Por ayudarme a ver resultados con distinto prisma, y por haber sido también un referente y un apoyo muy valioso en estos tres años y medio.

A todos los compañeros y compañeras del Instituto Pirenaico de Ecología, gracias por crear un maravilloso ambiente de compañerismo y sintonía. En especial a mis chicos del despacho 3, a los que no cambiaría por nada del mundo muchas gracias Esteban, Javi, Makki, Natalia y Paco. En especial quisiera agradecer a mi ~~*nieto*~~ *Fernando Domínguez*, por haber sido ese tercer director que la universidad nunca me dejó incluir. Y a *Fergus Reig*, por su infinita paciencia, constante apoyo y las mil y una risas que nos ha sacado a todos. Gracias a él he aprendido muchísimo, y un trocito importante de esta tesis también es suya.

Thanks so much to *Dr. Steven Quiring* and his team and *Dr. Anne Van Loon* for hosting me during the different research stays I had the oportunity to do in College Station, Columbus and Birmingham. Also I would like to mention and give a big thanks to *Doris Wendt* and *Sally Rangecroft* for their kindness and the guidance they provided me. Also to *Brent McRoberts*, I will never forget the Cup America 2016 and the trip to Fort Worth singing the best hits of Taylor Swift. I spent a wonderful time there and learnt a lot from all of them. Thank you so much.

A mis amigos *Laura González* y *José Martín*, por estar siempre al otro lado y apoyarme desde siempre, gracias chicos sois maravillosos.

A mis chicas *María Brazo* y *Luz María Martel*, amigas con mayúsculas. Gracias por hacer tan valiosos recuerdos tanto en Zaragoza como en Inglaterra durante estos años y por los reencuentros de sevillanas maneras.

Un gracias infinito que durará por siempre y para siempre a mi señora madre *Reyes Gallardo*, mi bola *Miguel A. Peña* y mi hermano *David Peña*. A mi abuelo *Antonio Gallardo* y a mi abuela *Ana María Calle*, ¡¡Que la Kiki ya casi es doctora, pero de las que no llevan bata blanca!!. Sin olvidar a todos mis tíos, tías, primos y primas.

Y gracias siempre a aquellas que no hablan, pero que poco les hace falta. Gracias a mi *Yuuki* bonita. Gracias a mi gordi *Luna* que aunque no está, sigue presente, te querremos siempre. Gracias a *Lili* y *Mimi* (aka. *Pili* y *Mili*) por la alegría que han traído a casa. Y un gracias mayúsculo a mi *Prim*, mi gata del alma, co-autora no oficial de gran parte de los trabajos aquí presentados.

Gracias a todos y todas los que habéis formado parte de un modo u otro de este camino.

Marina

To *my Nita*, for 17 precious years.

‘A dog is the only thing on Earth that loves you more than you love yourself. ‘
Josh Billings

The structure of the present dissertation follow the normative established by the University of Seville for the modality of published scientific articles. It is also articulated in two parts. Part A presents the complete estructure of the PhD dissertation in English and Part B provides the translation in Spanish of the main points that will be exposed in that language during the oral defese. The published/unpublished researches are indexed in Part A sections 4 and 5.

La estructura de la presente tesis sigue la normativa estipulada por la Universidad de Sevilla en referencia a la modalidad de compendio de artículos. El trabajo además se encuentra articulado en dos partes. La Parte A presenta la estructura completa de la tesis en inglés y la Parte B contiene la traducción al castellano de los principales puntos que serán expuestos en dicho idioma durante la defensa oral de la tesis. Los artículos publicados y sin publicar se encuentran indexados en las secciones 4 y 5 de la Parte A.

> Table of contents

PART **A** – Thesis in **English**

ABSTRACT

This PhD Thesis focuses in the evaluation of different drought indices on multiple systems and the spatio-temporal response of agriculture, forests and streamflow to drought conditions in two heterogeneous regions, the United States and Spain from the sixties to nowadays.

Knowing the importance of selecting appropriate tools for monitoring drought, the performance of seven of the most commonly used drought indices and their ability to capture impacts on vulnerable systems were validated. For this purpose, three multi-scalar drought indices (the SPI, the SPEI and the SPDI) and four uni-scalar Palmer family drought indices (the PDSI, the PHDI, the Z-index and the PMDI) were quantitatively compared.

The results obtained from the different analysis conducted demonstrated the superior performance of the SPEI, the SPI and the SPDI in comparison to the PDSIs. Independently on the type of crop, tree species, river basin and the temporal scale considered, drought indices calculated at different time scales have a superior capacity to reflect the different impacts of drought over diverse systems with a wide range of temporal responses to drought associated to specific characteristics that difficult even more this identification.

The varying responses of crops to drought indices time-scales observed in crop yields from US and Spain were mainly determined by the resilience of plants to develop strategies to deal with soil moisture depletion and by the resistance of the different types of crops during the sensitive vegetative stages of growth. Similarly, findings from forest sensitivity to drought in forests in Spain showed variations among species and climatic regions highlighting the role of resilience mechanisms to handle with extreme climatic conditions. In addition, seasonal variations predetermined the response of tree species to drought. In general, results suggested a lagged response to drought depending on the part of the tree decay cycle affected, thus secondary growth was found especially sensitive to humid conditions during summer months while photosynthetic activity was affected by drought conditions occurring during spring months. From the propagation of climatic drought to streamflow drought analysis, results suggested a primary response to drought at short-time scales in most of the near-natural basins analysed in the US and Spain. However, seasonal patterns and local differences in the response of streamflow demonstrated the influence of catchment properties (e.g. vegetation cover, land-use, climatic conditions or topographic characteristics such as elevation) on streamflow response to climatic drought.

This PhD Thesis provided quantitative evidences about the effectiveness of drought indices for quantification and monitoring purposes, and also improved the knowledge on the sensitivity and spatio-temporal response of different natural systems to the most hazardous and tricky climate phenomenon.

1. Introduction

1.1. Defining drought. Typologies and complexities of an extreme natural hazard

Drought is recognized as the most complex, recurrent and extreme climatic hazard occurring over most parts of the world and climate regions, from wet to arid. Drought arises when over a prolonged period of time a deficit in the amount of normal precipitation occurs, however many other factors are involved in the triggering of a drought event. The mechanisms are complex since the atmospheric evaporative demand (AED) may reinforce drought severity and other important feedbacks may cause a self-intensification of drought (e.g. by means of the complementary relationship between the actual evapotranspiration and the AED) (Seneviratne et al., 2010; Teuling, 2018). During severe drought episodes, soil moisture conditions and vapor pressure deficit suffer depletion, turning the probability of precipitation negligible since the synoptic atmospheric situation is dominated by vertical stability, only reversed by the arrived of a wet atmospheric disturbance (Mishra and Singh, 2010).

Sometimes the concepts of aridity, heat wave, and drought are employed without being clear what the distinction between these terms is intended to be. Unlike drought, aridity is defined as "the degree to which a climate lacks effective, life-promoting moisture", according to the Glossary of Meteorology from the American Meteorological Society. Namely, it is a characteristic of the climate itself, generally restricted to low rainfall regions (Wilhite, 2000), while droughts are usually an unforeseen event with an onset and termination in time. An anomalous period of low water availability in which it is not possible to cover the existing demands by different natural systems agriculture and/or different human activities (Wilhite and Pulwarty, 2017). For its part, a heat wave is a meteorological condition caused by an abnormal increase of temperature that usually last a few weeks, contrary drought can last for longer time scales such as months or years (Schubert et al., 2014). It is noteworthy indicating that recent studies have suggested strong connection between drought severity and heat wave occurrence (Hirschi et al., 2011; Miralles et al., 2014).

Among natural hazards, drought is often ranked as the most hazardous and insidious for its many direct and indirect effects, not only on the environment but also on human activities. The whole conceptualization of drought entails some aspects to take into consideration (Mishra and Singh, 2010). First, drought is a slow-onset 'creeping' hazard (Gilette, 1950) and usually its effects are perceived once the event has lasted for a long time or even ceased. For this reason, defining the beginning and the end of an ongoing drought event is a challenge. Second, drought causes very diverse impacts. Quantifying the scope of the caused impacts on multiple scenarios is tricky since drought affects equally vast or small regions, surface and groundwater resources and varies in multiple time scales. Besides, the quantification of drought impacts depends on the vulnerability of the specific impacted sector and its resilience to drought (Gazol et al., 2018a, 2017). Thus, environmental exposure to drought conditions is subject to inherent factors such as the climatic regime, the characteristics of hydrological processes, the type of vegetation, the lithology (presence/absence of permeable rocks) or the human activities of the targeted area (Kumar et

al., 2016; Leng et al., 2015; Sangüesa-Barreda et al., 2015; Vicente-Serrano et al., 2017b). This connects straightforward with the third aspect since anthropogenic influence plays a potential role triggering drought conditions. Certain human activities (e.g. water demands and land use changes) are prone to both exacerbate or mitigate drought situations (Van Loon et al., 2016).

Nonetheless, still nowadays it is not possible to find a consensus among the scientific community to define universally this phenomenon as there are as many impacts as sectors implied (Wilhite et al., 2007). At this respect, droughts are generally classified into four categories (Dracup and Kendall, 1990; Wilhite and Glantz, 1985) following the particular order of droughts occurrence:

i) *Meteorological droughts* are defined as an anomalous decrease of the amount of precipitation below averaged values over a region for a prolonged period of time. A meteorological drought can develop very quickly and last from short (days) to long time (years). The definition of this kind of droughts is site-specific since each region has its own climatic conditions.

ii) At short-term, the absence of precipitation causes the depletion of soil moisture in the surface layers. When dryness reaches the root zone the vegetation is affected, giving rise to an *agricultural drought*. Agricultural droughts develop before the surface and groundwater resources are constrained by the lack of precipitation and even when deeper soils maintain wetness conditions. Nevertheless, not only precipitation triggers the drought at this point, temperature influences the humidity requirements of the atmosphere and hence the potential evapotranspiration as a factor of the water demanded by plants. Depending on the physiological and phenological characteristics of the plants and the climatic conditions, agricultural drought may ultimately be responsible of crop fails (Vergni and Todisco, 2011).

iii) *Hydrological droughts* are mainly characterized by a low discharge of streams and generalized decline on water availability through the hydrological cycle, including surface (e.g. reservoirs, lakes) and subsurface (groundwater) supplies (Tallaksen et al., 1997). Streamflow levels are the most common indicator used for hydrologic drought assessment, integrating the climate signal along with the influence of human practices (Lorenzo-Lacruz et al., 2013). However, the connections between the different parts of the hydrological cycle are very complex, varying the response to drought conditions in time. For this reason, it is common to refer to *streamflow droughts* when low flows are recorded. Previous studies have demonstrated that not only climatic conditions but also physiographic characteristics of the basins influence the response of the hydrological system to drought, emphasizing the multilayered interaction of all the mechanism involved (Tijdeman et al., 2016; Van Loon and Laaha, 2015). When flows reduced, groundwater recharged ceases and if dry conditions persists, groundwater levels starts dropping until discharges decline. At this point a *groundwater drought* is developed (Bloomfield et al., 2015; Mishra and Singh, 2010).

iv) *Socio-economic droughts* are associated to the failure of water resources to meet the water demand from human activities, mainly due to weather-related deficits. The constant and increasing demand of water in many parts of the world due to the

growing population, the expansion of intensive agricultural practices among others, suppose risk factors for most of the socio-economic goods that depend directly or indirectly on water.

In recent years, a new drought type is gaining interest and research focus. Related to the ecological/environmental drought impacts in a variety of natural systems including, fauna, forests and water streams (Crausbay et al., 2017).

In addition to the classification types of drought, there is a wide terminology to characterize a drought episode. On one hand, conceptual descriptions provide an intelligible meaning of drought and its consequences; on the other hand, operational descriptions are more related to describe quantitatively the characteristics of a drought event. Following one of the most complete terminology announced by Salas, (1993) as mentioned by Zargar et al. (2011), droughts can be described by their:

i) Duration: As we mentioned before, droughts can last for days or years and the same region can experience an alternation of dry and wet periods at short and long-term.
ii) Magnitude: Refers to the positive sum of the precipitation deficit, generally in reference a particular threshold.
iii) Intensity: Defined as the ratio between the magnitude and duration of an event.
iv) Severity: Measured as the magnitude or the level of impact of the event.
v) Geographic extension: The spatial coverage of a drought over time. There is not a unique unit for measure it (e.g. pixels, regions, environmental units).
vi) Frequency: It is the estimated average time between drought events with equal or higher severity.

Additionally, drought is a multi-scalar phenomenon that can be described at different time-scales. The concept of quantifying drought at diverse times was first introduced by Mckee et al. (1993 ; 1995) to understand the response of the different parts from the hydrological cycle (surface water and groundwater) to precipitation shortages. It was demonstrated that the sensitivity of natural systems to precipitation deficits accumulated during different periods. For example, in natural vegetation, the response to drought varies significantly to drought time scales, depending, among other factors, on the species and the resistance to dry conditions. Thus, previous studies have shown the dissimilar temporal response of different species from a same region to drought conditions recorded on different time-scales (Gazol et al., 2018b; Vicente-Serrano et al., 2013). Similarly, the hydrological drought response to climatic drought is highly dependent on drought time-scales varying as a function on the system and target region (Bloomfield et al., 2015; López-Moreno et al., 2013; Lorenzo-Lacruz et al., 2013).

1.2. The impacts of drought on different natural systems and human sectors

According to the Special Report on Extreme Events and Disasters from the Fifth Report of the Intergovernmental Panel on Climate Change (IPCC, 2014), there is a medium confidence in the intensification and extended duration of droughts in southern Europe and central United

States in some seasons during the next decades due to the reduction of precipitation and increase of evapotranspiration.

Nevertheless, most of the semi-arid regions located in southwestern Europe and the United States are very likely to experience a serious dropping in freshwater resources as a consequence of an increase of the AED and a shifting on precipitation patterns (Fu and Feng, 2014; Sherwood and Fu, 2014). In addition, recent studies have suggested that future drought episodes may affect more extended areas, reaching levels of impact higher than any other climate-related hazard, especially on food supply activities (Romm, 2011). In short, the United States (US) and the Mediterranean area are two regions prone to suffer from potential impacts of climate change that may bring more severe weather extreme events affecting natural sectors.

Agriculture

Agriculture is the mainstay of food security and a sector highly dependent of water availability. The temporal variability of crop yields can respond to many non-climatic influences such as political conflicts, social crisis or healthy issues (Ben-Ari and Makowski, 2014; Schauberger et al., 2018) however, the main driver is the climate variability (Lobell et al., 2011). According to FAO (2019), in developing countries agriculture sector absorbs the 80 percent of the direct impacts caused by droughts while the 22% of economic impacts worldwide comes from crop loses produced by natural hazards, especially droughts.

The US is one of the three major cereal crop producers of the world accounting for the largest production of corn according to the USDA (2015). However, in the last few decades this country has suffered from various extreme drought episodes. The most intense occurred in 1988 and had a widespread critical impact over the agricultural regions, causing estimated costs about $87 billion (inflation-adjusted 2019); the 40% of those cost come from crop yield losses (approximately $38 billion) (Elliott et al., 2018; Smith and Katz, 2013). The 1988 drought episode was the second most costly natural hazard only behind hurricane Katrina (Smith and Matthews, 2015). However, another major drought event arisen in 2012 in the US, amounted about $30 billion (Smith and Matthews, 2015) in crop losses. In Mediterranean region, severe droughts have also caused substantial socio-economic losses in both, rain-fed and irrigated lands (Lopez-Nicolas et al., 2017). Only the episode from 2003 caused damages in agricultural sector around 13 billion euros and had a great repercussion particularly in Spain. Moreover, the most severe drought in the last 60 years occurred in 2005 caused a reduction in the European cereal production of the range of 10% (Blauhut et al., 2016). Similarly, another extreme event in 2012 produced severe economic and ecological impacts. Apart from the crop failure in most croplands of the country, especially Aragon and Andalusia, during this episode an increase of abrupt tree mortality and number of summer fires as a consequence of the lack of precipitation were reported (Navarro-Cerrillo et al., 2018). According to the Spanish National Statistical Institute, Spain is the second country in Europe on largest proportion of cultivated lands. Rain-fed and irrigated crops bear the impacts of water scarcity (Tigkas and Tsakiris, 2015), however the grade of resilience of species to water stress and the stage of crop growth at which the crop is affected determine different responses to drought (Lobell, 2014; Lobell and Field, 2007). Ultimately, if adverse weather conditions lasted for long and especially during the most sensitive stages of growth, droughts may cause complete loss of crops (Lobell and Field, 2007). Crop yields are therefore, extremely

vulnerable to drought conditions and their variations can bring catastrophic consequences to global food security and economy.

In this context, multiple studies have advertised the vulnerable situation of crop yields to changes in drought frequency and severity (Asseng et al., 2011; Olesen et al., 2011; Rossi and Niemeyer, 2010), as well as the response of crop yields to the interannual variability of drought (Capa-Morocho et al., 2016; Loukas and Vasiliades, 2004; Moorhead et al., 2015; Rohli et al., 2016). Nonetheless, there are still very few advances in the studied regions in connecting the multi temporal character of drought-related bearings to the different type of crops (Páscoa et al., 2016; Tian et al., 2018; Zipper et al., 2016). Besides, evidences of increasing interannual variability of crop yields due to a future increase of drought frequency and severity reflect the need to require effective monitoring tools that provide a reliable quantification of drought impacts on agriculture (Asseng et al., 2014; Rossi and Niemeyer, 2010; Tack et al., 2015).

Three of the researches here presented analyse the climatic and environmental main drivers that determine crop yields responses to different drought time-scales; at the same time, they provide a review of the performance of different drought indices for monitoring drought impacts on various crop types in the US and Spain.

Ecology

Forests are an essential part of terrestrial ecosystems for their main role on the release and absorption of greenhouse gases such as carbon dioxide (CO_2) (Heimann and Reichstein, 2008) and within the hydrological cycle (Horton, 1933). Forest decay and mortality episodes caused by drought have increased over the last decades worldwide (Greenwood et al., 2017; Young et al., 2017). Primary and secondary growth are processes closely dependent on water availability (Pasho et al., 2011). The Iberian Peninsula hosts a high diversity of species favoured by the wide range of climate types. A broad overview of the climatic map of this territory allows identifying humid Atlantic climate in the northwestern, continental Mediterranean climate in the Center and semi-arid Mediterranean climate in the southeastern (García-Ruiz et al., 2011). Mediterranean region have been object of frequent and severe drought episodes having historically induced extensive impacts on forests (Caminero et al., 2018; Granda et al., 2013; Sangüesa-Barreda et al., 2015). Determining the incidence of drought presents its own set of constraints as the response of forests varies significantly over regions showing also seasonal variations. Previous studies have pointed that adverse climatic conditions such as depletion on soil moisture and high rates of evapotranspiration before the growing season limit the Net Primary Production (NPP) causing a weakening on growth, a reduction on photosynthesis, and hence, eventually, forest die-off (Camarero et al., 2018, 2015; Lloret et al., 2012; Neumann et al., 2017).

The interannual variability characteristic of the precipitations in Mediterranean climates hinders determining the response times of tree growth to precipitation shortfalls. At this respect, Pasho et al. (2011) assessed the different responses of the impact of water scarcity on different tree species growth in Aragón (northeastern Spain) showing that, while short time-scales were mainly associated to tree growth response to low moisture conditions, longer time-scales responses were related to less frequent but intense drought episodes. Additionally, apart from local climatic and topographic conditions, the sensitivity to drought and the recovery capacity differ greatly

between species and even individuals of the same species (Forner et al., 2018; Peguero-Pina et al., 2011). At this respect, studies conducted in Spain observed different recoveries among Mediterranean species. Thus, some species reached pre-drought growth conditions earlier than others, independently on the declining state of the individuals (Camarero et al., 2018; Carnicer et al., 2011).

Overall, recent advances on this subject has warned about the general increase trend of crown defoliation in the Iberian Peninsula observed since the last decades (Carnicer et al., 2011). In a context of climate change with contrasted evidences of tree drought-related impacts it is important to address an in-depth analysis that encompasses the relationship between drought, NPP and the secondary growth of forests. For a comprehensive knowledge of drought impacts, the times of response of different species to drought conditions and an optimal monitoring, in this thesis, it has undertaken the ecological system as part of the analysis in the study entitled: *Drought Sensitiveness on Forest Growth in Peninsular Spain and the Balearic Islands*.

Hydrology

Among the multiple impacts caused by drought in the ecosystems, many of these are potentially hydrological related (Van Loon, 2015). Hydrological droughts are a complex phenomena partly understood that evolves multiple interactions between meteorological drought and the propagation of its effects throughout the entire hydrological cycle (Haslinger et al., 2014), from streamflow (López-Moreno et al., 2013; Lorenzo-Lacruz et al., 2010), lakes and reservoirs (McEvoy et al., 2012) to groundwater (Lorenzo-Lacruz et al., 2017; Marchant and Bloomfield, 2018).

Although climatic variability is closely linked to hydrological droughts, many other factors determine the characteristics of the event such as the duration, spatial extension and severity of the impacts. Thus, the intricate relationship between climate and water deficits through the different parts of the cycle is sometimes triggered by environmental and anthropogenic influences that determine the develop of extreme hydrological events (Bąk and Kubiak-Wójcicka, 2017; Tijdeman et al., 2018; Vicente-Serrano et al., 2012). The complex character of drought propagation makes a challenge disentangling the original causes of hydrological droughts, moreover when the nature of hydrological variables shows significant variations in the different times of response to moisture deficits conditions. Thus, soil moisture dryness conditions arise at short-term (Scaini et al., 2015) while groundwater or reservoir water storages do it at longer (Barker et al., 2016; López-Moreno et al., 2013; Lorenzo-Lacruz et al., 2017).

Particularly, this is more intricate in drainage basins where physiographical characteristics and human management practices have a major role on the complex response of streamflow to drought controlling its characteristics and, at the same time, the sensitivity to climatic conditions at different time-scales (Sheffield and Wood, 2011; Van Loon, 2015; Van Loon and Laaha, 2015). At this respect, many studies worldwide have demonstrated that catchment physiographical properties and vegetation coverage are a dealbreaker to understand the different responses of streamflow drought to climatic drought at different time-scales. For example, Barker et al. (2016) observed the great influence of the lithology and geological characteristics on the very diverse response of hydrological droughts to climatic droughts in different natural catchment in the UK.

Likewise, Vicente-Serrano et al. (2011) investigated the response to climatic drought time-scales in two near-natural upstream watersheds located in northeastern Spain. They found differentiated times of response attributable to the particular lithological characteristics. Thus, while one of the analysed watershed responded at very short time-scales (< 3 months), the other one did it at much longer time-scales (> 40 months). In Austrian catchments, Van Loon and Laaha, (2015) studied the controls on drought severity concluding that both streamflow drought duration and severity was mostly controlled by a combination of catchment properties.

Similarly, other studies have spotlighted the bias in the hydro-climatic relationship produced by anthropogenic activities related to water regulation and management practices (López-Moreno et al., 2009; Wu et al., 2017) as well as land-use changes (Van Loon and Laaha, 2015), acting either as driving or mitigating forces to streamflow drought events (AghaKouchak et al., 2015; Liu et al., 2019; López-Moreno et al., 2009; Terrado et al., 2014). These studies commonly assess the relationship between climatological and hydrological drought and its propagation through the hydrological cycle by using drought indices that relate climatic and streamflow data. For example in Tagus river (Spain) Lorenzo-Lacruz et al. (2010) found significant correlations between climatic drought indices and river discharges. Nonetheless, in Spain there is a gap of knowledge regarding drought monitor tools for hydrologic drought, having an absence of studies evaluating the performance of different climatic drought indices to provide a better comprehension of the response in hydrological droughts. Besides, most of the studies usually consider a large variety of basins generally disturbed by anthropogenic practices hindering the possibility of observing the response of streamflow to climatic droughts under natural conditions. Abatzoglou et al. (2014) performed multiple drought indices to address the streamflow anomalies and the relationship between climate and streamflow dynamics in some catchments located in the Pacific Northwest of the US. For its part, Tijdeman et al. (2016) analysed streamflow drought duration in more than 800 basins in the US finding that the duration of drought events varies depending on the climate and precipitation regime. Nevertheless, the influence of catchment characteristics on the propagation of climatic drought to streamflow has not been fully covered yet.

The studies compiled in this dissertation entitled: *Complex influences of meteorological drought time-scales on hydrological droughts in natural basins of the contiguous Unites States* and *Response of natural river basins to drought in Spain: Evaluation of different climatic drought indices* contribute to expand the knowledge relative to climatic drought propagation through the hydrologic system and identifying appropriate monitoring tools.

1.3. Drought indices

The physical processes involved in drought and the intrinsic non-linear associated dynamic are very complex (Lloyd-Hughes, 2014). Little can be done to mitigate the effects of drought, the broad scope of drought impacts propagating to many natural and human water resource systems has led to the scientific community to develop tools and management strategies such as mitigation and integrated action plans to characterize efficiently drought events (Ceglar et al., 2012; Vicente-Serrano et al., 2012). Drought indices are efficient tools, mostly based on climatic information, worldwide used for quantifying the impact of drought on multiple systems at real-time thanks to their ability in identifying multiple characteristics including

the onset, severity, duration and extension of drought conditions accurately (Shukla et al., 2011; WMO, 2012; GWP, 2016). Many studies have shown the high capacity of drought indices in identifying the temporal variability of drought impacts on multiple environmental variables such as crop yields (Mathieu and Aires, 2018; Sun et al., 2012; Tian et al., 2018), streamflow and groundwater (Fiorillo and Guadagno, 2010; López-Moreno et al., 2013; Lorenzo-Lacruz et al., 2017; Vasiliades and Loukas, 2009) or tree growth (Bhuyan et al., 2017; Pasho et al., 2011).

More than 100 drought indices have been proposed since last century to characterize different types of drought (meteorological, agricultural, hydrological…) (Heim, 2002). Recent studies have reviewed some of these indices providing a comprehensive and theoretical comparative of their potentials and weaknesses (Mishra and Singh, 2010; Zargar et al., 2011). However, few studies have performed statistical comparisons among different drought indices that may allow determining the preference application of a specific index depending on the system object of study. In this context, Trenberth et al. (2014) emphasizing the relevance of temperature as a variable input on drought indices in the actual global warming, provided a global quantitative study of the sensitivity of drought indices to changes in land surface air temperature. Vicente-Serrano et al. (2012) for their part, conducted a global analysis comparing the ability of the most widely used drought indices to explain drought impacts on different natural systems.

In this study, seven of the most widely used drought indices have analysed. In the next sub-sections, a description of each index is provided.

1.3.1. Palmer drought severity index (PDSI) family

The Palmer Drought Severity Index (PDSI) was a landmark in drought quantification and monitoring. Developed by Palmer, (1965) is a worldwide known meteorological drought index used for quantifying drought severity. Originally, the PDSI relies on the amount of moisture departure, defined as the 'Climatically Appropriate for Existing Conditions' (CAFEC), within a two-layered soil moisture simulation for a specific region. CAFEC is equivalent to a soil water balance that accounts for a supply-demand relationship in soil moisture storage (Alley, 1984).

Three PDSI-related drought indices where developed later (Heim, 2002):

i. The Palmer hydrological drought index (PHDI) measures the duration and intensity of long-term drought effects on hydrological systems. Hydrological impacts take longer to arise, thus PHDI changes are detected slower than the PDSI lasting low values for several month after the PDSI recovers normal levels.

ii. The Palmer moisture anomaly index (Z-index) accounts for short-term moisture conditions changes. It is especially sensitive to short-term drought detection identifying changes in soil moisture and river discharge related to dryness processes.

iii. The Palmer Modified Drought Index (PMDI) presented by Heddinghaus and Sabol, (1991) incorporates precedent wet and dry conditions into the anomalies accumulation. It was first developed for meteorological and agricultural drought monitoring purposes.

The four Palmer-related drought indices (PDSIs) present some major shortcomings that have been highlighted in later literature (Akinremi et al., 1996; Alley, 1984; Heim, 2002; Weber and Kkemdirim, 1998; Vicente-Serrano et al., 2011)(Vicente-Serrano et al., 2011a)(Vicente-Serrano et al., 2011a):

i. The indices lack of the ability to be comparable in space as it was conceived to monitor drought in western regions in the US.
ii. They are computed at a fixed time-scale (uni-scalar) limiting the capacity to monitor and quantify different types of drought precisely. Drought characteristics are described no lesser than 12-month time-scales.
iii. The large number of input variables required in the formulation (e.g. air temperature, evapotranspiration, soil water content) constrains the possibility of calculating these indices in regions where these data may not be available
iv. The indices do not account for delayed runoff and assumes that potential precipitation is equal to the available water content.
v. The calculation procedure is very complex in comparison to other drought indices. The complete methodology can be found described in Karl, (1986).

Nonetheless, notwithstanding the deficiencies the PDSI is currently one of the most used drought indices thanks to its ability to capture long-term drought conditions (Lloyd-Hughes and Saunders, 2002). In order to alleviate the issue of comparability, Wells et al. (2004) developed a self-calibrated version of Palmer indices that determine accurately regional coefficients.

1.3.2. The Standardized Precipitation Index (SPI)

The Standardized Precipitation Index (SPI) proposed by Mckee et al. (1993), introduced a novelty approach on drought quantification at multiple time-scales. Since its formulation, this index has been applied for identifying either wet and dry conditions at different time scales in multiple studies around the world, being recommended by The World Meteorological Organization as the universal meteorological drought index for monitoring and early warning purposes (WMO, 2012). The SPI is a precipitation-based index that transforms the variable into a selected probability function to later convert the probabilities into standardized units with mean equal to 0 and variance equal to 1.

Although Mckee et al. (1993) originally fitted a gamma distribution to adjust precipitation data, subsequent studies noticed that precipitation anomaly aggregation showed differences depending on the time-scale. The Pearson III distribution function has shown to get a better fitting of data at the any time-scale (López-Moreno et al., 2008; Vicente-Serrano, 2006). In this study the calculation of the SPI has been computed adjusting a Pearson III distribution function and obtaining the parameters of the distribution following the L-moments approach announced by Hosking, (1990).

The strengths of the SPI are multiple. First, the index only uses precipitation to characterize abnormal dryness or wetness that makes possible the ease of calculation. Second, the SPI improved the spatial comparison of drought conditions among regions with different climatic

conditions. Finally, it allows capturing the variable response to drought of any natural variable at different temporal scales which is the major differences respecting the PDSIs (Keyantash et al., 2002; Vicente-Serrano et al., 2012). Nonetheless, the SPI also has limitations. For example, the index does not consider the effects of the AED, ignoring the effects of the surface and atmospheric moisture feedback and hence providing a less reliable quantification of drought severity than other indices that consider the climatic water balance in their formulation.

1.3.3. The Standardized Precipitation and Evapotranspiration Index (SPEI)

The Standardized Precipitation and Evapotranspiration Index (SPEI) introduced by Vicente-Serrano et al. (2010) supposes a step forward on the quantification and characterization of drought. The SPEI overcomes the limitations of previous drought indices combining the sensitivity of the PDSI and the multi-temporal conceptualization of the SPI, incorporating the atmospheric evaporative demand as another important variable. Contrary to the basic assumption of the SPI that considers that drought depends only on temporal variability of precipitation, the SPEI take into account the role of temperature calculating a climatic water balance.

Previous studies have acknowledged the repercussion of warming on multiple natural systems stressing the importance of using drought indices that include the AED as a primary variable (Asseng et al., 2014; Cai and Cowan, 2008; Cheng and Huang, 2016; García-Ruiz et al., 2011; Vicente-Serrano et al., 2015). A shift in normal temperature patterns feedback dry conditions inducing negative impacts such as forest fires (Lindner et al., 2010), plagues (Logan et al., 2003), crop yields reduction (Lobell et al., 2011) or water resources depletion (Barnett et al., 2005).

The PDSI including the AED information in its formulation is able to identify warming-related drought impacts on natural systems, however it lacks of the multi-temporal ability for evaluating drought impacts on systems that response to drought at medium and short-time scales (Vicente-Serrano et al., 2012).

The SPEI computes monthly climate balances (D_i) using monthly precipitation and reference evapotranspiration values. Monthly D_i is aggregated at different time-scales and transformed to normal standardized units using a 3-parameter log-logistic distribution and later convert to standard deviations. The resulting values follow a normal distribution comparable to SPI values. This index henceforth enables the comparison of dry/wet conditions among regions independently of the specific climate characteristics. The complete description of the methodology of the SPEI and a comprehensive comparison with the PDSI and the SPI is provided by Vicente-Serrano et al. (2010), Vicente-Serrano and Beguería, (2016) and Beguería et al. (2014).

The SPEI shares the combined strengths of the SPI and the PDSI however, has more data requirements than the SPI and is sensitive to the method selected for calculating the AED.

1.3.4. The Standardized Palmer Drought Index (SPDI)

The standardized precipitation drought index (SPDI) is a recent drought index developed by Ma et al. (2014) based on the principal concept of supply-demand relationship in soil moisture departures (CAFEC) of the PDSI and the multi-scalar ability of the SPI and the SPEI. It is therefore a combined version of the methodologies proposed in the PDSI and the SPEI.

The SPDI accumulates the moisture departures anomalies following the same procedure of the PDSI scheme but at different time-scales. Accumulated anomalies are transformed to a standard variable with mean equal to 0 and standard deviation equal to 1 fitting a General Extreme Value (GEV) distribution. Vicente-Serrano et al. (2015) pointed out the suitability of fitting a log-logistic distribution function in order to avoid the limitations of GEV distribution to fit some extreme values (Vicente-Serrano and Beguería, 2016). Following the recommendation of these authors, in this study data have been fitted using the log-logistic distribution.

2. Objectives

In line with the mentioned in the Introduction section, the analysis performed in the present dissertation covers two wide and heterogeneous territories, peninsular Spain and the US.

Aware of the relevance of selecting appropriate tools for monitoring drought, the general objective of the study aims to provide a validation of the performance of seven of the most commonly used drought indices and their ability to capture impacts on vulnerable systems. For this purpose, three multi-scalar drought indices (the SPI, the SPEI and the SPDI) and four uni-scalar Palmer family drought indices (the PDSI, the PHDI, the Z-index and the PMDI) are compared.

This general objective can be broken down to more specific objectives here described according to the system assess.

Regarding the agrarian system, the specific objectives were to:

i. Analyse the temporal response of the annual crop yield in five main rain-fed cultivations in the United States (wheat, corn, soybean, cotton and barley) at county scale and two rain-fed cultivations in peninsular Spain (wheat and barley) at two scales, provincial and agricultural districts.
ii. Develop a new dataset for environmental variables with enough temporal and spatial coverage.
iii. Identify possible spatial patterns in the response of crop types to drought and defining the main environmental and climatic drivers that determine these patterns.

For vegetation activity, the analysis was only conducted in Spain and the specific objectives were to:

i. Provide a comparison between the response of three indicators of vegetation activity (tree-ring width, maximum annual greenness and a surrogate of the net primary production) to drought.
ii. Assess and compare the response of tree-ring width and NDVI to drought conditions for different species.

Finally, the specific objectives for the hydrological system were to:

i. Determine the climatic drought time-scales that better represent the hydrologic drought as reflected in normalized streamflow anomalies over a range of undisturbed basins in the conterminous US and peninsular Spain.
ii. Identify spatial patterns of streamflow response to climatic drought and possible non-stationarities in that relationship.
iii. Find the environmental and climatic factors that shape the vulnerability of streamflow to climatic droughts.

3. Results: brief summary

The results of this research have been published in four international journals indexed by the Journal Citation Report (Climate Research, Agricultural and Forest Meteorology, Forests and Journal of Hydrology). At the same time, part of the results here presented are part of a manuscript currently under review in another JCR journal (Natural Hazards and Earth System Sciences) and to a manuscript in preparation for submission. The published and unpublished researched can be found in sections 4 and 5 respectively.

In general terms, the relationship between any of the variables assessed (crop productions, tree ring width, greenness value, net primary production and streamflow) in this thesis and the seven drought indices evaluated demonstrated a superior performance of the multi-scalar drought indices. Thus, the highest values of Pearson's r coefficients were found between the SPI, the SPEI and the SPDI and each considered variable. A brief summary of the main results found in each of the studies conducted is provided in the next sub-sections.

3.1. Research Article 1 – results summary

In the US, correlations between the crop yields and the drought indices tended to be higher in soybeans crops than for the any other crop type analysed, while the lowest were found in cotton crops. The Palmer Drought Indices did not perform equally. With the exception of the Z-Index and the scZ-Index, in general PDSIs did not have statistically significant correlations with yields, regardless of the month of the year. On the contrary, correlations between the Z-Index, the SPI, the SPEI and the SPDI and crop yields tended to be statistically significant in the majority of counties analysed. The PDSIs were significantly correlated with crop yields in about 50% of the counties, reaching the self-calibrated versions the highest percentages. Among the three multi-scalar indices and crops, differences were observed. Thus, the SPI showed the highest percentage of counties with significant correlations for barley and soybeans, while the SPEI did best for cotton, corn and wheat. Similar performance was observed in the SPDI.

Attending to the seasonal and time-scales differences observed in each crop, little differences were found among multi-scalar drought indices results.

In general, barley best correlated in counties located in Montana and North Dakota states. The relationship with drought indices was higher during summer months at short time-scales (1 to 3-month). The SPDI was the most correlated drought index in ~30% of counties located along the Canada-U.S. border. The SPI was most correlated in ~ 28% of counties, and the SPEI in ~ 20% of counties mostly located in North Dakota and North Carolina.

Corn showed highest correlations in eastern Corn Belt (Illinois, Indiana and Ohio), southern Texas, southern Pennsylvania and southeastern Georgia and South Carolina reaching maximum agreement with the multi-scalar drought indices in July and August at short time-scales. In the Midwestern counties (51% of total), the maximum correlations were reached by the SPDI, while

the SPEI and the SPI resulted the most correlated indices in the 12.97% and 12.65% of counties respectively.

For cotton, correlations were exceptionally low in general. Maximum correlations were found during summer months also at short time-scales and the SPEI was the drought index with the largest proportion of counties (29.95%) in which the strongest agreement was found with these yields followed by the SPDI (26.82%) and the SPI (19.79%).

Soybeans correlated best in North and South Carolina, Central and Northern Plains of the US areas. August and September were the months in which this crop resulted more sensitive to drought conditions. The multi-scalar indices reached maximum values at 1 to 2-month time-scales, and the SPDI was the drought index that recorded the maximum correlations for most of the counties where soybeans are planted.

Finally, winter wheat presented the highest correlation in the Southern Plains area, mostly during spring months. This crop showed a higher variability regarding the time-scale at which the strongest correlations were detected ranging from short to long time-scales. The SPEI presented the highest number of counties where the strongest relationship between drought and annual winter wheat yields.

3.2. Research Article 2 – results summary

Results from this research highlighted the varied correlation patterns found between the SPEI and the crop yields. SPEI time-scales affected differently among crops, but also among regions, being especially evident on wheat results. In some counties, the response of wheat yields to the SPEI revealed a better agreement at longer time-scales, while in other counties did it at shorter. Overall, spatial patterns of crop yield response to drought at different time-scales demonstrated the need of performance a statistical approach in order to extract well-defined patterns of crop yield and SPEI time-scales. Conducting a Principal Component Analysis (PCA), different patterns were obtained depending on the crop type. Besides, a predictive discriminant analysis allowed to identify the factors that explained the different responses to SPEI time-scales.

For barley, wheat and soybeans, three components were extracted. In the case of barley, the first component explained the 78.3% of the variance and revealed that annual yield of barley was primarily affected by precipitation and AED conditions between January and July. Second and third components represented a low percentage of explained variance. Significant differences in the annual precipitation mainly controlled by the spatial patterns of spring precipitation among the different components were also observed.

Winter wheat showed in the first component positive correlations at 3 to 9-month time-scales in counties mainly located in the states of Nebraska, Kansas and Oklahoma. The second component did not show significant correlations and the third one presented significant correlations between wheat yields and the SPEI at time-scales ranging from short to long in most counties located in Eastern regions, Wisconsin and Illinois. Counties with positive loadings were characterized by more humid conditions than components characterized by negative loadings.

For soybeans, the pattern extracted from the first component was coherent; it presented high positive correlations with the SPEI at the time-scales from 1 to 4-months from July to September and from 4 to 13-months from July to December in counties located in the soybean belt. Second component showed positive correlations in August at 1-month but negative in June at 2 to 7-month in counties situated in Iowa, Missouri and Nebraska states. Third component was restricted to selected counties from Central Atlantic and Northeast showing a high positive correlation with the SPEI at long time-scales during mid and late summer. Among components, strong differences in the temperature and reference evapotranspiration (ETo) were found, as well as in average annual and seasonal values of temperature.

From corn yields, four components were extracted. The two first components shared the same region. The first component showed high positive correlations during summer months at time-scales from 1 to 4-month, while the second component presented negative correlations from January to July. The third and fourth component showed positive correlations at medium time-scales during late winter and spring mainly in central and north-central counties respectively. Differences among components were found characterized by differences in temperature and ETo.

Cotton showed a very specific cultivated area but presented a patchy correlation spatial pattern distributed in five components from which only the two firsts found significant positive correlations at medium and long time-scales in counties located within the cotton belt. In general, differences between the first and second components were likely controlled by the different average precipitation amount.

3.3. Research Article 3 – results summary

Results obtained from the spatial and temporal responses of tree variables to drought first showed significant variations in the magnitude of Pearson's correlations between drought indices and the tree ring width (TRW_i), the greenness range ($NDVI_{max}$) and the Net Primary Production (NPP, $NDVI_{annual}$). In general, TRW_i recorded the highest correlations with both, multi-scalar and uni-scalar indices.

On one hand, the spatial distribution of these correlations between the multi-scalar indices presented similar spatial patterns with maximums in forests mainly located in dry areas of Eastern Spain and the Balearic Islands. On the contrary, minimums were observed in hardwood-dominated forests from Northern Spain, region characterized for wet conditions. Regarding the results obtained specifically for each index, the SPI best correlations were found in the Northwest for $NDVI_{annual}$. For their part, correlations between the SPEI/SPDI and $NDVI_{annual}$ tended to be higher in the Southeast than for $NDVI_{max}$. Highest correlation values for the PDSIs showed spatial patterns similar to those found with the multi-scalar indices, although with lower magnitudes of correlation. Besides, no clear spatial differences in the correlations were found between the Palmer drought indices and $NDVI_{max}$ and $NDVI_{annual}$. In general, the results demonstrated that TRW_i had a higher response to the interannual variability of drought than the $NDVI_{max}$ and $NDVI_{annual}$ as noted from the comparison between maximum correlations of TRW_i than NDVI metrics.

On the other hand, the temporal response revealed dissimilar temporal patterns depending on the analyzed parameter. While secondary growth response to drought severity reached a maximum during summer months (July and August), annual vegetation growth and NPP exhibited a much earlier response to drought in springtime (April and May). Frequently species responded at medium (4 to 6-month) and long (> 6 months) time-scales drought conditions, suggesting that interannual variability of tree metrics to drought varies not only depending on the species, but also on the general hydro-climatic conditions of the region.

Attending to the relationship between vegetation variables and drought by species, no clear differences were found in the performance of any of the three multi-scalar drought indices and both NDVI metrics. Results at this respect suggested that species characteristics of moist and cold regions (e.g., *Abies alba* and *Pinus uncinata*) tended to show lower correlations than species of semi-arid climates (e.g., *Pinus halepensis*). In contrast, more variability was observed in the case of TRW_i that recorded stronger correlations in conifers species from dry regions (*Pinus halepensis*, *Pinus pinaster*, and *Juniperus thurifera*) in comparison to the low values achieved by conifers (*Abies pinsapo*) and hardwood species (*Castanea sativa* and *Fagus sylvatica*) from wet and temperate regions.

3.4. Research Article 4 – results summary

General patterns of response in undisturbed basins in the US to drought revealed differences in the streamflow response to climatic droughts likely controlled by catchment properties. Thus, high positive correlations in most of the analysed basins, except for the Rocky Mountains and Northeastern basins which showed lower correlations from February to April. In general, positive high correlation dominated the relationship between the SPEI and the standardized streamflow index (SSI) with maximum values reached at short time-scales with the exception of snow-regulated basins revealed to response better at longer time-scales.

From the performance of a PCA the existence of substantial variations on hydrological droughts response was confirmed. The 80% of the variance was achieved with seven components that represented the main spatial patterns of the month and time-scale correlation between the SPEI/SPI and the SSI. In general, the two firsts components representing the 55% of total variance, indicated a predominance of response to short time-scales in basins from Southeast and Midwest. While first component tended to be highly correlated at scales lower than 10 months, second component did it at very short time-scales between April and January. The third component representative of SPEI-SSI correlations found highest values in the Pacific Northwestern region at short time-scales from September to February. Longer time-scales found between May and August also showed strong correlations. Fourth component represented the basins located in Rocky Mountains and characterized sensitive responses to drought conditions occurred between June and February at time-scales from 8 to-18-month. Same analysis conducted between the SPI and the SSI showed similar spatial modes of variation to those found using the SPEI.

Among factors that explained the correlation patterns between the SPEI and the SSI, annual average NDVI presented strong differences between components. Particularly, components 1, 2, 6 and 7 correlated more strongly than components 3, 4 and 5. In addition, soil characteristics

varied especially the water field capacity and the depth of soil layers. At the same time, components 7 and 3 showed high intra-basin variability on average annual streamflow. Average basin elevation, temperature, and evapotranspiration differ between components too. Thus, components 3 and 4 were associated at basins located at higher elevations and lower temperatures than other components.

The analysis performed at different sub-periods showed some differences in the relationship between the climatic droughts and streamflow response in the US basins, but also demonstrated that the spatial patterns of the component loadings and the response of the basins were very similar in the analysis conducted by the two indices, the SPI and the SPEI. It was confirmed that the role of variations in the climatic water balance is secondary respecting the importance of precipitation variations. In general, the magnitude of the correlations observed in both sub-periods were very similar to the recorded at global period although differences in terms of the time-scales most correlated were observed.

3.5. Unpublished research 1 – results summary

Results of this analysis showed a stronger correlation for the drought indices in crops at district scale than at provincial scale. Additionally, more variability was found in the provincial data than in the district data, likely associated with the length of the available records. Annual wheat and barley yields depicted a similar spatial pattern among multi-scalar drought indices at the province scale. Strong correlations were found for the SPEI and the SPI in the provinces located in Castilla y León, Aragón, Castilla La Mancha, and the province of Valencia. On the contrary, the weakest correlations were observed in provinces from Southern Spain. The spatial distribution of correlations between annual wheat yields and the drought indices at the agricultural district scale presented clearer patterns. The magnitude of correlations was very similar to those observed at provincial scale, showing stronger correlations for the multi-scalar indices and weaker correlations for the Palmer indices, especially the PDSI and the PHDI. The most correlated agricultural districts were those located in Castilla y León, specifically in the provinces of Valladolid, Segovia, north of Ávila, and northeast of Salamanca. Similar correlations were found for districts in northeast Spain. Results for barley suggested a similar spatial relationship for the various drought indices. The highest coefficients were found for the multi-scalar indices, particularly in districts from the north of Cáceres and Galicia, and in Guadalajara; weaker correlations were registered in districts located in the south of Córdoba and Jaén. Among PDSIs, correlations were significantly high with the Z-index and the PMDI.

The time-scale at which these maximum correlations were found correspond principally to short time-scales in the case of both crops, and little differences were observed between the three multi-scalar drought indices. The scales varied from 1 to 3-month depending on the crop type. Thus, for wheat yields, more than the half of agricultural districts were strongly correlated with the 1-month time-scale while at provincial scale were correlated at 3-month. In the case of barley annual yields, the same temporal pattern was observed.

Although the three multi-scalar indices performed with practically no statistical differences, the SPEI was the most correlated drought index at provincial scale in both crops and at district scale in wheat crops. Districts were barley crops were cultivated correlated most with the SPDI.

From the application of a PCA, clear seasonal patterns were extracted from the relationship between annual yields and drought at district scale, albeit the available data for barley yields were limited. Provincial scale analysis on the contrary provided a less defined pattern. Two components were defined explaining the 60% of the total variance and among crops and spatial scales were reported some differences. Thus, for wheat yields at district scale, the first component corresponded to yields sensitive to drought during spring and autumn at short time-scales, and the second component only to spring months at medium time-scales. At provincial scale, yields in first and second component were found more sensitive in May at medium and long time-scales respectively. In the case of barley at district scale, there were few differences among components except for the time-scale of response. The influence of drought conditions varied from short to medium time-scales in the first component, to long time-scales in the second. At provincial scale, a higher variability in the magnitude of correlations was observed. In general terms, the response to drought was recorded at medium to long time-scales. Spring months were also found the most sensitive period of the year at both spatial scales.

3.6. Unpublished research 2 – results summary

The relationship between climatic drought indices and the standardized streamflow (SSI) from undisturbed basins in Spain was, in general, very strong in most of the basins. The multi-scalar drought indices performed better than the PDSIs, reflecting more efficiency on monitoring streamflow droughts. The particularity of these results was that the Z-index performed very similar to the multi-scalar indices.

The spatial distribution of the maximum correlations unveiled the good performance of the PHDI, the PDSI and the PMDI in selected basins located in the Segura, Guadiana and Ebro major basins, along with some others scattered sparsely located in the Guadalquivir, Tajo, Duero, Minho and Jucar major basins. For their part, multi-scalar drought indices and the Z-index (in lower grade) presented solid correlations equally distributed in the territory. The lower correlations between these indices and the SSI were observed in the basins of the Segura and Ebro, and the northern basins of Catalonia.

Especially, a high variability on the seasonal streamflow response to climate drought was observed. The maximum values of correlation were found, independently on the drought index considered, in months from February to September and the minimum during the months of November and December.

Some of the basins (12.24%) mostly located in eastern major river basins, revealed stronger agreement with one of the Palmer indices, being the Z-index the most representative. The SPDI was noticed as the index in which the greatest percentage of basins found the best agreement (41.92%) followed by the SPEI (25.33%) and the SPI (20.52%). Nevertheless, results from a t-test demonstrated the statistical similarities on the performance of any of the three multi-scalar indices and their capacity for relating with streamflow droughts in a similar form.

The seasonal response of the SSI to the different climatic indices, irrespective of the time-scale, demonstrated that during summer months this relationship reached the weakest values in most of the basins for any of the three multi-scalar drought indices. Results concerning to the response of the SSI to drought time-scales showed that more than the 62% of undisturbed basins presented high correlations at short time-scales (mostly at 2-month). However, focusing at the monthly correlations between the SPDI and the SSI seasonal and spatial differences were identified. The most evident were those observed in calcareous mountain streams that found maximum correlations in June corresponding to drought conditions at medium to long time-scales. This suggests complex associations of different mechanisms that determine the connection between climatic and hydrological droughts in river basins.

4. Published scientific articles

Vol. 75: 221–240, 2018
https://doi.org/10.3354/cr01519

CLIMATE RESEARCH
Clim Res

Published online August 28

Effectiveness of drought indices in identifying impacts on major crops across the USA

Marina Peña-Gallardo[1,*], Sergio M. Vicente-Serrano[1], Fernando Domínguez-Castro[1], Steven Quiring[2], Mark Svoboda[3], Santiago Beguería[4], Jamie Hannaford[5]

[1]Instituto Pirenaico de Ecología, Consejo Superior de Investigaciones Científicas (IPE–CSIC), Zaragoza, Spain
[2]Atmospheric Sciences Program, Department of Geography, The Ohio State University, Columbus, OH 43210, USA
[3]National Drought Mitigation Center, University of Nebraska-Lincoln, Lincoln, NE 68583, USA
[4]Estación Experimental de Aula Dei, Consejo Superior de Investigaciones Científicas (EEAD-CSIC), Zaragoza, Spain
[5]Centre for Ecology and Hydrology, Maclean Building, Crowmarsh Gifford, Wallingford OX10 8BB, UK

ABSTRACT: In North America, the occurrence of extreme drought events has increased significantly in number and severity over the last decades. Past droughts have contributed to lower agricultural productivity in major farming and ranching areas across the US. We evaluated the relationship between drought indices and crop yields across the US for the period 1961–2014. In order to assess the correlations with yields from the major cash crops in the country, we calculated several drought indices commonly used to monitor drought conditions, including 4 Palmer-based and 3 multiscalar indices (Standardized Precipitation Index, Standardized Precipitation Evapotranspiration Index, Standardized Precipitation Drought Index). The 3 multiscalar drought indices were aggregated at 1 to 12 mo timescales. Besides the quantification of the similarities or differences between these drought indices using Pearson correlation coefficients, we identified spatial patterns illustrating this relationship. The results demonstrate that the flexible multiscalar indices can identify drought impacts on different types of crops for a wide range of time periods. The differences in spatial and temporal distribution of the correlations depend on the crop and timescale analyzed, but can also be found within the same type of crop. The moisture conditions during summer and shorter timescales (1 to 3 mo) turn out to be a determining factor for barley, corn, cotton and soybean yields. Therefore, the use of multiscalar drought indices based on both precipitation and the atmospheric evaporative demand (SPEI and SPDI) seems to be a prudent recommendation.

KEY WORDS: Drought · Crop yields · Palmer drought indices · Standardized Precipitation Index · Standardized Precipitation Evapotranspiration Index · Standardized Precipitation Drought Index

1. INTRODUCTION

Many different natural hazards exist, but drought is recognized as one of the most costly and catastrophic (Andreadis & Lettenmaier 2006, Blauhut et al. 2016). Drought can cause a decrease or complete failure of crop yields in agricultural systems (Wilhite 2000, Quiring & Papakryiakou 2003, Lobell & Field 2007, Udmale et al. 2014). Crops are unable to meet their water requirements if insufficient water supplies are available as a result of weather conditions that determine water availability (decreased rainfall, increased atmospheric evaporative demand, or deficient topsoil moisture) during periods in which there is a demand for water by plants (Meze-Hausken 2004, Mishra & Singh 2010, Lobell et al. 2011). The impact of droughts on crop yields depends on the crop type, the stage of crop development and the biological characteristics of the specific crop and soil (Karim & Rahman 2015). Droughts usually reduce the capacity for active

*Corresponding author: marinapgallardo@ipe.csic.es

radiation absorption by the canopy (Earl & Davis 2003); thus the impact of droughts on crop yields depends on the crop type, the stage of crop development and the biological characteristics of the specific crop and soil (Karim & Rahman 2015).

The adverse impacts of drought on crop yields are unequally distributed geographically (Howitt et al. 2015). Natural hazards, including droughts, induced food crop disasters between 2003 and 2013 affecting more than 1.9 billion people in developing countries, causing over US$494 billion in estimated crop damages. In addition, these disasters slowed the economic growth in countries where agriculture is the main sector (30% of the GDP in most countries of Africa and 30% of the labor force in India, for example). On average, about 22% of the total economic impact caused by natural hazards, especially by droughts, occur in the agricultural sector (FAO 2015).

There are signals of increasing interannual variability in crop yields due to changes in drought frequency and severity (Rossi & Niemeyer 2010, Lobell et al. 2011, Olesen et al. 2011). However, quantification of the direct crop yield impacts due to drought is difficult given the complexity of drought events (Wilhite 1993, Wilhite et al. 2007, Geng et al. 2016). In addition, each crop has a differing degree of resilience to drought stress (Wilhelmi et al. 2002, Lobell et al. 2011, Tack et al. 2015, Liu et al. 2016). For these reasons, the quantification of the drought impacts on crop yields is very important.

Drought indices represent a reliable tool for monitoring and studying the impacts of droughts on different sectors, such as crop yields (Wilhite & Glantz 1985). Several studies have used drought indices to identify these impacts at different spatial scales in Europe (Mavromatis 2007, Ceglar et al. 2012, Di Lena et al. 2014, Páscoa et al. 2017), Australia (Lobell et al. 2015), Asia (Arshad et al. 2013, Sahoo et al. 2015, Kattelus et al. 2016, Wang et al. 2016), Africa (Blanc 2012, Elagib 2013), America (Kim et al. 2002, Quiring & Papakryiakou 2003) and at the global scale (Vicente-Serrano et al. 2012, Wang et al. 2014). In general, past research has shown that drought indices can be used to quantify reductions in yield that are associated with drought. Many drought indices have been developed since early last century (Zargar et al. 2011, Wilhite et al. 2014). However, not all drought indices perform equally well in accurately quantifying drought severity because of the different variables involved in their calculations (Morid et al. 2006, Vicente-Serrano et al. 2011). Therefore, it is necessary to compare the performance of different drought indices to determine which are most appropriate for assessing the impacts of drought for different crop types and in different regions. Although some studies have addressed this question at the regional scale (Keyantash & Dracup 2002, Quiring & Papakryiakou 2003, Wang et al. 2017), we are unaware of any studies comparing a variety of drought indices across different crop types and large regions (national to continental scale).

Some studies have suggested that drought vulnerability in the US is increasing (Mishra & Singh 2010, Carrão et al. 2016, Geng et al. 2016). For example, extreme droughts in the US (i.e. those covering >25% of the country) accounted for $6.7 billion in crop losses for 2000–2004 (Wilhite et al. 2007). Extreme drought events have been recorded in the past 2 decades in the southern Great Plains and Southwest (Hayes et al. 1999), the north-central US (McNeeley et al. 2016), South Carolina (Mizzell et al. 2010), California (Rippey, 2016), Midwest and the Great Plains (NOAA 2017, USDM 2017), causing widespread impacts across multiple sectors. Ross et al. (2003) reported that between 1980 and 2003, the US experienced at least one billion-dollar disaster in 20 of 23 years, including 10 major drought/heatwave episodes. NOAA's National Centers for Environmental Information (NCEI) (https://www.ncdc.noaa.gov/billions/) estimated that US losses from drought were $4.1 billion in 2014, US$4.6 billion in 2015, $10.7 billion in 2013 and $31.5 billion in 2012.

The objective of this study was to determine which drought indices are most suitable for monitoring agricultural drought impacts for different crop types at the regional level. Presently, there is no clear consensus about which index is the most appropriate for this purpose (Quiring 2009, Esfahanian et al. 2017). Here we compare the Standardized Precipitation Evapotranspiration Index (SPEI), the Standardized Precipitation Index (SPI), the Standardized Precipitation Drought Index (SPDI) and 4 Palmer-related drought indices (Palmer Drought Severity Index [PDSI], Palmer Hydrological Drought Index [PHDI], Palmer Moisture Anomaly Index [Z-index] and Palmer Modified Drought Index [PMDI]).

2. DATASETS AND METHODOLOGY

2.1. Crop data

Our analysis of drought indices focuses on the 5 crops with the broadest geographic distribution and highest production in the US: barley, corn, cotton, soybean and winter wheat (Fig. 1). Data on crop production for each county are collected by the United

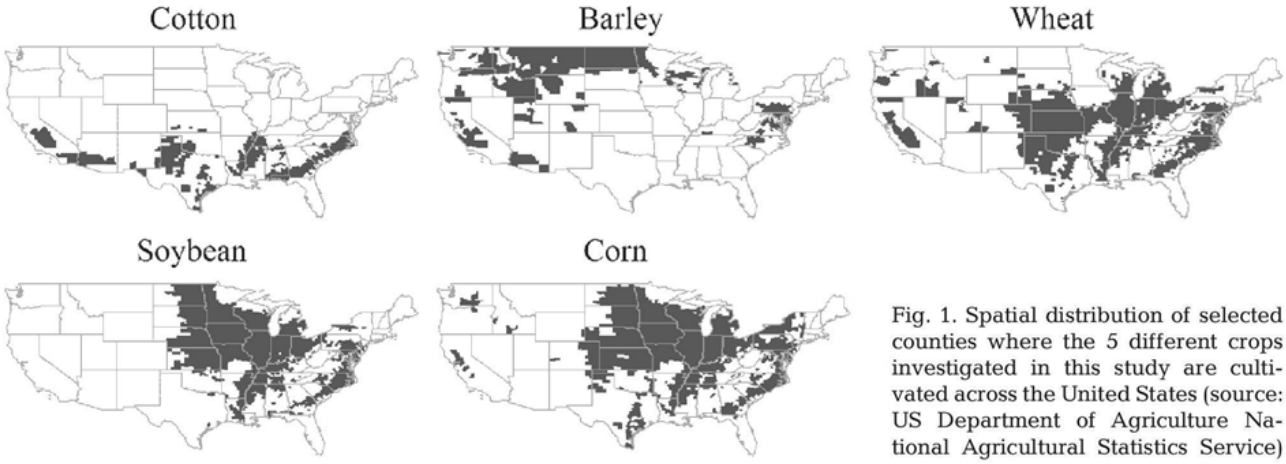

Fig. 1. Spatial distribution of selected counties where the 5 different crops investigated in this study are cultivated across the United States (source: US Department of Agriculture National Agricultural Statistics Service)

States Department of Agriculture (USDA) and made available by the National Agricultural Statistics Service (https://quickstats.nass.usda.gov). Only crop statistics under non-irrigated conditions were considered in this study. We created 5 masks based on the 5 crops considered in this analysis in order to identify the counties where there are representative areas of cultivation of these different crops. For this purpose, the available crop county maps were taken from the USDA (https://www.nass.usda.gov/Charts_and_Maps/Crops_County). Yield (t ha^{-1}) is based on the harvest in each county. The final data set used in this analysis comprised 373 counties for barley, 1542 counties for corn (maize), 388 counties for cotton, 1314 counties for soybeans and 1321 for winter wheat (Fig. 1). These counties have at least 25 years of data between 1961 and 2014.

Considering the importance of technology in enhancing efficiency in agriculture, but without knowing the weight of each technological advance that has occurred during the period of time analyzed in this work, crop yield series were de-trended to remove these non-climatic trends from yield data (Lobell & Field 2007, Xu et al. 2013). Based on the assumption that these improvements have changed linearly over time, the de-trending process was achieved by fitting a linear regression to obtain the yield data and calculating the residuals (e.g. Tigkas & Tsakiris 2015, Poudel & Shaw 2016, Zipper et al. 2016, Páscoa et al. 2017). These residuals were used in the subsequent analyses.

2.2. Climate data

To calculate the different drought indices at the county level, we used gridded data of monthly precipitation and maximum and minimum temperature, which were obtained from the Parameter-elevation Relationships on Independent Slopes Model (PRISM) gridded dataset (http://prism.oregonstate.edu). This dataset was developed and validated by Oregon State University (Daly et al. 2008) and has been used in many different climatological and environmental studies (Tilman et al. 2002, Loarie et al. 2009, Mayer 2012, Sanford & Selnick 2013, Wei et al. 2016).

Available water holding capacity of the soil is a necessary variable to calculate the Palmer drought indices. The National Resources Conservation Service (NRCS) State Soil Geographic (STATSGO) Database was used to determine the mean available water holding capacity of the soil for each county (https://water.usgs.gov/GIS/metadata/usgswrd/XML/ussoils.xml#stdorder).

2.3. Methods

2.3.1. Drought index calculations

Eleven drought indices were calculated: 8 versions of the Palmer Drought Indices suite and 3 drought indices that are generated at different timescales: SPI, SPEI and SPDI. These indices were selected because they are widely used in quantifying and monitoring droughts at both regional (Keyantash & Dracup 2002, Bonaccorso et al. 2003, Lorenzo-Lacruz et al. 2010, McEvoy et al. 2012, Rohli et al. 2016, Yan et al. 2016) and global scales (Dai et al. 2004, Vicente-Serrano et al. 2012, 2015, Trenberth et al. 2014, Geng et al. 2016).

(1) Palmer drought indices. The PDSI is a popular meteorological drought index that is commonly used in the US, as are the PHDI and the Z-index. Using precipitation and air temperature as inputs, the Palmer indices compute an estimation of moisture

supply and demand within a simple 2-layered soil moisture simulation. The PDSI has some issues related to the lack of comparability between regions (Alley 1984, Doesken & Garen 1991, Hayes et al. 1999, Heim 2002). To address this problem, Wells et al. (2004) developed self-calibrated (sc) Palmer indices to automatically determine appropriate regional coefficients. This scPDSI makes the Palmer indices more spatially comparable. Another limitation of the Palmer indices is that they are calculated at a fixed timescale, which limits their ability to accurately monitor and quantify different types of drought (Vicente-Serrano et al. 2011).

(2) SPI. Developed by McKee et al. (1993), the SPI quantifies and assesses precipitation shortages on multiple timescales. It is based on the conversion of the precipitation series using an incomplete Gamma distribution to a standard normal variable with mean = 0 and variance = 1. The SPI has been recommended by The World Meteorological Organization as the universal meteorological drought index (WMO 2012).

(3) SPEI. Proposed by Vicente- Serrano et al. (2010), the SPEI calculation rests on a monthly climate water balance (precipitation minus reference evapotranspiration, ETo), which is accumulated at different timescales and transformed to a normal standardized variable using a 3-parameter log-logistic distribution. Here the ETo was computed using the Hargreaves and Samani equation (Hargreaves & Samani 1985), which is recommended by FAO for data-scarce regions.

(4) Standardized Palmer Drought Index (SPDI). Developed by Ma et al. (2014), the SPDI is based on combining the methods of PDSI and SPI. This index shares the multiscalar concept and the statistical nature of the SPI and SPEI (Vicente-Serrano et al. 2015) and the water balance defined by Palmer (1965). The SPDI is transformed to a standard normal variable using a generalized extreme value distribution.

The different drought indices were calculated from the mean climate series generated for each county. The multiscalar indices (SPEI, SPI and SPDI) were calculated at timescales from 1 to 12 mo. The monthly drought indices for each county were de-trended using the same method that was applied for de-trending the crop yield data.

2.3.2. Relation between crop yields and drought indices

To analyze the relationships between the drought indices and crop yields in each county, we calculated Pearson correlation coefficients (Pearson's r). Since the month of the year when the highest correlation between the drought index and the crop yield were not known *a priori*, we correlated all 12 monthly series for each index with the annual yields.

Therefore, we obtained 12 correlations per index and crop. In addition, for the 3 multiscalar drought indices calculated from 1 to 12 mo timescales (SPI, SPEI and SPDI) we obtained 12 correlations (1 for each of the monthly series) for each timescale, resulting in a total of 144 correlations for each of the 3 drought indices for each crop type and each county. In addition, we also identified the timescale (in the case of multiscalar indices) and month in which the highest correlation was found within each county.

3. RESULTS

Fig. 2 shows the maximum Pearson's r correlations recorded in each county between the annual crop yields and the monthly drought indices used in this study. Generally, and independently of the crop type, Pearson's r coefficients showed higher values for the SPI, SPEI and SPDI. Among the 5 crop types, correlations tended to be higher for soybeans than for the other crop types. The lowest correlations tended to be obtained for cotton. The correlations between the Z-index, SPI, SPEI and SPDI and crop yields tended to be statistically significant in the majority of counties. The highest mean correlation for soybeans was about 0.56 for the SPEI, SPI and SPDI, and for wheat it was around 0.46 using the same indices. Moreover, we found that r = 0.44 for corn, 0.43 for barley and 0.38 for cotton. The Palmer drought indices, with the exception of the Z-index and the scZ-index, generally did not have statistically significant correlations with yield, regardless of the month of the year. Table 1 shows the percentage of counties in which significant correlations between crop yields and drought indices were found. In general, the different crop types have similar values; however, there are large differences between the drought indices. The Palmer indices are significantly correlated with crop yields in about 50% of the counties. The self-calibrated Palmer indices have a higher percentage of counties with significant correlations than the original (non-calibrated) Palmer indices for all crops. For this reason, we show only results of the self-calibrated version of the Palmer indices. In general, the 3 multiscalar indices used in this study performed much better than the Palmer indices. The SPI had the highest percentage of counties with significant correlations for barley and soy-

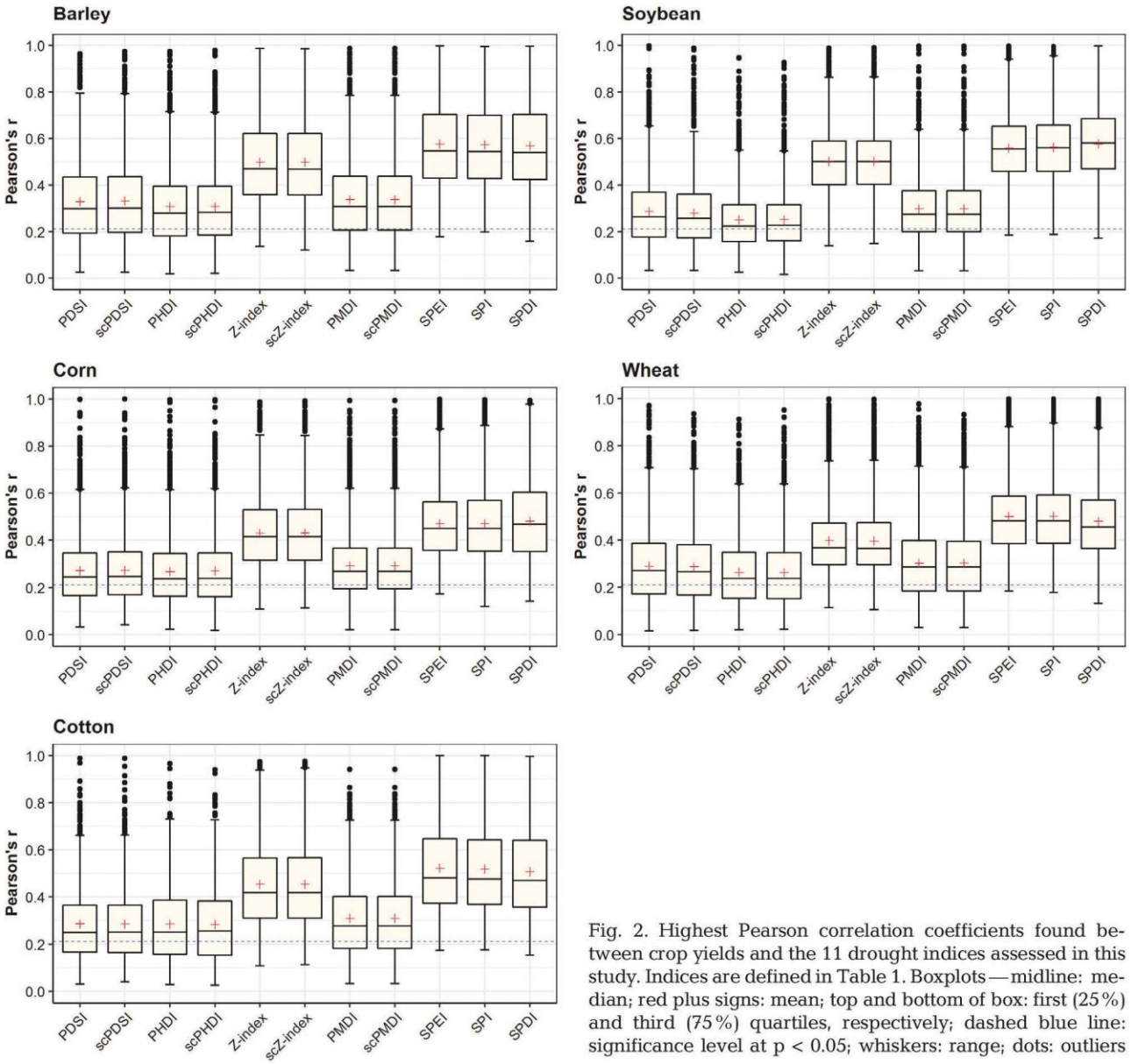

Fig. 2. Highest Pearson correlation coefficients found between crop yields and the 11 drought indices assessed in this study. Indices are defined in Table 1. Boxplots — midline: median; red plus signs: mean; top and bottom of box: first (25%) and third (75%) quartiles, respectively; dashed blue line: significance level at $p < 0.05$; whiskers: range; dots: outliers

Table 1. Percentage of US counties with significant correlations between crop yields and drought indices

Index	Abbreviation	Barley	Cotton	Corn	Soybean	Wheat
Palmer Drought Severity Index	PDSI	58.45	46.89	44.79	52.89	56.55
Self-calibrated PDSI	scPDSI	58.71	47.02	47.40	54.11	58.06
Palmer Hydrological Drought Index	PHDI	53.89	46.95	45.83	42.77	47.69
Self-calibrated PHDI	scPHDI	51.47	47.02	45.83	44.29	48.60
Palmer Moisture Anomaly Index	Z-index	90.62	92.93	85.42	97.34	90.01
Self-calibrated Z-index	scZ-index	90.88	93.00	85.16	97.34	90.16
Palmer Modified Drought Index	PMDI	62.73	58.50	50.30	59.20	61.10
Self-calibrated PMDI	scPMDI	63.27	60.05	51.30	61.19	62.91
Standardized Precipitation Evapotranspiration Index	SPEI	98.12	98.18	97.14	99.47	99.32
Standardized Precipitation Index	SPI	99.20	97.54	95.83	99.54	99.17
Standardized Palmer Drought Index	SPDI	95.44	94.36	93.23	98.17	97.05

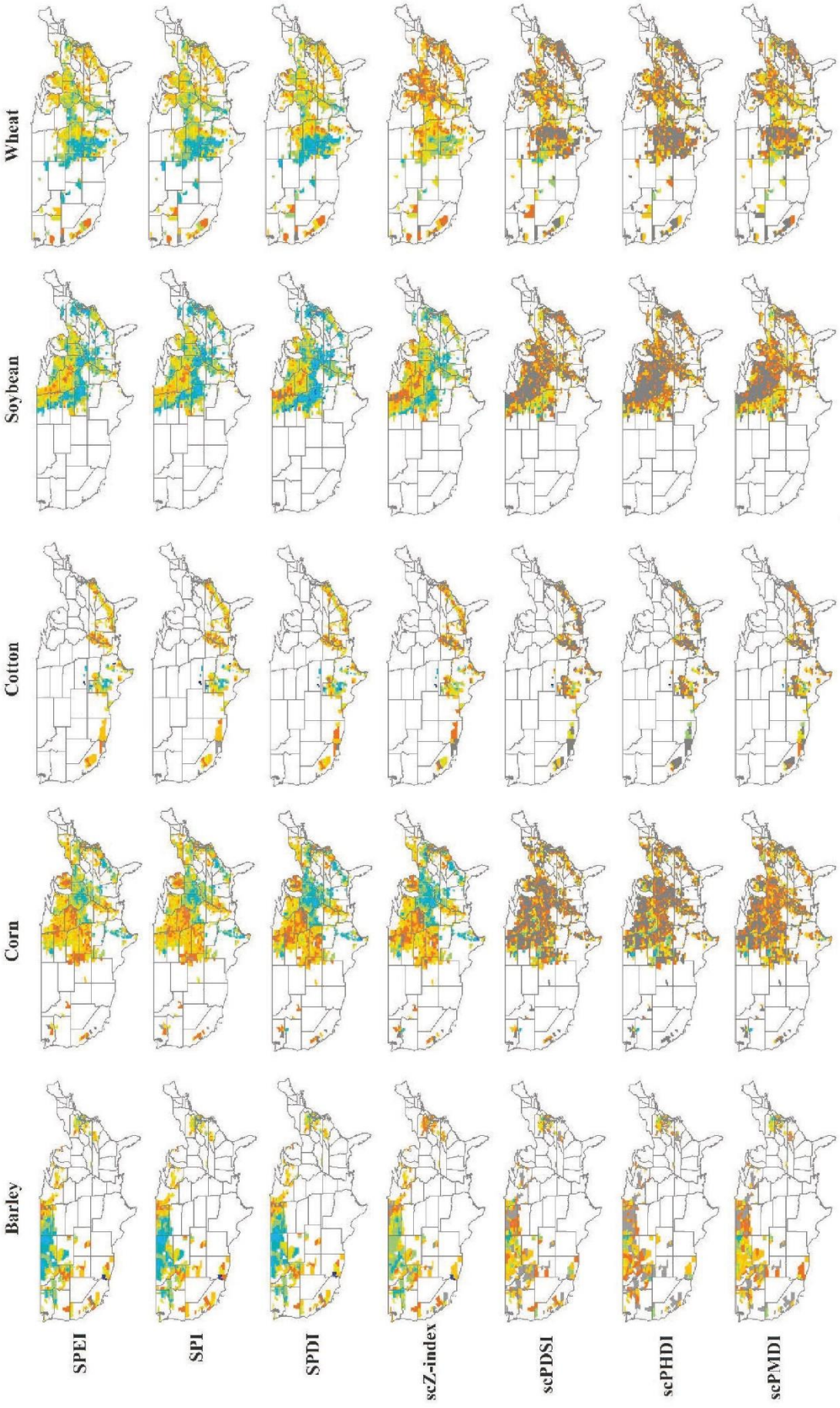

Fig. 3. Spatial distribution of the highest Pearson correlation coefficients obtained for the different indices and crop yields (indices are defined in Table 1). Counties with non-significant correlations ($p < 0.05$) are shown in grey

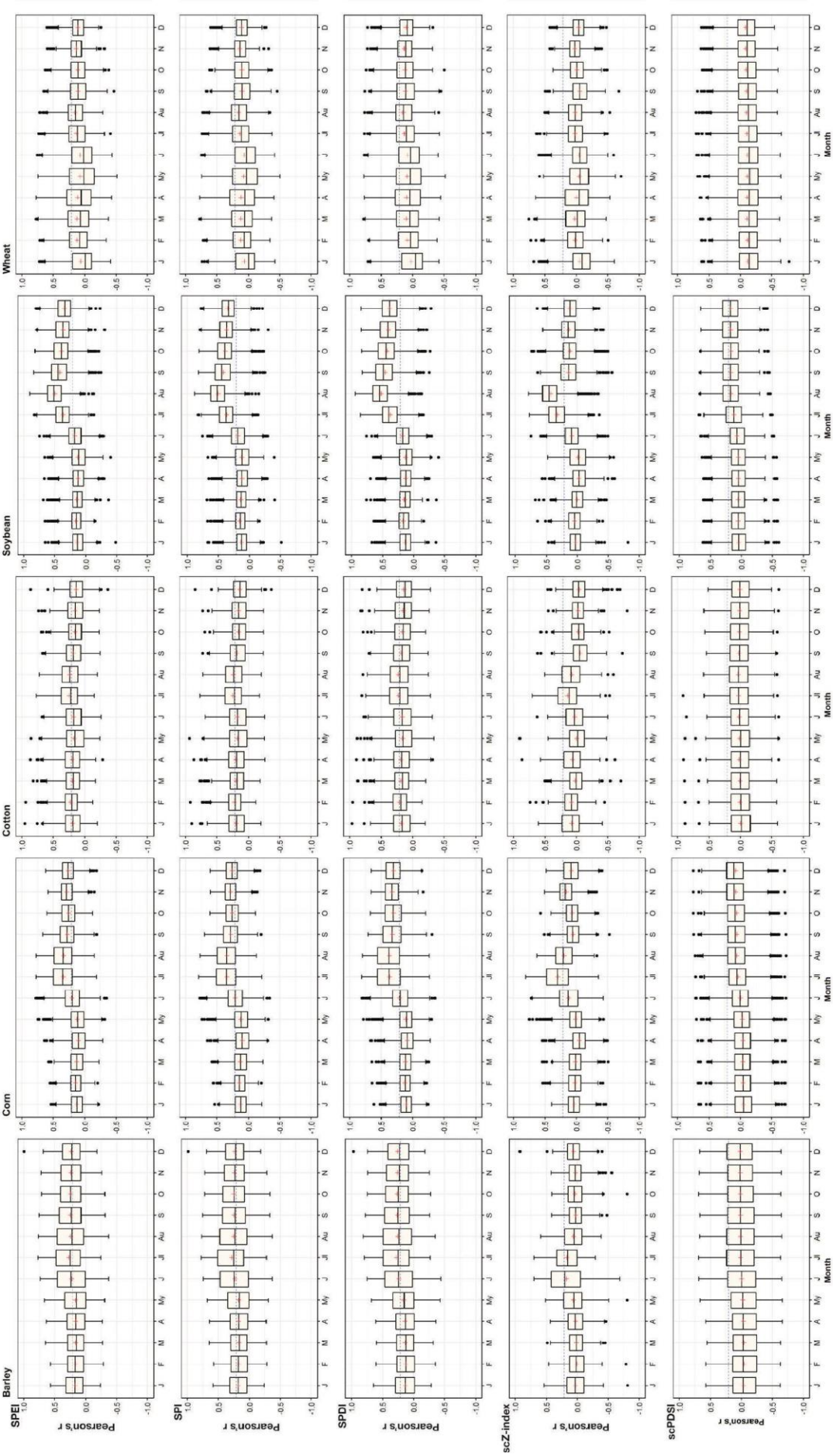

Fig. 4. Pearson correlation coefficients obtained between the monthly series of crop yields and the SPEI, SPI, SPDI, scZ-index and scPDSI. Boxplot parameters as in Fig. 2

Table 2. Percentage of the 373 analyzed US counties where barley, corn, cotton, soybeans and winter wheat are cultivated, and in which the maximum correlations with the 7 drought indices were found. Indices are defined in Table 1. Yearly totals are 100% in all cases

	Jan	Feb	Mar	Apr	May	Jun	Jul	Aug	Sep	Oct	Nov	Dec
Barley												
SPEI	5.90	4.56	3.49	2.68	1.61	14.75	21.72	8.04	10.72	6.70	6.43	13.40
SPI	5.90	4.29	3.22	5.36	1.07	15.01	23.59	9.12	7.51	5.63	5.36	13.94
SPDI	4.83	4.02	4.29	3.75	2.68	15.55	23.06	9.38	9.12	7.51	6.97	8.85
scPDSI	5.36	3.49	2.41	2.95	2.14	3.22	14.48	15.55	7.51	4.83	5.36	32.71
scPHDI	18.77	3.22	4.29	2.68	1.88	2.95	4.83	7.77	5.63	7.77	5.36	34.85
scZ-index	3.49	2.95	3.75	3.22	4.29	32.17	15.28	5.63	6.97	6.97	6.17	9.12
scPMDI	16.09	3.49	2.68	3.49	1.88	2.14	8.04	11.53	5.36	9.12	5.36	30.83
Corn												
SPEI	3.11	1.56	2.27	1.30	2.66	7.07	33.20	25.16	3.44	2.72	13.42	4.09
SPI	3.05	1.43	2.92	0.91	2.98	7.20	31.58	26.39	3.57	3.24	12.84	3.89
SPDI	2.14	1.30	2.27	0.52	2.01	6.49	30.61	29.51	3.76	2.59	15.05	3.76
scPDSI	4.35	1.62	2.79	0.58	1.43	1.49	4.67	12.39	7.72	4.73	17.38	40.86
scPHDI	4.35	1.88	2.27	0.45	0.84	0.71	2.53	6.36	4.41	4.35	15.95	55.90
scZ-index	2.08	1.49	2.59	0.65	2.98	11.41	41.12	13.68	2.08	2.59	16.67	2.66
scPMDI	3.31	1.56	3.05	0.58	1.17	0.52	3.05	8.43	6.55	3.76	17.90	50.13
Cotton												
SPEI	13.92	10.31	3.61	8.51	2.06	3.35	19.59	22.68	4.90	1.55	3.35	5.15
SPI	14.18	11.08	3.87	8.51	3.35	4.38	17.27	20.88	5.93	2.06	3.35	4.12
SPDI	15.72	11.60	3.87	8.76	2.32	2.58	17.78	20.88	6.19	2.06	2.06	4.38
scPDSI	9.54	8.51	3.87	8.76	2.58	3.61	9.02	23.45	5.93	6.96	6.44	11.34
scPHDI	10.31	10.57	5.67	4.90	2.84	2.06	5.41	15.98	8.76	6.44	10.57	15.46
scZ-index	12.37	8.76	6.44	7.47	2.84	4.38	25.77	14.95	5.41	2.58	1.55	6.44
scPMDI	11.60	10.57	3.87	7.47	2.58	2.32	5.67	23.20	7.99	5.15	5.93	12.63
Soybeans												
SPEI	1.07	1.45	0.99	0.99	0.68	0.15	3.58	68.42	10.20	6.09	2.97	3.20
SPI	1.37	1.29	0.76	0.46	0.99	0.68	3.65	68.57	9.21	5.86	3.50	3.65
SPDI	1.67	2.51	0.53	0.15	0.53	0.15	2.28	69.94	12.86	4.49	2.05	2.21
scPDSI	5.18	2.59	1.90	1.60	0.99	0.15	1.52	17.50	12.18	9.67	15.53	31.20
scPHDI	4.11	1.37	1.60	0.46	0.23	0.08	0.61	5.33	6.32	6.24	12.56	61.11
scZ-index	0.53	2.74	0.61	0.38	0.76	0.91	19.25	67.12	1.37	3.20	1.45	1.67
scPMDI	4.49	1.67	1.83	0.38	0.23	0.08	0.76	9.21	10.05	6.39	16.44	48.48
Winter wheat												
SPEI	3.56	4.69	10.07	14	6.81	2.04	9.92	16.5	5.83	6.43	13.32	6.74
SPI	3.48	5.00	8.33	16.28	7.04	2.35	9.84	16.43	5.53	6.06	13.02	6.66
SPDI	4.01	4.62	9.99	13.7	9.69	2.73	9.08	16.58	6.43	7.8	9.77	5.60
scPDSI	14.00	5.6	5.37	6.81	7.19	3.48	5.00	5.83	5.00	5.00	12.94	23.77
scPHDI	28.84	9.84	6.81	5.68	4.16	2.95	6.66	5.22	2.95	3.56	9.16	14.16
scZ-index	3.10	7.12	13.78	13.55	6.28	2.65	10.37	14.99	4.54	7.87	10.98	4.77
scPMDI	20.36	10.52	6.89	5.9	7.57	3.26	6.51	5.15	4.31	3.48	9.08	16.96

beans, while the SPEI did best for cotton, corn and wheat. The SPDI performed quite similar to the SPI and SPEI. The scZ-index also did relatively well.

The results are described separately for each crop. Fig. 3 shows the geographical distribution of the highest correlations between the drought indices and yield for the 5 crops. Fig. 4 displays the correlations between the different monthly series of drought indices and crop yields. Table 2 and Fig. A1 in the Appendix shows the seasonal differences in the performance of the drought indices to assess crop impacts. Fig. 5 and Fig. A2 illustrates the drought timescales that were found more useful for the SPI, SPDI and SPEI.

3.1. Barley

Barley yields show the highest correlations ($r > 0.7$) in the state of Montana and in eastern North Dakota.

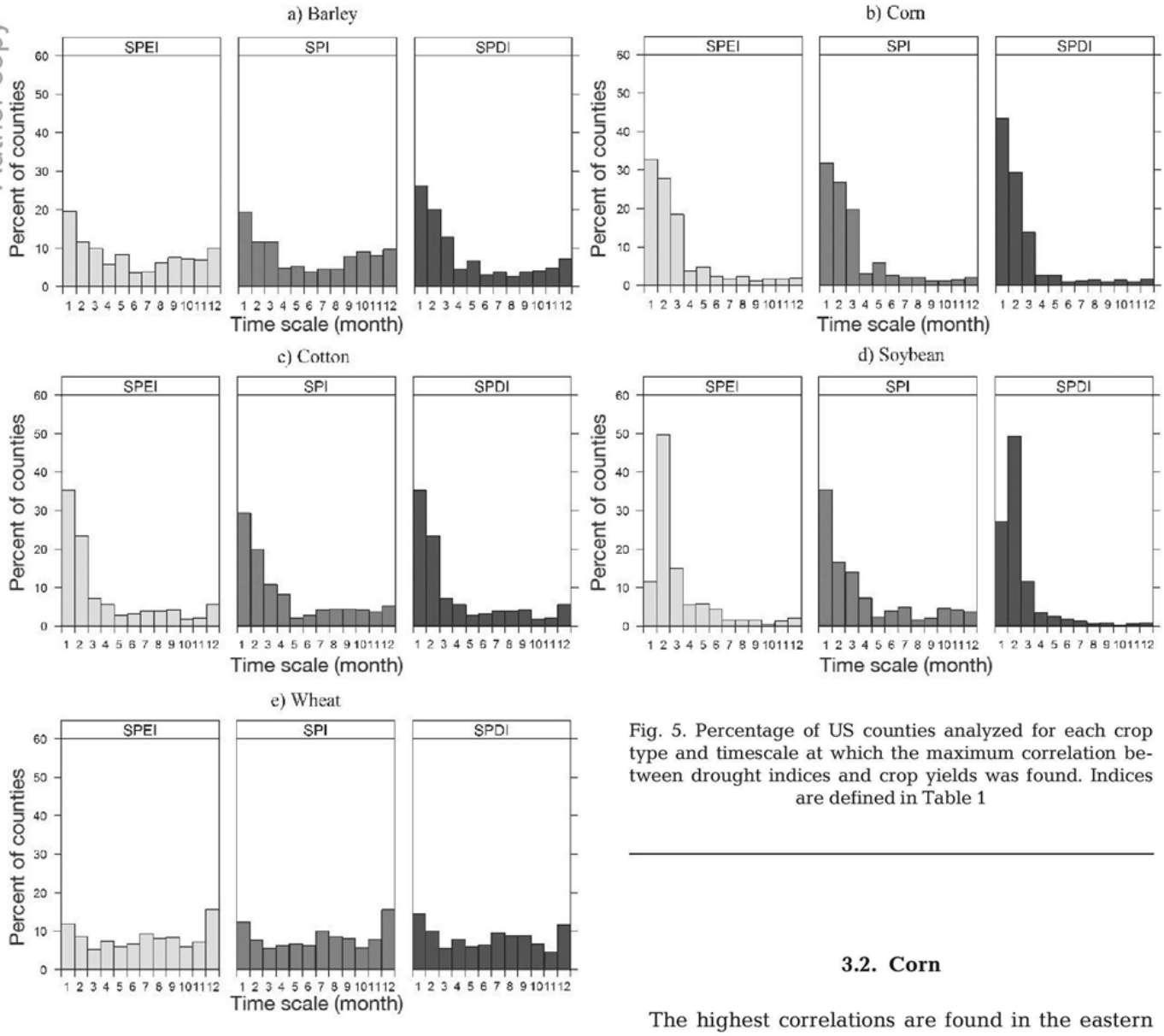

Fig. 5. Percentage of US counties analyzed for each crop type and timescale at which the maximum correlation between drought indices and crop yields was found. Indices are defined in Table 1

High correlations are recorded in these areas with the SPEI, SPI and SPDI. In contrast, the lowest correlations are found in the north central and eastern US barley-cultivated lands. Generally, the self-calibrated Palmer drought indices show lower correlations ($r < 0.5$) in the counties where the multiscalar indices show better results. The Z-index shows similar results to the multiscalar indices, but is characterized by lower r values (Fig. 4). Correlations tend to be higher in the summer months, and this pattern is identified with the SPEI, SPI, SPDI and Z-index (Table 2). In addition, barley is most sensitive to drought conditions on short timescales (1 to 3 mo) (Fig. 5a).

3.2. Corn

The highest correlations are found in the eastern Corn Belt (Illinois, Indiana and Ohio), southern Texas, southern Pennsylvania and southeastern Georgia and South Carolina, whereas the lowest correlations are found in central-northern states and Michigan. The drought indices with higher correlations are the SPEI, SPI, SPDI and scZ-index. The scPDSI, scPHDI and scPMDI show large areas with no statistically significant correlations with corn yield (Fig. 3). July and August are the months with the highest correlations for corn yields using the different multiscalar indices and the scZ-index. The scPDSI does not show as clear a pattern as the other indices (Fig. 4, Table 2). In general, the strongest response for multiscalar drought indices is found when considering the shorter (1 to 3 mo) timescales (Fig. 5b).

3.3. Cotton

The areas where cotton is planted are more geographically concentrated than the other crops. Correlations are low, in general, for all of the indices analyzed. Only the counties from northern Texas and Kansas present high correlations (Fig. 3). July and August have the highest correlations for all of the indices analyzed, although there is less seasonality than for the other crops (Fig. 4). The multiscalar indices, as well as the Palmer drought indices, also show maximum correlations in summer (Table 2). The highest correlations are found at shorter timescales (Fig. 5c).

3.4. Soybeans

North and South Carolina and the Central and Northern Plains of the US are the areas where the highest correlations are found between the multiscalar indices (along with the scZ-index) and soybean yields. These correlations present the same spatial distributions for the SPEI, SPI and SPDI results, while the area with correlations of $r > 0.7$ for the scZ-index is smaller. In general, these indices record lower correlations across northeastern Iowa, Minnesota, Michigan and eastern North Dakota. The results for the scPDSI, scPHDI and scPMDI show low significant correlations in most of the counties except for some counties in Nebraska, Kansas and Pennsylvania (Fig. 3). According to the months in which soybean crops are more vulnerable to drought, August and September clearly have the highest correlations (Fig. 4, Table 2). Again, the Palmer drought indices show lower correlations and no well-defined seasonal patterns. The 2 mo timescale has the greatest concentration of high correlations (Fig. 5d). The SPEI and SPDI agree with this pattern, while the SPI indicates that a 1 mo timescale is optimal. In 91% of counties in which soybeans are planted, the shorter timescales (1 to 2 mo) are optimal.

3.5. Winter wheat

Winter wheat presents a well-defined area in the Southern Plains with highest correlations between annual yields and the drought indices, while in the Atlantic Coastal Plains, West and the Midwest areas, the lowest correlations are found in the cases of the SPEI, SPI and SPDI. The correlation values of the SPEI are slightly higher than those of the SPI and SPDI. The scZ-index shows lower correlations in comparison with the multiscalar indices, but it performs better than the other Palmer drought indices. The scPDSI and scPMDI have higher correlations than the scPHDI (Fig. 3). March, April and May have the strongest response to moisture conditions, although the seasonal pattern for winter wheat is less defined than for the other crops (Fig. 4, Table 2). The best timescale is also more variable than in other crops (Fig. 5e). The 12 mo timescale for the SPEI and SPI was found to be the most suitable in ~15% of counties, while for the SPDI, the 1 mo timescale had the highest correlations in 12.5% of the counties. In general, only 40% of the counties show that shorter timescales (1 to 3 mo) are most suitable.

3.6. County response to drought indices

Fig. 6 identifies the drought index with the highest correlation in each county and for each crop. Table 3 shows the percentage of counties where each drought index has the highest correlation with crop yield for each crop. The SPDI is the best drought index for barley in ~30% of counties and these are mainly located along the Canada–US border. The SPI is the best index for barley in ~28% of counties. The SPEI is best in ~20% of counties, which are primarily located in North Dakota and North Carolina. The Palmer drought indices are much less important.

Corn has a well-defined area in the Midwestern US where SPDI has the highest correlation. In total, the SPDI is the best drought index for corn in nearly 51% of counties. The SPEI and SPI have similar numbers of counties where they are most strongly correlated with corn yield (12.97% and 12.65% respectively), and these regions are mainly located in southern and northern Texas, the South Atlantic region, and the states of North and South Dakota, Minnesota and New York. The scPHDI is the best drought index for corn in ~9% of counties, and these are primarily located in northwestern and central Iowa and Michigan. The scZ-index is the best index in only ~6% of counties and lacks a spatially coherent pattern.

For cotton, the SPEI is the drought index that was best in the largest proportion of counties (29.95%), followed by the SPDI (26.82%) and the SPI (19.79%). The scPHDI is the best drought index ~8% of counties, which are located principally in western Tennessee.

Soybeans and winter wheat show similar patterns, with 95% and 90% of the counties being highly correlated with 1 of the 3 multiscalar indices, respectively. In general, the SPDI is the best drought index

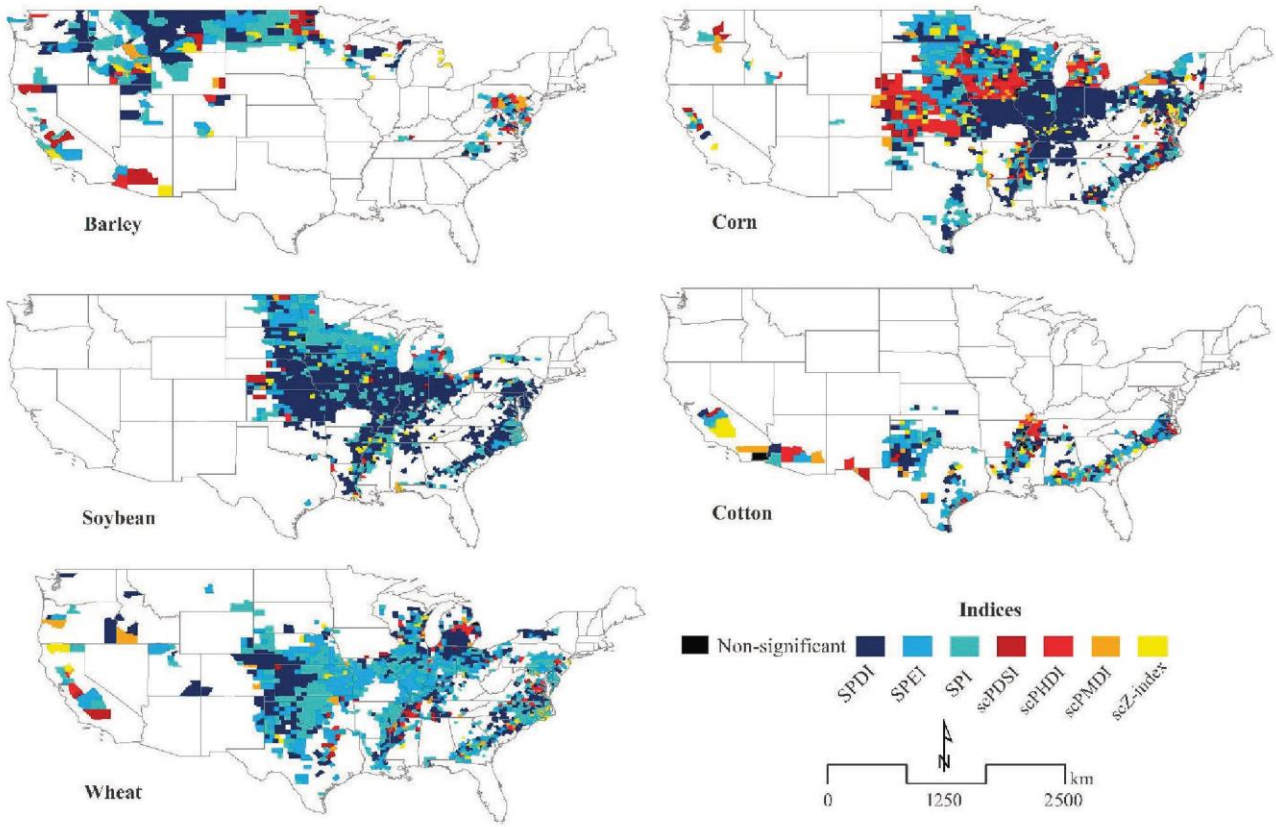

Fig. 6. Spatial classification of the US counties and crop types according to the drought indices that recorded the highest Pearson *r* correlation coefficient independently by timescale and month. Indices are defined in Table 1

Table 3. Percentage of US counties where each index recorded the highest correlation values between the drought index and crop yield. Values are expressed in percentages of the total of all counties. Indices are defined in Table 1

	SPEI	SPI	SPDI	scPDSI	scPHDI	scPMDI	scZ-index
Barley	20.38	27.61	30.29	7.77	4.83	4.29	4.83
Corn	12.97	12.65	50.97	5.25	9.53	2.85	5.77
Cotton	29.95	19.79	26.82	4.69	7.81	4.43	6.51
Soybeans	11.26	22.68	61.19	1.07	0.91	0.61	2.28
Wheat	30.66	31.04	28.61	2.65	2.73	2.2	2.12

for soybeans, and the SPEI is the best drought index for winter wheat. Kernel density curves for each crop and the correlations with drought indices are shown in Fig. 7. The scPDSI clearly stands out as the least correlated index (e.g. soybeans), while the multiscalar indices show greater variability. Fig. 8 shows maximum correlation scatterplots between pairs of drought indices (SPEI, SPI, SPDI and scZ-index) for the different crops, including the coefficient of determination (r^2) for each. The correlation differences between the 3 multiscalar drought indices are small (Fig. 8). The correlations for the multiscalar drought indices are significantly higher than the Palmer drought indices. There are minimal differences in the maximum correlation values between the 3 multiscalar indices. The scZ-index is also relatively similar.

The SPEI and SPI have the highest r^2 values (above 0.95) for the 5 crops, while the scZ-index and SPEI and scZ-index and SPDI have the lowest r^2 values (0.7). Based on the r^2, the multiscalar indices (SPEI, SPI and SPDI) are similar, and any one of these indices is suitable for monitoring drought and its impacts on crop yield.

4. DISCUSSION

In this study, we assessed the appropriateness of 11 drought indices for monitoring agricultural drought affecting the 5 main crops grown in the US. We identified spatial patterns illustrating the relationship

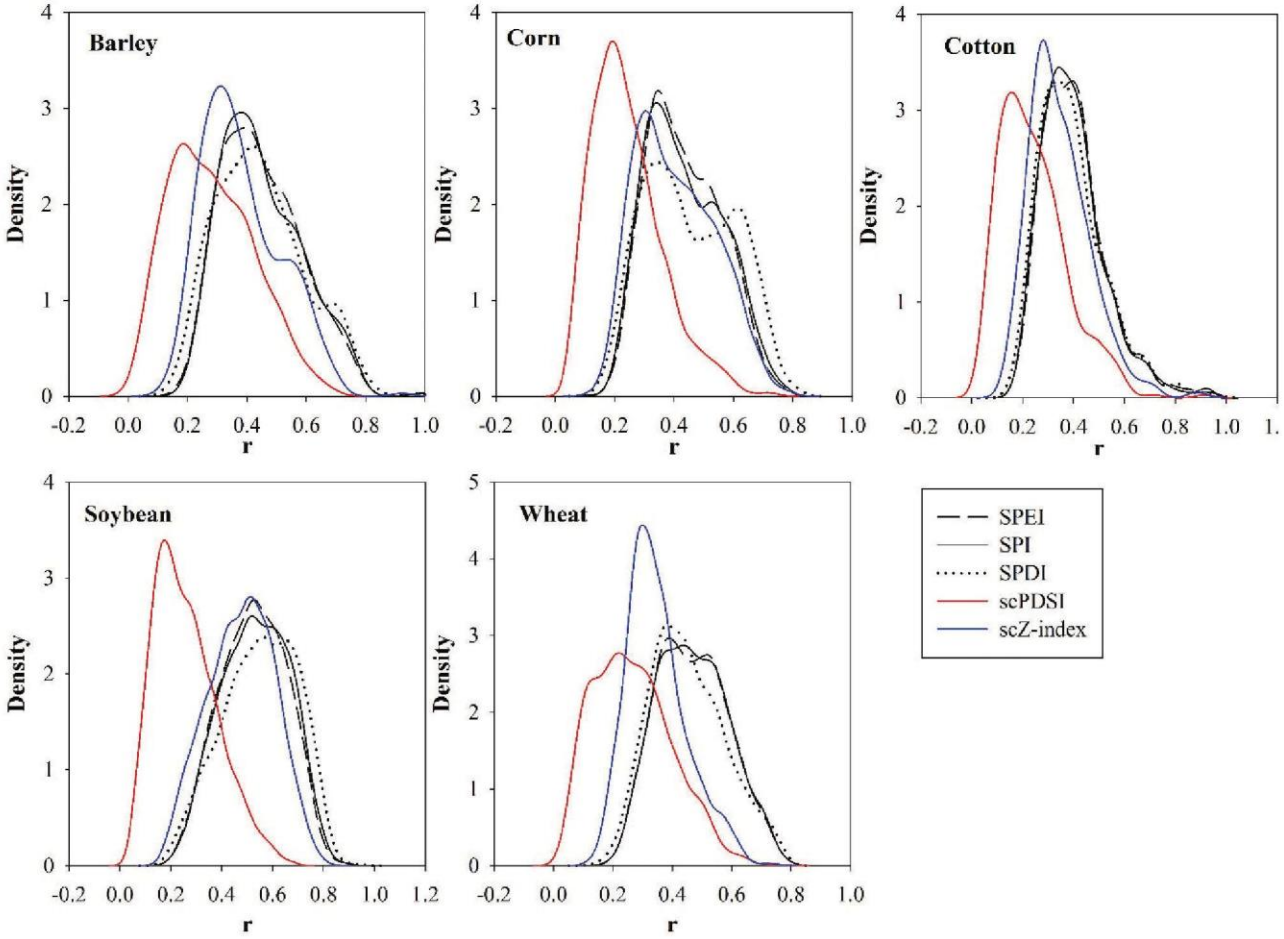

Fig. 7. Kernel density plots of the highest correlations found per index and for each crop. Indices are defined in Table 1

between crop yields and drought indices within the contiguous USA. For this, we used some of the most widespread drought indices employed for monitoring and scientific purposes, including different versions of the PDSI, the SPI, the SPEI and a recent multiscalar index based on the PDSI, the SPDI. The last 3 indices were obtained at several different timescales.

The Palmer drought indices have lower correlations with crop yields than the multiscalar drought indices, although the self-calibrated versions of the Palmer indices marginally improve their performance. In northern and central Greece, Mavromatis (2007) carried out an evaluation of the SPI and variations of the PDSI (the PDSI, the scPDSI and the scZ-index) for assessing common and durum wheat rain-fed yields. The results obtained suggested that drought indices based on Palmer's procedure have a weaker capacity for predicting yield losses than the multi-scalar ones. Nonetheless, the results also show that the self-calibrated PDSI versions performed best for wheat yields, and in general showed higher correlations than the non-calibrated ones.

Among the Palmer drought indices, the Z-index was more responsive to crop yields, recording more significant and higher correlations. These results are supported by previous studies; for example, Karl (1986) recommended the use of the Z-Index over the PDSI or PHDI in the USA. Quiring & Papakryiakou (2003) compared 4 drought indices (SPI, PDSI, Z-index and NOAA Drought Index) for estimating spring wheat yields on the Canadian prairies. They found that the Z-index was the most appropriate index for predicting yield when moisture stress occurs during the growing season, outperforming the PDSI. Sun et al. (2012) also found in the Canadian prairies that the PDSI was less relevant during the early stages of spring wheat growth than the Z-index. Finally, in the Czech Republic, Hlavinka et al. (2009) showed that the Z-index explained 81, 57 and 48% of the variability in barley, winter wheat and

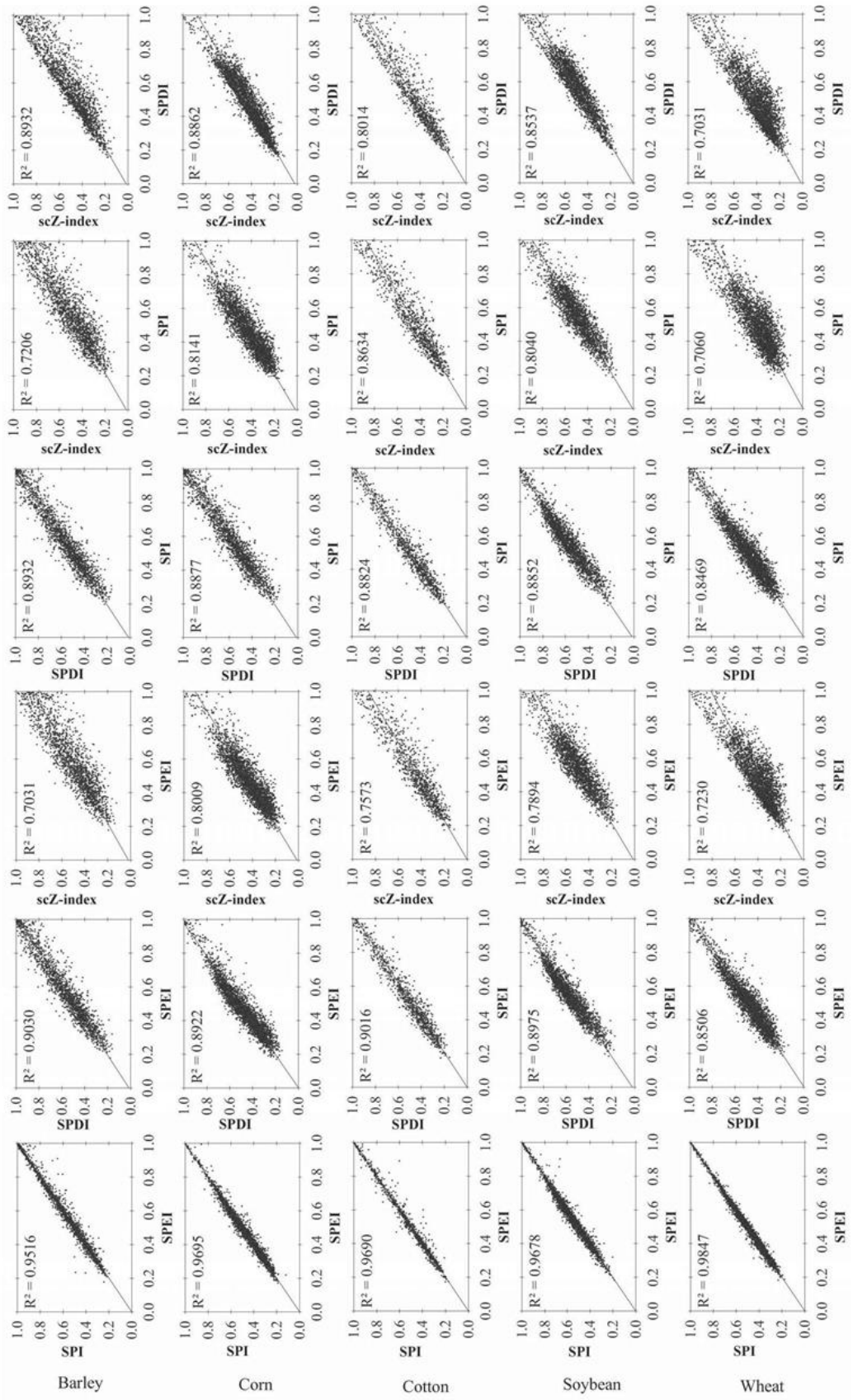

Fig. 8. Maximum correlation scatterplots of index pairs (SPEI, SPI, SPDI and scZ-index; indices are defined in Table 1) for each of the crops analyzed. Each point corresponds to the maximum correlation between drought index and crop yield recorded within each county. The coefficient of determination (R^2) is noted in each plot

corn, respectively. In our results, the highest percentage of counties where the scZ-index was found as the most suitable index was attained for cotton crops (6.51%).

We have shown that in general, independent of the type of crop, the 3 different multiscalar drought indices used in this study have higher correlations with crop yields than the Palmer drought indices. Although Palmer drought indices are used in current drought monitoring systems in the USA (e.g. US Drought Monitor, National Integrated Drought Information System and the National Weather Service's Climate Prediction Center), they still lack of the flexibility of the multiscalar indices (Vicente-Serrano et al. 2011). Our study demonstrates that multiscalar indices, such as the SPI, SPEI and SPDI, are better suited for quantifying drought impacts on a variety of crop types in the USA. The highest correlations between crop yields and drought indices ranged between 74 and 92% for multiscalar indices, whereas the Palmer indices had percentages ranging from 8 to 26%, depending on the crop. Several previous studies have noted the underperformance of the drought indices that are calculated on a single timescale. For example, McEvoy et al. (2012), Vicente-Serrano et al. (2012) and Q. Wang et al. (2017) highlighted the advantages of using multiscalar indices to identify crop failure and/or yield reductions associated with drought. This pattern can be explained by diverse environmental conditions (e.g. soil, climate, agricultural practices, disease and pests) that affect the direct response of crop yields to drought severity. For this reason, it is preferable to work with flexible indices, which may adapt to the different time lags of response between climate conditions and crop responses, mostly during the key stages of crop development.

In this study, we have revealed significant spatial variability in drought index performance, but also solid differences in the response to the drought indices amongst the different crop types. Thus, determining the best-suited drought index for a specific crop region is particularly difficult, since the response to drought varies depending on the crop's sensitivity to moisture shortage and the environmental characteristics of the study region (Mavromatis 2007). In addition, the response of the crop to drought indices also shows strong seasonality.

Non-irrigated crop moisture requirements, and for instance, the most sensitive stage to soil dryness, usually covers the vegetative growth stages (approximately the first 3 mo after planting), which would explain why meteorological drought is the main explanation for the strongest correlation values found at short timescales which, contrary to longer timescales, do not tend to have a smooth drought time series. As shown in the results, different types of crops are more sensitive, in general, to 1 to 3 mo timescale droughts in July (e.g. corn and barley) and August (e.g. soybean). This agrees with the planting times of the crops analyzed; for corn, these dates go from late March in some counties to May, while barley and soybean are planted between April and May. The results for cotton also indicated that a 1 mo timescale had the highest correlation, although longer timescales were found in ~30% of counties. The response of the month with the highest correlation was less clear, but it mainly corresponded to July and August. In contrast, winter wheat, planted in October and mostly active during spring months, presented a more heterogeneous response to timescales but a well-defined pattern of response to months as seen in the Great Plain where spring months are the most correlated at 3 to 4 mo timescales corresponding with the critical soil moisture recharge state during winter months.

In short, the moisture conditions during summer are important determinants for barley, corn, cotton and soybean yields. Summer months correspond to heading and reproductive stages of these crop types, and in these stages, the plants are more sensitive to water stress (Denmead & Shaw 1960, Çakir 2004, Zipper et al. 2016). In contrast, winter wheat showed a higher sensitivity to drought conditions during the spring, which corresponds to the period when winter wheat is more sensitive to water availability.

Generally, moisture conditions during shorter timescales (1 to 3 mo) were more important, except for winter wheat. These conclusions are consistent with the results of previous studies. For example, Moorhead et al. (2015) found that crop production of corn, soybeans and cotton was negatively impacted by drought conditions during July, suggesting a fast response to short-term precipitation deficits. Winter wheat responds in a different way since its growing season is different from the crops mentioned above. In a study carried out on the Iberian Peninsula, Páscoa et al. (2017) found that the months that showed the strongest control of drought on wheat yield were May and June, the period that corresponds to the grain filling and ripening phases. They also showed a response to longer SPEI timescales, since soil water availability in spring and early summer is strongly determined by winter soil moisture recharge given low evapotranspiration rates during the cold season (Austin et al. 1998). Wang et al. (2016) and H. Wang et al. (2017) showed a similar pattern in Northern

China and the Huang Hui Hai Plain, respectively, and noticed that the highest correlations between soil moisture and winter wheat yields were found in the months prior to the harvest season (i.e. October–December).

Zipper et al. (2016) examined the impact of drought on corn and soybeans in the US and confirmed our findings. Thus, corn results show the most sensitivity to drought occurring during July at a 1 mo timescale, while soybeans are most sensitive to droughts occurring in August at a 2 mo timescale. Similar results for soybeans using the SPEI were also found in Liaoning Province in China (Chen et al. 2016) and within the Elbe River Lowlands in Eastern Europe (Potopová et al. 2016).

Here we stress that agricultural drought impacts are directly dependent on the specific characteristics of each crop, its timing and sensitivity periods (Hlavinka et al. 2009). Thus, overall our results show that droughts are more prone to affect winter crops during the spring growing season (May through June in the US). Short timescales (1 to 3 mo) in agricultural systems respond to the state of the soil moisture levels as the first trigger of crop stress.

The analysis of the performance of a drought index to properly identify the derived drought impacts is key for accurate management and monitoring of drought risk. The indices selected for this study have been applied in many different studies concerning drought (Meyer et al. 1991, McEvoy et al. 2012, Feng et al. 2017).

The advantageous flexibility of the multiscalar drought indices calculated for different timescales (SPEI, SPI and SPDI) to identify drought impacts has been clearly identified in this study. Nevertheless, among the 3 multiscalar indices analyzed, the SPEI and SPDI showed higher correlations than the SPI for most of the crops. Although the difference in the magnitude of the correlation was small, the role of the atmospheric evaporative demand on drought severity and crop stress cannot be ignored. Different assessment methods have been used to estimate temperature impacts on different types of yields (Rosenzweig et al. 2014, Asseng et al. 2015). In a recent study, Liu et al. (2016) estimated a decrease between 4.1 and 6.4% of wheat yields with a 1°C global temperature increase, and it is suggested that in the US, a decrease of 7.6% in the wheat production for the period 1985–2013 may be associated with the increase in temperature, especially during the growing season (spring months) (Tack et al. 2015). Moreover, Lobell et al. (2014) indicated that the sensitivity of corn yields to drought stress in the USA increased in crops associated with high vapor pressure deficits, and stressed the need for considering the atmospheric evaporative demand in drought quantification. Therefore, the use of multiscalar drought indices based on both precipitation and the atmospheric evaporative demand (SPEI and SPDI) seems to be a prudent recommendation, to better quantify drought severity in comparison to the SPI, even more so when considering state-of-the-art climate change projections, which predict a significant drying in some of the major agricultural areas of the USA toward the end of this century, which will only be enhanced by warmer conditions (Feng et al. 2017).

5. CONCLUSIONS

The main results of this study are as follows:

(1) Differences exist between the performance of various drought indices used to identify drought impacts on crop yields, resulting in different temporal and spatial variations among crop types.

(2) Multiscalar drought indices outperform uniscalar drought indices for monitoring the impact of drought on crop yields.

(3) SPEI, SPI and SPDI all had very similar correlations, and in most cases, all of these indices are suitable for monitoring the impact of drought on various crops.

(4) Multiscalar drought indices have a high capacity to identify the seasonality of drought impacts. They can properly reflect drought conditions during the critical phenological stages of various crops.

(5) In general, shorter drought timescales (1 to 3 mo) are better at identifying drought impacts on crop yields, with the exception of winter wheat, the growth response of which is related to longer drought timescales.

(6) Before applying a specific drought index for agricultural drought monitoring, it is important to review any previous assessments to determine which indices and timescales are most suitable.

Acknowledgements. This work was supported by the research project I-Link1001 (Validation of climate drought indices for multi-sectorial applications in North America and Europe under a global warming scenario) financed by CSIC, PCIN-2015-220, CGL2014-52135-C03-01, Red de variabilidad y cambio climático RECLIM (CGL2014-517221-REDT) financed by the Spanish Commission of Science and Technology and FEDER, and IMDROFLOOD financed by the Water Works 2014 co-funded call of the European Commission. M.P.-G. received a grant from the Spanish Ministry of Economy and Competitiveness.

LITERATURE CITED

Alley WM (1984) The Palmer Drought Severity Index: limitations and assumptions. J Clim Appl Meteorol 23: 1100–1109

Andreadis KM, Lettenmaier DP (2006) Trends in 20th century drought over the continental United States. Geophys Res Lett 33:L10403

Arshad S, Morid S, Mobasheri MR, Alikhani MA, Arshad S (2013) Monitoring and forecasting drought impact on dryland farming areas. Int J Climatol 33:2068–2081

Asseng S, Ewert F, Martre P, Rötter RP and others (2015) Rising temperatures reduce global wheat production. Nat Clim Chang 5:143–147

Austin RB, Cantero-Martínez C, Arrúe JL, Playán E, Cano-Marcellánc P (1998) Yield–rainfall relationships in cereal cropping systems in the Ebro river valley of Spain. Eur J Agron 8:239–248

Blanc E (2012) The impact of climate change on crop yields in sub-Saharan Africa. Am J Clim Change 1:18072

Blauhut V, Stahl K, Stagge JH, Tallaksen LM, De Stefano L, Vogt J (2016) Estimating drought risk across Europe from reported drought impacts, drought indices, and vulnerability factors. Hydrol Earth Syst Sci 20:2779–2800

Bonaccorso B, Bordi I, Cancelliere A, Rossi G, Sutera A (2003) Spatial variability of drought: an analysis of the SPI in Sicily. Water Resour Manag 17:273–296

Çakir R (2004) Effect of water stress at different development stages on vegetative and reproductive growth of corn. Field Crops Res 89:1–16

Carrão H, Naumann G, Barbosa P (2016) Mapping global patterns of drought risk: an empirical framework based on sub-national estimates of hazard, exposure and vulnerability. Glob Environ Change 39:108–124

Ceglar A, Medved-Cvikl B, Moran-Tejeda E, Vicente-Serrano S, Kajfež-Bogataj L (2012) Assessment of multiscale drought datasets to quantify drought severity and impacts in agriculture: a case study for Slovenia. Int J Spat Data Infrastruct Res 7:464–487

Chen T, Xia G, Liu T, Chen W, Chi D (2016) Assessment of drought impact on main cereal crops using a Standardized Precipitation Evapotranspiration Index in Liaoning Province, China. Sustainability 8:1069

Dai A, Trenberth KE, Qian T (2004) A global dataset of Palmer Drought Severity Index for 1870–2002: relationship with soil moisture and effects of surface warming. J Hydrometeorol 5:1117–1130

Daly C, Halbleib M, Smith JI, Gibson WP and others (2008) Physiographically sensitive mapping of climatological temperature and precipitation across the conterminous United States. Int J Climatol 28:2031–2064

Denmead OT, Shaw RH (1960) The effects of soil moisture stress at different stages of growth on the development and yield of corn. Agron J 52:272–274

Di Lena B, Vergni L, Antenucci F, Todisco F, Mannocchi F (2014) Analysis of drought in the region of Abruzzo (Central Italy) by the Standardized Precipitation Index. Theor Appl Climatol 115:41–52

Doesken NJ, Garen D (1991) Drought monitoring in the Western United States using a surface water supply index. Seventh Conference on Applied Climatology, Salt Lake City, UT. American Meteorological Society, Boston, MA, p 266–269

Earl HJ, Davis RF (2003) Effect of drought stress on leaf and whole canopy radiation use efficiency and yield of maize. Agron J 95:688–696

Elagib NA (2013) Meteorological drought and crop yield in Sub-Saharan Sudan. Int J Water Resour Arid Environ 2: 164–171

Esfahanian E, Nejadhashemi AP, Abouali M, Adhikari U, Zhang Z, Daneshvar F, Herman MR (2017) Development and evaluation of a comprehensive drought index. J Environ Manag 185:31–43

FAO (Food and Agriculture Organization of the United Nations) (2015) The impact of natural hazards and disasters on agriculture and food security and nutrition. In: World Conference on Disaster Risk Reduction. Sendai, Japan.

Feng S, Trnka M, Hayes M, Zhang Y (2017) Why do different drought indices show distinct future drought risk outcomes in the U.S. Great Plains? J Clim 30:265–278

Geng G, Wu J, Wang Q, Lei T and others (2016) Agricultural drought hazard analysis during 1980–2008: a global perspective. Int J Climatol 36:389–399

Hargreaves GH, Samani ZA (1985) Reference crop evapotranspiration from temperature. Appl Eng Agric 1:96–99

Hayes MJ, Svoboda MD, Wilhite DA, Vanyarkho OV (1999) Monitoring the 1996 drought using the Standardized Precipitation Index. Bull Am Meteorol Soc 80:429–438

Heim RR (2002) A review of twentieth-century drought indices used in the United States. Bull Am Meteorol Soc 83:1149–1165

Hlavinka P, Trnka M, Semerádová D, Dubrovský M, Žalud Z, Možný M (2009) Effect of drought on yield variability of key crops in Czech Republic. Agric For Meteorol 149: 431–442

Howitt R, MacEwan D, Medellín-Azuara J, Lund J, Sumner D (2015) Economic analysis of the 2015 drought for California Agriculture. UC Davis Center for Watershed Sciences. Davis, CA

Karim MR, Rahman MA (2015) Drought risk management for increased cereal production in Asian Least Developed Countries. Weather Clim Extrem 7:24–35

Karl TR (1986) The sensitivity of the Palmer Drought Severity Index and Palmer's Z-index to their calibration coefficients including potential evapotranspiration. J Clim Appl Meteorol 25:77–86

Kattelus M, Salmivaara A, Mellin I, Varis O, Kummu M (2016) An evaluation of the Standardized Precipitation Index for assessing inter-annual rice yield variability in the Ganges-Brahmaputra-Meghna region. Int J Climatol 36:2210–2222

Keyantash J, Dracup JA (2002) The quantification of drought: an evaluation of drought indices. Bull Am Meteorol Soc 83:1167–1180

Kim TW, Valdés JB, Aparicio J (2002) Frequency and spatial characteristics of droughts in the Conchos River Basin, Mexico. Water Int 27:420–430

Liu B, Asseng S, Müller C, Ewert F and others (2016) Similar estimates of temperature impacts on global wheat yield by three independent methods. Nat Clim Chang 6: 1130–1136

Loarie SR, Duffy PB, Hamilton H, Asner GP, Field CB, Ackerly DD (2009) The velocity of climate change. Nature 462:1052–1055

Lobell DB, Field CB (2007) Global scale climate–crop yield relationships and the impacts of recent warming. Environ Res Lett 2:014002

Lobell DB, Schlenker W, Costa-Roberts J (2011) Climate trends and global crop production since 1980. Science 333:616–620

Lobell DB, Roberts MJ, Schlenker W, Braun N, Little BB, Rejesus RM, Hammer GL (2014) Greater sensitivity to drought accompanies maize yield increase in the U.S. Midwest. Science 344:516–519

Lobell DB, Hammer GL, Chenu K, Zheng B, McLean G, Chapman SC (2015) The shifting influence of drought and heat stress for crops in northeast Australia. Glob Change Biol 21:4115–4127

Lorenzo-Lacruz J, Vicente-Serrano SM, López-Moreno JI, Beguería S, García-Ruiz JM, Cuadrat JM (2010) The impact of droughts and water management on various hydrological systems in the headwaters of the Tagus River (central Spain). J Hydrol (Amst) 386:13–26

Ma M, Ren L, Yuan F, Jiang S, Liu Y, Kong H, Gong L (2014) A new standardized Palmer drought index for hydro-meteorological use. Hydrol Processes 28:5645–5661

Mavromatis T (2007) Drought index evaluation for assessing future wheat production in Greece. Int J Climatol 27: 911–924

Mayer TD (2012) Controls of summer stream temperature in the Pacific Northwest. J Hydrol (Amst) 475:323–335

McEvoy DJ, Huntington JL, Abatzoglou JT, Edwards LM (2012) An evaluation of multiscalar drought indices in Nevada and Eastern California. Earth Interact 16:18

McKee TB, Doesken NJ, Kleist J (1993) The relationship of drought frequency and duration to time scales. Eighth Conf Appl Climatol, 17–22 January 1993 Anaheim, CA. http://www.droughtmanagement.info/literature/AMS_Relationship_Drought_Frequency_Duration_Time_Scales_1993.pdf

McNeeley SM, Beeton TA, Ojima DS (2016) Drought risk and adaptation in the interior United States: understanding the importance of local context for resource management in times of drought. Weather Clim Soc 8:147–161

Meyer SJ, Hubbard KG, Wilhite DA (1991) The relationship of climatic indices and variables to corn (maize) yields: a principal components analysis. Agric For Meteorol 55: 59–84

Meze-Hausken E (2004) Contrasting climate variability and meteorological drought with perceived drought and climate change in northern Ethiopia. Clim Res 27:19–31

Mishra AK, Singh VP (2010) A review of drought concepts. J Hydrol (Amst) 391:202–216

Mizzell H, Carbone G, Dow K, Rhee J (2010) Addressing monitoring needs for drought management. Proc 2010 South Carolina Water Resources Conf, October 13–14, 2010, Columbia Metropolitan Convention Center. www.cisa.sc.edu/Pubs_Presentations_Posters/Conference%20Proceedings%20Papers/2010_Mizzell%20et%20al_Addressing%20monitoring%20needs%20for%20drought%20management.pdf

Moorhead JE, Gowda PH, Singh VP, Porter DO, Marek TH, Howell TA, Stewart BA (2015) Identifying and evaluating a suitable index for agricultural drought monitoring in the Texas High Plains. J Am Water Resour Assoc 51: 807–820

Morid S, Smakhtin V, Moghaddasi M (2006) Comparison of seven meteorological indices for drought monitoring in Iran. Int J Climatol 26:971–985

NOAA (National Oceanic and Atmospheric Administration (2017) State of the climate: drought for August 2017. www.ncdc.noaa.gov/sotc/drought/201708

Olesen JE, Trnka M, Kersebaum KC, Skjelvåg AO and others (2011) Impacts and adaptation of European crop production systems to climate change. Eur J Agron 34:96–112

Palmer WC (1965) Meteorological drought. Res Pap 45. U.S. Department of Commerce Weather Bureau, Washington, DC

Páscoa P, Gouveia CM, Russo A, Trigo RM (2017) The role of drought on wheat yield interannual variability in the Iberian Peninsula from 1929 to 2012. Int J Biometeorol 61:439–451

Potopová V, Štěpánek P, Farda A, Türkott L, Zahradníček P, Soukup J (2016) Drought stress impact on vegetable crop yields in the Elbe River lowland between 1961 and 2014. Cuad Invest Geogr 42:127–143

Poudel S, Shaw R (2016) The relationships between climate variability and crop yield in a mountainous environment: a case study in Lamjung District, Nepal. Climate 4:13

Quiring SM (2009) Developing objective operational definitions for monitoring drought. J Appl Meteorol Climatol 48:1217–1229

Quiring SM, Papakryiakou TN (2003) An evaluation of agricultural drought indices for the Canadian prairies. Agric For Meteorol 118:49–62

Rippey B (2016) U.S. drought coverage increases sharply in November. National Drought Mitigation Center News. http://drought.unl.edu/Publications/News.aspx?id=273

Rohli RV, Bushra N, Lam NSN, Zou L, Mihunov V, Reams MA, Argote JE (2016) Drought indices as drought predictors in the south-central USA. Nat Hazards 83:1567–1582

Rosenzweig C, Elliott J, Deryng D, Ruane AC and others (2014) Assessing agricultural risks of climate change in the 21st century in a global gridded crop model intercomparison. Proc Natl Acad Sci USA 111:3268–3273

Ross T, Lott N (2003) A climatology of 1980-2003 extreme weather and climate events. Tech Rep 2003-01. US Department of Commerce, NOAA/ NESDIS, National Climatic Data Center, Asheville, NC

Rossi S, Niemeyer S (2010) Monitoring droughts and impacts on the agricultural production: examples from Spain. In: López-Francos A (comp) Economics of drought and drought preparedness in a climate change context. Options Méditerranéennes Série A. Séminaires Méditerranéens 95. CHIHEAM, Zaragoza, p 35–40

Sahoo RN, Dutta D, Khanna M, Kumar N, Bandyopadhyay SK (2015) Drought assessment in the Dhar and Mewat Districts of India using meteorological, hydrological and remote-sensing derived indices. Nat Hazards 77: 733–751

Sanford WE, Selnick DL (2013) Estimation of evapotranspiration across the conterminous United States using a regression with climate and land-cover data. J Am Water Resour Assoc 49:217–230

Sun L, Mitchell SW, Davidson A (2012) Multiple drought indices for agricultural drought risk assessment on the Canadian prairies. Int J Climatol 32:1628–1639

Tack J, Barkley A, Nalley LL (2015) Effect of warming temperatures on US wheat yields. Proc Natl Acad Sci USA 112:6931–6936

Tigkas D, Tsakiris G (2015) Early estimation of drought impacts on rainfed wheat yield in Mediterranean climate. Environ Process 2:97–114

Tilman D, Cassman KG, Matson PA, Naylor R, Polasky S (2002) Agricultural sustainability and intensive production practices. Nature 418:671–677

Trenberth KE, Dai A, van der Schrier G, Jones PD, Barichivich J, Briffa KR, Sheffield J (2014) Global warming and changes in drought. Nat Clim Chang 4:17–22

Udmale P, Ichikawa Y, Manandhar S, Ishidaira H, Kiem AS

(2014) Farmers' perception of drought impacts, local adaptation and administrative mitigation measures in Maharashtra State, India. Int J Disaster Risk Reduct 10: 250–269

USDM (2017) National drought summary. http://droughtmonitor.unl.edu/DroughtSummary.aspx

Vicente-Serrano SM, Beguería S, López-Moreno JI (2010) A multiscalar drought index sensitive to global warming: the Standardized Precipitation Evapotranspiration Index. J Clim 23:1696–1718

Vicente-Serrano SM, Beguería S, López-Moreno JI (2011) Comment on 'Characteristics and trends in various forms of the Palmer Drought Severity Index (PDSI) during 1900–2008' by Aiguo Dai. J Geophys Res 116:D19112

Vicente-Serrano SM, Beguería S, Lorenzo-Lacruz J, Camarero JJ and others (2012) Performance of drought indices for ecological, agricultural, and hydrological applications. Earth Interact 16:10

Vicente-Serrano SM, van der Schrier G, Beguería S, Azorin-Molina C, Lopez-Moreno JI (2015) Contribution of precipitation and reference evapotranspiration to drought indices under different climates. J Hydrol (Amst) 526:42–54

Wang H, Vicente-Serrano SM, Tao F, Zhang X and others (2016) Monitoring winter wheat drought threat in Northern China using multiple climate-based drought indices and soil moisture during 2000–2013. Agric For Meteorol 228-229:1–12

Wang H, Pan Y, Chen Y (2017) Comparison of three drought indices and their evolutionary characteristics in the arid region of northwestern China. Atmos Sci Lett 18:132–139

Wang Q, Wu J, Lei T, He B and others (2014) Temporal-spatial characteristics of severe drought events and their impact on agriculture on a global scale. Quat Int 349: 10–21

Wang Q, Wu J, Li X, Zhou H and others (2017) A comprehensively quantitative method of evaluating the impact of drought on crop yield using daily multi-scale SPEI and crop growth process model. Int J Biometeorol 61:685–699

Wei J, Jin Q, Yang ZL, Dirmeyer PA (2016) Role of ocean evaporation in California droughts and floods. Geophys Res Lett 43:6554–6562

Wells N, Goddard S, Hayes MJ (2004) A self-calibrating Palmer Drought Severity Index. J Clim 17:2335–2351

Wilhelmi OV, Hubbard KG, Wilhite DA (2002) Spatial representation of agroclimatology in a study of agricultural drought. Int J Climatol 22:1399–1414

Wilhite DA (1993) The enigma of drought. In: Wilhite DA (ed) Drought assessment, management, and planning: theory and case studies. Kluwer, Boston, MA, p 3–15

Wilhite DA (2000) Drought as a natural hazard: concepts and definitions. In: Wilhite DA (ed) Drought: a global assessment, Vol I. Routledge, London, p 3–18

Wilhite DA, Glantz MH (1985) Understanding the drought phenomenon: the role of definitions. Water Int 10:111–120

Wilhite DA, Svoboda MD, Hayes MJ (2007) Understanding the complex impacts of drought: a key to enhancing drought mitigation and preparedness. Water Resour Manag 21:763–774

Wilhite DA, Sivakumar MVK, Pulwarty R (2014) Managing drought risk in a changing climate: the role of national drought policy. Weather Clim Extrem 3:4–13

WMO (World Meteorological Organization) (2012) Standardized Precipitation Index user guide. WMO-No. 1090. http://www.wamis.org/agm/pubs/SPI/WMO_1090_EN.pdf

Xu Z, Hennessy DA, Sardana K, Moschini G (2013) The realized yield effect of genetically engineered crops: U.S. maize and soybean. Crop Sci 53:735–745

Yan H, Wang S, Wang J, Lu H and others (2016) Assessing spatiotemporal variation of drought in China and its impact on agriculture during 1982–2011 by using PDSI indices and agriculture drought survey data. J Geophys Res Atmos 121:2283–2298

Zargar A, Sadiq R, Naser B, Khan FI (2011) A review of drought indices. Environ Rev 19:333–349

Zipper SC, Qiu J, Kucharik CJ (2016) Drought effects on US maize and soybean production: spatiotemporal patterns and historical changes. Environ Res Lett 11:094021

Agricultural and Forest Meteorology 264 (2019) 40–55

Contents lists available at ScienceDirect

Agricultural and Forest Meteorology

journal homepage: www.elsevier.com/locate/agrformet

Response of crop yield to different time-scales of drought in the United States: Spatio-temporal patterns and climatic and environmental drivers

Marina Peña-Gallardo[a,*], Sergio M. Vicente-Serrano[a], Steven Quiring[b], Marc Svoboda[c], Jamie Hannaford[d], Miquel Tomas-Burguera[e], Natalia Martín-Hernández[a], Fernando Domínguez-Castro[a], Ahmed El Kenawy[a,f]

[a] Instituto Pirenaico de Ecología, Consejo Superior de Investigaciones Científicas (IPE–CSIC), Spain
[b] Ohio State University, United States
[c] National Drought Mitigation Centre, University of Nebraska-Lincoln, United States
[d] Centre for Ecology and Hydrology, United Kingdom
[e] Estación Experimental de Aula Dei, Consejo Superior de Investigaciones Científicas (EEAD-CSIC), Spain
[f] Department of Geography, Mansoura University, Mansoura, Egypt

ARTICLE INFO

Keywords:
Drought index
SPEI
Drought impacts
Crop yields
Cultivations
Climatic change
Natural hazards

ABSTRACT

This article presents an analysis of the response of the annual crop yield in five main dryland cultivations in the United States to different time-scales of drought, and explores the environmental and climatic characteristics that determine the response. For this purpose we analysed barley, winter wheat, soybean, corn and cotton. Drought was quantified by means of the Standardized Precipitation Evapotranspiration Index (SPEI). The results demonstrate a strong response in the interannual variability of crop yields to the drought time-scales in the different cultivations. Moreover, the response is highly spatially variable. Crop types showed considerable differences in the month in which their yields are most strongly linked to drought conditions. Some crops (e.g. winter wheat) responded to drought at medium to long SPEI time-scales, while other crops (e.g. soybean and corn) responded to short or long drought time-scales. The study confirms that the differences in the patterns of crop yield response to drought time-scales are mostly controlled by average climate conditions, in general, and water availability (precipitation), in particular. Generally, we found that there is a weaker link between crop yield and drought severity in humid environments and also that the response tends to occur over longer time-scales.

1. Introduction

Long-term changes in large-scale crop production are driven by processes related to management and technical improvement (Fischer and Edmeades, 2010; Grassini et al., 2013). Thus, crop production has substantially increased at the global scale, supporting the needs of the increasing population. Nevertheless, the increase in crop productivity is a non-linear process over time, given that crop yields vary from year to year, with episodes characterized by yield reductions or crop failures (Ciais et al., 2005; Lobell et al., 2011a, b). There are numerous factors that can explain the temporal variability in crop yield. In addition to factors like diseases, social crisis and wars (Stanhill, 1976; Oerke, 2006; Wrather et al., 2001), climate variability is also a key controller of variations in crop yield (Lobell et al., 2007; Schlenker and Roberts, 2009). In particular, some meteorological hazards (e.g. frost, heat waves, hail, floods) may affect plant development and accordingly decrease crop production (Ciais et al., 2005; Lobell et al., 2011b; Asseng et al., 2011). Nevertheless, drought is considered the main climatic hazard impacting crop yield in many areas worldwide (Porter and Semenov, 2005; Barnabás et al., 2008; Farooq et al., 2009).

Although temperature and light are essential for plant growth, as they are important factors for photosynthetic activity (Nemani et al., 2003), water availability, in the form of soil moisture, is essential for plant growth and crop development, specifically during the critical phenological phases for a given crop (e.g. Barnabás et al., 2008; Ramadas and Govindaraju, 2015). However, assessing the impacts of drought on crop yield is not straight forward for a variety of reasons: i) vegetation types may have different resistance, times of response and resilience to water deficits as a consequence of different phenological, physiological and morphological strategies to cope with water deficits

* Corresponding author.
E-mail address: marinapgallardo@ipe.csic.es (M. Peña-Gallardo).

https://doi.org/10.1016/j.agrformet.2018.09.019
Received 25 July 2017; Received in revised form 26 January 2018; Accepted 28 September 2018

(Chaves et al., 2003), ii) drought is the most complex natural hazard, which makes it very difficult to study, particularly given the difficulty of establishing an unitary multidisciplinary definition of drought (Wilhite and Glantz, 1985; Lloyd-Hughes, 2014); iii) drought is difficult to quantify since there is no single climatic variable that can be employed to quantify drought severity, with the choice of variable (and appropriate timescale; McKee et al., 1993) being dependent on the type of impact that is of interest (Vicente-Serrano, 2016); iv) there are difficulties in defining the beginning, end, spatial extent and total severity of drought, which makes its quantification much more difficult; and v) the convergence of multiple climate factors trigger drought; although precipitation is the most important variable for determining drought severity, other variables that condition the atmospheric evaporative demand (AED) are also relevant and can be more important than precipitation (Narasimhan and Srinivasan, 2005; Hobbins et al., 2016; McEvoy et al., 2016).

The concept of drought time-scale, developed in the 1990s, altered the way in which drought is quantified and drought impacts are analysed. This concept was introduced to characterize the various response times, or lags, of different components of the terrestrial water cycle (streamflow, groundwater, etc.) to precipitation deficits (McKee et al., 1993), as hydrological drought conditions may be impacted by different climatic drought time-scales, as a function of different hydrological systems and regions (e.g. Lorenzo-Lacruz et al., 2010; 2012; Barker et al., 2015). The term time-scale has recently been applied in the quantification of the drought effects on natural vegetation communities, given the different resistance of vegetation types that makes their response highly dependent on drought time-scale (Ji and Peters, 2003; Pasho et al., 2011; Arzac et al., 2016; Vicente-Serrano et al., 2013, 2015). Robust and flexible drought indices can be calculated on different time scales, among them the Standardized Precipitation Index (SPI) (McKee et al., 1993), the Standardized Precipitation Evapotranspiration Index (SPEI) (Vicente-Serrano et al., 2010) and the Standardized Palmer Drought Index (SPDI) (Ma et al., 2014).

Drought indices have been widely used to explain crop yield anomalies (Easterling et al., 1988; Quiring and Papakryiakou, 2003; Kola et al., 2014; Tunalioclu and Durdu, 2012; Benitez and Domecq, 2014; Arshad et al., 2013) and to develop statistical models to predict crop yields (Vicente-Serrano and Cuadrat, 2006; Subash and Ram Mohan, 2011; Sadat Noori et al., 2012; Dutta et al., 2013; Ming et al., 2015; Scian, 2004; Potopova et al., 2016b). Nevertheless, multi-scalar drought indices are more skillful in identifying the influence of drought severity on crop yields, compared to other drought indices (Vicente-Serrano et al., 2012; Wang et al., 2016a,b). Among them, the SPEI has been widely used to analyse the impacts of crops on different cultivations in varied regions worldwide, including China (Ming et al., 2015; Wang et al., 2016a, b; Chen et al., 2016), the Iberian Peninsula (Pescoa et al., 2016), Slovakia (Labudova et al., 2016), Czech Republic (Potopova et al., 2016), Moldova (Potopova et al., 2015), South Africa (Araujo et al., 2016), U.S. (Moorhead et al., 2015) and the whole European continent (Gunst et al., 2015). These studies demonstrate that the SPEI performs better than other indices in identifying drought impacts on crop yields at regional and global scales (Vicente-Serrano et al., 2012; Gunst et al., 2015; Wang et al., 2016a, b; Chen et al., 2016; Labudova et al., 2016). The AED is included in the calculation of the SPEI. This is relevant since different studies have stressed the negative influence of temperature-driven evaporative demand and crop yields, given its influence on soil moisture and vegetation stress conditions (Asseng et al., 2004; Schlenker and Roberts, 2009; Lobell et al., 2003; 2007). A representative example is Lobell et al. (2014) who analysed the sensitivity of corn yields to drought in the U.S., indicating that the sensitivity to drought stress increased in crops associated with high vapor pressure deficits, thus underlining the need for considering AED in drought quantification tools.

The United States is one of the main crop producers in the world, with a high percentage of the total global production of some crops (e.g. corn, soybean and wheat) (FAO, 2013). Numerous studies have analysed the response of crop yields to interannual variability of drought indices in the United States (e.g. Easterling et al., 1988; Moorhead et al., 2015; Rohli et al., 2016). Nevertheless, there are very few studies that consider the connection between different drought time-scales and different crops (e.g. Zipper et al., 2016). Correspondingly, to the authors' knowledge there are no studies that determine the climatic and environmental drivers controlling crop yield responses to drought time-scales. Hence, in this study, we analyse the response of the annual crop yield in five main dryland cultivations in the United States to different time-scales of drought using the SPEI. The objective of this study is to identify possible spatial patterns in the response of crop types to drought at different time scales and to define the environmental and climatic characteristics that determine these patterns.

2. Data and methods

2.1. Data

2.1.1. Crop yield data

We used the entire dataset of the United States Department of Agriculture (National Agriculture Statistics Service), which was obtained through https://quickstats.nass.usda.gov/#AF9A0104-19EF-3BFE-90D2-C67700892F3E. This portal provides production statistics for different cultivations per unit of surface at the county level. We obtained the county production data for five different dryland cultivations: barley, winter wheat, soybean, corn and cotton. We did not include the yield of these cultivations in irrigated lands. Annual productions were obtained for each county and the information was scaled to the same units (Metric Tons/Ha). Data were obtained independently of the surface covered by the different crop types in each county. However, as crop types were not represented over large surfaces in some counties, we decided to exclude those counties with each crop type covering only a low percentage of the total surface of the county ($< 1\%$) (https://www.nass.usda.gov/Charts_and_Maps/Crops_County/#ctp) (Fig. 1).

Annual crop yield series in each county shows a strong positive trend since the 1960s, as a consequence of the ongoing technological and management improvements (Egli, 2008). To eliminate this effect, the series were de-trended by using a linear regression model fitted to crop yield series (dependent variable) and time (independent variable). The average crop yield of each series was added to the residual series of the model to produce the de-trended yield data in Metric Tons/Ha.

2.1.2. Climate data

We employed the PRISM (Parameter-elevation Relationships on Independent Slopes Model) gridded data set developed by the Oregon State University (http://www.prism.oregonstate.edu/). We used monthly data series for precipitation, maximum and minimum air temperatures from 1961 to 2014 at a grid interval of 30 s. PRISM data have already been validated (Daly et al., 2008) and widely used for climatic, hydrological, agricultural and environmental applications (e.g. Lutz et al., 2010; Bandaru et al., 2017; Bodner and Robles, 2017).

2.1.3. Normalized Difference Vegetation Index data and water field capacity

We used the NOAA-AVHRR NDVI dataset (https://www.star.nesdis.noaa.gov/smcd/emb/vci/VH/vh_browse.php) (Vargas et al., 2009) at a spatial resolution of 16 km^2 to characterise the different responses of crop yield to drought time-scales. NDVI is calculated as:

$$\mathrm{NDVI} = \frac{(NIR - VIS)}{(NIR + VIS)}$$

Where NIR and VIS refer to the near-infrared' and visible wavelengths of spectrum.

The NDVI is closely related to the total biomass and leaf area index

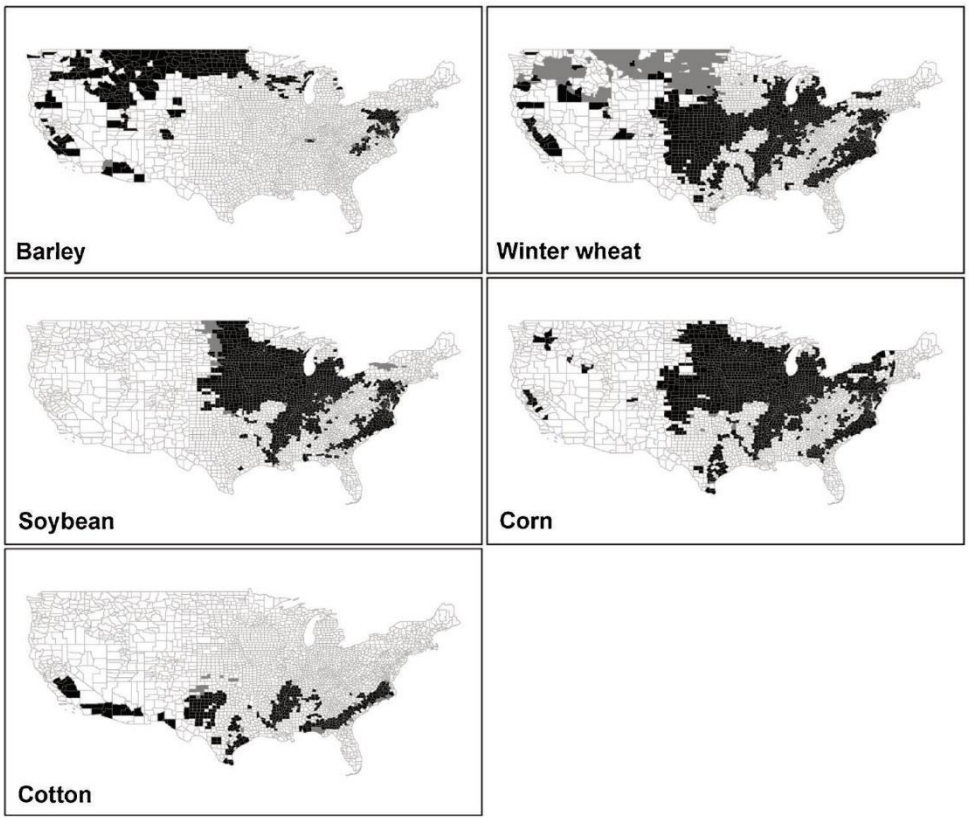

Fig. 1. Spatial distribution of the US counties with a high/low percentage of lands cultivated by one of the five different crops (black/grey).

(Baret and Guyot, 1991; Gutman, 1991; Carlson and Ripley, 1997). Seasonal and annual averages were obtained for each county for the period 1981-2014. In addition, vegetation phenology metrics (i.e. green-up and maximum NDVI dates) were calculated from the average NDVI series of each county (Fischer, 1994; Doktor et al., 2009). Finally, high resolution water field capacity data were obtained from the State Soil Geographic (STATSGO) Database for the contiguous United States (https://water.usgs.gov/GIS/metadata/usgswrd/XML/ussoils.xml#stdorder).

2.2. Methods

2.2.1. SPEI calculation

The Standardized Precipitation Evapotranspiration Index (SPEI) developed by Vicente-Serrano et al. (2010) is equally sensitive to precipitation and AED (Vicente-Serrano et al., 2015). In comparison with other drought indices based on precipitation alone, this property allows for better identification of the impact of extreme warm air temperatures and heat waves on drought severity (Beguería et al., 2014). Using the average monthly precipitation and maximum and minimum air temperature series corresponding to each county, we calculated the SPEI series at time scales ranging from 1 to 18 months. For this purpose, we derived a monthly climatic water balance time series (i.e. the difference between precipitation and AED) and then fitted a log-logistic distribution (Vicente-Serrano et al., 2015) to obtain the SPEI in standardized units. For the complete mathematical procedure, please refer to Vicente-Serrano et al. (2010).

This procedure allows for comparing drought characteristics in space, time and at different time-scales, regardless of the magnitude and seasonality of climate in each region. To account for AED we used reference evapotranspiration (ETo) in the SPEI calculation and applied the Hargreaves method (Hargreaves and Samani, 1985) using maximum and minimum air temperatures and extraterrestrial solar radiation data calculated using latitude and Julian day. In accordance with crop yield time series and considering the existence of a linear tendency in each SPEI time series the 1- to 18-month SPEI series were also detrended for the period 1961–2014.

2.2.2. Correlation between SPEI and crop yields

The influence of droughts on the annual yield of different crops was assessed using the Pearson correlation coefficient. The correlation was computed between the time series of the de-trended annual crop yield and de-trended SPEI for all months of the year, using SPEI aggregation periods of 1- to 18-months (i.e. the month in question and then aggregating two to 18 months prior) for each county independently. Thus, for each crop and county, we obtained 216 correlations (12 months × 18 time-scales).

2.2.3. Identification of the main patterns of crop yield response to SPEI time-scales

To summarize the high variability in the correlations computed between the crop yield series and the many SPEI series at different time-scales, we performed a Principal Component Analysis (PCA) in S mode, in which each vector was the 12 (months) x 18 (time-scale) correlations (216 cases) obtained between SPEI and crop yield in each county. The correlation matrix was used to extract the components (Richman, 1986; Barry and Carleton, 2001). This approach enabled us to classify, at the broad scale, the patterns of response recorded in individual counties, on the basis of the similarities of the obtained correlations. The number of the extracted components was defined based on the percentage of the total explained variance, as suggested by the scree-plots. The retained components showed strong differences in the explained variance in comparison to the rest of the components. The classification was based on the PCA loadings and following the maximum loading rule. The loadings indicate the degree of similarity of the patterns of correlations between crop yields and SPEI in each county, and the pattern representing a number of counties that correspond to a particular principal component (PC). In other words, mapping the loadings allows us

to identify counties with a similar crop yield response to drought.

2.2.4. Driving factors of crop yield responses to droughts

We applied two different methods to define the factors responsible for the varying responses of crop yields to different SPEI time-scales. First, we analysed whether there are differences in the values of different independent variables between the various classes of crop yield response to drought, as identified using the methods outlined in 2.2.3. These included climate variables, such as mean, maximum and minimum annual and seasonal air temperature averages, seasonal and annual mean precipitation and ETo. We also incorporated climatic balance variables, such as Precipitation minus ETo, the long term average of the NDVI green-up and maximum NDVI dates, and soil water field capacity. Specifically, for each crop type, we employed the Tukey post-hoc test within the Analysis of Variance (ANOVA) to compare the differences among means of the different variables, as a function of the general patterns of crop yield response to the SPEI.

Second, the contribution of the various factors in explaining the different types of crop yield response to drought time-scales was estimated using predictive discriminant analysis (PDA) for each crop type. PDA is commonly used to explain the value of a dependent categorical variable based on its relationship to one or more predictors (Huberty, 1994). Given a set of independent variables, PDA attempts to identify linear combinations of those variables (e.g. climatic conditions, phenology and soil water field capacity) that best separate the groups of cases of the dependent variable (i.e. groups of crop yield response to the SPEI). These combinations are termed discriminant functions (Hair et al., 1998). This procedure automatically defines the first function that separates the groups as much as possible. It then chooses a second function that does not correlate with the first function and provides as much separation as possible. This procedure considers further functions until the maximum number of functions is reached, based on the number of predictors and categories in the dependent variable. The PDA enables defining predictors that contribute to most of the inter-category differences of the dependent variable, which is the groups of crop yield response to SPEI time-scales in our case.

3. Results

3.1. Diverse response of crop yield to SPEI time-scales

Fig. 2 illustrates an example of the varied correlation patterns between the SPEI (1- to 18-month) and winter wheat yield in the US from 1961 to 2014. As depicted, in the case of Valley County, Nebraska, the maximum correlation is recorded in April for an SPEI time-scale of 8 months. In Decatur County, Kansas, the correlation is much stronger during May for an SPEI time-scale of 11 months. Results also reveal that while longer SPEI time-scales impact wheat crop yields in some counties, the response of wheat yield to drought in other counties (e.g. Thomas County, Georgia) is more pronounced at shorter time-scales. Overall, these findings underline the need for PCA to summarize the spatial patterns of crop yield response to drought at different time-scales. Results demonstrate that the PCA identified well-defined patterns of crop yield and SPEI time-scales across the US. As illustrated in Fig. 3, the scree-plots suggest three patterns for barley, wheat and soybean, four patterns for the corn and five patterns for the cotton. In the next sections, we explain in-depth the characteristics and spatial distribution of these patterns.

3.2. General spatial patterns within the main cultivations

3.2.1. Barley

Fig. 4 shows the main patterns of response of barley crop yields to the SPEI time-scales. The first component (PC1), which explains the main percentage of the total variance (78.3%) reveals a pattern of barley response to short to medium SPEI time-scales (3–7 months in July). This finding demonstrates that the annual yield of barley is mainly impacted by precipitation and AED conditions between January and July. Spatially, this pattern represents those areas located in the north-central counties, close to the Canadian boundaries. PC2 shows a different pattern, with negative correlations between barley annual yield and SPEI time-scales between 8–14 months from February to April. This pattern explains a low percentage of the total variance and is recorded in the counties located in the northwestern limit of the barley cultivation belt. Finally, PC3 is representative of the Northwest US region, suggesting dominant negative correlations with the SPEI in the months of April and May, though not statistically significant at $p < 0.05$.

3.2.2. Winter wheat

Fig. 5 summarizes correlations between the SPEI and winter wheat yields. PC1 represents a large spatial extent, comprised mostly in the central counties of the country and located mainly in the states of Nebraska, Kansas and Oklahoma. This component is characterized by positive correlations between winter wheat yields and the SPEI at time scales between 3 and 9 months in the months of April and May. The maximum correlation is recorded at the time scale of 5 months. Conversely, counties located in the Northeast, Mid-west, and the East Coast show negative correlations between winter-spring SPEI and winter wheat yields. PC2 exhibited no significant correlations between winter wheat yields and the SPEI for almost all time-scales. This pattern is bimodal, with negative correlations in the counties located in the Central U.S. and positive correlations in a large number of counties in Wyoming, Nebraska and Colorado. Finally, PC3 informs that there are significant correlations between winter wheat yields and the SPEI at time-scales ranging from short to long, particularly over the second half of the year. This component is mostly situated in the counties located in the Eastern US, besides Wisconsin, Illinois and Michigan. The same pattern, albeit with a negative sign, is distributed over the Central US, particularly in Iowa and Missouri.

3.2.3. Soybean

The correlations between soybean yield and the SPEI indicates a coherent pattern, with high positive correlations with the SPEI at time-scales from 1 to 4 months from July to September but also 4 to 13 months from July to the end of the year (Fig. 6). This pattern is observed over the majority of the counties located within the soybean belt in the US. On the other hand, PC2 suggests negative correlations with the SPEI in June at time-scales from 2 to 7 months, compared to positive correlations with the 1-month SPEI during August. Spatially, this component is restricted to a few counties situated mainly within the states of Iowa, Missouri and Nebraska. In comparison to PC1 and PC2, PC3 is devoted particularly to some counties in the Central Atlantic and Northeast, with a generally high positive correlation between soybean yield and the SPEI at long time-scales during the mid and late summer.

3.2.4. Corn

Corn yields show similar patterns to those identified for soybean, with the two first components being specific to the same regions (Fig. 7). PC1 demonstrates high positive correlations with the SPEI at time-scales between 1 and 4 months during summer months, while PC2 shows dominant negative correlations between the SPEI and corn yield during the cold half of the year (January-May) and at the beginning of summer. For PC3, positive and significant correlations dominate between the annual corn yields and the SPEI at the 4–7 month scales in late winter and spring. This pattern prevails over the central counties of the U.S. in which corn is cultivated. Finally, PC4 suggests positive and significant correlations between the annual yield of corn and long SPEI time-scales, albeit with a limited spatial coverage, mainly over few counties in north-central US.

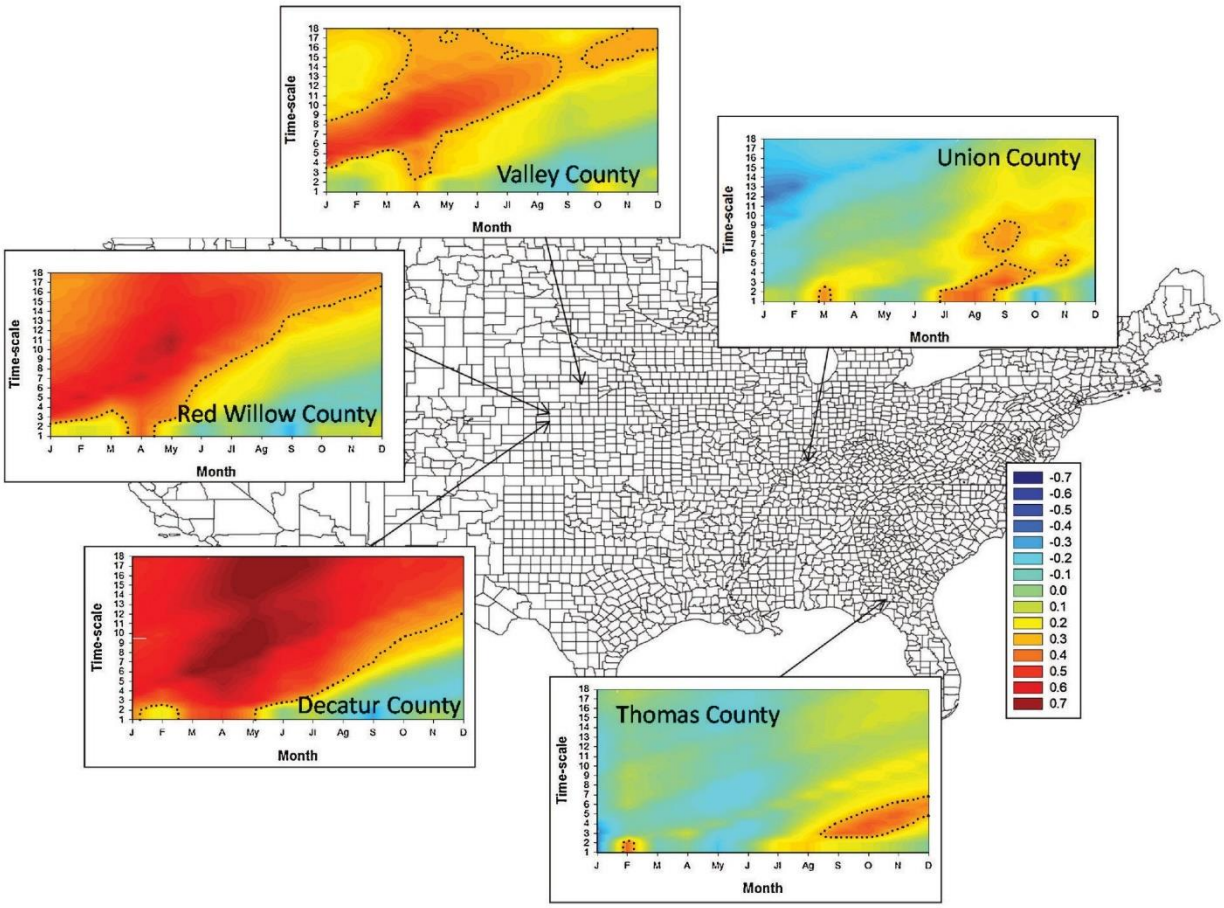

Fig. 2. Example of the diverse patterns of correlation between annual winter wheat yields and 1- to 18-month SPEI timescales. Colors in the scale represent Person's r correlations and dotted lines outline only significant correlations at the 95% significance level ($p < 0.05$).

3.2.5. Cotton

Although cotton is cultivated in fewer areas, mainly in the Southern US, it shows more spatially fragmented correlation patterns, with five main components, compared to other investigated crops (Fig. 8). The first two components exhibit positive and significant correlations with the SPEI, at medium (4–7 months) and long (10–12 months) time-scales. PC1 is broadly distributed in counties located within the cotton belt. On the other hand, PC2 dominates over central-south counties across the cotton belt. The remaining components do not show any distinctive response of cotton annual yields to the SPEI at the different time-scales, indicating that the spatial distribution of PC loadings is patchy across the area of cotton cultivation.

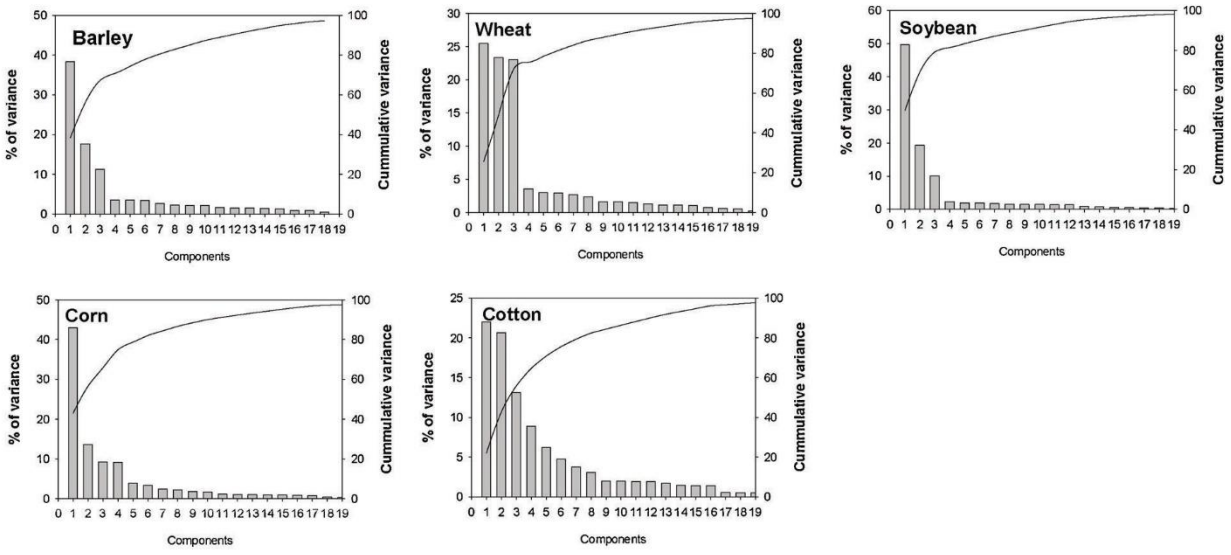

Fig. 3. Scree plots summarizing the number of retained components for each crop type, following the PCA results applied to the different patterns of correlations between SPEI and crop yields.

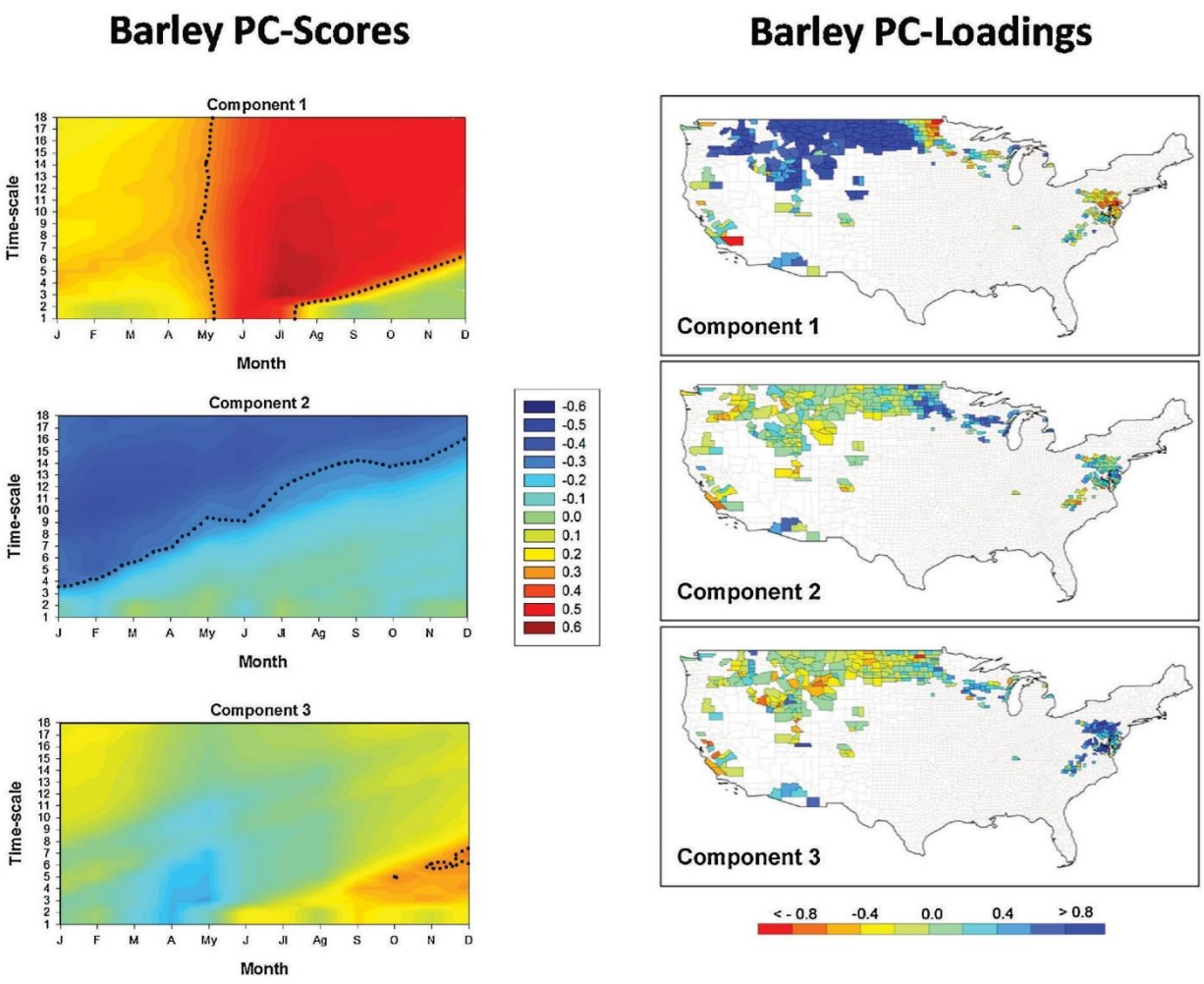

Fig. 4. Left: PC-scores that represent extracted main patterns of correlation between 1- to 18-month SPEI time-scales and barley yields. Right: Spatial distribution of the PC-loadings of the extracted components. Dotted lines outline significant correlations at the 95% significance level ($p < 0.05$).

3.3. Factors explaining the different responses of crops to SPEI time-scales

To account for the possible influences of climatic and environmental conditions on the response of the selected crops to the different time-scales of the SPEI, we analysed the magnitudes in mean precipitation, mean air temperature, total ETo, the climatic balance, the information obtained from the NDVI series (i.e. green up day and the day in which the maximum annual NDVI is recorded) and the soil water field capacity for the five cultivations.

Supplementary Figs. 1 and 2 illustrates the annual and seasonal values corresponding to barley crop yields. The significance of the values of the different variables among groups and seasons is also listed in the different tables of the supplementary information. There are statistically significant differences in the annual precipitation among the different groups of counties characterized by different correlations between SPEI time-scales and the barley crop yields. These differences are mainly controlled by the spatial patterns of spring precipitation. In general, counties represented by PC1+ (i.e. with maximum positive loadings on this component) are characterized by low annual precipitation and low annual air temperature and in general lower NDVI values than other components. As opposed to PC1+, the counties represented by PC2+ are characterized by higher annual precipitation, which is clearly identified in spring and summer. These areas are also characterized by higher annual air temperatures, higher ETo and humid conditions identified by the climatic water balance. Vegetation activity in counties corresponding to PC2+ is also high, in comparison to that observed for the areas of PC1 +. The counties represented by the PC3+ have low precipitation and ETo; however summer water balance is similar to that observed for the most humid counties represented by PC2 +. Winter, spring and autumn mean NDVI values in each county are strongly different among the PC groups, although the average water field capacity, the average day of the year recording the maximum NDVI and the green up day do not show statistically significant different values among the different PC groups.

Supplementary Figs. 3 and 4 shows the corresponding violin plots for winter wheat yields and the different SPEI time-scales. There are strong differences between the counties belonging to PC1+, PC2+ and PC3+and those counties with negative (opposite) loadings on the same components. Counties with positive loadings are characterized by more humid conditions, as represented by precipitation and climatic balance, than components characterized by negative loadings. Specifically, counties represented by PC1-, PC2- and PC3- show average annual precipitation values below 700 mm coupled with very negative climate balances, especially for PC1-. Thus, there are statistically significant differences in annual precipitation and climatic balance between the counties corresponding to these groups (see Supplementary information). This pattern is evident for all seasons of the year. In addition, there are also some differences among counties represented by positive and negative loadings in temperatures and ETo, which is clearly observed during summertime.

Soybean shows that PC1+ and PC3+ correspond to counties that receive more annual precipitation than PC2+ (Supplementary Fig. 5) and during the cold season (i.e. winter and spring; Supplementary Fig. 6). As illustrated, PC1+ and PC3+ are characterized by strong

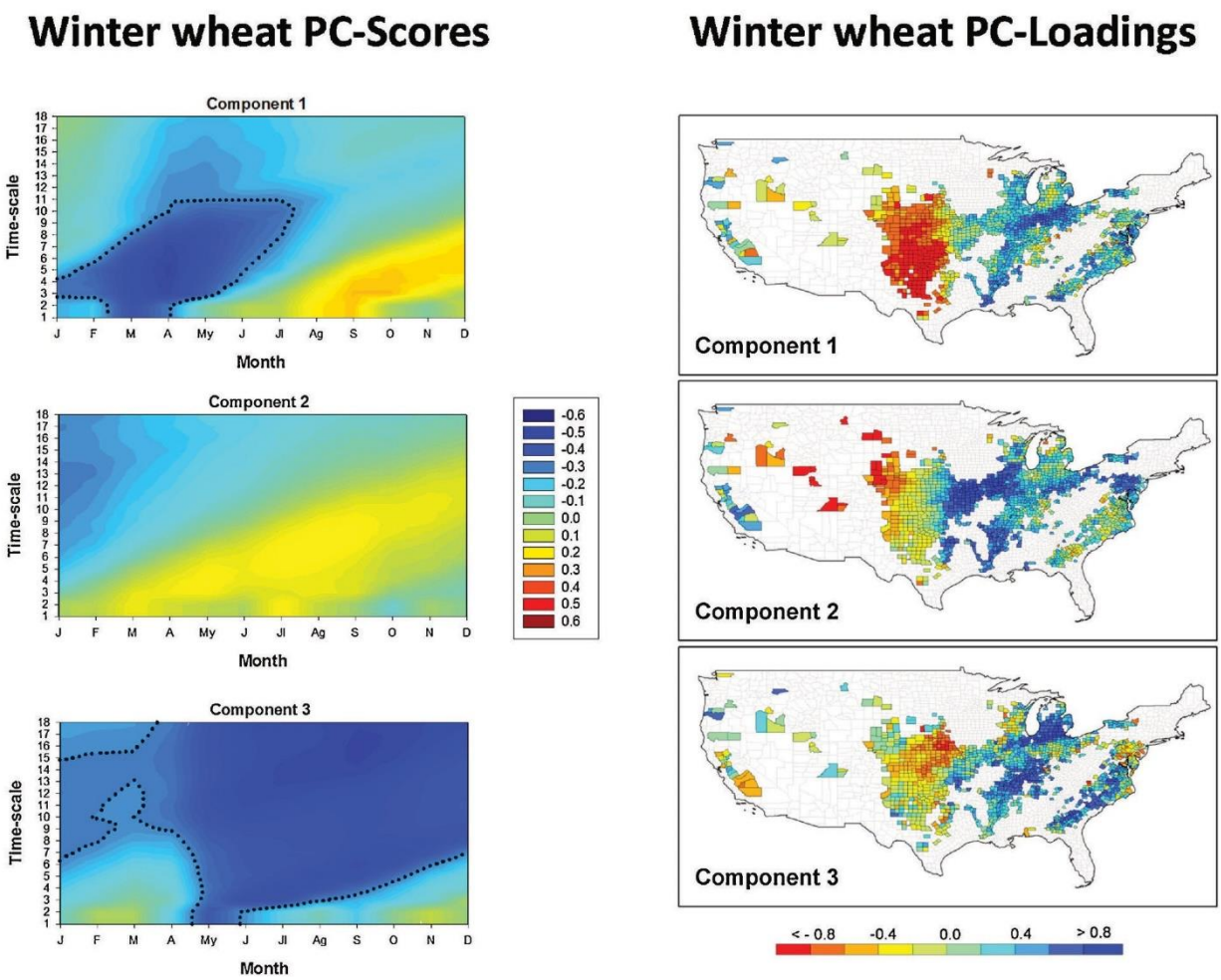

Fig. 5. Left: PC-scores that represent extracted main patterns of correlation between 1- to 18-month SPEI time-scales and winter wheat yields. Right: Spatial distribution of the PC-loadings of the extracted components. Dotted lines outline significant correlations at the 95% significance level ($p < 0.05$).

correlation between the SPEI and the annual soybean yields, albeit with correlations recorded at very different time-scales. These different patterns could be explained by the strong differences in the temperature and ETo between these two patterns, given that PC1+ is recorded in warmer counties than PC3+ either on the seasonal or annual scales. Average annual and seasonal values of temperature are statistically different between these two components; a similar finding is also found for ETo during the warm season (summer and autumn). The local differences to these general patterns, which are characterized by negative loadings, could be related to aridity, recalling the low water balance of PC3- and the water field capacity of PC1- and PC2-.

The four main groups of corn yield show more complex patterns, in response to the different environmental variables (Supplementary Figs. 7 and 8); but again the different climate variables play the main role in explaining the patterns of corn yield response to the SPEI at different time-scales. Average annual and cold season precipitation is much higher in the two components (PC1+ and PC4+) characterized by a strong response of the corn yield to the SPEI. Thus, these two components show lower values of the climate water balance. The different patterns that characterise PC1+ and PC4+ are mostly driven by the differences in temperature and ETo, which are higher in PC1. The water field capacity and the phenological variables (e.g. green-up and maximum NDVI dates) do not show any considerable differences among patterns. Nevertheless, there are significant differences in the average NDVI values in the counties represented by the different PCs that might highlight some control of the pattern of corn yield response to the SPEI as a function of the crop biomass/leaf area. Overall, the number of statistically significant differences is lower than that found using the average climate variables.

Finally, the patterns found for cotton yields show much more complex features, with a higher identified number of patterns (Supplementary Figures 9 and 10). In general, the differences between the first two PCs, which represent the highest percentage of the total variance, are likely controlled by the different average precipitation amount. PC1+, with a response of cotton yields to short SPEI time-scale, is more specific to counties that receive much more precipitation (800 mm in average of difference) than PC2+, which shows low precipitation values, mainly during the winter season. Annual and seasonal air temperatures and ETo do not show significant differences among the different patterns of response of the cotton yields to the SPEI time-scales.

Table 1 shows the structure matrix of the first three discriminant functions of the predictive discriminant analysis applied to the five crop types, while Fig. 9indicates the centroids of the different PC groups corresponding to the first three discriminant functions. This analysis identifies the factors that are controlling the different crop yield responses to the various SPEI time-scales, including seasonal and annual averages of the analysed climatic and environmental variables. This approach allows us to coherently extract the main determinants of the patterns of response of the crop yields to the SPEI time-scales.

The different barley groups show contrasted differences in function 1. This function is mostly represented by the annual and seasonal precipitation (with the exception of winter precipitation). The centroids of the different PC groups show negative values for function 1 in the

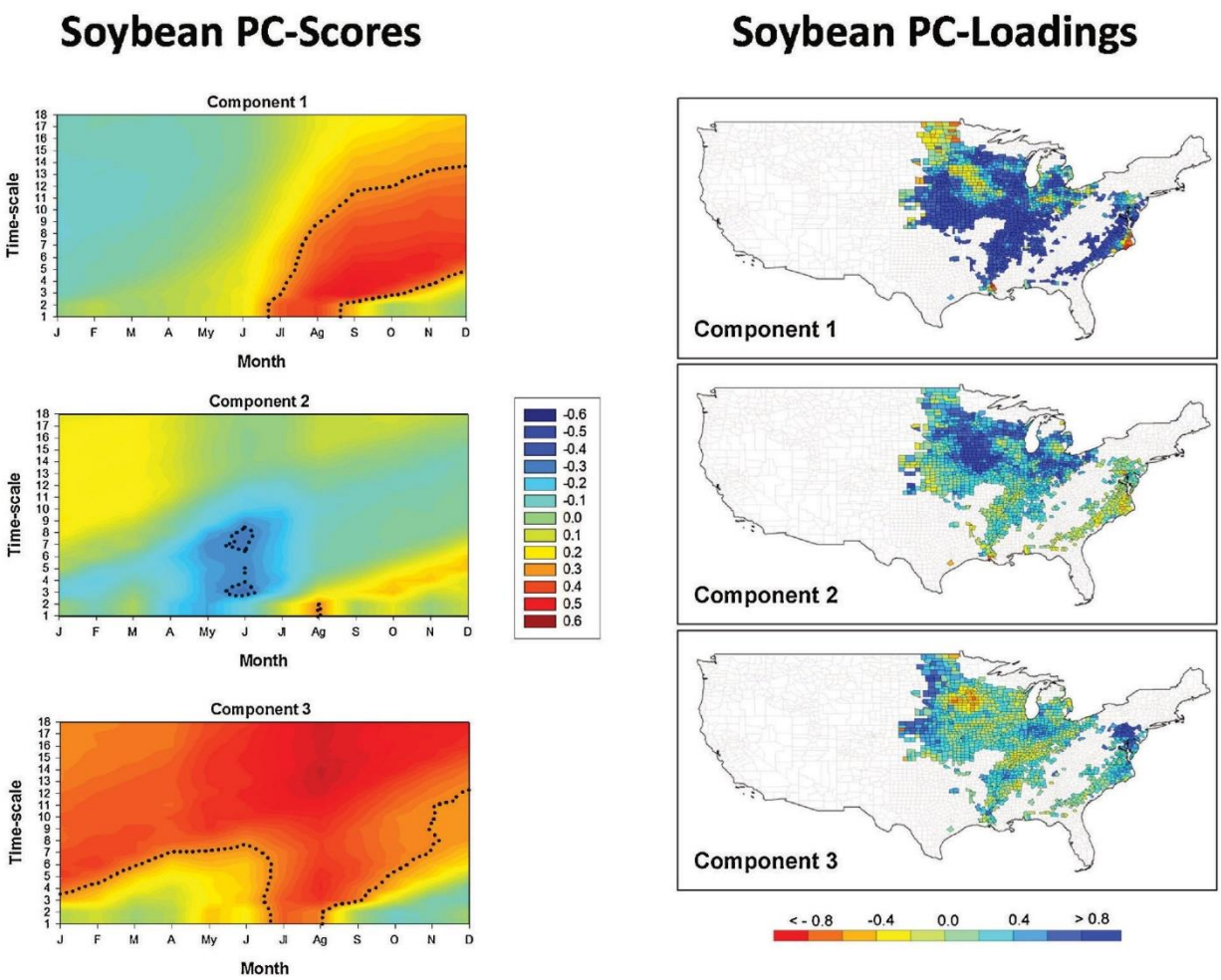

Fig. 6. Left: PC-scores that represent extracted main patterns of correlation between 1- to 18-month SPEI time-scales and soybean yields. Right: Spatial distribution of the PC-loadings of the extracted components. Dotted lines outline significant correlations at the 95% significance level ($p < 0.05$).

PC1+, which contrasts with positive values found for PC2+ and PC3 + . Functions 2 and 3 explain a low percentage of the total variance. Function 2 mostly represents winter temperature conditions, but it does not show a clear separation between PC groups. Therefore, the areas in which a clear response of the barley yields to the SPEI is identified correspond to dry environments. On the other hand, the most humid areas assigned to PC2+ and PC3+ do not show a clear response to drought.

The different PC groups of the wheat yield response to the SPEI time scales show clear different response in the discriminant function 1 between positive (PC1+, PC2+ and PC3+) and negative groups (PC1-, PC2- and PC3-). Discriminant function 1 for wheat yields is mostly representing water availability, with negative coefficients for the precipitation and the climatic balance at the annual and seasonal scales. Moreover, this function shows a positive coefficient for ETo during summer months, in which a high AED has a negative influence on water availability. Negative wheat yield patterns (PC1-, PC2- and PC3-) are characterized by positive correlations between the SPEI and the winter wheat yields for different seasons and SPEI time-scales before the wheat harvesting. These patterns are characterized by drier areas than positive groups. The areas represented by positive patterns (PC1+, PC2+ and PC3+) are dominated by negative or insignificant correlations between the SPEI and the winter wheat yields. Therefore, this behavior is principally assigned for humid areas (positive coefficients in the precipitation and the climatic water balance in the discriminant function 1). In these humid areas, it is found that even drought conditions may have a positive effect on the winter wheat crop yields. Nevertheless, although negative PC patterns are characterized by drier conditions than positive patterns, the discriminant function 1 establishes clear differences between PC1- and PC3- (positive values in the function) and PC2- (values close to 0). This finding stresses that PC1- and PC3-, which show the clearest patterns of wheat yield response to the SPEI, are representative of the most arid areas in the winter wheat belt. The different pattern found between PC1- and PC2- is explained by the function 2, which is positively represented by warm season temperatures. PC3- pattern would be characteristic of the colder areas than PC1- pattern, which would explain the later response of yields to longer SPEI timescales as wheat harvesting will be later.

The patterns of soybean response to the SPEI time-scales show little separation for the discriminant function 1. This function shows positive values for the different climatic variables, with the exception of the climate balance. It implies that average climate conditions are not the main driver of the spatial differences found in the response of the soybean yields to the different drought time-scales. Discriminant function 2 shows positive values for summer ETo, but there are no significant differences in the centroids of the positive PCs (which are clearly dominant for the soybean crop) in the function 2.

The discriminant analysis also shows complex results for the different groups of response of the corn yields to the various SPEI time-scales. In any case, function 1 shows the most clear separation between the four extracted PCs, with negative values for PC2+ and PC3+ and values close to 0 in PC1+ and PC4 + . The main weight in the function 1 is recorded for precipitation and climatic balance variables, mainly during the cold season, confirming that, as opposed to other crops, a

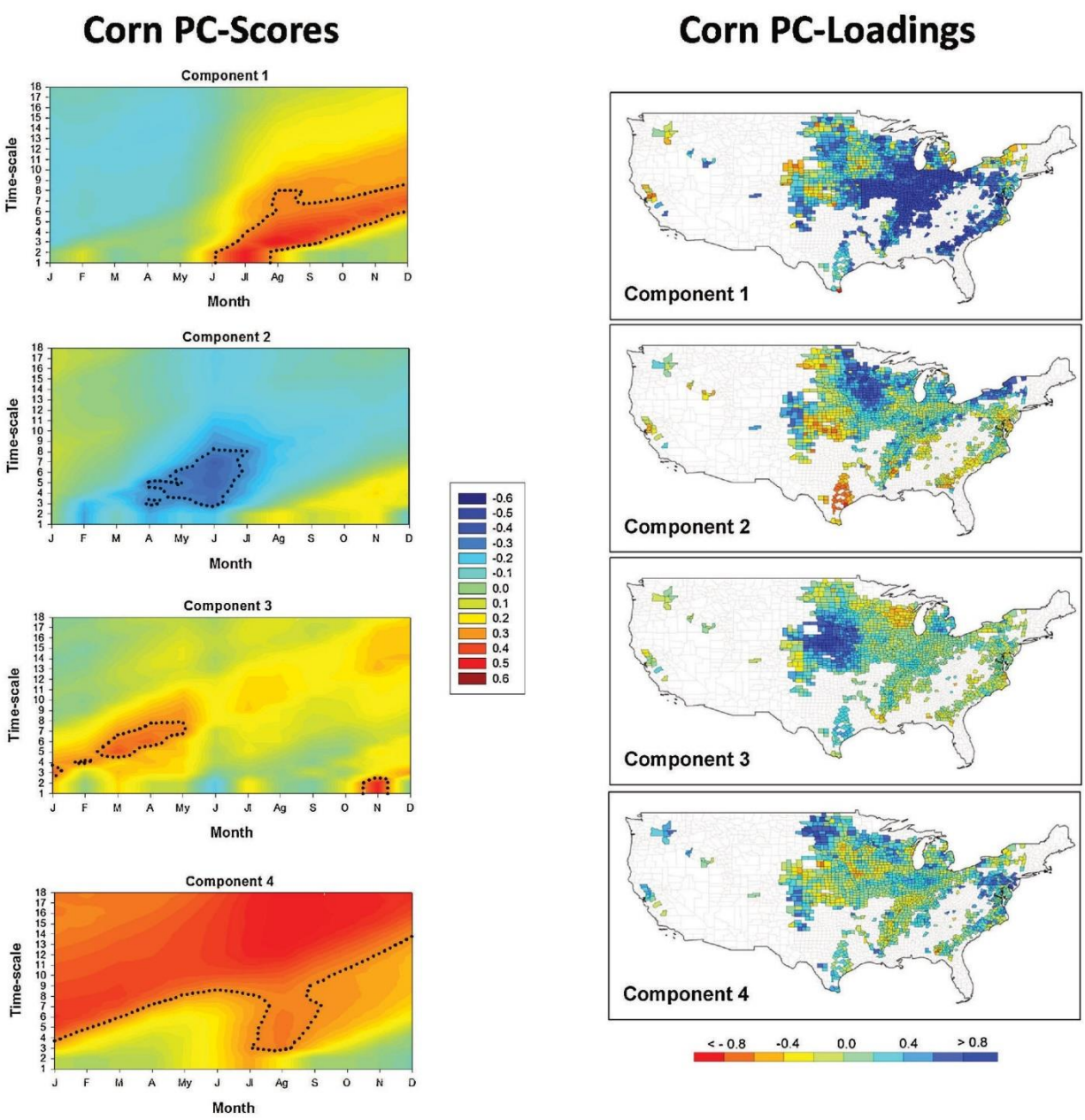

Fig. 7. Left: PC-scores that represent extracted main patterns of correlation between 1- to 18-month SPEI time-scales and corn yields. Right: Spatial distribution of the PC-loadings of the extracted components. Dotted lines outline significant correlations at the 95% significance level ($p < 0.05$).

higher response of the interannual variability of yields to the SPEI is recorded in the most arid counties. Temperatures show a positive weight in the discriminant function 1, confirming that PC2+ and PC3+ are also characteristic of the colder areas than PC1+ and PC4+. Function 2 mostly represents the warm season climatic balance (with a positive weight) and the cold season temperature (with a negative weight in the function). This function mostly separates between positive and negative patterns for PC1 and PC2, which would indicate that patterns characterized by negative loadings in PC1 and PC2 are characterized by warmer and drier conditions than patterns characterized by positive loadings. Function 3 mostly represents the warm season temperature and separates the most between PC2+ and PC3+.

Finally, for cotton yields, function 1 mainly represents annual and cold season humidity conditions (both for precipitation and the climatic balance, showing a negative weight on function 1). PC2+ shows the centroid on positive values of this function, confirming again that this pattern is representative of dry counties.

4. Discussion

This study assessed the response patterns of crop yields to drought in different cultivations across the United States. Drought severity was quantified at different time-scales using the Standardized Precipitation Evapotranspiration Index (SPEI). In general, results demonstrate a strong response in the interannual variability of crop yields to the SPEI time-scales in the different cultivations.

Nevertheless, this study clearly illustrated that the relationship between the interannual variability of droughts and crop yields may be highly spatially variable and dependent on the time-scale at which drought is measured. Table 2 summarises the well-defined patterns of crop yield response to drought time-scales found in this study. They correspond to very coherent spatial patterns and a clear response of the crop yields to a characteristic drought time-scale recorded for a certain period. Different studies have already showed this characteristic for natural vegetation (Ji and Peters, 2003; Pasho et al., 2011; Vicente-

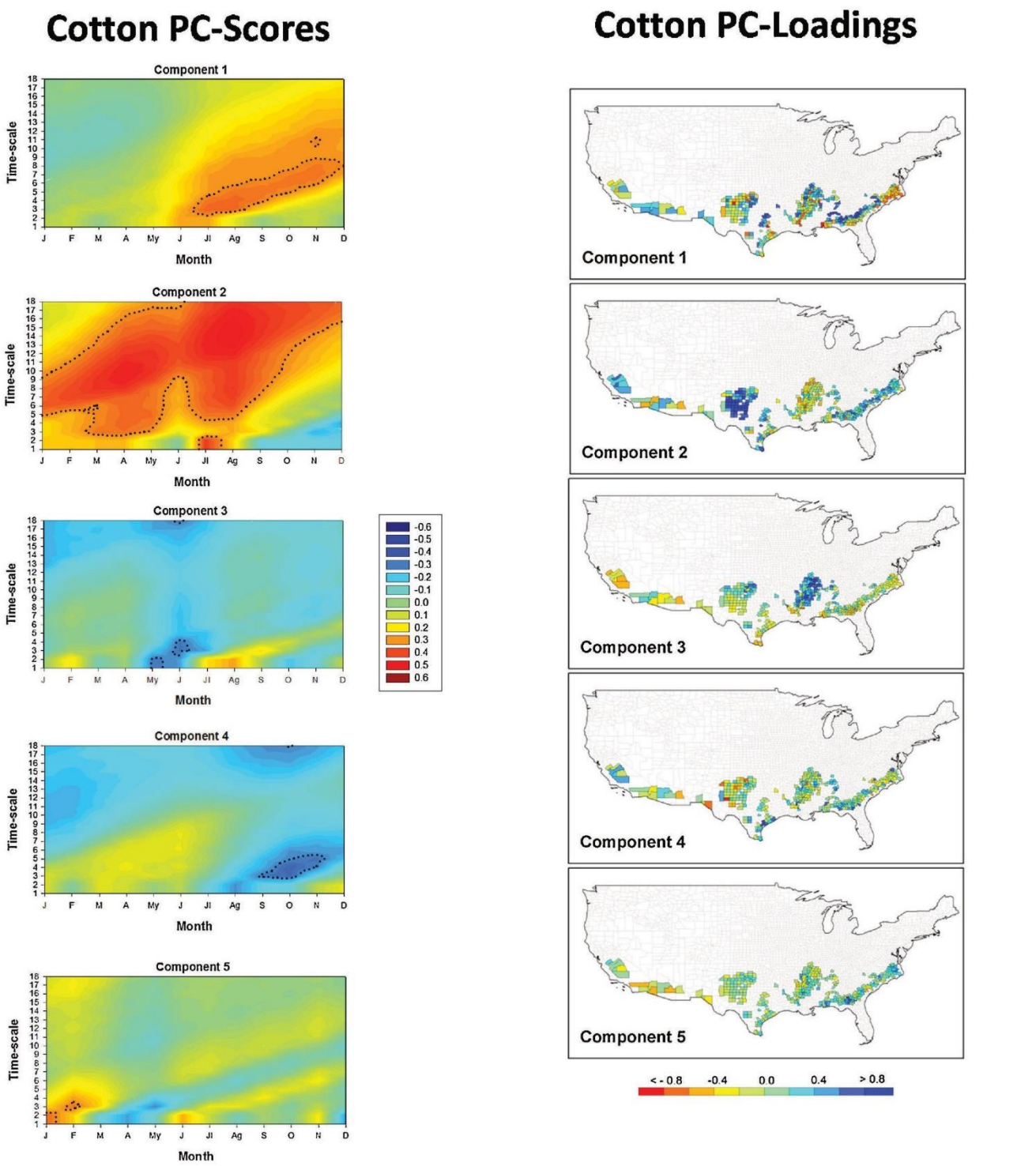

Fig. 8. Left: PC-scores that represent extracted main patterns of correlation between 1- to 18-month SPEI time-scales and cotton yields. Right: Spatial distribution of the PC-loadings of the extracted components. Dotted lines outline significant correlations at the 95% significance level ($p < 0.05$).

Serrano et al., 2014). Thus, the global response of different vegetation metrics (e.g. activity, growth and biomass) to drought in natural (i.e. uncultivated) areas is highly dependent on the time-scale of the drought index we use to measure drought (Vicente-Serrano et al., 2013), given the different resistance of vegetation types to water deficits. Previous studies analysed drought impacts on crops, suggesting different impacts, in response to different time-scales of drought indices (Wang et al., 2016a, b; Zipper et al., 2016). Here, we found that the selected crops (barley, winter wheat, soybean, corn and cotton) show different patterns of the yield response to the various SPEI time-scales. These crop types showed considerable differences in the month in which their yields are mostly controlled by drought conditions. Barley showed more spatially homogeneous patterns in terms of its yield response to the SPEI time-scales. Thus, the majority of counties in which barley is cultivated show the same response, with a maximum correlation with the 3-month SPEI in July. The rest of the cultivations show more spatial differences. While the yield of some selected crops (e.g. winter wheat) responded to drought at medium-long SPEI time-scales in some counties, other cultivations responded to short or long drought time-scales in different regions.

Table 1
Structure matrix of the first three functions (the explained variance by each function is indicated in parentheses) of the predictive discriminant analysis (PDA) for each one of the five crop types. The correlation values computed for each predictor variable with the three discriminant functions are also included. The variables represented in each of the functions are depicted in bold according to $p < 0.05$.

	Barley			Wheat			Soybean			Corn			Cotton		
	Function 1 (78.3%)	Function 2 (13.2%)	Function 3 (6.8%)	Function 1 (78.3%)	Function 2 (10.6%)	Function 3 (6.4%)	Function 1 (45.7%)	Function 2 (30.0%)	Function 3 (17.1%)	Function 1 (36.7%)	Function 2 (26.4%)	Function 3 (22.9%)	Function 1 (36.7%)	Function 2 (25.0%)	Function 3 (11.4%)
Precipitation (annual)	**0.67**	0.33	−0.11	**−0.62**	0.10	0.17	**0.55**	0.23	0.27	**0.71**	0.23	0.11	**−0.59**	**0.41**	−0.20
Precipitation (winter)	0.35	0.41	0.35	−0.43	−0.10	**0.44**	**0.54**	0.32	0.14	**0.75**	0.06	0.10	**−0.62**	0.37	0.00
Precipitation (spring)	**0.59**	0.36	−0.18	**−0.55**	0.13	−0.03	**0.66**	0.03	0.22	**0.62**	0.30	0.25	**−0.75**	0.23	−0.16
Precipitation (summer)	**0.59**	−0.02	−0.52	−0.44	0.25	0.02	0.07	0.15	**0.49**	0.27	0.40	−0.04	−0.17	**0.50**	−0.34
Precipitation (autumn)	**0.68**	0.27	−0.14	**−0.61**	0.19	−0.08	**0.50**	0.20	0.25	**0.70**	0.10	0.01	**−0.59**	0.39	−0.31
Mean temp. (annual)	0.39	0.37	0.19	0.02	0.37	0.21	**0.73**	0.37	0.30	**0.49**	**−0.40**	**0.49**	0.20	0.38	**0.42**
Mean temp. (winter)	0.25	**0.49**	0.30	0.02	0.24	0.32	**0.69**	0.39	0.24	**0.52**	**−0.40**	**0.45**	0.26	**0.50**	**0.42**
Mean temp. (spring)	0.42	0.35	0.14	0.01	0.39	0.19	**0.74**	0.35	0.33	**0.50**	−0.37	**0.48**	0.17	0.31	0.36
Mean temp. (summer)	0.42	0.09	−0.07	0.08	**0.51**	0.03	**0.75**	0.32	0.31	0.34	−0.36	**0.57**	0.11	0.07	0.38
Mean temp. (autumn)	0.45	0.30	0.19	−0.02	**0.40**	0.20	**0.71**	0.36	0.33	**0.52**	**−0.41**	**0.45**	0.17	0.43	**0.42**
Max. temp. (annual)	0.30	0.40	0.25	0.12	0.35	0.23	**0.75**	0.38	0.25	0.42	**−0.41**	**0.53**	0.36	0.22	**0.48**
Max. temp. (winter)	0.24	**0.51**	0.33	0.10	0.25	0.31	**0.70**	0.42	0.23	0.45	**−0.41**	**0.47**	0.41	0.39	0.40
Max. temp. (spring)	0.36	0.39	0.20	0.10	0.38	0.23	**0.76**	0.36	0.27	0.44	−0.37	**0.52**	0.37	0.16	**0.41**
Max. temp. (summer)	0.22	0.14	0.09	0.24	**0.44**	0.04	**0.77**	0.31	0.19	0.23	**−0.42**	**0.64**	0.25	−0.17	**0.50**
Max. temp. (autumn)	0.34	0.35	0.26	0.09	0.36	0.21	**0.74**	0.36	0.27	0.44	**−0.41**	**0.53**	0.25	0.30	**0.51**
Min. temp. (annual)	0.47	0.32	0.11	−0.09	0.38	0.19	**0.69**	0.34	0.35	**0.56**	−0.37	0.42	0.04	**0.47**	0.32
Min. temp. (winter)	0.26	**0.46**	0.27	−0.09	0.22	0.32	**0.67**	0.35	0.26	**0.59**	−0.38	0.42	0.08	**0.58**	**0.41**
Min. temp. (spring)	0.48	0.30	0.07	−0.09	0.39	0.14	**0.70**	0.33	0.39	**0.54**	−0.36	0.41	−0.01	0.40	0.27
Min. temp. (summer)	**0.56**	0.05	−0.21	−0.06	**0.55**	0.01	**0.71**	0.31	0.39	0.40	−0.29	**0.47**	−0.04	0.26	0.18
Min. temp. (autumn)	**0.55**	0.22	0.11	−0.13	**0.42**	0.18	**0.65**	0.34	0.38	**0.59**	−0.38	0.35	0.09	0.50	0.32
ETo (annual)	0.23	0.37	0.35	0.23	0.35	0.26	**0.74**	0.37	0.20	0.34	**−0.42**	**0.54**	0.45	−0.05	**0.51**
ETo (winter)	0.30	**0.47**	0.37	0.12	0.29	0.31	**0.66**	**0.44**	0.28	0.43	**−0.46**	**0.40**	0.43	0.29	0.38
ETo (spring)	0.34	0.38	0.27	0.17	0.38	0.29	**0.74**	0.36	0.21	0.39	−0.35	**0.53**	**0.50**	−0.05	0.40
ETo (summer)	−0.07	0.18	0.31	**0.51**	0.30	0.10	**0.69**	0.22	−0.08	0.01	−0.39	**0.63**	0.31	−0.40	**0.46**
ETo (autumn)	0.29	0.39	0.38	0.16	0.34	0.24	**0.74**	0.35	0.25	0.40	−0.42	**0.53**	0.30	0.10	**0.54**
Clim. Balance (annual)	0.43	0.07	−0.28	**−0.83**	−0.16	−0.02	0.16	0.01	0.21	**0.52**	**0.52**	−0.25	**−0.62**	0.37	−0.30
Clim. Balance (winter)	0.27	0.28	0.24	**−0.59**	−0.28	0.37	0.40	0.22	0.05	**0.70**	0.31	−0.08	**−0.68**	0.29	−0.08

(*continued on next page*)

Table 1 (*continued*)

	Barley			Wheat			Soybean			Corn			Cotton		
	Function 1 (78.3%)	Function 2 (13.2%)	Function 3 (6.8%)	Function 1 (78.3%)	Function 2 (10.6%)	Function 3 (6.4%)	Function 1 (45.7%)	Function 2 (30.0%)	Function 3 (17.1%)	Function 1 (36.7%)	Function 2 (26.4%)	Function 3 (22.9%)	Function 1 (36.7%)	Function 2 (25.0%)	Function 3 (11.4%)
Clim. Balance (spring)	0.27	0.06	−0.31	**−0.66**	−0.18	−0.26	0.20	−0.26	0.09	0.36	**0.55**	−0.11	**−0.77**	0.21	−0.24
Clim. Balance (summer)	0.46	−0.08	−0.51	**−0.60**	0.07	−0.03	−0.29	0.02	**0.46**	0.21	**0.49**	−0.31	−0.22	**0.51**	**−0.39**
Clim. Balance (autumn)	0.43	0.02	−0.33	**−0.68**	−0.07	−0.26	0.01	−0.04	0.10	0.42	0.38	−0.34	**−0.60**	0.30	**−0.43**
NDVI (winter)	**0.56**	0.20	−0.24	−0.27	0.08	0.26	0.02	0.19	−0.23	0.34	0.08	−0.15	−0.02	0.33	−0.11
NDVI (spring)	0.49	0.08	−0.32	−0.22	0.19	0.31	0.02	0.19	−0.23	0.30	0.06	−0.06	−0.08	0.20	−0.06
NDVI (summer)	−0.02	−0.08	−0.20	−0.06	0.09	0.35	0.07	0.01	−0.04	0.25	0.07	0.13	−0.11	−0.20	0.17
NDVI (autumn)	0.38	−0.04	−0.26	−0.22	0.16	**0.41**	0.07	0.02	−0.09	0.39	0.14	0.00	−0.12	0.03	0.08
Day maximum NDVI	−0.05	−0.06	0.18	−0.03	0.01	0.14	0.10	−0.13	0.22	0.10	0.10	0.11	−0.04	−0.01	0.15
Day gree up NDVI	−0.11	−0.09	0.18	0.01	−0.04	0.04	0.08	−0.12	0.19	0.05	0.08	0.05	−0.01	−0.05	0.11
Soil water capacity	0.11	0.01	0.07	0.03	0.10	**−0.40**	0.01	0.09	0.30	0.00	−0.14	0.17	−0.11	0.08	−0.14

Some studies have suggested that vegetation conditions may respond to rapid changes in soil water content, which would be reflected in the response to short SPEI time-scales (Hunt et al., 2014; Zipper et al., 2016). This behaviour could explain why the crop yields respond to short SPEI time-scales in some counties. For example, the main response of corn yields to the SPEI timescales in large areas of the central U.S. is recorded during August over a 3 month SPEI time-scale. In the same context, soybean yields also show a dominant response to the September 4-month SPEI in a large percentage of the counties. The maximum correlations in these dominant patterns are recorded between July and September, confirming the seasonality in the response of crop yields to drought. This seasonality would be related to the phenology, as numerous works suggest that the response of crops to drought is higher during the key phenological stages in which soil water availability is necessary (e.g. Araujo et al., 2016; Zipper et al., 2016). A representative example is corn, where the months with the maximum correlation with the SPEI corresponding to silking and reproductive phenological phases (Wu et al., 2004). But also for barley since in the East Coast planting starts on fall and in this region is clearly identified a specific pattern (PC3) that shows a different response to drought timescales and in which drought indices during the fall period have the main role on crop yields. For soybean, we found a high response to the 4-month drought conditions recorded in September. Soybean is commonly planted between May and June; but soybean is usually at the pod fill stage in early September, showing very high sensitivy to soil water stress at that time (Wu et al., 2004).

Nevertheless, although the dominant pattern of crop yield response to drought was typically recorded for short drought time-scales during the key vegetative periods, there are noticeable spatial differences, with some crop areas showing a dominant response to medium (6–9 months) and long SPEI time-scales (9–12 months). As mentioned earlier, these patterns mainly correspond to winter wheat cultivation. The cycle of winter wheat is very different to those recorded for the other four crops. Winter wheat is usually planted in September-October and harvested between May and August, as a function of the climate characteristics. Winter wheat is mostly active during the cold season; the soil moisture recharge in winter wheat fields mostly occurs in winter months, as a consequence of the low AED (Austin et al., 1998; Liu et al., 2002; Burba and Verma, 2005). This would explain the high sensitivity to long SPEI time-scales, given that spring wheat growth depends on the soil moisture recharge some months in advance. Similar to winter wheat, a response to long SPEI time-scales has been also identified in some regions for the other four crops (e.g. in South central for cotton, in North central for corn and counties in the east and the center for soybean). In these areas, there is a strong control of crop yields by drought severity, albeit with the strongest relationships over long SPEI time-scales. Indeed, this pattern is not specific to US crops, recalling that a range of studies that link drought indices with crop yields have already shown closer relationships of crop yield to long time-scales of the drought indices in China (Ming et al., 2015), Brazil (Fernandes and Heinemann, 2011) and the Great Plains of Nebraska (Yamoah et al., 2000).

Studies focusing on natural vegetation have suggested that general environmental conditions may explain the differences found in the patterns of response of vegetation growth/activity to the different timescales at which drought indices are calculated. Among these different environmental conditions, climate characteristics seem to be the main controller of the different types of response (Pasho et al., 2011; Vicente-Serrano et al., 2013). Overall, the varying responses to SPEI time-scales can be explained by the different resistance of vegetation types to water deficits (Chaves et al., 2003), and the varied strategies of vegetation to cope with drought periods (McDowell et al., 2012).

Based on the selected five main crop types across the US, this study confirms that the differences in the patterns of crop yield response to drought time-scales are mostly controlled by climatology in general and water availability in particular. Overall, independently of the crop type, a stronger response in crop yield to the SPEI is recorded in more arid

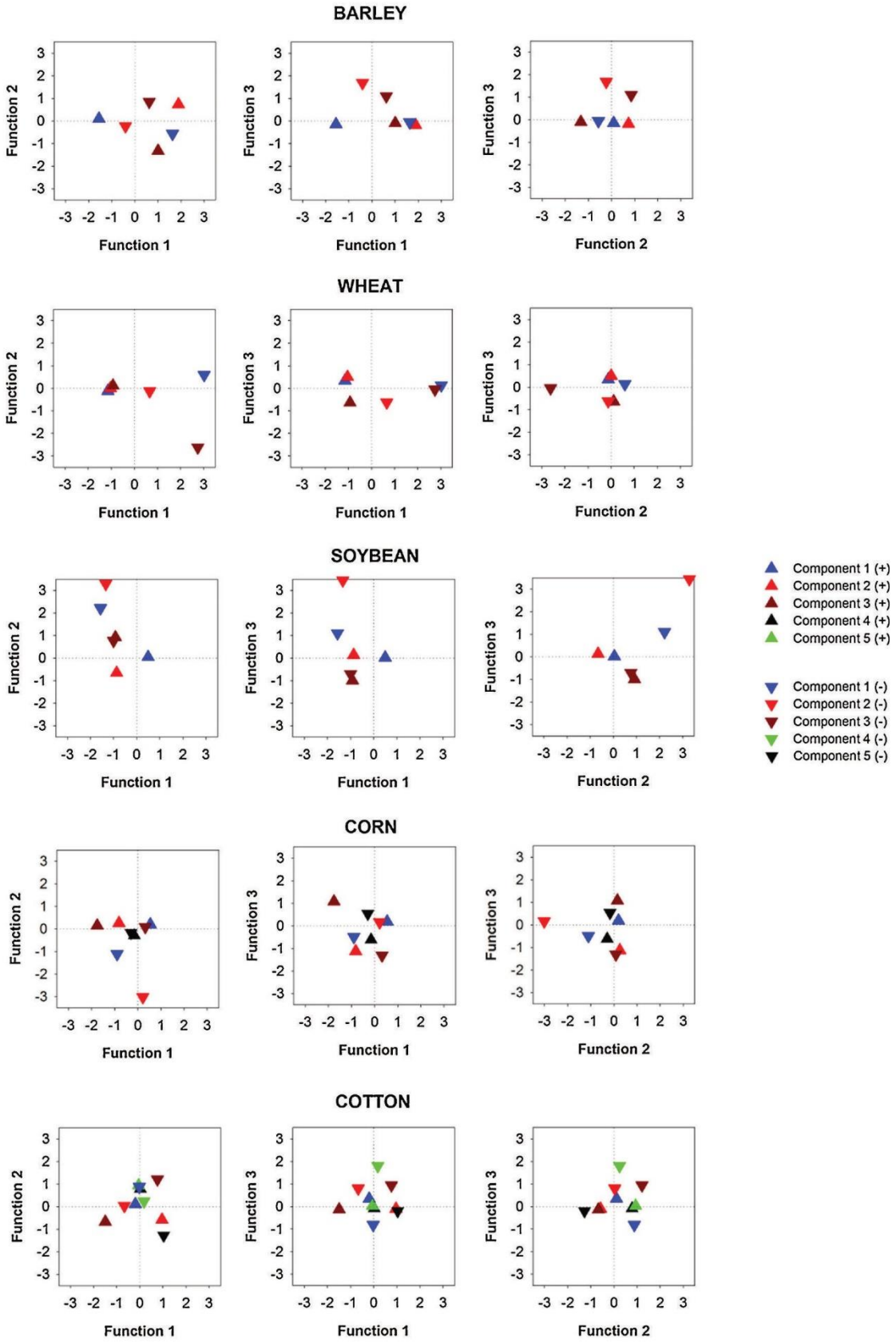

Fig. 9. Centroids of the groups obtained through a principal component analysis.
corresponding to the first three functions of the predictive discriminant analysis (PDA) for each one of the five crop types.

Table 2
Best defined patterns of crop yield response to drought time-scales in the different crop types across U.S.

Crop type	Geographical region	Most correlated drought time-scale	Month of maximum correlation
Barley	Central North U.S.	4 month	July
Winter wheat	Central U.S.	6 month	April
Soybean	The majority of the area of distribution	4 month	September
Corn	East and Northeast U.S.	4 month	August
Corn	Central U.S.	6 month	April

sites. For example, in the barley belt, the majority of the areas assigned to the general pattern, as suggested by PC results, are recorded across the driest counties with negative climate balances. In contrast, those counties that show a divergence to this general pattern are characterized by higher humidity conditions, with low sensitivity to the SPEI variability. This is also observed in some spatial patterns obtained for corn and cotton. Previous studies identified a non-linear response of crop yields to drought indices. Zipper et al. (2016) showed that the response of corn and soybean yields to the SPEI is mostly recorded for negative SPEI values, resulting in a dramatic reduction of yields. In contrast, high positive SPEI values do not guarantee a proportional increase in annual yields of these crops. A similar pattern was observed by Meyer et al. (1991) for the Great Plains and the Midwest of the US, where below-normal precipitation during the corn growing season was closely related with drought severity. Our results concur with these findings, given that we also identified a lower response to drought severity in humid environments and also that the response tends to be recorded on longer time-scales. Here, it is worth noting that although the standardized drought indices (e.g. the SPEI) are comparable in space and time, independently of the climate magnitude and climate regimes (Heim, 2002; Vicente-Serrano et al., 2011), the same SPEI may represent strongly different magnitudes of the climatic balance. In humid environments, where water availability is usually above the current needs of cultivations, the negative SPEI values may correspond to an available total water magnitude that meets crop water requirements. Also, these environments are expected to respond to longer SPEI time-scales since the impacts of drought on soil moisture availability and crop stress conditions will be observed only when persistent long-term drought conditions are recorded.

However, although water availability is the main factor explaining the spatial differences in the response patterns of some crops to drought severity, the spatial differences of temperature and ETo also play an important role for other crops. This aspect is clearly identified for soybean crops, given that the most representative pattern of the yield response to the SPEI does not differ significantly from the other two identified spatial patterns in terms of the annual climate balance, albeit with strong differences (> 200 mm) in the average ETo. This pattern suggests that, within the soybean belt, warmer counties are more sensitive, and their response is observed at shorter drought time-scales than cold counties; this pattern could be explained by differences in phenology related to temperature variations (Piper and Boote, 1999), as well as the indirect effects of temperature on soil water availability, given reduced AED and consequently soil and plant evaporation.

Under changing climate conditions, drought management and monitoring will be even more essential today. In the U.S. although in general there is a complex situation with different SPEI time-scales needed for different seasons, crops and locations, here we have found a very coherent response of crop yields to SPEI time-scales over some homogeneous regions and crop types (see Table 2). In these regions, drought monitoring based on the identified SPEI time-scales during key periods of the year may contribute to better risk assessment and even to improve crop yield forecasting some months in advance. Moreover, given the spatial diversity of situations among crop types and regions, the results of this work reinforces the need for evaluating the crop response to drought characteristics prior developing predictive crop yield statistical models and proper drought monitoring and early warning/forecast systems.

5. Conclusions

The major conclusions of this study are:

(i) Spatial differences that depend on the time-scale selected to measure drought exist when characterize the relationship between drought events and crop yields.
(ii) There are clear differentiate response patterns for each type of crop to the month in which the yields are more prone to be affected by drought conditions.
(iii) Short time-scales (1–3 months) are the dominant pattern of crop yields response to drought corresponding to the key vegetative growth periods. Nonetheless, some crop areas show a response to medium (6–9 months) and long (9–12 months) SPEI time-scales.
(iv) The different patterns of crop yields response to drought time-scales are controlled, in general, by climate conditions and, in particular, by water availability.
(v) Temperature variations and ETo may condition the response of some crops to drought severity. Counties with a humid climate have a low response to drought severity and a high response to longer time-scales while counties with a warm climate are more sensitive to shorter drought time-scales.

Acknowledgements

This work was supported by the research project I-Link1001 (Validation of climate drought indices for multi-sectorial applications in North America and Europe under a global warming scenario) financed by CSIC, PCIN-2015-220, CGL2014-52135-C03-01, *Red de variabilidad y cambio climático* RECLIM (CGL2014-517221-REDT) financed by the Spanish Commission of Science and Technology and FEDER, and IMDROFLOOD financed by the Water Works 2014 co-funded call of the European Commission. Marina Peña-Gallardo was granted by the Spanish Ministry of Economy and Competitiveness; Natalia Martin-Hernandez was supported by a doctoral grant by the Aragón Regional Government; and Miquel Tomas-Burguera was supported by a doctoral grant by el Ministerio de Educación, Cultura y Deporte. Jamie Hannaford was supported by the Belmont Forum project 'DrIVER', NERC Grant Number (grant NE/L010038/1).

Appendix A. Supplementary data

Supplementary material related to this article can be found, in the online version, at doi:https://doi.org/10.1016/j.agrformet.2018.09.019.

References

Araujo, J.A., Abiodun, B.J., Crespo, O., 2016. Impacts of drought on grape yields in Western Cape, South Africa. Theor. Appl. Climatol. 123 (1-2), 117–130.
Arshad, S., Morid, S., Mobasheri, M.R., Alikhani, M.A., Arshad, S., 2013. Monitoring and forecasting drought impact on dryland farming areas. Int. J. Climatol. 33, 2068–2081.
Arzac, R., García-Cervigón, A.I., Vicente-Serrano, S.M., Loidi, J., Olano, J.M., 2016. Phenological shifts in climatic response of secondary growth allow Juniperus sabina L. To cope with altitudinal and temporal climate variability. Agric. For. Meteorol. 217, 35–45.
Asseng, S., Jamieson, P.D., Kimball, B., Pinter, P., Sayre, K., Bowden, J.W., Howden, S.M., 2004. Simulated wheat growth affected by rising temperature, increased water deficit and elevated atmospheric CO2. Field Crops Res. 85 (2-3), 85–102.
Asseng, S., Foster, I., Turner, N.C., 2011. The impact of temperature variability on wheat yields. Glob. Chang. Biol. 17, 997–1012.

Austin, R.B., Cantero-Martínez, C., Arrue, J.L., Playan, E., Cano-Marcellán, P., 1998. Yield–rainfall relationships in cereal cropping systems in the Ebro river valley of Spain. Eur. J. Agron. 8, 239–248.
Bandaru, V., Pei, Y., Hart, Q., Jenkins, B.M., 2017. Impact of biases in gridded weather datasets on biomass estimates of short rotation woody cropping systems. Agric. For. Meteorol. 233, 71–79.
Baret, F., Guyot, G., 1991. Potential and limits of vegetation indices for LAI and APAR assessment. Remote Sens. Environ. 35, 161–173.
Barker, L.J., Hannaford, J., Chiverton, A., Svensson, C., 2015. From meteorological to hydrological drought using standardised indicators. Hydrol. Earth Syst. Sci. Discuss. 12, 12827–12875.
Barnabás, B., Jäger, K., Fehér, A., 2008. The effect of drought and heat stress on reproductive processes in cereals. Plant Cell Environ. 31, 11–38.
Barry, R.G., Carleton, A.M., 2001. Synoptic and Dynamic Climatology. Routledge, London.
Beguería, S., Vicente-Serrano, S.M., Reig, Fergus, Latorre, Borja, 2014. Standardized Precipitation Evapotranspiration Index (SPEI) revisited: parameter fitting, evapotranspiration models, kernel weighting, tools, datasets and drought monitoring. Int. J. Climatol. 34, 3001–3023.
Benitez, J.B., Domecq, R.M., 2014. Analysis of meteorological drought episodes in Paraguay. Clim. Change 127, 15–25.
Bodner, G.S., Robles, M.D., 2017. Enduring a decade of drought: patterns and drivers of vegetation change in a semi-arid grassland. J. Arid Environ. 136, 1–14.
Burba, G.G., Verma, S.B., 2005. Seasonal and interannual variability in evapotranspiration of native tallgrass prairie and cultivated wheat ecosystems. Agric. For. Meteorol. 135 (1-4), 190–201.
Carlson, T.N., Ripley, D.A., 1997. On the relation between NDVI, fractional vegetation cover, and leaf area index. Remote Sens. Environ. 62, 241–252.
Chaves, M.M., Maroco, J.P., Pereira, J.S., 2003. Understanding plant responses to drought—from genes to the whole plant. Funct. Plant Biol. 30 (3), 239–264.
Chen, T., Xia, G., Liu, T., Chen, W., Chi, D., 2016. Assessment of drought impact on main cereal crops using a standardized precipitation evapotranspiration index in Liaoning Province, China. Sustainability (Switzerland) 8 (10) art. no. 1069.
Ciais, Ph., Reichstein, M., Viovy, N., et al., 2005. Europe-wide reduction in primary productivity caused by the heat and drought in 2003. Nature 437, 529–533.
Daly, C., Halbleib, M., Smith, J.I., et al., 2008. Physiographically sensitive mapping of climatological temperature and precipitation across the conterminous United States. Int. J. Climatol. 28 (15), 2031–2064.
Doktor, D., Bondeau, A., Koslowski, D., Badeck, F.W., 2009. Influence of heterogeneous landscapes on computed green-up dates based on daily AVHRR NDVI observations. Remote Sens. Environ. 113, 2618–2632.
Dutta, D., Kundu, A., Patel, N.R., 2013. Predicting agricultural drought in eastern Rajasthan of India using NDVI and standardized precipitation index. Geocarto Int. 28, 192–209.
Easterling, W.E., Isard, S.A., Warren, P., Guinan, P., Shafer, M., 1988. Improving the detection of agricultural drought: a case study of illinois corn production. Agric. For. Meteorol. 43, 37–47.
Egli, D.B., 2008. Comparison of corn and soybean yields in the United States: historical trends and future prospects. Agron. J. 100 (3 SUPPL), S79–S88.
FAO, 2013. Statistical Yearbook. FAO Rome.
Farooq, M., Wahid, A., Kobayashi, N., Fujita, D., Basra, S.M.A., 2009. Plant drought stress: effects, mechanisms and management. Agron. Sustain. Dev. 29, 185–212.
Fernandes, D.S., Heinemann, A.B., 2011. Rice yield variability estimates at different time scales of SPI index. Pesqui. Agropecu. Bras. 46 (4), 335–343.
Fischer, A., 1994. A model for the seasonal variations of vegetation indices in coarse resolution data and its inversion to extract crop parameters. Remote Sens. Environ. 48, 220–230.
Fischer, R.A., Edmeades, G.O., 2010. Breeding and cereal yield progress. Crop Sci. 50 S-85-S-98.
Grassini, P., Eskridge, K.M., Cassman, K.G., 2013. Distinguishing between yield advances and yield plateaus in historical crop production trends. Nat. Commun. 4, 2918.
Gunst, L., Rego, F.C., Dias, S., Bifulco, C., Stagge, J.H., Rocha, M., von Lanen, H.A.J., 2015. Impact of meteorological drought on crop yield on pan-European scale, 1979-2009. Drought: Research and Science-Policy Interfacing - Proceedings of the International Conference on Drought: Research and Science-Policy Interfacing. pp. 113–118.
Gutman, G., 1991. Vegetation indices from AVHRR: an update and future prospects. Remote Sens. Environ. 35, 121–136.
Hair, J.F., Anderson, R.E., Tatham, R.L., Black, W.C., 1998. Multivariate Data Analysis. Prentice Hall, New York, NY.
Hargreaves, G.L., Samani, Z.A., 1985. Reference crop evapotranspiration from temperature. Appl. Eng. Agric. 1, 96–99.
Heim, R.R., 2002. A review of twentieth-century drought indices used in the United States. Bull. Am. Meteorol. Soc. 83, 1149–1165.
Hobbins, M.T., Wood, A., McEvoy, D.J., Huntington, J.L., Morton, C., Verdin, J., 2016. The Evaporative Demand Drought Index. Part I: linking drought evolution to variations in evaporative demand. J. Hydrometeor. 17, 1745–1761.
Huberty, C.J., 1994. Applied Discriminant Analysis. Wiley, New York, NY.
Hunt, E.D., Svoboda, M., Wardlow, B., Hubbard, K., Hayes, M., Arkebauer, T., 2014. Monitoring the effects of rapid onset of drought on non-irrigated maize with agronomic data and climate-based drought indices. Agric. For. Meteorol. 191, 1–11.
Ji, L., Peters, A.J., 2003. Assessing vegetation response to drought in the northern Great Plains using vegetation and drought indices. Remote Sens. Environ. 87, 85–98.
Kola, P., Trnka, M., Brazdil, R., Hlavinka, P., 2014. Influence of climatic factors on the low yields of spring barley and winter wheat in Southern Moravia (Czech Republic) during the 1961-2007 period. Theor. Appl. Climatol. 117, 707–721.
Labudova, L., Labuda, M., Taka, A., 2016. Comparison of SPI and SPEI applicability for drought impact assessment on crop production in the Danubian Lowland and the East Slovakian Lowland. Theor. Appl. Climatol. 1–16 Article in Press.
Liu, C., Zhang, X., Zhang, Y., 2002. Determination of daily evaporation and evapotranspiration of winter wheat and maize by large-scale weighing lysimeter and micro-lysimeter. Agric. For. Meteorol. 111 (2), 109–120.
Lloyd-Hughes, B., 2014. The impracticality of a universal drought definition. Theor. Appl. Climatol. 117 (3-4), 607–611.
Lobell, D.B., Asner, G.P., 2003. Climate and management contributions to recent trends in U.S. Agricultural yields. Science 299 (5609), 1032.
Lobell, D.B., Cahill, K.N., Field, C.B., 2007. Historical effects of temperature and precipitation on California crop yields. Clim. Change 81, 187–203.
Lobell, D.B., Schlenker, W., Costa-Roberts, J., 2011a. Climate trends and global crop production since 1980. Science 333, 616–620.
Lobell, D.B., Bänziger, M., Magorokosho, C., Vivek, B., 2011b. Nonlinear heat effects on African maize as evidenced by historical yield trials. Nat. Clim. Chang. 1, 42–45.
Lobell, D.B., Roberts, M.J., Schlenker, W., Braun, N., Little, B.B., Rejesus, R.M., Hammer, G.L., 2014. Greater sensitivity to drought accompanies maize yield increase in the U.S. Midwest. Science 344 (6183), 516–519.
Lorenzo-Lacruz, J., Vicente-Serrano, S.M., López-Moreno, J.I., Beguería, S., García-Ruiz, J.M., Cuadrat, J.M., 2010. The impact of droughts and water management on various hydrological systems in the headwaters of the Tagus River (central Spain). J. Hydrol. (Amst.) 386, 13–26.
Lutz, J.A., van Wagtendonk, J.W., Franklin, J.F., 2010. Climatic water deficit, tree species ranges, and climate change in Yosemite National Park. J. Biogeogr. 37 (5), 936–950.
Ma, M., Ren, Liliang, Yuan, Fei, Jiang, Shanhu, Liu, Yi, Kong, Hao, Gong, Luyan, 2014. A new standardized Palmer drought index for hydro-meteorological use. Hydrol. Process. https://doi.org/10.1002/hyp.10063.
McEvoy, D.J., Huntington, J.L., Hobbins, M.T., Woodd, A., Morton, C., Anderson, M., Hain, C., 2016. The evaporative demand drought index. Part II: CONUS-Wide assessment against common drought indicators. J. Hydrometeorol. https://doi.org/10.1175/JHM-D-15-0122.1.
McKee, T.B.N., Doesken, J., Kleist, J., 1993. The Relationship of Drought Frequency and Duration to Time Scales, Paper Presented at Eighth Conference on Applied Climatology. Am. Meteorol. Soc., Anaheim, Calif.
Meyer, S.J., Hubbard, K.G., Wilhite, D.A., 1991. The relationship of climatic indices and variables to corn (maize) yields: a principal components analysis. Agric. For. Meteorol. 55 (1-2), 59–84.
Ming, B., Guo, Y.-Q., Tao, H.-B., Liu, G.-Z., Li, S.-K., Wang, P., 2015. SPEIPM-based research on drought impact on maize yield in North China Plain. J. Integr. Agric. 14, 660–669.
Moorhead, J.E., Gowda, P.H., Singh, V.P., Porter, D.O., Marek, T.H., Howell, T.A., Stewart, B.A., 2015. Identifying and evaluating a suitable index for agricultural drought monitoring in the Texas High Plains. J. Am. Water Resour. Assoc. 51 (3), 807–820.
Narasimhan, B., Srinivasan, R., 2005. Development and evaluation of Soil Moisture Deficit Index (SMDI) and Evapotranspiration Deficit Index (ETDI) for agricultural drought monitoring. Agric. For. Meteorol. 133 (1-4), 69–88.
Nemani, R.R., Keeling, C.D., Hashimoto, H., et al., 2003. Climate-driven increases in global terrestrial net primary production from 1982 to 1999. Science 300 (5625), 1560–1563.
Oerke, E.-C., 2006. Crop losses to pests. J. Agric. Sci. 144, 31–43.
Pasho, E., Julio Camarero, J., Martín de Luis and Vicente-Serrano, S.M, 2011. Impacts of drought at different time scales on forest growth across a wide climatic gradient in north-eastern Spain. Agric. For. Meteorol. 151, 1800–1811.
Pescoa, P., Gouveia, C.M., Russo, A., Trigo, R.M., 2016. The role of drought on wheat yield interannual variability in the Iberian Peninsula from 1929 to 2012. Int. J. Biometeorol. 1–13.
Piper, E.L., Boote, K.J., 1999. Temperature and cultivar effects on soybean seed oil and protein concentrations. J. Am. Oil Chem. Soc. 76 (10), 1233–1242.
Porter, J.R., Semenov, M.A., 2005. Crop responses to climatic variation. Philos. Trans. Biol. Sci. 360, 2021–2035.
Potopova, V., Boroneant, C., Boincean, B., 2015. Multi-scalar drought and its impact on crop yield in the Republic of Moldova. Drought: Research and Science-Policy Interfacing - Proceedings of the International Conference on Drought: Research and Science-Policy Interfacing. pp. 85–90.
Potopova, V., Boroneant, C., Boincean, B., Soukup, J., 2016. Impact of agricultural drought on main crop yields in the Republic of Moldova. Int. J. Climatol. 36, 2063–2082.
Potopova, V., Stepanek, P., Farda, A., Tarkott, L., Zahradna, P., Soukup, J., 2016b. Drought stress impact on vegetable crop yields in the elbe river lowland between 1961 and 2014. Cuadernos de Investigacion Geografica 42 (1), 127–143.
Quiring, S.M., Papakryiakou, T.N., 2003. An evaluation of agricultural drought indices for the Canadian prairies. Agric. For. Meteorol. 118, 49–62.
Ramadas, M., Govindaraju, R.S., 2015. Probabilistic assessment of agricultural droughts using graphical models. J. Hydrol. (Amst) 526, 151–163.
Richman, M.B., 1986. Rotation of principal components. J. Climatol. 6, 293–335.
Rohli, R.V., Bushra, N., Lam, N.S.N., Zou, L., Mihunov, V., Reams, M.A., Argote, J.E., 2016. Drought indices as drought predictors in the south-central US. Nat. Hazards 83 (3), 1567–1582.
Sadat Noori, S.M., Liaghat, A.M., Ebrahimi, K., 2012. Prediction of crop production using drought indices at different time scales and climatic factors to manage drought risk. J. Am. Water Resour. Assoc. 48, 1–9.
Schlenker, W., Roberts, M.J., 2009. Nonlinear temperature effects indicate severe damages to U.S. Crop yields under climate change. Proc. Natl. Acad. Sci. U. S. A. 106 (37), 15594–15598.

Scian, B.V., 2004. Environmental variables for modeling wheat yields in the southwest pampa region of Argentina. Int. J. Biometeorol. 48, 206–212.
Stanhill, G., 1976. Trends and deviations in the yield of the English wheat crop during the last 750 years. AgroEcosystems 3, 1–10.
Subash, N., Ram Mohan, H.S., 2011. A simple rationally integrated drought Indicator for rice-wheat productivity. Water Resour. Manag. 25 (10), 2425–2447.
Tunalioclu, R., Durdu, O.F., 2012. Assessment of future olive crop yield by a comparative evaluation of drought indices: A case study in western Turkey. Theor. Appl. Climatol. 108, 397–410.
Vargas, M., Kogan, F., Guo, W., 2009. Empirical normalization for the effect of volcanic stratospheric aerosols on AVHRR NDVI. Geophys. Res. Lett. 36 (7), L07701.
Vicente-Serrano, S.M., 2016. Cuadernos de Investigación Geográfica 42, 7–11.
Vicente-Serrano, S.M., Beguería, Santiago, López-Moreno, Juan I., 2010. A Multi-scalar drought index sensitive to global warming: the Standardized Precipitation Evapotranspiration Index – SPEI. J. Clim. 23, 1696–1718.
Vicente-Serrano, S.M., Beguería, S., López-Moreno, Juan I., 2011. Comment on "Characteristics and trends in various forms of the Palmer Drought Severity Index (PDSI) during 1900-2008" by A. Dai. J. Geophys. Res. Atmos. 116, D19112. https://doi.org/10.1029/2011JD016410.
Vicente-Serrano, S.M., Beguería, Santiago, Lorenzo-Lacruz, Jorge, Camarero, Jesús Julio, López-Moreno, Juan I., Azorin-Molina, Cesar, Revuelto, Jesús, Morán-Tejeda, Enrique, Sánchez-Lorenzo, Arturo, 2012. Performance of drought índices for ecological, agricultural and hydrological applications. Earth Interact. 16, 1–27.
Vicente-Serrano, S.M., Gouveia, C.élia, Camarero, Jesús Julio, Beguería, Santiago, Trigo, Ricardo, López-Moreno, Juan I., Azorín-Molina, C.ésar, Pasho, Edmond, Lorenzo-Lacruz, Jorge, Revuelto, Jesús, Morán-Tejeda, Enrique, Sanchez-Lorenzo, Arturo, 2013. The response of vegetation to drought time-scales across global land biomes. Proc. Natl. Acad. Sci. U. S. A. 110, 52–57.
Vicente-Serrano, S.M., Camarero, J.J., Azorín-Molina, C., 2014. Diverse responses of forest growth to drought time-scales in the northern hemisphere. Glob. Ecol. Biogeogr. 23, 1019–1030.
Vicente-Serrano, S.M., Van der Schrier, Gerard, Beguería, Santiago, Azorin–Molina, Cesar, Lopez–Moreno, Juan-I., 2015. Contribution of precipitation and reference evapotranspiration to drought indices under different climates. J. Hydrol. (Amst) 426, 42–54.
Vicente-Serrano, S.M., Cuadrat, J.M. y Romo, A., (2006), Early prediction of crop productions using drought indices at different time scales and remote sensing data: application in the Ebro valley (North-east Spain). International Journal of Remote Sensing 27: 511-518.
Wang, H., Vicente-Serrano, S.M., Tao, F., Zhang, X., Wang, P., Zhang, C., Chen, Y., Zhu, D., Kenawy, A.E., 2016a. Monitoring winter wheat drought threat in Northern China using multiple climate-based drought indices and soil moisture during 2000-2013. Agric. For. Meteorol. 228–229.
Wang, Q., Wu, J., Li, X., Zhou, H., Yang, J., Geng, G., An, X., Liu, L., Tang, Z., 2016b. A comprehensively quantitative method of evaluating the impact of drought on crop yield using daily multi-scale SPEI and crop growth process model. Int. J. Biometeorol. 1–15.
Wilhite, D.A., Glantz, M.H., 1985. Understanding the drought phenomenon: the role of definitions. Water Int. 10, 111–120.
Wrather, J.A., Stienstra, W.C., Koenning, S.R., 2001. Soybean disease loss estimates for the United States from 1996 to 1998. Can. J. Plant Pathol. 23, 122–131.
Wu, H., Hubbard, K.G., Wilhite, D.A., 2004. An agricultural drought risk-assessment model for corn and soybeans. Int. J. Climatol. 24 (6), 723–741.
Yamoah, C.F., Walters, D.T., Shapiro, C.A., Francis, C.A., Hayes, M.J., 2000. Standardized precipitation index and nitrogen rate effects on crop yields and risk distribution in maize. Agric. Ecosyst. Environ. 80 (1-2), 113–120.
Zipper, S.C., Qiu, J., Kucharik, C.J., 2016. Drought effects on US maize and soybean production: spatiotemporal patterns and historical changes. Environ. Res. Lett. 11 (9), 094021.

forests

MDPI

Article

Drought Sensitiveness on Forest Growth in Peninsular Spain and the Balearic Islands

Marina Peña-Gallardo [1,*], Sergio M. Vicente-Serrano [1], J. Julio Camarero [1], Antonio Gazol [1], Raúl Sánchez-Salguero [2], Fernando Domínguez-Castro [1], Ahmed El Kenawy [1,3], Santiago Beguería-Portugés [4], Emilia Gutiérrez [5], Martin de Luis [6], Gabriel Sangüesa-Barreda [1], Klemen Novak [6,7], Vicente Rozas [8], Pedro A. Tíscar [9], Juan C. Linares [2], Edurne Martínez del Castillo [6], Montserrat Ribas Matamoros [5], Ignacio García-González [10], Fernando Silla [11], Álvaro Camisón [12], Mar Génova [13], José M. Olano [8], Luis A. Longares [6], Andrea Hevia [14] and J. Diego Galván [15]

1 Instituto Pirenaico de Ecología (IPE-CSIC), 50192 Zaragoza, Spain; svicen@ipe.csic.es (S.M.V.-S.); jjcamarero@ipe.csic.es (J.J.C.); agazol@ipe.csic.es (A.G.); f.dominguez@ipe.csic.es (F.D.-C.); kenawy@ipe.csic.es (A.E.K.); gsanguesa@ipe.csic.es (G.S.-B.)
2 Departamento de Sistemas Físicos, Químicos y Naturales, Universidad de Pablo de Olavide, 41013 Sevilla, Spain; rsanchez@upo.es (R.S.-S.); jclincal@upo.es (J.C.L.)
3 Department of Geography, Mansoura University, 35516 Mansoura, Egypt
4 Estación Experimental Aula Dei, Consejo Superior de Investigaciones Científicas (EEAD-CSIC), 50192 Zaragoza, Spain; santiago.begueria@csic.es
5 Department of Evolutionary Biology, Ecology and Environmental Sciences, Barcelona University, 08028 Barcelona, Spain; emgutierrez@ub.edu (E.G.); mribas@porthos.bio.ub.es (M.R.M.)
6 Departamento de Geografía y Ordenación del Territorio—IUCA, Universidad de Zaragoza, 50009 Zaragoza, Spain; mdla@unizar.es (M.d.L.); kn4@alu.ua.es (K.N.); edurne@unizar.es (E.M.d.C.); lalongar@unizar.es (L.A.L.)
7 Departamento de Ecología, Universidad de Alicante, Carretera San Vicente del Raspeig s/n, 03080 Alicante, Spain
8 Departamento de Ciencias Agroforestales, EU de Ingenierias Agrarias, iuFOR—Universidad de Valladolid, 42004 Soria, Spain; vicentefernando.rozas@uva.es (V.R.); josemiguel.olano@uva.es (J.M.O.)
9 Centro de Capacitación y Experimentación Forestal. C/. Vadillo-Castril, 23470 Cazorla, Spain; pedroa.tiscar@juntadeandalucia.es
10 Departamento de Botánica, Escola Politécnica Superior de Enxeñaría Campus Terra, Universidade de Santiago de Compostela, 27002 Lugo, Spain; ignacio.garcia@usc.es
11 Departamento de Biología Animal, Parasitología, Ecología, Edafología y Química Agrícola, Universidad de Salamanca, 37071 Salamanca, Spain; fsilla@usal.es
12 Ingeniería Forestal y del Medio Natural, Universidad de Extremadura, 10600 Plasencia, Spain; alvarocc@unex.es
13 Departamento de Sistemas y Recursos Naturales, Universidad de Politécnica de Madrid, 28040 Madrid, Spain; mar.genova@upm.es
14 Forest and Wood Technology Research Centre (CETEMAS), 33936 Asturias, Spain; ahevia@cetemas.es
15 Ionplus AG. Lerzenstrasse 12, 8953 Dietikon, Switzerland; galvan@ionplus.ch
* Correspondence: marinapgallardo@ipe.csic.es

Received: 23 July 2018; Accepted: 27 August 2018; Published: 30 August 2018

Abstract: Drought is one of the key natural hazards impacting net primary production and tree growth in forest ecosystems. Nonetheless, tree species show different responses to drought events, which make it difficult to adopt fixed tools for monitoring drought impacts under contrasting environmental and climatic conditions. In this study, we assess the response of forest growth and a satellite proxy of the net primary production (NPP) to drought in peninsular Spain and the Balearic Islands, a region characterized by complex climatological, topographical, and environmental characteristics. Herein, we employed three different indicators based on

in situ measurements and satellite image-derived vegetation information (i.e., tree-ring width, maximum annual greenness, and an indicator of NPP). We used seven different climate drought indices to assess drought impacts on the tree variables analyzed. The selected drought indices include four versions of the Palmer Drought Severity Index (PDSI, Palmer Hydrological Drought Index (PHDI), Z-index, and Palmer Modified Drought Index (PMDI)) and three multi-scalar indices (Standardized Precipitation Evapotranspiration Index (SPEI), Standardized Precipitation Index (SPI), and Standardized Precipitation Drought Index (SPDI)). Our results suggest that—irrespective of drought index and tree species—tree-ring width shows a stronger response to interannual variability of drought, compared to the greenness and the NPP. In comparison to other drought indices (e.g., PDSI), and our results demonstrate that multi-scalar drought indices (e.g., SPI, SPEI) are more advantageous in monitoring drought impacts on tree-ring growth, maximum greenness, and NPP. This finding suggests that multi-scalar indices are more appropriate for monitoring and modelling forest drought in peninsular Spain and the Balearic Islands.

Keywords: normalized difference vegetation index; tree-rings; drought indices; forest productivity; Spain

1. Introduction

Drought is a major hydroclimatic hazard that is difficult to quantify, analyze, monitor and, thus, mitigate [1]. This is because drought has a complex nature, given that it is the result of the synergy among a wide range of variables (e.g., precipitation, temperature, land use, human activities, etc.). Additionally, assessing the impacts of drought on natural and human environments can vary among regions and systems depending on their response and vulnerability. Furthermore, it is difficult to prevent droughts, due to their slow and less evident onset compared to other natural hazards (e.g., floods, landslides, volcanic eruptions), on one hand, and their serious and adverse socioeconomic and environmental impacts, on the other hand [2,3].

Droughts may trigger forest decay and mortality episodes [4,5], which have increased over the last decades in many regions worldwide [6,7]. The Mediterranean region has witnessed frequent and severe drought episodes, inducing important impacts to forests [8,9] given that both primary and secondary growth are constrained by water availability [10]. Some tree species and phenotypes are more sensitive to drought-triggered growth decline and damage [11,12]. Local environmental and climatic conditions can complicate further the response of forests to drought [13,14]. However, assessing forest response to drought is a challenging task, as species [15], and even individuals [16], differ in their sensitivity to this phenomenon. Moreover, spatial variability in climatic and topographic conditions adds a finer grain to drought pattern predictions.

The Iberian Peninsula (IP) is characterized by a great heterogeneity of climate types, ranging from a humid Atlantic climate in the northwest and north to semi-arid Mediterranean conditions in the east and southeast [17]. As such, the response of forests to drought incidence vary markedly over space. In this context, changing climatic conditions (e.g., abnormal low precipitation, temperature rise), mostly during the previous winter of the growing season, cause a reduction in Net Primary Production (NPP), growth decline, as well as forest die-off in some extreme cases [5,18–20]. In Mediterranean forests, radial growth sensitivity to drought intensity varies depending on soil moisture and precipitation, both factors being highly variable in space and time in the region. In particular, while tree growth responses at short time scales are more associated with consecutive periods of dryness and moisture conditions, responses at longer time scales are linked to less frequent, but more intense, drought events [10]. Some Mediterranean species experience a higher recovery to pre-drought growth level at short-term than at long-term timescale, either for declining or non-declining individuals [18]. Nonetheless, a general increase of crown defoliation trend has

been observed in the IP over the last decades, especially in drier areas, where tree mortality is also related to dynamic changes at the trophic level as a consequence of drought impacts related to climate warming [21].

Forests are an important component of the terrestrial ecosystems dynamics, given its capital role in the hydrological and carbon cycles [22,23]. Furthermore, forests are sources for minerals, agricultural products, recreation and other benefits to mankind [4]. In this respect, Zhao et al. [24] found that drought is the leading cause of global NPP depletion. The eco-physiological impacts drought causes in vegetation are diverse [25], with some plant responses to drought stress related to stomata regulation, osmotic adjustment, and anti-oxidative defense [26]. However, reduction of photosynthesis is the ultimate impact of drought. Dramatic changes in primary metabolism lead to a decline in leaf net carbon uptake as a consequence of a decrease in water availability [27]. A prolonged reduced photosynthetic activity may lead to the decrease of molecular oxygen and the increase of reactive oxygen species inducing important damage to the photosynthetic apparatus [28]. Accordingly, the response of forests to drought has been a matter of interest in the scientific community [29–31]. In this context, a comprehensive assessment of the links between drought, NPP, and secondary growth among different forest ecosystems is still lacking.

Dendrochronological techniques have quantified secondary growth over time in a wealth of tree species [10,11,32,33]. Tree-rings provide short- to long-term information about annual radial growth, a proxy of carbon uptake and NPP [34]. Tree-ring width data have been used to identify the effects of drought on forest growth and vitality [20,35]. However, few dendrochronological studies have related tree-ring width data with surrogates of primary growth and NPP at consistent temporal (long) and spatial (broad coverage) scales [36]. Vegetation indices derived from satellite remote-sensing data, have proven valuable to monitor forests from local [37–39] to global scales [40]. The Normalized Difference Vegetation Index (NDVI) is commonly used to quantify the photosynthetic activity, which is closely related to the total biomass production and the vegetation NPP [41,42]. In the same context, a wide range of drought indices have been developed over the last decades [43,44]. These indices are well-recognized as useful tools for assessing drought under different hydrological and agricultural conditions [3,45–47].

The aims of this work are two-fold. First, it aims at comparing and assessing the performance of a range of drought indices for monitoring the response of vegetation activity, as summarized by tree-ring width, maximum annual greenness, and a surrogate of the NPP, to drought impacts. Second, it assesses and contrasts the response of tree-ring width and NDVI to drought conditions for different species. To accomplish this task, we linked seven widely used drought indices: Standardized Precipitation Evapotranspiration Index (SPEI), Standardized Precipitation Index (SPI), Standardized Palmer Drought Severity Index (SPDSI), and four Palmer-related drought indices (Palmer Drought Severity Index (PDSI), Palmer Hydrological Drought Index (PHDI), Palmer Z-Index (Z), and Palmer Modified Drought Index (PMDI)) with climatic, NDVI, and dendrochronological data for the IP and the Balearic Islands for the period 1981–2015. As a result we should be able to assess the validity of these drought indices to assessing and monitor the impacts of drought on forest growth and vitality [48–50].

2. Data and Methods

2.1. Datasets Description

We employed a daily dataset of meteorological variables (precipitation, maximum and minimum air temperatures, wind speed, sunshine duration and relative humidity) provided by the Spanish National Meteorological Agency (AEMET). The original dataset was subjected to a rigorous procedure to ensure data quality and homogeneity. Daily records were aggregated to weekly data and gridded at a 1.1 km resolution. Further details about data development are outlined in Vicente-Serrano et al. [51]. Based on the available input variables, we also calculated reference evapotranspiration (ETo) using

the Penman-Monteith equation recommended by the FAO [52]. For this analysis, we aggregated the weekly gridded data at monthly scale for the period 1981–2015.

2.2. NDVI Data

The Normalized Difference Vegetation Index (NDVI) is widely-used to assess vegetation activity, with a good agreement with the photosynthetically-active radiation absorbed by vegetation [41,53]. Here, we employed NDVI data at 1.1 km resolution for the period 1981 to 2015 at a monthly time scale aggregation [54]. The original data were obtained from the National Oceanic and Atmospheric Administration (NOAA) polar orbiting satellites that used the Advanced Very High Resolution Radiometer (AVHRR) sensors to provide daily satellite images. Our selection allowed to characterize vegetation activity with more detailed spatial coverage and finer temporal resolution than other publicly available data sets such as the Global Inventory Monitoring and Mapping Studies (GIMMS) and the Moderate-Resolution Imaging Spectroradiometer (MODIS) [41,51,52]. In order to obtain the final NDVI product, the original data were subjected to a series of data processing, including radiometric calibration [55,56], geometric and topographic corrections [57,58], cloud cover removal [59] to obtain semi-monthly composite images by maximum NDVI value (two images per month) [60]. A comprehensive explanation of this procedure is found in Vicente-Serrano et al. [54].

2.3. Tree-Ring Width Data

We compiled annual tree-ring width chronologies of 568 forest stands covering the majority of forest areas across the IP and the Balearic Islands from 1981 to 2015 (Figure 1). Chronologies were obtained using the basic dendrochronological protocol [34]. At least 10 dominant or codominant trees located in undisturbed stands were selected and cored at 1.3 m using increment borers to obtain 2–3 cores per tree in each forest. The selected study sites represent a wide sample of conifers and hardwood species subjected to different climatic and edaphic conditions along the Spanish territory. Latitude, longitude, and mean elevation were recorded at each sample. Wood samples were air-dried and sanded until rings were clearly visible and then visually cross-dated. Tree-ring width was measured to at least the nearest 0.01 mm using binocular microscopes and measuring device systems (Lintab, RinnTech, Heidelberg, Germany; Velmex Inc., Bloomfirld, NY, USA). In order to check the accuracy of visual cross-dating and measurements, we used the COFECHA program, based on moving correlations between each individual tree-ring series and the mean site series [61]. Additionally, to remove the trends in tree-ring width due to tree aging and the enlargement of the stem, we used traditional dendrochronological protocols [34]. Specifically, we detrended each individual tree-ring width series by fitting negative exponential curves and then obtained the residuals through dividing the observed values by the fitted ones. Then, we averaged the detrended series of tree-ring width indices (hereafter TRWi) for each forest by computing bi-weight robust means. The mean site-level chronology represents the average growth series of a variable number of trees of the same species growing at the same forest stand. Since no autoregressive modelling was performed, we removed the low- to mid-frequency variability, while keeping the high-frequency variability and the first-order autocorrelation. The procedure of chronology building was implemented using the 'dplR' package within the R platform [62]. Table 1 summarizes the main characteristics of the tree species used in this study.

Table 1. List of tree species, abbreviations, and number of the sampled forests stands; including the average mean annual temperature and precipitation of each tree species location.

Gymnosperms					Angiosperms				
Tree Species	**Abbreviation**	**Number of Sampled Forests Stands**	**Mean Annual Temperature (°C)**	**Annual Precipitation (mm)**	**Tree Species**	**Abbreviation**	**Number of Sampled Forests Stands**	**Mean Annual Temperature (°C)**	**Annual Precipitation (mm)**
Abies alba	ABAL	48	13.10	1439.98	*Fagus sylvatica*	FASY	51	14.36	1212.98
Abies pinsapo	ABPN	15	17.53	1467.33	*Quercus pyrenaica*	QUPY	34	16.20	878.27
Pinus halepensis	PIHA	119	19.93	599.87	*Quercus robur*	QURO	34	16.19	1484.53
Pinus sylvestris	PISY	76	14.80	958.32	*Quercus faginea*	QUFA	19	16.89	975.97
Pinus nigra	PINI	66	17.05	754.00	*Quercus ilex*	QUIL	5	17.32	786.00
Pinus uncinata	PIUN	39	10.11	1442.68	*Quercus petraea*	QUPE	7	15.58	1062.13
Pinus pinaster	PIPI	20	18.52	705.30	*Castanea sativa*	CASA	10	17.50	928.00
Pinus pinea	PIPN	9	19.98	550.89					
Juniperus thurifera	JUTH	16	17.22	690.59					

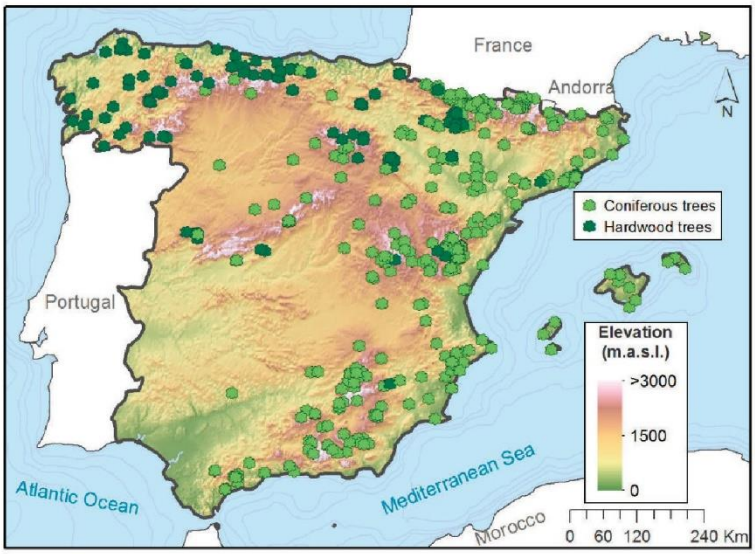

Figure 1. Location of the sampled forest stands in the study domain. Note that the conifer forests (n = 408 sites) dominate in the driest regions (Mediterranean climate) of Eastern and Southeastern Spain, and also in mountainous terrain, while hardwood forests prevail in the wettest and temperate regions (Atlantic climate) in Northwestern and Northern Spain (n = 160 sites).

2.4. Drought Indices

We computed the seven drought indices based on the monthly climate data for each location to each sampled forest stand as the time of response to drought indices is not known beforehand, described as follows.

2.4.1. Palmer Drought Severity Indices (PDSIs)

The Palmer Drought Severity Index (PDSI) is a well-known meteorological drought index proposed by Palmer [63] along with the Palmer Hydrological Drought Index (PHDI), the Palmer Moisture Anomaly Index (Z-index), and the Palmer Modified Drought Index (PMDI). While Palmer indices account for supply-demand relationship of soil moisture using precipitation and air temperature data, our preference was to use a modification of the original methodology to limit the possible impact of lack of comparability between differentiated regions [64–66]. This issue was solved by Wells et al. [62] who employed the self-calibrated Palmer indices algorithm, which automatically determines the appropriate and spatially-comparable regional coefficients. Hereafter, we will use the original acronyms to refer to the self-calibrated versions of Palmer drought indices. As opposed to multiscalar drought indices (e.g., SPI, SPEI, SPDI), PDSIs are uni-scalar.

2.4.2. Standardized Precipitation Index (SPI)

The Standardized Precipitation Index (SPI) was developed by McKee et al. [67]. The SPI introduced for the very first time a new functional definition of drought based on the standardized precipitation and time scales to quantify precipitation shortages along time. The index is based on the conversion of the precipitation series using an incomplete Gamma distribution to a standard normal variable with the mean equal to zero and variance equal to one. The SPI is the universal reference meteorological index according to the World Meteorological Organization [68].

2.4.3. Standardized Precipitation Evapotranspiration Index (SPEI)

The Standardized Precipitation Evapotranspiration Index (SPEI) was proposed by Vicente-Serrano et al. [69], accounting for the possible impact of reference evapotranspiration

on drought. In particular, the SPEI is based on the computation of monthly climate water balances (precipitation minus reference evapotranspiration) accumulated at different timescales. The resulting values are later transformed to a normal standardized variable using a three-parameter log-logistic distribution, allowing for direct comparison over space. The SPEI has been widely used in multiple drought-related studies, with a main focus on evaluation of drought impacts, recurrence, variability, or reconstruction.

2.4.4. Standardized Precipitation Drought Index (SPDI)

The Standardized Precipitation Drought Index (SPDI) was introduced by Ma et al. [70]. It is defined as a combination of the PDSI and SPI. It also implements the timescale concept and the statistical nature of the SPI and SPEI [71] as well as the water balance concept defined by Palmer [64]. For its calculation, the SPDI-accumulated values are transformed to a standard normal variable using a generalized extreme value distribution.

Herein, the multi-scalar indices (i.e., SPEI, SPI and SPDI) were calculated at 1- to 12-, 18-, and 24-timescale. It is noteworthy emphasizing that the monthly drought indices, for each sampled tree, were detrended by fitting a linear regression with the time series. This procedure removes any possible trend that can disturb the comparison among drought and tree-ring growth, given that tree-ring series were already detrended. Finally, the residual of each series was obtained from linear models, and summed to the average of the period to obtain the detrended drought indices.

2.5. Statistical Methods

We assessed the response of vegetation activity to the interannual variations of drought for the common period of time 1981–2015. To achieve the mentioned purpose, three indicators were considered: TRWi, maximum annual NDVI value (NDVI max) and annual integrated NDVI. The NDVI max was obtained from the biweekly series of the NDVI, providing information on the maximum potential vegetation activity in each sampled forest stand. As such, it is considered a reliable indicator of the annual vegetation growth [72]. In this work, the annual cumulative NDVI (NDVI annual) is used as a surrogate of NPP. This is simply because the NPP, defined as the net carbon accumulated by plants per unit and time [73], is closely related to the amount of photosynthetically active radiation (PAR) captured by green foliage. Thus, the NPP depends on the fraction of photosynthetically active radiation (FPAR) absorbed by the canopy [74].

We computed the Pearson correlation coefficient between the TRWi, NDVI max, and NDVI annual and each drought index for the common period 1981–2015. To keep consistency among all variables, we also detrended the NDVI variables. Since the response of vegetation to drought is expected to vary at different time scales [40], and the month when the vegetation is most susceptible to drought is not known a priori, we correlated the 12 monthly series of each drought index with the annual series of TRWi, NDVI max, and NDVI annual and kept the maximum correlation value for analyzing spatial and temporal responses of tree variables to drought and the relationship between vegetation variables and drought by species. We calculated the indices at 1- to 12-, 18-, and 24-month time-scales for the multi-scalar indices (SPEI, SPI, and SPDI). This procedure resulted in 168 correlation values (12 correlations for each time-scale) for the multi-scalar indices and 12 correlations for the uni-scalar indices. We also calculated the climatic water balance as the difference between precipitation and evapotranspiration (P—ETo) at each sampled forest stand.

3. Results

3.1. Spatial and Temporal Responses of Tree Variables to Drought

The magnitude of maximum Pearson correlations found between each of the selected drought indices and the three tree variables (TRWi, NDVI max, and NDVI annual) varied considerably between the two main groups of drought indices: multi-scalar vs. uni-scalar (Figure 2). In general,

multi-scalar indices had higher correlations than for uni-scalar indices. Remarkably, TRWi had higher correlations with drought indices than NDVI max and NDVI annual. This pattern was evident for all drought indices (Figure 2). Correlation values averaged 0.60 for TRWi, and 0.45 and 0.40 for NDVI annual and NDVI max, respectively. Among the uni-scalar drought indices, the Z-index showed the highest correlations, particularly with TRWi, although a high percentage of correlations for the four Palmer indices was statistically non-significant. Among multiscalar indices, SPEI showed the highest correlations with TRWi and NDVI max, while the SPI correlated better with the NDVI annual (Table 2).

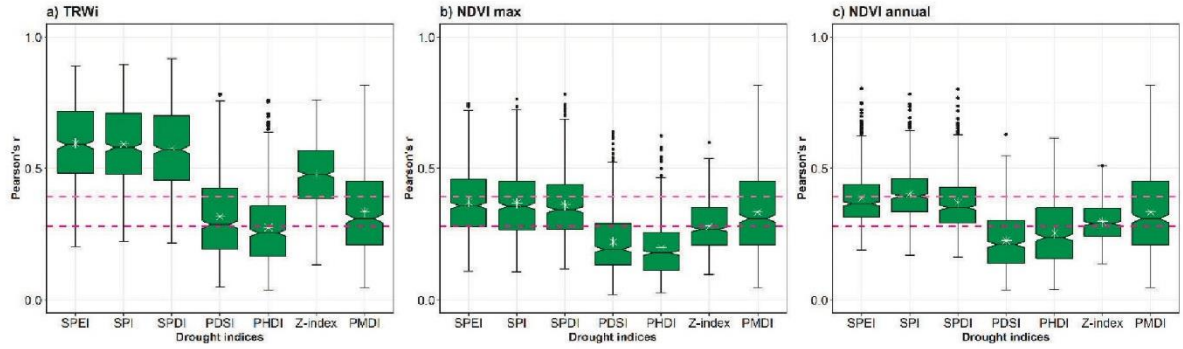

Figure 2. Box plots showing the Pearson correlation coefficients computed between the seven drought indices and ring-width indices, including (**a**) TRWi, (**b**) NDVI max, and (**c**) NDVI annual. The solid black line corresponds to the median, the white asterisks denote the mean and dashed lines show the significant level at $p < 0.05$ (light pink) and $p < 0.01$ (dark pink).

Table 2. Percentage of the sampled forest stands, with the maximum Pearson correlation coefficients found for each forest variable and with each drought index.

	TRWi	NDVI Max	NDVI Annual
SPEI	38.97	43.25	33.50
SPI	35.73	32.48	53.16
SPDI	25.30	24.27	13.33

The spatial distribution of maximum Pearson correlations between the seven drought indices and vegetation variables in each sampled forest stand is shown in Figure 3. The three multi-scalar drought indices showed similar spatial patterns, with higher values (r = 0.6–1.0) in forests located mostly in dry areas of Eastern Spain and the Balearic Islands (Figure 3). In contrast, correlations were lower in Northern Spain, where wet conditions prevail and hardwood forests dominate. The highest correlation values for the Palmer drought indices showed spatial patterns similar to those of the multi-scalar indices, albeit with lower magnitudes of correlation. Among the uni-scalar indices, Z-index and TRWi showed the highest correlations followed by PMDI and TRWi, with values ranging between 0.4 and 0.6. In contrast, PDSI and PHDI had the lowest correlations. The differences between PMDI–Z-index and PDSI–PHDI results were less evident for other variables (i.e., NDVI max and NDVI annual), with low (r = 0.2–0.4) and spatially homogeneous correlations. Similar results are found for the magnitude and the distribution of the maximum correlations for the NDVI max and NDVI annual. Regarding the SPI, higher correlations (r = 0.4–0.6) are found in Northwestern Spain for NDVI annual. The correlations between the SPEI/SPDI and NDVI annual tend to be higher in Southeast Spain than for NDVI max. Additionally, we noted that there are no clear spatial differences in the correlations found between the Palmer drought indices and NDVI max and NDVI annual.

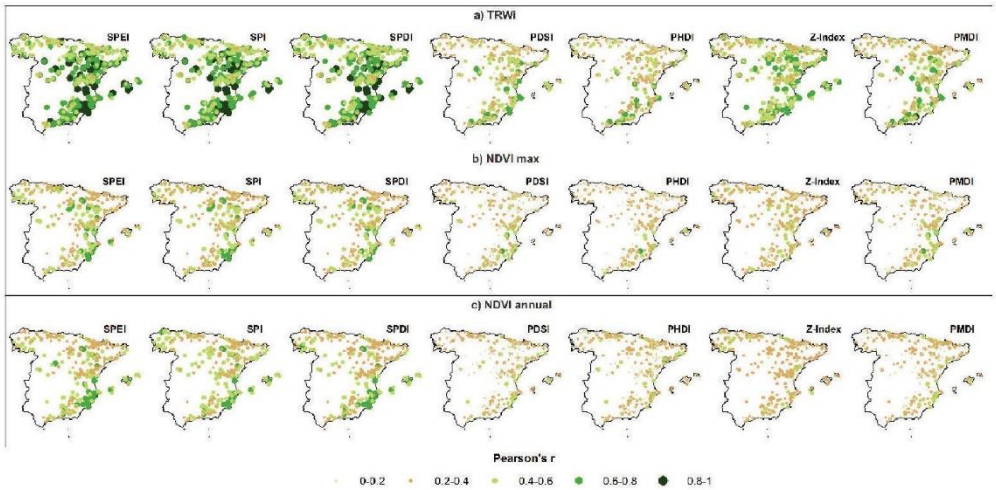

Figure 3. Spatial distribution of the maximum Pearson correlation coefficients computed between the seven drought indices and ring-width indices TRWi (**a**), NDVI max (**b**), and integrated annual NDVI (**c**).

In general, it is evident that TRWi shows a higher response to the interannual variability of drought than the NDVI max and NDVI annual. Figure 4 shows the relationship between the maximum correlations obtained relating TRWi and drought indices and those obtained for the NDVI annual and NDVI max. It can be noted that maximum correlations are much higher considering TRWi than NDVI metrics. Moreover, there are no clear relationships between the spatial patterns of the correlations. In particular, the highest correlations between drought indices and TRWi did not imply the highest correlations with NDVi metrics. The highest percentages of maximum correlations between TRWi and multi-scalar drought indices were in July (43.08%) and August (40.69%) (Table S1). SPEI correlated better with TRWi in July (17.09%), while the SPI and SPDI showed better association with TRWi in August (15.9% and 12.65%, respectively). In contrast, NDVI max showed highest percentage of maximum correlations in April (63.16%) and May (32.99%); the three drought indices also correlated most in April, with very similar percentages (SPEI: 21.28%, SPI: 21.11% and SPDI: 20.77%). For NDVI annual, the majority of forests showed their best correlations in May (90.94%), particularly for the SPEI (37.61%), the SPI (32.48%), and the SPDI (20.85%). Thus, two distinct temporal patterns could be observed depending on the analyzed parameter, whereas secondary growth response to drought severity reached a maximum in July and August, annual vegetation growth (NDVI max) and NPP (NDVI annual) showed a much earlier response to drought in springtime (April and May).

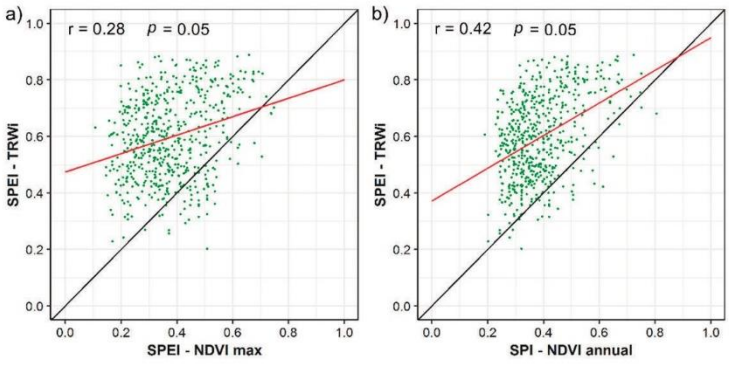

Figure 4. Scatterplots showing maximum Pearson correlation coefficients found for SPEI-TRWi and SPI-NDVIannual (**a**) and SPEI-TRWi and SPEI-NDVImax (**b**). The solid red line corresponds to the fitted linear regression model and black line, 1:1.

3.2. Relationship between Vegetation Variables and Drought by Species

Among tree species, there are no clear differences in the correlations between the multi-scalar drought indices and NDVI annual and NDVI max (Figure 5). In contrast, the correlations with TRWi show higher variability amongst tree species. Generally, the NDVI metrics suggest that species characteristics of moist and cold regions (e.g., *Abies alba* and *Pinus uncinata*) tend to show lower correlations than species of semi-arid climates (e.g., *Pinus halepensis*).

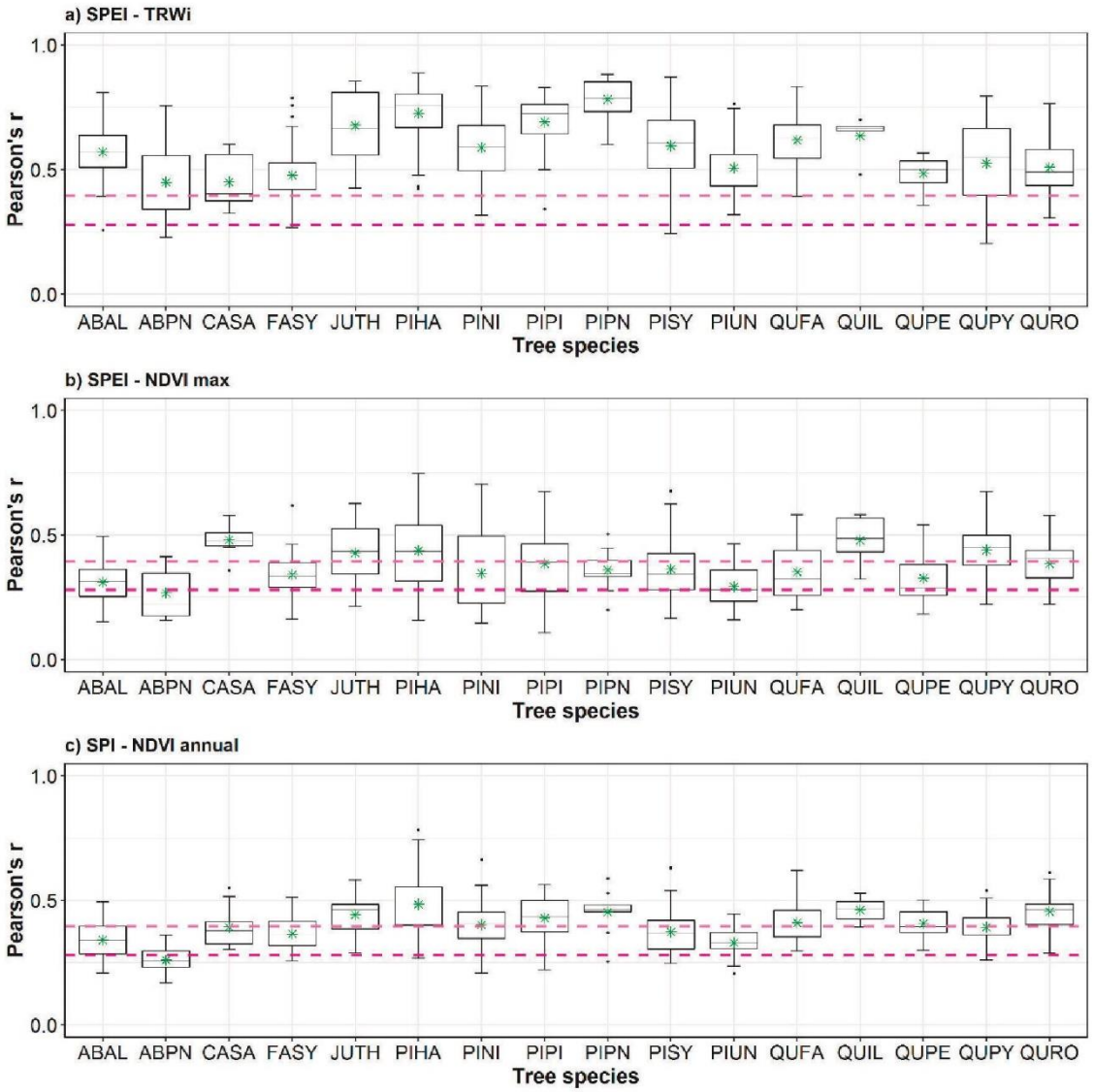

Figure 5. Box plots showing maximum Pearson correlation coefficients computed between ring-width indices (TRWi, (**a**)), NDVI max (**b**), NDVI annual (**c**), and the most correlated drought index for each tree species. The solid black line corresponds to the median, green asterisks mark the mean and dashed lines show the significance level at $p < 0.05$ (light pink) and $p < 0.01$ (dark pink). Species' codes correspond to those listed in Table 1.

Conifers from dry regions (*Pinus halepensis*, *Pinus pinaster*, and *Juniperus thurifera*) recorded the highest correlation coefficients in the case of TRWi (r = 0.70); on the contrary, conifers (*Abies pinsapo*) and hardwood species (*Castanea sativa* and *Fagus sylvatica*) from wet and temperate regions recorded lower correlations (r = 0.45). The response of the species to NDVI max—SPEI relationship was more evident for two species dominant in dry areas: *Pinus halepensis* and *Quercus ilex* (r = 0.5). In Figures S1 and S2

are displayed the maximum correlations (S1) and Pearson's partial correlations (S2) for the rest of the indices and variables considered in the analysis for each tree species respectively.

According to Figure 6, the response to medium (4–6 months) to long (>6 months) drought time-scales are frequently observed. Several tree species (e.g., *Quercus ilex*, *Quercus faginea*, *Pinus pinaster*, *Pinus pinea*, *Pinus halepensis*, and *Castanea sativa*) exhibited similar long time-scale responses in the three forest variables. It seems that the response of the interannual variability of tree metrics to drought was not only driven by the differences among species, but also by the general hydro-climatic conditions. Figure S3 illustrates the most correlated time-scale found for the rest of the multi-scalar drought indices and variables considered in the analysis for each tree species respectively.

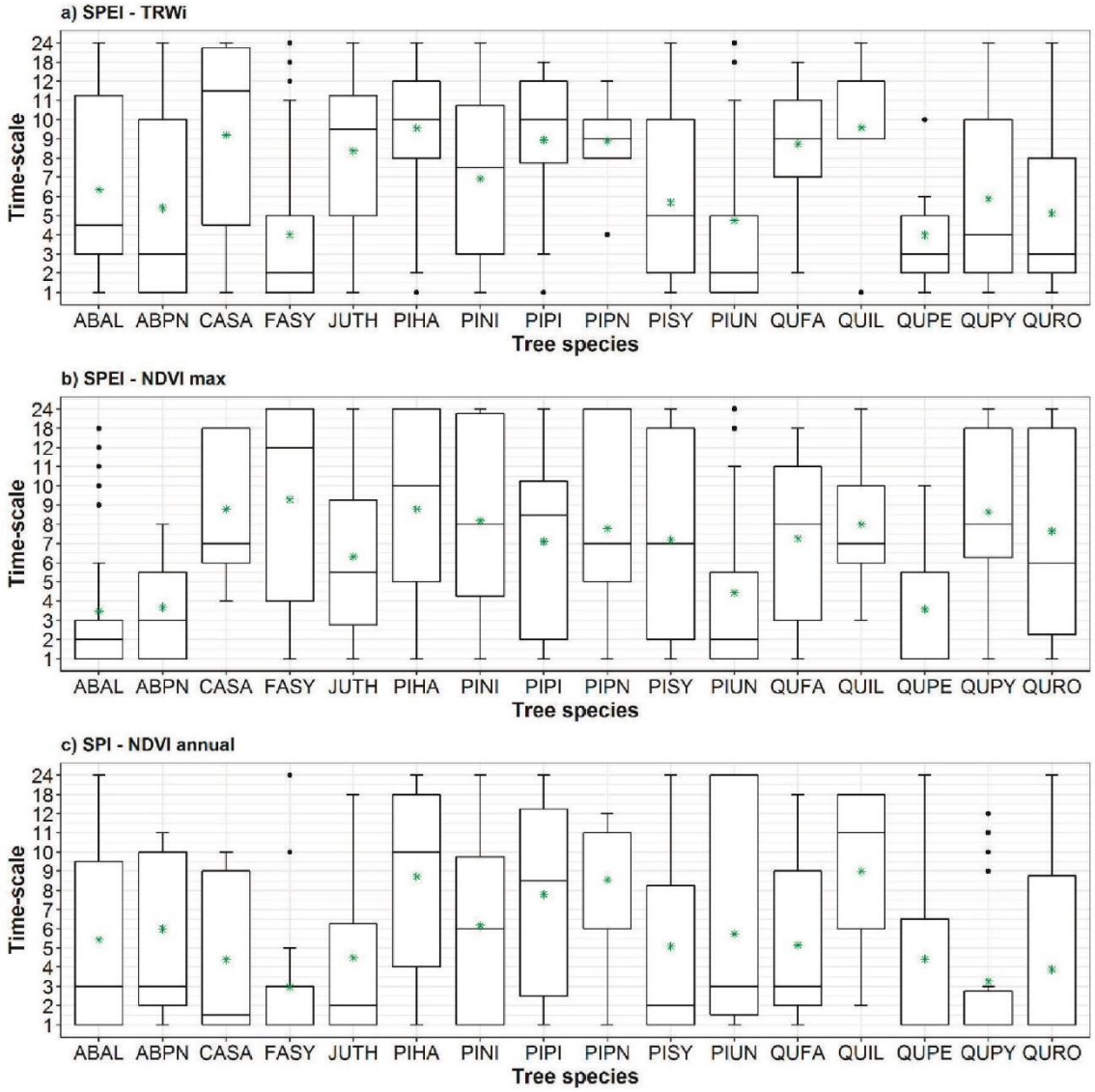

Figure 6. Box plots showing the most correlated timescale found for ring-width indices (TRWi, (**a**)), NDVI max (**b**), NDVI annual (**c**), and the most correlated drought index. The solid black line corresponds to the median, green asterisks mark the means. Species' codes correspond to those listed in Table 1.

Figure 7 illustrates the relationship between the average annual hydro-climatic balance for hardwoods and coniferous species and the correlation found between the most correlated drought index and each of the three variables. As depicted, most conifer forests were characterized by negative

annual hydro-climatic balances, while half of hardwood forests, mainly those located in humid and mountainous regions, showed a positive hydro-climatic balance. Figures S6–S8 summarize this relationship for each species and variable.

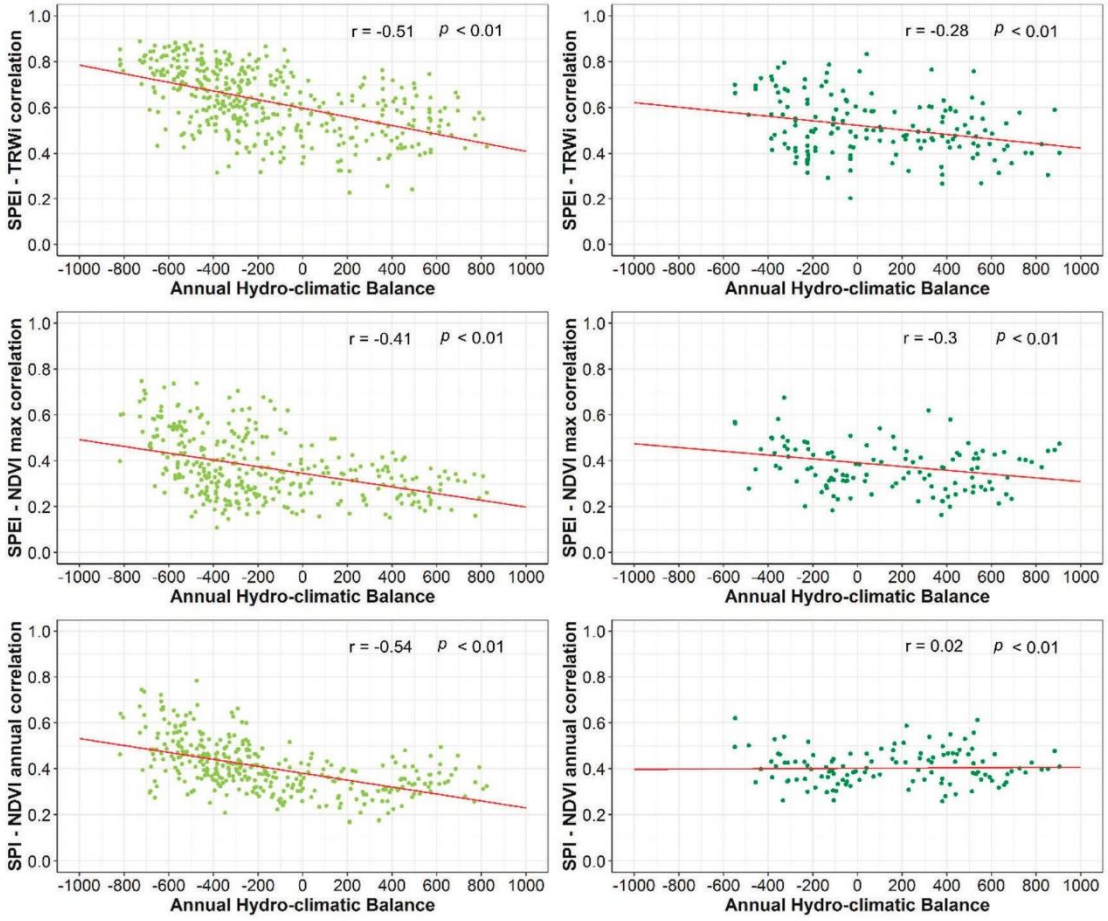

Figure 7. Scatter plots showing the relationship between maximum Pearson correlations found for SPEI-TRWi, SPEI-NDVImax, SPI-NDVIannual, and the average annual water balance of hardwood species (**right**, dark green) and conifers (**left**, light green). Solid red line corresponds to the fitted lines of regression models.

4. Discussion

This study addressed the sensitivity of several drought indices to record responses of NDVI metrics and tree growth to water shortage. In general, we found that multi-scalar drought indices (e.g., SPI, SPEI) outperform uni-scalar drought indices (PDSIs) in terms of capturing the impacts of water shortage on forest growth and NDVI metrics. Likewise, this study assesses the performance of different drought indices to adequately monitor the impact of drought on forests under different climatic and geographical conditions, and taxonomic origins. Our analysis is based on two promising datasets covering the IP and the Balearic Islands. The first comprises tree-ring width data from a dense network of 568 forests for 16 tree species [75]. The second includes a 1.1 km spatial resolution NDVI dataset that allows for detecting the growth and NDVI signal in each forest stand, reducing the interferences associated with the non-related vegetation cover [54]. Changes in vegetation due to adverse environmental conditions have been addressed in the scientific literature from different methodological perspectives. Tardieu et al. [76] proposed a probabilistic approach based on the genetic variability to study the adaptive mechanisms of vegetation to uncertain climatic conditions as drought to contribute to the tolerance of major crops to deal with them. For its part, Almeida et al. [77]

developed a systematic methodology to study the spectral differences of vegetation, discriminate between vegetation assemblages, and assess the phenology of plants applying a principal component analysis to band ratios. They found significant differences in comparison to most traditional approaches such as the NDVI. Previous studies also examined the links between vegetation activity and drought events assessing the response of NDVI to drought using drought indices for finding links between vegetation activity and drought events [78]. Some studies also quantified the impacts of drought on forest growth using dendrochronological methods and multi-scalar drought indices [10], while others assessed the relationship between NDVI and tree-ring width data [32,38,79].

However, very few studies have assessed the varying response of vegetation to various drought indices [48,80,81], considering NDVI and tree-ring width data for different tree species, taxonomic groups and biogeographical regions.

This study demonstrates that TRWi and NDVI metrics show different responses to multi-scalar drought indices (Figures S4 and S5), highlighting the different relationship between wood production and canopy greenness or activity (NPP) with drought. TRWi was more responsive to drought severity than the NDVI metrics. Similar results have been observed by Gazol et al. [75] for Spain, as they noted that tree growth is more sensitive to extreme climate events than the above-ground photosynthetic biomass. They attributed this pattern to: (1) the dependence of leaf and wood formation processes on water availability, (2) the distortion of NDVI signal as a consequence of the spatial resolution, and (3) the effect of nearby vegetation. A similar finding was also observed by Aaltonen et al. [82] who indicated that drought led to a decline in the growth of Scots pine seedlings due to stress. In contrast, the photosynthetic rates did not decrease due to drought, confirming the physiological adaptations (e.g., larger root network) to deal with water scarcity. Similarly, McDowell et al. [83] described different mechanisms to explain mortality caused by drought and water stress. These mechanisms include biotic stressors, hydraulic failure, and carbon starvation. Additonally, numerous studies confirmed that—under soil moisture deficit scenarios—forests can maintain their photosynthetic capacity [84], while dehydration associated with long periods of xylem conductivity loss inevitably can induce tree dieback [85,86]. Thus, it is acceptable that sensitivity of secondary growth to drought is greater than that of the photosynthetic activity. It is also important to consider that, albeit with the high dependence of spectral measurements on the amount of leafy biomass and primary production [41], remotely-sensed vegetation indices (e.g., NDVI) are limited, given that saturation problems can occur, especially in regions with high biomass and strong chlorophyll absorption in the red and near-infrared bands [87,88]. This feature may add further uncertainty to the obtained results, particularly at regional scales.

Our findings on the performance of the different drought indices stress the superiority of multi-scalar indices over the uni-scalar indices. This is clearly evident for the three vegetation indicators considered in this study. In this context, Bhuyan et al. [80] employed a range of drought indices to evaluate the connection between drought and tree growth of nine tree species across Europe. In their comparison of multi-scalar drought indices (i.e., SPI and SPEI) and the self-calibrated PDSI, they found a good agreement for *F. sylvatica* forests between the correlation values found for the Palmer index and the SPEI-SPI at long time scales (>12 months). On the other hand, the SPEI and SPI captured drought signals in the growth series of all tree species, especially in temperate and cold forests. Our results suggest that the Z-Index and the PMDI show more significant and higher correlations with TRWi compared with the PDSI. In this regard, Karl [89] stated that, for some agricultural and forest fires applications, the Z-Index outperforms PDSI given its competence to respond to short-term moisture variances. In our case, the highest correlations of the Z-Index were found for TRWi. In their global assessment, Vicente-Serrano et al. [48] indicated that growth-drought correlations were stronger for the SPI and SPEI indices than for the PDSI and the Z-Index. They also found that a higher percentage of forests from different biomes across the world correlated better with the SPEI than with the SPI. For its part, Bachmair et al. [50] assessed the relationship between meteorological indicators and forests in Europe, suggesting slight differences between the SPEI and SPI. Nonetheless, they noted

that—at shorter time scales—the SPEI shows a stronger response in the forests of southern Europe, a result that is in agreement with the findings of our study.

Our findings also demonstrate that the strength of correlations and timing response to drought vary spatially depending on the species and climatic conditions. Specifically, hardwood species under moist climate in Northern Spain are less correlated with drought indices than the remaining species. The deciduous species (e.g., *Fagus sylvatica*, *Quercus petraea*, *Quercus pyrenaica*, and *Quercus robur*) were, however, more sensitive to drought at short (1–3 months) and medium time scales than most of evergreen coniferous trees, particularly in the dry eastern IP under Mediterranean climate that responded to longer time scales (e.g., *Pinus halepensis*). This entails the resilience capacity of the species to endure with droughts. Gazol et al. [75] found that the same pine species inhabiting southern and eastern dry regions in the IP showed a low resistance to drought and a high post-drought recovery capacity. In semiarid areas, soil water availability is the main constraint for forest growth [72]. This dependence on moisture deficit at medium to longer temporal scales was also found by Rimkus et al. [78] for the Baltic region and Quiring and Ganesh [90] for Texas (USA).

Overall, species growing under humid climate conditions present a weaker correlation with drought indices. Nonetheless, these species are most sensitive to extreme or prolonged drought events, due to the absence of resilience mechanisms to reduce the damage caused by severe water shortage [91], although they can show high resistance to drought in terms of growth loss [75]. In these humid regions, precipitation seems to be the main limiting factor, given the stronger response of SPI to NDVI cumulative annual series (NDVI annual), compared to drought indices that account for precipitation as well as atmospheric evaporative demand (i.e., SPEI) [40]. Furthermore, vegetation from humid regions may respond in a different manner to mild droughts, as suggest by Zhang et al. [92]. This behavior can be interpreted within a context where temperature rise and low cloudiness could increase the incoming photosynthetically-active radiation simultaneously with increased evapotranspiration.

Interestingly, the response of species to drought differs among species belonging of the same genus, and also between sites in the same species, indicating the relevance of local site climatic and soil conditions. Thus, some species dominating in cold and continental mountainous areas (e.g., *Pinus sylvestris* and *Pinus uncinata*) tend to respond to shorter temporal scales because of their higher dependence on water availability [93]. In contrast, *Pinus halepensis* and *Pinus nigra*, which are dominant in dry regions, are less sensitive to moisture deficit, especially during prolonged droughts [94].

In addition, the response of forests to drought indices shows a strong seasonality. For tree-ring growth, moisture conditions during summer, especially in July and August, are determinant of wood formation. On the other hand, for the NDVI (max and annual), late spring months (April and May) are more relevant. The higher sensitivity of wood formation to summer water availability is probably related to phenological patterns of each species [95]. A similar pattern was observed over arid and semi-arid regions of Mongolia and China [92]. Even if spring droughts may lead to severe impacts, these impacts may be lagged to subsequent months, leading to photosynthesis reduction as well as accelerated respiration rates in summer. All these factors together reduced the annual net carbon uptake and, thus, wood formation [96].

5. Conclusions

To sum up, our study reflects some key findings:

1. The multi-scalar drought indices (e.g., SPEI, SPI, and SPDI) perform better than uni-scalar indices (e.g., PDSI) to identify drought impacts on forests for different species.
2. Among the multi-scalar indices, SPEI and SPI correlate better with TRWi and NDVI than the SPDI for most species.
3. Albeit with the few differences in the magnitude of correlations between the SPEI and SPI, our results suggest a major role of the atmospheric evaporative demand in drought severity across forests located in dry Mediterranean areas.

4. Droughts are more prone to impact forest secondary growth (TRWi) during summertime, and annual production and greenness (NDVI) during springtime.
5. The response of the forests to drought is mainly driven by short time scales (1–3 months) in humid-temperate hardwood forests, compared to long to medium (>4 months) time scales in warm-dry conifer forests.
6. Tree-ring growth seems a more reliable indicator of the response of forests to drought, due to its higher association with drought indices.

Supplementary Materials: The following are available online at http://www.mdpi.com/1999-4907/9/9/524/s1, Figure S1. Box plots showing the maximum Pearson correlation coefficients computed between NDVI annual (a,f), ring-width indices (TRWi (b,d), and NDVImax (c,e), and the multi-scalar drought indices (SPEI, SPI, and SPDI), Figure S2. Box plots showing the maximum partial Pearson correlation coefficients found between TRWi (b,d), NDVI max (c,e), NDVI annual (a,f), and the multi-scalar drought indices. Figure S3. Box plots showing the most correlated time-scale found for TRWi (b,d), NDVI max (c,e), NDVI annual (a,f), and the multi-scalar drought indices. Figure S4. Scatterplots showing the maximum Pearson correlation coefficients found for SPEI-TRWi and SPI-NDVI annual by species. Figure S5. Scatterplots showing the maximum Pearson correlation coefficients found for SPEI-TRWi and SPEI-NDVI max by species. Figure S6. Scatterplots showing the maximum Pearson correlation coefficients found for SPEI-TRWi and the average annual hydro-climatic balance by species. Figure S7. Same as Figure S6, but for SPEI-NDVI max. Figure S8. Same as Figure S6, but for SPEI-NDVI annual. Table S1. Percentage of sampled forests per drought index and time-scale (number of months) in which the maximum correlation value was found with ring-width indices (TRWi, a), NDVI max (b), and NDVI annual (c).

Author Contributions: Conceptualization, S.M.V.-S.; Data curation, S.M.V.-S., J.J.C., A.G., R.S.-S., E.G., M.d.L., G.S.-B., K.N., V.R., P.A.T., J.C.L., E.M.d.C., M.R.M., I.G.-G., F.S., A.C., M.G., J.M.O., L.A.L., A.H. and J.D.G.; Formal analysis, M.P.-G.; Methodology, M.P.-G. and S.M.V.-S.; Supervision, S.M.V.-S., J.J.C.; Visualization, M.P.-G.; Writing—original draft, M.P.-G.; Writing—review & editing, S.M.V.-S., J.J.C., F.D.-C., A.E.K., S.B.-P., G.S.-B., J.M.O. and A.H.

Funding: This study was financially supported by the Spanish Ministry of Economy projects: CGL2015-69186-C2-1-R (Fundiver), CGL2015-69985-R (CLIMED), CGL2013-48843-C2-1-R (CoMo-ReAdapt), AGL2014-53822-C2-1-R (SATIVA), XIRONO (BFU2010-21451), CGL2014-52135-C03-01, PCIN-2015-220, and CGL2016-81706-REDT (Ecometas Network), 1560/2015 (ECOHIPRO). The study was also funded by IMDROFLOOD (Water Works 2014, EC) and INDECIS (European Research Areas for Climate Services) projects. This work also benefited from funding from Xunta de Galicia (PGIDIT06PXIB502262PR, GRC GI-1809, ROCLIGAL-10MDS291009PR), INIA (RTA200600117), and Interreg V-A POCTEFA (CANOPEE, 2014-2020-FEDER funds) projects. Marina Peña-Gallardo was granted by the Spanish Ministry of Economy and Competitiveness. Raúl Sánchez-Salguero and Antonio Gazol were supported by postdoctoral grants (IJCI-2015-25845 and MINECO-FPDI 2013-16600; FEDER funds).

Conflicts of Interest: The authors declare no conflict of interest.

References

1. Wilhite, D.A.; Pulwarty, R.S. *Drought and Water Crises: Integrating Science, Management, and Policy*; CRC Press: Boca Raton, FL, USA, 2017; ISBN 9781138035645.
2. Bachmair, S.; Kohn, I.; Stahl, K. Exploring the link between drought indicators and impacts. *Nat. Hazards Earth Syst. Sci.* **2015**, *15*, 1381–1397. [CrossRef]
3. Wilhite, D.A.; Svoboda, M.D.; Hayes, M.J. Understanding the complex impacts of drought: A key to enhancing drought mitigation and preparedness. *Water Resour. Manag.* **2007**, *21*, 763–774. [CrossRef]
4. Allen, C.D.; Macalady, A.K.; Chenchouni, H.; Bachelet, D.; McDowell, N.; Vennetier, M.; Kitzberger, T.; Rigling, A.; Breshears, D.D.; Hogg, E.H.; et al. A global overview of drought and heat-induced tree mortality reveals emerging climate change risks for forests. *For. Ecol. Manag.* **2010**, *259*, 660–684. [CrossRef]
5. Zhang, Q.; Shao, M.; Jia, X.; Wei, X. Relationship of Climatic and Forest Factors to Drought- and Heat-Induced Tree Mortality. *PLoS ONE* **2017**, *12*, e0169770. [CrossRef] [PubMed]
6. Young, D.J.N.; Stevens, J.T.; Earles, J.M.; Moore, J.; Ellis, A.; Jirka, A.L.; Latimer, A.M. Long-term climate and competition explain forest mortality patterns under extreme drought. *Ecol. Lett.* **2017**, *20*, 78–86. [CrossRef] [PubMed]
7. Greenwood, S.; Ruiz-Benito, P.; Martínez-Vilalta, J.; Lloret, F.; Kitzberger, T.; Allen, C.D.; Fensham, R.; Laughlin, D.C.; Kattge, J.; Bönisch, G.; et al. Tree mortality across biomes is promoted by drought intensity, lower wood density and higher specific leaf area. *Ecol. Lett.* **2017**, *20*, 539–553. [CrossRef] [PubMed]

8. Vicente-Serrano, S.M.; Lopez-Moreno, J.-I.; Beguería, S.; Lorenzo-Lacruz, J.; Sanchez-Lorenzo, A.; García-Ruiz, J.M.; Azorin-Molina, C.; Morán-Tejeda, E.; Revuelto, J.; Trigo, R.; et al. Evidence of increasing drought severity caused by temperature rise in southern Europe. *Environ. Res. Lett.* **2014**, *9*, 44001–44009. [CrossRef]
9. Dai, A. Increasing drought under global warming in observations and models. *Nat. Clim. Chang.* **2013**, *3*, 52–58. [CrossRef]
10. Pasho, E.; Camarero, J.J.; de Luis, M.; Vicente-Serrano, S.M. Impacts of drought at different time scales on forest growth across a wide climatic gradient in north-eastern Spain. *Agric. For. Meteorol.* **2011**, *151*, 1800–1811. [CrossRef]
11. Gazol, A.; Camarero, J.J.; Anderegg, W.R.L.; Vicente-Serrano, S.M. Impacts of droughts on the growth resilience of Northern Hemisphere forests. *Glob. Ecol. Biogeogr.* **2017**, *26*, 166–176. [CrossRef]
12. Sánchez-Salguero, R.; Navarro-Cerrillo, R.M.; Camarero, J.J.; Fernández-Cancio, Á. Selective drought-induced decline of pine species in southeastern Spain. *Clim. Chang.* **2012**, *113*, 767–785. [CrossRef]
13. Arzac, A.; Rozas, V.; Rozenberg, P.; Olano, J.M. Water availability controls Pinus pinaster xylem growth and density: A multi-proxy approach along its environmental range. *Agric. For. Meteorol.* **2018**, *250–251*, 171–180. [CrossRef]
14. Arzac, A.; García-Cervigón, A.I.; Vicente-Serrano, S.M.; Loidi, J.; Olano, J.M. Phenological shifts in climatic response of secondary growth allow Juniperus sabina L. to cope with altitudinal and temporal climate variability. *Agric. For. Meteorol.* **2016**, *217*, 35–45. [CrossRef]
15. Forner, A.; Valladares, F.; Bonal, D.; Granier, A.; Grossiord, C.; Aranda, I. Extreme droughts affecting Mediterranean tree species' growth and water-use efficiency: The importance of timing. *Tree Physiol.* **2018**. [CrossRef] [PubMed]
16. Peguero-Pina, J.J.; Sancho-Knapik, D.; Cochard, H.; Barredo, G.; Villarroya, D.; Gil-Pelegrin, E. Hydraulic traits are associated with the distribution range of two closely related Mediterranean firs, Abies alba Mill. and Abies pinsapo Boiss. *Tree Physiol.* **2011**, *31*, 1067–1075. [CrossRef] [PubMed]
17. Martín Vide, J.; Olcina Cantos, J. *Climas y Tiempos de España*; Alianza Editorial: Madrid, Spain, 2001; ISBN 8420657778.
18. Camarero, J.J.; Gazol, A.; Sangüesa-Barreda, G.; Cantero, A.; Sánchez-Salguero, R.; Sánchez-Miranda, A.; Granda, E.; Serra-Maluquer, X.; Ibáñez, R. Forest Growth Responses to Drought at Short- and Long-Term Scales in Spain: Squeezing the Stress Memory from Tree Rings. *Front. Ecol. Evol.* **2018**, *6*, 9. [CrossRef]
19. Neumann, M.; Mues, V.; Moreno, A.; Hasenauer, H.; Seidl, R. Climate variability drives recent tree mortality in Europe. *Glob. Chang. Biol.* **2017**, *23*, 4788–4797. [CrossRef] [PubMed]
20. Camarero, J.J.; Gazol, A.; Sangüesa-Barreda, G.; Oliva, J.; Vicente-Serrano, S.M. To die or not to die: Early warnings of tree dieback in response to a severe drought. *J. Ecol.* **2015**, *103*, 44–57. [CrossRef]
21. Carnicer, J.; Coll, M.; Ninyerola, M.; Pons, X.; Sánchez, G.; Peñuelas, J. Widespread crown condition decline, food web disruption, and amplified tree mortality with increased climate change-type drought. *Proc. Natl. Acad. Sci. USA* **2011**, *108*, 1474–1478. [CrossRef] [PubMed]
22. Bonan, G.B. Forests and climate change: Forcings, feedbacks, and the climate benefits of forests. *Science* **2008**, *320*, 1444–1449. [CrossRef] [PubMed]
23. Frank, D.C.; Poulter, B.; Saurer, M.; Esper, J.; Huntingford, C.; Helle, G.; Treydte, K.; Zimmermann, N.E.; Schleser, G.H.; Ahlström, A.; et al. Water-use efficiency and transpiration across European forests during the Anthropocene. *Nat. Clim. Chang.* **2015**, *5*, 579–583. [CrossRef]
24. Zhao, M.; Running, S.W. Drought-Induced Reduction in Global Terrestrial Net Primary Production from 2000 Through 2009. *Science* **2010**, *329*, 940–943. [CrossRef] [PubMed]
25. Gursoy, M.; Balkan, A.; Ulukan, H. Ecophysiological Responses to Stresses in Plants: A General Approach. *Pak. J. Biol. Sci.* **2012**, *15*, 506–516. [CrossRef] [PubMed]
26. Li, J.; Cang, Z.; Jiao, F.; Bai, X.; Zhang, D.; Zhai, R. Influence of drought stress on photosynthetic characteristics and protective enzymes of potato at seedling stage. *J. Saudi Soc. Agric. Sci.* **2017**, *16*, 82–88. [CrossRef]
27. Pinheiro, C.; Chaves, M.M. Photosynthesis and drought: can we make metabolic connections from available data? *J. Exp. Bot.* **2011**, *62*, 869–882. [CrossRef] [PubMed]
28. Basu, S.; Ramegowda, V.; Kumar, A.; Pereira, A. Plant adaptation to drought stress. *F1000Research* **2016**, *5*. [CrossRef] [PubMed]

29. Granda, E.; Escudero, A.; Valladares, F. More than just drought: Complexity of recruitment patterns in Mediterranean forests. *Oecologia* **2014**, *176*, 997–1007. [CrossRef] [PubMed]
30. Lloret, F.; Escudero, A.; Iriondo, J.M.; Martínez-Vilalta, J.; Valladares, F. Extreme climatic events and vegetation: The role of stabilizing processes. *Glob. Chang. Biol.* **2012**, *18*, 797–805. [CrossRef]
31. Vidal-Macua, J.J.; Ninyerola, M.; Zabala, A.; Domingo-Marimon, C.; Pons, X. Factors affecting forest dynamics in the Iberian Peninsula from 1987 to 2012. The role of topography and drought. *For. Ecol. Manag.* **2017**, *406*, 290–306. [CrossRef]
32. Vicente-Serrano, S.M.; Camarero, J.J.; Olano, J.M.; Martín-Hernández, N.; Peña-Gallardo, M.; Tomás-Burguera, M.; Gazol, A.; Azorin-Molina, C.; Bhuyan, U.; El Kenawy, A. Diverse relationships between forest growth and the Normalized Difference Vegetation Index at a global scale. *Remote Sens. Environ.* **2016**, *187*, 14–29. [CrossRef]
33. Babst, F.; Poulter, B.; Trouet, V.; Tan, K.; Neuwirth, B.; Wilson, R.; Carrer, M.; Grabner, M.; Tegel, W.; Levanic, T.; et al. Site- and species-specific responses of forest growth to climate across the European continent. *Glob. Ecol. Biogeogr.* **2013**, *22*, 706–717. [CrossRef]
34. Fritts, H.C. *Tree Rings and Climate*; Academic Press: Cambridge, MA, USA, 1976; ISBN 9780122684500.
35. Gazol, A.; Sangüesa-Barreda, G.; Granda, E.; Camarero, J.J. Tracking the impact of drought on functionally different woody plants in a Mediterranean scrubland ecosystem. *Plant Ecol.* **2017**, *218*, 1009–1020. [CrossRef]
36. Vicente-Serrano, S.M.; Martín-Hernández, N.; Camarero, J.J.; Gazol, A.; Sánchez-Salguero, R.; Peña-Gallardo, M.; El Kenawy, A.; Domínguez-Castro, F.; Tomas-Burguera, M.; Gutiérrez, E.; et al. Spatial, temporal and climatic determinants of the responses of tree-ring growth to satellite-derived primary growth in multiple forest biomes. *Sci. Total Environ.* **2018**. under review.
37. Poulter, B.; Pederson, N.; Liu, H.; Zhu, Z.; D'Arrigo, R.; Ciais, P.; Davi, N.; Frank, D.; Leland, C.; Myneni, R.; Piao, S.; Wang, T. Recent trends in Inner Asian forest dynamics to temperature and precipitation indicate high sensitivity to climate change. *Agric. For. Meteorol.* **2013**, *178–179*, 31–45. [CrossRef]
38. Wang, J.; Rich, P.M.; Price, K.P.; Kettle, W.D. Relations between NDVI and tree productivity in the central Great Plains. *Int. J. Remote Sens.* **2004**, *25*, 3127–3138. [CrossRef]
39. Bochenek, Z.; Ziolkowski, D.; Bartold, M.; Orlowska, K.; Ochtyra, A. Monitoring forest biodiversity and the impact of climate on forest environment using high-resolution satellite images. *Eur. J. Remote Sens.* **2018**, *51*, 166–181. [CrossRef]
40. Vicente-Serrano, S.M.; Gouveia, C.; Camarero, J.J.; Beguería, S.; Trigo, R.; López-Moreno, J.I.; Azorín-Molina, C.; Pasho, E.; Lorenzo-Lacruz, J.; Revuelto, J.; et al. Response of vegetation to drought time-scales across global land biomes. *Proc. Natl. Acad. Sci. USA* **2013**, *110*, 52–57. [CrossRef] [PubMed]
41. Tucker, C.J. Red and photographic infrared linear combinations for monitoring vegetation. *Remote Sens. Environ.* **1979**, *8*, 127–150. [CrossRef]
42. Tucker, C.J.; Sellers, P.J. Satellite remote sensing of primary production. *Int. J. Remote Sens.* **1986**, *7*, 1395–1416. [CrossRef]
43. Keyantash, J.; Dracup, J.A.; Keyantash, J.; Dracup, J.A. The Quantification of Drought: An Evaluation of Drought Indices. *Bull. Am. Meteorol. Soc.* **2002**, *83*, 1167–1180. [CrossRef]
44. Zargar, A.; Sadiq, R.; Naser, B.; Khan, F.I. A review of drought indices. *Environ. Rev.* **2011**, *19*, 333–349. [CrossRef]
45. Shukla, S.; Steinemann, A.C.; Lettenmaier, D.P.; Shukla, S.; Steinemann, A.C.; Lettenmaier, D.P. Drought Monitoring for Washington State: Indicators and Applications. *J. Hydrometeorol.* **2011**, *12*, 66–83. [CrossRef]
46. Lorenzo-Lacruz, J.; Vicente-Serrano, S.M.; López-Moreno, J.I.; Beguería, S.; García-Ruiz, J.M.; Cuadrat, J.M. The impact of droughts and water management on various hydrological systems in the headwaters of the Tagus River (central Spain). *J. Hydrol.* **2010**, *386*, 13–26. [CrossRef]
47. Peña-Gallardo, M.; Vicente-Serrano, S.M.; Domínguez-Castro, F.; Quiring, S.M.; Svoboda, M.D.; Beguería-Portugués, S.; Hannaford, J. Effectiveness of drought indices in identifying impacts on major crops over the USA. *Clim. Res.* **2018**, in press. [CrossRef]
48. Vicente-Serrano, S.M.; Beguería, S.; Lorenzo-Lacruz, J.; Camarero, J.J.; López-Moreno, J.I.; Azorin-Molina, C.; Revuelto, J.; Morán-Tejeda, E.; Sanchez-Lorenzo, A.; Vicente-Serrano, S.M.; et al. Performance of Drought Indices for Ecological, Agricultural, and Hydrological Applications. *Earth Int.* **2012**. [CrossRef]

49. Kempes, C.P.; Myers, O.B.; Breshears, D.D.; Ebersole, J.J. Comparing response of Pinus edulis tree-ring growth to five alternate moisture indices using historic meteorological data. *J. Arid Environ.* **2008**, *72*, 350–357. [CrossRef]
50. Bachmair, S.; Tanguy, M.; Hannaford, J.; Stahl, K. How well do meteorological indicators represent agricultural and forest drought across Europe? *Environ. Res. Lett.* **2018**, *13*, 034042. [CrossRef]
51. Vicente-Serrano, S.M.; Tomas-Burguera, M.; Beguería, S.; Reig, F.; Latorre, B.; Peña-Gallardo, M.; Luna, M.Y.; Morata, A.; González-Hidalgo, J.C. A High Resolution Dataset of Drought Indices for Spain. *Data* **2017**, *2*, 22. [CrossRef]
52. Allen, R.G.; Rick, G. Food and Agriculture Organization of the United Nations. In *Crop Evapotranspiration: Guidelines for Computing Crop Water Requirements*; Allen, R.G., Pereira, L.S., Raes, D., smith, M., Eds.; Food and Agriculture Organization of the United Nations: Rome, Italy, 1998; ISBN 9251042195.
53. Pettorelli, N.; Vik, J.O.; Mysterud, A.; Gaillard, J.-M.; Tucker, C.J.; Stenseth, N.C. Using the satellite-derived NDVI to assess ecological responses to environmental change. *Trends Ecol. Evol.* **2005**, *20*, 503–510. [CrossRef] [PubMed]
54. Vicente-Serrano, M.; Martín-Hernández, N.; Camarero, J.J.; Gazol, A.; Sánchez-Salguero, R.; Peña-Gallardo, M.; El Kenawy, A.; Domínguez-Castro, F.; Tomás-Burquera, M.; Gutiérrez, E.; et al. Linking tree-ring growth and satellite-derived gross primary growth in multiple forest biomes. Temporal-scale matters. *Sci. Total Environ.* **2018**. under review.
55. Nagaraja Rao, C.R.; Zhang, N.; Sullivan, J.T. Inter-calibration of meteorological satellite sensors in the visible and near-infrared. *Adv. Space Res.* **2001**, *28*, 3–10. [CrossRef]
56. Robel, J. NOAA KLM User's Guide—Satellite and Data Description of NOAA's Polar-Orbiting Satellites from NOAA-15 and Later. 2009. Available online: https://www1.ncdc.noaa.gov/pub/data/satellite/publications/podguides/N-15%20thru%20N-19/pdf/0.0%20NOAA%20KLM%20Users%20Guide.pdf (accessed on 28 August 2018).
57. Riano, D.; Chuvieco, E.; Salas, J.; Aguado, I. Assessment of different topographic corrections in landsat-TM data for mapping vegetation types (2003). *IEEE Trans. Geosci. Remote Sens.* **2003**, *41*, 1056–1061. [CrossRef]
58. Baena-Calatrava, R. *Georreferenciación Automática de Imágenes NOAA-AVHRR*; University of Jaén: Jaen, Spain, 2002.
59. Azorin-Molina, C.; Baena-Calatrava, R.; Echave-Calvo, I.; Connell, B.H.; Vicente-Serrano, S.M.; López-Moreno, J.I. A daytime over land algorithm for computing AVHRR convective cloud climatologies for the Iberian Peninsula and the Balearic Islands. *Int. J. Climatol.* **2013**, *33*, 2113–2128. [CrossRef]
60. Holben, B.N. Characteristics of maximum-value composite images from temporal AVHRR data. *Int. J. Remote Sens.* **1986**, *7*, 1417–1434. [CrossRef]
61. Holmes, R.L. Computer-assisted quality control in tree-ring dating and measurements. *Tree-Ring Bull.* **1983**, *43*, 69–78.
62. Bunn, A.G. A dendrochronology program library in R (dplR). *Dendrochronologia* **2008**, *26*, 115–124. [CrossRef]
63. Palmer, W.C. *Meteorological Drought*; U.S. Department of Commerce: Washington, DC, USA, 1965.
64. Alley, W.M. The Palmer Drought Severity Index: Limitations and Assumptions. *J. Clim. Appl. Meteorol.* **1984**, *23*, 1100–1109. [CrossRef]
65. Doesken, N.J.; Garen, D. Drought monitoring in the Western United States using a surface water supply index. In Proceedings of the 7th Conference on Applied Climatology, Salt Lake City, UT, USA, 10–13 September 1991; Doesken, N.J., Mckee, T.B., Kleist, J., Eds.; Colorado State University: Fort Collins, CO, USA, 1991.
66. Heim, R.R. A Review of Twentieth-Century Drought Indices Used in the United States. *Bull. Am. Meteorol. Soc.* **2002**, *83*, 1149–1165. [CrossRef]
67. Mckee, T.B.; Doesken, N.J.; Kleist, J. The Relationship of Drought Frequency and Duration to Time Scales. In Proceedings of the 8th Conference on Applied Climatology, Anaheim, CA, USA, 17–22 January 1993.
68. Svoboda, M.; Hayes, M.; Wood, D. *Standardized Precipitation Index User Guide*; World Meteorological Organization: Geneva, Swizerland, 2012.
69. Vicente-Serrano, S.M.; Beguería, S.; López-Moreno, J.I.; Vicente-Serrano, S.M.; Beguería, S.; López-Moreno, J.I. A Multiscalar Drought Index Sensitive to Global Warming: The Standardized Precipitation Evapotranspiration Index. *J. Clim.* **2010**, *23*, 1696–1718. [CrossRef]
70. Ma, M.; Ren, L.; Yuan, F.; Jiang, S.; Liu, Y.; Kong, H.; Gong, L. A new standardized Palmer drought index for hydro-meteorological use. *Hydrol. Process.* **2014**, *28*, 5645–5661. [CrossRef]

71. Vicente-Serrano, S.M.; Van der Schrier, G.; Beguería, S.; Azorin-Molina, C.; Lopez-Moreno, J.-I. Contribution of precipitation and reference evapotranspiration to drought indices under different climates. *J. Hydrol.* **2015**, *526*, 42–54. [CrossRef]
72. Vicente-Serrano, S.; Cabello, D.; Tomás-Burguera, M.; Martín-Hernández, N.; Beguería, S.; Azorin-Molina, C.; Kenawy, A. Drought Variability and Land Degradation in Semiarid Regions: Assessment Using Remote Sensing Data and Drought Indices (1982–2011). *Remote Sens.* **2015**, *7*, 4391–4423. [CrossRef]
73. Bian, J.; Li, A.; Deng, W. Estimation and analysis of net primary Productivity of Ruoergai wetland in China for the recent 10 years based on remote sensing. *Procedia Environ. Sci.* **2010**, *2*, 288–301. [CrossRef]
74. Kuenzer, C.; Dech, S.W.; Wagner, W. *Remote Sensing Time Series: Revealing Land Surface Dynamics*; Springer: Berlin, Germany, 2015; ISBN 9783319159676.
75. Gazol, A.; Camarero, J.J.; Vicente-Serrano, S.M.; Sánchez-Salguero, R.; Gutiérrez, E.; de Luis, M.; Sangüesa-Barreda, G.; Novak, K.; Rozas, V.; Tíscar, P.A.; Linares, J.C.; et al. Forest resilience to drought varies across biomes. *Glob. Chang. Biol.* **2018**, *24*, 2143–2158. [CrossRef] [PubMed]
76. Tardieu, F.; Simonneau, T.; Muller, B. The Physiological Basis of Drought Tolerance in Crop Plants: A Scenario-Dependent Probabilistic Approach. *Annu. Rev. Plant Biol.* **2018**, *69*, 733–759. [CrossRef] [PubMed]
77. Almeida, T.I.R.; Filho, D.S. Principal component analysis applied to feature-oriented band ratios of hyperspectral data: A tool for vegetation studies. *Int. J. Remote Sens.* **2004**, *25*, 5005–5023. [CrossRef]
78. Rimkus, E.; Stonevicius, E.; Kilpys, J.; Maciulyte, V.; Valiukas, D. Drought identification in the eastern Baltic region using NDVI. *Earth Syst. Dyn.* **2017**, *85194*, 627–637. [CrossRef]
79. He, J.; Shao, X. Relationships between tree-ring width index and NDVI of grassland in Delingha. *Chin. Sci. Bull.* **2006**, *51*, 1106–1114. [CrossRef]
80. Bhuyan, U.; Zang, C.; Menzel, A. Different responses of multispecies tree ring growth to various drought indices across Europe. *Dendrochronologia* **2017**, *44*, 1–8. [CrossRef]
81. Vilhar, U. Comparison of drought stress indices in beech forests: A modelling study. *iForest* **2016**, *9*, 635. [CrossRef]
82. Aaltonen, H.; Lindén, A.; Heinonsalo, J.; Biasi, C.; Pumpanen, J. Effects of prolonged drought stress on Scots pine seedling carbon allocation. *Tree Physiol.* **2016**, *37*, 418–427. [CrossRef] [PubMed]
83. McDowell, N.; Allen, C.D.; Anderson-Teixeira, K.; Brando, P.; Brienen, R.; Chambers, J.; Christoffersen, B.; Davies, S.; Doughty, C.; Duque, A.; et al. Drivers and mechanisms of tree mortality in moist tropical forests. *New Phytol.* **2018**. [CrossRef] [PubMed]
84. Rowland, L.; Lobo-do-Vale, R.L.; Christoffersen, B.O.; Melém, E.A.; Kruijt, B.; Vasconcelos, S.S.; Domingues, T.; Binks, O.J.; Oliveira, A.A.R.; Metcalfe, D.; et al. After more than a decade of soil moisture deficit, tropical rainforest trees maintain photosynthetic capacity, despite increased leaf respiration. *Glob. Chang. Biol.* **2015**, *21*, 4662–4672. [CrossRef] [PubMed]
85. McDowell, N.G.; Fisher, R.A.; Xu, C.; Domec, J.C.; Hölttä, T.; Mackay, D.S.; Sperry, J.S.; Boutz, A.; Dickman, L.; Gehres, N.; et al. Evaluating theories of drought-induced vegetation mortality using a multimodel-experiment framework. *New Phytol.* **2013**, *200*, 304–321. [CrossRef] [PubMed]
86. Rowland, L.; da Costa, A.C.L.; Galbraith, D.R.; Oliveira, R.S.; Binks, O.J.; Oliveira, A.A.R.; Pullen, A.M.; Doughty, C.E.; Metcalfe, D.B.; Vasconcelos, S.S.; et al. Death from drought in tropical forests is triggered by hydraulics not carbon starvation. *Nature* **2015**, *528*, 119. [CrossRef] [PubMed]
87. Wang, Q.; Adiku, S.; Tenhunen, J.; Granier, A. On the relationship of NDVI with leaf area index in a deciduous forest site. *Remote Sens. Environ.* **2005**, *94*, 244–255. [CrossRef]
88. Mutanga, O.; Skidmore, A.K. Narrow band vegetation indices overcome the saturation problem in biomass estimation. *Int. J. Remote Sens.* **2004**, *25*, 3999–4014. [CrossRef]
89. Karl, T.R. The Sensitivity of the Palmer Drought Severity Index and Palmer's Z-Index to their Calibration Coefficients Including Potential Evapotranspiration. *J. Clim. Appl. Meteorol.* **1986**, *25*, 77–86. [CrossRef]
90. Quiring, S.M.; Ganesh, S. Evaluating the utility of the Vegetation Condition Index (VCI) for monitoring meteorological drought in Texas. *Agric. For. Meteorol.* **2010**, *150*, 330–339. [CrossRef]
91. Jump, A.S.; Ruiz-Benito, P.; Greenwood, S.; Allen, C.D.; Kitzberger, T.; Fensham, R.; Martínez-Vilalta, J.; Lloret, F. Structural overshoot of tree growth with climate variability and the global spectrum of drought-induced forest dieback. *Glob. Chang. Biol.* **2017**, *23*, 3742–3757. [CrossRef] [PubMed]

92. Zhang, L.; Xiao, J.; Zhou, Y.; Zheng, Y.; Li, J.; Xiao, H. Drought events and their effects on vegetation productivity in China. *Ecosphere* **2016**, *7*, e01591. [CrossRef]
93. Irvine, J.; Perks, M.P.; Magnani, F.; Grace, J. The response of Pinus sylvestris to drought: stomatal control of transpiration and hydraulic conductance. *Tree Physiol.* **1998**, *18*, 393–402. [CrossRef] [PubMed]
94. Klein, T.; Cohen, S.; Yakir, D. Hydraulic adjustments underlying drought resistance of Pinus halepensis. *Tree Physiol.* **2011**, *31*, 637–648. [CrossRef] [PubMed]
95. Camarero, J.J.; Olano, J.M.; Parras, A. Plastic bimodal xylogenesis in conifers from continental Mediterranean climates. *New Phytol.* **2010**, *185*, 471–480. [CrossRef] [PubMed]
96. Noormets, A.; McNulty, S.G.; DeForest, J.L.; Sun, G.; Li, Q.; Chen, J. Drought during canopy development has lasting effect on annual carbon balance in a deciduous temperate forest. *New Phytol.* **2008**, *179*, 818–828. [CrossRef] [PubMed]

Journal of Hydrology 568 (2019) 611–625

Contents lists available at ScienceDirect

Journal of Hydrology

journal homepage: www.elsevier.com/locate/jhydrol

Review papers

Complex influences of meteorological drought time-scales on hydrological droughts in natural basins of the contiguous Unites States

Marina Peña-Gallardo[a,*], Sergio M. Vicente-Serrano[a], Jamie Hannaford[b,h], Jorge Lorenzo-Lacruz[c], Mark Svoboda[d], Fernando Domínguez-Castro[a], Marco Maneta[e], Miquel Tomas-Burguera[f], Ahmed El Kenawy[a,g]

[a] Instituto Pirenaico de Ecología, Consejo Superior de Investigaciones Científicas (IPE–CSIC), Spain
[b] Centre for Ecology and Hydrology, UK
[c] University of the Balearic Islands, Spain
[d] National Drought Mitigation Centre, University of Nebraska-Lincoln, United States
[e] Geosciences Department, University of Montana, Missoula, United States
[f] Estación Experimental de Aula Dei, Consejo Superior de Investigaciones Científicas (EEAD-CSIC), Spain
[g] Department of Geography, Mansoura University, Mansoura, Egypt
[h] Irish Climate Analysis and Research UnitS (ICARUS) Maynooth University, Ireland.

ARTICLE INFO

This manuscript was handled by Marco Borga, Editor-in-Chief, with the assistance of Yuting Yang, Associate Editor

Keywords:
Hydrological drought
Climatic drought
Time-scales
Drought propagation
SPEI
Natural basins
Climate variability

ABSTRACT

We analyzed the relationships between meteorological drought and hydrological drought using very dense and diverse network of gauged natural drainage basins across the conterminous U.S. Specifically, this work utilized a dataset of 289 gauging stations, covering the period 1940–2013. Drainage basins were obtained for each gauging station using a digital terrain model. In addition to meteorological data (e.g., precipitation, air temperature and the atmospheric evaporative demand), we obtained a number of topographic, soil and remote sensing variables for each defined drainage basin. A hydrological drought index (the Standardized Streamflow Index; SSI) was computed for each basin and linked to the Standardized Precipitation Evapotranspiration Index (SPEI), which was used as a metric of climatic drought severity. The relationships between different SPEI time-scales and their corresponding SSI were assessed by means of a Pearson correlation coefficient. Also, the general patterns of response of hydrological droughts to climatic droughts were identified using a principal component analysis. Overall, results demonstrate a positive response of SSI to SPEI at shorter time-scales, with strong seasonality and clear spatial differences. We also assessed the role of some climatic and environmental factors in explaining these different responses using a predictive discriminant analysis. Results indicate that elevation and vegetation coverage are the main drivers of the diverse response of SSI to SPEI time-scales. Similar analyses were made for three sub-periods (1940–1964, 1965–1989 and 1989–2013), whose results confirm considerable differences in the response of SSI to SPEI over the past eighty years.

1. Introduction

Hydrological drought has the potential for having severe economic, social and environmental consequences (Van Loon, 2015), being a complex phenomenon that is yet not fully understood (Tallaksen and Van Lanen, 2004). While there is an evident connection between hydrological droughts and climatic variability, other human and environmental factors may impact the duration, extent, and severity of hydrological droughts along with their associated damage (Lorenzo-Lacruz et al., 2013; Bąk and Kubiak-Wójcicka, 2017; Tijdeman et al., 2018). Furthermore, correctly attributing the causes of hydrological droughts remains a challenge given the varying and complex relationship between climate moisture deficits and water deficits in different systems, which is a consequence of the complex character of drought propagation throughout the hydrological cycle, particularly in drainage basins with diverse physical characteristics and management practices (Tallaksen et al., 2004; Sheffield and Wood, 2011; Van Loon, 2015).

McKee et al. (1993) developed the concept of drought time-scale to characterize the system response period from the arrival of water inputs to the time water is available for different usable resources (e.g., soil moisture, groundwater, snowpack, streamflow, lake levels and reservoir storages). Indeed, the response time to a climatic drought condition

* Corresponding author.
E-mail address: marinapgallardo@ipe.csic.es (M. Peña-Gallardo).

https://doi.org/10.1016/j.jhydrol.2018.11.026
Received 10 July 2018; Received in revised form 28 September 2018; Accepted 7 November 2018
Available online 17 November 2018

varies significantly between these different usable water sources. For example, soil moisture usually responds at short climate drought time-scales (Scaini et al., 2015), while reservoir storages and groundwater levels respond to drought at longer time-scales (Bloomfield et al., 2015; Lorenzo-Lacruz et al., 2010 and 2017). Streamflows show a complex response that is dependent on a variety of natural and anthropogenic factors, including –among others- climatic and topographic characteristics, land cover and use, and management practices (López-Moreno et al., 2013; Lorenzo-Lacruz et al., 2013; Barker et al., 2016). Recent studies show that the response of streamflows to climatic droughts of different time scales is complex and multifaceted (Merheb et al., 2016; Huang et al., 2017; Wu et al., 2017; Tijdeman et al., 2018).

Although some studies have argued that anthropogenic factors (e.g., water management practices, water regulation and use) are the most important in determining the response of streamflow droughts to different climatic drought time-scales (López-Moreno et al., 2009; Lorenzo-Lacruz et al., 2013; Wu et al., 2017), the physical characteristics of a basin area are also very important factors and contribute critical information to explaining the different response of streamflow droughts to climatic drought time-scales. For example, Vicente-Serrano et al. (2011) analyzed the response of two relatively undisturbed upstream watersheds located in northeastern Spain, and found they presented a complex and contrasting response to climatic drought time-scales. In particular, while one of these two watersheds responded to short (< 3 months) climatic drought time-scales, the other responded to a very long (> 40 months) time-scales. This contrasting response was mainly attributed to the differing dominant lithology of each basin. Similarly, Barker et al. (2016) analyzed the relationship between hydrological and climatic droughts in different natural catchments in the UK. They reported strong differences in the response of hydrological droughts to climatic droughts linked to the different lithology and aquifer characteristics of the catchments.

For instance physiographic variables (e.g., area, topography, slope, etc.), and vegetation coverage are important controls mediating the effect of climatological drought on streamflows, as confirmed by many studies worldwide. One representative example is Van Loon and Laaha (2015), who concluded that streamflow drought duration in Austria is controlled primarily by catchment properties that define storage and release dynamics (e.g. geology and land use). What these studies show is that biophysical factors control not only streamflow drought characteristics (e.g. duration and severity), but also the sensitivity of streamflow drought to climatic drought at different time-scales. However, disentangling the role of individual factors and attributing their contribution to the response of hydrological drought to climatic drought conditions is an unresolved problem, which is complicated by anthropogenic modifications as well as by the intrinsic non-linear dynamics of hydrologic systems.

In the United States, Abatzoglou et al. (2014) used a range of drought indices to analyze streamflow anomalies in the U.S. Pacific Northwest and the stationarity of the relationship between climatic and streamflow dynamics, while Tijdeman et al. (2016) analyzed streamflow drought duration in > 800 catchments across the US. They found that drought duration characteristics vary among the different climate regimes, with precipitation playing the main role in these spatial variations. However, these studies did not analyze the role that catchment characteristics play on the propagation of climatic drought to streamflows.

In this study we fill a gap in our understanding of how climatic droughts propagate through the hydrologic system. The objectives of this study are fourfold: (i) to determine the climatic drought time-scales that better explain the hydrologic drought as reflected in streamflow anomalies over a wide range of natural basins across the conterminous United States (CONUS), (ii) to identify and analyze spatial patterns and gradients in the climatic-hydrologic drought response, (iii) to explore the role that different environmental factors play in shaping the sensitivity of streamflows to climatic drought, and (iv) to identify possible non-stationarities in the climate-streamflow relationship. This study employs long-term monthly streamflow records from the USGS Hydro-Climatic Data Network, which covers all hydroclimatic regions in the CONUS and provides a solid base from which we can gain insight into how streamflow responds to climatic drought.

2. Data and methods

2.1. Datasets

2.1.1. Streamflow time series

Streamflow time series for our analysis were obtained from the USGS Hydro-Climatic Data Network 2009 (HCDN-2009), which includes monthly streamflow records from 702 hydrological gauges located in catchments with low anthropogenic perturbations. Further details about the characteristics of this dataset (e.g. data quality, data completeness, spatial and temporal coverage, etc.) can be obtained at (http://water.usgs.gov/osw/hcdn-2009/). From the 702 gauges included in the HCDN-2009, we restricted our analysis to those gauges covering the period 1940–2013 and with less than 15% missing data. Following these criteria, we selected 289 stations, whose spatial distribution is illustrated in Fig. 1. The selected gauges cover the entire CONUS, although sampling densities are higher along the eastern and western coasts, the Inter-mountain West and the Midwest regions of the country. Gaps in the streamflow time series were completed using data from a standardized composite reference series built from the most correlated series with the target series, and using percentiles with the purpose of maintaining the temporal variance of the series.

2.1.2. Climatic information

Monthly gridded precipitation and temperature data were obtained from the PRISM (Parameter-elevation Relationships on Independent Slopes Model) product developed by Oregon State University (http://www.prism.oregonstate.edu/, \Daly et al., 2008). PRISM has been widely used for climatic, hydrological, agricultural and environmental applications in the U.S. (e.g. Lutz et al., 2010; Bandaru et al., 2017; Bodner and Robles, 2017). In this study, we employed monthly precipitation, maximum and minimum air temperatures from 1940 to 2013, provided by PRISM at 30 s (approximately 10 km) resolution. Monthly Reference Evapotranspiration (ETo) was calculated from using the Hargreaves method (Hargreaves and Samani, 1985). The Hargreaves-Samani method is recommended under data scarcity conditions (Allen, 1998), as it estimates ETo using only maximum and minimum air temperatures and the extraterrestrial solar radiation calculated using the latitude and the Julian day. Finally, precipitation and ETo grids were used to calculate the climatic balance, defined as the difference between precipitation and ETo.

2.1.3. Physiography and land cover

Elevation data for the CONUS was obtained from the USGS Digital Elevation Model (DEM) (https://lta.cr.usgs.gov/GMTED2010). Vegetation characteristics were assessed using the Normalized Difference Vegetation Index (NDVI) dataset derived from reflectance bands obtained by the Advanced Very high Resolution Radiometer (AVHRR) sensor (https://www.star.nesdis.noaa.gov/smcd/emb/vci/VH/vh_browse.php) at a spatial resolution of 1.1 km. The NDVI is a reflectance-based variable, closely related to the vegetation coverage, biomass and leaf area index (Carlson and Ripley, 1997).

Relevant high-resolution soil variables (e.g., depth of soil layer, soil drainage, water field capacity, infiltration capacity and soil permeability) were obtained from the USDA's State Soil Geographic (STATSGO, 1991) database (USDA, 1991). Data of all variables were derived for each individual basin incorporating some of the selected streamflow gauges. The boundaries of each drainage basin were defined using the DEM data within the ArcGIS platform. Average monthly and seasonal climate data were obtained for each basin independently.

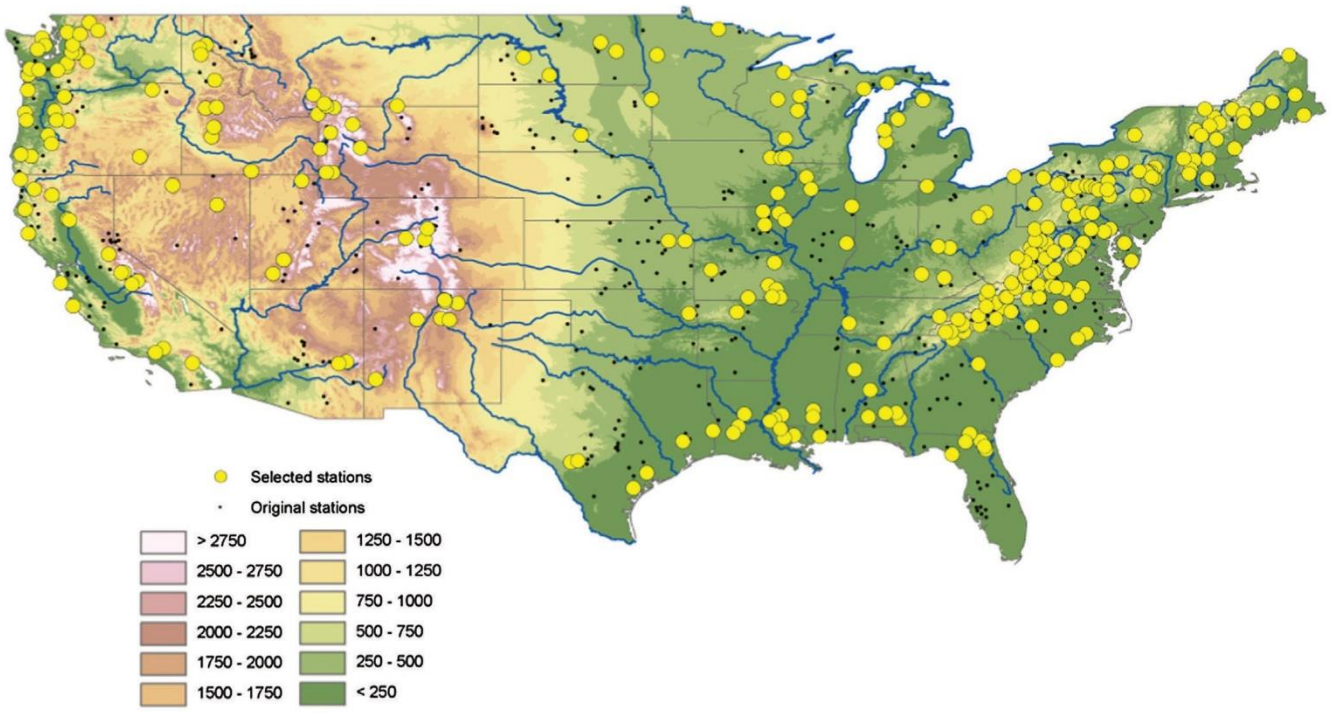

Fig. 1. Spatial distribution of the available (black dots) and the selected (yellow circles) near-natural streamflow gauges across the U.S. Elevation is given in meters. (For interpretation of the references to colour in this figure legend, the reader is referred to the web version of this article.)

Seasons were defined as: cold season (ONDJFM) and warm season (AMJJAS).

2.2. Methods

2.2.1. Hydrological drought definition

We used the Standardized Streamflow Index (SSI) to quantify streamflow drought severity (Vicente-Serrano et al., 2012). Since the SSI is a standardized quantity, it permits direct comparison between gauges, and between different time periods, irrespective of the magnitude and seasonality of streamflow series. The SSI transforms monthly streamflow time series into a time series of probabilities by first calculating a dimensionless time series of standardized streamflow anomalies using different distribution fits for each month/station. We used a wide range of candidate probability distributions, including the general extreme value, the Pearson Type III (PIII), the log-logistic, the log-normal, the generalized Pareto and the Weibull distributions. The selection based on the minimum orthogonal distance between the L-moments of the sampled dataset and the L-moment of a candidate continuous distribution.

More details on the SSI calculation can be found in Vicente-Serrano et al. (2012).

2.2.2. Climatic drought indices

There is a large amount of drought indices based on climate information (Heim, 2002), existing recent developments like the Evaporative Demand Drought Index (EDDI) (Hobbins et al., 2016) or the Standardized Evapotranspiration Deficit Index (SEDI) (Vicente-Serrano et al., 2018). Here, to characterize climatic anomalies, we used two of the most common climatic drought indices, the Standardization Precipitation Index (SPI) and the Standardization Precipitation Evapotranspiration Index (SPEI). The SPI was proposed by McKee et al. (1993) and has been widely used during the last two decades due to its solid theoretical development, robustness, and versatility in drought analyses (Redmond, 2002). As such, it has been recommended by the World Meteorological Organization as the reference index for meteorological drought (WMO, 2012). Like the SSI, the SPI is based on the conversion of precipitation anomalies to probabilities using long-term records. The anomalies are accumulated over periods of a specified length, which produce a time series of anomalies representing a characteristic time-scale. The main advantage of the SPI is that it allows for analyzing drought impacts at different temporal scales, which can then be compared to anomalies from datasets representing other drought types (i.e. meteorological, hydrological and economic). The SPI has been widely used for this purpose in several studies (e.g. Vicente-Serrano and López-Moreno 2005; Fiorillo and Guadagno 2010; Lorenzo-Lacruz et al., 2010; Vicente-Serrano et al., 2011).

The main criticism of the SPI is that its calculation is based solely on precipitation data and does not account for other meteorological factors (e.g., Atmospheric Evaporative Demand (AED)), which may have a strong influence on drought severity, as evidenced in many hydrological (Vicente-Serrano et al., 2014) and ecological (Allen et al., 2015; Adams et al., 2017) applications. To overcome this we have also included in our analysis another popular drought index, the Standardized Precipitation Evapotranspiration Index (SPEI). Unlike the SPI, the SPEI accounts for both Precipitation (P) and Reference Evapotranspiration (ETo) as a representative metric to quantify the AED. The SPEI is based on a monthly climatic water balance (P-ETo), and is equally sensitive to variations in these two input variables (Vicente-Serrano et al., 2015). The P-ETo series of anomalies are adjusted using a three-parameter log–logistic distribution. The anomalies are accumulated at different time-scales, following the same approach used in the SPI, and converted to standard deviations with respect to average value (z-scores). Details on the calculation procedure of the SPEI can be found in Vicente-Serrano et al. (2010) and Beguería et al. (2014). The ETo was computed from air temperature data using the Hargreaves-Samani method (Hargreaves and Samani, 1985) as explained in the Section 2.1.2.

2.2.3. Statistical analysis

To quantify drought severity for each watershed and the sensitivity of streamflows to anomalies in each month of the year, we calculated the SPI and SPEI at time-scales varying from 1 to 48 months for each month of the year using the corresponding spatially-averaged series of P and ETo. For each watershed we obtained 576 series (12 months × 48

time-scales) for each drought index. Then, to account for the links between climatic droughts and hydrological droughts, we used the Pearson correlation coefficient, computed between the time series of SPEI/SPI for each time-scale and month of the year. All calculations were made for the entire study period (1940–2013), as well as for some selected sub-periods: 1940–1964, 1965–1989 and 1990–2013 to evaluate the stationarity of this correlation.

To summarize the high spatial variability exhibited by the relationship between SSI and SPEI/SPI, we performed a Principal Component Analysis (PCA) in S mode (Richman, 1986). In this mode, the data (i.e. correlations between SPEI/SPI and SSI in each basin) were structured in a matrix with 12 (months) rows by 48 (time-scales) columns per site, which represent the SPI-SSI or SPEI-SSI correlation structure in a month-time scale space. PCA analysis decomposes this month-time scale correlation space into a series of modes that represent independent amounts of the complexity (variance) in the SPI-SSI and/or SPEI-SSI correlation space.

The PCA procedure allows for the classification of 289 basins on the basis of the similarities of the principal components of the correlations between the SPEI/SPI and the SSI, and permits us to identify general patterns in these correlations. The number of the retained components was defined based on the percentage of the variance of the original month-time series correlation space explained by each component according to a scree-plot. We also mapped the PCA loadings for each watershed, which in our case is equivalent to the square root of the variance of the original space retained by each component, and identifies how much each principal component relates to the SPI/SPEI-SSI relationship of each watershed. We also classified the watersheds according to the maximum loading rule, in which each watershed was assigned to the PC that showed the highest loading. This analysis was conducted for the three selected sub-periods of the data record to analyze stationarity.

We also integrated information on soil, climate, topography and NDVI variables (see Section 2.1) in each watershed and analyzed how well they explain the spatial distribution of the loading patterns. This was done by spatially averaging and plotting the values of these biophysical variables and the PC Groups obtained from the maximum loading rule by means of boxplots for the entire period 1940–2013 as well as the three selected sub-periods.

Finally, to quantify the relative contribution of each of the biophysical variables explaining the spatial differences in SSI response to the SPEI at different time-scales, we applied a predictive discriminant analysis (PDA). The PDA explains the value of a dependent categorical variable based on its relationship to one or more predictors (Huberty, 1994). Given the presence of different independent variables, the PDA identifies the possible linear combinations of those predictors that best separate the groups of cases of the predicted; these combinations are termed discriminant functions (Hair et al., 1998). The PDA allowed identifying which predictors contributed more to the inter-category differences of the PC modes that summarize SSI–SPEI dependency.

3. Results

3.1. General patterns of response (1940–2013)

Fig. 2 shows the spatial distribution of the maximum correlation of the series of timescales between SPEI and SSI for each month and for the series of all months. Results are presented for the entire study period (1940–2013) and irrespective of any climatic and hydrological seasonal variations. Overall, Fig. 2 reveals high positive correlations in the majority of the analyzed basins, with only a few exceptions. One example of such an exception is the lower correlation found between SPEI and SSI along the Rocky Mountains and in the northeastern U.S. for the period February to April. These spatial patterns are very similar to the correlations between the SPEI and SSI (Supplementary Fig. 1). In both cases, there is clear dominance of positive and high correlations between SSI and SPEI during the different months of the year (Supplementary Fig. 2).

In general, maximum correlations between SPEI and SSI tend to be achieved at shorter time-scales, with averages ranging between 2- and 3-month SPEI (Supplementary Fig. 3), however, there are some regions that present maximum correlations at longer time scales. Notably, the snow regulated basins, particularly those in the western portions of the country, respond to longer SPEI time-scales than other basins. This pattern is evident for all months of the year and for the series of all months. This suggests differences in how these watersheds mediate the response of streamflow to climatic droughts (see Fig. 3).

The Principal Component Analysis confirms the existence of substantial variability in the patterns of hydrological droughts response. Specifically, it takes seven principal components to account for more than 80% of the total explained variance (Supplementary Fig. 4), each representing different spatial patterns of the month and time scale correlation between the SPEI and SSI.

Figs. 4 and 5 show the principal components and the principal component loadings, respectively. These figures identify the main hydrological drought response patterns to the range of climatic drought time-scales used in this analysis. The figures show substantial variations in the response of the analyzed basins, with coherent geographical patterns. In general, the PCs indicate a dominance of response to short SPEI time-scales, which is clearly represented in the first two components (Fig. 4). These two PCs explain 55% of the total variance. The loadings of PC1 show that this PC is representative of watersheds in the Southeast and the Midwest U.S. (Fig. 5). The mode of variation for PC1 (Fig. 4) show high correlations at SPEI time-scales lower than 10 months (Fig. 4), while the loadings of PC 2 show that this mode represents northeastern basins (Fig. 5), which show the strongest response at very short SPEI time-scales (less than 3 months) between April and January (Fig. 4). PC3 is representative of SPEI-SSI correlations in the US Pacific northwest region, with the highest correlation found at short SPEI time-scales between September and February. Significant correlations are also found between May and August, but only for longer SPEI time-scales. The loadings of PC 4 represents the SPEI-SSI relationship in the watersheds located in the Rocky Mountains, and the PC scores indicate that these basins are most responsive to climatic anomalies occurring between June and February at time-scales ranging from 8 to 18 months. The remaining PCs (PCs 5–7) represent local patterns, and small clusters of basins.

The PC analysis showing the spatial patterns of the SPI-SSI correlations are presented in Supplementary Figs. 5 through 7. These results show that the spatial modes of variation are similar to those analyzed using the SPEI and increases our confidence that the response of hydrological drought to climatic drought time-scales shows consistent spatial patterns, irrespective of the selected drought index.

3.2. Factors explaining the general response of SSI to SPEI time-scales

Fig. 6 shows the average values of the different topographic and environmental variables as a function of the PCs that summarize correlation patterns between SPEI and SSI. Annual average NDVI presents strong differences between PCs, with PCs 1, 2, 6 and 7 correlating with higher average NDVI than PCs 3, 4 and 5. Notably, PCs 3 and 6 show high intra-basin variability. Also, soil characteristics vary significantly between PCs, especially those related to water field capacity and depth of soil layer (the highest being recorded for PC 1). In contrast, soil drainage, infiltration and soil permeability do not present substantial differences between the different PCs. Similarly, basin area does not differ significantly between PCs. Average annual streamflow shows higher values for PCs 7 and 3, with high intra-basin variability among the basins belonging to these components. Average basin elevation presents noticeable differences between the PCs, with PCs 3 and 4 associated with higher elevations than the remaining components. Similarly, the PCs seem to vary with average annual minimum, maximum

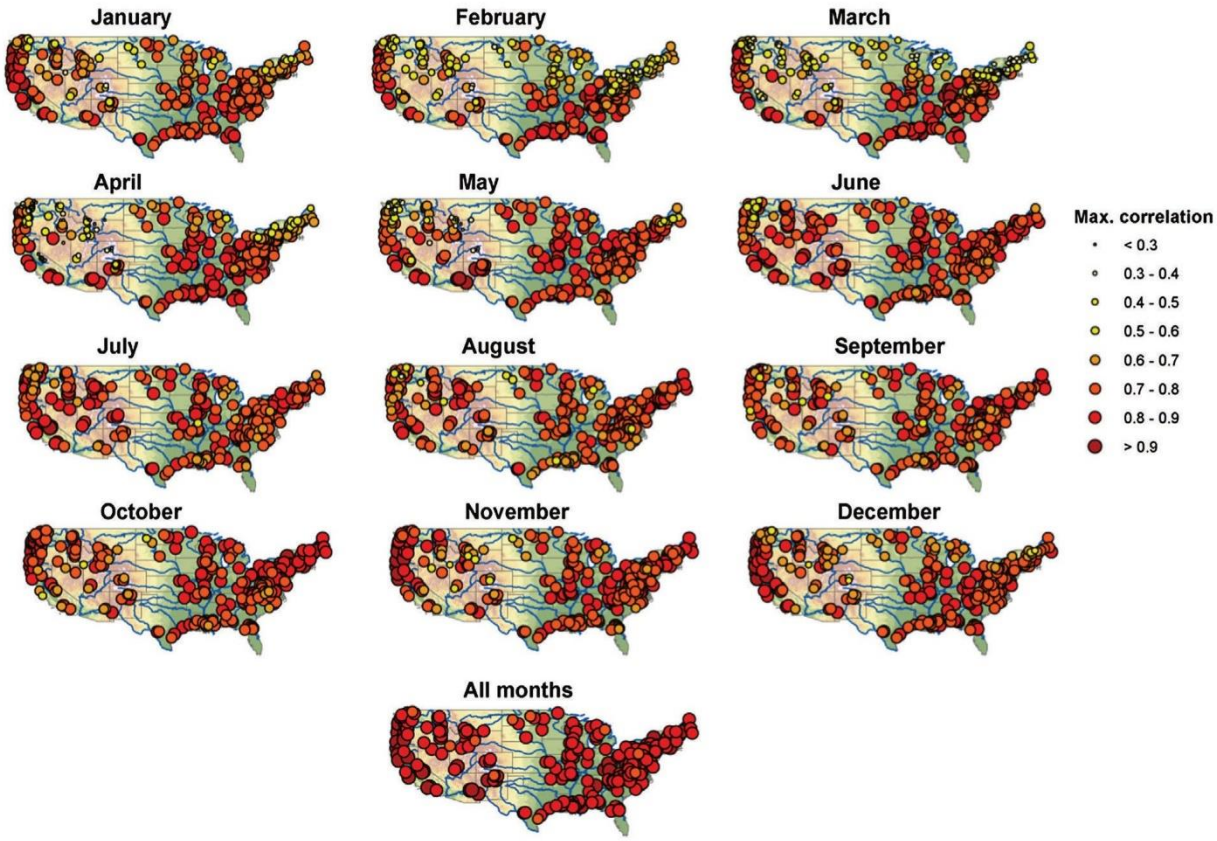

Fig. 2. Spatial distribution of maximum correlation between SPEI time-scales and SSI for each month independently and also for the series of all months.

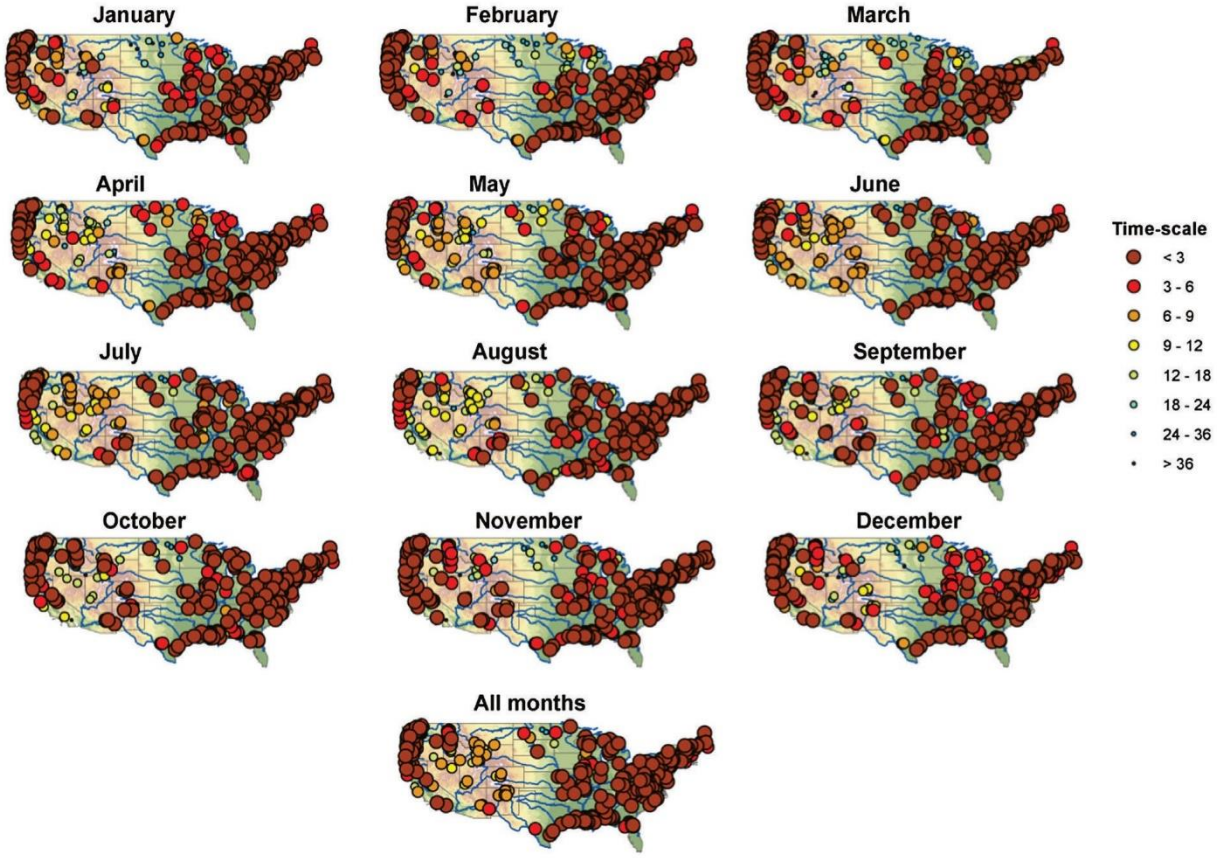

Fig. 3. Spatial distribution of the SPEI time-scale at which maximum correlation between SPEI time-scales and SSI is found for each month independently and also for the series of all months).

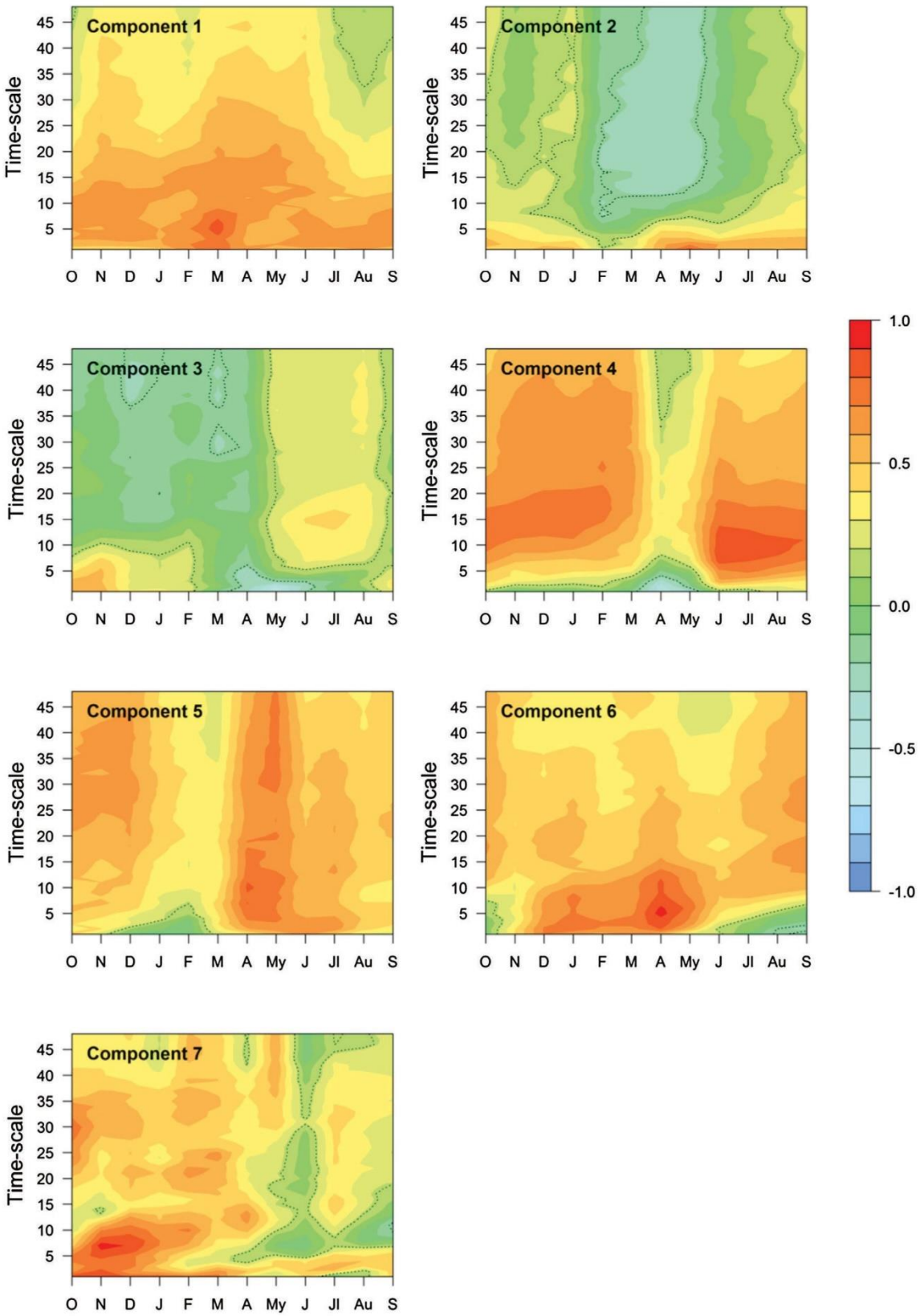

Fig. 4. Principal component scores obtained from correlations between SPEI time-scales and SSI (1940–2013). Dotted lines indicate significant correlations at $p < 0.05$.

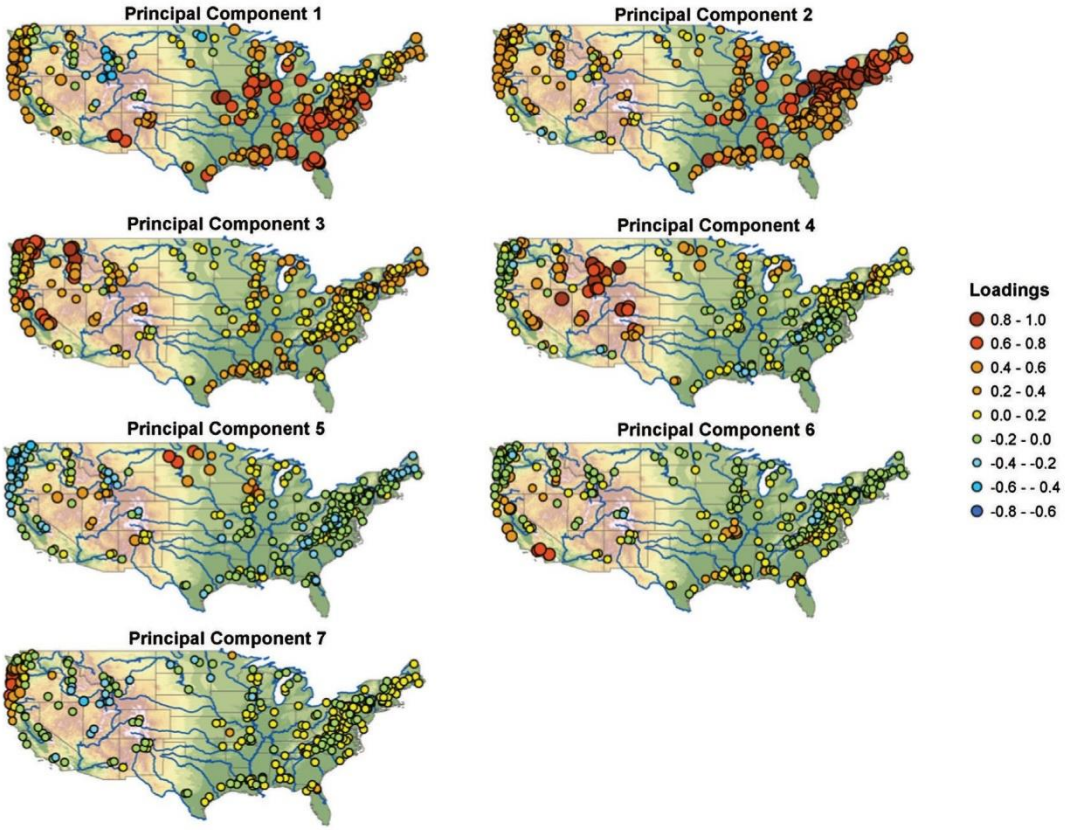

Fig. 5. Spatial distribution of the loadings of the extracted PCs, which summarize the patterns of correlation between SPEI time-scales and SSI.

temperature and ETo. PCs 3, 4 and 5 are characterized by lower temperatures than other components.

Table 1 shows the structure matrix following the results of the Predictive Discriminant Analysis (PDA), with three functions representing 43.8%, 27.7% and 10.5% of the total variance, respectively. Table 2 shows the centroids of the different components for the three predictive discriminant functions (PDFs). PC 1 and PC 2 show negative values for PDF 1, which has the greatest power to discriminate between the different independent variables. On the other hand, PCs 3, 4, 6 and 7 show positive values in PDF 1, indicating that the pattern of relationship between climatic and hydrologic droughts characteristics of PCs 1 and 2 is favored in areas with high vegetation coverage (NDVI). This feature is particularly evident during the warm season, when vegetation is more active. Positive values in PDF 1 are also associated with low elevations, high temperatures during the warm season, high precipitation during the warm season and low precipitation during the cold season. The patterns of relationship summarized by PCs 3 and 4, and to less extent PCs 6 and 7, are dominant in basins with opposite characteristics (i.e. low NDVI, high elevation, low temperatures and low precipitation during the warm season and high precipitation during the cold season). PDF 2 mostly discriminates between PCs 4 and 5 on the one hand and PC 7 on the other hand, demonstrating that PCs 4 and 5 are dominant in basins with low vegetation coverage, high elevation and low precipitation, while PC7 characterize watershed with high vegetation coverage in low elevation areas with relatively high precipitation. PDF 3 had low discrimination capacity and low values for the different variables. PDA also indicated that soil characteristics, average streamflow magnitude, and total surface area of the basins contributed less to discriminating between the different patterns of response of SSI to SPEI time-scales.

3.3. Temporal differences in the response of SSI to SPEI time-scales

The analysis applied for the different sub-periods (1940–1964, 1964–1989 and 1990–2013) reveal some differences in the relationship between climatic drought and hydrologic response in the U.S. The monthly correlation patterns in the month-time scale space between SSI and the SPEI shows that the general patterns for the entire period (1940–2013) are not exactly stationary in time. Between 1940 and 1964, the percentage of the variance absorbed by the first few PCs is similar to the variance absorbed by the PCs in the analysis of the entire period (Fig. 7). However, the subperiod 1965–1989 distributes the total variance between the PCs more evenly, and during the 1990–2013 period PC1 clearly represents a higher percentage of the total variance (Supplementary Fig. 8). The first two components of the 1940–1964 period maintain the response of SSI to SPEI at short time-scales, but with clear monthly differences (Fig. 7). The remaining components present a SSI response to longer SPEI time-scales, also with strong monthly differences. Nonetheless, these patterns have less spatial coherence, compared to those defined for the entire period (Supplementary Fig. 9).

The dominant patterns during 1965–1989 show some differences from those of the earlier period (Fig. 8). PC 1 shows higher correlations from medium to long time-scales between February and June and between July and November, while PC 2 exhibits significant correlations considering short SPEI time-scales between October and February. Similarly, PC 3 shows significant correlations at very short time-scales (1–2 months) between May and July. PC 4 presents a similar pattern than the same component calculated for the entire period, with significant correlations at longer time-scales, with the exception of April. These components show more coherent spatial patterns and are representative of larger regions than those of the earlier period (Supplementary Fig. 10). Compared to 1940–1964 and 1965–1989, the PCs in the analysis of the 1990–2013 period shows more granularity

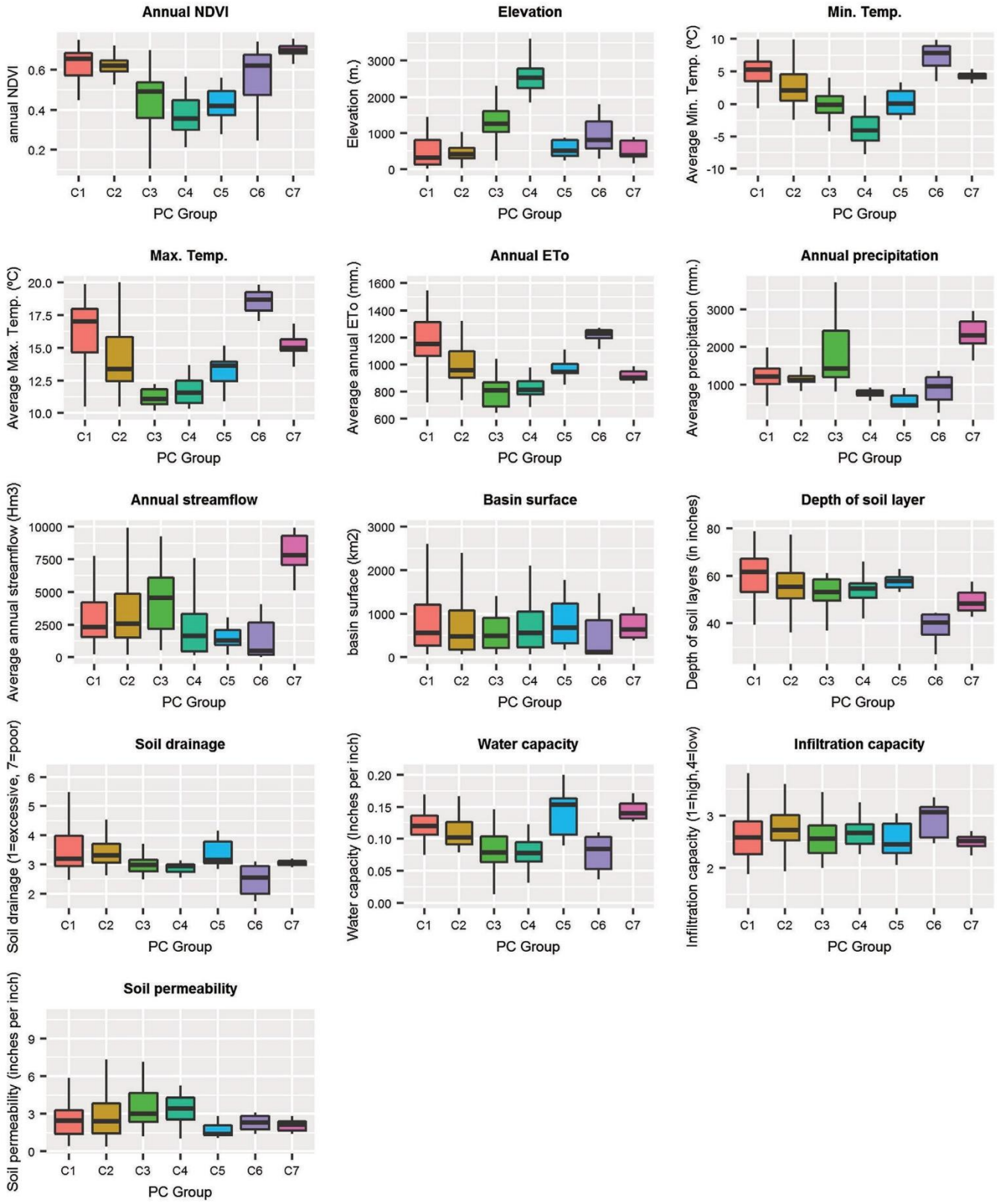

Fig. 6. Box-plots showing the average values of the different topographic and environmental variables corresponding to the seven retained PCs, which summarize the patterns of correlation between SSI and SPEI time-scales.

and variation (Fig. 9). The correlation patterns show distinct monthly responses to the range of SPEI time-scales, with smoother and more coherent spatial patterns. We noted PCs that represents the basins located in the northeastern (PC 1), southeastern U.S. (PC 2) and the Rocky Mountains (PC 5) (Supplementary Fig. 11). Overall, the spatial patterns of PC loadings and the analyzed response of the basins was very similar in the analysis done with any of the two drought indices -i.e. SPI and SPEI (Supplementary Figs. 12–18). This may indicate that

Table 1
Structure matrix of the PDA. Significant values ($p < 0.05$) are marked in bold.

	Function 1 (43.8%)	Function 2 (27.7%)	Function 3 (10.5%)
NDVI (annual)	**−0.459**	**0.551**	0.035
NDVI (cold season)	−0.365	**0.504**	0.11
NDVI (warm season)	**−0.515**	**0.545**	−0.053
Elevation	**0.488**	**−0.458**	−0.019
Min. Temperature (cold season)	−0.121	0.376	0.245
Min. Temperature (warm season)	**−0.45**	0.189	0.215
Min. Temperature (annual)	−0.286	0.299	0.24
Max. Temperature (annual)	−0.296	0.185	0.3
Max. Temperature (cold season)	−0.193	0.219	0.284
Max. Temperature (warm season)	−0.414	0.127	0.301
Eto (annual)	−0.303	0.073	0.298
Eto (cold season)	−0.223	0.078	0.237
Eto (warm season)	−0.358	0.064	0.337
Precipitation (annual)	0.199	**0.584**	−0.071
Precipitation (cold season)	0.431	**0.621**	−0.012
Precipitation (warm season)	−0.444	0.226	−0.179
Streamflow (annual)	0.137	0.222	−0.001
Streamflow (cold season)	0.09	0.402	0.16
Streamflow (warm season)	0.155	0.016	−0.147
Surface area	0.009	−0.155	0.277
Soil depth layer	−0.172	−0.041	0.065
Soil drainage	−0.213	0.038	−0.008
Soil water capacity	−0.259	0.179	0.478
Soil infiltration capacity	−0.022	−0.011	−0.126
Soil Permeability	0.094	−0.068	−0.169

Table 2
Centroids for the different components for the three discriminant functions.

Principal components	PDF 1	PDF 2	PDF 3
1	−0.857	0.014	0.503
2	−1,243	0.275	−0.703
3	3,557	0.523	−0.914
4	2,080	−2,571	0.15
5	−0.475	−2,319	2,282
6	2,002	0.313	0.626
7	2,252	4,888	1,917

the role of variations in the climatological water balance (P-ETo) is of secondary importance on the development of hydrological drought in the selected basins compared to variations in precipitation, which is the common input variable in the calculation of both SPI and SPEI. Our comparison also indicates that there is a general agreement on the magnitude of the maximum correlations found for the different sub-periods (Supplementary Figs. 19 and 20). However, and despite the overall agreement, there are some differences in terms of the SPEI time-scales at which the maximum correlations are recorded (Supplementary Figs. 21 and 22).

For the sub-periods 1940–1964 and 1965–1989, there are clear differences in the maximum correlation patterns found between SPEI and SSI (Supplementary Fig. 23). One representative example is the Rocky Mountains, where correlations increased from January to March, while decreased in April. In December, the magnitude of correlations clearly increased over the basins located in eastern and western portions of the country. On the other hand, while there are differences in the magnitude of maximum correlation patterns between the 1965–1989 and 1990–2013 periods (see for example, northern basins in January and February and western basins in April), their spatial patterns are more random than those found in the previous period (Supplementary Fig. 24). Notably, SPEI time-scales of maximum correlation are very different between sub-periods for some basins. In some cases, maximum correlations were found at longer SPEI time scales in one period, but at short time scales in the other (Supplementary Figs. 25 and 26). These findings indicate that the mechanisms that connect climatic and hydrological droughts may interact and reinforce or cancel each other out between the two periods. These mechanisms and their interactions are difficult to identify and evaluate because the small number of instances when maximum correlations shifted differently between SPEI time-scales in two periods makes comparisons with environmental and climatic variables (Supplementary Tables 1–4). Positive differences in maximum correlations between 1940 and 1964 and 1965–1989 (i.e. correlation of second period minus correlation of first period) are preferentially recorded for basins characterized by low NDVI values, high elevations, low ETo and temperature, but with clearly higher temperatures during the second period (Supplementary Table 1). This analysis seems to indicate that correlation differences between these two periods follow a spatial pattern related to the spatial distribution of these climatic and physiographical variables. However, the spatial patterns of differences in the SPEI time-scales at which maximum correlation is obtained between the two sub-periods do not show clear relationship with any of the analyzed climatologic or physiographical variables, with the exception of some monthly significant correlations (Supplementary Table 2).

The same analysis for sub-periods 1965–1989 and 1990–2013 show that the spatial patterns of maximum correlation difference may be controlled by the spatial patterns of precipitation, and mostly by the observed change in precipitation between the two sub-periods. Specifically, higher correlations during the second period tend to be primarily recorded for basins with low average precipitation, which makes an increase in annual and seasonal precipitation during the second sub-period more likely (Supplementary Table 3). Finally, differences in the time-scales at which the maximum correlation was recorded between these two periods did not reveal spatial patterns that correlate with the environmental and climatic variables analyzed here.

4. Discussion

In this study, we analyzed the response of a hydrological drought index (the Standardized Streamflow Index, SSI) to different time-scales of the Standardized Precipitation Evapotranspiration Index (SPEI) in different low anthropogenic perturbation watersheds across the U.S. Our findings indicate high correlations between the SPEI and SSI during a range of months of the year, confirming that the magnitude of hydrological droughts in the conterminous U.S. is strongly controlled by climatic droughts. The correlations found in this study are stronger than those obtained for basins impacted by water regulation and human management (e.g. Lorenzo-Lacruz et al., 2013; Vicente-Serrano et al., 2017b; Wu et al., 2017). With the exception of the February and April period, when correlations are generally lower, average correlations were around 0.8 or higher. For the all-months series, the average correlation was 0.9. These results highlight that hydrological droughts in natural basins are more influenced by climatic drought than in highly regulated basins, in which the temporal variability of hydrological droughts is controlled by other non-climatic factors, such as water storage capacity (Lorenzo-Lacruz et al., 2013) and dam operation rules (López-Moreno et al., 2009). Furthermore, water extraction and reallocation for different uses can also disrupt the relationship between climate variability and hydrological droughts (Tijdeman et al., 2018). However, the U.S. basins included in the analysis are considered to be relatively unperturbed by direct human action. Nevertheless, in some cases they can be affected by change in vegetation cover (e.g. recovery from past forest fires, ecological transitions), which can also affect the relationship between climatic and hydrologic droughts (García-Ruiz et al., 2008). Nevertheless, these potential vegetation cover changes are expected to have a local impact and it is most likely that hydrological drought responses in the studied basins are mainly controlled by climate variability.

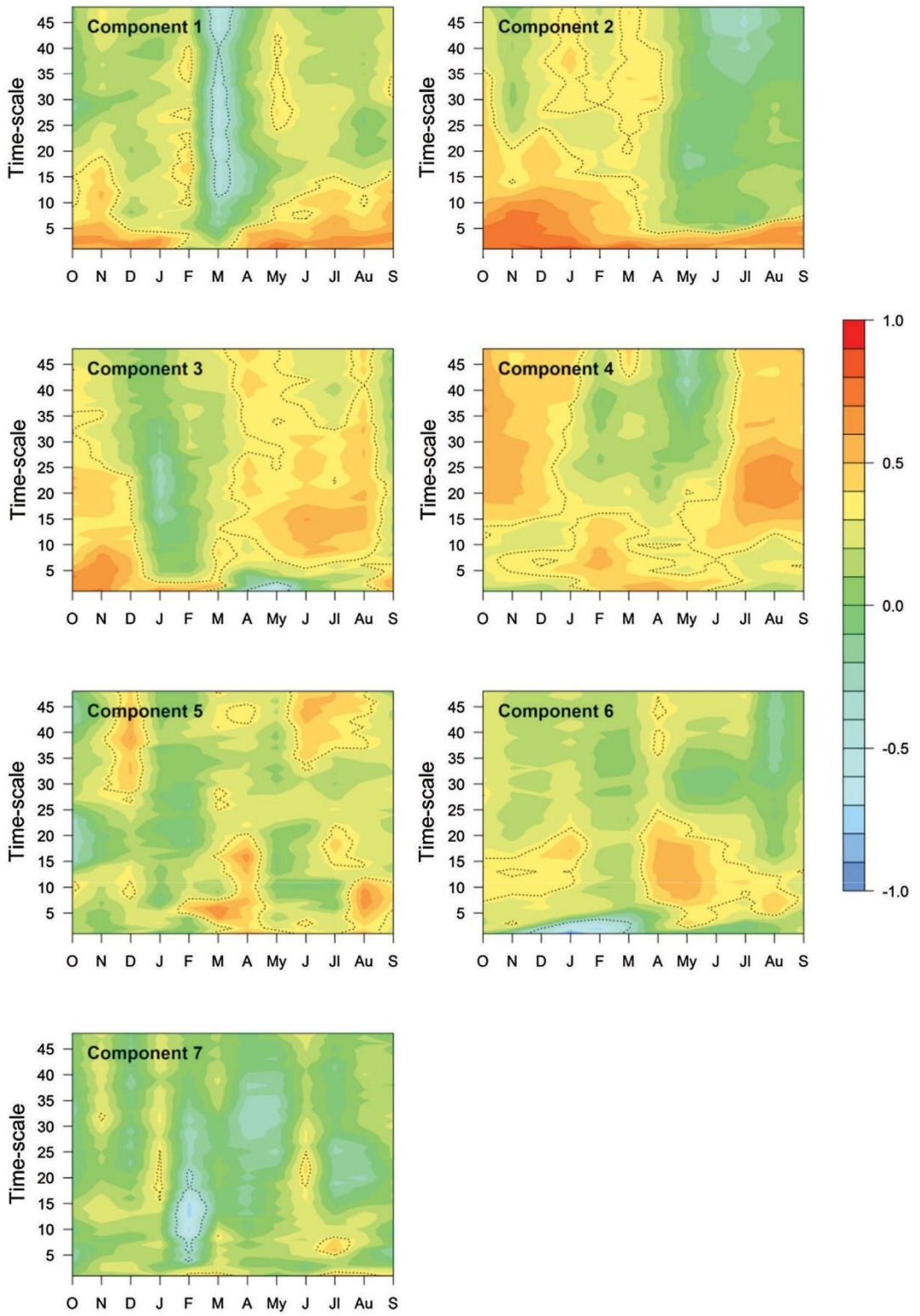

Fig. 7. Principal component scores obtained from monthly correlations between SPEI time-scales and SSI for the whole period 1940–1964. Dotted lines outline significant correlations at $p < 0.05$.

Another important finding is that SSI variability is mostly controlled by climatic droughts having characteristically short time-scales in the majority of the studied basins. Generally, our results show that the SPEI at time-scales between two and four months are often the most correlated with SSI. This clearly suggests that SSI in these natural basins responds to high frequency climate variability. Once again, these results are in contrast with results found in other studies for regulated basins (e.g. Lorenzo-Lacruz et al., 2010 and 2013), where variability of hydrological drought is mostly linked to climatic droughts of longer characteristic time scales and to streamflow drought conditions prolonged and exacerbated by water abstractions, transfers or impoundments (Tijdeman et al., 2018). These differences can reflect increased watershed storage, (e.g., reservoir storage), which modulates high frequency variations of upstream rain and streamflows, which induces

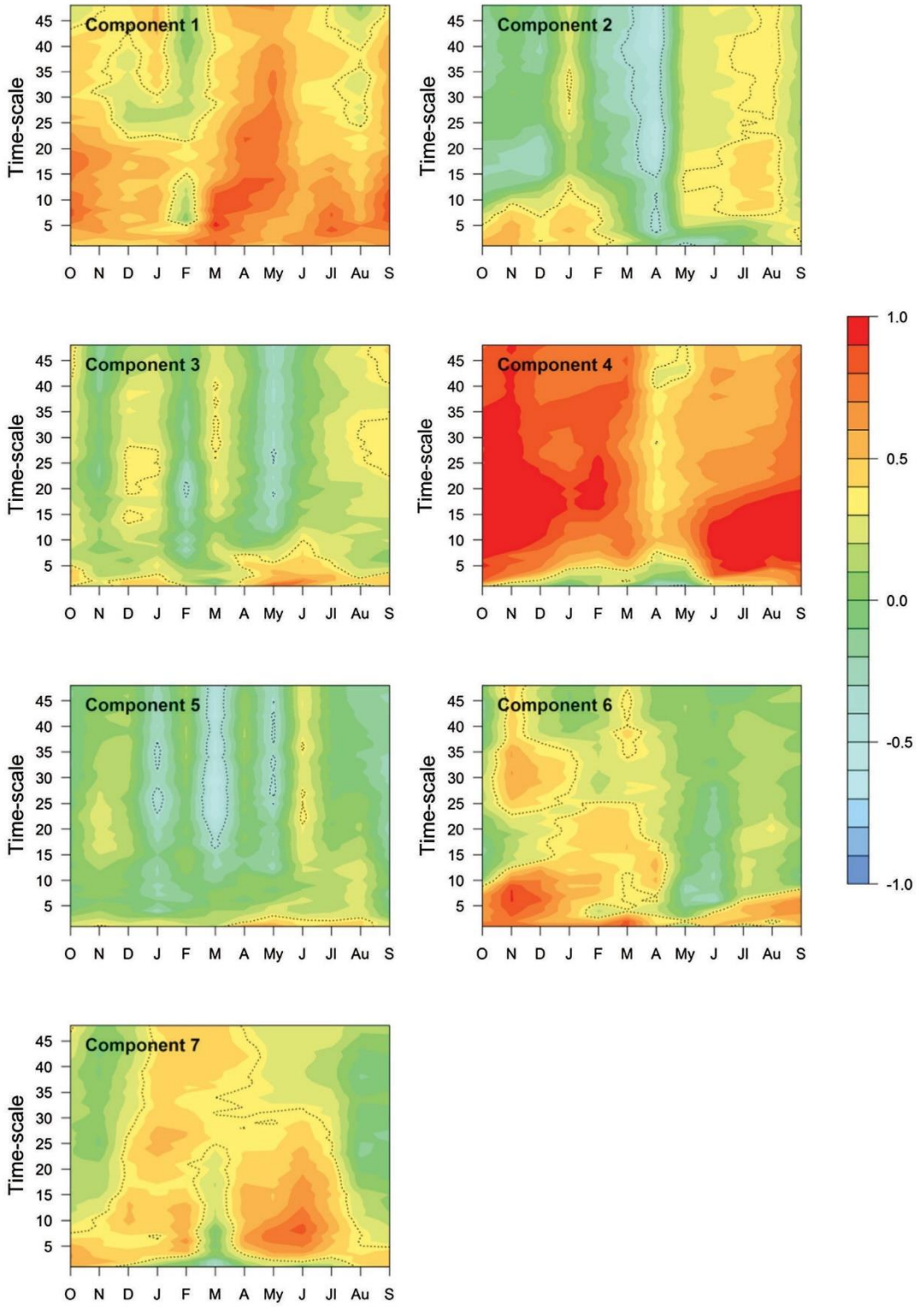

Fig. 8. Principal component scores obtained from the monthly correlations between SPEI time-scales and SSI for the sub-period 1965–1989. Dotted lines outline significant correlations at $p < 0.05$.

temporal autocorrelation and decreases the frequency of high peaks downstream (Lorenzo-Lacruz et al., 2010). In general, because of their higher capacity, hydrological drought conditions in reservoirs occur less frequently than in streamflows (Vicente-Serrano and López-Moreno, 2005; Wu et al., 2017) and even less frequently in groundwater systems (Bloomfield et al., 2015; Lorenzo-Lacruz et al., 2017). Our results align with the expectation that hydrologic drought response of the natural basins used in this study is mostly controlled by climatic drought.

We did, however, find some exceptions to the pattern of generally short timescales between meteorological and hydrological droughts. Some watersheds, mostly located in the Rocky Mountains, showed low correlations between the SPEI and SSI during the summer and winter months at shorter time scales, and appeared more responsive to long-

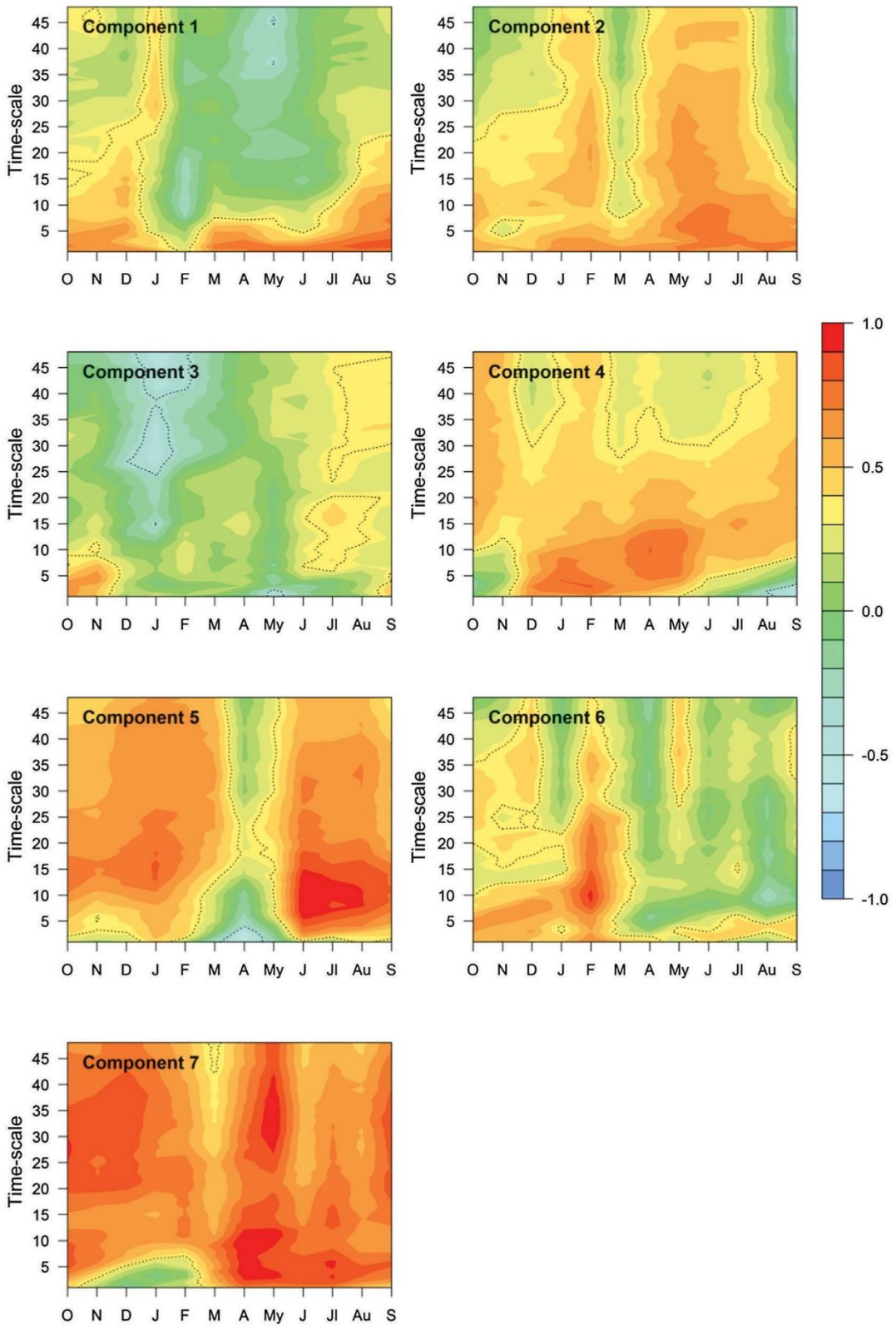

Fig. 9. Principal component scores obtained from correlations between SPEI time-scales and SSI for the sub-period 1990–2013. Dotted lines outline significant correlations at $p < 0.05$.

term SPEI time-scales during the spring and fall. This may be explained by the specific characteristics of the rivers located in this region, with streamflow driven by snow accumulation and melting, which are strongly controlled by temperature variability, instead of being directly controlled by rainfall variability. This was also found by Haslinger et al. (2014) and Rimkus et al. (2013), who found strong connections between hydrological and climatic droughts in Austria and Lithuania, except for those basins and seasons in which snow processes are important.

To ensure the results are robust and consistent, we conducted the

analysis with two widely used drought indices, the SPI (based only on precipitation data) and the SPEI (calculated using both precipitation and atmospheric evaporative demand). Vicente-Serrano et al. (2012) analyzed the relationship between streamflow variability and different drought indices in different basins worldwide. They reported that a higher correlation between climatic and streamflow anomalies was obtained when the SPEI was used instead of the SPI. However, increased AED also affects streamflow drought severity (e.g. Cai and Cowan, 2008; Cho et al., 2011; Teuling et al., 2013; Vicente-Serrano et al., 2017a). In this study there were negligible differences not only in the magnitude of correlations found between the SPI or the SPEI and the SSI, but also in the time scales and the seasonal patterns of these correlations. This finding suggests that in natural hydrological basins precipitation would have the greater influence on streamflow drought severity. Vicente-Serrano et al. (2014) showed that SSI in the Iberian Peninsula rivers responded better to SPEI than to SPI, especially in the summer months when the role of the AED is higher. However, they also reported that correlations between SPEI and SSI and SPI and SSI were similar for watersheds located in the headwaters where human intervention is more restricted and the effects of AED is lower. As the rivers reach their medium and low courses, temporal variability of streamflows is affected by AED, especially in the most regulated basins, where there is high surface coverage by irrigated lands (Vicente-Serrano et al., 2017b). In these circumstances, the SPEI explained streamflow anomalies better than the SPI.

Although we do not expect that the hydrological drought response patterns of the undisturbed watersheds analyzed in this study have the same degree of complexity than the regulated basins, we found remarkable spatial variations. This heterogeneity in the response of natural basins was also found by Barker et al. (2016) in > 120 catchments across the UK.

With a few exceptions, U.S. watersheds dominantly respond to climatic drought of short characteristic time-scales, but there were clear seasonal differences that confound homogeneous patterns in the correlations between SSI and climatic drought time-scales. Differences in the month-time scale correlation space of the different watersheds are mainly associated to differences in temperature, vegetation cover/use, as well as by topography (elevation).

Physiographic characteristics and vegetation coverage vary significantly from one river basin to another. In this analysis, we are considering a wide heterogeneous scenario to assess the response of hydrological drought to the climatic drought in a very diverse number of basins.

At this respect, we found out, as well as other studies related to this topic (Haslinger et al., 2014; Van Loon and Laaha, 2015), that not only precipitation but also elevation is one of the natural drivers that control the seasonality of the streamflows as AED directly depends on it (e.g. snow melt contribution to streamflows) and hence, the response of SSI to SPEI time-scales.

Regarding to the land use, vegetation has a major role as soil structure is directly related to the hydrological cycle processes (e.g. the runoff occurred during a heavy precipitation event or the water drainage from the aquifers to the watersheds). In addition, natural vegetation consumes water for respiration processes, being this the main disturbing factor that explains climate vs. streamflow relationships. This topic has been widely studied in the scientific literature (e.g. Bosch and Hewlett, 1982; de Jong et al., 2009; García-Ruiz et al., 2011; Llorens and Domingo, 2007)

The magnitude of streamflow, precipitation, soil characteristics and basin area also bring secondary contributions to these differences. The muted contribution of average annual and seasonal precipitation to explaining patterns of response of hydrologic drought contrasts with the findings of Tijdeman et al. (2016), who concluded that the characteristics and duration of hydrological drought in natural basins of the U.S. is mostly controlled by the precipitation characteristics of each basin.

This study also suggests that the mechanisms that propagate climatic droughts to streamflows may not be time stationary. This suggestion is based on the differences we have found in the magnitude of correlations and the time scales of maximum correlation between different periods in the record. The factors that drive this behavior are unclear, but they could be related to the non-linearity in the dynamics of watersheds during wet and dry periods, which affect how meteorological droughts propagate to become hydrological droughts (Haslinger et al., 2014). During the mega drought recorded in southeastern Australia in the 2000s, Yang et al. (2017) showed that the rainfall-runoff relationship was non-stationary, and that there were feedback mechanisms such that the duration and intensity of meteorological droughts were lengthened and amplified by the hydrological drought it generated. Non-stationarity driven by drought severity and catchment/land feedbacks adds some uncertainty to how climatological droughts propagate throughout the hydrological cycle. None of the explanatory variables used obtain insight into the spatial patterns of hydrologic drought were able to explain adequately why the magnitude of the differences and time-scales of maximum correlation was not stable between the analyzed sub-periods. The lack of explanatory power of the variables used in this study aligns with the results presented by Yang et al. (2017), who found that the times of recovery of hydrological drought conditions in relation to climatic droughts are not related to the catchment landscape. They confirmed that the impact of other hydro-climatic factors and catchment properties is minimal.

Recent studies have suggested the use of climatic information to predict hydrological droughts (e.g. Zhu et al., 2016; Yuan, et al., 2017), which is especially appealing to characterize hydrological drought in regions where streamflow data is not available. However, results from this study, and specifically the evidence of non-stationary mechanisms in the response of hydrological droughts to climate variability, suggest that making robust predictions using only climatological information will be a challenging task, even in natural basins, where most of streamflow behavior is expected to respond to climate variability. The complexity of physiographic, climatic, edaphic and mostly vegetation characteristics drive a complex and non-stationary behavior, which is very difficult to determine.

In summary, we have showed that the response of hydrological droughts to climatic droughts is complex, especially in terms of the climatic drought time-scales that are more likely to control hydrological drought severity. This is expected in strongly modified and regulated basins, where water management and/or dam operation rules may strongly alter this behavior. In this study it has been demonstrated that the response of hydrological droughts to climatic drought conditions can be complex and non-stationary, even in natural basins. Within the conterminous U.S. very different patterns of hydrological drought responses to climatic drought time-scales have been detected. These natural basins are characterized by different climatological, physiographical and vegetation conditions. Further research is necessary to understand the role of vegetation cover change on the non-stationary behavior of hydrological drought response detected in this study, and to define to what extent the connection between climatic and hydrologic drought is disrupted by different levels of human management and practices in the United States.

5. Conclusions

In conclusion, we summarize the main findings of this study:

- The magnitude of hydrological droughts in U.S. depends directly on climatic droughts, and this relationship is stronger in natural basins than in regulated basins.
- In natural basins, the SSI responds predominantly to high frequency climate variability.
- The time scales and seasonal response of SSI to SPEI and SPI suggest that hydrological basins precipitation would have the greatest

influence on streamflow drought severity.

- However, in the contiguous U.S., a noteworthy spatial variation and heterogeneity in the response of natural basins exist. In mountainous river basins, hydrological droughts were found exceptionally to be controlled not only by precipitation variability but also by temperature at long-term.
- At this respect, not only climatic conditions influence hydrological droughts. Soil characteristics, vegetation or physical characteristics of the basins also determine the different patterns of response found in natural regimes.

Acknowledgements

This work was supported by the research project I-Link1001 (Validation of climate drought indices for multi-sectorial applications in North America and Europe under a global warming scenario) financed by CSIC, PCIN-2015-220 and CGL2014-52135-C03-01 financed by the Spanish Commission of Science and Technology and FEDER, IMDROFLOOD financed by the Water Works 2014 co-funded call of the European Commission and INDECIS, which is part of ERA4CS, an ERA-NET initiated by JPI Climate, and funded by FORMAS (SE), DLR (DE), BMWFW (AT), IFD (DK), MINECO (ES), ANR (FR) with co-funding by the European Union (Grant 690462). Marina Peña-Gallardo was granted by the Spanish Ministry of Economy and Competitiveness. Miquel Tomas-Burguera was supported by a doctoral grant by the Spanish Ministry of Education, Culture and Sport. Jamie Hannaford was supported by the Belmont Forum project 'DrIVER', NERC Grant Number (grant NE/L010038/1). Marco Maneta acknowledges support from the USDA NIFA grant 2016-67026-25067.

Appendix A. Supplementary material

Supplementary data to this article can be found online at https://doi.org/10.1016/j.jhydrol.2018.11.026.

References

Adams, H.D., Zeppel, M.J.B., Anderegg, W.R.L., Hartmann, H., Landhäusser, S.M., Tissue, D.T., Huxman, T.E., Hudson, P.J., Franz, T.E., Allen, C.D., Anderegg, L.D.L., Barron-Gafford, G.A., Beerling, D.J., Breshears, D.D., Brodribb, T.J., Bugmann, H., Cobb, R.C., Collins, A.D., Dickman, L.T., Duan, H., Ewers, B.E., Galiano, L., Galvez, D.A., Garcia-Forner, N., Gaylord, M.L., Germino, M.J., Gessler, A., Hacke, U.G., Hakamada, R., Hector, A., Jenkins, M.W., Kane, J.M., Kolb, T.E., Law, D.J., Lewis, J.D., Limousin, J.-M., Love, D.M., Macalady, A.K., Martínez-Vilalta, J., Mencuccini, M., Mitchell, P.J., Muss, J.D., O'Brien, M.J., O'Grady, A.P., Pangle, R.E., Pinkard, E.A., Piper, F.I., Plaut, J.A., Pockman, W.T., Quirk, J., Reinhardt, K., Ripullone, F., Ryan, M.G., Sala, A., Sevanto, S., Sperry, J.S., Vargas, R., Vennetier, M., Way, D.A., Xu, C., Yepez, E.A., McDowell, N.G., 2017. A multi-species synthesis of physiological mechanisms in drought-induced tree mortality. Nat. Ecol. Evol. 1, 1285–1291. https://doi.org/10.1038/s41559-017-0248-x.

Allen, C.D., Breshears, D.D., McDowell, N.G., 2015. On underestimation of global vulnerability to tree mortality and forest die-off from hotter drought in the Anthropocene. Ecosphere 6, art129. https://doi.org/10.1890/ES15-00203.1.

Allen, R.G., 1998. Crop evapotranspiration: guidelines for computing crop water requirements. Food Agric. Org. United Nations.

Bąk, B., Kubiak-Wójcicka, K., 2017. Impact of meteorological drought on hydrological drought in Toruń (central Poland) in the period of 1971–2015. J. Water L. Dev. 32. https://doi.org/10.1515/jwld-2017-0001.

Bandaru, V., Pei, Y., Hart, Q., Jenkins, B.M., 2017. Impact of biases in gridded weather datasets on biomass estimates of short rotation woody cropping systems. Agric. For. Meteorol. 233, 71–79. https://doi.org/10.1016/J.AGRFORMET.2016.11.008.

Barker, L.J., Hannaford, J., Chiverton, A., Svensson, C., 2016. From meteorological to hydrological drought using standardised indicators. Hydrol. Earth Syst. Sci. 20, 2483–2505. https://doi.org/10.5194/hess-20-2483-2016.

Beguería, S., Vicente-Serrano, S.M., Reig, F., Latorre, B., 2014. Standardized precipitation evapotranspiration index (SPEI) revisited: parameter fitting, evapotranspiration models, tools, datasets and drought monitoring. Int. J. Climatol. 34, 3001–3023. https://doi.org/10.1002/joc.3887.

Bloomfield, J.P., Marchant, B.P., Bricker, S.H., Morgan, R.B., 2015. Regional analysis of groundwater droughts using hydrograph classification. Hydrol. Earth Syst. Sci. 19, 4327–4344. https://doi.org/10.5194/hess-19-4327-2015.

Bodner, G.S., Robles, M.D., 2017. Enduring a decade of drought: patterns and drivers of vegetation change in a semi-arid grassland. J. Arid Environ. 136, 1–14. https://doi.org/10.1016/J.JARIDENV.2016.09.002.

Bosch, J.M., Hewlett, J.D., 1982. A review of catchment experiments to determine the effect of vegetation changes on water yield and evapotranspiration. J. Hydrol. 55, 3–23. https://doi.org/10.1016/0022-1694(82)90117-2.

Cai, W., Cowan, T., 2008. Dynamics of late autumn rainfall reduction over southeastern Australia. Geophys. Res. Lett. 35, L09708. https://doi.org/10.1029/2008GL033727.

Carlson, T.N., Ripley, D.A., 1997. On the relation between NDVI, fractional vegetation cover, and leaf area index. Remote Sens. Environ. 62, 241–252. https://doi.org/10.1016/S0034-4257(97)00104-1.

Cho, J., Komatsu, H., Pokhrel, Y., Yeh, P.J.-F., Oki, T., Kanae, S., 2011. The effects of annual precipitation and mean air temperature on annual runoff in global forest regions. Clim. Change 108, 401–410. https://doi.org/10.1007/s10584-011-0197-3.

Daly, C., Halbleib, M., Smith, J.I., Gibson, W.P., Doggett, M.K., Taylor, G.H., Curtis, J., Pasteris, P.P., 2008. Physiographically sensitive mapping of climatological temperature and precipitation across the conterminous United States. Int. J. Climatol. 28, 2031–2064. https://doi.org/10.1002/joc.1688.

de Jong, C., Lawler, D., Essery, R., 2009. Mountain Hydroclimatology and Snow Seasonality- Perspectives on climate impacts, snow seasonality and hydrological change in mountain environments. Hydrol. Process. 23, 955–961. https://doi.org/10.1002/hyp.7193.

Fiorillo, F., Guadagno, F.M., 2010. Karst spring discharges analysis in relation to drought periods, using the SPI. Water Resour. Manage. 24, 1867–1884. https://doi.org/10.1007/s11269-009-9528-9.

García-Ruiz, J.M., Regüés, D., Alvera, B., Lana-Renault, N., Serrano-Muela, P., Nadal-Romero, E., Navas, A., Latron, J., Martí-Bono, C., Arnáez, J., 2008. Flood generation and sediment transport in experimental catchments affected by land use changes in the central Pyrenees. J. Hydrol. 356, 245–260. https://doi.org/10.1016/j.jhydrol.2008.04.013.

García-Ruiz, J.M., López-Moreno, J.I., Vicente-Serrano, S.M., Lasanta–Martínez, T., Beguería, S., 2011. Mediterranean water resources in a global change scenario. Earth-Science Rev. 105, 121–139. https://doi.org/10.1016/J.EARSCIREV.2011.01.006.

Hair, J.F., Black, W.C., Babin, B.J., Anderson, R.E., 1998. Multivariate Data Analysis. Prentice Hall, New York.

Hargreaves, G.H., Samani, Z.A., 1985. Reference crop evapotranspiration from temperature. Appl. Eng. Agric. 1, 96–99. https://doi.org/10.13031/2013.26773.

Haslinger, K., Koffler, D., Schöner, W., Laaha, G., 2014. Exploring the link between meteorological drought and streamflow: effects of climate-catchment interaction. Water Resour. Res. 50, 2468–2487. https://doi.org/10.1002/2013WR015051.

Heim, R.R., 2002. A Review of Twentieth-Century Drought Indices Used in the United States. Bull. Am. Meteorol. Soc. 83, 1149–1165. https://doi.org/10.1175/1520-0477(2002)083<1149:AROTDI>2.3.CO;2.

Hobbins, M.T., Wood, A., McEvoy, D.J., Huntington, J.L., Morton, C., Anderson, M., Hain, C., Hobbins, M.T., Wood, A., McEvoy, D.J., Huntington, J.L., Morton, C., Anderson, M., Hain, C., 2016. The Evaporative Demand Drought Index. Part I: Linking Drought Evolution to Variations in Evaporative Demand. J. Hydrometeorol. 17, 1745–1761. https://doi.org/10.1175/JHM-D-15-0121.1.

Huang, S., Li, P., Huang, Q., Leng, G., Hou, B., Ma, L., 2017. The propagation from meteorological to hydrological drought and its potential influence factors. J. Hydrol. 547, 184–195. https://doi.org/10.1016/J.JHYDROL.2017.01.041.

Huberty, C.J., 1994. Why multivariable analyses? Educ. Psychol. Meas. 54, 620–627. https://doi.org/10.1177/0013164494054003005.

Llorens, P., Domingo, F., 2007. Rainfall partitioning by vegetation under Mediterranean conditions. A review of studies in Europe. J. Hydrol. 335, 37–54. https://doi.org/10.1016/J.JHYDROL.2006.10.032.

López-Moreno, J.I., Vicente-Serrano, S.M., Beguería, S., García-Ruiz, J.M., Portela, M.M., Almeida, A.B., 2009. Dam effects on droughts magnitude and duration in a transboundary basin: The Lower River Tagus, Spain and Portugal. Water Resour. Res. 45. https://doi.org/10.1029/2008WR007198.

López-Moreno, J.I., Vicente-Serrano, S.M., Zabalza, J., Beguería, S., Lorenzo-Lacruz, J., Azorin-Molina, C., Morán-Tejeda, E., 2013. Hydrological response to climate variability at different time scales: a study in the Ebro basin. J. Hydrol. 477, 175–188. https://doi.org/10.1016/J.JHYDROL.2012.11.028.

Lorenzo-Lacruz, J., Garcia, C., Morán-Tejeda, E., 2017. Groundwater level responses to precipitation variability in Mediterranean insular aquifers. J. Hydrol. 552, 516–531. https://doi.org/10.1016/J.JHYDROL.2017.07.011.

Lorenzo-Lacruz, J., Vicente-Serrano, S., González-Hidalgo, J., López-Moreno, J., Cortesi, N., 2013. Hydrological drought response to meteorological drought in the Iberian Peninsula. Clim. Res. 58, 117–131. https://doi.org/10.3354/cr01177.

Lorenzo-Lacruz, J., Vicente-Serrano, S.M., López-Moreno, J.I., Beguería, S., García-Ruiz, J.M., Cuadrat, J.M., 2010. The impact of droughts and water management on various hydrological systems in the headwaters of the Tagus River (central Spain). J. Hydrol. 386, 13–26. https://doi.org/10.1016/j.jhydrol.2010.01.001.

Lutz, J.A., van Wagtendonk, J.W., Franklin, J.F., 2010. Climatic water deficit, tree species ranges, and climate change in Yosemite National Park. J. Biogeogr. 37, 936–950. https://doi.org/10.1111/j.1365-2699.2009.02268.x.

Mckee, T.B., Doesken, N.J., Kleist, J., 1993. The relationshio of drought frequency and duration to time scales. Eighth Conf. Appl. Climatol. 17–22.

Merheb, M., Moussa, R., Abdallah, C., Colin, F., Perrin, C., Baghdadi, N., 2016. Hydrological response characteristics of Mediterranean catchments at different time scales: a meta-analysis. Hydrol. Sci. J. 61, 2520–2539. https://doi.org/10.1080/02626667.2016.1140174.

Redmond, K.T., 2002. The depiction of drought. Bull. Am. Meteorol. Soc. 83, 1143–1148. https://doi.org/10.1175/1520-0477-83.8.1143.

Richman, M.B., 1986. Rotation of principal components. J. Climatol. 6, 293–335. https://doi.org/10.1002/joc.3370060305.

Rimkus, E., Stonevičius, E., Korneev, V., Kažys, J., Valiuškevičius, G., Pakhomau, A., 2013. Dynamics of meteorological and hydrological droughts in the Neman river

basin. Environ. Res. Lett. 8, 045014. https://doi.org/10.1088/1748-9326/8/4/045014.
Scaini, A., Sánchez, N., Vicente-Serrano, S.M., Martínez-Fernández, J., 2015. SMOS-derived soil moisture anomalies and drought indices: a comparative analysis using in situ measurements. Hydrol. Process. 29, 373–383. https://doi.org/10.1002/hyp.10150.
Sheffield, J., Wood, E.F., 2011. In: Sheffield, J., Wood, E.F. (Eds.), GNHRE. Earthscan, London and Washington DC.
State Soil Geographic (STATSG0), 1991. Data Base Data use information. Publication Number 1492. U.S. Department of Agriculture, Natural Resources Conservation Service. Fort Worth, Texas.
Tallaksen, L.M., Van Lanen, H.A., 2004. Hydrological drought : processes and estimation methods for streamflow and groundwater. Developments in Water Science, 48th ed. Elsevier Science B.V., Amsterdam, the Netherlands.
Tallaksen, L.M., Madsen, H., Hisdal, H., 2004. Frequency analysis. In: Tallaksen, L.M., van Lanen, H.A.J. (Eds.), Hydrological Drought Processes and Estimation Methods for Streamflow and Groundwater. Elsevier Science, Amsterdam, pp. 199–271.
Teuling, A.J., Van Loon, A.F., Seneviratne, S.I., Lehner, I., Aubinet, M., Heinesch, B., Bernhofer, C., Grünwald, T., Prasse, H., Spank, U., 2013. Evapotranspiration amplifies European summer drought. Geophys. Res. Lett. 40, 2071–2075. https://doi.org/10.1002/grl.50495.
Tijdeman, E., Bachmair, S., Stahl, K., 2016. Controls on hydrologic drought duration in near-natural streamflow in Europe and the USA. Hydrol. Earth Syst. Sci. 20, 4043–4059. https://doi.org/10.5194/hess-20-4043-2016.
Tijdeman, E., Hannaford, J., Stahl, K., 2018. Human influences on streamflow drought characteristics in England and Wales. Hydrol. Earth Syst. Sci. 22, 1051–1064. https://doi.org/10.5194/hess-22-1051-2018.
Van Loon, A.F., 2015. Hydrological drought explained. Wiley Interdiscip. Rev. Water 2, 359–392. https://doi.org/10.1002/wat2.1085.
Van Loon, A.F., Laaha, G., 2015. Hydrological drought severity explained by climate and catchment characteristics. J. Hydrol. 526, 3–14. https://doi.org/10.1016/J.JHYDROL.2014.10.059.
Vicente-Serrano, S.M, Miralles, Diego Gonzalez, Domínguez-Castro, Fernando, Azorin-Molina, Cesar, El Kenawy, Ahmed, McVicar, Tim R, Tomás-Burguera, Miquel, Beguería, Santiago, Maneta, Marco, Peña-Gallardo, Marina, 2018. Global Assessment of the Standardized Evapotranspiration Deficit Index (SEDI) for Drought Analysis and Monitoring. J.Climate 31 (14), 5371–5393.
Vicente-Serrano, S.M., Beguería, S., López-Moreno, J.I., 2011. Comment on "Characteristics and trends in various forms of the Palmer Drought Severity Index (PDSI) during 1900–2008" by Aiguo Dai. J. Geophys. Res. 116, D19112. https://doi.org/10.1029/2011JD016410.
Vicente-Serrano, S.M., Beguería, S., López-Moreno, J.I., Vicente-Serrano, S.M., Beguería, S., López-Moreno, J.I., 2010. A multiscalar drought index sensitive to global warming: the standardized precipitation evapotranspiration index. J. Clim. 23, 1696–1718. https://doi.org/10.1175/2009JCLI2909.1.
Vicente-Serrano, S.M., Lopez-Moreno, J.-I., Beguería, S., Lorenzo-Lacruz, J., Sanchez-Lorenzo, A., García-Ruiz, J.M., Azorin-Molina, C., Morán-Tejeda, E., Revuelto, J., Trigo, R., Coelho, F., Espejo, F., 2014. Evidence of increasing drought severity caused by temperature rise in southern Europe. Environ. Res. Lett. Environ. Res. Lett. 9, 44001–44009. https://doi.org/10.1088/1748-9326/9/4/044001.
Vicente-Serrano, S.M., López-Moreno, J.I., 2005. Hydrological response to different time scales of climatological drought: an evaluation of the Standardized Precipitation Index in a mountainous Mediterranean basin. Hydrol. Earth Syst. Sci. 9, 523–533. https://doi.org/10.5194/hess-9-523-2005.
Vicente-Serrano, S.M., López-Moreno, J.I., Beguería, S., Lorenzo-Lacruz, J., Azorin-Molina, C., Morán-Tejeda, E., 2012. Accurate computation of a streamflow drought index. J. Hydrol. Eng. 17, 318–332. https://doi.org/10.1061/(ASCE)HE.1943-5584.0000433.
Vicente-Serrano, S.M., Van der Schrier, G., Beguería, S., Azorin-Molina, C., Lopez-Moreno, J.-I., 2015. Contribution of precipitation and reference evapotranspiration to drought indices under different climates. J. Hydrol. 526, 42–54. https://doi.org/10.1016/j.jhydrol.2014.11.025.
Vicente-Serrano, S.M., Zabalza-Martínez, J., Borràs, G., López-Moreno, J.I., Pla, E., Pascual, D., Savé, R., Biel, C., Funes, I., Azorin-Molina, C., Sanchez-Lorenzo, A., Martín-Hernández, N., Peña-Gallardo, M., Alonso-González, E., Tomas-Burguera, M., El Kenawy, A., 2017a. Extreme hydrological events and the influence of reservoirs in a highly regulated river basin of northeastern Spain. J. Hydrol. Reg. Stud. 12, 13–32. https://doi.org/10.1016/j.ejrh.2017.01.004.
Vicente-Serrano, S.M., Zabalza-Martínez, J., Borràs, G., López-Moreno, J.I., Pla, E., Pascual, D., Savé, R., Biel, C., Funes, I., Martín-Hernández, N., Peña-Gallardo, M., Beguería, S., Tomas-Burguera, M., 2017b. Effect of reservoirs on streamflow and river regimes in a heavily regulated river basin of Northeast Spain. CATENA 149, 727–741. https://doi.org/10.1016/j.catena.2016.03.042.
WMO, 2012. Standardized Precipitation Index User Guide.
Wu, J., Chen, X., Yao, H., Gao, L., Chen, Y., Liu, M., 2017. Non-linear relationship of hydrological drought responding to meteorological drought and impact of a large reservoir. J. Hydrol. 551, 495–507. https://doi.org/10.1016/J.JHYDROL.2017.06.029.
Yang, Y., McVicar, T.R., Donohue, R.J., Zhang, Y., Roderick, M.L., Chiew, F.H.S., Zhang, L., Zhang, J., 2017. Lags in hydrologic recovery following an extreme drought: assessing the roles of climate and catchment characteristics. Water Resour. Res. 53, 4821–4837. https://doi.org/10.1002/2017WR020683.
Yuan, X., Zhang, M., Wang, L., Zhou, T., 2017. Understanding and seasonal forecasting of hydrological drought in the Anthropocene. Hydrol. Earth Syst. Sci. 21, 5477–5492. https://doi.org/10.5194/hess-21-5477-2017.
Zhu, Y., Wang, W., Singh, V.P., Liu, Y., 2016. Combined use of meteorological drought indices at multi-time scales for improving hydrological drought detection. Sci. Total Environ. 571, 1058–1068. https://doi.org/10.1016/J.SCITOTENV.2016.07.096.

5. Unpublished researches

The impact of drought on the productivity of two rainfed crops in Spain

Marina Peña-Gallardo[1], Sergio Martín Vicente-Serrano[1], Fernando Domínguez-Castro[1], Santiago Beguería[2]

[1] Instituto Pirenaico de Ecología, Consejo Superior de Investigaciones Científicas (IPE-CSIC), Zaragoza, Spain.
[2] Estación Experimental de Aula Dei, Consejo Superior de Investigaciones Científicas (EEAD-CSIC), Zaragoza, Spain.

Abstract

Drought events are of great importance in most Mediterranean climate regions because of the diverse and costly impacts they have in various economic sectors and on the environment. The effects of this natural hazard on rainfed crops are particularly evident. In this study the impacts of drought on two representative rainfed crops in Spain (wheat and barley) were assessed. As the agriculture sector is vulnerable to climate, it is especially important to identify the most appropriate tools for monitoring the impact of the weather on crops, and particularly the impact of drought. Drought indices are the most effective tool for that purpose. Various drought indices have been used to assess the influence of drought on crop yields in Spain, including the standardized precipitation and evapotranspiration index (SPEI), the standardized precipitation index (SPI), the Palmer drought indices (PDSI, Z-Index, PHDI, PMDI), and the standardized Palmer drought index (SPDI). Two sets of crop yield data at different spatial scales and temporal periods were used in the analysis. The results showed that drought indices calculated at different time scales (SPI, SPEI) most closely correlated with crop yield. The results also suggested that different patterns of yield response to drought occurred depending on the region, period of the year, and the drought time scale. The differing responses across the country were related to season and the magnitude of various climate variables.

Key words: crop yields, drought, Spain, standardized precipitation index, standardized precipitation evapotranspiration index, standardized Palmer drought severity index

1. Introduction

The Mediterranean region is one of the major areas in Europe likely to be subject to the potential impacts of climate change. Many semiarid regions of southwestern Europe are expected to undergo a critical decline in water availability as a consequence of reduced precipitation and an increase in interannual and intra-annual rainfall variability (IPCC, 2014, EEA, 2017). It is also expected that future changes in the precipitation regime, along with a rise in temperature, will inevitably bring more extreme and severe weather events (Giorgi and Lionello, 2008; Webber et al., 2018; Wigley, 2009) that will impact ecosystems and economic sectors (Asseng et al., 2014; Tack et al., 2015). It has been suggested that precipitation and temperature changes in the western Mediterranean region will lead to more severe and longer drought events in coming decades (Alcamo et al., 2007; Dai, 2011; Forzieri et al., 2016; Giorgi and Lionello, 2008; Spinoni et al., 2018; Vicente-Serrano et al., 2014). This is significant because agriculture plays a key role in food supply; in 2017 it accounted for 2.59% of GDP in Spain, 1.92% in Italy, and 3.53% in Greece (World Bank, 2017).

The agriculture sector is highly vulnerable to drought, as it depends directly on water availability (Hanjra and Qureshi, 2010; Meng et al., 2016; Tsakiris and Tigkas, 2007). Although each crop differs in its resilience to water stress (Liu et al., 2016; Lobell et al., 2011), droughts can cause crop failure if the weather conditions are adverse during the most sensitive stage of crop growth (Lobell and Field, 2007). The adverse impacts of drought have been highlighted in recent severe events, including in 2003 when the agricultural and forestry losses from drought in France, Italy, Germany, Spain, Portugal, and Austria were approximately 13 billion Euros (Fink et al., 2004; García-Herrera et al., 2010). The most recent drought, which mostly affected north–central Europe, caused European farmers to claim agricultural aid because of the low production that resulted (European Commission, 2018).

For these reasons the vulnerability of agricultural production to extreme events, and the quantification of drought impacts on crop yields, have become a focus of interest. In recent years diverse studies in the Mediterranean region have assessed these issues from multiple perspectives. For example, Capa-Morocho et al. (2016) investigated the link between seasonal climate forecasts and crop models in Spain, Loukas and Vasiliades, (2004) used a probabilistic approach to evaluate the spatio-temporal characteristics of drought in an agricultural plain region in Greece, and Moore and Lobell, (2014) estimated the impacts of climate projections on various crop types across Europe.

Droughts are difficult to measure and quantify (Vicente-Serrano et al., 2016), and consequently a wide range of drought indices has been developed to provide tools for quantifying the effects of drought across different sectors (Zargar et al., 2011). In this respect, drought indices are the most widely used method for monitoring drought impacts on agriculture; examples of their use available in the scientific literature include in Europe (Hernandez-Barrera et al., 2016; Potopová et al., 2016a; Sepulcre-Canto et al., 2012; Vergni and Todisco, 2011), America (McEvoy et al., 2012; Quiring and Papakryiakou, 2003) and Asia (Ebrahimpour et al., 2015;Wang et al., 2016a). However, there is no general consensus on the most suitable indices for this purpose (Esfahanian et al., 2017). Despite the existing literature, very few studies (Peña-Gallardo et al., 2018a; Tian et

al., 2018) have compared drought indices to identify their appropriateness for monitoring drought impacts on agriculture and for various crop types.

Among Mediterranean countries, agriculture in Spain is particularly sensitive to climate because of the low average precipitation level and its marked interannual variability (Vicente-Serrano, 2006). Spain has been subject to multiple episodes of drought (Domínguez-Castro et al., 2012), with those in the last century being amongst the most severe to have occurred in Europe (González-Hidalgo et al., 2018; Vicente-Serrano, 2006). In 2017 the agricultural and livestock losses caused by drought were estimated to be at least 3600 million Euros (UPA, 2017), highlighting the need to establish appropriate tools for monitoring drought impacts on crops.

Information on crop production is commonly limited in terms of spatial or temporal availability. Recent studies in Spain have analyzed the impact of drought on various crops since the early 21st century at national or provincial scales (Cantelaube et al., 2004; Hernandez-Barrera et al., 2016; Páscoa et al., 2016), but few have used yield data at finer resolution (García-León et al., 2019) . In this study we compared different drought indices using two datasets at different spatial scales: provincial information provided by the national statistical services, and a regional dataset specifically developed for the study. The objectives of this study were: (1) to determine the most appropriate and functional drought index among four Palmer-related drought indices (Palmer drought severity index: PDSI; Palmer hydrological drought index: PHDI; Palmer Z index: Z-index; Palmer modified drought index: PMDI), and the standardized precipitation evapotranspiration index (SPEI), the standardized precipitation index (SPI), and the standardized Palmer drought index (SPDI); (2) to identify the temporal response of two main herbaceous rainfed crops (wheat and barley) to drought; and (3) to determine whether there were common spatial patterns, by comparing the two datasets at different spatial scales.

2. Methods and datasets

2.1.Crop yield data

The statistical analysis was conducted using an annual dataset of crop yields for peninsular Spain and the Balearic Islands at two spatial scales for the two main herbaceous rainfed crops (barley and wheat). We obtained provincial annual yield data from the National Agricultural Statistics Annuaries published by the Spanish Ministry of Agriculture, Fishing and Environment (MAPA), available at: https://www.mapa.gob.es/es/estadistica/temas/publicaciones/anuario-de-estadistica/default.aspx (last accessed: March 2018); these include agricultural statistics since the early 20th century. We used data from 1962 to 2014, to match climate data that was available for this period. The Gipuzkoa and Vizcaya provinces were not used in the analysis at the province scale as wheat has not been cultivated there since 1973 and 1989, respectively. We used crop production data collected by the *Encuesta sobre Superficies y Rendimientos de Cultivos-Survey on surface and crop yields (Esyrce)*, an agrarian yield survey undertaken by the MAPA since 1990. This survey records information about crop production at parcel scale every year from a sample of parcels. Yield observations were aggregated to the main spatial unit defined for agricultural districts by the MAPA (Fig. 1). As not all territories were included in this survey until 1993, we only considered the period 1993–2015. Data on barley production is limited in the Esyrce database, and the agricultural districts considered in this study did not correspond to all the areas where this crop is cultivated.

For both datasets the unit of measure was the harvested production per unit of harvested area (kg/ha); it did not include any measure of production related to the area of the crop planted in each province or region. To consider the total area covered by the crops we used the defined rainfed crop delimited area for Spain, derived from the Corine land cover 2000 database (http://centrodedescargas.cnig.es/CentroDescargas/catalogo.do?Serie=MPPIF ; last accessed: March 2018).

The spatial resolution of yield data can influence the interpretation of drought impacts on agriculture. Figure 2 shows a comparison of crop yields for the common period of available information in both datasets (1993–2014). Overall, the average production was greater at the agricultural district scale than at the provincial scale. Tables S1 and S2 summarize the relationships between the datasets for each province for the available common period, based on Pearson's correlations coefficients for wheat and barley yields, respectively. It was surprising that both datasets showed very different temporal variability in crop yields in the analyzed provinces. Wheat yields showed good agreement and highly significant correlations between both datasets in provinces including Ávila (r = 0.77), Barcelona (r = 0.69), Burgos (r = 0.82), Cuenca (r = 0.86), Guadalajara (r = 0.87), León (r = 0.69), Palencia (r = 0.73), Salamanca (r = 0.87), Segovia (r = 0.94), Teruel (r = 0.83), Valladolid (r = 0.92), and Zamora (r = 0.75), while in other provinces including Castellón, Málaga, Murcia, and Navarra the correlations were non significant or negative. Thus, the national statistics for these districts were unreliable. For barley yields the available regional data were more limited, but similar relationships with good agreement and more highly significant correlations were found among the datasets for the provinces where wheat was also cultivated, including Cáceres (r = 0.48), Cuenca (r = 0.88), Granada (r = 0.51), Guadalajara (r = 0.86), La Rioja (r = 0.76), and Tarragona (r = 0.88); however, for Sevilla the correlation was negative and significant (r = –0.35).

Mechanization and innovation in agriculture have increased since last century, resulting in a trend of increased yields (Lobell and Field, 2007), that is also evident in data for Spain. To remove bias introduced by non-climate factors, and to enable comparison of yields between the two crop types, the original series were transformed to standardized yield residuals series (SYR), using the following quadratic polynomial equation:

$$SYRS = \frac{y_{d-\mu}}{\sigma}$$

where y_d is the residuals of the de-trended yield obtained by fitting a linear regression model, μ is the mean of the de-trended series, and σ is the standard deviation of the de-trended yield.

This methodology has been applied in other similar studies (Chen et al., 2016; Potopová et al., 2015; Tian et al., 2018). the full procedure is described by Lobell and Asner, (2003), Lobell et al. (2011) and Potopová et al. (2015).

2.2. Climate data

We used a weekly gridded dataset of meteorological variables (precipitation, maximum and minimum temperature, relative humidity and sunshine duration) at 1.1 km resolution for peninsular Spain and the Balearic Islands for the period 1962–2015. The grids were generated from a daily meteorological dataset provided by the Spanish National Meteorological Agency (AEMET), following quality control and homogenization of the data. Further details on the method

and the gridding procedure are provided by Vicente-Serrano et al. (2017). Reference evapotranspiration (ETo) was calculated using the FAO-56 Penman-Monteith equation (Allen et al., 1998). Weekly data were aggregated at the monthly scale for calculation of the various drought indices.

2.3. Methods

2.3.1. Drought indices

Palmer Drought Severity Indices (PDSIs)

Palmer (1965) developed the Palmer drought severity index (PDSI). Variations of this index include the Palmer hydrological drought index (PHDI), the Palmer moisture anomaly index (Z-index), and the Palmer modified drought index (PMDI). Computation of the Palmer indices (PDSIs) is mainly based on estimation of the ratio between the surface moisture and the atmospheric humidity demand. Subsequent studies have revealed that spatial comparison among regions is problematic (Alley, 1984; Doesken and Garen, 1991; Heim, 2002). In this context we followed the variation introduced by Wells et al. (2004); this enables spatial comparison when determining a suitable regional coefficient, developing the self-calibrated PDSIs. PDSIs are also referred to as uni-scalar indices, which can only be calculated at fixed and unknown timescales (Guttman, 1998; Vicente-Serrano et al., 2010); this is a limitation of these indices.

Standardized Precipitation Index (SPI)

The standardized precipitation index (SPI) was introduced by Mckee et al. (1993), and provided a new approach to the quantification of drought at multiple time scales. The index is based on the conversion of precipitation series to a standard normal variable having a mean equal to 0 and variance equal to 1, by adjusting an incomplete Gamma distribution. The SPI is a meteorological index used worldwide, and is especially recommended by The World Meteorological Organization (WMO, 2012) for drought monitoring and early warning.

Standardized Precipitation Evapotranspiration Index (SPEI)

Vicente-Serrano et al. (2010) proposed the standardized precipitation evapotranspiration index (SPEI) as a drought index that takes into consideration the effect of atmospheric evaporative demand on drought severity. It provides monthly climate balances (precipitation minus reference evapotranspiration), and the values are transformed to normal standardized units using a 3-parameter log-logistic distribution. Following the concept of the SPI, the SPEI enables comparison of drought characteristics at various time scales among regions, independently of their climatic conditions. The SPEI has been widely used in drought-related studies, including to investigate the impacts of drought on various crops worldwide (Chen et al., 2016; Kuhnert et al., 2016; Peña-Gallardo et al., 2018b; Potopová et al., 2016b; Vicente-Serrano et al., 2012).

Standardized Precipitation Drought Index (SPDI)

The standardized precipitation drought index (SPDI) was developed by Ma et al (2014), and relies on the concept of time scales. It is considered to be a combined version of the PDSI and the SPEI, because the SPDI accumulates the internal water balance anomalies (D) obtained in the PDSI scheme at various time scales, and the values are later transformed into z-units following a General Extreme Value distribution function. For this purpose a log-logistic distribution has been

used, because this has been shown to be effective at the global scale (Vicente-Serrano et al., 2015).

The SPEI, SPI, and SPDI are referred to here as multi-scalar indices, and the PDSIs as uni-scalar indices. Thus, the multi-scalar indices were computed at scales of 1, 12, 18, and 24 months, and along with the PDSIs series were de-trended by adjusting a linear regression model to enable accurate comparisons with de-trended crop yield information. Following the same procedure used for the yield series, the residual of each monthly series was summed to the average value for the period.

2.3.2. Correlation between drought indices and crop yields

The relationship between the drought indices and the SYRS for both datasets was assessed by calculating polynomial correlation coefficients (c) (Baten and Frame, 1959). We used a second-order polynomial regression model, given the common nonlinear relationship between drought indices and crop production (Páscoa et al., 2016; Zipper et al., 2016). Hereafter, the references made to correlations refer to results obtained using the polynomial approach. The months of August and September were excluded from the analysis because they correspond to the post harvest period, and we were considering only the period from sowing to harvest.

As the month of the year when the greatest correlation between the drought index and the crop yield was not known beforehand, all 10 monthly series for each index were correlated with the annual yield, and the highest correlation value was used. In the case of the multi-scalar indices, for each monthly series and time scale we obtained 10 correlations (one for each of the 10 months and the 14 time scales considered in the analysis). Thus, 120 correlations were obtained for each crop and spatial unit considered in the analysis (only correlations significant at $p < 0.05$ were considered). In addition, we used the time scale (in the case of multi-scalar drought indices) and the month in which the strongest correlation was found.

A t-test was performed to assess the significance of the differences in the polynomial regression correlation coefficients obtained from the drought–yield relationships, to determine whether there were significant similarities or differences among the indices.

2.4. Identification of spatial patterns for crop yield response to drought.

A principal component analysis (PCA) was performed to identify general patterns in the effect of drought on crop yields, in relation to seasonality of the effects. PCA is a mathematical technique that enables the dimensionality of a large range of variables to be reduced, by fitting linear combinations of variables. We conducted a T-mode analysis, and used the varimax method to rotate the components to obtain more spatially robust patterns (Richman, 1986). The monthly series of the monthly maximum correlation values found from the yield–drought relationship were the variables (one data point per month), and the provinces and agricultural districts were the cases. We selected two principal components (PC) that in combination explained > 60% of the variance (individually the other components explained < 5% of the variance), and aggregated each province or agricultural district according to the maximum loading rule (i.e., assigning each spatial unit to the PC for which the highest loading value was found). The loadings were expressed in the original correlation magnitudes using the matrix of component weights.

3. Results

3.1. Relationship of drought indices to crop yields

Figure 3 shows the strongest correlation found between the crop yield for each dataset and the monthly drought indices. The correlations differed substantially between the two groups of indices. Independently of the crop type, month of the year, or the drought time scale considered, the correlation coefficients for the multi-scalar indices were much higher than those for the uni-scalar indices. In both cases weaker correlations were found for the wheat crops compared with the barley crops. The PDSI, PHDI, and PMDI correlations were non significant ($p < 0.05$), but the correlations for the Z-index and the multi-scalar indices were significant for most provinces and agricultural districts. The correlation values for the three multi-scalar drought indices were similar. At district scale the average values were $c = 0.57$ and $c = 0.6$ for wheat and barley, respectively, and $c = 0.41$ and $c = 0.48$ at the provincial scale. Thus, the datasets showed a stronger correlation for the drought indices at district scale than at the provincial scale. In addition, more variability was found in the provincial data than in the regional data, associated with the length of the available records.

The spatial distribution of the maximum correlation coefficients between the drought indices and the crop yields are shown in figures 4 and 5, for the province and district scales, respectively. The wheat and barley yield–drought correlations showed a similar spatial pattern among indices at the province scale. Stronger correlations ($c \geq 0.7$) were found for the SPEI and SPI for the provinces of Castilla y León (Valladolid, Zamora, Segovia, and Soria), Aragón (Zaragoza and Teruel), Castilla La Mancha (Guadalajara, Albacete, and Toledo), and the province of Valencia (particularly the cereal agricultural districts). The weakest correlations were found for the southern (Andalusian) provinces. For the Palmer drought indices, the PMDI and Z-index showed similar spatial patterns to the multi-scalar indices (especially in the central and northern provinces), but the correlations were weaker ($c = 0.25–0.6$). For most provinces the weakest correlations were found for the PDSI and PHDI ($c = 0.1–0.25$) for both crops, with no clear spatial difference in the correlations.

The spatial distribution of correlations between wheat yields and the drought indices at the agricultural district scale showed clearer patterns than those for the province level. Thus, the response of drought indices at district scale is similar to the response observed at provincial scale, showing stronger correlations for the multi-scalar indices and weaker correlations for the Palmer indices, especially the PDSI and PHDI. The distribution of correlations among the multi-scalar indices was very similar. The most correlated agricultural districts ($c \geq 0.8$) were in Castilla y León, especially Valladolid, Segovia, north of Ávila, and northeast of Salamanca. Similar correlations were found for areas of northeast Spain. There was a gradient in correlations from north to south, with the exception of some districts in northwestern Málaga, where wheat is extensively cultivated. In addition, in some districts of Galicia, where expansion of the planted wheat area has not been large, there was a strong relationship between drought indices and crop yields. The results for barley suggest a similar spatial relationship for the various drought indices. The highest coefficients were found for the multi-scalar indices, followed by the Z-index and the PMDI, with districts north of Cáceres, north of Galicia, and in Guadalajara showing correlations in the order of $c = 0.8$, while the correlations were weaker ($c = 0.25–0.4$) in districts in the south of Córdoba and Jaén.

3.2. Relationship of drought indices to crop yields: temporal responses

Table 1 summarizes the time scales at which the strongest correlations were found for each of the three multi-scalar indices. Strongest correlations were found for short time scales (1–3 months) for both datasets and both crops, in general with little difference between the indices. For wheat, for 52.6% of the agricultural districts the yield was most strongly correlated with all three drought indices at a time scale of 1–3 months; this was also the case for 49.6% of provinces. In agricultural districts where wheat is cultivated the strongest correlations were predominantly at the 1-month scale (20.37%), especially for the SPDI, while for most of the provinces this occurred at the 3-month scale, particular for the SPEI and SPI (23.26%). For barley, 57.4% of the districts and 58.7% of provinces where this crop was grown the strongest correlations were predominantly at 1- to 3-month time scales. Among the various indices for districts, the SPI showed the strongest correlation at the 1-month scale, while for provinces the SPEI showed the strongest correlation at the 3-month scale (33.33%).

The multi-scalar drought indices showed similar results. Among these, the SPEI was the index most strongly correlated with yield in the highest percentage of provinces and districts (Table 2). For wheat crops the SPEI was the most strongly correlated index with yield in ~37% of the agricultural districts and ~58% of the provinces; these correlations were found predominantly at the 3-month time scale. For this crop the SPDI was most strongly correlated with yield in a similar proportion of districts (~33%), primarily at the 1-month scale, but only ~14% at the province scale. In general, most of the maximum correlations corresponded to short time scales.

Figure 6 shows the spatial distribution of the most strongly correlated drought indices. For most of the provinces the SPEI was the index most strongly correlated with crop yield. For the agricultural districts there was substantial spatial variability and, along with the provincial results, no well-defined spatial pattern that distinguished specific areas for which one index was most effective at monitoring drought. For barley the SPDI showed the best correlation with yield among districts (~44%), while in provinces the SPEI was best correlated (~69%). No clear spatial patterns were evident. The similarities in the magnitude of the correlations between multi-scalar drought indices and crop yields were statistically significant. A t-test (Fig. S1) was used to determine whether there were significant differences in the magnitude of correlations obtained using the various multi-scalar drought indices. This showed significant differences between the SPEI and the SPDI in ~30% of agricultural districts where wheat was grown; these were districts that showed a weaker correlation of yield with drought indices. The results suggest that, for districts having strong correlations between drought indices and crop yields, the two indexes were equally useful. A lower proportion of districts where barley is planted showed that statistical differences among indices exist. In contrast, for provinces no significant differences were found. Overall, this suggests the appropriateness of using any of these multi-scalar indices indistinctly.

3.3. Spatial patterns of drought index correlations at the monthly scale

Regionalization of the crop yield response to drought based on monthly correlations with the drought indices was undertaken in relation to the most correlated drought index in each region, independently of the month in which this maximum correlation occurred. Thus, in this analysis the results obtained using the various multi-scalar drought indices were merged. General spatial patterns in the effect of drought conditions on yield were identified using a T-mode PCA. Figures

7 and 8 show the results for the provincial and regional datasets, respectively. We selected two components that explained more than the 60% of the variance in each case. This classification reinforced the north–south pattern of correlations previously found for both datasets. Figure 9 shows the time scales for which the maximum monthly correlations were found for the provinces and agricultural districts for each of the defined components, using a maximum loading rule.

3.3.1. Wheat

Agricultural district scale

At the district scale the PCA for wheat (Figure 7a) showed more defined spatial patterns than did the PCA at the provincial scale. PC1 explained 43.36% of the variance, and was characterized by stronger correlations (c = 0.7–0.9) in districts mainly located on the north and central plateau; these were stronger than those recorded for the same locations at the provincial scale. Weaker correlations (c = 0.15–0.5) were dispersed, although these were found predominantly in the south and northwest. The scores for PC1 showed particular sensitivity to drought during spring, although strong correlations were also found during autumn. PC2 explained 18.63% of the variance, and the loading coefficients also showed a clear spatial pattern, with the agricultural districts north of Sevilla and east of Castilla La Mancha having the highest values. The weakest correlations were found for the districts of Andalucía, Extremadura, and Aragón. Lower scores in PC2 characterized the interannual response to drought relative to PC1. These districts in PC2 also showed a stronger response during spring but not autumn, as was found for PC1. The distribution of PCs according to the maximum loading rule enabled identification of a north–south component in the sensitivity of wheat yields to the drought index. The time scales at which wheat yields in agricultural districts responded most during spring varied from shorter time scales (3-month) in districts in PC1 to longer time scales (5- to 6-month) for those in PC2 (Fig. 9e, 9f), which also showed greater variability in most months relative to districts from PC1. Greater variability for wheat at the district scale was observed relative to that at the provincial scale. Due to the major number of observations considered, the response to drought in Spain when considering district scale shows more heterogeneity than at provincial scale.

Provincial scale

The results for wheat at the provincial scale (Fig. 7b) showed that the first (PC1) and second (PC2) components explained 51.7% and 20.8% of the variance, respectively. The loadings of the first component were higher for the central plateau and the east of Spain. These represent provinces in the Castilla y León and Castilla y La Mancha districts, and the provinces of Castellón, Valencia, Alicante, Cantabria and Huelva, and Sevilla and Almería in Andalucía. In these provinces there was a strong correlation between drought indices and crop yields, especially during spring, with particularly strong correlations in May. In contrast, during winter the correlations were weaker, especially in February. PC2 showed greater spatial heterogeneity, with strong correlations in the east (Zaragoza and Tarragona provinces) and south (Cádiz, Córdoba, Málaga, Granada, and Jaén provinces) of Spain. For this component the temporal response to drought was not as strong as that for PC1, but the maximum correlation was also found during May. The distribution of the maximum loadings showed a dispersed pattern, with PC1 grouping provinces in the central plateau and east of Spain, and PC2 grouping those in southern and some northeastern provinces. The averaged temporal response to drought during spring is set at medium time scales (4–7

months). In particular, in May most of the provinces correlated at 5 months (Fig. 9a, 9b), indicating the importance of climatic conditions during winter and spring to the crop yields obtained. This was also evident for the longer time scales at which most of the provinces correlated during the winter months (11–18 months). It is noteworthy that there was great variability in the temporal response of provinces in PC1 in October, February, March, and April.

3.3.2. Barley

Agricultural district *scale*

For barley crops (Fig. 8a) both components showed strong correlations (c = 0.6–0.9) in most of the agricultural districts. In general, the districts showing the strongest correlations in PC1 and PC2 were those located in Castilla La Mancha, and north of Cáceres and Córdoba. Scores for PC1 for barley crops were similar to those for PC1 for wheat during spring and autumn, but the results for PC2 suggest that there was little interannual sensitivity to drought. Most of the correlations for spring indicate that barley responded to drought conditions at the 3–4 month scale, mainly in those districts associated with PC1. Barley yields in districts associated with PC2 were more affected by drought conditions in May at 7–9 month time scales (Fig. 9g, 9h).

Provincial scale

For barley at the provincial scale (Fig. 8b) we found more variability in the magnitude of correlations. For PC1 (explaining 43.22% of the variance) strong correlations (r = 0.7–0.9) were found for the north and central provinces of Castilla y León, the central provinces of Castilla y la Mancha, and Madrid, Teruel, Valencia and Castellón. The provinces associated with PC2 (explaining 27.91% of the variance) were more dispersed than those in PC1, and those showing show strong correlations included Zaragoza and Guadalajara in the north, Barcelona and Balearic Islands in the northeast and east, Cáceres in the west, and Cádiz, Córdoba, Málaga, Granada and Jaén in the south. Provinces showing weaker correlations in PC1 were spread in the northeast (e.g., Navarra, Zaragoza, and Lleida) and west of Spain (e.g., Cáceres and Badajoz). Component scores for PC1 were higher than for PC2, although for wheat crops both showed maximum scores during spring (March) and minimum scores in autumn and winter. More provinces in May were correlated with drought indices at medium drought time scales (4–8 months). During spring, provinces in PC1 showed correlations at longer time scales (7–8 months), while provinces in PC2 showed responses at shorter time scales (3–4 months) (Fig. 9c, 9d).

3.3.3. General climatological characteristics for the PCA components

Figures S2-11 show the distribution of climatic characteristics including precipitation, atmospheric evaporative demand (AED), maximum and minimum temperature, and the hydroclimatic balance (precipitation minus AED) at the district scale for the two PCA components. For those districts where wheat was cultivated, no major differences in AED values were found among the components. However, minor differences were observed in precipitation among districts belonging to different PCA components. Those in PC2 had on average less precipitation than those in PC1, especially during autumn, but the difference was not substantial. Greater differences were observed for temperature, with PC1 mainly characterized by districts that had higher maximum temperatures in autumn and spring, and with higher minimum temperatures

than the districts in PC2. These results highlight the important role of temperature in the different responses of crop yield to drought, and demonstrate that, contrary to what may have been expected, temperature and not precipitation was the main factor constraining crop growth. Thus, changes in extreme temperature levels may influence future crop yields. Districts in PC2 where the barley yield correlated with drought indices were characterized by lower levels of precipitation and higher maximum and minimum temperatures than districts represented by PC1, and by higher AED, especially from April to July. Extremes of temperature also seemed to be the major factor determining barley crop yield.

4. Discussion

In this study we investigated the impacts of drought on two rainfed crops in Spain, as measured by a variety of drought indices. We used two datasets of annual crop yields, one from agricultural statistics at the provincial scale spanning the period 1962–2013, and the other a new database at the agricultural district scale from the available parcel data from the national survey covering the period 1993–2015. To identify the best indicator of the impact of drought on yields and their sensitivity to climate, we evaluated the performance of seven drought indices. The selection of drought indices was based on those commonly used to monitoring droughts worldwide, including the standardized precipitation and evapotranspiration index (SPEI), the standardized precipitation index (SPI), the Palmer drought indices (PDSI, Z-Index, PHDI, and PMDI), and the standardized Palmer drought index (SPDI).

Independently of the type of crop and the temporal scale considered, our results showed that drought indices calculated at different time scales (the SPEI, the SPI, and the SPDI) had greater capacity to reflect the impacts of climate on crop yields, relative to uni-scalar drought indices. The better performance of these multi-scalar drought indices was mainly because of their flexibility in reflecting the negative impacts of drought over a range of regions having very different characteristics (Vicente-Serrano et al., 2011). This issue is especially relevant in agriculture, as vegetation components do not respond equally to water deficit. The sensitivity and vulnerability of each type of crop to drought, and the characteristics of the specific region influence the variability evident in the response to droughts (Contreras and Hunink, 2015). Nonetheless, the results of the assessment of the performance of the PDSIs demonstrated that correlations varied markedly among them, showing some exceptions that may affect their usefulness for monitoring purposes. Overall, our results showed that the PHDI had the weakest relationship to crop yields, followed by the PDSI and the PMDI. The better performance of the PDSI over the PHDI was expected, as the latter was primarily developed for hydrological purposes. Likewise, our results confirmed a better performance of the PMDI (a modified version of the PDSI) over the original PDSI for both crops. Our results are consistent with those of previous studies assessing agricultural drought impacts on crop yields at the global (Vicente-Serrano et al., 2012) and regional (Peña-Gallardo et al., 2018b) scales. The Z-index was the best uni-scalar index among the set analyzed in our study. This index measures short-term moisture conditions, which is a major factor in crop stress (Quiring and Papakryiakou, 2003). Thus, the Z-index was more closely correlated with crop yield than any of the other Palmer indices, indicating its usefulness relative to other PDSIs (Karl, 1986).

Although our findings point to poorer performance of the Palmer drought indices relative to the multi-scalar drought indices, they remain among the most widely accepted indices. Numerous

studies have used the Palmer indices in assessments of the use of drought indices for monitoring agricultural drought in various regions worldwide, and have reported the superiority of the Z-index (Mavromatis, 2007; Quiring and Papakryiakou, 2003; Sun et al., 2012; Tunalıoğlu and Durdu, 2012) ; our results confirm it usefulness among the Palmer drought indices.

Nevertheless, it is important to stress that the usefulness of PDSIs is less than drought indices that can be computed at different time scales (Vicente-Serrano et al. 2012). We demonstrated that the three multi-scalar drought indices in our study (SPEI, SPI, and SPDI) were able to detect drought at different time scales, enabling past weather conditions to be related to present conditions in regions characterized by diverse climatic conditions. This is consistent with previous comparative studies in various regions that reported multi-scalar drought indices were effective for monitoring drought impacts on agricultural lands (Blanc, 2012; Kim et al., 2012; Potopová, 2011; Potopová et al., 2016a; Tian et al., 2018; Zhu et al., 2016; Zipper et al., 2016). Although previous studies reported differences among some of the above three indices (e.g., the SPDI and the SPEI; Ghabaei Sough et al., 2018), others have reported similarities in their performance in assessing agricultural drought impacts (Labudová et al., 2016; Peña-Gallardo et al., 2018a). The similar magnitudes of their correlations suggest a similar ability to characterize the impact of drought on crop yields. However, minor differences among these indices suggested the SPEI performed best. First, for both crops slightly stronger correlations were observed with the SPEI, although the SPDI was superior in relation to barley yields at the agricultural district scale. In general, the SPEI was found to be the most suitable drought index in the majority of agricultural districts and provinces. This suggests that inclusion of AED in the drought index calculation, as occurs in the SPEI, provides greater capacity to predict drought impacts on crop yields compared with the use of precipitation only. Variation in the maximum and minimum temperatures has been found to be the major factor differentiating agricultural districts and provinces having greater sensitivity to drought. Previous studies have stressed the risks associated with an increase in global temperatures, particularly maximum temperatures, and the possible effects on crop yields (Lobell and Field, 2007; Moore and Lobell, 2014). Thus, a ~5.4% reduction in grain yields resulting from an increase in average temperature is expected to occur under the current global warming scenario (Asseng et al., 2014; Zhao et al., 2017).

The temporal and spatial effects of drought on yields seem to be very complex, given the observed variability in Spain. In this respect, significant yield effects of drought were found in both datasets. Nevertheless, at the agricultural district scale there was a more evident spatial effect of drought on agricultural yields. This is a key finding for spatial-scale analyses, although the lack of long time series datasets on regional yields is a common constraint.

Drought effects on barley and wheat were similar in space and time, although their sensitivity to drought differed, as shown by differences in the magnitude of the correlations with the drought indices, with wheat yields showing stronger correlations than barley yields. This can be explained by the different physiological characteristics of the two crops, as barley is less dependent on water availability at germination and the grain filling stage than wheat (Mamnouie et al., 2006). Although the transpiration coefficient for barley is higher, this crop is not as subject as wheat to water stress under drought conditions (Fischer et al., 1998). Our results indicate that the temporal responses of barley and wheat to drought conditions were very similar, despite the fact that in Spain barley is typically cultivated later than wheat, and in soils having poor moisture retention.

Therefore, the phenological characteristics of each type of crop determine how drought affects yields. The results showed that temperature had a more important role than precipitation, suggesting that extreme variations in average temperature conditions during the most sensitive growth stages may have a negative impact on crops.

Overall, crop yields in Spain tend to respond to short drought time scales (1–3 months). However, the sensitivity of crops to drought is greater during spring at medium (4–6 months) time scales. This highlights that moisture conditions during winter (the period corresponding to planting, and the first growth stages of tillering and stem elongation), are crucial for the successful development of the plants (Çakir, 2004; Moorhead et al., 2015; Wang et al., 2016a, 2016b).

We found a stronger response of crops to climatic conditions in provinces and agricultural districts in the central plateau, and unexpectedly a weaker response in southwestern districts. This reflects the inconsistencies reported for the Iberian Peninsula by Páscoa et al. (2016) , who argued that spatial differences can be explained mainly by the differing productivities in the various districts; we noted this for the mainly agrarian areas of peninsular Spain (Castilla y León and Castilla La Mancha), and the characteristically heterogeneity of this territory. In the southwestern agricultural areas, where the precipitation rates are lower and temperatures higher, the correlations of yield with drought were weaker. This can be attributed to episodes of abnormal extreme temperatures, such as the very low temperatures in early spring or warmer than usual temperatures in winter; these would affect the expected low evapotranspiration rates during the cold season (Fontana et al., 2015; Kolář et al., 2014). A recent study by Hernandez-Barrera et al. (2016) demonstrated that during autumn and spring, precipitation deficit is the most influential climate factor affecting wheat growth, while an increase in the diurnal temperature range causes a reduction in wheat yield. We found no major differences in precipitation among districts belonging to any of the two defined components, but found other differences including in the average maximum and minimum temperatures. These findings highlight the complexity in choosing a useful drought index that encompasses the specificities of each crop, including its sensitivity to moisture and environmental conditions throughout the entire growth cycle, and its seasonality. This underscores the importance of testing and comparing the appropriateness of different drought indices to ensure accurate identification of the multi-temporal impacts of drought on natural systems.

5. Conclusions

The main findings of this study are summarized below.

(1) Assessment of the efficacy of drought indices for monitoring the effect of climate on agricultural yields demonstrated the better performance of multi-scalar indices. The ability to calculate these indices at various time scales enabled drought impacts to be more precisely defined than with the use of indices lacking this characteristic. The multi-scalar drought indices assessed also had fewer computational and data requirements (particularly the SPEI and the SPI), which is a significant consideration when performing analyses based on scarce climate data.

(2) From a quantitative evaluation of the relationship of drought indices to crop yields we determined that both of the multi-scalar drought indices tested were useful for

assessment of agricultural drought in Spain. However, the SPEI had slightly better correlations and is the most highly recommended for the purpose.

(3) The spatial definition of yield responses to drought was clearer at the district scale, where the finer spatial resolution enabled better definition of the patterns of responses because the climatic variability of each region was better captured at this scale.

(4) Barley and wheat yields were more vulnerable to drought during spring, both at short (1–3 months) and medium (4–6 months) time scales. Moisture conditions during late autumn and winter also had an impact on the crop yields.

(5) The strongest relationships between drought indices and crop yields were found for the northern and central agricultural districts. The relationships for the southern districts were weaker because of the difficulty of characterizing drought impacts over the diverse and complex territory involved.

(6) The climatic and agricultural conditions in Spain are very diverse. The large spatial diversity and complexity of droughts highlights the need to establish accurate and effective indices to monitor the variable evolution of drought in vulnerable agriculture areas. Climate change is likely to lead to yield losses because of increased drought stress on crops, so in this context effective monitoring tools are of utmost importance. The authors consider that further analysis complementing this study may help to unravel the climate mechanisms that influence the spatio-temporal responses of yields to climate in Spain.

Acknowledgments

This work was supported by the research projects PCIN-2015-220 and CGL2014-52135-C03-01 financed by the Spanish Commission of Science and Technology and FEDER, IMDROFLOOD financed by the Water Works 2014 co-funded call of the European Commission and INDECIS, which is part of ERA4CS, and ERA-NET initiated by JPI Climate, and funded by FORMAS (SE), DLR (DE), BMWFW (AT), IFD (DK), MINECO (ES), ANR (FR) with co-funding by the European Union (Grant 690462). Peña-Gallardo Marina was granted by the Spanish Ministry of Economy and Competitiveness (BES-2015-072022).

Bibliography

Alcamo, J., Flörke, M. and Märker, M.: Future long-term changes in global water resources driven by socio-economic and climatic changes, Hydrol. Sci. J., 52(2), 247–275, doi:10.1623/hysj.52.2.247, 2007.

Allen, R. G., Pereira, L. S., Raes, D. and Smith, M.: No Title, Crop Evapotranspiration Guidel. Comput. Crop Water Requir., 1998.

Alley, W. M.: The Palmer Drought Severity Index: Limitations and Assumptions, J. Clim. Appl. Meteorol., 23(7), 1100–1109, doi:10.1175/1520-0450(1984)023<1100:TPDSIL>2.0.CO;2, 1984.

Asseng, S., Foster, I. and Turner, N. C.: The impact of temperature variability on wheat yields, Glob. Chang. Biol., 17(2), 997–1012, doi:10.1111/j.1365-2486.2010.02262.x, 2011.

Asseng, S., Ewert, F., Martre, P., Rötter, R. P., Lobell, D. B., Cammarano, D., Kimball, B. A., Ottman, M. J., Wall, G. W., White, J. W., Reynolds, M. P., Alderman, P. D., Prasad, P. V. V., Aggarwal, P. K.,

Anothai, J., Basso, B., Biernath, C., Challinor, A. J., De Sanctis, G., Doltra, J., Fereres, E., Garcia-Vila, M., Gayler, S., Hoogenboom, G., Hunt, L. A., Izaurralde, R. C., Jabloun, M., Jones, C. D., Kersebaum, K. C., Koehler, A.-K., Müller, C., Naresh Kumar, S., Nendel, C., O'Leary, G., Olesen, J. E., Palosuo, T., Priesack, E., Eyshi Rezaei, E., Ruane, A. C., Semenov, M. A., Shcherbak, I., Stöckle, C., Stratonovitch, P., Streck, T., Supit, I., Tao, F., Thorburn, P. J., Waha, K., Wang, E., Wallach, D., Wolf, J., Zhao, Z. and Zhu, Y.: Rising temperatures reduce global wheat production, Nat. Clim. Chang., 5(2), 143–147, doi:10.1038/nclimate2470, 2014.

Blanc, E.: The Impact of Climate Change on Crop Yields in Sub-Saharan Africa, Am. J. Clim. Chang., 01(01), 1–13, doi:10.4236/ajcc.2012.11001, 2012.

Çakir, R.: Effect of water stress at different development stages on vegetative and reproductive growth of corn, F. Crop. Res., 89(1), 1–16, doi:10.1016/j.fcr.2004.01.005, 2004.

Cantelaube, P., Terres, J. and Doblas-Reyes, F.: Influence of climate variability on European agriculture-analysis of winter wheat production, Clim. Res., 27(2), 135–144, doi:10.3354/cr027135, 2004.

Capa-Morocho, M., Ines, A. V. M., Baethgen, W. E., Rodríguez-Fonseca, B., Han, E. and Ruiz-Ramos, M.: Crop yield outlooks in the Iberian Peninsula: Connecting seasonal climate forecasts with crop simulation models, Agric. Syst., 149, 75–87, doi:10.1016/J.AGSY.2016.08.008, 2016.

Chen, T., Xia, G., Liu, T., Chen, W., Chi, D., Chen, T., Xia, G., Liu, T., Chen, W. and Chi, D.: Assessment of Drought Impact on Main Cereal Crops Using a Standardized Precipitation Evapotranspiration Index in Liaoning Province, China, Sustainability, 8(10), 1069, doi:10.3390/su8101069, 2016.

Contreras, S. and Hunink, J. E.: Drought effects on rainfed agriculture using standardized indices: A case study in SE Spain, in Drought: Research and Science-Policy Interfacing., 2015.

Dai, A.: Drought under global warming: a review, Wiley Interdiscip. Rev. Clim. Chang., 2(1), 45–65, doi:10.1002/wcc.81, 2011.

Doesken, N. J. and Garen, D.: Drought monitoring in the Western United States using a surface water supply index. Presented at: 7th Conference on Applied Climatology, Sept. 10-13, 1991 in Salt Lake City, Utah, in Development of a Surface Water Supply Index (SWSI) for the Western United States, 1991, edited by D. of A. S. Fort Collins, CO: Colorado State University, pp. 77–80., 1991.

Domínguez-Castro, F., Ribera, P., García-Herrera, R., Vaquero, J. M., Barriendos, M., Cuadrat, J. M. and Moreno, J. M.: Assessing extreme droughts in Spain during 1750–1850 from rogation ceremonies, Clim. Past, 8(2), 705–722, doi:10.5194/cp-8-705-2012, 2012.

Ebrahimpour, M., Rahimi, J., Nikkhah, A. and Bazrafshan, J.: Monitoring Agricultural Drought Using the Standardized Effective Precipitation Index, J. Irrig. Drain. Eng., 141(1), 04014044, doi:10.1061/(ASCE)IR.1943-4774.0000771, 2015.

Esfahanian, E., Nejadhashemi, A. P., Abouali, M., Adhikari, U., Zhang, Z., Daneshvar, F. and Herman, M. R.: Development and evaluation of a comprehensive drought index, J. Environ. Manage., 185, 31–43, doi:10.1016/j.jenvman.2016.10.050, 2017.

European Commission. Agriculture and Rural Development: Commission offers further support to European farmers dealing with droughts [online] Available from: https://ec.europa.eu/info/news/commission-offers-further-support-european-farmers-dealing-droughts-2018-aug-02-0_en (Accessed 26 October 2018), 2018.

European Environment Agency (EEA): Climate change, impacts and vulnerability in Europe 2016. An indicator-based report., Luxembourg., 2017.

Fink, A. H., Brücher, T., Krüger, A., Leckebusch, G. C., Pinto, J. G. and Ulbrich, U.: The 2003 European summer heatwaves and drought -synoptic diagnosis and impacts., 2004.

Fischer, R. A., Rees, D., Sayre, K. D., Lu, Z.-M., Condon, A. G. and Saavedra, A. L.: Wheat Yield Progress Associated with Higher Stomatal Conductance and Photosynthetic Rate, and Cooler Canopies, Crop Sci., 38(6), 1467, doi:10.2135/cropsci1998.0011183X003800060011x, 1998.

Fontana, G., Toreti, A., Ceglar, A. and De Sanctis, G.: Early heat waves over Italy and their impacts on durum wheat yields, Nat. Hazards Earth Syst. Sci., 15(7), 1631–1637, doi:10.5194/nhess-15-1631-2015, 2015.

Forzieri, G., Feyen, L., Russo, S., Vousdoukas, M., Alfieri, L., Outten, S., Migliavacca, M., Bianchi, A., Rojas, R. and Cid, A.: Multi-hazard assessment in Europe under climate change, Clim. Change, 137(1–2), 105–119, doi:10.1007/s10584-016-1661-x, 2016.

García-Herrera, R., Díaz, J., Trigo, R. M., Luterbacher, J. and Fischer, E. M.: A Review of the European Summer Heat Wave of 2003, Crit. Rev. Environ. Sci. Technol., 40(4), 267–306, doi:10.1080/10643380802238137, 2010.

García-León, D., Contreras, S. and Hunink, J.: Comparison of meteorological and satellite-based drought indices as yield predictors of Spanish cereals, Agric. Water Manag., 213, 388–396, doi:10.1016/J.AGWAT.2018.10.030, 2019.

Ghabaei Sough, M., Zare Abyaneh, H. and Mosaedi, A.: Assessing a Multivariate Approach Based on Scalogram Analysis for Agricultural Drought Monitoring, Water Resour. Manag., 32(10), 3423–3440, doi:10.1007/s11269-018-1999-0, 2018.

Giorgi, F. and Lionello, P.: Climate change projections for the Mediterranean region, Glob. Planet. Change, 63(2–3), 90–104, doi:10.1016/j.gloplacha.2007.09.005, 2008.

Guttman, N. B.: Comparing the Palmer Drought Index and The Standardized Precipitation Index, J. Am. Water Resour. Assoc., 34(1), 113–121, doi:10.1111/j.1752-1688.1998.tb05964.x, 1998.

Hanjra, M. A. and Qureshi, M. E.: Global water crisis and future food security in an era of climate change, Food Policy, 35(5), 365–377, doi:10.1016/J.FOODPOL.2010.05.006, 2010.

Heim, R. R.: A Review of Twentieth-Century Drought Indices Used in the United States, Bull. Am. Meteorol. Soc., 83(8), 1149–1165, doi:10.1175/1520-0477(2002)083<1149:AROTDI>2.3.CO;2, 2002.

Hernandez-Barrera, S., Rodriguez-Puebla, C. and Challinor, A. J.: Effects of diurnal temperature range and drought on wheat yield in Spain, Theor. Appl. Climatol., doi:10.1007/s00704-016-1779-9, 2016.

IPCC, 2014: Climate Change 2014: Mitigation of Climate Change. Contribution of Working Group III to the Fifth Assessment Report of the Intergovernmental Panel on Climate Change [Edenhofer, O., R. Pichs-Madruga, Y. Sokona, E. Farahani, S. Kadner, K. Seyboth, A. Adler, I. Baum, S. Brunner, P. Eickemeier, B. Kriemann, J. Savolainen, S. Schlömer, C. von Stechow, T. Zwickel and J.C. Minx (eds.)]. Cambridge University Press, Cambridge, United Kingdom and New York, NY, USA.

Karl, T. R.: The Sensitivity of the Palmer Drought Severity Index and Palmer's Z-Index to their Calibration Coefficients Including Potential Evapotranspiration, J. Clim. Appl. Meteorol., 25(1), 77–86, doi:10.1175/1520-0450(1986)025<0077:TSOTPD>2.0.CO;2, 1986.

Kim, B.-S., Sung, J.-H., Kang, H.-S. and Cho, C.-H.: Assessment of Drought Severity over South Korea using Standardized Precipitation Evapo-transpiration Index (SPEI), J. Korea Water Resour. Assoc., 45(9), 887–900, doi:10.3741/JKWRA.2012.45.9.887, 2012.

Kolář, P., Trnka, M., Brázdil, R. and Hlavinka, P.: Influence of climatic factors on the low yields of spring barley and winter wheat in Southern Moravia (Czech Republic) during the 1961–2007 period, Theor. Appl. Climatol., 117(3–4), 707–721, doi:10.1007/s00704-013-1037-3, 2014.

Kuhnert, M., Yeluripati, J., Smith, P., Hoffmann, H., van Oijen, M., Constantin, J., Coucheney, E., Dechow, R., Eckersten, H., Gaiser, T., Grosz, B., Haas, E., Kersebaum, K.-C., Kiese, R., Klatt, S., Lewan, E., Nendel, C., Raynal, H., Sosa, C., Specka, X., Teixeira, E., Wang, E., Weihermüller, L., Zhao, G., Zhao, Z., Ogle, S. and Ewert, F.: Impact analysis of climate data aggregation at different spatial scales on simulated net primary productivity for croplands, Eur. J. Agron., doi:10.1016/j.eja.2016.06.005, 2016.

Labudová, L., Labuda, M. and Takáč, J.: Comparison of SPI and SPEI applicability for drought impact assessment on crop production in the Danubian Lowland and the East Slovakian Lowland, Theor. Appl. Climatol., 1–16, doi:10.1007/s00704-016-1870-2, 2016.

Liu, B., Asseng, S., Müller, C., Ewert, F., Elliott, J., Lobell, D. B., Martre, P., Ruane, A. C., Wallach, D., Jones, J. W., Rosenzweig, C., Aggarwal, P. K., Alderman, P. D., Anothai, J., Basso, B., Biernath, C., Cammarano, D., Challinor, A., Deryng, D., Sanctis, G. D., Doltra, J., Fereres, E., Folberth, C., Garcia-Vila, M., Gayler, S., Hoogenboom, G., Hunt, L. A., Izaurralde, R. C., Jabloun, M., Jones, C. D., Kersebaum, K. C., Kimball, B. A., Koehler, A.-K., Kumar, S. N., Nendel, C., O'Leary, G. J., Olesen, J. E., Ottman, M. J., Palosuo, T., Prasad, P. V. V., Priesack, E., Pugh, T. A. M., Reynolds, M., Rezaei, E. E., Rötter, R. P., Schmid, E., Semenov, M. A., Shcherbak, I., Stehfest, E., Stöckle, C. O., Stratonovitch, P., Streck, T., Supit, I., Tao, F., Thorburn, P., Waha, K., Wall, G. W., Wang, E., White, J. W., Wolf, J., Zhao, Z. and Zhu, Y.: Similar estimates of temperature impacts on global wheat yield by three independent methods, Nat. Clim. Chang., 6(12), 1130–1136, doi:10.1038/nclimate3115, 2016.

Lobell, D. B. and Asner, G. P.: Climate and management contributions to recent trends in U.S. agricultural yields., Science (80-.)., 299(5609), 1032, doi:10.1126/science.1078475, 2003.

Lobell, D. B. and Field, C. B.: Global scale climate–crop yield relationships and the impacts of recent warming, Environ. Res. Lett., 2(1), 014002, doi:10.1088/1748-9326/2/1/014002, 2007.

Lobell, D. B., Schlenker, W. and Costa-Roberts, J.: Climate Trends and Global Crop Production Since 1980, Science (80-)., 333(6042), 2011.

Loukas, A. and Vasiliades, L.: Probabilistic analysis of drought spatiotemporal characteristics in Thessaly region, Greece, Nat. Hazards Earth Syst. Sci., 4(5/6), 719–731, doi:10.5194/nhess-4-719-2004, 2004.

Ma, M., Ren, L., Yuan, F., Jiang, S., Liu, Y., Kong, H. and Gong, L.: A new standardized Palmer drought index for hydro-meteorological use, Hydrol. Process., 28(23), 5645–5661, doi:10.1002/hyp.10063, 2014.

Mamnouie, E., Ghazvini, R. F., Esfahany, M. and Nakhoda, B.: The Effects of Water Deficit on Crop Yield and the Physiological Characteristics of Barley (Hordeum vulgare L.) Varieties. [online] Available from: http://jast.modares.ac.ir/article-23-5420-en.pdf (Accessed 24 November 2018), 2006.

Mavromatis, T.: Drought index evaluation for assessing future wheat production in Greece, Int. J. Climatol., 27(7), 911–924, doi:10.1002/joc.1444, 2007.

McEvoy, D. J., Huntington, J. L., Abatzoglou, J. T., Edwards, L. M., McEvoy, D. J., Huntington, J. L., Abatzoglou, J. T. and Edwards, L. M.: An Evaluation of Multiscalar Drought Indices in Nevada and Eastern California, Earth Interact., 16(18), 1–18, doi:10.1175/2012EI000447.1, 2012.

Mckee, T. B., Doesken, N. J. and Kleist, J.: The relationshio of drought frequency and duration to

time scales, Eighth Conf. Appl. Climatol., 17–22 [online] Available from: http://www.droughtmanagement.info/literature/AMS_Relationship_Drought_Frequency_Duration_Time_Scales_1993.pdf (Accessed 30 May 2018), 1993.

Meng, Q., Chen, X., Lobell, D. B., Cui, Z., Zhang, Y., Yang, H. and Zhang, F.: Growing sensitivity of maize to water scarcity under climate change, Sci. Rep., 6, 19605, doi:10.1038/srep19605, 2016.

Moore, F. C. and Lobell, D. B.: Adaptation potential of European agriculture in response to climate change, Nat. Clim. Chang., 4(7), 610–614, doi:10.1038/nclimate2228, 2014.

Moorhead, J. E., Gowda, P. H., Singh, V. P., Porter, D. O., Marek, T. H., Howell, T. A. and Stewart, B. A.: Identifying and Evaluating a Suitable Index for Agricultural Drought Monitoring in the Texas High Plains, JAWRA J. Am. Water Resour. Assoc., 51(3), 807–820, doi:10.1111/jawr.12275, 2015.

Palmer, W. C.: Meteorological Drought. Research Paper No. 45, 1965, 58 p., U.S. Dep. Commer. Weather Bur. Washington, DC., Research P, 1965.

Páscoa, P., Gouveia, C. M., Russo, A. and Trigo, R. M.: The role of drought on wheat yield interannual variability in the Iberian Peninsula from 1929 to 2012, Int. J. Biometeorol., 1–13, doi:10.1007/s00484-016-1224-x, 2016.

Peña-Gallardo, M., Vicente-Serrano, S., Domínguez-Castro, F., Quiring, S., Svoboda, M., Beguería, S. and Hannaford, J.: Effectiveness of drought indices in identifying impacts on major crops across the USA, Clim. Res., 75(3), 221–240, doi:10.3354/cr01519, 2018a.

Peña-Gallardo, M., Quiring, S., Svoboda, M., Hannaford, J., Tomas-Burguera, M., Martín-Hernández, N., Domínguez-Castro, F. and El Kenawy, A.: Response of crop yield to different time-scales of drought in the United States: Spatio-temporal patterns and climatic and environmental drivers, Agric. For. Meteorol., 264, 40–55, doi:10.1016/j.agrformet.2018.09.019, 2018b.

Potopová, V.: Evolution of drought severity and its impact on corn in the Republic of Moldova, Theor. Appl. Climatol., 105(3–4), 469–483, doi:10.1007/s00704-011-0403-2, 2011.

Potopová, V., Štěpánek, P., Možný, M., Türkott, L. and Soukup, J.: Performance of the standardised precipitation evapotranspiration index at various lags for agricultural drought risk assessment in the Czech Republic, Agric. For. Meteorol., 202, 26–38, doi:10.1016/J.AGRFORMET.2014.11.022, 2015.

Potopová, V., Štěpánek, P., Farda, A., Türkott, L., Zahradníček, P. and Soukup, J.: Drought stress impact on vegetable crop yields in the Elbe River lowland between 1961 and 2014, Cuad. Investig. Geográfica, 42(1), 127, doi:10.18172/cig.2924, 2016a.

Potopová, V., Boroneanţ, C., Boincean, B. and Soukup, J.: Impact of agricultural drought on main crop yields in the Republic of Moldova, Int. J. Climatol., 36(4), 2063–2082, doi:10.1002/joc.4481, 2016b.

Quiring, S. M. and Papakryiakou, T. N.: An evaluation of agricultural drought indices for the Canadian prairies, Agric. For. Meteorol., 118(1), 49–62, doi:10.1016/S0168-1923(03)00072-8, 2003.

Richman, M. B.: Rotation of principal components, J. Climatol., 6(3), 293–335, doi:10.1002/joc.3370060305, 1986.

Sepulcre-Canto, G., Horion, S., Singleton, A., Carrao, H. and Vogt, J.: Development of a Combined Drought Indicator to detect agricultural drought in Europe, Nat. Hazards Earth Syst. Sci., 12(11), 3519–3531, doi:10.5194/nhess-12-3519-2012, 2012.

Spinoni, J., Vogt, J. V., Naumann, G., Barbosa, P. and Dosio, A.: Will drought events become more

frequent and severe in Europe?, Int. J. Climatol., 38(4), 1718–1736, doi:10.1002/joc.5291, 2018.

Sun, L., Mitchell, S. W. and Davidson, A.: Multiple drought indices for agricultural drought risk assessment on the Canadian prairies, Int. J. Climatol., 32(11), 1628–1639, doi:10.1002/joc.2385, 2012.

Tack, J., Barkley, A. and Nalley, L. L.: Effect of warming temperatures on US wheat yields., Proc. Natl. Acad. Sci. U. S. A., 112(22), 6931–6, doi:10.1073/pnas.1415181112, 2015.

Tian, L., Yuan, S. and Quiring, S. M.: Evaluation of six indices for monitoring agricultural drought in the south-central United States, Agric. For. Meteorol., 249, 107–119, doi:10.1016/J.AGRFORMET.2017.11.024, 2018.

Tsakiris, G. and Tigkas, D.: Drought Risk in Agriculture in Mediterranean Regions. Case Study: Eastern Crete, in Methods and Tools for Drought Analysis and Management, pp. 399–414, Springer Netherlands, Dordrecht., 2007.

Tunalıoğlu, R. and Durdu, Ö. F.: Assessment of future olive crop yield by a comparative evaluation of drought indices: a case study in western Turkey, Theor. Appl. Climatol., 108(3–4), 397–410, doi:10.1007/s00704-011-0535-4, 2012.

UPA, Unión de Pequeños Agricultores y Ganaderos: La sequía y sus efectos sobre la agricultura y la ganadería, [online] Available from: https://www.upa.es/upa/uControlador/index.php?nodo=1021&hn=2232 (Accessed 25 October 2018), 2017.

Vergni, L. and Todisco, F.: Spatio-temporal variability of precipitation, temperature and agricultural drought indices in Central Italy, Agric. For. Meteorol., 151(3), 301–313, doi:10.1016/j.agrformet.2010.11.005, 2011.

Vicente-Serrano, S. M.: Spatial and temporal analysis of droughts in the Iberian Peninsula (1910–2000), Hydrol. Sci. J., 51(1), 83–97, doi:10.1623/hysj.51.1.83, 2006.

Vicente-Serrano, S. M., Beguería, S., López-Moreno, J. I., Vicente-Serrano, S. M., Beguería, S. and López-Moreno, J. I.: A Multiscalar Drought Index Sensitive to Global Warming: The Standardized Precipitation Evapotranspiration Index, J. Clim., 23(7), 1696–1718, doi:10.1175/2009JCLI2909.1, 2010.

Vicente-Serrano, S. M., Beguería, S. and López-Moreno, J. I.: Comment on “Characteristics and trends in various forms of the Palmer Drought Severity Index (PDSI) during 1900–2008” by Aiguo Dai, J. Geophys. Res., 116(D19), D19112, doi:10.1029/2011JD016410, 2011.

Vicente-Serrano, S. M., Beguería, S., Lorenzo-Lacruz, J., Camarero, J. J., López-Moreno, J. I., Azorin-Molina, C., Revuelto, J., Morán-Tejeda, E., Sanchez-Lorenzo, A., Vicente-Serrano, S. M., Beguería, S., Lorenzo-Lacruz, J., Camarero, J. J., López-Moreno, J. I., Azorin-Molina, C., Revuelto, J., Morán-Tejeda, E. and Sanchez-Lorenzo, A.: Performance of Drought Indices for Ecological, Agricultural, and Hydrological Applications, http://dx.doi.org/10.1175/2012EI000434.1, doi:10.1175/2012EI000434.1, 2012.

Vicente-Serrano, S. M., Lopez-Moreno, J.-I., Beguería, S., Lorenzo-Lacruz, J., Sanchez-Lorenzo, A., García-Ruiz, J. M., Azorin-Molina, C., Morán-Tejeda, E., Revuelto, J., Trigo, R., Coelho, F. and Espejo, F.: Evidence of increasing drought severity caused by temperature rise in southern Europe, Environ. Res. Lett. Environ. Res. Lett, 9, 44001–9, doi:10.1088/1748-9326/9/4/044001, 2014.

Vicente-Serrano, S. M., Van der Schrier, G., Beguería, S., Azorin-Molina, C. and Lopez-Moreno, J.-I.: Contribution of precipitation and reference evapotranspiration to drought indices under

different climates, J. Hydrol., 526, doi:10.1016/j.jhydrol.2014.11.025, 2015.

Vicente-Serrano, S. M., Camarero, J. J., Olano, J. M., Martín-Hernández, N., Peña-Gallardo, M., Tomás-Burguera, M., Gazol, A., Azorin-Molina, C., Bhuyan, U. and El Kenawy, A.: Diverse relationships between forest growth and the Normalized Difference Vegetation Index at a global scale, Remote Sens. Environ., 187, doi:10.1016/j.rse.2016.10.001, 2016.

Vicente-Serrano, S. M., Tomas-Burguera, M., Beguería, S., Reig, F., Latorre, B., Peña-Gallardo, M., Luna, M. Y., Morata, A. and González-Hidalgo, J. C.: A High Resolution Dataset of Drought Indices for Spain, Data, 2(3), 22, doi:10.3390/data2030022, 2017.

Wang, H., Vicente-serrano, S. M., Tao, F., Zhang, X., Wang, P., Zhang, C., Chen, Y., Zhu, D. and Kenawy, A. El: Monitoring winter wheat drought threat in Northern China using multiple climate-based drought indices and soil moisture during 2000–2013, Agric. For. Meteorol., 228–229, 1–12, doi:10.1016/j.agrformet.2016.06.004, 2016a.

Wang, Q., Wu, J., Li, X., Zhou, H., Yang, J., Geng, G., An, X., Liu, L. and Tang, Z.: A comprehensively quantitative method of evaluating the impact of drought on crop yield using daily multi-scale SPEI and crop growth process model, Int. J. Biometeorol., 1–15, doi:10.1007/s00484-016-1246-4, 2016b.

Webber, H., Ewert, F., Olesen, J. E., Müller, C., Fronzek, S., Ruane, A. C., Bourgault, M., Martre, P., Ababaei, B., Bindi, M., Ferrise, R., Finger, R., Fodor, N., Gabaldón-Leal, C., Gaiser, T., Jabloun, M., Kersebaum, K.-C., Lizaso, J. I., Lorite, I. J., Manceau, L., Moriondo, M., Nendel, C., Rodríguez, A., Ruiz-Ramos, M., Semenov, M. A., Siebert, S., Stella, T., Stratonovitch, P., Trombi, G. and Wallach, D.: Diverging importance of drought stress for maize and winter wheat in Europe, Nat. Commun., 9(1), 4249, doi:10.1038/s41467-018-06525-2, 2018.

Wells, N., Goddard, S., Hayes, M. J., Wells, N., Goddard, S. and Hayes, M. J.: A Self-Calibrating Palmer Drought Severity Index, J. Clim., 17(12), 2335–2351, doi:10.1175/1520-0442(2004)017<2335:ASPDSI>2.0.CO;2, 2004.

Wigley, T. M. L.: The effect of changing climate on the frequency of absolute extreme events, Clim. Change, 97(1–2), 67–76, doi:10.1007/s10584-009-9654-7, 2009.

WMO: Standardized Precipitation Index User Guide, 2012.

World Bank: World Bank Data. Agriculture, forestry, and fishing, value added (% of GDP) | Data, [online] Available from: https://data.worldbank.org/indicator/nv.agr.totl.zs (Accessed 25 October 2018), 2017.

Zargar, A., Sadiq, R., Naser, B. and Khan, F. I.: A review of drought indices, Environ. Rev., 19(NA), 333–349, doi:10.1139/a11-013, 2011.

Zhao, C., Liu, B., Piao, S., Wang, X., Lobell, D. B., Huang, Y., Huang, M., Yao, Y., Bassu, S., Ciais, P., Durand, J.-L., Elliott, J., Ewert, F., Janssens, I. A., Li, T., Lin, E., Liu, Q., Martre, P., Müller, C., Peng, S., Peñuelas, J., Ruane, A. C., Wallach, D., Wang, T., Wu, D., Liu, Z., Zhu, Y., Zhu, Z. and Asseng, S.: Temperature increase reduces global yields of major crops in four independent estimates., Proc. Natl. Acad. Sci. U. S. A., 114(35), 9326–9331, doi:10.1073/pnas.1701762114, 2017.

Zhu, Y., Wang, W., Singh, V. P. and Liu, Y.: Combined use of meteorological drought indices at multi-time scales for improving hydrological drought detection, Sci. Total Environ., 571, 1058–1068, doi:10.1016/J.SCITOTENV.2016.07.096, 2016.

Zipper, S. C., Qiu, J. and Kucharik, C. J.: Drought effects on US maize and soybean production: spatiotemporal patterns and historical changes, Environ. Res. Lett., 11(9), 094021, doi:10.1088/1748-9326/11/9/094021, 2016.

Tables

Table 1. Percentage of analyzed agricultural districts and provinces where wheat and barley are cultivated, at which the maximum correlations per time scale were found using the multi-scalar indices.

Time-scale		1	2	3	4	5	6	7	8	9	10	11	12	18	24
a) Agricultural district data															
Wheat	SPI	18.38	15.38	13.68	9.83	4.27	7.26	2.56	5.13	1.28	3.42	6.41	2.14	5.98	4.27
	SPEI	16.67	14.96	17.09	9.83	6.41	3.42	5.13	4.7	3.42	2.56	3.85	4.27	5.13	2.56
	SPDI	26.07	21.79	13.68	5.13	3.42	2.99	2.56	2.56	2.14	5.13	1.71	3.85	3.42	5.56
Averaged %		**20.37**	**17.38**	**14.82**	**8.26**	**4.70**	**4.56**	**3.42**	**4.13**	**2.28**	**3.70**	**3.99**	**3.42**	**4.84**	**4.13**
Barley	SPI	29.63	14.81	14.81	12.96	0	3.7	3.7	1.85	3.7	1.85	1.85	3.7	3.7	3.7
	SPEI	24.07	12.96	22.22	9.26	1.85	3.7	5.56	3.7	3.7	1.85	0	5.56	1.85	3.7
	SPDI	24.07	14.81	14.81	7.41	7.41	3.7	11.11	1.85	0	3.7	0	0	3.7	7.41
Averaged %		**25.92**	**14.19**	**17.28**	**9.88**	**3.09**	**3.70**	**6.79**	**2.47**	**2.47**	**2.47**	**0.62**	**3.09**	**3.08**	**4.94**
b) Provincial data															
Wheat	SPI	6.98	13.95	23.26	6.98	2.33	6.98	6.98	6.98	6.98	2.33	4.65	4.65	4.65	2.33

	SPEI	9.3	11.63	23.26	11.63	9.3	0	6.98	6.98	2.33	2.33	4.65	4.65	4.65	2.33
	SPDI	13.95	32.56	13.95	2.33	2.33	4.65	4.65	6.98	0	2.33	6.98	2.33	0	6.98
Averaged %		**10.08**	**19.38**	**20.16**	**6.98**	**4.65**	**3.88**	**6.20**	**6.98**	**3.10**	**2.33**	**5.43**	**3.88**	**3.10**	**3.88**
Barley	SPI	7.14	19.05	30.95	9.52	4.76	7.14	0	2.38	2.38	0	0	11.9	0	4.76
	SPEI	11.9	11.9	33.33	7.14	4.76	4.76	7.14	4.76	7.14	0	0	2.38	2.38	2.38
	SPDI	9.52	38.1	14.29	4.76	4.76	7.14	0	0	7.14	0	2.38	4.76	2.38	4.76
Averaged %		**9.52**	**23.02**	**26.19**	**7.14**	**4.76**	**6.35**	**2.38**	**2.38**	**5.55**	**0.00**	**0.79**	**6.35**	**1.59**	**3.97**

Table 2. Percentage of analyzed agricultural districts and provinces where wheat and barley are cultivated, where the maximum correlations with the multi-scalar indices were found. Information in parentheses show the time scale at which the provinces and agricultural districts correlate most and the percentage of the provinces and district.

		SPEI	SPDI	SPI
Agricultural districts	Wheat	36.75 (3, 7.26)	33.33 (1, 7.69)	29.91 (2, 4.70)
	Barley	35.19 (3, 11.11)	44.44 (1, 12.96)	20.37 (1, 11.11)
Provinces	Wheat	58.14 (3, 18.60)	13.95 (24, 4.65)	27.9 (3, 4.65)
	Barley	69.04 (3, 16.66)	9.52 (1, 7.14)	21.42 (5,24, 4.76)

Figures

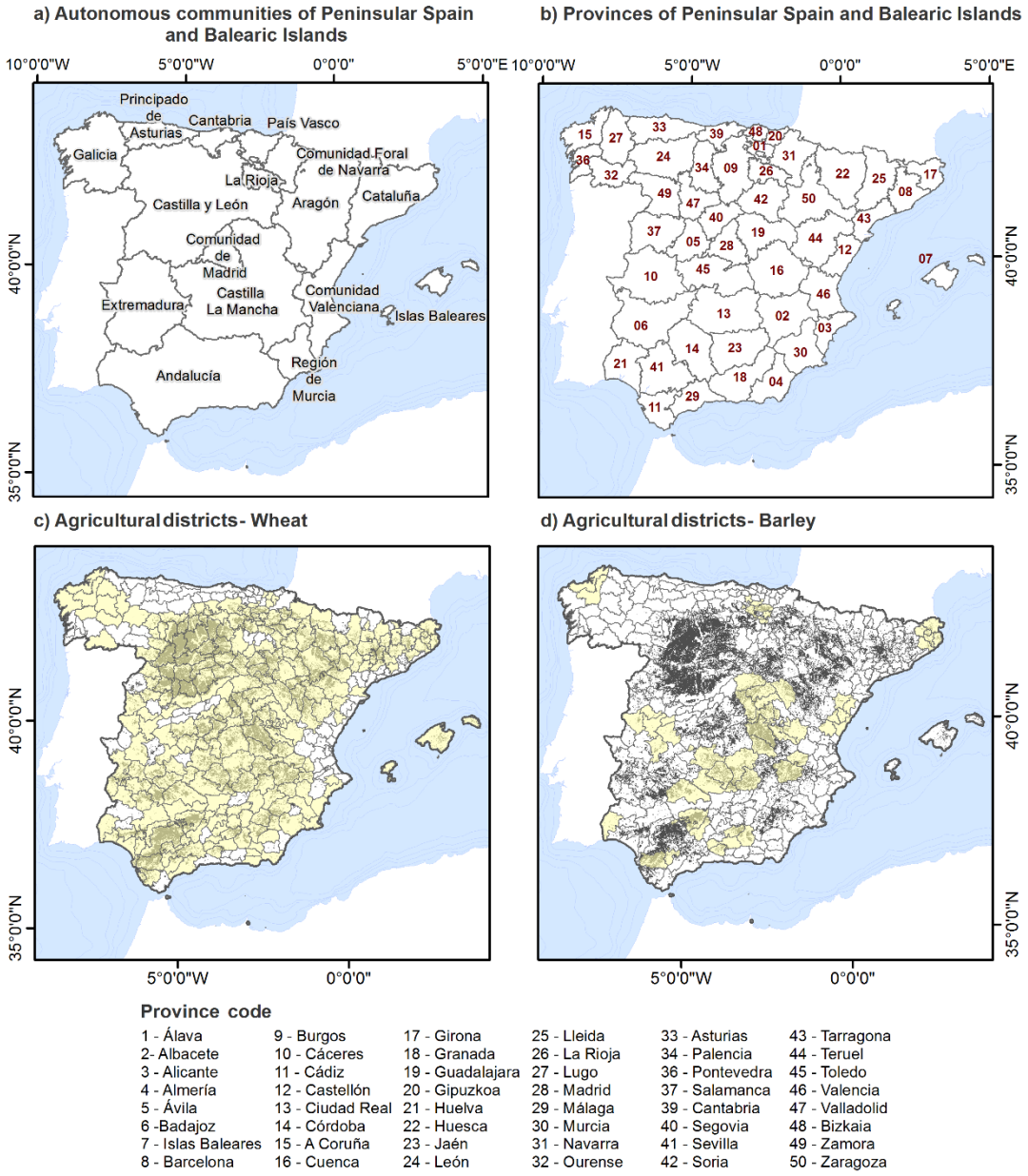

Fig. 1. Location of Spanish Autonomous Communities (a) and provinces (b), and the distribution of agricultural districts having data available (yellow) for wheat (c) and barley (d) yields for the period 1993–2015. Areas where rainfed cereal crops are cultivated (Corine Land Cover 2006) are shown in grey.

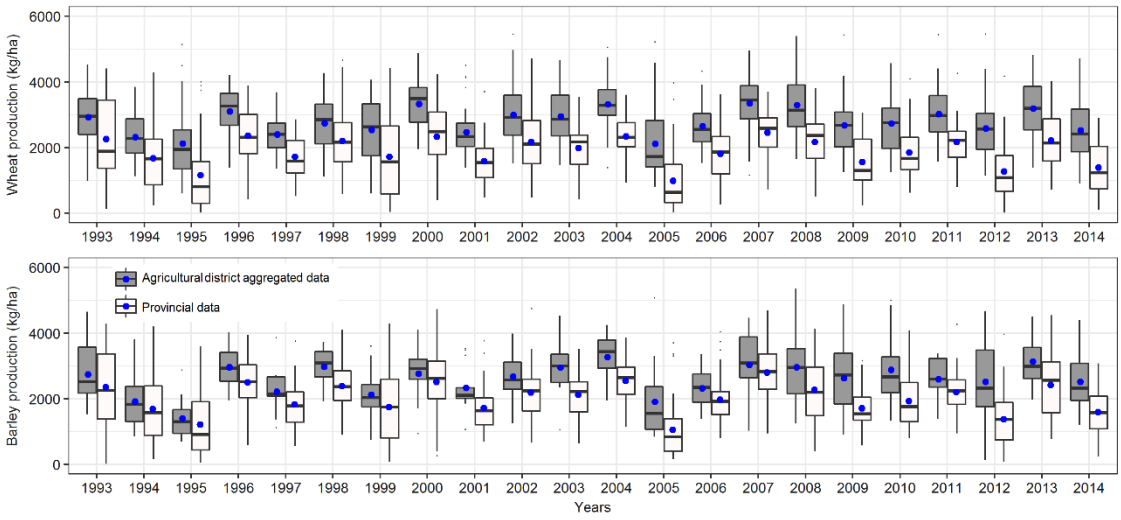

Fig. 2. Temporal series of wheat (top) and barley (bottom) yields for the provincial data, and the aggregated agricultural district data at the province scale for the common period 1993–2014. The solid black line shows the median and the blue dot shows the mean.

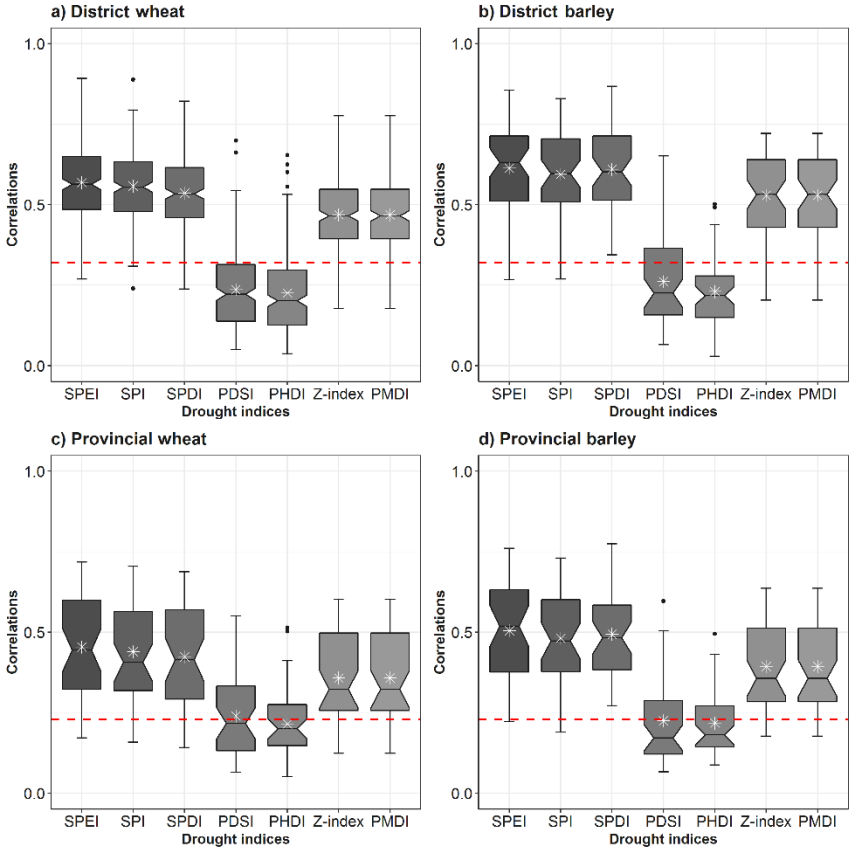

Fig. 3. Box plots showing the strongest correlation coefficients found between drought indices and wheat and barley yields at the agricultural district (a and b) and provincial (c and d) scales, respectively. The solid black line shows the median, the white asterisk shows the mean, and the dashed red lines show the $p < 0.05$ significance level.

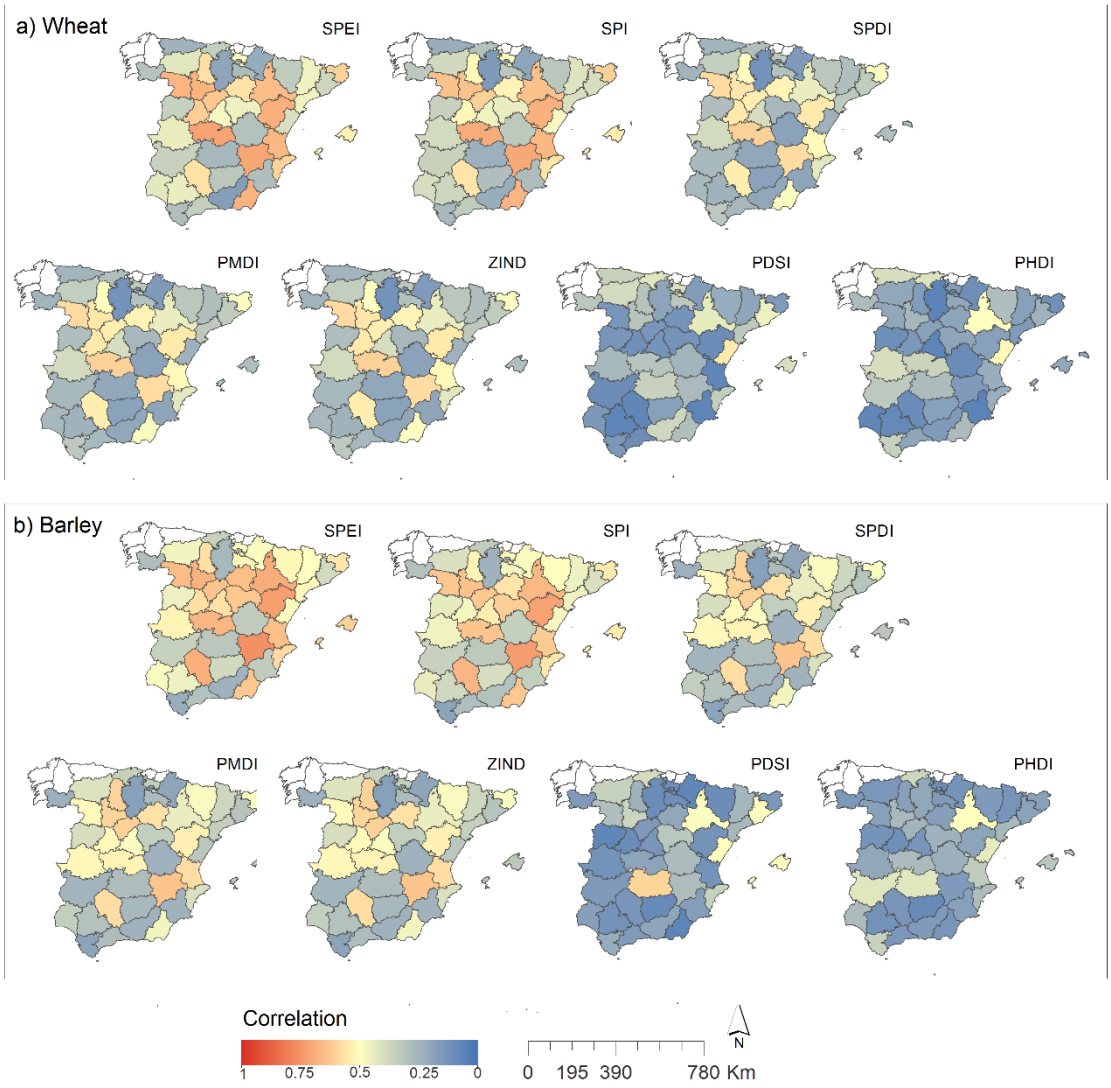

Fig. 4. Spatial distribution of the highest correlation coefficients between the drought indices and the wheat (a) and barley (b) yields at the provincial scale, independently of the time scale.

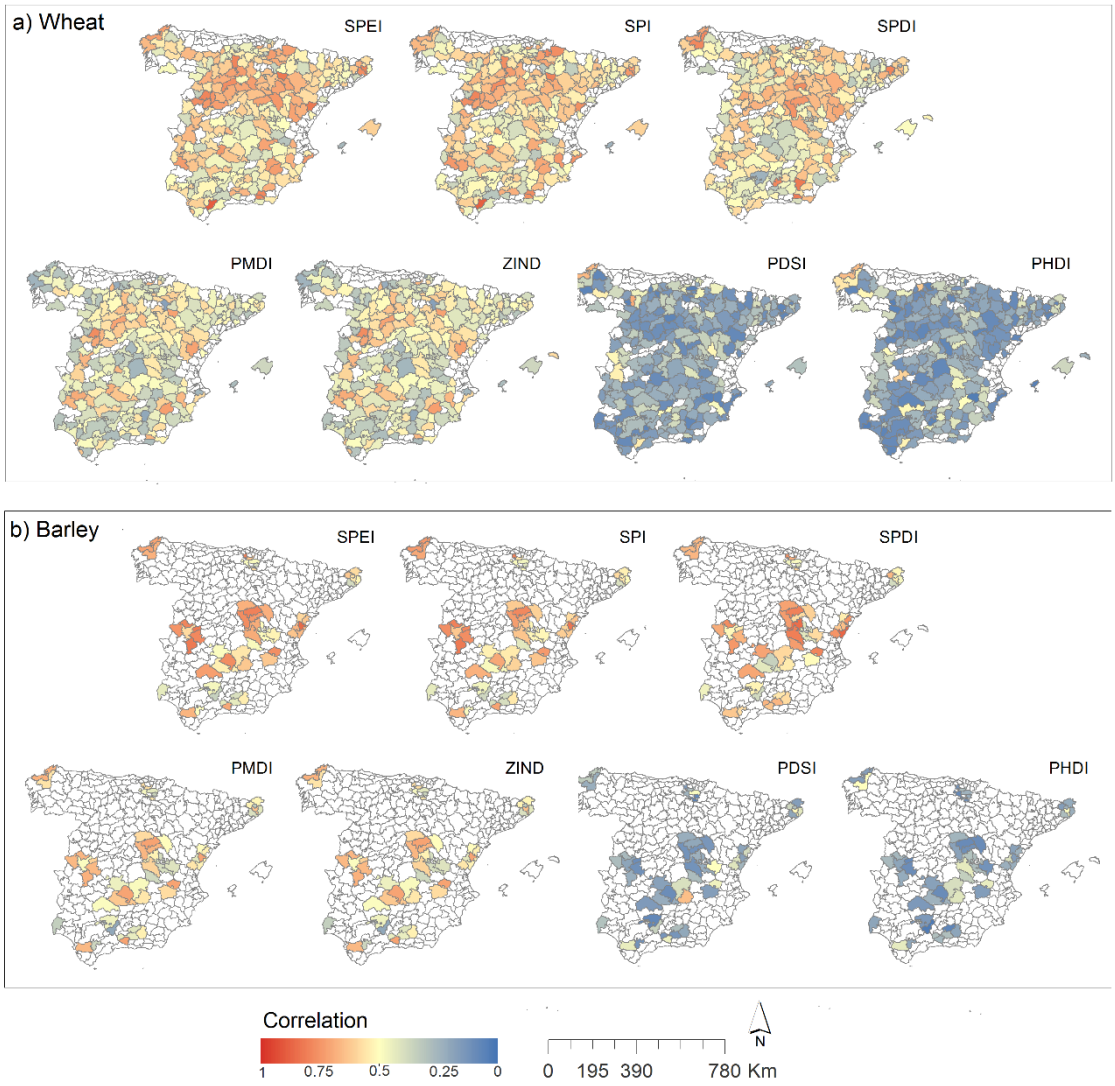

Fig. 5. Spatial distribution of the highest correlation coefficients between the drought indices and the wheat (a) and barley (b) yields at the agricultural district scale, independently of the time scale.

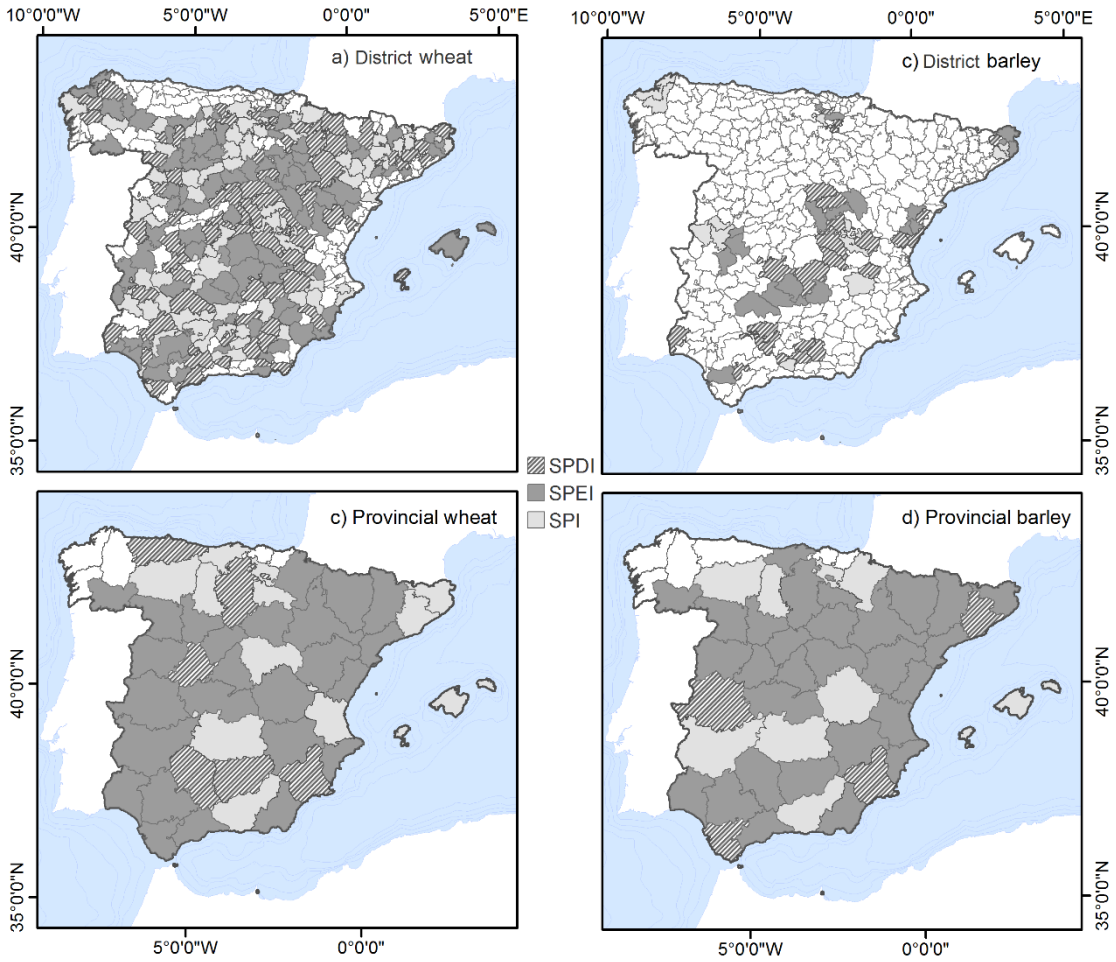

Fig. 6. Spatial distribution of the drought indices having the strongest correlations with wheat (left) and barley (right) at the province (bottom) and agricultural district (top) scales.

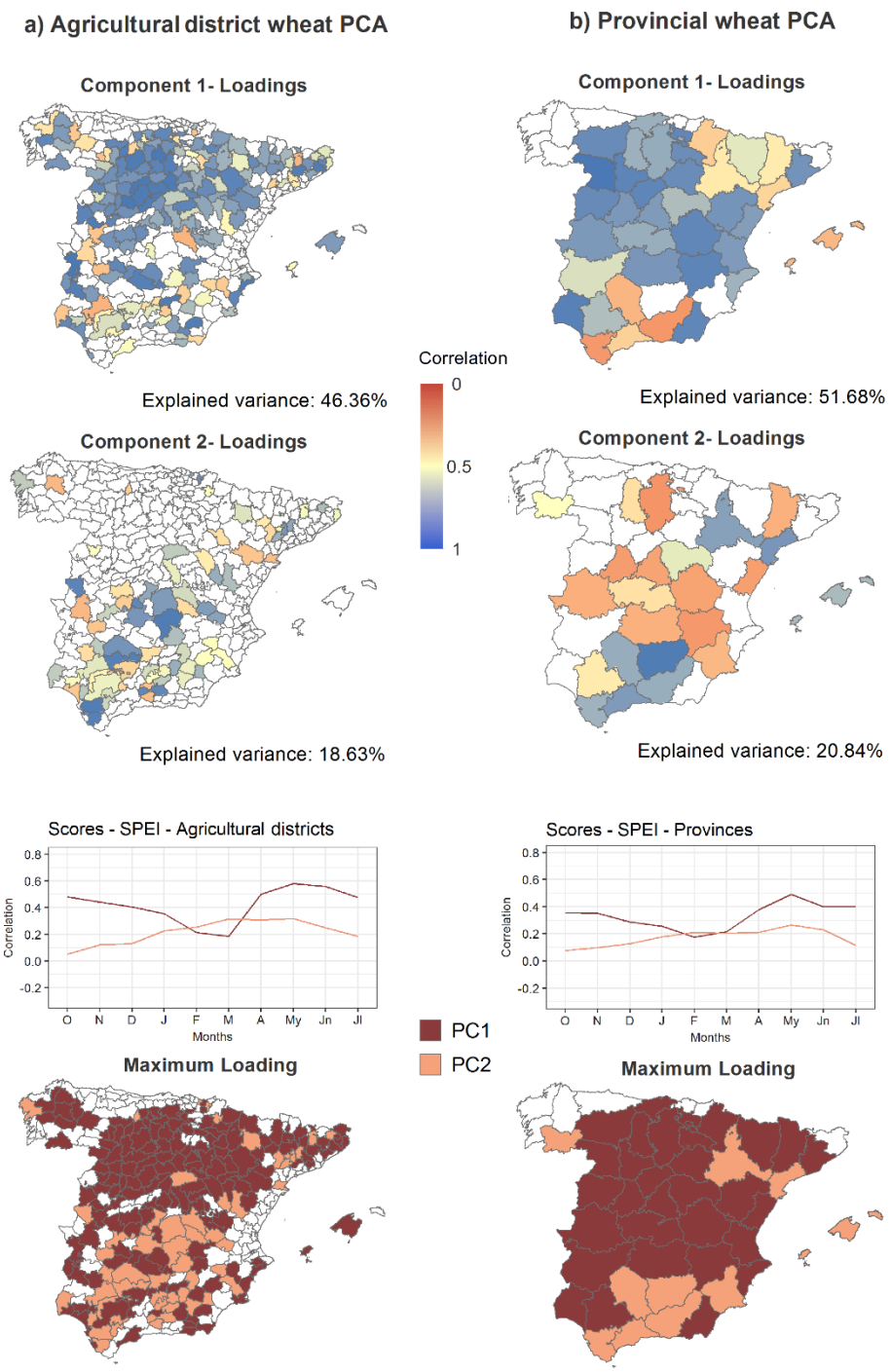

Fig. 7. PC loadings, PC scores, time scales, and maximum loading rules from the PCA for monthly maximum correlation coefficients between the SPEI and wheat yields at the agricultural district (a) and provincial (b) scales, independently of the time scale. The PC loadings and maximum loadings were significant at $p < 0.05$.

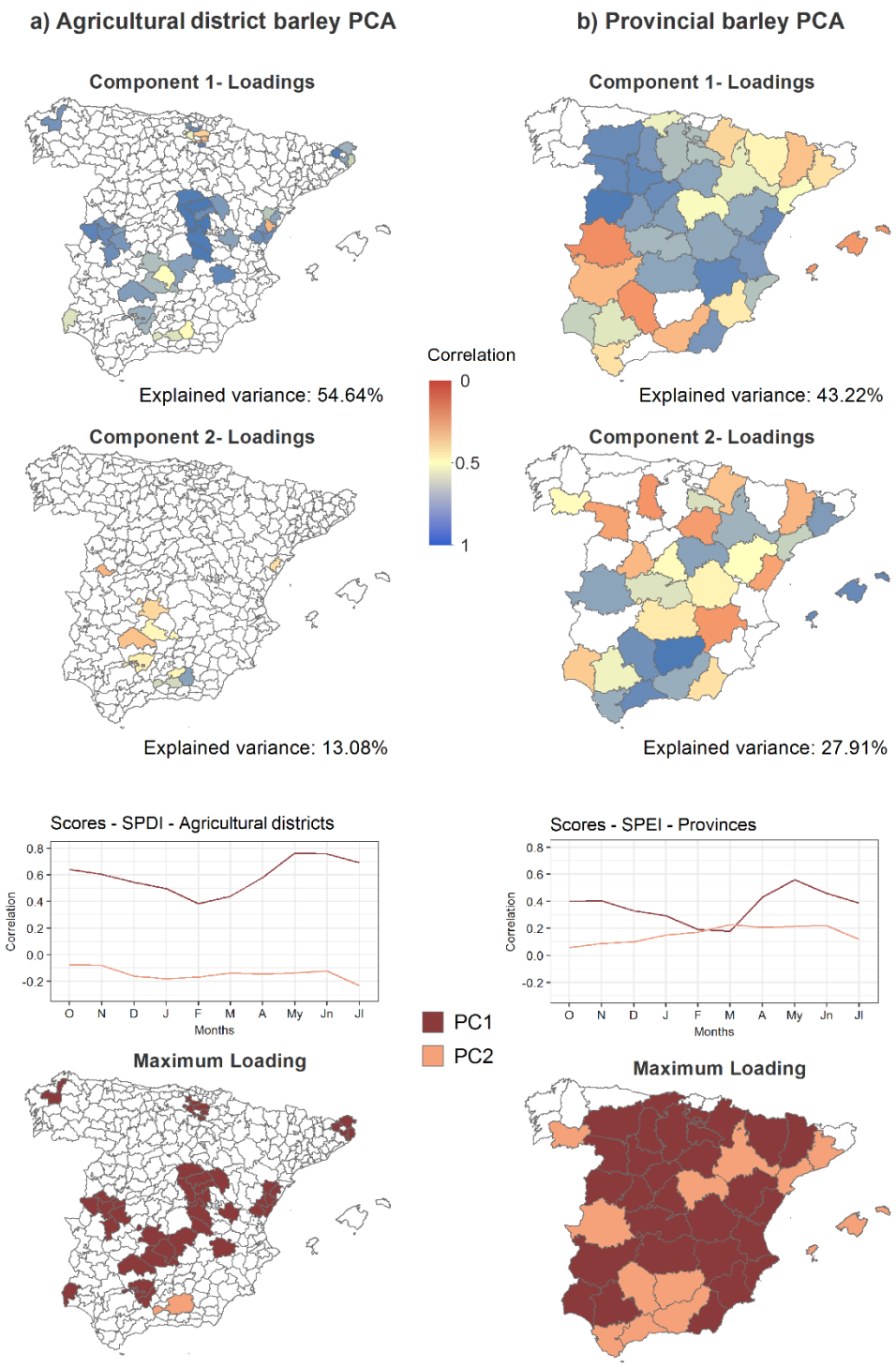

Fig 8. PC loadings, PC scores, time scales, and maximum loading rules from the PCA for monthly maximum correlation coefficients between the SPEI and barley yields at the agricultural district scale (a), and the SPDI and barley yields at the provincial scale (b), independently of the time scale. The PC loadings and maximum loadings were significant at $p < 0.05$.

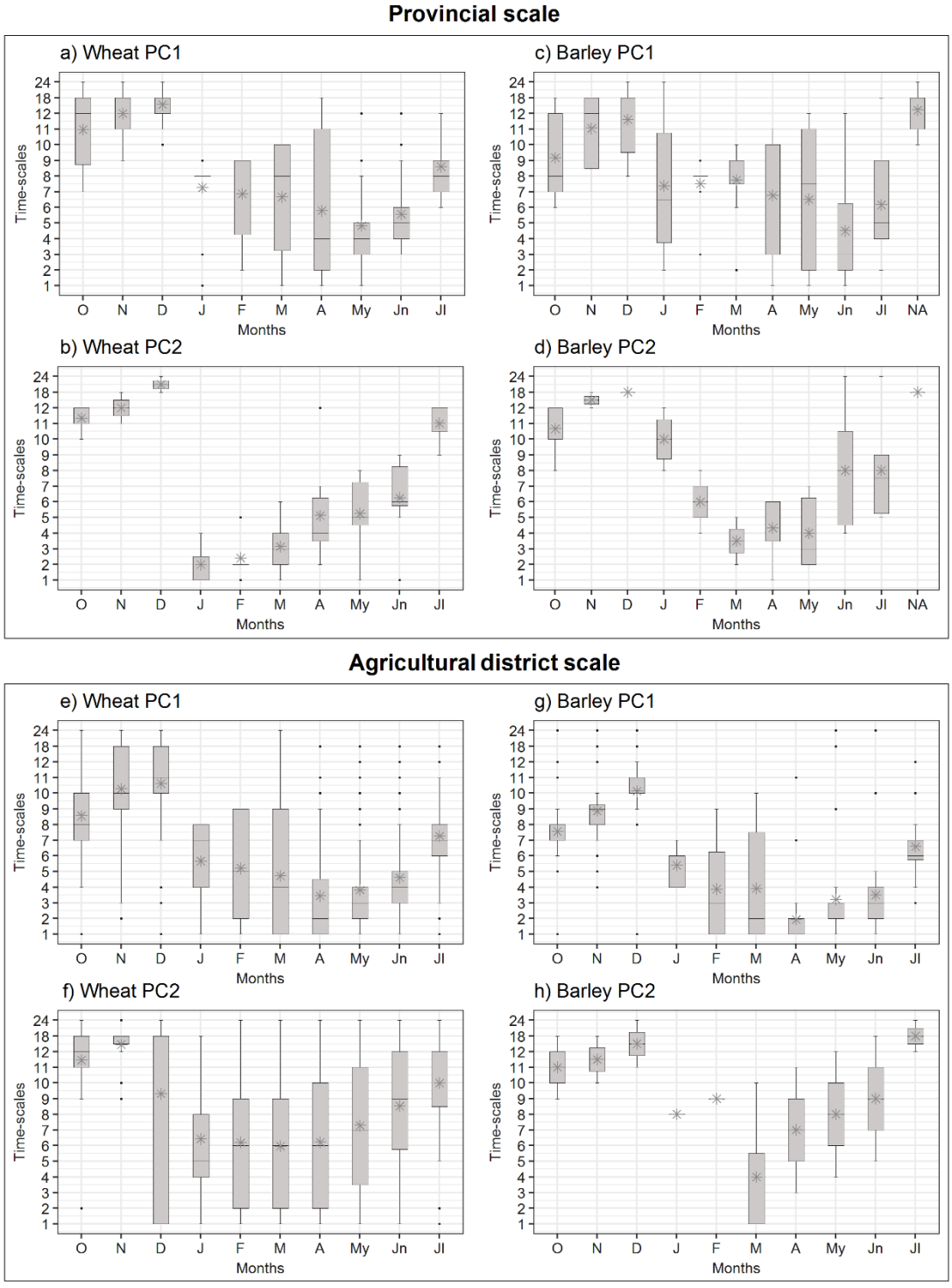

Fig. 9. Box plots showing the time scale at which significant monthly correlations were found in the provinces (top) and agricultural districts (bottom) for wheat and barley for each of the components defined in the PCA

Response of natural river basins to drought in Spain: Evaluation of different climatic drought indices

Marina Peña-Gallardo[1], Sergio Martín Vicente-Serrano[1], Fernando Domínguez-Castro[1], Santiago Beguería[2], Anne Van Loon[3]

[1] Instituto Pirenaico de Ecología, Consejo Superior de Investigaciones Científicas (IPE-CSIC), Zaragoza, Spain.
[2] Estación Experimental de Aula Dei, Consejo Superior de Investigaciones Científicas (EEAD-CSIC), Zaragoza, Spain.
[3] School of Geography, Earth and Environmental Sciences, University of Birmingham, Edgbaston, Birmingham, UK

Abstract

In this study, we use seven climatic drought indices to determine the influence of climatic drought to streamflow droughts in 226 undisturbed river basins in peninsular Spain covering the period 1962-2013. At the same time, we define spatial patterns in the response of streamflow to climatic drought. The study was conducted relating the climatic component represented by three multi-scalar drought indices -the Standardized Precipitation and Evapotranspiration Index (SPEI), the Standardized Precipitation Index (SPI), the Standardized Precipitation Drought Index (SPDI)- and the self-calibrated version of four Palmer's indices (PDSI, PHDI, Z-index and PMDI) with the hydrological-based Standardized Streamflow Index (SSI). Results demonstrated that multi-scalar drought indices outperform the Palmer drought indices (uni-scalars) thanks to their ability of determining climatic anomalies for different cumulative periods. Undisturbed river basins mainly responded at short time-scales of the different climate indices and the precipitation variability is the main driver of streamflow drought severity. Our results also showed that different non-climate factors have a great influence to explain the different times of response of hydrological drought to climate drought characteristics.

Key words

Hydrological drought, streamflow, drought indices, time scales.

1. Introduction

Among natural extreme hazards, drought entails one of the most difficult to define and characterize due to the complexity of defining the onset and not only the climatic, but also the anthropogenic factors involved in the development of an event (Lloyd-Hughes, 2014; Van Loon et al., 2016; Wilhite and Glantz, 1985). The main cause (but not the unique) of drought is the anomalous reduction of precipitations over a certain period of time, triggering what is known as meteorological drought. Climate anomalies such as precipitation shortages and/or increased atmospheric evaporative demand may propagate to the hydrological cycle by means of soil moisture deficits, streamflow, lake levels, reservoir storages etc., producing a hydrological drought (Barker et al., 2016; Tallaksen and Van Lanen, 2004; Van Loon, 2015; Van Loon and Laaha, 2015).

There are several knowledge gaps on the whole interaction between meteorological droughts and their propagation throughout the entire hydrological system, including streamflow (Haslinger et al., 2014) and groundwater (Lorenzo-Lacruz et al., 2017; Marchant and Bloomfield, 2018). This inherent complexity contribute to the uncertainty of pinpointing the beginning of the event, identifying the trigger mechanisms and constraining factors – naturals or not – and quantifying the impacts caused on water resources (generally linked to socio-economic activities) and the environmental damages associated to a drop in flow regime (e.g. increase of water temperature, changes in aquatic ecosystems, etc.)(Mosley, 2015).

Besides, the different response times of the hydrological system to precipitation deficits vary significantly. Previous studies have shown that the nature of hydrological variables determine different temporalities, for example, lowering in water retained by soils shows up faster than groundwater levels or reservoir storages rates (Barker et al., 2016; Bloomfield et al., 2015; Lorenzo-Lacruz et al., 2010; Peters et al., 2005; Scaini et al., 2015). Catchment physiographical properties also determine different temporal patterns. In a recent study, Peña-Gallardo et al. (2019) analyzed the hydrological response to drought in relatively undisturbed river basins across the U.S. emphasizing the importance of environmental and physical characteristics to explain different modes in the response of hydrological to meteorological droughts. For their part, Van Loon and Laaha, (2015) demonstrated that catchment properties related to climate control are the main explaining factors on streamflow drought duration in Austria. Similarly, many studies (Batalla et al., 2004; López-Moreno et al., 2009; Tijdeman et al., 2018; Vicente-Serrano et al., 2017) have focus the attention on how the human influence, mainly reflected on water regulation, management and demand, but also land-use/land-cover conditions, biases the hydrological response to meteorological droughts, sometimes mitigating or intensifying the intensity, frequency or duration of these events (Liu et al., 2019; López-Moreno et al., 2009; Vicente-Serrano et al., 2017).

Given the importance of the effects of hydrological droughts, proper management strategies as mitigation plans and early warning systems are necessary in order to assess adequately and effectively drought severity (Huang et al., 2017). There are multiple methods for characterizing the effects of drought (e.g. remote sensing derived information (Ayehu et al., 2019)) but since last century, scientific community have made an effort developing multiple drought indices, commonly used nowadays for operative monitoring purposes. Reviews as the conducted by

Mishra and Singh, (2010) or more recently Mukherjee et al. (2018) provide a comprehensive evaluation of the very diverse drought indices designed to quantitatively analyse drought characteristics (duration, severity and intensity). Particular consideration should be given to Palmer (1965) who proposed for the very first time a drought index, the Palmer Drought Severity Index (PDSI) that allows identifying independent drought periods and objectively determining their severity. For their part, Mckee et al. (1993) introduced the time-scale concept with the Standardized Precipitation Index (SPI), recognized by the World Meteorological Organization as the reference drought index (Hayes et al., 2011; WMO, 2012). This novel concept let identifying drought events in any natural system and region under very diverse climatic conditions at different time scales (Vicente-Serrano et al., 2012), in particular the hydrological system response time to climate conditions, which is well known that fluctuate in time and among regions (Barker et al., 2016; López-Moreno et al., 2013; Tetzlaff et al., 2008).

Many studies have assessed the relationship between climatological and hydrological drought and the propagation through different parts of the hydrological system by performing meteorological drought indices and relating them with streamflow discharged data. For example, Lorenzo-Lacruz et al. (2010) evaluated the impact of climatic droughts in a highly regulated basin in the Tagus river (Spain), finding significant correlations between two multi-scalar drought indices and river discharges. Barker et al. (2016) studied the propagation of drought in the 121 near-natural UK catchment identifying significant temporal and spatial differences in the relationship between the SPI and standardized streamflow. For their part, Loukas and Vasiliades, (2004) reported significant and strong correlations between the 2 to-4-month SPI and surface runoff in Greece, whereas soil moisture responded better at 1 to-3-month SPI. Similar results were noticed in the river flows of ten regions in China by Zhai et al. (2010).

The stated drought indices are generally climate-based (precipitation and the AED are the main input variables). Wittingly the non-linear processes associated to climate and natural systems interactions, it is often discussed the appropriateness or not, of applying a single climate-based drought index to characterize a particular drought event (e.g. using a meteorological index to analyse a hydrological drought) (Van Lanen et al., 2013). Integrated systems specifically designed for a risk management also wander incorporating meteorological variables to assess other types of drought (Bachmair et al., 2016) (e.g. European Drought Observatory (EDO), http://edo.jrc.ec.europa.eu or the South Asia Drought Monitoring System, http://dms.iwmi.org).

Mediterranean region is characterized by a high seasonal and interannual variability of precipitation, being recurrent the long and severe drought events. Climatic characteristics cause that water resources are very limited in Mediterranean river basins. It is therefore necessary the identification of appropriate management tools able to quantify the impact of climatic drought on streamflow.

Previous studies have characterized the connections of drought through the hydrological cycle in Spain (e.g. López-Moreno et al. (2013); Lorenzo-Lacruz et al. (2013), (2017), Vicente-Serrano et al.,(2015), (2017)), however there are no previous studies evaluating the performance of different climatic drought indices. Moreover, the existing studies focused on a large diversity of basins, several of them affected by large human influences, making impossible to isolate the

possible differences in the response of hydrologic to climatic droughts in natural basins. For these reasons, in this study we analyzed the spatio-temporal response of a hydrological drought index in 226 headwaters basin (avoiding the anthropogenic signal), to climatic drought. To achieve this goal, we provide a performance review for seven of the most well-known multi-scalar (the Standardized Precipitation Index –SPI- , the Standardized Precipitation and Evapotranspiration Index –SPEI-, the Standardized Palmer Drought Index – SPDI-) and uni-scalar (the Palmer Drought Severity Index –PDSI-, the Palmer Drought Hydrological Index –PHDI-, the Palmer Moisture Anomaly Index –Z-Index-, the Palmer Modified Drought Index – PMDI -) drought indices in Peninsular Spain in the period 1962-2013. At the same time, we analysed temporal and spatial patterns of streamflow response to climatic droughts in these basins.

2. Data and methods

2.1. Datasets

2.1.1. Climatic data

Meteorological information (precipitation, maximum and minimum temperature) was obtained from a gridded dataset at 1.1 km resolution available for peninsular Spain and the Balearic Islands at weekly scale for the period 1962-2013. This dataset comprises a larger number of meteorological variables such as relative humidity, wind speed and sunshine duration. The Spanish National Meteorological Agency (AEMET) provided original data. An exhaustive quality control and homogenization of data were conducted before gridding process. More detailed description about the complete procedure of the dataset construction can be found in Vicente-Serrano et al. (2017). The AED was inferred using the available information and following the Penman-Monteith's parametrization recommended by FAO (Allen et al., 1998). Weekly data was transformed to monthly for the different analysis. The water holding capacity information was obtained from the European LUCAS based topsoil data (Ballabio et al., 2016).

2.1.2. Streamflow data

Most of the streamflow series used in this study were provided by the Ministry of Agriculture's CEDEX (http://ceh-flumen64.cedex.es/general/default.htm), while the stations located within the autonomous communities of Andalusia (https://www.agenciamedioambienteyagua.es/) , Basque Country (http://www.uragentzia.euskadi.eus/u81-0002/es/) and Catalonia (http://aca.gencat.cat/ca/inici) were obtained from the corresponding autonomic agencies websites. A network of 1204 gaugin stations in peninsular Spain were collected, however the selection was restricted to those stations with less than the 25% of missing data for the analysed period. In order to work with no missing values in the series, we developed a reconstruction and gap filling procedure based on nearby neighbour and using the whole available stations. Series from 472 gaugin stations widespread distributed were filled. Further details about the followed methodology and the statistical validation of the reconstructed series are outlined in Vicente-Serrano et al. (2019, *submitted*). From the final series, we selected a total of 226 stations located in the headwater of major basins, excluding those affected by reservoirs or any other known human regulation activity that may affected the natural signal of streamflow. Figure 1 illustrates the spatial distribution of the selected gauging stations.

2.1.3. Physiographical and land cover information

A digital elevation model (DEM) at 400 m resolution for the entire Iberian Peninsula was obtained from the National Center for Geographic Information (CNIG) (http://centrodedescargas.cnig.es/CentroDescargas/catalogo.do?Serie=LIDAR). This DEM served to create drainage and direct flood grids that served to delimitate the drainage basins boundaries associated to each gaugin station. For this purpose we used ArcGis watershed tool and the gauging stations were used as the pour points. The resulting drainage basins were used as masks to extract the average climatic and physiographical characteristicis in each basin.

The National Geological Map provided by the Spanish Geological Survey (IGME) (http://info.igme.es/cartografiadigital/geologica/Magna50.aspx?language=en) was employed to classify the lithological units of Spain. The three major soil classes considered are: chalky, clay and siliceous soils. The land cover map (1980 - 1990) developed by the Spanish Ministry of Agriculture (https://www.mapa.gob.es/es/cartografia-y-sig/publicaciones/agricultura/mac_1980_1990.aspx), originally at the spatial scale of 1:50,000 and later rasterized at 1.1 km resolution was used to a better knowledge of the land classes present in each basins.

2.2. Methodology

2.2.1. Hydrological drought identification

Standardized Streamflow Index (SSI)

Streamflow magnitude and seasonality change considerably depending on the river regime and time, making difficult to compare time series from different regions. To solve this matter, streamflow series are usually standardized letting the comparison among stations not just in space but also in time. Despite streamflow data do not adjust to a unique statistical distribution function, many of the standardized indices in the literature lack of the flexibility to find the most suitable distribution in each time series (Lorenzo-Lacruz et al., 2013). Here, for standardizing the monthly streamflow series we used the Standardized Streamflow Index (SSI) following the methodology described in Vicente-Serrano et al. (2012). Thus, probabilities are obtained by fitting one of the multiple candidate probability functions (e.g. the General Extreme Value, the Pearson type III, the log-logistic, the log-normal, the generalized Pareto or the Weibull distributions). Depending on the robustness found in the adjustment between the L-moments of the sampled station and the L-moments of the specific selected distribution, one or another distribution is fitted. Probabilities are ultimately transformed to *z*-scores using Abramowitz and Stegun (1970) approximation.

2.2.2. Climatic drought indices

Palmer Drought Severity Indices (PDSIs)

The Palmer Drought Severity Index (PDSI) was enunciated by Palmer, (1965), it is a worldwide known meteorological drought index used for estimating relative dryness. Originally, the PDSI is based on the amount of moisture departure, defined as the 'Climatically Appropriate for Existing Conditions' (CAFEC), within a two-layered soil moisture simulation for a specific region. Variations of this index include the Palmer hydrological drought index (PHDI), the Palmer moisture anomaly

index (Z-index), and the Palmer modified drought index (PMDI). Even though these indices are broadly applied for monitoring purposes and quantification of droughts, they have important limitations to monitor drought conditions (Vicente-Serrano et al., 2011), lacking of multi-scalar features, having a complicated formulation and not being comparable among regions (Alley, 1984; Doesken and Garen, 1991; Guttman, 1998). In this study we used the modified version of PDSIs, the self-calibrated, introduced by Wells et al. (2004), which allows better spatial comparability.

Standardized Precipitation Index (SPI)

Introduced by Mckee et al. (1993), the Standardized Precipitation Index (SPI) provides the possibility of identifying either wet and dry conditions at different time scales. This index is worldwide recognized for been a useful tool for monitoring and early warning purposes (WMO, 2012). Among its strengths, it is worth mentioning the less number of variables required in the calculation in comparison to other drought indices. The SPI transforms the sum of monthly precipitation into a probability function fitting a gamma distribution and probability is transformed to standardized units (with mean equal to 0 and variance equal to 1), enabling spatial comparison across regions with different climates characteristics.

Standardized Precipitation Evapotranspiration Index (SPEI)

Vicente-Serrano et al. (2010) developed the Standardized Precipitation Evapotranspiration extending the conceptualization of the SPI considering the AED as another relevant factor that affects drought severity. Previous studies have acknowledged the repercussion of warming on crop productions (Asseng et al., 2014), forests decay (Camarero et al., 2015) and streamflow (Vicente-Serrano et al., 2014) around the world, highlighting the importance of using drought indices that include temperature as principal variable. The SPEI first computes monthly climate balances (D_i) using monthly precipitation and reference evapotranspiration values. Monthly D_i are later aggregated at different time scales and transformed to normal standardized units using a 3-parameter log-logistic distribution.

Standardized Precipitation Drought Index (SPDI)

The standardized precipitation drought index (SPDI) presented by Ma et al. (2014), combines PDSI and SPEI schemes. The SPDI accumulates at various time scales internal water balance anomalies calculated in the PDSI scheme, which are transformed into standardized units fitting a standard normal distribution.

Hereafter, we used the terminology multi-scalar to designate those indices that can be calculated at different time scales - SPEI, SPI, and SPDI – and uni-scalar to the PDSIs.

2.2.3. Statistical analysis

Considering the whole series of streamflow, that is not differentiating between high and low flows periods, we first examined the link between the SSI and the different climatic drought indices and determined which index or indices resulted the most suitable for monitoring streamflow drought conditions. This relationship between the climatic drought indices -summary of the climatic conditions-, and the standardized streamflow represented by the SSI was conducted calculating Pearson's correlation coefficients. As multi-scalar drought indices were calculated at scales from

1- to 48-months, a total of 576 series (12 months x 48 time-scales) of correlations were obtained for each basins in the case of SSI and multi-scalar indices and 12 series for the SSI and uni-scalar indices.

The time-scale (in the case of multi-scalar indices) at which the strongest correlation occurs between climatic drought indices and SSI is a priori unknown. For this reason, we calculated the correlations at time-scales between 1- and 48-months and for the different monthly series, retaining the maximum *r* value in each basin independently on the time-scale or month in which it is recorded (only significant correlations $p < 0.05$ were account). A t-test was conducted to investigate possible significant differences or similarities in the correlation coefficients obtained between the SSI and the different climatic drought indices. Once the index with best response to streamflow was determined, we aimed to explain the relationship between the maximum correlations and the climatological characteristics in order to find similarities, or not, in the response to drought of the selected basins with different averaged climatic conditions. At the same time, we extracted the percentage of surface in each basin corresponding to the three basic lithological categories (clay, chalk and siliceous soils) and vegetation cover (irrigated and rain-fed croplands, meadows and shrubs, conifers and deciduous forests).

3. Results

3.1. Relationship between climatic drought indices and the standardized streamflow index

The magnitude of the Pearson's correlation coefficients between the seven climate drought indices and the SSI revealed, in general, that strong and significant relationship exist among the SSI and the climate drought indices in the majority of basins (Figure 2). However, substantial differences were glimpsed between indices. Independently on the month of the year and the drought time-scale, higher correlation coefficients were found considering the different multi-scalar indices (SPI, SPEI and SPDI), with average correlation higher than 0.8 in all of the cases, while correlations tended to be lower with the Palmer indices. The PHDI resulted the drought index with the weakest relation with SSI ($r = 0.52$). The PDSI and the PMDI showed higher median correlation values ($r = 0.57$ and $r = 0.58$ respectively) and almost all the basins recorded significant correlations. Among the Palmer indices, the Z-index showed the strongest correlation with the standardized streamflow, this index was among PDSIs the one that performed very similar to the multi-scalar. The median correlation value was high ($r = 0.78$) but also presented higher dispersion between basins and recorded non-significant correlations. On the other hand, the SPEI, the SPI and the SPDI reached the highest median correlations (SPEI $r = 0.86$, SPI $r = 0.85$, SPDI $r = 0.86$) with little differences among them. Multi-scalar drought indices tended to perform better than the PDSIs, being able to monitor streamflow droughts more effectively.

The spatial distribution of the maximum correlations between the SSI and the different climate indices is illustrated in Figure 3. In the case of the PDSI, the PHDI and the PMDI low to medium correlations values (r = 0.4 - 0.6) were found in almost all the territory. The PHDI showed high correlations ($r \geq 0.8$) in the headwater basins located in the Segura, Guadiana and Ebro major basins, these values were recorded by the PDSI and the PMDI in the same basins and a few others located in the Guadalquivir, Tajo, Duero, Minho and Jucar major basins. The pattern showed by the Z-index varied significantly respecting the other PDSIs. Medium to high ($r = 0.5 – 0.8$)

correlations predominated in almost all the basins. Exceptionally, low correlations were registered in the basins of the Segura river, as well as in southwestern regions of Ebro river basin and basins located in northern Spain. High correlations between the multi-scalar drought indices and the SSI with the strongest correlations coefficients (average $r \geq 0.8$) were found equally distributed in the territory. On the contrary, lower correlations (average $r = 0.5 - 0.6$) were observed, once again, in the basins of the Segura river and northern of the internal basins of Catalonia.

The monthly correlations between the SSI and the seven drought indices are showed in the Figure 4. In general, higher correlations were observed from February to May, especially in the multi-scalar indices (average $r \geq 0.8$) and the Z-index (average $r > 0.6$), but they are also in general high from May to September. The magnitude of the correlations considering the PDSI, the PHDI and the PMDI tended to be low and under significance level in February and March, while the months with lower correlations for the multi-scalar indices and the Z-index were November and December with average correlations below 0.6 and 0.4 respectively. The three multi-scalar drought indices showed little differences in the magnitude of their correlations.

Figure 5 shows the similar magnitudes in the maximum correlations found between the multi-scalar drought indices and the standardized streamflow. Little differences have been observed between the SPEI, the SPI and the SPDI, the level of agreement between pairs of indices is quite notable: the SPEI/SPDI or the SPEI/SPI were $r = 0.98$, while the SPDI/SPI was $r = 0.97$. Comparing the magnitudes of these multi-scalar drought indices with the Z-index, we noticed that the agreement was weaker.

Among the analysed climatic drought indices correlated with the SSI, the multi-scalar drought indices were those that recorded the maximum number of basins where highest correlations were found (Figure 6). Some of the basins, mainly located in the eastern of major river basins, showed stronger agreement with one of the PDSIs, but that percentage ranked for the 12.24% of basins, being the Z-index the most representative (8.30%) and the PDMI the last (0.44%). The SPDI pointed out as the index in which the greatest percentage of basins found the best agreement (41.92%) followed by the SPEI (25.33%) and the SPI (20.52%). Nevertheless, there are not significant differences among the different multi-scalar indices. The results of the t-test performed with the complete correlation matrices (i.e. considering the 48 time steps and months of the year) showed that in less than the 15% of the basins there were significant differences between the correlations recorded between the SPEI and the SPDI, and less than the 30% between the SPEI/SPI and the SPDI/SPI. Next section uses the results based on the SPDI that shows in general a bit higher correlations.

3.2. Seasonal response of the SSI to the different climatic drought indices

Figure 7 displays the spatial distribution of the monthly maximum correlations recorded between the SPDI and the SSI irrespective on the time-scale. In general, high correlations were recorded in most of stations but during summer months, the weakest correlations were observed. Similar spatial patterns and magnitude of correlations were found with the SPI and the SPEI results (Supplementary Figure 1 and Supplementary Figure 2).

Table 1 summarized the percentage of basins with the highest correlations between the three climate drought indices and the SSI as a function of the drought time scale at which this correlation is found. More than the 62% of basins presented strongest correlations at short time-scales. The 11% of basins correlated more at 1-month, the 14.83% did it at 3-month while more than the 37% found the best agreement with climatic conditions at the 2-month scale.

Maximum monthly correlations between the SPDI and the SSI tended to correspond to short time-scales (1 to-3 months) in more than the 80% of the analysed basins (Figure 8). This percentage varied depending on the observed month. For example, in June approximately the 35% of the basins found the highest correlations at medium to longer time-scales (ranging between 7 and >25 months). It is noteworthy that the majority of the basins, mainly located in Iberian (northeast) and Central System, and Cantabrian range (north) showed, systematically, a stronger dependency to long time-scales (> 10 months). Results for the SPEI/SSI and SPI/SSI (Supplementary Figure 3 and Supplementary Figure 4). Overall, the differences in the times of response of streamflow droughts to climatic drought suggest the complexity associated to the different mechanisms that determine this link in river basins.

3.3. Physiographical and climatological characteristics

In supplementary figures 5-9 we summarized the temporal relationship between the maximum correlations found between the SSI and the SPDI, and the climatic variables. Regarding precipitation (Supplementary figure 5), during autumn and winter months a more disperse pattern than the rest of the months, in the magnitude of correlations was observed. Strong values were recorded in basins either with low or high averaged precipitations. Similarly, maximum and minimum temperatures (Supplementary figures 6 and 7), atmospheric evaporative demand (Supplementary figure 8) and average streamflow (Supplementary figure 9) showed a similar response to climatic drought independently on the average climatic conditions and month at which the maximum correlation is found in the basins.

Physiographical characteristics displayed in Figure 9 showed that the average water holding capacity (whc) in most of the basins is estimated in the range of 45-55 mm (Figure 9a). Spatial differences demonstrated that some basins present higher rates of whc, mostly corresponding to those basins that recorded the maximum correlations between the SSI and the climatic drought indices at longer time-scales. These basins also matched with those characterized by high percentages of chalky soils (Figure 9b) mostly located in the north and east of Spain (corresponding with calcareous mountain streams). Probably, chalk aquifers associated to these basins are the responsible to low infiltration dynamics that determine the slow response to drought observed in previous results. Clay soils mainly dominate in basins from the north and northeastern Spain although in the south, also most of the basins from Andalusia Mediterranean basins showed a high percentage of clays (Figure 9c). These basins also presented high to medium rates of whc due to the high retention capacity of these type of permeable soils, tended to response also at medium to longer time-scales. Lastly, most of the basins with major percentage of siliceous soils are located in humid regions of Spain (northwest and central of Spain) and in some tributaries of Guadalquivir river with headwaters located in Sierra Morena) (Figure 9d). Basins from central Spain and Sierra Morena showed the lowest rates of whc but in contrast, the rates recorded by Galician basins were higher.

4. Discussion.

In this study we have performed a dual analysis. On one hand, we provided a comprehensive view of the performance of seven climatic drought indices and their efficacy to detect streamflow response in 226 unregulated basins in peninsular Spain for the period 1962-2013. On the other hand, we tried to identify spatial patterns in the response of streamflow to climatic drought indices. To this end, we regarded the association of the SPEI, the SPI, the SPDI and the PDSIs with the standardized streamflow (SSI) by calculating Pearson's correlation coefficients. A comparison between the seven drought indices results revealed that the magnitude of the correlation coefficients vary significantly among type of indices. Aware of the shortcomings associated to the PDSIs (Vicente-Serrano et al., 2011), authors noticed that the median magnitude of the maximum correlations achieved by any of the PDSIs was relatively higher than what it was expected. More specifically, the Z-index showed to be more sensitive in reflecting the manifestation of streamflow droughts compared to the rest of the PDSIs. In Iberian Peninsula little references to previous studies performing any of the PDSIs for hydro-climatological purposes were found (Ortega-Gómez et al., 2018; Vicente-Serrano et al., 2012; Von Gunten et al., 2016). In the context of Mediterranean region, Vasiliades and Loukas, (2009) conducted a similar investigation in a basin located in Thessaly (Greece) where they correlated simulated streamflow values with three Palmer drought indices and a modification of the PDSI. The observed correlations ranged between 0.69 and 0.74 in the case of the Z-index, 0.78 and 0.80 for the PDSI and 0.69 and 0.71 for the PHDI. These magnitudes are in line with the ones observed in our study. Even the PHDI, was also found by these authors as the Palmer family index which exhibited the lowest maximum correlations. Contrary to their results that set up the maximum correlations of the PDSIs analysed in December and January, we found May as the month in which any of the four PDSIs registered the highest median maximum correlations. We interpret these high correlations in May as a consequence of the soil moisture conditions of the preceding months, usually corresponding with the rainy season over a large part of the region. The PDSI drought detection ability relates with annual time-scales while the Z-index, as a soil moisture-drought index, is more sensitive to water deficiencies at shorter time-scales (Wang et al., 2015). At this respect and as we will tackle later, the Z-index was found the fourth best-correlated drought index here assessed, displaying a similar performance to the multi-scalar drought indices and depicting an outperformance in comparison with the other PDSIs. Similarly to our observations, Vicente-Serrano et al. (2012) observed by over different river basins at global scale higher magnitudes in the correlations between the Z-index and standardized streamflow than with any other PDSIs. However, contrary to our results concerning the PDSIs performance, Haslinger et al. (2014) observed in their study conducted in Austria a stronger relationship between the self-calibrated version of the PDSI and streamflow than the Z-index, attributing this to the weaker performance of the latter in low flow scenarios. Here we considered the whole period, not distinguishing between low and high flow periods, for this reason we found our results consistent, as we support the initial hypothesis on the response of undisturbed basins to droughts at short time-scales.

Yet, our results demonstrated that the multi-scalar drought indices, calculated at different time-scales (the SPEI, the SPI, the SPDI), presented a superior capability to capture the hydro-climatological associations in comparison to the uni-scalar drought indices (PDSIs). The flexibility and comparability over time and space, independently on the climatological or environmental characteristics these indices provide, is the main reason for their primacy (Liu et al., 2019;

Vicente-Serrano et al., 2011). The median magnitude of the correlations recorded with the SSI showed a high agreement during all months of the year, especially from February to May (r ~ 0.85). The months of November and December were an exception as the averaged correlations were generally lower in all the indices (r ~ 0.55). This is in consistency with previous comparative studies in different regions where multi-scalar drought indices demonstrated a great efficacy on hydrological drought characterization (Dogan et al., 2012; Lorenzo-Lacruz et al., 2013; Peña-Gallardo et al., 2019; Wang et al., 2015; Zhai et al., 2010). Comparing to prior studies, it was observed that the magnitude of the correlations between the climatic drought indices and the streamflow vary significantly depending on the degree of the anthropogenic impact on river basins. For example, in the analysis conducted by López-Moreno et al. (2013), Lorenzo-Lacruz et al. (2013b) and Zhai et al. (2010) in highly regulated river basins , the association between climatic droughts and streamflow was lower than the observed under near-natural conditions. In these cases, the response of streamflow to drought is not limited to natural mechanisms but to disruptive factors which may mitigate or sharpen the effects of climatic droughts on streamflow (Rangecroft et al., 2018; Tijdeman et al., 2018).

Precipitation proved to be the major limiting factor that would cause effect on streamflow over the influence role that AED would have. Yang et al. (2018) recently demonstrated the major sensitivity of surface runoff to changes in potential evapotranspiration in comparison to changes in precipitation over past observation and projections for the 21st century globally. However little seasonal variations in the performance of the SPI in comparison to the SPEI/SPDI demonstrated a slightly diminish in the magnitude of the correlations recorded by the SPI and the SSI in August.. At this respect, in Iberian Peninsula this task has been already assessed by Vicente-Serrano et al. (2014) under unregulated conditions. These authors found a greater response of the SPEI to the SSI during summer months due to the increase of the AED even when precipitation variability was the main responsible of streamflow's sensitivity to humid/dry conditions. In a comparable setup, the differences in the relationship observed in our study, during summer months among these two indices and the SSI were insignificant.

Overall, we did not find significant general differences among the three multi-scalar drought indices, and the seasonal variations were minor. The median maximum correlation coefficient for the SPI was r = 0.84 while for the SPEI and the SPDI was r = 0.85. Although the SPDI was found the most correlated index in a greater percentage of basins, the differences in the magnitudes of these correlations are negligible. Consequently, we consider correct the applicability of any of them for analysis of the impact of drought on the streamflow response.

The results also reflected the existence of different times of response of streamflow to climatic drought in peninsular Spain. Thus, we observed that strongest correlations were recorded at short time-scales in a major percentage of basins, especially on a 2-month time-scale with maxima reaching in November, April and July. In line with our results, Vicente-Serrano and López-Moreno, (2005) also found in a closed and unregulated basin located in the central Spanish Pyrenees high correlations in the month of November at short time-scales (1 to-2-month). In contrast, studies performed in regulated river basins found that streamflow drought and climatic droughts were more related at longer time-scales (López-Moreno et al., 2013; Lorenzo-Lacruz et al., 2010, 2013b), mostly due to the multiple practices associated to the regulation of water

resources. In keeping with this latter idea, we found out some exceptions indicating a complex heterogeneity response in typically headwater basins not regulated, as already has been reported by Peña-Gallardo et al. (2019) in 289 undisturbed basins in the U.S. and Barker et al. (2016) in 121 near-natural basins in the UK. Thus, no dissimilarities in the climatic conditions from the 226 basins analysed were observed when comparing with the maximum correlations achieved between the SSI and the climatic drought indices. However, when we attended to the physiographical characteristics of the surface occupied by the basins, we noticed that mostly lithological characteristics in conjunction with the water holding capacity helped to understand the differences observed on the timings of response to drought conditions on streams from basins located in diverse regions of Spain. These results emphasized the basic assumption that many non-climatic local factors also influence the link between climate and streamflow even under unregulated regimens (Van Loon and Laaha, 2015). At this respect, physiographic characteristics were decisive to explain the behavior of these basins. Thus, these basins previously mentioned where located in the main chalky regions. This lithology is characterized by its permeability and high transmissivity and it is associated to chalk aquifers that operate as a reservoir in these regimens thanks to the aquifer recharge any time a precipitation deficit occurs. Our findings were supported by Lorenzo-Lacruz et al. (2013a) who showed similar results to ours in a selection of 58 unregulated basins in Iberian Peninsula (specifically most of these basins are located in Iberian System). At the same time, the elevation, the vegetation cover and the land-use are influential factors that influence the hydrological cycle processes making a substantial difference in the response of basins with diverse characteristics to drought.

5. Conclusions.

- Strong correlations were found between the seven drought indices here assessed and the standardized streamflow. Multi-scalar drought indices excelled as the most suitable tools for hydrological drought purposes. Not having found significant differences in the performance of the SPEI, the SPI or the SPDI, authors suggest the interchangeably use of any of them.
- There is a seasonal component in the response of streamflow to climate that determine the propagation from climatic drought to hydrological drought.
- Undisturbed river basins in peninsular Spain mainly respond to short time-scales, emphasizing the role of precipitation as the major climatic driver in streamflow droughts.
- In line with the latter point, there is a complexity associated to the propagation of climatic drought to streamflow under near-natural conditions. We identified a wide range of temporal responses in peninsular Spain river basins related to local non-climatic characteristics such physiography and vegetation cover.

Authors are aware of the limitations involved in this kind of general analysis and are encouraged to work on further analysis necessary to fully understand the influence of the non-climatic mechanisms controlling the delayed response of streamflow to climatic drought in the basins here assessed.

Acknowledgments

This work was supported by the research projects PCIN-2015-220 and CGL2014-52135-C03-01 financed by the Spanish Commission of Science and Technology and FEDER, IMDROFLOOD financed by the Water Works 2014 co-funded call of the European Commission and INDECIS, which is part of ERA4CS, and ERA-NET initiated by JPI Climate, and funded by FORMAS (SE), DLR (DE), BMWFW (AT), IFD (DK), MINECO (ES), ANR (FR) with co-funding by the European Union (Grant 690462). Peña-Gallardo Marina was granted by the Spanish Ministry of Economy and Competitiveness (BES-2015-072022).

References

Abramowitz, M., Stegun, I.A., 1970. Handbook of mathematical functions : with formulas, graphs, and mathematical tables. Dover Publications.

Allen, R.G., Pereira, L.S., Raes, D., Smith, M., 1998. Crop Evapotranspiration: Guidelines for Computing Crop Water Requirements.

Alley, W.M., 1984. The Palmer Drought Severity Index: Limitations and Assumptions. J. Clim. Appl. Meteorol. 23, 1100–1109. https://doi.org/10.1175/1520-0450(1984)023<1100:TPDSIL>2.0.CO;2

Asseng, S., Ewert, F., Martre, P., Rötter, R.P., Lobell, D.B., Cammarano, D., Kimball, B.A., Ottman, M.J., Wall, G.W., White, J.W., Reynolds, M.P., Alderman, P.D., Prasad, P.V. V., Aggarwal, P.K., Anothai, J., Basso, B., Biernath, C., Challinor, A.J., De Sanctis, G., Doltra, J., Fereres, E., Garcia-Vila, M., Gayler, S., Hoogenboom, G., Hunt, L.A., Izaurralde, R.C., Jabloun, M., Jones, C.D., Kersebaum, K.C., Koehler, A.-K., Müller, C., Naresh Kumar, S., Nendel, C., O'Leary, G., Olesen, J.E., Palosuo, T., Priesack, E., Eyshi Rezaei, E., Ruane, A.C., Semenov, M.A., Shcherbak, I., Stöckle, C., Stratonovitch, P., Streck, T., Supit, I., Tao, F., Thorburn, P.J., Waha, K., Wang, E., Wallach, D., Wolf, J., Zhao, Z., Zhu, Y., 2014. Rising temperatures reduce global wheat production. Nat. Clim. Chang. 5, 143–147. https://doi.org/10.1038/nclimate2470

Ayehu, G., Tadesse, T., Gessesse, B., Yigrem, Y., Ayehu, G., Tadesse, T., Gessesse, B., Yigrem, Y., 2019. Soil Moisture Monitoring Using Remote Sensing Data and a Stepwise-Cluster Prediction Model: The Case of Upper Blue Nile Basin, Ethiopia. Remote Sens. 11, 125. https://doi.org/10.3390/rs11020125

Bachmair, S., Stahl, K., Collins, K., Hannaford, J., Acreman, M., Svoboda, M., Knutson, C., Smith, K.H., Wall, N., Fuchs, B., Crossman, N.D., Overton, I.C., 2016. Drought indicators revisited: the need for a wider consideration of environment and society. Wiley Interdiscip. Rev. Water 3, 516–536. https://doi.org/10.1002/wat2.1154

Ballabio, C., Panagos, P., Monatanarella, L., 2016. Mapping topsoil physical properties at European scale using the LUCAS database. Geoderma 261, 110–123. https://doi.org/10.1016/J.GEODERMA.2015.07.006

Barker, L.J., Hannaford, J., Chiverton, A., Svensson, C., 2016. From meteorological to hydrological drought using standardised indicators. Hydrol. Earth Syst. Sci. 20, 2483–2505. https://doi.org/10.5194/hess-20-2483-2016

Batalla, R.J., Gómez, C.M., Kondolf, G.M., 2004. Reservoir-induced hydrological changes in the Ebro River basin (NE Spain). J. Hydrol. 290, 117–136. https://doi.org/10.1016/J.JHYDROL.2003.12.002

Beguería, S., López-Moreno, J.I., Lorente, A., Seeger, M., García-Ruiz, J.M., 2003. Assessing the effect of climate oscillations and land-use changes on streamflow in the central Spanish Pyrenees. Ambio 32, 283–6.

Bloomfield, J.P., Marchant, B.P., Bricker, S.H., Morgan, R.B., 2015. Regional analysis of groundwater droughts using hydrograph classification. Hydrol. Earth Syst. Sci. 19, 4327–4344. https://doi.org/10.5194/hess-19-4327-2015

Camarero, J.J., Gazol, A., Sangüesa-Barreda, G., Oliva, J., Vicente-Serrano, S.M., 2015. To die or not to die: early warnings of tree dieback in response to a severe drought. J. Ecol. 103, 44–57. https://doi.org/10.1111/1365-2745.12295

Doesken, N.J., Garen, D., 1991. Drought monitoring in the Western United States using a surface water supply index. Presented at: 7th Conference on Applied Climatology, Sept. 10-13, 1991 in Salt Lake City, Utah, in: Fort Collins, CO: Colorado State University, D. of A.S. (Ed.), Development of a Surface Water Supply Index (SWSI) for the Western United States, 1991. pp. 77–80.

Dogan, S., Berktay, A., Singh, V.P., 2012. Comparison of multi-monthly rainfall-based drought severity indices, with application to semi-arid Konya closed basin, Turkey. J. Hydrol. 470–471, 255–268. https://doi.org/10.1016/J.JHYDROL.2012.09.003

Guttman, N.B., 1998. Comparing the Palmer Drought Index and the Standardized Precipitation Index. J. Am. Water Resour. Assoc. 34, 113–121. https://doi.org/10.1111/j.1752-1688.1998.tb05964.x

Haslinger, K., Koffler, D., Schöner, W., Laaha, G., 2014. Exploring the link between meteorological drought and streamflow: Effects of climate-catchment interaction. Water Resour. Res. 50, 2468–2487. https://doi.org/10.1002/2013WR015051

Hayes, M., Svoboda, M., Wall, N., Widhalm, M., 2011. The Lincoln Declaration on Drought Indices Universal Meteorological Drought Index: Recommended Interregional Workshop on Indices and Early Warning Systems for Drought. Bull. Am. Meteorol. Soc. 92(4), 485–488. https://doi.org/10.1175/2010BAMS3103.1

Huang, S., Li, P., Huang, Q., Leng, G., Hou, B., Ma, L., 2017. The propagation from meteorological to hydrological drought and its potential influence factors. J. Hydrol. 547, 184–195. https://doi.org/10.1016/J.JHYDROL.2017.01.041

Liu, Y., Zhu, Y., Ren, L., Singh, V.P., Yong, B., Jiang, S., Yuan, F., Yang, X., 2019. Understanding the spatiotemporal links between meteorological and hydrological droughts from a three-dimensional perspective. J. Geophys. Res. Atmos. 2018JD028947. https://doi.org/10.1029/2018JD028947

Lloyd-Hughes, B., 2014. The impracticality of a universal drought definition. Theor. Appl. Climatol. 117, 607–611. https://doi.org/10.1007/s00704-013-1025-7

López-Moreno, J.I., Vicente-Serrano, S.M., Beguería, S., García-Ruiz, J.M., Portela, M.M., Almeida, A.B., 2009. Dam effects on droughts magnitude and duration in a transboundary basin: The Lower River Tagus, Spain and Portugal. Water Resour. Res. 45. https://doi.org/10.1029/2008WR007198

López-Moreno, J.I., Vicente-Serrano, S.M., Zabalza, J., Beguería, S., Lorenzo-Lacruz, J., Azorin-Molina, C., Morán-Tejeda, E., 2013. Hydrological response to climate variability at different time scales: A study in the Ebro basin. J. Hydrol. 477, 175–188. https://doi.org/10.1016/J.JHYDROL.2012.11.028

Lorenzo-Lacruz, J., Garcia, C., Morán-Tejeda, E., 2017. Groundwater level responses to precipitation variability in Mediterranean insular aquifers. J. Hydrol. 552, 516–531. https://doi.org/10.1016/J.JHYDROL.2017.07.011

Lorenzo-Lacruz, J., Morán-Tejeda, E., Vicente-Serrano, S.M., López-Moreno, J.I., 2013a. Streamflow droughts in the Iberian Peninsula between 1945 and 2005: spatial and temporal patterns. Hydrol. Earth Syst. Sci. 17, 119–134. https://doi.org/10.5194/hess-17-119-2013

Lorenzo-Lacruz, J., Vicente-Serrano, S., González-Hidalgo, J., López-Moreno, J., Cortesi, N., 2013b. Hydrological drought response to meteorological drought in the Iberian Peninsula. Clim. Res. 58, 117–131. https://doi.org/10.3354/cr01177

Lorenzo-Lacruz, J., Vicente-Serrano, S.M., López-Moreno, J.I., Beguería, S., García-Ruiz, J.M., Cuadrat-Prats, J.M., 2010. The impact of droughts and water management on various hydrological systems in the headwaters of the Tagus River (central Spain). J. Hydrol. 386, 13–26. https://doi.org/10.1016/j.jhydrol.2010.01.001

Loukas, A., Vasiliades, L., 2004. Probabilistic analysis of drought spatiotemporal characteristics inThessaly region, Greece. Nat. Hazards Earth Syst. Sci. 4, 719–731. https://doi.org/10.5194/nhess-4-719-2004

Ma, M., Ren, L., Yuan, F., Jiang, S., Liu, Y., Kong, H., Gong, L., 2014. A new standardized Palmer drought index for hydro-meteorological use. Hydrol. Process. 28, 5645–5661. https://doi.org/10.1002/hyp.10063

Marchant, B.P., Bloomfield, J.P., 2018. Spatio-temporal modelling of the status of groundwater droughts. J. Hydrol. 564, 397–413. https://doi.org/https://doi.org/10.1016/j.jhydrol.2018.07.009

Mckee, T.B., Doesken, N.J., Kleist, J., 1993. The relationshio of drought frequency and duration to time scales. Eighth Conf. Appl. Climatol. 17–22.

Mishra, A.K., Singh, V.P., 2010. A review of drought concepts. J. Hydrol. 391, 202–216. https://doi.org/10.1016/j.jhydrol.2010.07.012

Mosley, L.M., 2015. Drought impacts on the water quality of freshwater systems; review and integration. Earth-Science Rev. 140, 203–214. https://doi.org/10.1016/J.EARSCIREV.2014.11.010

Mukherjee, S., Mishra, A., Trenberth, K.E., 2018. Climate Change and Drought: a Perspective on Drought Indices. Curr. Clim. Chang. Reports 4, 145–163. https://doi.org/10.1007/s40641-018-0098-x

Ortega-Gómez, T., Pérez-Martín, M.A., Estrela, T., 2018. Improvement of the drought indicators system in the Júcar River Basin, Spain. Sci. Total Environ. 610–611, 276–290. https://doi.org/10.1016/j.scitotenv.2017.07.250

Palmer, W.C., 1965. Meteorological Drought. Research Paper No. 45, 1965, 58 p. U.S. Dep. Commer. Weather Bur. Washington, DC. Research P.

Peña-Gallardo, M., Vicente-Serrano, S.M., Hannaford, J., Lorenzo-Lacruz, J., Svoboda, M., Domínguez-Castro, F., Maneta, M., Tomas-Burguera, M., Kenawy, A. El, 2019. Complex influences of meteorological drought time-scales on hydrological droughts in natural basins of the contiguous Unites States. J. Hydrol. 568, 611–625. https://doi.org/10.1016/J.JHYDROL.2018.11.026

Peters, E., van Lanen, H.A.J., Torfs, P.J.J.F., Bier, G., 2005. Drought in groundwater—drought distribution and performance indicators. J. Hydrol. 306, 302–317. https://doi.org/10.1016/j.jhydrol.2004.09.014

Rangecroft, S., Van Loon, A.F., Coxon, G., Breña-Naranjo, J.A., Van Ogtrop, F., Van Lanen, H.A.J., 2018. Using paired catchments to quantify the human influence on hydrological droughts. Hydrol. Earth Syst. Sci. Discuss. 1–23. https://doi.org/10.5194/hess-2018-215

Scaini, A., Sánchez, N., Vicente-Serrano, S.M., Martínez-Fernández, J., 2015. SMOS-derived soil moisture anomalies and drought indices: a comparative analysis using *in situ* measurements. Hydrol. Process. 29, 373–383. https://doi.org/10.1002/hyp.10150

Tallaksen, L.M., Van Lanen, H.A., 2004. Hydrological drought : processes and estimation methods for streamflow and groundwater, 48th ed, Developments in Water Science. Elsevier Science B.V., Amsterdam, the Netherlands.

Tetzlaff, D., McDonnell, J.J., Uhlenbrook, S., McGuire, K.J., Bogaart, P.W., Naef, F., Baird, A.J., Dunn, S.M., Soulsby, C., 2008. Conceptualizing catchment processes: simply too complex? Hydrol. Process. 22, 1727–1730. https://doi.org/10.1002/hyp.7069

Tijdeman, E., Hannaford, J., Stahl, K., 2018. Human influences on streamflow drought characteristics in England and Wales. Hydrol. Earth Syst. Sci. 22, 1051–1064. https://doi.org/10.5194/hess-22-1051-2018

Van Lanen, H.A.J., Wanders, N., Tallaksen, L.M., Van Loon, A.F., 2013. Hydrological drought across the world: impact of climate and physical catchment structure. Hydrol. Earth Syst. Sci 17, 1715–1732. https://doi.org/10.5194/hess-17-1715-2013

Van Loon, A.F., 2015. Hydrological drought explained. Wiley Interdiscip. Rev. Water 2, 359–392. https://doi.org/10.1002/wat2.1085

Van Loon, A.F., Gleeson, T., Clark, J., Van Dijk, A.I.J.M., Stahl, K., Hannaford, J., Di Baldassarre, G., Teuling, A.J., Tallaksen, L.M., Uijlenhoet, R., Hannah, D.M., Sheffield, J., Svoboda, M., Verbeiren, B., Wagener, T., Rangecroft, S., Wanders, N., Van Lanen, H.A.J., 2016. Drought in the Anthropocene. Nat. Geosci. 9, 89–91. https://doi.org/10.1038/ngeo2646

Van Loon, A.F., Laaha, G., 2015. Hydrological drought severity explained by climate and catchment characteristics. J. Hydrol. 526, 3–14. https://doi.org/10.1016/J.JHYDROL.2014.10.059

Vasiliades, L., Loukas, A., 2009. Hydrological response to meteorological drought using the Palmer drought indices in Thessaly, Greece. Desalination 237, 3–21. https://doi.org/10.1016/J.DESAL.2007.12.019

Vicente-Serrano, S.M., Beguería, S., López-Moreno, J.I., 2011. Comment on "Characteristics and trends in various forms of the Palmer Drought Severity Index (PDSI) during 1900–2008" by Aiguo Dai. J. Geophys. Res. 116, D19112. https://doi.org/10.1029/2011JD016410

Vicente-Serrano, S.M., Beguería, S., López-Moreno, J.I., Vicente-Serrano, S.M., Beguería, S., López-Moreno, J.I., 2010. A Multiscalar Drought Index Sensitive to Global Warming: The Standardized Precipitation Evapotranspiration Index. J. Clim. 23, 1696–1718. https://doi.org/10.1175/2009JCLI2909.1

Vicente-Serrano, S.M., Beguería, S., Lorenzo-Lacruz, J., Camarero, J.J., López-Moreno, J.I., Azorin-Molina, C., Revuelto, J., Morán-Tejeda, E., Sanchez-Lorenzo, A., Vicente-Serrano, S.M., Beguería, S., Lorenzo-Lacruz, J., Camarero, J.J., López-Moreno, J.I., Azorin-Molina, C., Revuelto, J., Morán-Tejeda, E., Sanchez-Lorenzo, A., 2012. Performance of Drought Indices for Ecological, Agricultural, and Hydrological Applications. http://dx.doi.org/10.1175/2012EI000434.1. https://doi.org/10.1175/2012EI000434.1

Vicente-Serrano, S.M., Lopez-Moreno, J.-I., Beguería, S., Lorenzo-Lacruz, J., Sanchez-Lorenzo, A., García-Ruiz, J.M., Azorin-Molina, C., Morán-Tejeda, E., Revuelto, J., Trigo, R., Coelho, F., Espejo, F., 2014. Evidence of increasing drought severity caused by temperature rise in southern Europe. Environ. Res. Lett. Environ. Res. Lett 9, 44001–9. https://doi.org/10.1088/1748-9326/9/4/044001

Vicente-Serrano, S.M., López-Moreno, J.I., 2005. Hydrological response to different time scales of climatological drought: an evaluation of the Standardized Precipitation Index in a mountainous Mediterranean basin. Hydrol. Earth Syst. Sci. 9, 523–533. https://doi.org/10.5194/hess-9-523-2005

Vicente-Serrano, S.M., Tomas-Burguera, M., Beguería, S., Reig, F., Latorre, B., Peña-Gallardo, M., Luna, M.Y., Morata, A., González-Hidalgo, J.C., 2017. A High Resolution Dataset of Drought Indices for Spain. Data 2, 22. https://doi.org/10.3390/data2030022

Vicente-Serrano, S.M., Zabalza-Martínez, J., Borràs, G., López-Moreno, J.I., Pla, E., Pascual, D., Savé, R., Biel, C., Funes, I., Azorin-Molina, C., Sanchez-Lorenzo, A., Martín-Hernández, N., Peña-Gallardo, M., Alonso-González, E., Tomas-Burguera, M., El Kenawy, A., 2017. Extreme hydrological events and the influence of reservoirs in a highly regulated river basin of northeastern Spain. J. Hydrol. Reg. Stud. 12. https://doi.org/10.1016/j.ejrh.2017.01.004

Vicente-Serrano, S.M., Zabalza-Martínez, J., Borràs, G., López-Moreno, J.I., Pla, E., Pascual, D., Savé, R., Biel, C., Funes, I., Martín-Hernández, N., Peña-Gallardo, M., Beguería, S., Tomas-Burguera, M., 2015. Effect of reservoirs on streamflow and river regimes in a heavily regulated river basin of Northeast Spain. Catena. https://doi.org/10.1016/j.catena.2016.03.042

Von Gunten, D., Wöhling, T., Haslauer, C.P., Merchán, D., Causapé, J., Cirpka, O.A., 2016. Using an integrated hydrological model to estimate the usefulness of meteorological drought indices in a changing climate. Hydrol. Earth Syst. Sci 20, 4159–4175. https://doi.org/10.5194/hess-20-4159-2016

Wang, H., Rogers, J.C., Munroe, D.K., Wang, H., Rogers, J.C., Munroe, D.K., 2015. Commonly Used Drought Indices as Indicators of Soil Moisture in China. J. Hydrometeorol. 16, 1397–1408. https://doi.org/10.1175/JHM-D-14-0076.1

Wells, N., Goddard, S., Hayes, M.J., Wells, N., Goddard, S., Hayes, M.J., 2004. A Self-Calibrating Palmer Drought Severity Index. J. Clim. 17, 2335–2351. https://doi.org/10.1175/1520-0442(2004)017<2335:ASPDSI>2.0.CO;2

Wilhite, D.A., Glantz, M.H., 1985. Understanding: the Drought Phenomenon: The Role of Definitions. Water Int. 10, 111–120. https://doi.org/10.1080/02508068508686328

WMO, 2012. Standardized Precipitation Index User Guide. http://www.wamis.org/agm/pubs/SPI/WMO_1090_EN.pdf (Last access, 22 February 2019)

Yang, Y., Zhang, S., McVicar, T.R., Beck, H.E., Zhang, Y., Liu, B., 2018. Disconnection Between Trends of Atmospheric Drying and Continental Runoff. Water Resour. Res. 54, 4700–4713. https://doi.org/10.1029/2018WR022593

Zargar, A., Sadiq, R., Naser, B., Khan, F.I., 2011. A review of drought indices. Environ. Rev. 19, 333–349. https://doi.org/10.1139/a11-013

Zhai, J., Su, B., Krysanova, V., Vetter, T., Gao, C., Jiang, T., Zhai, J., Su, B., Krysanova, V., Vetter, T., Gao, C., Jiang, T., 2010. Spatial Variation and Trends in PDSI and SPI Indices and Their Relation to Streamflow in 10 Large Regions of China. J. Clim. 23, 649–663. https://doi.org/10.1175/2009JCLI2968.1

Tables

Table 1. Percentage of basins per index and time-scale at which the maximum correlations were found. Notice that long time-scales from 13 to 48-month where summarized in two groups (13-24 and >24-month) due the low percentages recorded individually.

	1	2	3	4	5	6	7	8	9	10	11	12	13-24	> 24
SPI	7.93	33.04	14.54	7.93	8.37	3.08	4.41	3.52	0.44	1.32	1.32	1.76	4.41	7.93
SPDI	14.98	42.29	14.10	5.73	3.52	3.08	0.88	1.32	0.88	1.32	0.88	0.88	2.64	7.49
SPEI	10.13	36.12	15.86	8.37	6.61	3.52	0.88	2.20	0.88	1.32	0.44	0.44	4.41	8.81
Averaged (%)	11.01	37.15	14.83	7.34	6.17	3.23	2.06	2.35	0.73	1.32	0.88	1.03	3.82	8.08

Figures

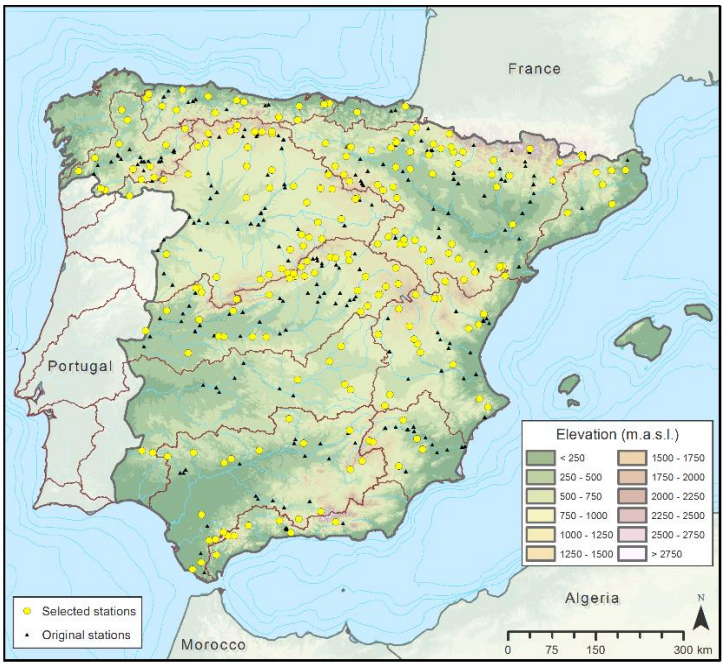

Figure 1. Location of the available (black dots) and selected (yellow dots) streamflow gauging stations.

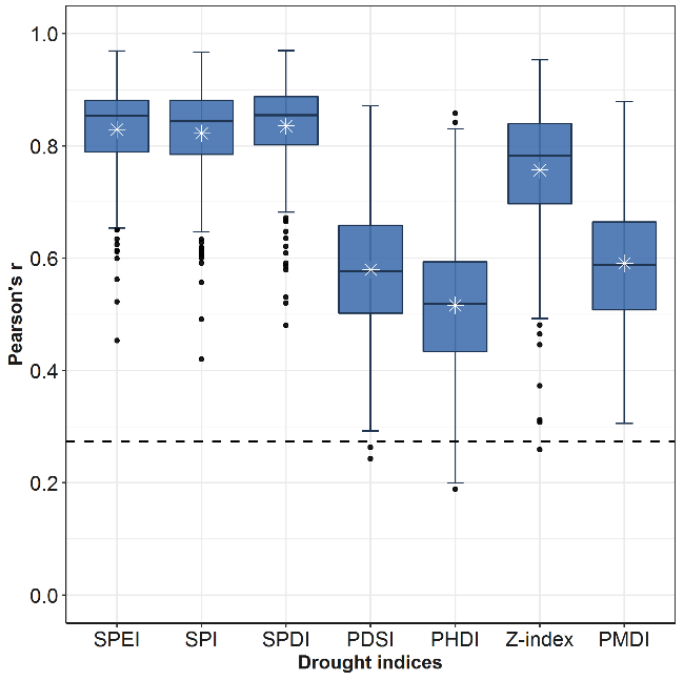

Figure 2. Box plots showing the strongest correlation coefficients found between climatic drought indices and the SSI for the 226 natural basins considered in this study. The solid black line shows the median, the white asterisk shows the mean, and the dashed black line shows the $p < 0.05$ significance level.

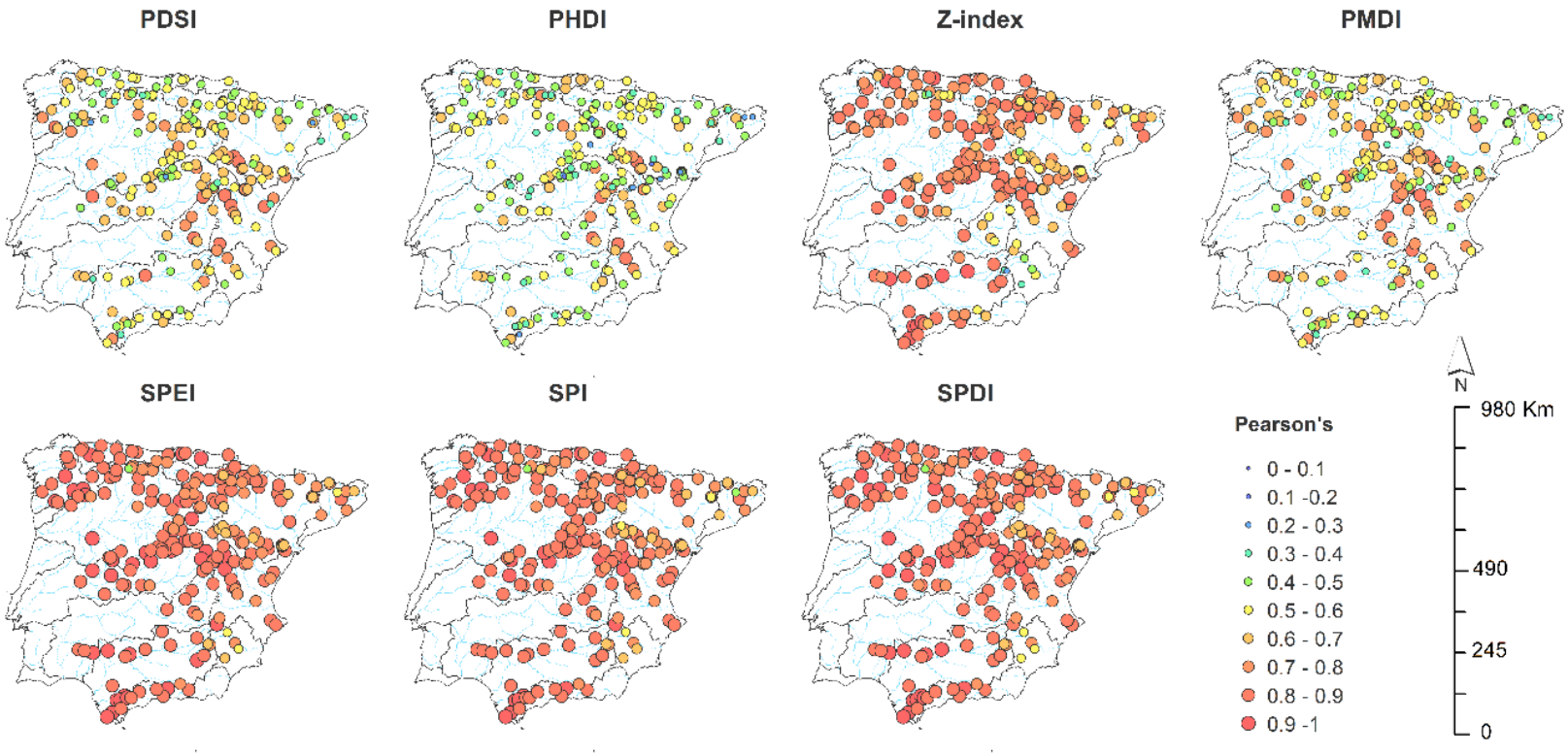

Figure 3. Spatial distribution of the highest correlation coefficients between the climatic drought indices and the SSI independently of the month of the year and drought time-scale.

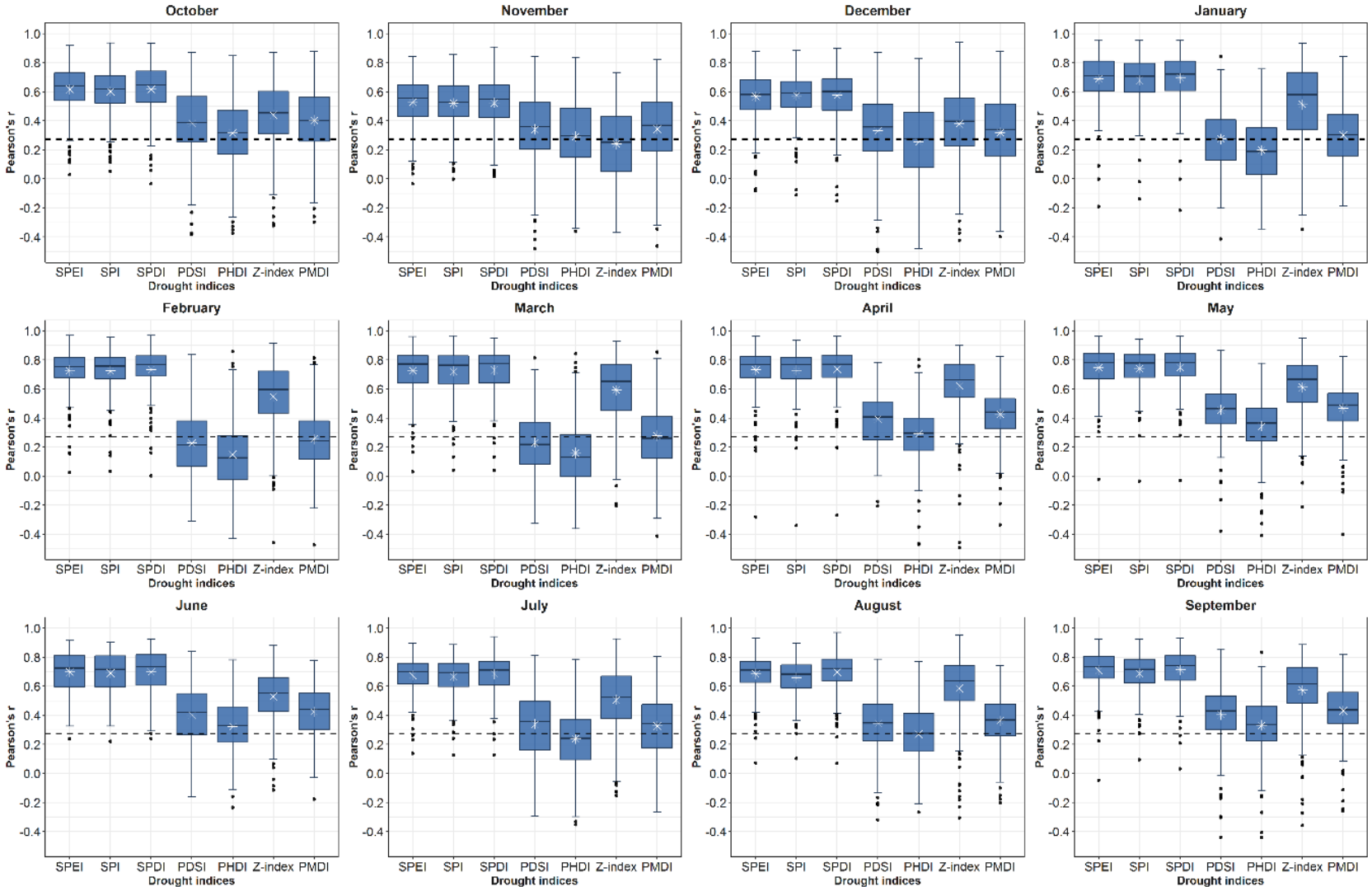

Figure 4. Boxplots showing the monthly Pearson correlation coefficients obtained between series of the SSI and the seven drought indices. The dashed solid black line corresponds to the median, the white asterisk the mean and the dashed black line the $p < 0.05$ significance level.

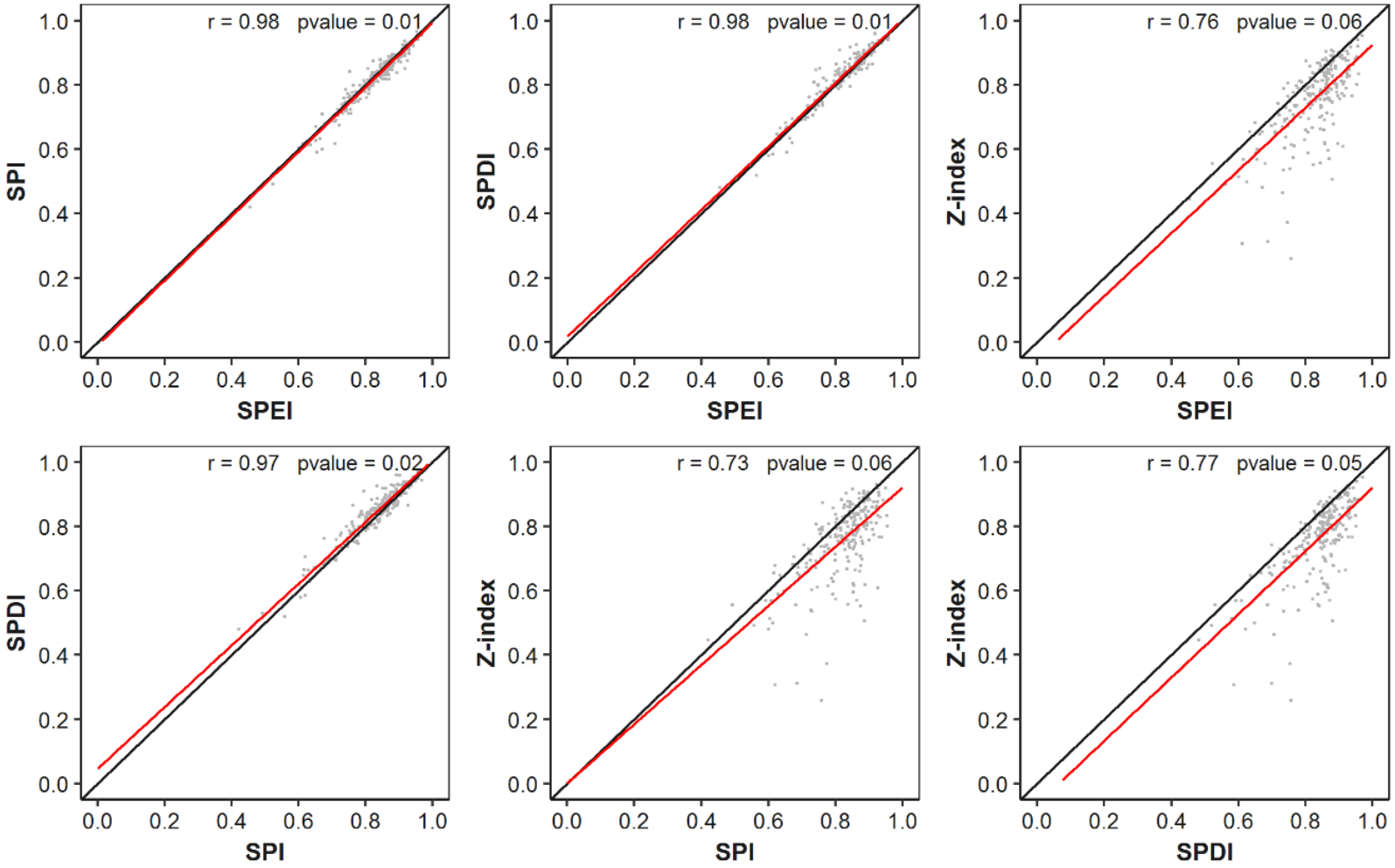

Figure 5. Maximum correlation scatterplots of index pairs (SPEI, SPI, SPDI and Z-index). Each point corresponds to the highest Pearson's correlation coefficient recorded in each basin.

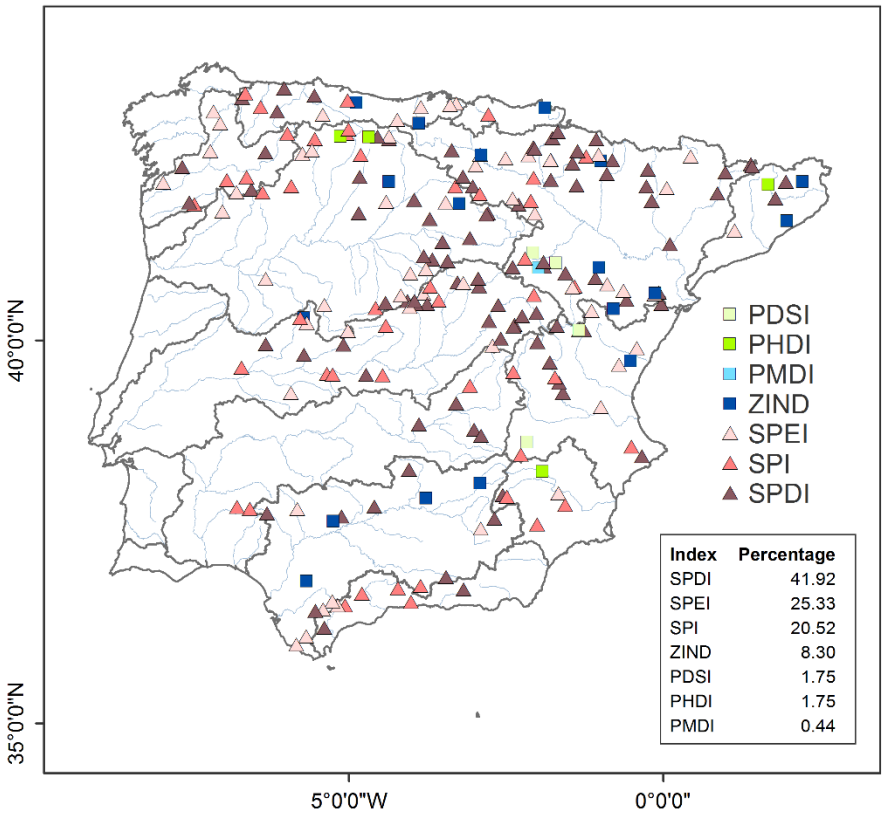

Figure 6. Spatial distribution of the drought indices having the strongest correlations with the SSI and the percentage in each case.

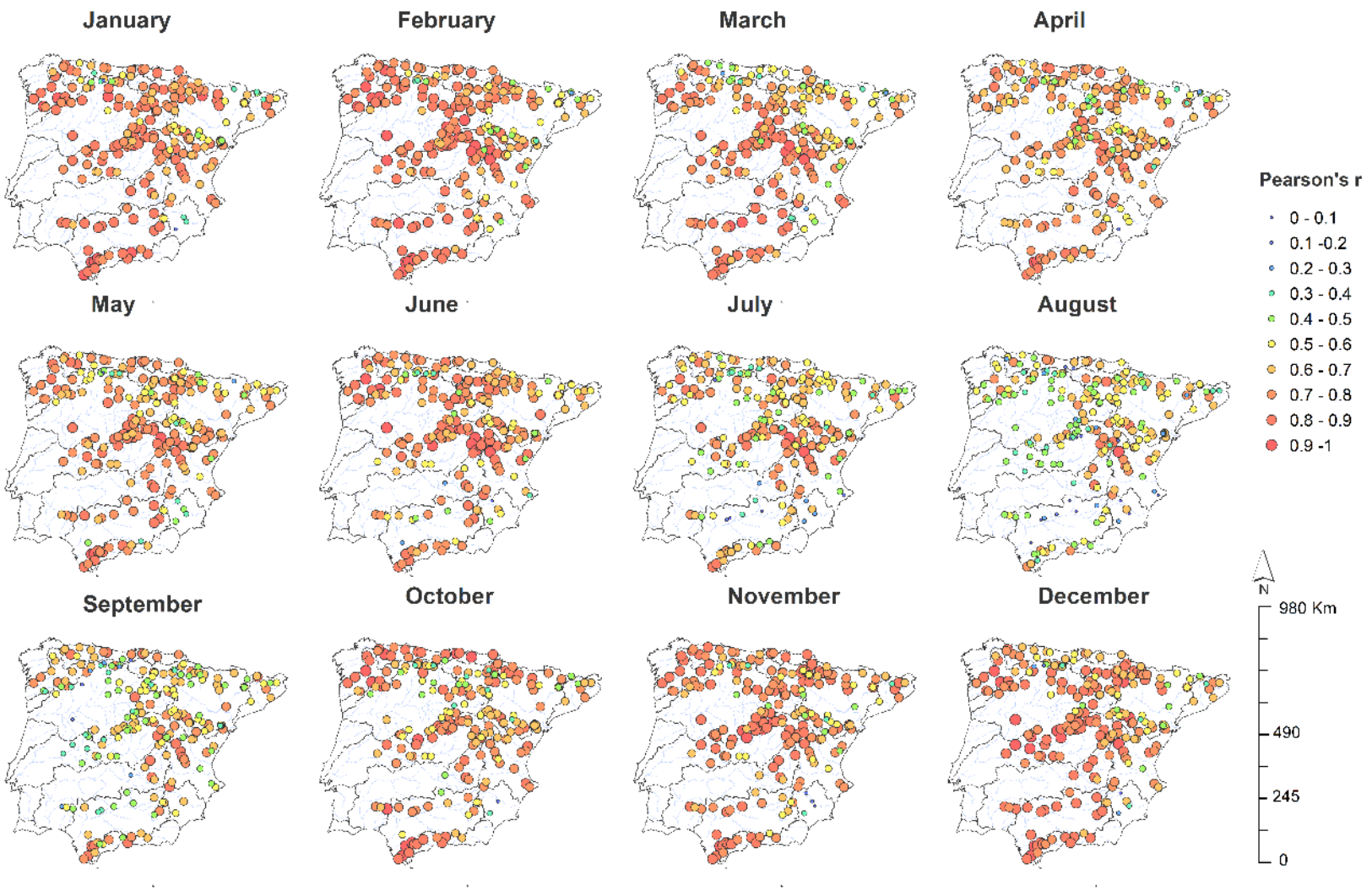

Figure 7. Spatial distribution of the monthly highest correlation coefficients between the SPDI and the SSI independently of the month and time-scale.

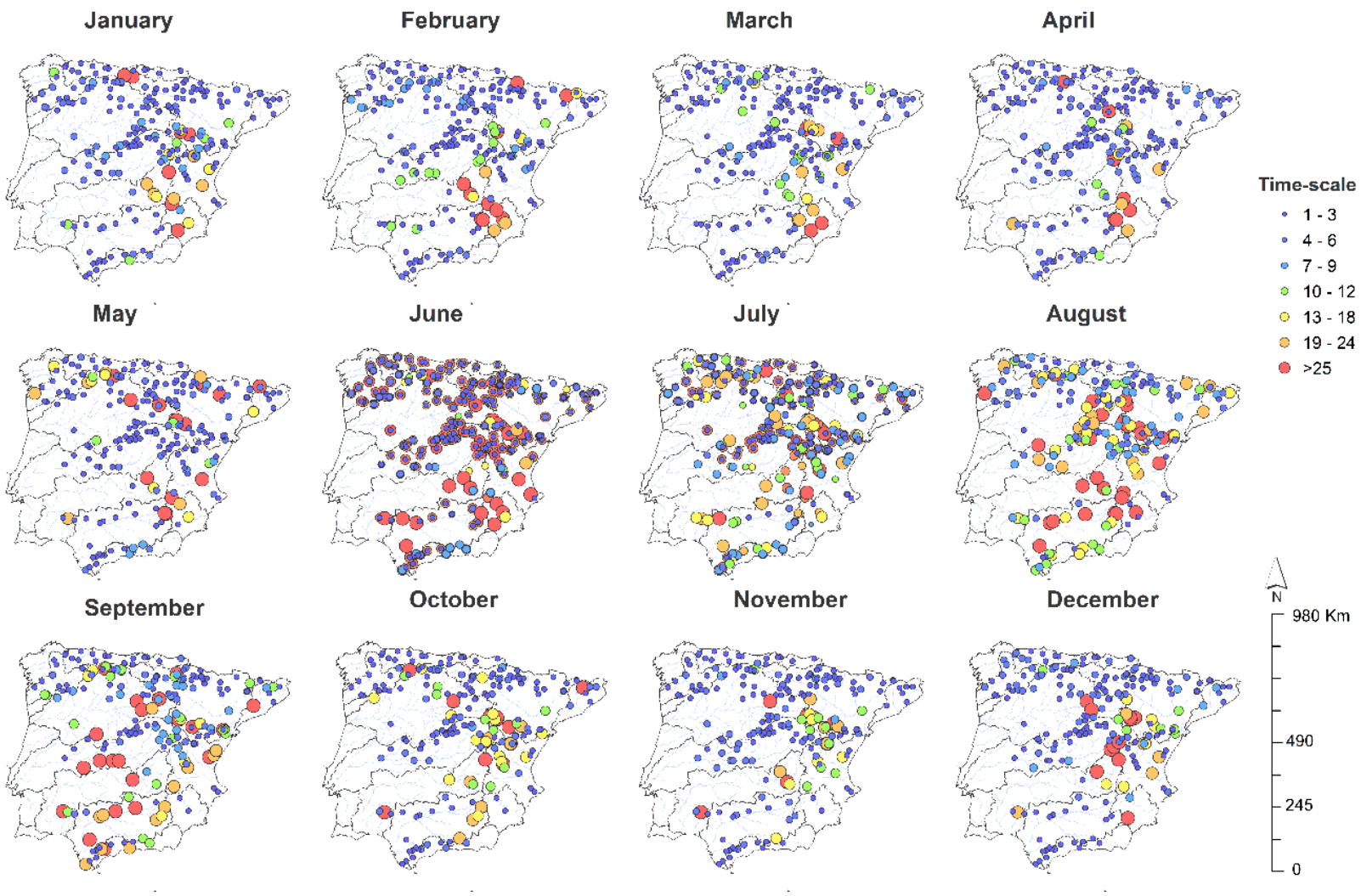

Figure 8. Spatial distribution of the time-scales at which monthly highest correlation coefficients between the SPDI and the SSI were found.

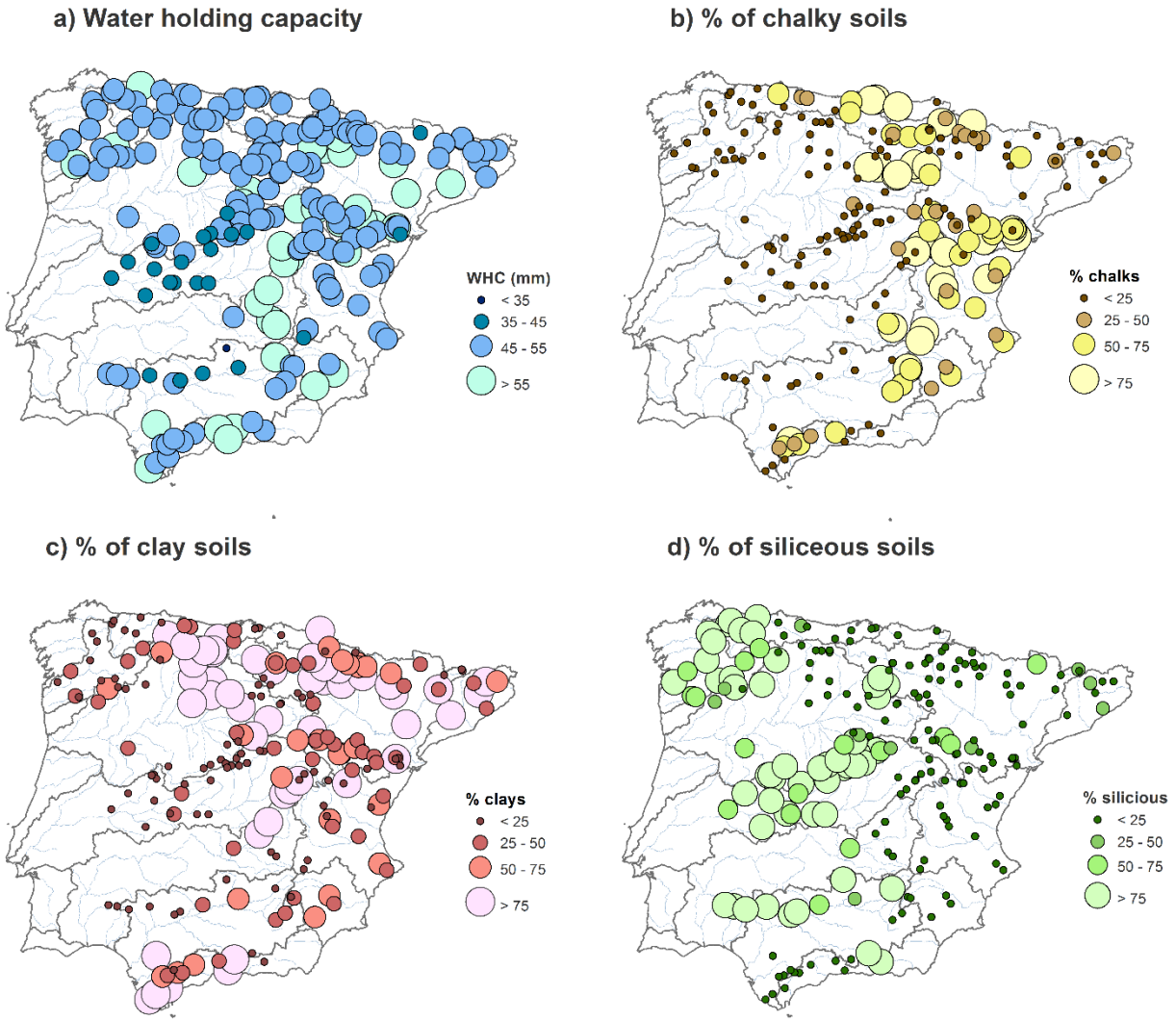

Figure 9. Water holding capacity (a) and percentage of surface characterized by the dominant lithology (b, c, d) of the analysed basins.

6. General discussion

This thesis has provided a comprehensive analysis on the evaluation of different drought indices on multiple systems and, at the same time, has assessed the spatio-temporal response of agriculture, forests and streamflow to drought conditions in two heterogeneous regions, the United States and Spain. The relevance of the results obtained from the different studies conducted aims (i) to improving the knowledge about the correct and effective monitoring and quantification of a complex climatic hazard as is the drought, and (ii) to the creation of climatic services that allow an appropriate risk management.

6.1. Evaluation of the adequacy of drought indices

In four of the researches conducted, the appropriateness of different climatic drought indices for monitoring purposes on different systems and their efficacy to detect the response of these systems to drought conditions were assessed. The drought indices selected are worldwide used, and have been widely covered in the scientific literature and used on operational drought monitoring. For the systems analysed in this thesis similar results were observed regarding the association between the two groups of indices (multi-scalars and uni-scalars) and the different agricultural, hydrological and environmental variables. A stronger response of the variability of crop yields, tree growth metrics and streamflow to drought was noticed in the multi-scalar drought indices than in the uni-scalars. As observed from the magnitude of obtained correlations, this varies significantly among type of indices.

The assessment of the performance of the PDSIs showed in general low correlations with either of the variables assessed, even when the self-calibrated version improved significantly the performance of these indices as seen in *Article 1* for predicting yield loses. This result was supported by Mavromatis, (2007) results obtained from wheat rain-fed yields in Greece. Nonetheless, and despite the results of these indices in comparison to the multi-scalars, the PDSIs proved that correlations varied noticeably among them finding some exceptions. For example, the Z-index demonstrated to be more sensitive in reflecting the manifestation of impacts of drought on yields, streamflow and forests more efficiently than any other PDSIs, recording more significant and higher correlations. This index has already stated measure short-term moisture conditions matching the averaged temporal response of vegetation and undisturbed streamflow regimes to dry conditions (Lorenzo-Lacruz et al., 2013; Quiring and Papakryiakou, 2003; Vicente-Serrano et al., 2013). Moreover, results from *Unpublished Research 2* showed that the median magnitude of correlations achieved by the PDSIs and the streamflow was the highest among the systems analysed in this thesis. In fact, similar magnitudes of correlations achieved in that research were observed in a natural basin from Thessaly region in Greece by Vasiliades and Loukas, (2009), also demonstrating that among PDSIs, the PHDI resulted the worst index to assess drought impacts on streamflow as the analysis in undisturbed basins in Spain also showed. At this respect, the PHDI was the index that presented the weakest relationship to any of the variables analysed, followed by the PDSI and the PMDI.

Notwithstanding what here has said, many previous studies have applied the PDSIs with successful results for either monitoring or impacts-related investigation purposes and sometimes their findings contrasted with the results here obtained. That is the case for example of Karl, (1986) whose study showed that for agricultural and forest fires analysis in the US, the Z-index was better at recording short-term moisture variability than the PDSI. Similar conclusions were obtained in Canadian prairies by Quiring and Papakryiakou, (2003) and in the Czech Republic by Hlavinka et al. (2009). For their part, Bhuyan et al. (2017) conducting a similar analysis to this over nine tree species in Europe, compared the SPEI, the SPI and the PDSIs finding similar agreement with the PDSIs and the multi-scalar indices at long time-scales superior to 12 months.

Yet, the PDSIs lack of the flexibility to identify the impact of drought at different time-scales. As the studies here conducted demonstrate, and many other previous studies support, differences on the temporal response in agriculture, vegetation and hydrology to water deficit hidden the complexity and hence the need of using drought indices that allow connecting past weather characteristics to present conditions in regions with complex climate conditions (García-León et al., 2019; Vicente-Serrano et al., 2011). Thus, in agreement with this, comparative studies in various regions as the conducted by McEvoy et al. (2012), Wang et al. (2014) or Tian et al. (2018) highlighted the superior performance of the multi-scalar drought indices for monitoring drought impacts on agricultural lands. Vicente-Serrano et al. (2012) on tree growth showed same results at global scale, and similarly Liu et al. (2019), Lorenzo-Lacruz et al. (2013) or Dogan et al. (2012) did it on river basins.

The similar magnitudes of correlations observed between the drought multi-scalar indices and the different variables proved the analogous ability to characterize the impact of drought. At this respect, Labudová et al. (2016) found similar performance of the SPEI (calculated using both precipitation and atmospheric evaporative demand) and the SPI (based only on precipitation data) for assessing the impact of drought on crop production in the Danubian Lowland and the East Slovakian Lowland. However, slight differences in the magnitude of correlations observed between the SPI and the SPEI and the variables representative of the three systems here analysed suggested the relevance of the AED in drought index calculation. Thus, observed the general higher correlations achieved by the SPEI in comparison to the SPI it is important consider the sensitivity that crops, streamflow and forests present to variations in the AED. Regarding to this, previous studies have also noticed the effects of AED on the response of different systems to drought. In relation to this finding, Lobell and Field, (2007) demonstrated the risk on crop yields associated to a global increase of maximum temperatures. Bachmair et al. (2018) found same differences between the SPEI and the SPI associated to the role of temperature on the response of forest in southern Europe. Even when AED also affects streamflow drought severity, it was less evident to appreciate this on natural basins according to the results obtained from this analysis. Thus, differences not as evident as detected by the other analysed variables were found between the SSI/SPI and the SSI/SPEI relationship in the undisturbed basins selected. In consonance to this are the results presented by Vicente-Serrano et al. (2014) which noticed that the role of the AED was major in those basins with any type of anthropogenic intervention than in those less regulated. In the hydrological analysis a close relationship between climate and natural streamflow was observed proving precipitation is more decisive in streamflow drought development, as already suggested at the global scale under current and future scenarios (Yang et al., 2018).

Overall, the performance of the SPEI, the SPI and the SPDI was superior to the PDSIs. Independently on the type of crop, tree species, river basin and the temporal scale considered, results relative to the performance of drought indices demonstrated that drought indices calculated at different time scales (the SPEI, the SPI, and the SPDI) have a superior capacity to reflect the impacts of drought.

6.2. Drought impact on rain-fed crop yields, temporal and spatial characteristics

The global response of crops to drought has strong seasonal character and it is highly reliant on the time-scale of the drought index used to quantify drought severity. Besides, more of the characteristics that represent the response of yields to drought are very dependent on the different levels of resistance that crop types present to water scarcity conditions (Contreras and Hunink, 2015; Vicente-Serrano et al., 2013). While previous studies also showed that impacts varies depending on the time-scale (Wang et al., 2016; Zipper et al., 2016), here it was demonstrated that moisture conditions at short time-scales enhance or constrain the growth of cereal cultivations as barley, corn, soybeans, cotton and wheat.

Nonetheless, there are considerable differences in the month in which yields are mostly controlled by drought conditions. In general, moisture conditions during summer months were determinant for barley, corn, cotton and soybeans yields. In the US, barley yields presented the most homogeneous pattern of response to SPEI time-scales correlating mostly at 3-month in July. Main response of corn yields to the SPEI timescales in wide regions of central US was recorded in August at 3-month time-scale, while in the case of soybeans dominant patterns showed a high response to drought in September at 4-month time-scale. For its part, winter wheat responded to limited water availability during spring months at medium and long time-scales. In Spain barley and wheat yields mostly responded at short time-scales although, the most sensitive response was found in spring at medium time-scales.

At this respect, previous studies demonstrated that vegetation conditions tends to be affected first by changes in soil moisture content (Capa-Morocho et al., 2016; García-León et al., 2019; Moorhead et al., 2015), fact that could explain the general response of crops to short time-scales. In line with the results here discussed, Zipper et al. (2016) evaluated the impact of drought on corn and soybeans in the US finding that corn was more sensitivity to drought occurring during July at a 1-month time-scale, while soybeans were more sensitive to droughts occurring in August at a 2-month timescale. For their part, Moorhead et al. (2015) also found negative impacts caused by drought conditions in July on cereal crops.

Ultimately, the seasonality observed in the crop response to drought is related to the phenology. As many previous studies suggested before, the response of crops to drought is major during the most sensitive phenological states to soil water availability (Chaves et al., 2003; Poulter et al., 2013; Zipper et al., 2016). Winter corresponds to the first growth stages of plants, and summer with the heading and reproductive stages. Moisture conditions during winter determine the correct development of crops (Çakir, 2004), thus sensitive response to medium time-scales during summer months observed in some crops (e.g. corn recording maximum correlations at silking and

reproductive phenological stages) was related to the phenological response to moisture or dryness conditions during winter months. Nonetheless, not always the temporal pattern of response is the same. Winter wheat in the US showed a strong relationship with drought from medium to long time-scales (in contrast to wheat yields in Spain that mostly correlated with drought indices at short and medium time-scales). Due to the different time of cultivation, winter wheat planted in September and October is mostly active during cold season, moment when the moisture recharge occurs and more sensitive to water shortages is (Tian et al., 2018; Wang et al., 2016).

In addition, physiological characteristics determine the resilience of the crops to cope with drought conditions even during the sensitive stages of growth. That was evident on the differences found in the magnitude of correlations in Spanish crops, as wheat demonstrated to correlate better with drought indices than barley. In this case, barley is a less dependent on water availability to complete successfully the germination and grain filling stage thanks to its own physiological mechanisms to grow under adverse moisture conditions (Mamnouie et al., 2006). Noticeable differences among crop types demonstrated that in some areas responses to medium and long time-scales are more common.

Besides the logical explanation that phenology provides to the rapid response to moisture conditions in the majority of crops, differences in temporal response to drought not related to cultivation periods observed in areas of the US (e.g. northcentral located counties in the US for corn yields) highlighted the relevance of environmental conditions in crop growth, particularly climate characteristic (Pasho et al., 2011; Vicente-Serrano et al., 2013). Regional further explanations on how climate predetermine the impact of drought on crop yields are detailed in discussion section from *Article 1*, *Article 2* and *Unpublished Research 1*. Overall, the varying responses of crops to drought indices time-scales are mainly explained, on one hand by the resilience of plants to develop strategies to deal with soil moisture depletion and on the other hand by the resistance of the different types of crops during the different vegetative stages of growth.

6.3. The sensitivity of forest growth to water shortage

In line with the above mentioned, negative environmental and climatic conditions cause changes in vegetation, especially drought that impacts on ecosystems degrading vegetation activity (Granda et al., 2013). From the study conducted in *Article 3* it was shown that TRW_i was more responsive to drought severity than the photosynthetic biomass defined by the NDVI metrics. Primarily, this is because water availability constrains the leaf and wood formation, but also due to the limitations of satellite measurements. Sometimes, remote sensing derived information provides distorted signal either because of the spatial resolution or the influence of nearby vegetation (Gazol et al., 2018b). Nonetheless, the major sensitivity of secondary growth in comparison to the photosynthetic activity is not solely explained by technical limitations. Previous scientific researches (Aaltonen et al., 2016; Mcdowell et al., 2008) noticed the role of regulated mechanisms of trees to deal with water stress. Thus, unchanged photosynthetic rates but diminishing in the growth under drought conditions is explained by these mechanisms,

however, after long periods of dehydration cannot avoid from drought-induced tree mortality (Martínez-Vilalta and Lloret, 2016; McDowell et al., 2013; Sangüesa-Barreda et al., 2015).

Findings from forest sensitivity to drought showed clear variations among species and climatic regions. As already noticed with crop types, different resilience methods determine different manners species can handle extreme climatic conditions. Thus, under humid conditions, the response of trees to drought (e.g. hardwood species from northern Spain) to drought was weaker than the response from trees growing under Mediterranean climate conditions (e.g. *Quercus* species). Nonetheless, it was observed that temporal response to drought was highly dependent on the adaptive mechanisms of the different species. Therefore, results demonstrated that deciduous species, characteristics of humid regions, were more sensitive to drought at short to medium time-scales, while most of the evergreen coniferous trees characteristics from Mediterranean regions responded to much longer time-scales. This aspect was also stressed by other studies similar to the one here conducted (Gazol et al., 2018b; Quiring and Ganesh, 2010; Rimkus et al., 2017), agreeing all authors with the superior capacity of species from dry regions to recovery from recurrent limited soil water situations in comparison to species accustomed to humid conditions. These species are more vulnerable to extreme and prolonged drought episodes, due to the lack of resilience mechanisms to buffer the impacts caused by severe water shortage.

Seasonal variations also predetermined the response of tree species to drought in Spain. In general, secondary growth was especially sensitive to humid conditions during summer months and is probably explained by specific phenological behaviours of each species (Camarero et al., 2010). Photosynthetic activity was affected by drought conditions occurring during April and May. The lagged impact of drought is the result of the cycle of tree decay that starts with a reduction of photosynthesis, carbon uptake and ultimately wood formation (Noormets et al., 2008).

6.4. Streamflow response to drought under near-natural conditions

Streamflow from undisturbed catchments were found strongly correlated with climatic drought indices. Average correlations in US and Spain basins were around r ~ 0.8, much higher than the correlations observed in previous studies conducted in regulated basins (López-Moreno et al., 2013; Lorenzo-Lacruz et al., 2013; Vicente-Serrano et al., 2017a). Thus, comparing to the magnitude of the correlations between anthropogenic influenced basins and climatic drought, it is more evident the closer influence of climatic conditions on streamflow under natural conditions. This is because regulated basins are controlled by non-climatic factors that disrupt the natural change of streamflow regimens to climatic conditions (Tijdeman et al., 2018). These disruptions can be produced either by water storage capacity (Lorenzo-Lacruz et al., 2013) or regulated interventions (Rangecroft et al., 2018).

An important finding was that the SSI variability in most of the analysed basins from the US and Spain was mainly controlled by droughts at short time-scales. In general, results shown that strongest correlations were found at time-scales between 1 to 4-month, suggesting that under natural conditions, streamflow responds rapidly to climatic variations. Particularly, in Spanish basins a major percentage of cases found maximum correlations at 2-month drought time-scales

in the months of November, April and July. In consistency with this, Vicente-Serrano and López-Moreno (2005) also found similar results in an undisturbed basin in the central Spanish Pyrenees. Nonetheless, in contrast to this pattern of temporal response, other studies conducted in disturbed basins proved that hydrological droughts were mostly linked to climatic droughts at longer time-scales (Huang et al., 2017; Lorenzo-Lacruz et al., 2013; Lorenzo-Lacruz et al., 2010). However, this was expected since these type of catchments are characterized for regulation practices and human influences that can mitigate or reinforce the effect of climate on water resources. Sometimes, non-natural influences act to cushion the effects of droughts by increasing catchment storage and hence modulating the streamflow downstream (López-Moreno et al., 2009; Lorenzo-Lacruz et al., 2010).

Even though regulated basins are characterized by complex response patterns to drought, results from undisturbed basins also showed a wide heterogeneity in the response to dry events. Thus in the US some exceptions to the common response of natural basins at short time-scales were found in basins located in the Rocky Mountains. These basins showed very low correlations between the SPEI and the SSI during summer and winter months at short time-scales, in contrast were more sensitive to SPEI long time-scales during spring and autumn. In Spain also some exceptions were found as many basins located in Iberian System, head of Ebro river major basin and some other scattered basins located in south, southeast and north of peninsular Spain, responded to climate variability at very long time-scales. On one hand, the US case was easily attributed to local characteristics common from mountainous basins. In these basins streamflow are more influenced by snow accumulation during cold season and melting from spring on, than by precipitation interannual variability. Similarly, Haslinger et al. (2014) and Rimkus et al. (2013) noticed that basins controlled by snow processes responded at longer term to drought conditions. On the other hand, the factor that explained the Spanish basins responding to long time-scales and not being conditioned by snow regulation resulted to be the lithology. Emphasizing the statement of the role that non-climatic local factors have in the link between meteorological droughts and hydrological drought under natural conditions, physiographical characteristics determined the temporal response of these basins to drought (Van Loon and Laaha, 2015). Chalk catchments are characterized by a high permeability and a transmissivity operating as natural reservoirs that delay the effects of precipitation shortages. Results found by Lorenzo-Lacruz et al. (2013) also showed the distinct response of catchments in Spain with different lithology.

Overall, even when dominant homogeneous temporal response to drought at short time-scales operates in most of the analysed basins, there were also seasonal patterns and differences in the response of natural basins associated to catchment properties (e.g. vegetation cover, land-use, climatic conditions or topographic characteristics such as elevation).

7. Conclusions

The conclusions of the present dissertation are articulated, on one hand in main conclusions obtained from the general and common objective of the different conducted analysis. On the other hand, specific conclusions from the specific objectives are described in base on the three natural systems assessed (agriculture, vegetation and hydrology). In the second part, a synthesis of the key points resulted from the different analysed systems is provided as follow:

Main conclusions:

i. Assessed the effectiveness of the seven drought indices for monitoring the effect of climate extreme events as droughts on agricultural yields, tree growth and streamflow, the called multi-scalar drought indices (the SPI, the SPEI and the SPDI) demonstrated a better performance than the uni-scalar drought indices (PDSIs).

ii. Thanks to the ability to accumulate climatic anomalies at various time scales drought impacts were more precisely defined by the multi-scalar drought indices that showed a high capacity to identify the seasonality of drought impacts on the different natural systems.

iii. When performing analyses under scarce climate data conditions, the multi-scalar drought indices result more appropriate given the fewer computational and data requirements (particularly the SPEI and the SPI).

iv. Among the three multi-scalar drought indices, significant statistical differences were not found. The SPI, the SPI and the SPDI showed very similar correlations with the environmental variables analysed and hence any of the three indices are consider suitable for monitoring the impact of drought on natural systems.

v. Slightly stronger correlations were recorded by the SPEI and the SPDI than the SPI. In line with the previous point, this conclusion highlights the major role of the atmospheric evaporative demand, and hence the influence of temperature variations in the effects of drought severity on crop yields, forest growth and in a lesser extent on streamflow in undisturbed basins.

Specific conclusions:

Agriculture in the US

i. Different patterns of response exist among types of crops and the month of the year in which each crop is more sensitive to drought conditions. The spatial differences mainly depend on the time-scale at which drought is quantified. In general, the different patterns are controlled by climate conditions and more specifically by the available water.

ii. Shorter time-scales (1 to 3 months) are the foremost at identifying drought impacts on crop yields, corresponding with the most sensitive vegetative growing periods. Exceptionally, some areas where winter wheat is the main crop cultivated show a response to medium (6 to-9 months) and long (9 to-12 months).

iii. Crops growing in humid climates present a lower response to drought severity and a higher response to longer time-scales in comparison to those crops cultivated in temperate and warm climates where the sensitive response of crop yields to drought is more related to short time-scales.

Agriculture in peninsular Spain

i. Finer spatial resolution enables to define clearer patterns that explain the crop yields response to drought impact. Thus, conducting analysis on the relationship between drought and yields using the district scale allows to better capture the climatic variability of regions in Spain contrary to the coarser provincial scale used in most of the studies conducted on the issue.

ii. The relationship between drought impacts and rain-fed crops in a diverse and complex territory as Spain showed contrasted responses. While northern and central agricultural districts showed the strongest associations between drought indices and crop yields, southern agricultural districts presented a weaker sensitiveness to droughts.

iii. The spatial diversity and complexity of drought over a heterogeneous territory underscore the necessity of an effective tool for quantifying its impact on vulnerable areas.

iv. There were clear seasonal patterns in the response of wheat and barley yields to drought. Spring months were the most vulnerable for both crops showing a high agreement at short (1 to 3-month) and medium (4 to 6-month) time-scales. For its part, wetness/dryness conditions during late autumn and winter also determine the subsequent correct growth of crops.

Vegetation activity and growth

i. Tree ring width showed a better response to the SPEI and the SPI while the indicators derived from NDVI correlated better with the SPDI.

ii. Species located in driest Mediterranean areas showed a particular higher correlation with the SPEI, supporting one of the main conclusions regarding the major role of the atmospheric evaporative demand in drought severity.

iii. Secondary growth (tree ring width) resulted to be more prone to be affected by drought conditions during summer months while annual production and greenness during spring months. Besides, secondary growth showed the highest response to drought resulting to be the most reliable indicator to study the effects of drought on forests.

iv. In humid-temperate hardwood forests, the response of vegetation to drought is mostly explain by short time-scales (1 to 3-month) and in warm-dry conifer forests by long to medium time-scales (>4 months).

Hydrology in the US

i. In natural basins, climatic droughts are the main driver that controls the magnitude of hydrological droughts.

ii. The standardized streamflow under natural conditions mainly respond to high frequency climate variability suggesting that precipitation has the greatest influence on streamflow drought severity as observed in the response of the SSI to the SPEI and the SPI.

iii. The response of streamflow to drought in natural basins present a notable spatial heterogeneity. For example, in mountainous basins, two principal climate variables control hydrological droughts, precipitation variability and temperature at long-term. However, physiographical characteristics and vegetation cover also determine the different patterns of response found under natural conditions in streamflow.

Hydrology in peninsular Spain

i. Undisturbed headwater basins in peninsular Spain present a seasonal component in the response of streamflow to climate. The response to drought mostly occurs at short time-scales enhancing the role of precipitation as the major climatic driver in streamflow droughts, however some basins respond to very long time-scales.

ii. There is a wide range of responses to drought in natural basins that cannot be solely explained by climate variability. To the contrary, local physiographical characteristics predetermine the temporality of streamflow drought effects.

8. Bibliography

Aaltonen, H., Lindén, A., Heinonsalo, J., Biasi, C., Pumpanen, J., 2016. Effects of prolonged drought stress on Scots pine seedling carbon allocation. Tree Physiol. 37, 418–427. https://doi.org/10.1093/treephys/tpw119

Abatzoglou, J.T., Barbero, R., Wolf, J.W., Holden, Z.A., Abatzoglou, J.T., Barbero, R., Wolf, J.W., Holden, Z.A., 2014. Tracking Interannual Streamflow Variability with Drought Indices in the U.S. Pacific Northwest. J. Hydrometeorol. 15, 1900–1912. https://doi.org/10.1175/JHM-D-13-0167.1

AghaKouchak, A., Feldman, D., Hoerling, M., Huxman, T., Lund, J., 2015. Water and climate: Recognize anthropogenic drought. Nature 524, 409–411. https://doi.org/10.1038/524409a

Agriculture and climate change, 2019. . FAO, Rome, Italy.

Akinremi, O.O., McGinn, S.M., Barr, A.G., Akinremi, O.O., McGinn, S.M., Barr, A.G., 1996. Evaluation of the Palmer Drought Index on the Canadian Prairies. J. Clim. 9, 897–905. https://doi.org/10.1175/1520-0442(1996)009<0897:EOTPDI>2.0.CO;2

Alley, W.M., 1984. The Palmer Drought Severity Index: Limitations and Assumptions. J. Clim. Appl. Meteorol. 23, 1100–1109. https://doi.org/10.1175/1520-0450(1984)023<1100:TPDSIL>2.0.CO;2

Asseng, S., Ewert, F., Martre, P., Rötter, R.P., Lobell, D.B., Cammarano, D., Kimball, B.A., Ottman, M.J., Wall, G.W., White, J.W., Reynolds, M.P., Alderman, P.D., Prasad, P.V. V., Aggarwal, P.K., Anothai, J., Basso, B., Biernath, C., Challinor, A.J., De Sanctis, G., Doltra, J., Fereres, E., Garcia-Vila, M., Gayler, S., Hoogenboom, G., Hunt, L.A., Izaurralde, R.C., Jabloun, M., Jones, C.D., Kersebaum, K.C., Koehler, A.-K., Müller, C., Naresh Kumar, S., Nendel, C., O'Leary, G., Olesen, J.E., Palosuo, T., Priesack, E., Eyshi Rezaei, E., Ruane, A.C., Semenov, M.A., Shcherbak, I., Stöckle, C., Stratonovitch, P., Streck, T., Supit, I., Tao, F., Thorburn, P.J., Waha, K., Wang, E., Wallach, D., Wolf, J., Zhao, Z., Zhu, Y., 2014. Rising temperatures reduce global wheat production. Nat. Clim. Chang. 5, 143–147. https://doi.org/10.1038/nclimate2470

Asseng, S., Foster, I., Turner, N.C., 2011. The impact of temperature variability on wheat yields. Glob. Chang. Biol. 17, 997–1012. https://doi.org/10.1111/j.1365-2486.2010.02262.x

Bachmair, S., Tanguy, M., Hannaford, J., Stahl, K., 2018. How well do meteorological indicators represent agricultural and forest drought across Europe? Environ. Res. Lett. 13, 034042. https://doi.org/10.1088/1748-9326/aaafda

Bąk, B., Kubiak-Wójcicka, K., 2017. Impact of meteorological drought on hydrological drought in Toruń (central Poland) in the period of 1971–2015. J. Water L. Dev. 32. https://doi.org/10.1515/jwld-2017-0001

Barker, L.J., Hannaford, J., Chiverton, A., Svensson, C., 2016. From meteorological to hydrological drought using standardised indicators. Hydrol. Earth Syst. Sci. 20, 2483–2505. https://doi.org/10.5194/hess-20-2483-2016

Barnett, T.P., Adam, J.C., Lettenmaier, D.P., 2005. Potential impacts of a warming climate on water availability in snow-dominated regions. Nature 438, 303–309. https://doi.org/10.1038/nature04141

Baten, W.D., Frame, J.S., 1959. The Polynomial Correlation Coefficient. Am. Math. Mon. 66, 283. https://doi.org/10.2307/2309635

Beguería, S., Vicente-Serrano, S.M., Reig, F., Latorre, B., 2014. Standardized precipitation evapotranspiration index (SPEI) revisited: parameter fitting, evapotranspiration models, tools, datasets and drought monitoring. Int. J. Climatol. 34, 3001–3023. https://doi.org/10.1002/joc.3887

Ben-Ari, T., Makowski, D., 2014. Decomposing global crop yield variability. Environ. Res. Lett. 9, 114011. https://doi.org/10.1088/1748-9326/9/11/114011
Bhuyan, U., Zang, C., Menzel, A., 2017. Different responses of multispecies tree ring growth to various drought indices across Europe. Dendrochronologia 44, 1–8. https://doi.org/10.1016/J.DENDRO.2017.02.002
Blauhut, V., Stahl, K., Stagge, J.H., Tallaksen, L.M., De Stefano, L., Vogt, J., 2016. Estimating drought risk across Europe from reported drought impacts, drought indices, and vulnerability factors. Hydrol. Earth Syst. Sci. 20, 2779–2800. https://doi.org/10.5194/hess-20-2779-2016
Bloomfield, J.P., Marchant, B.P., Bricker, S.H., Morgan, R.B., 2015. Regional analysis of groundwater droughts using hydrograph classification. Hydrol. Earth Syst. Sci. 19, 4327–4344. https://doi.org/10.5194/hess-19-4327-2015
Cai, W., Cowan, T., 2008. Evidence of impacts from rising temperature on inflows to the Murray-Darling Basin. Geophys. Res. Lett. 35, n/a-n/a. https://doi.org/10.1029/2008GL033390
Çakir, R., 2004. Effect of water stress at different development stages on vegetative and reproductive growth of corn. F. Crop. Res. 89, 1–16. https://doi.org/10.1016/j.fcr.2004.01.005
Camarero, J.J., Gazol, A., Sangüesa-Barreda, G., Cantero, A., Sánchez-Salguero, R., Sánchez-Miranda, A., Granda, E., Serra-Maluquer, X., Ibáñez, R., 2018. Forest Growth Responses to Drought at Short- and Long-Term Scales in Spain: Squeezing the Stress Memory from Tree Rings. Front. Ecol. Evol. 6, 9. https://doi.org/10.3389/fevo.2018.00009
Camarero, J.J., Gazol, A., Sangüesa-Barreda, G., Oliva, J., Vicente-Serrano, S.M., 2015. To die or not to die: early warnings of tree dieback in response to a severe drought. J. Ecol. 103, 44–57. https://doi.org/10.1111/1365-2745.12295
Camarero, J.J., Olano, J.M., Parras, A., 2010. Plastic bimodal xylogenesis in conifers from continental Mediterranean climates. New Phytol. 185, 471–480. https://doi.org/10.1111/j.1469-8137.2009.03073.x
Caminero, L., Génova, M., Camarero, J.J., Sánchez-Salguero, R., 2018. Growth responses to climate and drought at the southernmost European limit of Mediterranean Pinus pinaster forests. Dendrochronologia 48, 20–29. https://doi.org/10.1016/J.DENDRO.2018.01.006
Capa-Morocho, M., Ines, A.V.M., Baethgen, W.E., Rodríguez-Fonseca, B., Han, E., Ruiz-Ramos, M., 2016. Crop yield outlooks in the Iberian Peninsula: Connecting seasonal climate forecasts with crop simulation models. Agric. Syst. 149, 75–87. https://doi.org/10.1016/J.AGSY.2016.08.008
Carnicer, J., Coll, M., Ninyerola, M., Pons, X., Sánchez, G., Peñuelas, J., 2011. Widespread crown condition decline, food web disruption, and amplified tree mortality with increased climate change-type drought. Proc. Natl. Acad. Sci. U. S. A. 108, 1474–8. https://doi.org/10.1073/pnas.1010070108
Ceglar, A., Medved-Cvikl, B., Moran-Tejeda, E., Vicente-Serrano, S., Kajfež-Bogataj, L., 2012. Assessment of multi-scale drought datasets to quantify drought severity and impacts in agriculture: a case study for Slovenia. Int. J. Spat. Data Infrastructures Res. 7, 464–487. https://doi.org/10.2902/IJSDIR.V7I0.271
Chaves, M.M., Maroco, J.P., Pereira, J.S., 2003. Understanding plant responses to drought - From genes to the whole plant. Funct. Plant Biol. 30, 239–264. https://doi.org/10.1071/FP02076
Cheng, S., Huang, J., n.d. Enhanced soil moisture drying in transitional regions under a warming climate. https://doi.org/10.1002/2015JD024559
Contreras, S., Hunink, J.E., 2015. Drought effects on rainfed agriculture using standardized indices: A case study in SE Spain, in: Drought: Research and Science-Policy Interfacing. https://doi.org/10.1201/b18077-13
Core Writing Team, 2014. IPCC,2014: Climate Change 2014: Synthesis Report. Contribution of Working Groups I,II and III to the Fifth Assessment Report of the Intergovemmental Panel

on Climate Change. Geneva, Switzerland.
Crausbay, S.D., Ramirez, A.R., Carter, S.L., Cross, M.S., Hall, K.R., Bathke, D.J., Betancourt, J.L., Colt, S., Cravens, A.E., Dalton, M.S., Dunham, J.B., Hay, L.E., Hayes, M.J., McEvoy, J., McNutt, C.A., Moritz, M.A., Nislow, K.H., Raheem, N., Sanford, T., Crausbay, S.D., Ramirez, A.R., Carter, S.L., Cross, M.S., Hall, K.R., Bathke, D.J., Betancourt, J.L., Colt, S., Cravens, A.E., Dalton, M.S., Dunham, J.B., Hay, L.E., Hayes, M.J., McEvoy, J., McNutt, C.A., Moritz, M.A., Nislow, K.H., Raheem, N., Sanford, T., 2017. Defining Ecological Drought for the Twenty-First Century. Bull. Am. Meteorol. Soc. 98, 2543–2550. https://doi.org/10.1175/BAMS-D-16-0292.1
Dogan, S., Berktay, A., Singh, V.P., 2012. Comparison of multi-monthly rainfall-based drought severity indices, with application to semi-arid Konya closed basin, Turkey. J. Hydrol. 470–471, 255–268. https://doi.org/10.1016/J.JHYDROL.2012.09.003
Dracup, J.A., Kendall, D.R., 1990. Floods and droughts, in: Waggoner, P. (Ed.), Climate Change and US Water Resources. Wiley, New York, pp. 243–267.
Elliott, J., Glotter, M., Ruane, A.C., Boote, K.J., Hatfield, J.L., Jones, J.W., Rosenzweig, C., Smith, L.A., Foster, I., 2018. Characterizing agricultural impacts of recent large-scale US droughts and changing technology and management. Agric. Syst. 159, 275–281. https://doi.org/10.1016/J.AGSY.2017.07.012
Fiorillo, F., Guadagno, F.M., 2010. Karst Spring Discharges Analysis in Relation to Drought Periods, Using the SPI. Water Resour. Manag. 24, 1867–1884. https://doi.org/10.1007/s11269-009-9528-9
Forner, A., Valladares, F., Bonal, D., Granier, A., Grossiord, C., Aranda, I., 2018. Extreme droughts affecting Mediterranean tree species' growth and water-use efficiency: the importance of timing. Tree Physiol. https://doi.org/10.1093/treephys/tpy022
Fu, Q., Feng, S., 2014. Responses of terrestrial aridity to global warming. J. Geophys. Res. 119, 7863–7875. https://doi.org/10.1002/2014JD021608
García-León, D., Contreras, S., Hunink, J., 2019. Comparison of meteorological and satellite-based drought indices as yield predictors of Spanish cereals. Agric. Water Manag. 213, 388–396. https://doi.org/10.1016/J.AGWAT.2018.10.030
García-Ruiz, J.M., López-Moreno, J.I., Vicente-Serrano, S.M., Lasanta–Martínez, T., Beguería, S., 2011. Mediterranean water resources in a global change scenario. Earth-Science Rev. 105, 121–139. https://doi.org/10.1016/J.EARSCIREV.2011.01.006
Gazol, A., Camarero, J.J., Anderegg, W.R.L., Vicente-Serrano, S.M., 2017. Impacts of droughts on the growth resilience of Northern Hemisphere forests. Glob. Ecol. Biogeogr. 26, 166–176. https://doi.org/10.1111/geb.12526
Gazol, A., Camarero, J.J., Sangüesa-Barreda, G., Vicente-Serrano, S.M., 2018a. Post-drought Resilience After Forest Die-Off: Shifts in Regeneration, Composition, Growth and Productivity. Front. Plant Sci. 9, 1546. https://doi.org/10.3389/fpls.2018.01546
Gazol, A., Camarero, J.J., Vicente-Serrano, S.M., Sánchez-Salguero, R., Gutiérrez, E., de Luis, M., Sangüesa-Barreda, G., Novak, K., Rozas, V., Tíscar, P.A., Linares, J.C., Martín-Hernández, N., Martínez del Castillo, E., Ribas, M., García-González, I., Silla, F., Camisón, A., Génova, M., Olano, J.M., Longares, L.A., Hevia, A., Tomás-Burguera, M., Galván, J.D., 2018b. Forest resilience to drought varies across biomes. Glob. Chang. Biol. 24, 2143–2158. https://doi.org/10.1111/gcb.14082
Gilette, H.P., 1950. A creeping drought under way. Water Sew. Work. 104–195.
Granda, E., Camarero, J.J., Gimeno, T.E., Martínez-Fernández, J., Valladares, F., 2013. Intensity and timing of warming and drought differentially affect growth patterns of co-occurring Mediterranean tree species. Eur. J. For. Res. 132, 469–480. https://doi.org/10.1007/s10342-013-0687-0
Greenwood, S., Ruiz-Benito, P., Martínez-Vilalta, J., Lloret, F., Kitzberger, T., Allen, C.D., Fensham, R., Laughlin, D.C., Kattge, J., Bönisch, G., Kraft, N.J.B., Jump, A.S., 2017. Tree mortality across biomes is promoted by drought intensity, lower wood density and higher

specific leaf area. Ecol. Lett. 20, 539–553. https://doi.org/10.1111/ele.12748
Haslinger, K., Koffler, D., Schöner, W., Laaha, G., 2014. Exploring the link between meteorological drought and streamflow: Effects of climate-catchment interaction. Water Resour. Res. 50, 2468–2487. https://doi.org/10.1002/2013WR015051
Heddinghaus, T.R., Sabol, P., 1991. A Review of the Palmer Drought Severity index and Where Do We Go From Here. PROC. 7TH Conf . Appl. Clim. Am. Meteorol. Soc.
Heim, R.R., 2002. A Review of Twentieth-Century Drought Indices Used in the United States. Bull. Am. Meteorol. Soc. 83, 1149–1165. https://doi.org/10.1175/1520-0477(2002)083<1149:AROTDI>2.3.CO;2
Heimann, M., Reichstein, M., 2008. Terrestrial ecosystem carbon dynamics and climate feedbacks. Nature 451, 289–292. https://doi.org/10.1038/nature06591
Hirschi, M., Seneviratne, S.I., Alexandrov, V., Boberg, F., Boroneant, C., Christensen, O.B., Formayer, H., Orlowsky, B., Stepanek, P., 2011. Observational evidence for soil-moisture impact on hot extremes in southeastern Europe. Nat. Geosci. 4, 17–21. https://doi.org/10.1038/ngeo1032
Hlavinka, P., Trnka, M., Semerádová, D., Dubrovský, M., Žalud, Z., Možný, M., 2009. Effect of drought on yield variability of key crops in Czech Republic. Agric. For. Meteorol. 149, 431–442. https://doi.org/10.1016/j.agrformet.2008.09.004
Horton, R.E., 1933. The Rôle of infiltration in the hydrologic cycle. Trans. Am. Geophys. Union 14, 446. https://doi.org/10.1029/TR014i001p00446
Hosking, J.R.M., 1990. L-Moments: Analysis and Estimation of Distributions Using Linear Combinations of Order Statistics. J. R. Stat. Soc. Ser. B. https://doi.org/10.2307/2345653
Huang, S., Li, P., Huang, Q., Leng, G., Hou, B., Ma, L., 2017. The propagation from meteorological to hydrological drought and its potential influence factors. J. Hydrol. 547, 184–195. https://doi.org/10.1016/J.JHYDROL.2017.01.041
Karl, T.R., 1986. The Sensitivity of the Palmer Drought Severity Index and Palmer's Z-Index to their Calibration Coefficients Including Potential Evapotranspiration. J. Clim. Appl. Meteorol. 25, 77–86. https://doi.org/10.1175/1520-0450(1986)025<0077:TSOTPD>2.0.CO;2
Keyantash, J., Dracup, J.A., Keyantash, J., Dracup, J.A., 2002. The Quantification of Drought: An Evaluation of Drought Indices. Bull. Am. Meteorol. Soc. 83, 1167–1180. https://doi.org/10.1175/1520-0477(2002)083<1191:TQODAE>2.3.CO;2
Kumar, R., Musuuza, J.L., Van Loon, A.F., Teuling, A.J., Barthel, R., Ten Broek, J., Mai, J., Samaniego, L., Attinger, S., 2016. Multiscale evaluation of the Standardized Precipitation Index as a groundwater drought indicator. Hydrol. Earth Syst. Sci. 20, 1117–1131. https://doi.org/10.5194/hess-20-1117-2016
Labudová, L., Labuda, M., Takáč, J., 2016. Comparison of SPI and SPEI applicability for drought impact assessment on crop production in the Danubian Lowland and the East Slovakian Lowland. Theor. Appl. Climatol. 1–16. https://doi.org/10.1007/s00704-016-1870-2
Leng, G., Huang, M., Tang, Q., Leung, L.R., 2015. A modeling study of irrigation effects on global surface water and groundwater resources under a changing climate. J. Adv. Model. Earth Syst. 7, 1285–1304. https://doi.org/10.1002/2015MS000437
Lindner, M., Maroschek, M., Netherer, S., Kremer, A., Barbati, A., Garcia-Gonzalo, J., Seidl, R., Delzon, S., Corona, P., Kolström, M., Lexer, M.J., Marchetti, M., 2010. Climate change impacts, adaptive capacity, and vulnerability of European forest ecosystems. For. Ecol. Manage. 259, 698–709. https://doi.org/10.1016/J.FORECO.2009.09.023
Liu, Y., Zhu, Y., Ren, L., Singh, V.P., Yong, B., Jiang, S., Yuan, F., Yang, X., 2019. Understanding the spatiotemporal links between meteorological and hydrological droughts from a three-dimensional perspective. J. Geophys. Res. Atmos. 2018JD028947. https://doi.org/10.1029/2018JD028947
Lloret, F., Escudero, A., Iriondo, J.M., Martínez-Vilalta, J., Valladares, F., 2012. Extreme climatic events and vegetation: the role of stabilizing processes. Glob. Chang. Biol. 18, 797–805.

https://doi.org/10.1111/j.1365-2486.2011.02624.x
Lloyd-Hughes, B., 2014. The impracticality of a universal drought definition. Theor. Appl. Climatol. 117, 607–611. https://doi.org/10.1007/s00704-013-1025-7
Lloyd-Hughes, B., Saunders, M.A., 2002. A drought climatology for Europe. Int. J. Climatol. 22, 1571–1592. https://doi.org/10.1002/joc.846
Lobell, D.B., 2014. Climate change adaptation in crop production: Beware of illusions. Glob. Food Sec. 3, 72–76. https://doi.org/10.1016/j.gfs.2014.05.002
Lobell, D.B., Field, C.B., 2007. Global scale climate–crop yield relationships and the impacts of recent warming. Environ. Res. Lett. 2, 014002. https://doi.org/10.1088/1748-9326/2/1/014002
Lobell, D.B., Schlenker, W., Costa-Roberts, J., 2011. Climate Trends and Global Crop Production Since 1980. Science (80-.). 333.
Logan, J.A., Régnière, J., Powell, J.A., 2003. Assessing the impacts of global warming on forest pest dynamics. Front. Ecol. Environ. 1, 130–137. https://doi.org/10.1890/1540-9295(2003)001[0130:ATIOGW]2.0.CO;2
López-Moreno, J.I., Vicente-Serrano, S.M., Beguería, S., García-Ruiz, J.M., Portela, M.M., Almeida, A.B., 2009. Dam effects on droughts magnitude and duration in a transboundary basin: The Lower River Tagus, Spain and Portugal. Water Resour. Res. 45. https://doi.org/10.1029/2008WR007198
López-Moreno, J.I., Vicente-Serrano, S.M., López-Moreno, J.I., Vicente-Serrano, S.M., 2008. Positive and Negative Phases of the Wintertime North Atlantic Oscillation and Drought Occurrence over Europe: A Multitemporal-Scale Approach. J. Clim. 21, 1220–1243. https://doi.org/10.1175/2007JCLI1739.1
López-Moreno, J.I., Vicente-Serrano, S.M., Zabalza, J., Beguería, S., Lorenzo-Lacruz, J., Azorin-Molina, C., Morán-Tejeda, E., 2013. Hydrological response to climate variability at different time scales: A study in the Ebro basin. J. Hydrol. 477, 175–188. https://doi.org/10.1016/J.JHYDROL.2012.11.028
Lopez-Nicolas, A., Pulido-Velazquez, M., Macian-Sorribes, H., 2017. Economic risk assessment of drought impacts on irrigated agriculture. J. Hydrol. 550, 580–589. https://doi.org/10.1016/J.JHYDROL.2017.05.004
Lorenzo-Lacruz, J., Garcia, C., Morán-Tejeda, E., 2017. Groundwater level responses to precipitation variability in Mediterranean insular aquifers. J. Hydrol. 552, 516–531. https://doi.org/10.1016/J.JHYDROL.2017.07.011
Lorenzo-Lacruz, J., Morán-Tejeda, E., Vicente-Serrano, S.M., López-Moreno, J.I., 2013. Streamflow droughts in the Iberian Peninsula between 1945 and 2005: spatial and temporal patterns. Hydrol. Earth Syst. Sci. 17, 119–134. https://doi.org/10.5194/hess-17-119-2013
Lorenzo-Lacruz, J., Vicente-Serrano, S., González-Hidalgo, J., López-Moreno, J., Cortesi, N., 2013. Hydrological drought response to meteorological drought in the Iberian Peninsula. Clim. Res. 58, 117–131. https://doi.org/10.3354/cr01177
Lorenzo-Lacruz, J., Vicente-Serrano, S.M., López-Moreno, J.I., Beguería, S., García-Ruiz, J.M., Cuadrat-Prats, J.M., 2010a. The impact of droughts and water management on various hydrological systems in the headwaters of the Tagus River (central Spain). J. Hydrol. 386, 13–26. https://doi.org/10.1016/j.jhydrol.2010.01.001
Lorenzo-Lacruz, J., Vicente-Serrano, S.M., López-Moreno, J.I., Beguería, S., García-Ruiz, J.M., Cuadrat, J.M., 2010b. The impact of droughts and water management on various hydrological systems in the headwaters of the Tagus River (central Spain). J. Hydrol. 386, 13–26. https://doi.org/10.1016/j.jhydrol.2010.01.001
Loukas, A., Vasiliades, L., 2004. Probabilistic analysis of drought spatiotemporal characteristics inThessaly region, Greece. Nat. Hazards Earth Syst. Sci. 4, 719–731. https://doi.org/10.5194/nhess-4-719-2004
Ma, M., Ren, L., Yuan, F., Jiang, S., Liu, Y., Kong, H., Gong, L., 2014. A new standardized Palmer

drought index for hydro-meteorological use. Hydrol. Process. 28, 5645–5661. https://doi.org/10.1002/hyp.10063
Mamnouie, E., Ghazvini, R.F., Esfahany, M., Nakhoda, B., 2006. The Effects of Water Deficit on Crop Yield and the Physiological Characteristics of Barley (Hordeum vulgare L.) Varieties, J. Agric. Sci. Technol.
Marchant, B.P., Bloomfield, J.P., 2018. Spatio-temporal modelling of the status of groundwater droughts. J. Hydrol. 564, 397–413. https://doi.org/https://doi.org/10.1016/j.jhydrol.2018.07.009
Martínez-Vilalta, J., Lloret, F., 2016. Drought-induced vegetation shifts in terrestrial ecosystems: The key role of regeneration dynamics. Glob. Planet. Change 144, 94–108. https://doi.org/10.1016/J.GLOPLACHA.2016.07.009
Mathieu, J.A., Aires, F., 2018. Assessment of the agro-climatic indices to improve crop yield forecasting. Agric. For. Meteorol. 253–254, 15–30. https://doi.org/10.1016/J.AGRFORMET.2018.01.031
Mavromatis, T., 2007. Drought index evaluation for assessing future wheat production in Greece. Int. J. Climatol. 27, 911–924. https://doi.org/10.1002/joc.1444
Mcdowell, N., Pockman, W.T., Allen, C.D., Breshears, D.D., Cobb, N., Kolb, T., Plaut, J., Sperry, J., West, A., Williams, D.G., Yepez, E.A., 2008. Tansley review Mechanisms of plant survival and mortality during drought: why do some plants survive while others succumb to drought? https://doi.org/10.1111/j.1469-8137.2008.02436.x
McDowell, N.G., Fisher, R.A., Xu, C., Domec, J.C., Hölttä, T., Mackay, D.S., Sperry, J.S., Boutz, A., Dickman, L., Gehres, N., Limousin, J.M., Macalady, A., Martínez-Vilalta, J., Mencuccini, M., Plaut, J.A., Ogée, J., Pangle, R.E., Rasse, D.P., Ryan, M.G., Sevanto, S., Waring, R.H., Williams, A.P., Yepez, E.A., Pockman, W.T., 2013. Evaluating theories of drought-induced vegetation mortality using a multimodel-experiment framework. New Phytol. 200, 304–321. https://doi.org/10.1111/nph.12465
McEvoy, D.J., Huntington, J.L., Abatzoglou, J.T., Edwards, L.M., McEvoy, D.J., Huntington, J.L., Abatzoglou, J.T., Edwards, L.M., 2012. An Evaluation of Multiscalar Drought Indices in Nevada and Eastern California. Earth Interact. 16, 1–18. https://doi.org/10.1175/2012EI000447.1
Mckee, T.B., Doesken, N.J., Kleist, J., 1993. The relationshio of drought frequency and duration to time scales. Eighth Conf. Appl. Climatol. 17–22.
McKee, T.B., Doesken, N.J., Kleist, J., Society, A.M., 1995. Drought Monitoring with Multiple Time Scales, in: Conference on Applied Climatology. The Society, Dallas, pp. 233–236.
Miralles, D.G., Teuling, A.J., Van Heerwaarden, C.C., De Arellano, J.V.-G., 2014. Mega-heatwave temperatures due to combined soil desiccation and atmospheric heat accumulation. Nat. Geosci. 7, 345–349. https://doi.org/10.1038/ngeo2141
Mishra, A.K., Singh, V.P., 2010. A review of drought concepts. J. Hydrol. 391, 202–216. https://doi.org/10.1016/j.jhydrol.2010.07.012
Moorhead, J.E., Gowda, P.H., Singh, V.P., Porter, D.O., Marek, T.H., Howell, T.A., Stewart, B.A., 2015. Identifying and Evaluating a Suitable Index for Agricultural Drought Monitoring in the Texas High Plains. JAWRA J. Am. Water Resour. Assoc. 51, 807–820. https://doi.org/10.1111/jawr.12275
Navarro-Cerrillo, R., Rodriguez-Vallejo, C., Silveiro, E., Hortal, A., Palacios-Rodríguez, G., Duque-Lazo, J., Camarero, J., 2018. Cumulative Drought Stress Leads to a Loss of Growth Resilience and Explains Higher Mortality in Planted than in Naturally Regenerated Pinus pinaster Stands. Forests 9, 358. https://doi.org/10.3390/f9060358
Neumann, M., Mues, V., Moreno, A., Hasenauer, H., Seidl, R., 2017. Climate variability drives recent tree mortality in Europe. Glob. Chang. Biol. 23, 4788–4797. https://doi.org/10.1111/gcb.13724
Noormets, A., McNulty, S.G., DeForest, J.L., Sun, G., Li, Q., Chen, J., 2008. Drought during canopy development has lasting effect on annual carbon balance in a deciduous temperate forest.

New Phytol. 179, 818–828. https://doi.org/10.1111/j.1469-8137.2008.02501.x
Olesen, J.E., Trnka, M., Kersebaum, K.C., Skjelvåg, A.O., Seguin, B., Peltonen-Sainio, P., Rossi, F., Kozyra, J., Micale, F., 2011. Impacts and adaptation of European crop production systems to climate change. Eur. J. Agron. 34, 96–112. https://doi.org/10.1016/j.eja.2010.11.003
Palmer, W.C., 1965. Meteorological Drought. Research Paper No. 45, 1965, 58 p. U.S. Dep. Commer. Weather Bur. Washington, DC. Research P.
Páscoa, P., Gouveia, C.M., Russo, A., Trigo, R.M., 2016. The role of drought on wheat yield interannual variability in the Iberian Peninsula from 1929 to 2012. Int. J. Biometeorol. 1–13. https://doi.org/10.1007/s00484-016-1224-x
Pasho, E., Camarero, J.J., de Luis, M., Vicente-Serrano, S.M., 2011. Impacts of drought at different time scales on forest growth across a wide climatic gradient in north-eastern Spain. Agric. For. Meteorol. 151, 1800–1811. https://doi.org/10.1016/j.agrformet.2011.07.018
Peguero-Pina, J.J., Sancho-Knapik, D., Cochard, H., Barredo, G., Villarroya, D., Gil-Pelegrin, E., 2011. Hydraulic traits are associated with the distribution range of two closely related Mediterranean firs, Abies alba Mill. and Abies pinsapo Boiss. Tree Physiol. 31, 1067–1075. https://doi.org/10.1093/treephys/tpr092
Poulter, B., Pederson, N., Liu, H., Zhu, Z., D'Arrigo, R., Ciais, P., Davi, N., Frank, D., Leland, C., Myneni, R., Piao, S., Wang, T., 2013. Recent trends in Inner Asian forest dynamics to temperature and precipitation indicate high sensitivity to climate change. Agric. For. Meteorol. 178–179, 31–45. https://doi.org/10.1016/J.AGRFORMET.2012.12.006
Quiring, S.M., Ganesh, S., 2010. Evaluating the utility of the Vegetation Condition Index (VCI) for monitoring meteorological drought in Texas. Agric. For. Meteorol. 150, 330–339. https://doi.org/10.1016/j.agrformet.2009.11.015
Quiring, S.M., Papakryiakou, T.N., 2003. An evaluation of agricultural drought indices for the Canadian prairies. Agric. For. Meteorol. 118, 49–62. https://doi.org/10.1016/S0168-1923(03)00072-8
Rangecroft, S., Van Loon, A.F., Coxon, G., Breña-Naranjo, J.A., Van Ogtrop, F., Van Lanen, H.A.J., 2018. Using paired catchments to quantify the human influence on hydrological droughts. Hydrol. Earth Syst. Sci. Discuss. 1–23. https://doi.org/10.5194/hess-2018-215
Rimkus, E., Stonevicius, E., Kilpys, J., Maciulyte, V., Valiukas, D., 2017. Drought identification in the eastern Baltic region using NDVI. Earth Syst. Dynam 85194, 627–637. https://doi.org/10.5194/esd-8-627-2017
Rimkus, E., Stonevičius, E., Korneev, V., Kažys, J., Valiuškevičius, G., Pakhomau, A., 2013. Dynamics of meteorological and hydrological droughts in the Neman river basin. Environ. Res. Lett. 8, 045014. https://doi.org/10.1088/1748-9326/8/4/045014
Rohli, R. V., Bushra, N., Lam, N.S.N., Zou, L., Mihunov, V., Reams, M.A., Argote, J.E., 2016. Drought indices as drought predictors in the south-central USA. Nat. Hazards 83. https://doi.org/10.1007/s11069-016-2376-z
Romm, J., 2011. The next dust bowl. Nature 478, 450–451. https://doi.org/10.1038/478450a
Rossi S, Niemeyer S, 2010. Monitoring droughts and impacts on the agricultural production: Examples from Spain. MARM Options Méditerranéennes Série A. Séminaires Méditerranéens 35–40.
Salas, J., 1993. Analysis and modeling of hydrologic time series, in: McGraw-Hill (Ed.), Handbook of Hydrology. New York, pp. 1–72.
Sangüesa-Barreda, G., Linares, J.C., Camarero, J.J., 2015. Reduced growth sensitivity to climate in bark-beetle infested Aleppo pines: Connecting climatic and biotic drivers of forest dieback. For. Ecol. Manage. 357, 126–137. https://doi.org/10.1016/J.FORECO.2015.08.017
Scaini, A., Sánchez, N., Vicente-Serrano, S.M., Martínez-Fernández, J., 2015. SMOS-derived soil moisture anomalies and drought indices: a comparative analysis using *in situ* measurements. Hydrol. Process. 29, 373–383. https://doi.org/10.1002/hyp.10150
Schauberger, B., Ben-Ari, T., Makowski, D., Kato, T., Kato, H., Ciais, P., 2018. Yield trends,

variability and stagnation analysis of major crops in France over more than a century. Sci. Rep. 8, 16865. https://doi.org/10.1038/s41598-018-35351-1
Schubert, S.D., Wang, H., Koster, R.D., Suarez, M.J., Groisman, P.Y., Schubert, S.D., Wang, H., Koster, R.D., Suarez, M.J., Groisman, P.Y., 2014. Northern Eurasian Heat Waves and Droughts. J. Clim. 27, 3169–3207. https://doi.org/10.1175/JCLI-D-13-00360.1
Seneviratne, S.I., Corti, T., Davin, E.L., Hirschi, M., Jaeger, E.B., Lehner, I., Orlowsky, B., Teuling, A.J., 2010. Investigating soil moisture-climate interactions in a changing climate: A review. Earth-Science Rev. 99, 125–161. https://doi.org/10.1016/j.earscirev.2010.02.004
Sheffield, J., Wood, E.F., 2011. Drought: Past Problems & Future Scenarios (J. Sheffield & E.F. Wood) - GNHRE. Earthscan, London and Washington DC.
Sherwood, S., Fu, Q., 2014. A drier future? Science (80-.). 343, 737–739. https://doi.org/10.1126/science.1247620
Shukla, S., Steinemann, A.C., Lettenmaier, D.P., Shukla, S., Steinemann, A.C., Lettenmaier, D.P., 2011. Drought Monitoring for Washington State: Indicators and Applications. J. Hydrometeorol. 12, 66–83. https://doi.org/10.1175/2010JHM1307.1
Smith, A.B., Katz, R.W., 2013. US billion-dollar weather and climate disasters: data sources, trends, accuracy and biases. Nat. Hazards 67, 387–410. https://doi.org/10.1007/s11069-013-0566-5
Smith, A.B., Matthews, J.L., 2015. Quantifying uncertainty and variable sensitivity within the US billion-dollar weather and climate disaster cost estimates. Nat. Hazards 77, 1829–1851. https://doi.org/10.1007/s11069-015-1678-x
Sun, L., Mitchell, S.W., Davidson, A., 2012. Multiple drought indices for agricultural drought risk assessment on the Canadian prairies. Int. J. Climatol. 32, 1628–1639. https://doi.org/10.1002/joc.2385
Tack, J., Barkley, A., Nalley, L.L., 2015. Effect of warming temperatures on US wheat yields. Proc. Natl. Acad. Sci. U. S. A. 112, 6931–6. https://doi.org/10.1073/pnas.1415181112
Tallaksen, L.M., Madsen, H., Clausen, B., 1997. On the definition and modelling of streamflow drought duration and deficit volume. Hydrol. Sci. J. 42, 15–33. https://doi.org/10.1080/02626669709492003
Terrado, M., Acuña, V., Ennaanay, D., Tallis, H., Sabater, S., 2014. Impact of climate extremes on hydrological ecosystem services in a heavily humanized Mediterranean basin. Ecol. Indic. 37, 199–209. https://doi.org/10.1016/J.ECOLIND.2013.01.016
Teuling, A.J., 2018. A hot future for European droughts. Nat. Clim. Chang. 8, 364–365. https://doi.org/10.1038/s41558-018-0154-5
Tian, L., Yuan, S., Quiring, S.M., 2018. Evaluation of six indices for monitoring agricultural drought in the south-central United States. Agric. For. Meteorol. 249, 107–119. https://doi.org/10.1016/J.AGRFORMET.2017.11.024
Tigkas, D., Tsakiris, G., 2015. Early Estimation of Drought Impacts on Rainfed Wheat Yield in Mediterranean Climate. Environ. Process. 2, 97–114. https://doi.org/10.1007/s40710-014-0052-4
Tijdeman, E., Bachmair, S., Stahl, K., 2016. Controls on hydrologic drought duration in near-natural streamflow in Europe and the USA. Hydrol. Earth Syst. Sci. 20, 4043–4059. https://doi.org/10.5194/hess-20-4043-2016
Tijdeman, E., Hannaford, J., Stahl, K., 2018. Human influences on streamflow drought characteristics in England and Wales. Hydrol. Earth Syst. Sci. 22, 1051–1064. https://doi.org/10.5194/hess-22-1051-2018
Trenberth, K.E., Dai, A., van der Schrier, G., Jones, P.D., Barichivich, J., Briffa, K.R., Sheffield, J., 2014. Global warming and changes in drought. Nat. Clim. Chang. 4, 17–22. https://doi.org/10.1038/nclimate2067
Van Loon, A.F., 2015. Hydrological drought explained. Wiley Interdiscip. Rev. Water 2, 359–392. https://doi.org/10.1002/wat2.1085
Van Loon, A.F., Gleeson, T., Clark, J., Van Dijk, A.I.J.M., Stahl, K., Hannaford, J., Di Baldassarre, G.,

Teuling, A.J., Tallaksen, L.M., Uijlenhoet, R., Hannah, D.M., Sheffield, J., Svoboda, M., Verbeiren, B., Wagener, T., Rangecroft, S., Wanders, N., Van Lanen, H.A.J., 2016. Drought in the Anthropocene. Nat. Geosci. 9, 89–91. https://doi.org/10.1038/ngeo2646

Van Loon, A.F., Laaha, G., 2015. Hydrological drought severity explained by climate and catchment characteristics. J. Hydrol. 526, 3–14. https://doi.org/10.1016/J.JHYDROL.2014.10.059

Vasiliades, L., Loukas, A., 2009. Hydrological response to meteorological drought using the Palmer drought indices in Thessaly, Greece. Desalination 237, 3–21. https://doi.org/10.1016/J.DESAL.2007.12.019

Vergni, L., Todisco, F., 2011. Spatio-temporal variability of precipitation, temperature and agricultural drought indices in Central Italy. Agric. For. Meteorol. 151, 301–313. https://doi.org/10.1016/j.agrformet.2010.11.005

Vicente-Serrano, S.M., 2006. Differences in Spatial Patterns of Drought on Different Time Scales : An Analysis of the Iberian Peninsula. Water Resour. Manag. 20, 37–60. https://doi.org/10.1007/s11269-006-2974-8

Vicente-Serrano, S.M., Beguería, S., 2016. Comment on "Candidate distributions for climatological drought indices (SPI and SPEI)" by James H. Stagge et al. Int. J. Climatol. 36. https://doi.org/10.1002/joc.4474

Vicente-Serrano, S.M., Beguería, S., López-Moreno, J.I., 2011a. Comment on "Characteristics and trends in various forms of the Palmer Drought Severity Index (PDSI) during 1900–2008" by Aiguo Dai. J. Geophys. Res. 116, D19112. https://doi.org/10.1029/2011JD016410

Vicente-Serrano, S.M., Beguería, S., López-Moreno, J.I., 2011b. Comment on "Characteristics and trends in various forms of the Palmer Drought Severity Index (PDSI) during 1900–2008" by Aiguo Dai. J. Geophys. Res. 116, D19112. https://doi.org/10.1029/2011JD016410

Vicente-Serrano, S.M., Beguería, S., López-Moreno, J.I., Vicente-Serrano, S.M., Beguería, S., López-Moreno, J.I., 2010. A Multiscalar Drought Index Sensitive to Global Warming: The Standardized Precipitation Evapotranspiration Index. J. Clim. 23, 1696–1718. https://doi.org/10.1175/2009JCLI2909.1

Vicente-Serrano, S.M., Beguería, S., Lorenzo-Lacruz, J., Camarero, J.J., López-Moreno, J.I., Azorin-Molina, C., Revuelto, J., Morán-Tejeda, E., Sanchez-Lorenzo, A., Vicente-Serrano, S.M., Beguería, S., Lorenzo-Lacruz, J., Camarero, J.J., López-Moreno, J.I., Azorin-Molina, C., Revuelto, J., Morán-Tejeda, E., Sanchez-Lorenzo, A., 2012. Performance of Drought Indices for Ecological, Agricultural, and Hydrological Applications. http://dx.doi.org/10.1175/2012EI000434.1. https://doi.org/10.1175/2012EI000434.1

Vicente-Serrano, S.M., Gouveia, C., Camarero, J.J., Beguería, S., Trigo, R., López-Moreno, J.I., Azorín-Molina, C., Pasho, E., Lorenzo-Lacruz, J., Revuelto, J., Morán-Tejeda, E., Sanchez-Lorenzo, A., 2013a. Response of vegetation to drought time-scales across global land biomes. Proc. Natl. Acad. Sci. U. S. A. 110, 52–7. https://doi.org/10.1073/pnas.1207068110

Vicente-Serrano, S.M., Gouveia, C., Camarero, J.J., Beguería, S., Trigo, R., López-Moreno, J.I., Azorín-Molina, C., Pasho, E., Lorenzo-Lacruz, J., Revuelto, J., Morán-Tejeda, E., Sanchez-Lorenzo, A., 2013b. Response of vegetation to drought time-scales across global land biomes. Proc. Natl. Acad. Sci. U. S. A. 110, 52–7. https://doi.org/10.1073/pnas.1207068110

Vicente-Serrano, S.M., Lopez-Moreno, J.-I., Beguería, S., Lorenzo-Lacruz, J., Sanchez-Lorenzo, A., García-Ruiz, J.M., Azorin-Molina, C., Morán-Tejeda, E., Revuelto, J., Trigo, R., Coelho, F., Espejo, F., 2014. Evidence of increasing drought severity caused by temperature rise in southern Europe. Environ. Res. Lett. Environ. Res. Lett 9, 44001–9. https://doi.org/10.1088/1748-9326/9/4/044001

Vicente-Serrano, S.M., López-Moreno, J.I., 2005. Hydrological response to different time scales of climatological drought: an evaluation of the Standardized Precipitation Index in a mountainous Mediterranean basin. Hydrol. Earth Syst. Sci. 9, 523–533.

https://doi.org/10.5194/hess-9-523-2005
Vicente-Serrano, S.M., López-Moreno, J.I., Beguería, S., Lorenzo-Lacruz, J., Azorin-Molina, C., Morán-Tejeda, E., 2012. Accurate Computation of a Streamflow Drought Index. J. Hydrol. Eng. 17. https://doi.org/10.1061/(ASCE)HE.1943-5584.0000433
Vicente-Serrano, S.M., Van der Schrier, G., Beguería, S., Azorin-Molina, C., Lopez-Moreno, J.-I., 2015. Contribution of precipitation and reference evapotranspiration to drought indices under different climates. J. Hydrol. 526, 42–54. https://doi.org/10.1016/j.jhydrol.2014.11.025
Vicente-Serrano, S.M., Zabalza-Martínez, J., Borràs, G., López-Moreno, J.I., Pla, E., Pascual, D., Savé, R., Biel, C., Funes, I., Azorin-Molina, C., Sanchez-Lorenzo, A., Martín-Hernández, N., Peña-Gallardo, M., Alonso-González, E., Tomas-Burguera, M., El Kenawy, A., 2017a. Extreme hydrological events and the influence of reservoirs in a highly regulated river basin of northeastern Spain. J. Hydrol. Reg. Stud. 12. https://doi.org/10.1016/j.ejrh.2017.01.004
Vicente-Serrano, S.M., Zabalza-Martínez, J., Borràs, G., López-Moreno, J.I., Pla, E., Pascual, D., Savé, R., Biel, C., Funes, I., Martín-Hernández, N., Peña-Gallardo, M., Beguería, S., Tomas-Burguera, M., 2017b. Effect of reservoirs on streamflow and river regimes in a heavily regulated river basin of Northeast Spain. CATENA 149, 727–741. https://doi.org/10.1016/j.catena.2016.03.042
Wang, H., Vicente-serrano, S.M., Tao, F., Zhang, X., Wang, P., Zhang, C., Chen, Y., Zhu, D., Kenawy, A. El, 2016. Monitoring winter wheat drought threat in Northern China using multiple climate-based drought indices and soil moisture during 2000–2013. Agric. For. Meteorol. 228–229, 1–12. https://doi.org/10.1016/j.agrformet.2016.06.004
Wang, Q., Wu, J., Lei, T., He, B., Wu, Z., Liu, M., Mo, X., Geng, G., Li, X., Zhou, H., Liu, D., 2014. Temporal-spatial characteristics of severe drought events and their impact on agriculture on a global scale, Quaternary International. https://doi.org/10.1016/j.quaint.2014.06.021
Wang, Q., Wu, J., Li, X., Zhou, H., Yang, J., Geng, G., An, X., Liu, L., Tang, Z., 2016. A comprehensively quantitative method of evaluating the impact of drought on crop yield using daily multi-scale SPEI and crop growth process model. Int. J. Biometeorol. 1–15. https://doi.org/10.1007/s00484-016-1246-4
Weber, L., Kkemdirim, L., 1998. Palmer's Drought Indices Revisited. Geogr. Ann. Ser. A Phys. Geogr. 80, 153–172. https://doi.org/10.1111/j.0435-3676.1998.00033.x
Wells, N., Goddard, S., Hayes, M.J., Wells, N., Goddard, S., Hayes, M.J., 2004. A Self-Calibrating Palmer Drought Severity Index. J. Clim. 17, 2335–2351. https://doi.org/10.1175/1520-0442(2004)017<2335:ASPDSI>2.0.CO;2
Wilhite, D.A., 2000. Drought as a Natural Hazard: Concepts and Definitions, in: Wilhite, D.A. (Ed.), Drought: A Global Assessment. Vol.1. Drought Mitigation Center Faculty Publications, pp. 3–18.
Wilhite, D.A., Glantz, M.H., 1985. Understanding: the Drought Phenomenon: The Role of Definitions. Water Int. 10, 111–120. https://doi.org/10.1080/02508068508686328
Wilhite, D.A., Pulwarty, R.S., 2017. Drought as Hazard: Understanding the Natural and Social Context, in: Drought and Water Crises: Integrating Science, Management, and Policy. pp. 3–22.
Wilhite, D.A., Svoboda, M.D., Hayes, M.J., 2007. Understanding the complex impacts of drought: A key to enhancing drought mitigation and preparedness. Water Resour. Manag. 21, 763–774. https://doi.org/10.1007/s11269-006-9076-5
WMO, 2012. Standardized Precipitation Index User Guide.
World Meteorological Organization (WMO) and Global Water Partnership (GWP), 2016. Handbook of Drought Indicators and Indices (M. Svoboda and B.A. Fuchs). Integrated Drought Management Programme (IDMP), Integrated Drought Management Tools and Guidelines Series 2. Geneva.
Wu, J., Chen, X., Yao, H., Gao, L., Chen, Y., Liu, M., 2017. Non-linear relationship of hydrological

drought responding to meteorological drought and impact of a large reservoir. J. Hydrol. 551, 495–507. https://doi.org/10.1016/J.JHYDROL.2017.06.029
Yang, Y., Zhang, S., McVicar, T.R., Beck, H.E., Zhang, Y., Liu, B., 2018. Disconnection Between Trends of Atmospheric Drying and Continental Runoff. Water Resour. Res. 54, 4700–4713. https://doi.org/10.1029/2018WR022593
Young, D.J.N., Stevens, J.T., Earles, J.M., Moore, J., Ellis, A., Jirka, A.L., Latimer, A.M., 2017. Long-term climate and competition explain forest mortality patterns under extreme drought. Ecol. Lett. 20, 78–86. https://doi.org/10.1111/ele.12711
Zargar, A., Sadiq, R., Naser, B., Khan, F.I., 2011. A review of drought indices. Environ. Rev. 19, 333–349. https://doi.org/10.1139/a11-013
Zipper, S.C., Qiu, J., Kucharik, C.J., 2016. Drought effects on US maize and soybean production: spatiotemporal patterns and historical changes. Environ. Res. Lett. 11, 094021. https://doi.org/10.1088/1748-9326/11/9/094021

9. Appendix

Supplementary material from published an unpublished articles

Appendix. Additional data

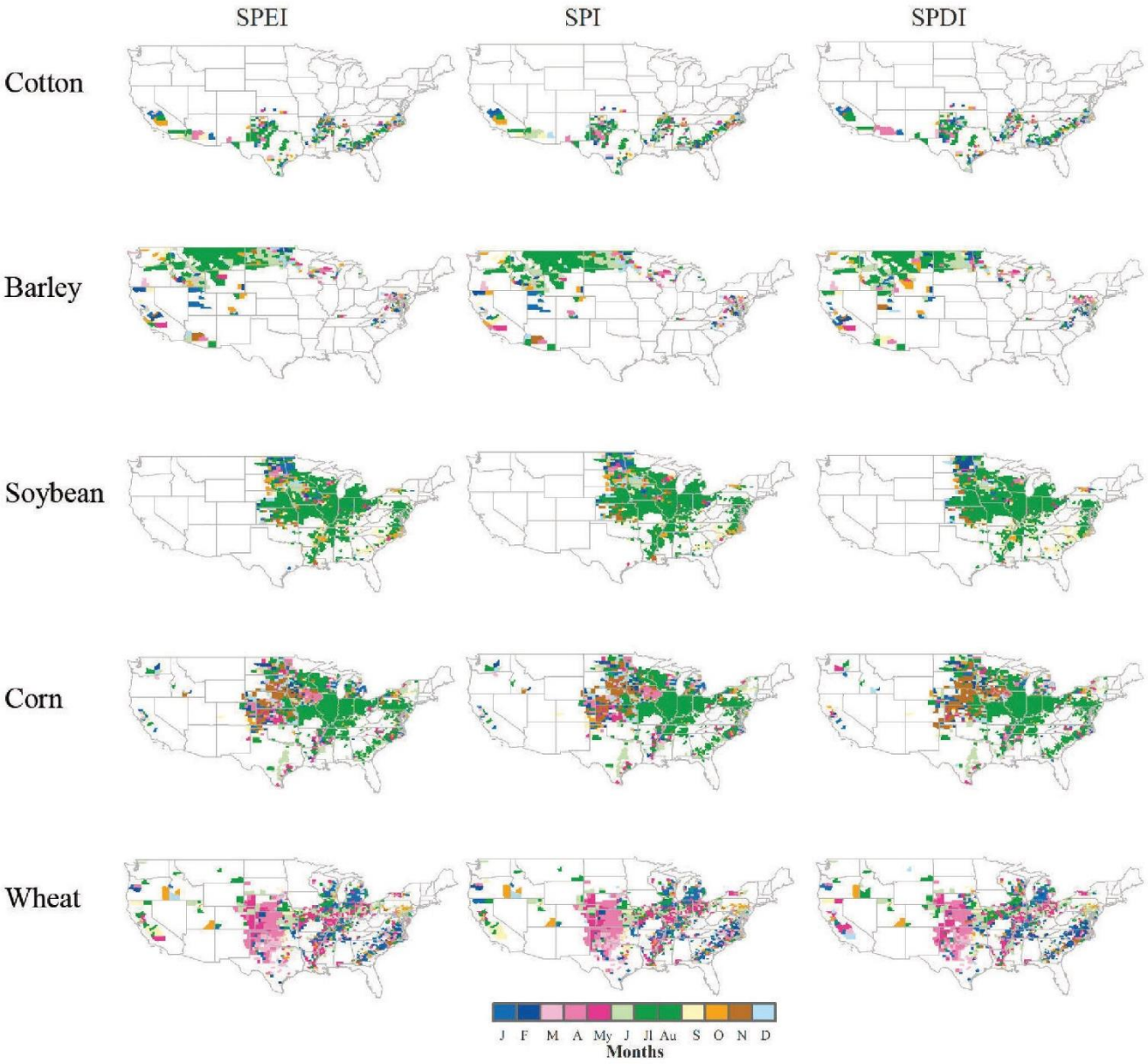

Fig. A1. Spatial distribution of the months in which the highest Pearson correlation coefficients were obtained for the SPEI, SPI and SPDI and crop yields. Indices are defined in Table 1

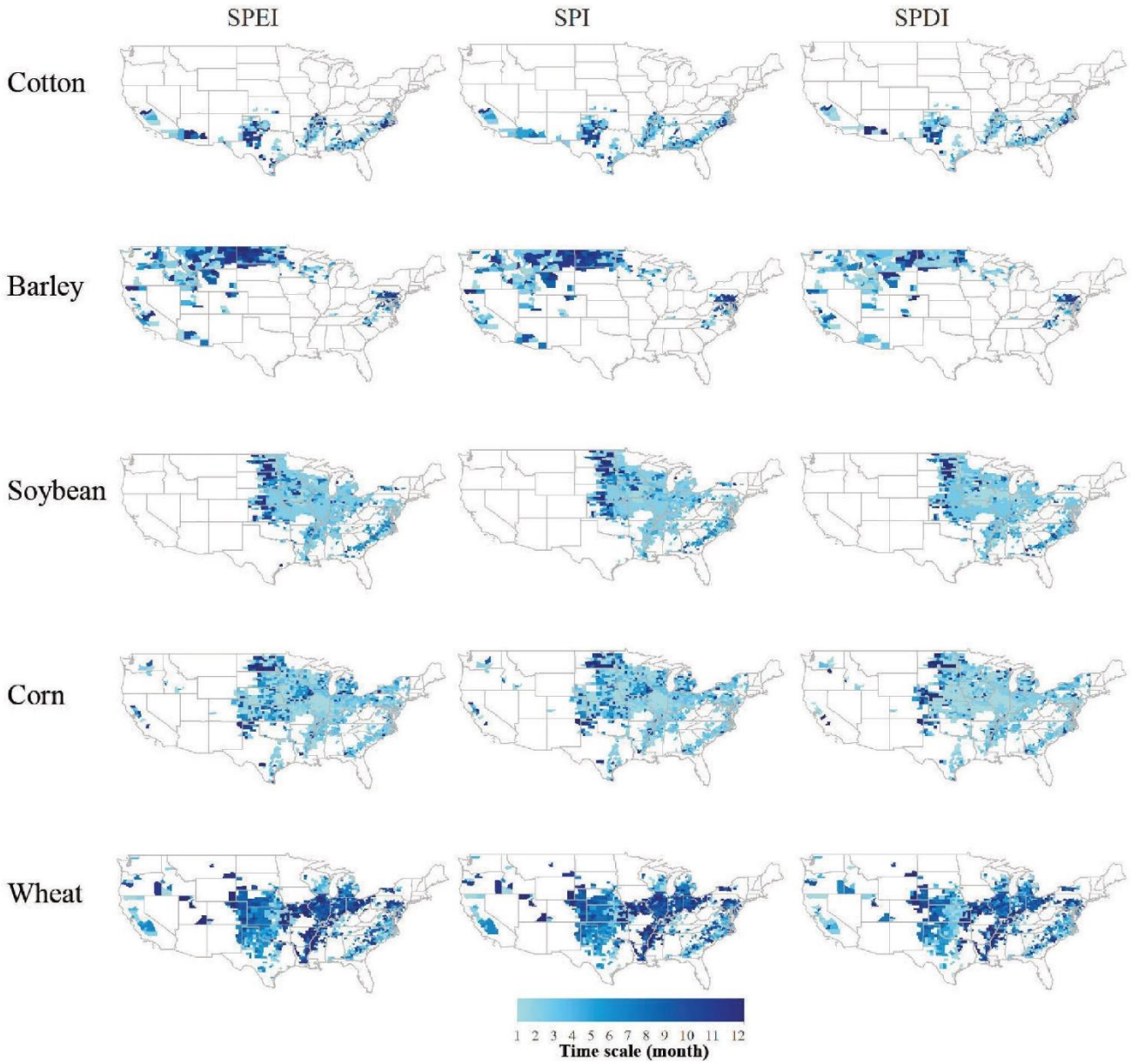

Fig. A2. Spatial distribution of the timescales at which the highest Pearson correlation coefficients were obtained for the SPEI, SPI and SPDI and crop yields. Indices are defined in Table 1

Editorial responsibility: Toshichika Iizumi, Tsukuba, Japan

Submitted: January 25, 2018; Accepted: May 7, 2018
Proofs received from author(s): July 26, 2018

Supplementary material:

Response of crop yield to different time-scales of drought in the United States: spatio-temporal patterns and climatic and environmental drivers

Marina Peña-Gallardo[1], Sergio M. Vicente-Serrano[1], Steven Quiring[2], Marc Svoboda[3], Jamie Hannaford[4], Miquel Tomas-Burguera[5], Natalia Martin-Hernandez[1], Fernando Domínguez-Castro[1], Ahmed El Kenawy[1,6]

[1]Instituto Pirenaico de Ecología, Consejo Superior de Investigaciones Científicas (IPE–CSIC), Spain
[2]Ohio State University, US
[3]National Drought Mitigation Centre, University of Nebraska-Lincoln, US
[4]Centre for Ecology and Hydrology, United Kingdom
[5] Estación Experimental de Aula Dei, Consejo Superior de Investigaciones Científicas (EEAD-CSIC), Spain
[6] Department of Geography, Mansoura University, Mansoura, Egypt

This document contains supplementary figures and statistical analysis

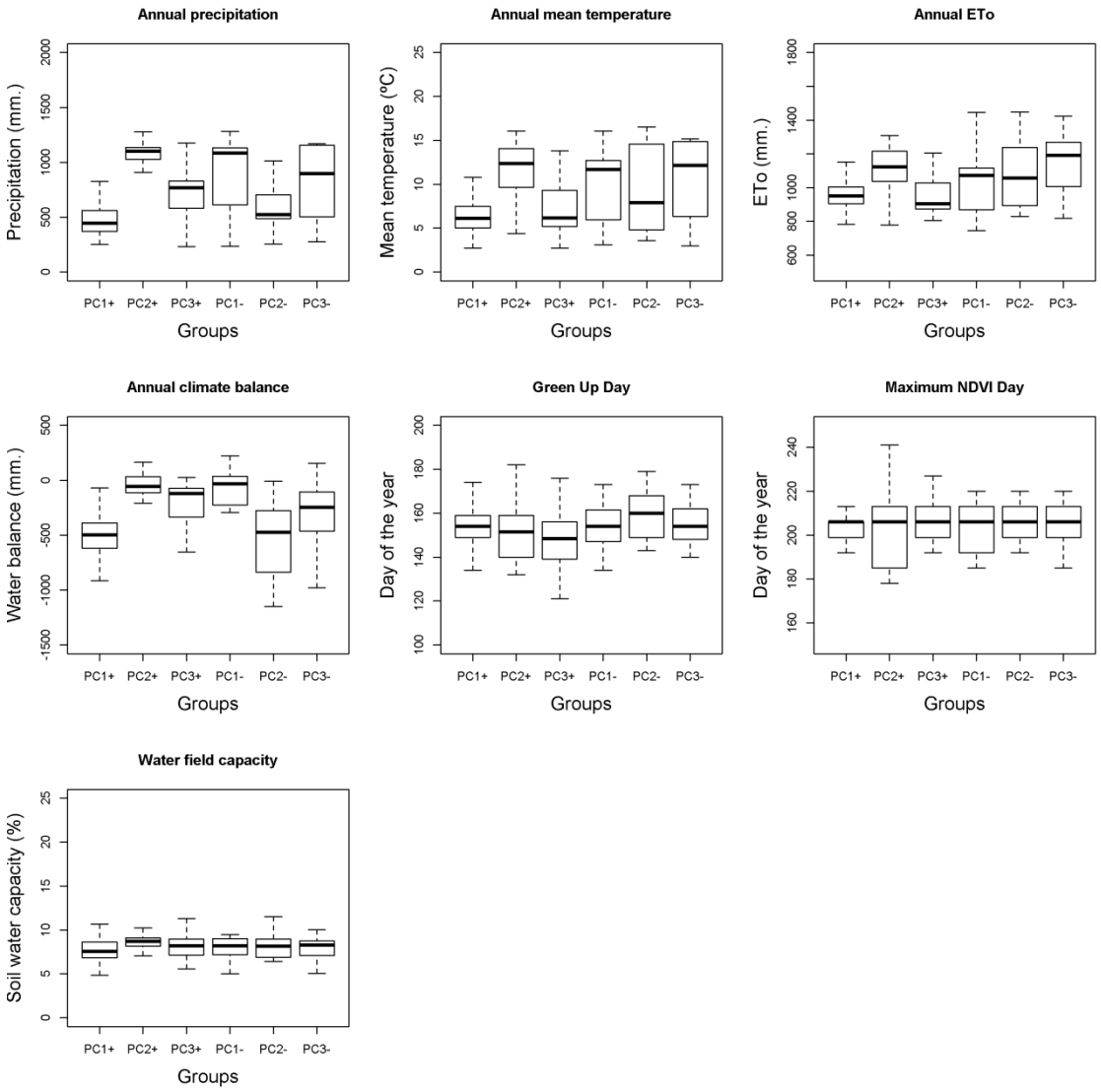

Supplementary Figure 1: Boxplots showing the statistical distribution of different annual climate and environmental variables corresponding to the different groups of response of the annual barley crop yields to different time-scales of the SPEI.

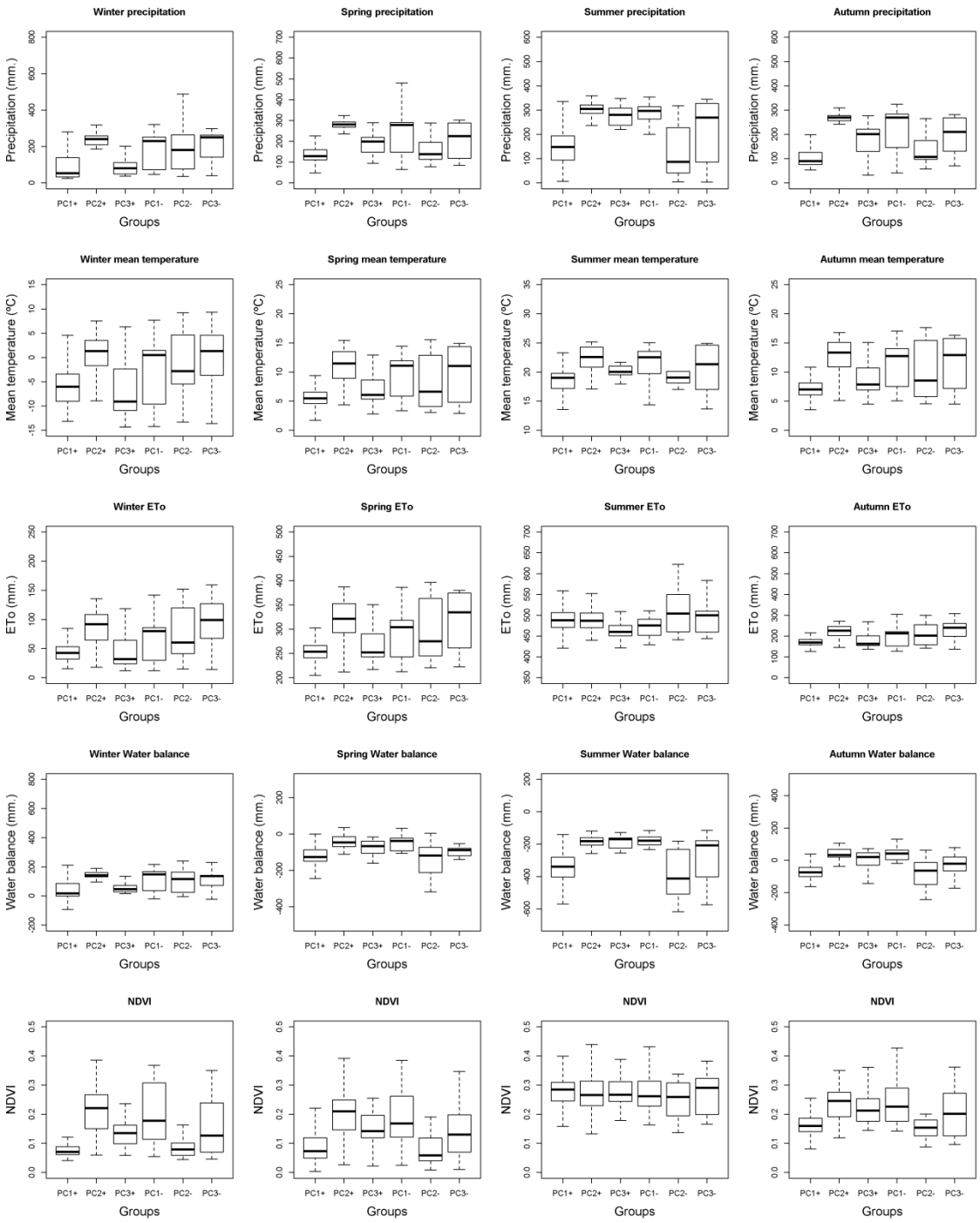

Supplementary Figure 2: Boxplots showing the statistical distribution of different seasonal climate variables and the NDVI corresponding to the different groups of response of the annual barley crop yields to different time-scales of the SPEI obtained by means of the PCA.

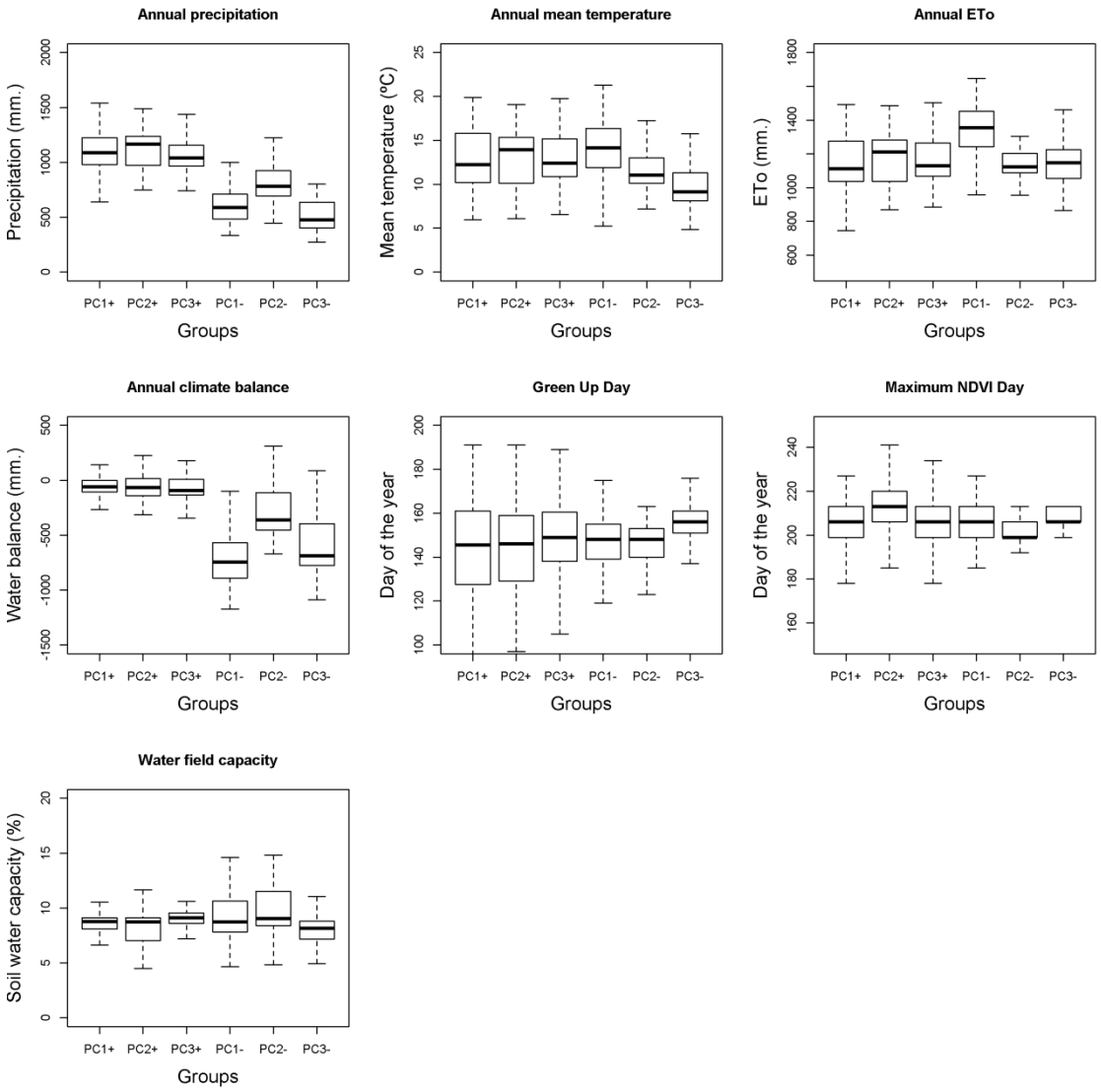

Supplementary Figure 3: Same as Supplementary Figure 1, but for winter wheat crop yields.

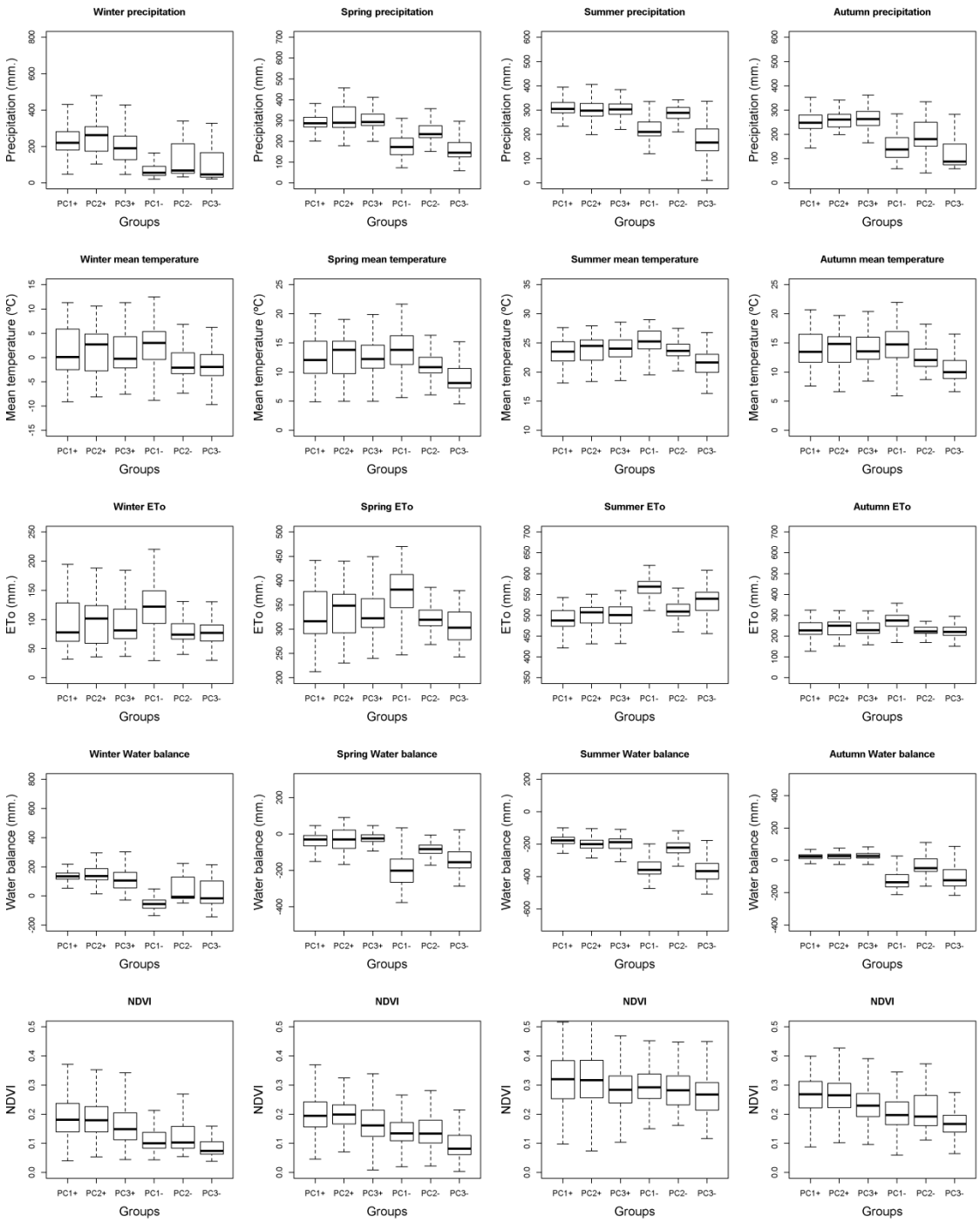

Supplementary Figure 4: Same as Supplementary Figure 2, but for winter wheat yields.

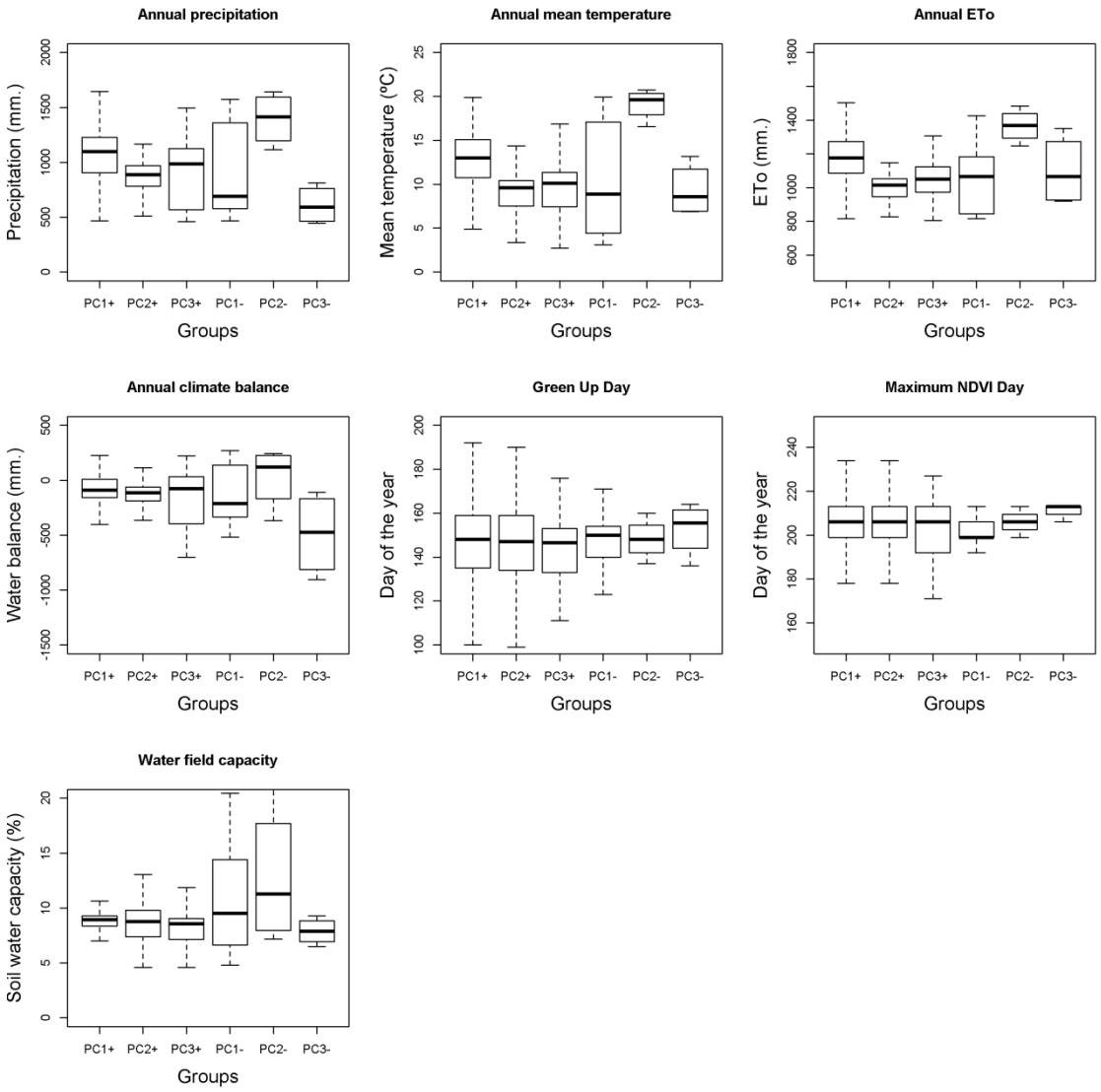

Supplementary Figure 5: Same as Supplementary Figure 1, but for soybean crop yields.

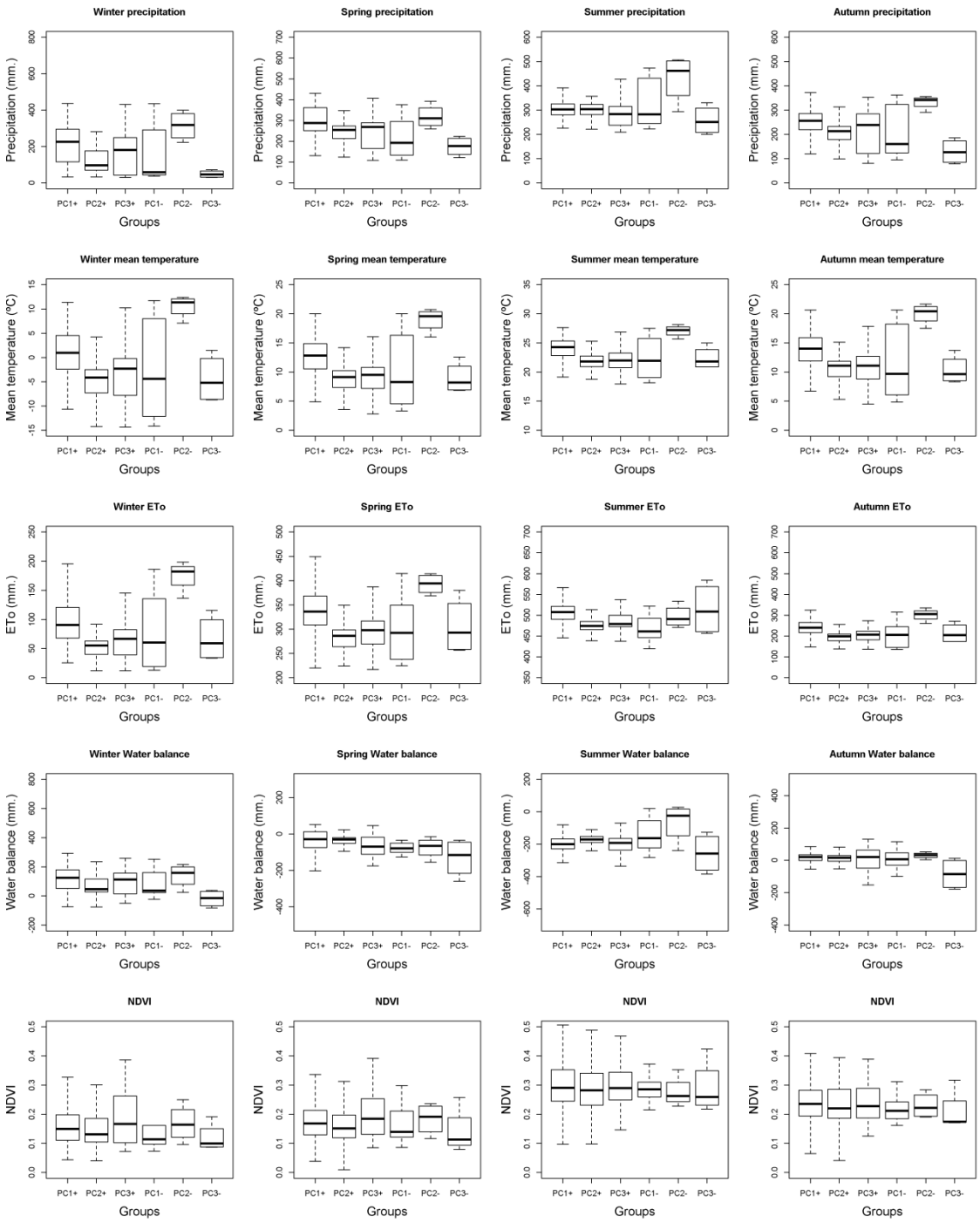

Supplementary Figure 6: Same as Supplementary Figure 2,but for soybean yields.

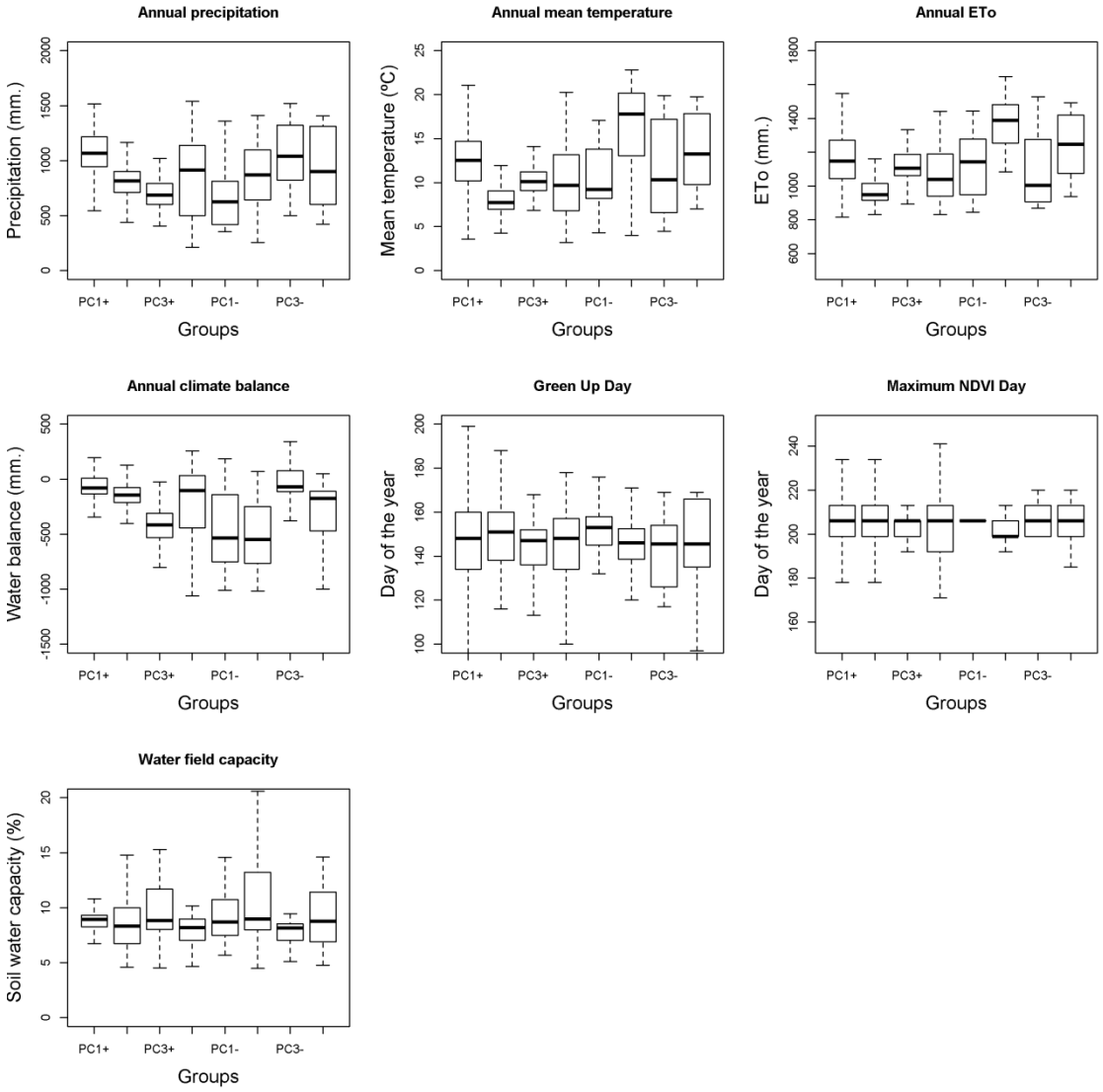

Supplementary Figure 7: Same as Supplementary Figure 1, but for corn crop yields.

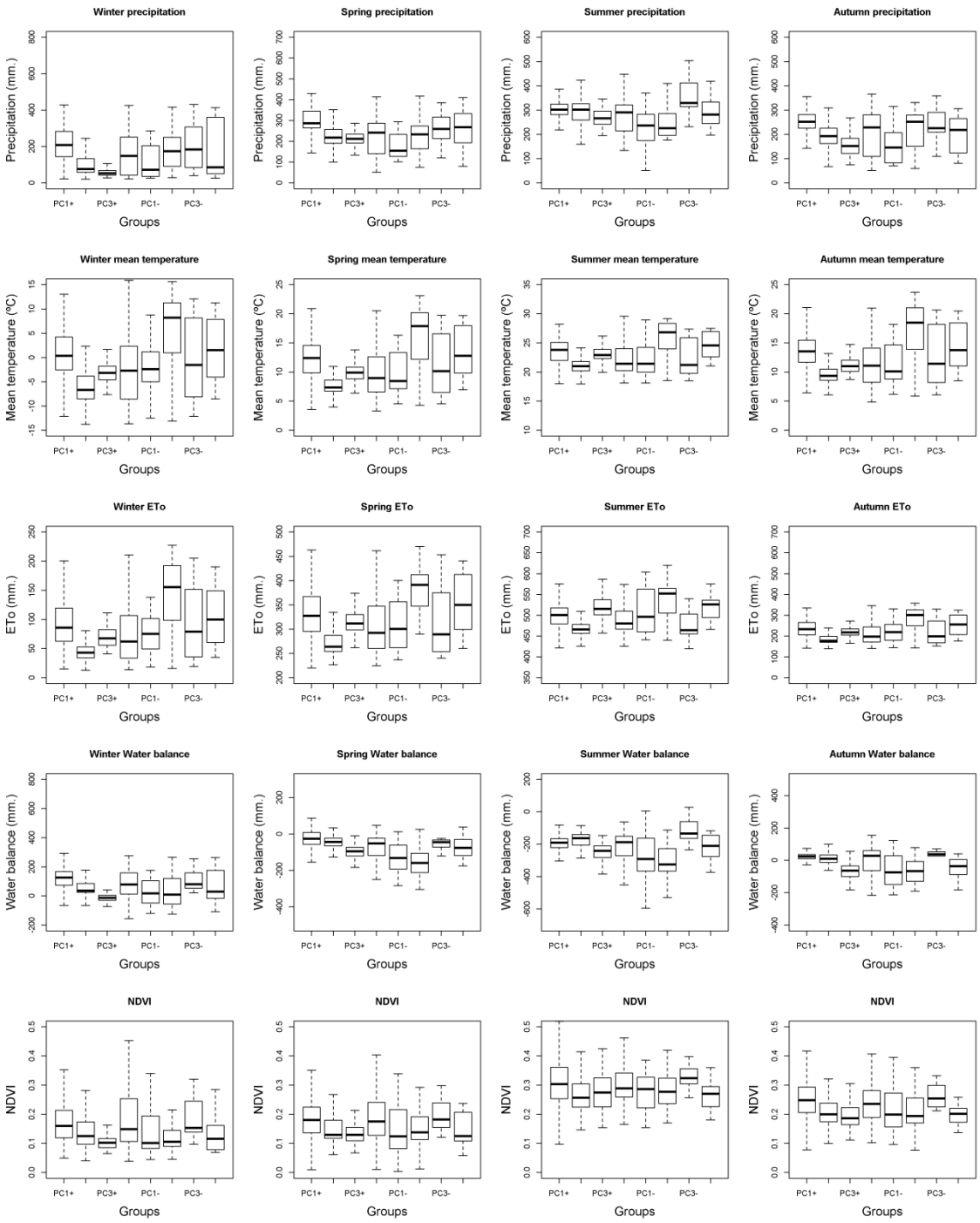

Supplementary Figure 8: Same as Supplementary Figure 2, but for corn yields.

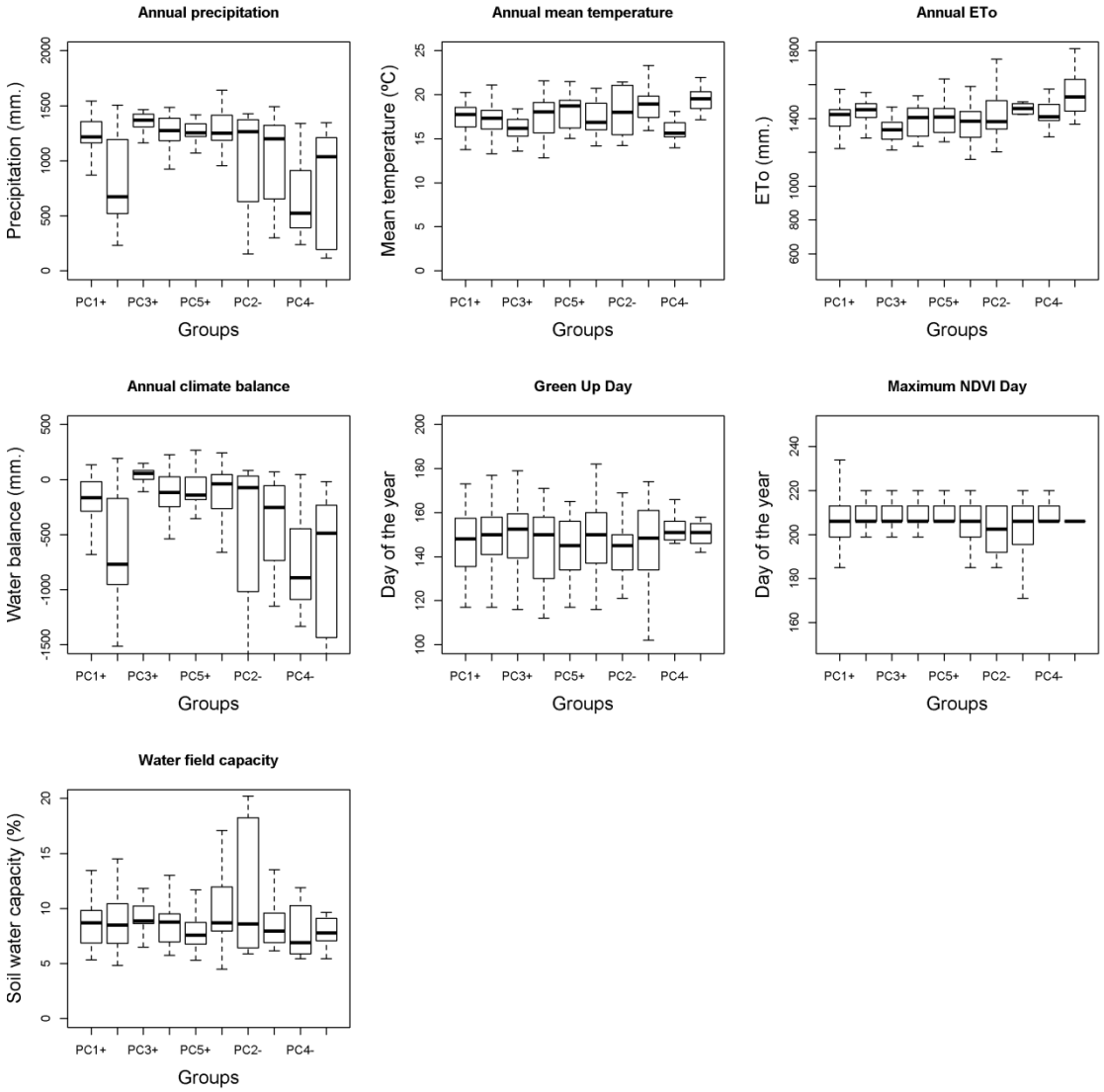

Supplementary Figure 9: Same as Supplementary Figure 1, but for cotton crop yields.

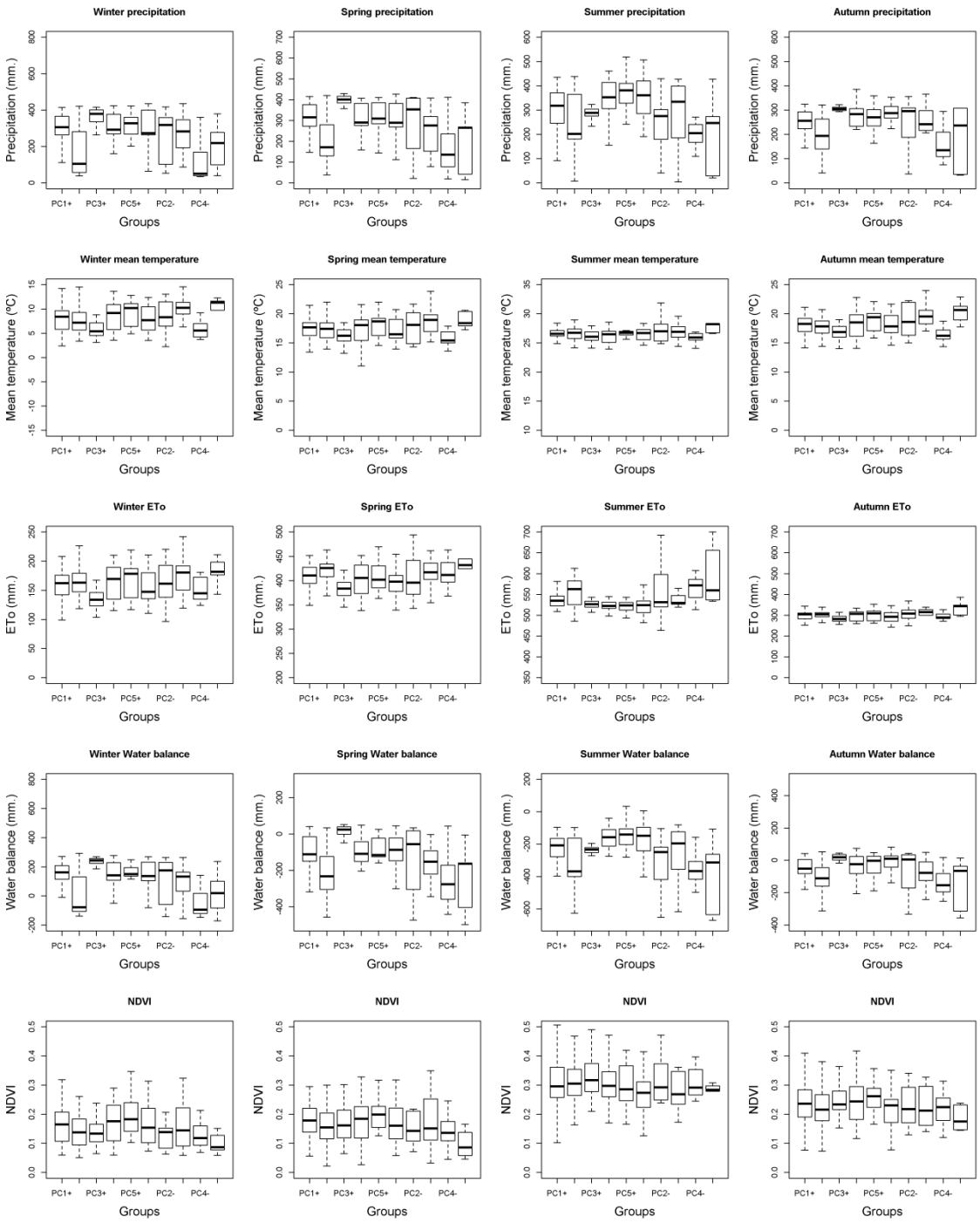

Supplementary Figure 10: Same as Supplementary Figure 2, but for cotton yields.

Supplementary statistical analysis:

Post-hoc statistical tests to determine the significance of the differences between climate and NDVI variables among the different groups of crop-yield response to the SPEI time-scales obtained by means of the PCA.

SIGNIFICATION CODES:

Signif. codes: 0 '***' 0.001 '**' 0.01 '*' 0.05 '.' 0.1 ' ' 1
(Adjusted p values reported -- single-step method)

1. BARLEY

Annual precipitation

	Estimate	Std. Error	t value	Pr(>|t|)	
Comp1(+) - Comp1(-) == 0	70.17	16.88	4.156	< 0.001	***
Comp2(-) - Comp1(-) == 0	80.75	26.27	3.074	0.02436	*
Comp2(+) - Comp1(-) == 0	-23.75	18.43	-1.289	0.77463	
Comp3(-) - Comp1(-) == 0	16.80	28.64	0.586	0.99088	
Comp3(+) - Comp1(-) == 0	117.76	20.32	5.796	< 0.001	***
Comp2(-) - Comp1(+) == 0	10.58	22.51	0.470	0.99676	
Comp2(+) - Comp1(+) == 0	-93.92	12.48	-7.523	< 0.001	***
Comp3(-) - Comp1(+) == 0	-53.37	25.23	-2.115	0.26236	
Comp3(+) - Comp1(+) == 0	47.59	15.13	3.144	0.01965	*
Comp2(+) - Comp2(-) == 0	-104.50	23.69	-4.412	< 0.001	***
Comp3(-) - Comp2(-) == 0	-63.95	32.28	-1.981	0.33332	
Comp3(+) - Comp2(-) == 0	37.01	25.18	1.469	0.66293	
Comp3(-) - Comp2(+) == 0	40.55	26.29	1.542	0.61485	
Comp3(+) - Comp2(+) == 0	141.51	16.84	8.403	< 0.001	***
Comp3(+) - Comp3(-) == 0	100.96	27.65	3.651	0.00363	**

Winter precipitation

	Estimate	Std. Error	t value	Pr(>|t|)	
Comp1(+) - Comp1(-) == 0	-1.150	18.720	-0.061	1.00000	
Comp2(-) - Comp1(-) == 0	1.319	29.129	0.045	1.00000	
Comp2(+) - Comp1(-) == 0	-25.796	20.432	-1.263	0.78932	
Comp3(-) - Comp1(-) == 0	-34.371	31.758	-1.082	0.87775	
Comp3(+) - Comp1(-) == 0	46.116	22.526	2.047	0.29726	
Comp2(-) - Comp1(+) == 0	2.469	24.952	0.099	1.00000	
Comp2(+) - Comp1(+) == 0	-24.646	13.841	-1.781	0.45594	
Comp3(-) - Comp1(+) == 0	-33.221	27.977	-1.187	0.82909	
Comp3(+) - Comp1(+) == 0	47.266	16.779	2.817	0.05145	.
Comp2(+) - Comp2(-) == 0	-27.115	26.261	-1.033	0.89767	
Comp3(-) - Comp2(-) == 0	-35.690	35.788	-0.997	0.91051	
Comp3(+) - Comp2(-) == 0	44.797	27.921	1.604	0.57317	
Comp3(-) - Comp2(+) == 0	-8.575	29.150	-0.294	0.99966	
Comp3(+) - Comp2(+) == 0	71.912	18.670	3.852	0.00168	**
Comp3(+) - Comp3(-) == 0	80.488	30.654	2.626	0.08501	.

Spring precipitation

	Estimate	Std. Error	t value	Pr(>|t|)	
Comp1(+) - Comp1(-) == 0	-99.59	16.39	-6.075	< 0.001	***
Comp2(-) - Comp1(-) == 0	-88.27	25.51	-3.460	0.00703	**
Comp2(+) - Comp1(-) == 0	27.21	17.89	1.521	0.62917	
Comp3(-) - Comp1(-) == 0	-31.16	27.81	-1.120	0.86121	
Comp3(+) - Comp1(-) == 0	-55.48	19.73	-2.812	0.05217	.
Comp2(-) - Comp1(+) == 0	11.32	21.85	0.518	0.99487	

```
Comp2(+) - Comp1(+) == 0   126.80     12.12  10.461  < 0.001 ***
Comp3(-) - Comp1(+) == 0    68.43     24.50   2.793  0.05503 .
Comp3(+) - Comp1(+) == 0    44.11     14.69   3.002  0.03050 *
Comp2(+) - Comp2(-) == 0   115.48     23.00   5.021  < 0.001 ***
Comp3(-) - Comp2(-) == 0    57.11     31.34   1.822  0.42932
Comp3(+) - Comp2(-) == 0    32.79     24.45   1.341  0.74407
Comp3(-) - Comp2(+) == 0   -58.37     25.53  -2.286  0.18671
Comp3(+) - Comp2(+) == 0   -82.70     16.35  -5.058  < 0.001 ***
Comp3(+) - Comp3(-) == 0   -24.33     26.85  -0.906  0.93895
```

Summer precipitation

```
                      Estimate Std. Error t value Pr(>|t|)
Comp1(+) - Comp1(-) == 0  -63.071     18.060  -3.492  0.00642 **
Comp2(-) - Comp1(-) == 0   17.343     28.103   0.617  0.98849
Comp2(+) - Comp1(-) == 0   10.074     19.712   0.511  0.99519
Comp3(-) - Comp1(-) == 0   16.343     30.639   0.533  0.99413
Comp3(+) - Comp1(-) == 0  -18.962     21.733  -0.872  0.94774
Comp2(-) - Comp1(+) == 0   80.414     24.073   3.340  0.01071 *
Comp2(+) - Comp1(+) == 0   73.144     13.353   5.478  < 0.001 ***
Comp3(-) - Comp1(+) == 0   79.414     26.991   2.942  0.03619 *
Comp3(+) - Comp1(+) == 0   44.109     16.187   2.725  0.06582 .
Comp2(+) - Comp2(-) == 0   -7.269     25.336  -0.287  0.99970
Comp3(-) - Comp2(-) == 0   -1.000     34.527  -0.029  1.00000
Comp3(+) - Comp2(-) == 0  -36.304     26.937  -1.348  0.73985
Comp3(-) - Comp2(+) == 0    6.269     28.123   0.223  0.99991
Comp3(+) - Comp2(+) == 0  -29.035     18.012  -1.612  0.56801
Comp3(+) - Comp3(-) == 0  -35.304     29.574  -1.194  0.82592
```

Autumn precipitation

```
                      Estimate Std. Error t value Pr(>|t|)
Comp1(+) - Comp1(-) == 0   31.323     18.622   1.682   0.5210
Comp2(-) - Comp1(-) == 0    1.583     28.977   0.055   1.0000
Comp2(+) - Comp1(-) == 0   16.689     20.325   0.821   0.9595
Comp3(-) - Comp1(-) == 0    6.829     31.592   0.216   0.9999
Comp3(+) - Comp1(-) == 0  -41.768     22.408  -1.864   0.4030
Comp2(-) - Comp1(+) == 0  -29.741     24.821  -1.198   0.8236
Comp2(+) - Comp1(+) == 0  -14.634     13.768  -1.063   0.8857
Comp3(-) - Comp1(+) == 0  -24.495     27.830  -0.880   0.9458
Comp3(+) - Comp1(+) == 0  -73.091     16.691  -4.379   <0.001 ***
Comp2(+) - Comp2(-) == 0   15.107     26.124   0.578   0.9915
Comp3(-) - Comp2(-) == 0    5.246     35.601   0.147   1.0000
Comp3(+) - Comp2(-) == 0  -43.350     27.775  -1.561   0.6026
Comp3(-) - Comp2(+) == 0   -9.861     28.998  -0.340   0.9993
Comp3(+) - Comp2(+) == 0  -58.457     18.572  -3.148   0.0196 *
Comp3(+) - Comp3(-) == 0  -48.596     30.494  -1.594   0.5804
```

Annual mean temperature

```
                      Estimate Std. Error t value Pr(>|t|)
Comp1(+) - Comp1(-) == 0  104.841     17.209   6.092  < 0.001 ***
Comp2(-) - Comp1(-) == 0   78.094     26.778   2.916  0.03913 *
Comp2(+) - Comp1(-) == 0    4.179     18.783   0.222  0.99991
Comp3(-) - Comp1(-) == 0   41.943     29.195   1.437  0.68432
Comp3(+) - Comp1(-) == 0   74.350     20.708   3.590  0.00455 **
Comp2(-) - Comp1(+) == 0  -26.747     22.938  -1.166  0.83971
Comp2(+) - Comp1(+) == 0 -100.661     12.723  -7.911  < 0.001 ***
```

Comp3(-) - Comp1(+) == 0 -62.898 25.718 -2.446 0.13109
Comp3(+) - Comp1(+) == 0 -30.491 15.424 -1.977 0.33599
Comp2(+) - Comp2(-) == 0 -73.915 24.141 -3.062 0.02550 *
Comp3(-) - Comp2(-) == 0 -36.151 32.899 -1.099 0.87062
Comp3(+) - Comp2(-) == 0 -3.744 25.667 -0.146 0.99999
Comp3(-) - Comp2(+) == 0 37.764 26.797 1.409 0.70182
Comp3(+) - Comp2(+) == 0 70.171 17.163 4.089 < 0.001 ***
Comp3(+) - Comp3(-) == 0 32.407 28.180 1.150 0.84742

Winter mean temperature

	Estimate	Std. Error	t value	Pr(>|t|)	
Comp1(+) - Comp1(-) == 0	-50.725	18.473	-2.746	0.0625	.
Comp2(-) - Comp1(-) == 0	-13.830	28.745	-0.481	0.9964	
Comp2(+) - Comp1(-) == 0	11.319	20.163	0.561	0.9925	
Comp3(-) - Comp1(-) == 0	14.471	31.340	0.462	0.9970	
Comp3(+) - Comp1(-) == 0	-30.516	22.229	-1.373	0.7246	
Comp2(-) - Comp1(+) == 0	36.895	24.623	1.498	0.6440	
Comp2(+) - Comp1(+) == 0	62.045	13.658	4.543	<0.001	***
Comp3(-) - Comp1(+) == 0	65.197	27.608	2.362	0.1587	
Comp3(+) - Comp1(+) == 0	20.209	16.557	1.221	0.8120	
Comp2(+) - Comp2(-) == 0	25.150	25.915	0.970	0.9196	
Comp3(-) - Comp2(-) == 0	28.302	35.316	0.801	0.9634	
Comp3(+) - Comp2(-) == 0	-16.686	27.553	-0.606	0.9894	
Comp3(-) - Comp2(+) == 0	3.152	28.766	0.110	1.0000	
Comp3(+) - Comp2(+) == 0	-41.836	18.424	-2.271	0.1932	
Comp3(+) - Comp3(-) == 0	-44.988	30.250	-1.487	0.6515	

Spring mean temperature

	Estimate	Std. Error	t value	Pr(>|t|)	
Comp1(+) - Comp1(-) == 0	91.09	18.18	5.010	< 0.001	***
Comp2(-) - Comp1(-) == 0	59.40	28.29	2.100	0.27013	
Comp2(+) - Comp1(-) == 0	37.72	19.84	1.901	0.38059	
Comp3(-) - Comp1(-) == 0	23.73	30.85	0.769	0.96932	
Comp3(+) - Comp1(-) == 0	87.51	21.88	4.000	< 0.001	***
Comp2(-) - Comp1(+) == 0	-31.69	24.23	-1.308	0.76366	
Comp2(+) - Comp1(+) == 0	-53.38	13.44	-3.970	0.00114	**
Comp3(-) - Comp1(+) == 0	-67.37	27.17	-2.479	0.12144	
Comp3(+) - Comp1(+) == 0	-3.58	16.30	-0.220	0.99992	
Comp2(+) - Comp2(-) == 0	-21.68	25.51	-0.850	0.95309	
Comp3(-) - Comp2(-) == 0	-35.67	34.76	-1.026	0.90002	
Comp3(+) - Comp2(-) == 0	28.11	27.12	1.037	0.89610	
Comp3(-) - Comp2(+) == 0	-13.99	28.31	-0.494	0.99590	
Comp3(+) - Comp2(+) == 0	49.80	18.13	2.746	0.06242	.
Comp3(+) - Comp3(-) == 0	63.79	29.77	2.142	0.24908	

Summer mean temperature

	Estimate	Std. Error	t value	Pr(>|t|)	
Comp1(+) - Comp1(-) == 0	-110.826	15.351	-7.219	< 0.001	***
Comp2(-) - Comp1(-) == 0	-85.838	23.887	-3.593	0.00454	**
Comp2(+) - Comp1(-) == 0	35.931	16.755	2.144	0.24795	
Comp3(-) - Comp1(-) == 0	-23.886	26.043	-0.917	0.93588	
Comp3(+) - Comp1(-) == 0	-30.128	18.473	-1.631	0.55519	
Comp2(-) - Comp1(+) == 0	24.988	20.462	1.221	0.81162	
Comp2(+) - Comp1(+) == 0	146.757	11.350	12.930	< 0.001	***
Comp3(-) - Comp1(+) == 0	86.940	22.942	3.790	0.00221	**
Comp3(+) - Comp1(+) == 0	80.698	13.759	5.865	< 0.001	***
Comp2(+) - Comp2(-) == 0	121.769	21.535	5.654	< 0.001	***

Comp3(-) - Comp2(-) == 0 61.952 29.348 2.111 0.26430
Comp3(+) - Comp2(-) == 0 55.710 22.897 2.433 0.13530
Comp3(-) - Comp2(+) == 0 -59.817 23.905 -2.502 0.11515
Comp3(+) - Comp2(+) == 0 -66.059 15.310 -4.315 < 0.001 ***
Comp3(+) - Comp3(-) == 0 -6.242 25.138 -0.248 0.99985

Autumn mean temperature

	Estimate	Std. Error	t value	Pr(>|t|)
Comp1(+) - Comp1(-) == 0	107.8434	16.0900	6.703	< 0.001 ***
Comp2(-) - Comp1(-) == 0	68.1397	25.0369	2.722	0.06647 .
Comp2(+) - Comp1(-) == 0	-18.5099	17.5619	-1.054	0.88933
Comp3(-) - Comp1(-) == 0	-0.1143	27.2969	-0.004	1.00000
Comp3(+) - Comp1(-) == 0	93.2894	19.3617	4.818	< 0.001 ***
Comp2(-) - Comp1(+) == 0	-39.7037	21.4465	-1.851	0.41075
Comp2(+) - Comp1(+) == 0	-126.3533	11.8964	-10.621	< 0.001 ***
Comp3(-) - Comp1(+) == 0	-107.9577	24.0463	-4.490	< 0.001 ***
Comp3(+) - Comp1(+) == 0	-14.5539	14.4214	-1.009	0.90624
Comp2(+) - Comp2(-) == 0	-86.6496	22.5718	-3.839	0.00186 **
Comp3(-) - Comp2(-) == 0	-68.2540	30.7601	-2.219	0.21431
Comp3(+) - Comp2(-) == 0	25.1498	23.9987	1.048	0.89165
Comp3(-) - Comp2(+) == 0	18.3956	25.0551	0.734	0.97497
Comp3(+) - Comp2(+) == 0	111.7993	16.0472	6.967	< 0.001 ***
Comp3(+) - Comp3(-) == 0	93.4037	26.3479	3.545	0.00527 **

Annual ETo

	Estimate	Std. Error	t value	Pr(>|t|)
Comp1(+) - Comp1(-) == 0	89.029	17.491	5.090	<0.001 ***
Comp2(-) - Comp1(-) == 0	19.486	27.217	0.716	0.9776
Comp2(+) - Comp1(-) == 0	-3.104	19.091	-0.163	1.0000
Comp3(-) - Comp1(-) == 0	9.343	29.674	0.315	0.9995
Comp3(+) - Comp1(-) == 0	68.681	21.048	3.263	0.0136 *
Comp2(-) - Comp1(+) == 0	-69.543	23.314	-2.983	0.0321 *
Comp2(+) - Comp1(+) == 0	-92.133	12.932	-7.124	<0.001 ***
Comp3(-) - Comp1(+) == 0	-79.686	26.140	-3.048	0.0265 *
Comp3(+) - Comp1(+) == 0	-20.348	15.677	-1.298	0.7693
Comp2(+) - Comp2(-) == 0	-22.590	24.537	-0.921	0.9349
Comp3(-) - Comp2(-) == 0	-10.143	33.439	-0.303	0.9996
Comp3(+) - Comp2(-) == 0	49.196	26.088	1.886	0.3897
Comp3(-) - Comp2(+) == 0	12.447	27.237	0.457	0.9972
Comp3(+) - Comp2(+) == 0	71.785	17.444	4.115	<0.001 ***
Comp3(+) - Comp3(-) == 0	59.339	28.642	2.072	0.2841

Winter ETo

	Estimate	Std. Error	t value	Pr(>|t|)
Comp1(+) - Comp1(-) == 0	-3.058	18.957	-0.161	1.000
Comp2(-) - Comp1(-) == 0	-24.200	29.498	-0.820	0.960
Comp2(+) - Comp1(-) == 0	-10.713	20.691	-0.518	0.995
Comp3(-) - Comp1(-) == 0	-36.843	32.160	-1.146	0.849
Comp3(+) - Comp1(-) == 0	-44.004	22.811	-1.929	0.364
Comp2(-) - Comp1(+) == 0	-21.142	25.268	-0.837	0.956
Comp2(+) - Comp1(+) == 0	-7.655	14.016	-0.546	0.993
Comp3(-) - Comp1(+) == 0	-33.785	28.331	-1.193	0.827
Comp3(+) - Comp1(+) == 0	-40.946	16.991	-2.410	0.143
Comp2(+) - Comp2(-) == 0	13.487	26.593	0.507	0.995
Comp3(-) - Comp2(-) == 0	-12.643	36.241	-0.349	0.999
Comp3(+) - Comp2(-) == 0	-19.804	28.275	-0.700	0.980
Comp3(-) - Comp2(+) == 0	-26.130	29.519	-0.885	0.945

```
Comp3(+) - Comp2(+) == 0  -33.292     18.906  -1.761    0.469
Comp3(+) - Comp3(-) == 0   -7.161     31.042  -0.231    1.000
(Adjusted p values reported -- single-step method)
```

Spring ETo

```
                    Estimate Std. Error t value Pr(>|t|)
Comp1(+) - Comp1(-) == 0   -70.05      16.29  -4.299  < 0.001 ***
Comp2(-) - Comp1(-) == 0   -13.83      25.35  -0.545  0.99348
Comp2(+) - Comp1(-) == 0    59.20      17.78   3.329  0.01107 *
Comp3(-) - Comp1(-) == 0    47.09      27.64   1.703  0.50679
Comp3(+) - Comp1(-) == 0   -52.71      19.61  -2.688  0.07232 .
Comp2(-) - Comp1(+) == 0    56.22      21.72   2.589  0.09318 .
Comp2(+) - Comp1(+) == 0   129.25      12.05  10.729  < 0.001 ***
Comp3(-) - Comp1(+) == 0   117.13      24.35   4.810  < 0.001 ***
Comp3(+) - Comp1(+) == 0    17.34      14.60   1.188  0.82900
Comp2(+) - Comp2(-) == 0    73.03      22.86   3.195  0.01703 *
Comp3(-) - Comp2(-) == 0    60.91      31.15   1.955  0.34813
Comp3(+) - Comp2(-) == 0   -38.88      24.30  -1.600  0.57626
Comp3(-) - Comp2(+) == 0   -12.12      25.37  -0.478  0.99650
Comp3(+) - Comp2(+) == 0  -111.91      16.25  -6.886  < 0.001 ***
Comp3(+) - Comp3(-) == 0   -99.79      26.68  -3.740  0.00272 **
```

Summer ETo

```
                    Estimate Std. Error t value Pr(>|t|)
Comp1(+) - Comp1(-) == 0   52.233     18.304   2.854  0.04629 *
Comp2(-) - Comp1(-) == 0   73.319     28.482   2.574  0.09670 .
Comp2(+) - Comp1(-) == 0   45.704     19.979   2.288  0.18605
Comp3(-) - Comp1(-) == 0   60.057     31.053   1.934  0.36062
Comp3(+) - Comp1(-) == 0  -28.427     22.026  -1.291  0.77339
Comp2(-) - Comp1(+) == 0   21.086     24.398   0.864  0.94974
Comp2(+) - Comp1(+) == 0   -6.529     13.533  -0.482  0.99633
Comp3(-) - Comp1(+) == 0    7.825     27.355   0.286  0.99971
Comp3(+) - Comp1(+) == 0  -80.660     16.406  -4.916  < 0.001 ***
Comp2(+) - Comp2(-) == 0  -27.615     25.678  -1.075  0.88061
Comp3(-) - Comp2(-) == 0  -13.262     34.993  -0.379  0.99884
Comp3(+) - Comp2(-) == 0 -101.746     27.301  -3.727  0.00293 **
Comp3(-) - Comp2(+) == 0   14.353     28.503   0.504  0.99552
Comp3(+) - Comp2(+) == 0  -74.131     18.255  -4.061  < 0.001 ***
Comp3(+) - Comp3(-) == 0  -88.484     29.974  -2.952  0.03523 *
```

Autumn ETo

```
                    Estimate Std. Error t value Pr(>|t|)
Comp1(+) - Comp1(-) == 0  -55.9744    16.5216  -3.388  0.00900 **
Comp2(-) - Comp1(-) == 0    6.3095    25.7086   0.245  0.99986
Comp2(+) - Comp1(-) == 0   63.0403    18.0330   3.496  0.00624 **
Comp3(-) - Comp1(-) == 0   70.2857    28.0292   2.508  0.11380
Comp3(+) - Comp1(-) == 0  -55.3137    19.8811  -2.782  0.05645 .
Comp2(-) - Comp1(+) == 0   62.2840    22.0218   2.828  0.04989 *
Comp2(+) - Comp1(+) == 0  119.0147    12.2155   9.743  < 0.001 ***
Comp3(-) - Comp1(+) == 0  126.2601    24.6913   5.114  < 0.001 ***
Comp3(+) - Comp1(+) == 0    0.6608    14.8083   0.045  1.00000
Comp2(+) - Comp2(-) == 0   56.7308    23.1773   2.448  0.13103
Comp3(-) - Comp2(-) == 0   63.9762    31.5853   2.026  0.30869
Comp3(+) - Comp2(-) == 0  -61.6232    24.6425  -2.501  0.11561
Comp3(-) - Comp2(+) == 0    7.2454    25.7272   0.282  0.99973
Comp3(+) - Comp2(+) == 0 -118.3540    16.4776  -7.183  < 0.001 ***
Comp3(+) - Comp3(-) == 0 -125.5994    27.0547  -4.642  < 0.001 ***
```

Annual climate balance

	Estimate	Std. Error	t value	Pr(>|t|)	
Comp1(+) - Comp1(-) == 0	-23.0208	18.8935	-1.218	0.8132	
Comp2(-) - Comp1(-) == 0	-23.1937	29.3994	-0.789	0.9658	
Comp2(+) - Comp1(-) == 0	2.4645	20.6219	0.120	1.0000	
Comp3(-) - Comp1(-) == 0	-27.3286	32.0531	-0.853	0.9525	
Comp3(+) - Comp1(-) == 0	-51.2975	22.7353	-2.256	0.1991	
Comp2(-) - Comp1(+) == 0	-0.1728	25.1833	-0.007	1.0000	
Comp2(+) - Comp1(+) == 0	25.4853	13.9692	1.824	0.4280	
Comp3(-) - Comp1(+) == 0	-4.3078	28.2361	-0.153	1.0000	
Comp3(+) - Comp1(+) == 0	-28.2767	16.9342	-1.670	0.5293	
Comp2(+) - Comp2(-) == 0	25.6581	26.5047	0.968	0.9204	
Comp3(-) - Comp2(-) == 0	-4.1349	36.1198	-0.114	1.0000	
Comp3(+) - Comp2(-) == 0	-28.1039	28.1803	-0.997	0.9105	
Comp3(-) - Comp2(+) == 0	-29.7930	29.4207	-1.013	0.9050	
Comp3(+) - Comp2(+) == 0	-53.7620	18.8432	-2.853	0.0467	*
Comp3(+) - Comp3(-) == 0	-23.9689	30.9388	-0.775	0.9684	

Winter climate balance

	Estimate	Std. Error	t value	Pr(>|t|)	
Comp1(+) - Comp1(-) == 0	-41.620	18.333	-2.270	0.193	
Comp2(-) - Comp1(-) == 0	1.189	28.528	0.042	1.000	
Comp2(+) - Comp1(-) == 0	-45.136	20.010	-2.256	0.199	
Comp3(-) - Comp1(-) == 0	-10.700	31.103	-0.344	0.999	
Comp3(+) - Comp1(-) == 0	40.191	22.061	1.822	0.429	
Comp2(-) - Comp1(+) == 0	42.809	24.437	1.752	0.475	
Comp2(+) - Comp1(+) == 0	-3.516	13.555	-0.259	1.000	
Comp3(-) - Comp1(+) == 0	30.920	27.399	1.128	0.857	
Comp3(+) - Comp1(+) == 0	81.811	16.432	4.979	<0.001	***
Comp2(+) - Comp2(-) == 0	-46.325	25.719	-1.801	0.443	
Comp3(-) - Comp2(-) == 0	-11.889	35.049	-0.339	0.999	
Comp3(+) - Comp2(-) == 0	39.002	27.345	1.426	0.691	
Comp3(-) - Comp2(+) == 0	34.436	28.548	1.206	0.820	
Comp3(+) - Comp2(+) == 0	85.327	18.285	4.667	<0.001	***
Comp3(+) - Comp3(-) == 0	50.891	30.022	1.695	0.512	

Spring climate balance

	Estimate	Std. Error	t value	Pr(>|t|)	
Comp1(+) - Comp1(-) == 0	-45.745	17.561	-2.605	0.0896	.
Comp2(-) - Comp1(-) == 0	-23.832	27.326	-0.872	0.9478	
Comp2(+) - Comp1(-) == 0	56.788	19.168	2.963	0.0343	*
Comp3(-) - Comp1(-) == 0	29.843	29.793	1.002	0.9090	
Comp3(+) - Comp1(-) == 0	-3.573	21.132	-0.169	1.0000	
Comp2(-) - Comp1(+) == 0	21.914	23.407	0.936	0.9303	
Comp2(+) - Comp1(+) == 0	102.533	12.984	7.897	<0.001	***
Comp3(-) - Comp1(+) == 0	75.588	26.245	2.880	0.0431	*
Comp3(+) - Comp1(+) == 0	42.172	15.740	2.679	0.0744	.
Comp2(+) - Comp2(-) == 0	80.620	24.635	3.273	0.0131	*
Comp3(-) - Comp2(-) == 0	53.675	33.572	1.599	0.5770	
Comp3(+) - Comp2(-) == 0	20.258	26.193	0.773	0.9686	
Comp3(-) - Comp2(+) == 0	-26.945	27.346	-0.985	0.9146	
Comp3(+) - Comp2(+) == 0	-60.361	17.514	-3.446	0.0074	**
Comp3(+) - Comp3(-) == 0	-33.416	28.757	-1.162	0.8417	

Summer climate balance

	Estimate	Std. Error	t value	Pr(>|t|)

Comp1(+) - Comp1(-) == 0 147.228 13.866 10.618 < 0.001 ***
Comp2(-) - Comp1(-) == 0 165.710 21.576 7.680 < 0.001 ***
Comp2(+) - Comp1(-) == 0 4.312 15.135 0.285 0.99971
Comp3(-) - Comp1(-) == 0 74.757 23.524 3.178 0.01782 *
Comp3(+) - Comp1(-) == 0 12.347 16.686 0.740 0.97410
Comp2(-) - Comp1(+) == 0 18.481 18.482 1.000 0.90954
Comp2(+) - Comp1(+) == 0 -142.916 10.252 -13.940 < 0.001 ***
Comp3(-) - Comp1(+) == 0 -72.471 20.723 -3.497 0.00634 **
Comp3(+) - Comp1(+) == 0 -134.881 12.428 -10.853 < 0.001 ***
Comp2(+) - Comp2(-) == 0 -161.397 19.452 -8.297 < 0.001 ***
Comp3(-) - Comp2(-) == 0 -90.952 26.509 -3.431 0.00763 **
Comp3(+) - Comp2(-) == 0 -153.362 20.682 -7.415 < 0.001 ***
Comp3(-) - Comp2(+) == 0 70.445 21.592 3.263 0.01364 *
Comp3(+) - Comp2(+) == 0 8.035 13.829 0.581 0.99126
Comp3(+) - Comp3(-) == 0 -62.410 22.706 -2.749 0.06189 .

Autumn climate balance

Estimate Std. Error t value Pr(>|t|)
Comp1(+) - Comp1(-) == 0 -110.310 16.014 -6.888 <0.001 ***
Comp2(-) - Comp1(-) == 0 -103.606 24.918 -4.158 <0.001 ***
Comp2(+) - Comp1(-) == 0 21.646 17.479 1.238 0.8026
Comp3(-) - Comp1(-) == 0 -55.257 27.167 -2.034 0.3043
Comp3(+) - Comp1(-) == 0 -42.307 19.270 -2.195 0.2246
Comp2(-) - Comp1(+) == 0 6.704 21.345 0.314 0.9995
Comp2(+) - Comp1(+) == 0 131.956 11.840 11.145 <0.001 ***
Comp3(-) - Comp1(+) == 0 55.053 23.932 2.300 0.1810
Comp3(+) - Comp1(+) == 0 68.003 14.353 4.738 <0.001 ***
Comp2(+) - Comp2(-) == 0 125.252 22.465 5.576 <0.001 ***
Comp3(-) - Comp2(-) == 0 48.349 30.614 1.579 0.5900
Comp3(+) - Comp2(-) == 0 61.300 23.885 2.566 0.0987 .
Comp3(-) - Comp2(+) == 0 -76.903 24.936 -3.084 0.0240 *
Comp3(+) - Comp2(+) == 0 -63.953 15.971 -4.004 <0.001 ***
Comp3(+) - Comp3(-) == 0 12.950 26.223 0.494 0.9959

Winter NDVI

Estimate Std. Error t value Pr(>|t|)
Comp1(+) - Comp1(-) == 0 -144.48 14.21 -10.168 < 0.001 ***
Comp2(-) - Comp1(-) == 0 -132.92 22.11 -6.012 < 0.001 ***
Comp2(+) - Comp1(-) == 0 10.51 15.51 0.677 0.98247
Comp3(-) - Comp1(-) == 0 -69.56 24.11 -2.885 0.04261 *
Comp3(+) - Comp1(-) == 0 -43.59 17.10 -2.549 0.10274
Comp2(-) - Comp1(+) == 0 11.56 18.94 0.610 0.98908
Comp2(+) - Comp1(+) == 0 154.98 10.51 14.752 < 0.001 ***
Comp3(-) - Comp1(+) == 0 74.92 21.24 3.528 0.00556 **
Comp3(+) - Comp1(+) == 0 100.89 12.74 7.922 < 0.001 ***
Comp2(+) - Comp2(-) == 0 143.43 19.93 7.195 < 0.001 ***
Comp3(-) - Comp2(-) == 0 63.37 27.16 2.333 0.16912
Comp3(+) - Comp2(-) == 0 89.33 21.19 4.215 < 0.001 ***
Comp3(-) - Comp2(+) == 0 -80.06 22.13 -3.618 0.00404 **
Comp3(+) - Comp2(+) == 0 -54.10 14.17 -3.817 0.00202 **
Comp3(+) - Comp3(-) == 0 25.97 23.27 1.116 0.86314

Spring NDVI

Estimate Std. Error t value Pr(>|t|)
Comp1(+) - Comp1(-) == 0 -123.17 15.04 -8.187 <0.001 ***
Comp2(-) - Comp1(-) == 0 -136.11 23.41 -5.814 <0.001 ***
Comp2(+) - Comp1(-) == 0 18.26 16.42 1.112 0.8648

Comp3(-) - Comp1(-) == 0 -59.66 25.52 -2.337 0.1673
Comp3(+) - Comp1(-) == 0 -24.14 18.10 -1.333 0.7484
Comp2(-) - Comp1(+) == 0 -12.94 20.05 -0.645 0.9859
Comp2(+) - Comp1(+) == 0 141.43 11.12 12.715 <0.001 ***
Comp3(-) - Comp1(+) == 0 63.51 22.48 2.825 0.0502 .
Comp3(+) - Comp1(+) == 0 99.03 13.48 7.344 <0.001 ***
Comp2(+) - Comp2(-) == 0 154.37 21.11 7.314 <0.001 ***
Comp3(-) - Comp2(-) == 0 76.45 28.76 2.658 0.0783 .
Comp3(+) - Comp2(-) == 0 111.97 22.44 4.990 <0.001 ***
Comp3(-) - Comp2(+) == 0 -77.92 23.43 -3.326 0.0111 *
Comp3(+) - Comp2(+) == 0 -42.40 15.00 -2.826 0.0503 .
Comp3(+) - Comp3(-) == 0 35.52 24.64 1.442 0.6811

Summer NDVI

	Estimate	Std. Error	t value	Pr(>|t|)	
Comp1(+) - Comp1(-) == 0	17.950	19.035	0.943	0.928	
Comp2(-) - Comp1(-) == 0	-26.137	29.620	-0.882	0.945	
Comp2(+) - Comp1(-) == 0	-1.722	20.776	-0.083	1.000	
Comp3(-) - Comp1(-) == 0	6.586	32.293	0.204	1.000	
Comp3(+) - Comp1(-) == 0	9.977	22.906	0.436	0.998	
Comp2(-) - Comp1(+) == 0	-44.086	25.372	-1.738	0.484	
Comp2(+) - Comp1(+) == 0	-19.672	14.074	-1.398	0.709	
Comp3(-) - Comp1(+) == 0	-11.364	28.448	-0.399	0.999	
Comp3(+) - Comp1(+) == 0	-7.973	17.061	-0.467	0.997	
Comp2(+) - Comp2(-) == 0	24.415	26.703	0.914	0.937	
Comp3(-) - Comp2(-) == 0	32.722	36.390	0.899	0.941	
Comp3(+) - Comp2(-) == 0	36.114	28.391	1.272	0.784	
Comp3(-) - Comp2(+) == 0	8.308	29.641	0.280	1.000	
Comp3(+) - Comp2(+) == 0	11.699	18.984	0.616	0.989	
Comp3(+) - Comp3(-) == 0	3.391	31.171	0.109	1.000	

Autumn NDVI

	Estimate	Std. Error	t value	Pr(>|t|)	
Comp1(+) - Comp1(-) == 0	-109.035	16.295	-6.691	<0.001	***
Comp2(-) - Comp1(-) == 0	-126.868	25.356	-5.004	<0.001	***
Comp2(+) - Comp1(-) == 0	3.615	17.785	0.203	0.9999	
Comp3(-) - Comp1(-) == 0	-44.757	27.644	-1.619	0.5633	
Comp3(+) - Comp1(-) == 0	-13.605	19.608	-0.694	0.9805	
Comp2(-) - Comp1(+) == 0	-17.833	21.720	-0.821	0.9595	
Comp2(+) - Comp1(+) == 0	112.650	12.048	9.350	<0.001	***
Comp3(-) - Comp1(+) == 0	64.278	24.352	2.639	0.0821	.
Comp3(+) - Comp1(+) == 0	95.430	14.605	6.534	<0.001	***
Comp2(+) - Comp2(-) == 0	130.483	22.859	5.708	<0.001	***
Comp3(-) - Comp2(-) == 0	82.111	31.152	2.636	0.0830	.
Comp3(+) - Comp2(-) == 0	113.263	24.304	4.660	<0.001	***
Comp3(-) - Comp2(+) == 0	-48.372	25.374	-1.906	0.3771	
Comp3(+) - Comp2(+) == 0	-17.220	16.251	-1.060	0.8870	
Comp3(+) - Comp3(-) == 0	31.152	26.683	1.167	0.8390	

Average day of the year recording the maximum NDVI

	Estimate	Std. Error	t value	Pr(>|t|)	
Comp1(+) - Comp1(-) == 0	-1.9603	0.6685	-2.932	0.0373	*
Comp2(-) - Comp1(-) == 0	-1.0159	1.0402	-0.977	0.9176	
Comp2(+) - Comp1(-) == 0	0.9158	0.7296	1.255	0.7934	
Comp3(-) - Comp1(-) == 0	-0.8571	1.1341	-0.756	0.9716	
Comp3(+) - Comp1(-) == 0	-0.1584	0.8044	-0.197	1.0000	
Comp2(-) - Comp1(+) == 0	0.9444	0.8910	1.060	0.8869	

Comp2(+) - Comp1(+) == 0 2.8761 0.4943 5.819 <0.001 ***
Comp3(-) - Comp1(+) == 0 1.1032 0.9990 1.104 0.8683
Comp3(+) - Comp1(+) == 0 1.8019 0.5992 3.007 0.0300 *
Comp2(+) - Comp2(-) == 0 1.9316 0.9378 2.060 0.2904
Comp3(-) - Comp2(-) == 0 0.1587 1.2780 0.124 1.0000
Comp3(+) - Comp2(-) == 0 0.8575 0.9971 0.860 0.9508
Comp3(-) - Comp2(+) == 0 -1.7729 1.0410 -1.703 0.5068
Comp3(+) - Comp2(+) == 0 -1.0741 0.6667 -1.611 0.5686
Comp3(+) - Comp3(-) == 0 0.6988 1.0947 0.638 0.9866

Average day of the year recording the green up

	Estimate	Std. Error	t value	Pr(>|t|)	
Comp1(+) - Comp1(-) == 0	-4.73862	2.35722	-2.010	0.31724	
Comp2(-) - Comp1(-) == 0	1.29841	3.66797	0.354	0.99917	
Comp2(+) - Comp1(-) == 0	0.01209	2.57286	0.005	1.00000	
Comp3(-) - Comp1(-) == 0	-3.11429	3.99906	-0.779	0.96766	
Comp3(+) - Comp1(-) == 0	-8.06149	2.83653	-2.842	0.04800	*
Comp2(-) - Comp1(+) == 0	6.03704	3.14196	1.921	0.36829	
Comp2(+) - Comp1(+) == 0	4.75071	1.74284	2.726	0.06571	.
Comp3(-) - Comp1(+) == 0	1.62434	3.52284	0.461	0.99704	
Comp3(+) - Comp1(+) == 0	-3.32287	2.11277	-1.573	0.59441	
Comp2(+) - Comp2(-) == 0	-1.28632	3.30681	-0.389	0.99869	
Comp3(-) - Comp2(-) == 0	-4.41270	4.50643	-0.979	0.91668	
Comp3(+) - Comp2(-) == 0	-9.35990	3.51587	-2.662	0.07752	.
Comp3(-) - Comp2(+) == 0	-3.12637	3.67063	-0.852	0.95273	
Comp3(+) - Comp2(+) == 0	-8.07358	2.35094	-3.434	0.00743	**
Comp3(+) - Comp3(-) == 0	-4.94720	3.86003	-1.282	0.77862	

Soil water capacity

	Estimate	Std. Error	t value	Pr(>|t|)	
Comp1(+) - Comp1(-) == 0	-39.124	18.083	-2.164	0.239	
Comp2(-) - Comp1(-) == 0	-60.457	28.138	-2.149	0.246	
Comp2(+) - Comp1(-) == 0	41.492	19.737	2.102	0.269	
Comp3(-) - Comp1(-) == 0	-12.886	30.678	-0.420	0.998	
Comp3(+) - Comp1(-) == 0	-31.283	21.760	-1.438	0.684	
Comp2(-) - Comp1(+) == 0	-21.333	24.103	-0.885	0.945	
Comp2(+) - Comp1(+) == 0	80.615	13.370	6.030	<0.001	***
Comp3(-) - Comp1(+) == 0	26.238	27.025	0.971	0.919	
Comp3(+) - Comp1(+) == 0	7.841	16.208	0.484	0.996	
Comp2(+) - Comp2(-) == 0	101.949	25.368	4.019	<0.001	***
Comp3(-) - Comp2(-) == 0	47.571	34.570	1.376	0.723	
Comp3(+) - Comp2(-) == 0	29.174	26.971	1.082	0.878	
Comp3(-) - Comp2(+) == 0	-54.377	28.159	-1.931	0.362	
Comp3(+) - Comp2(+) == 0	-72.775	18.035	-4.035	<0.001	***
Comp3(+) - Comp3(-) == 0	-18.398	29.612	-0.621	0.988	

2. WHEAT

Annual precipitation

	Estimate	Std. Error	t value	Pr(>|t|)	
Comp1(+) - Comp1(-) == 0	-229.87	34.19	-6.722	< 0.001	***
Comp2(-) - Comp1(-) == 0	-13.82	45.93	-0.301	0.99964	
Comp2(+) - Comp1(-) == 0	-218.49	30.48	-7.168	< 0.001	***
Comp3(-) - Comp1(-) == 0	-125.98	53.36	-2.361	0.15981	
Comp3(+) - Comp1(-) == 0	-185.10	30.41	-6.086	< 0.001	***
Comp2(-) - Comp1(+) == 0	216.05	46.64	4.633	< 0.001	***
Comp2(+) - Comp1(+) == 0	11.38	31.53	0.361	0.99913	
Comp3(-) - Comp1(+) == 0	103.89	53.97	1.925	0.36983	
Comp3(+) - Comp1(+) == 0	44.77	31.46	1.423	0.69837	
Comp2(+) - Comp2(-) == 0	-204.67	43.99	-4.653	< 0.001	***
Comp3(-) - Comp2(-) == 0	-112.16	62.07	-1.807	0.44394	
Comp3(+) - Comp2(-) == 0	-171.28	43.94	-3.898	0.00129	**
Comp3(-) - Comp2(+) == 0	92.51	51.70	1.790	0.45505	
Comp3(+) - Comp2(+) == 0	33.39	27.38	1.220	0.81680	
Comp3(+) - Comp3(-) == 0	-59.12	51.66	-1.145	0.85366	

Winter precipitation

	Estimate	Std. Error	t value	Pr(>|t|)	
Comp1(+) - Comp1(-) == 0	-311.48	31.88	-9.770	< 0.001	***
Comp2(-) - Comp1(-) == 0	38.47	42.82	0.898	0.94290	
Comp2(+) - Comp1(-) == 0	-325.63	28.42	-11.458	< 0.001	***
Comp3(-) - Comp1(-) == 0	-149.63	49.75	-3.008	0.02935	*
Comp3(+) - Comp1(-) == 0	-392.19	28.35	-13.832	< 0.001	***
Comp2(-) - Comp1(+) == 0	349.94	43.48	8.049	< 0.001	***
Comp2(+) - Comp1(+) == 0	-14.15	29.40	-0.481	0.99652	
Comp3(-) - Comp1(+) == 0	161.85	50.32	3.217	0.01527	*
Comp3(+) - Comp1(+) == 0	-80.71	29.33	-2.752	0.06114	.
Comp2(+) - Comp2(-) == 0	-364.09	41.01	-8.879	< 0.001	***
Comp3(-) - Comp2(-) == 0	-188.09	57.87	-3.250	0.01367	*
Comp3(+) - Comp2(-) == 0	-430.66	40.96	-10.513	< 0.001	***
Comp3(-) - Comp2(+) == 0	176.00	48.20	3.652	0.00342	**
Comp3(+) - Comp2(+) == 0	-66.56	25.53	-2.607	0.08878	.
Comp3(+) - Comp3(-) == 0	-242.56	48.16	-5.037	< 0.001	***

Spring precipitation

	Estimate	Std. Error	t value	Pr(>|t|)	
Comp1(+) - Comp1(-) == 0	445.16	29.22	15.237	<0.001	***
Comp2(-) - Comp1(-) == 0	156.38	39.24	3.985	<0.001	***
Comp2(+) - Comp1(-) == 0	489.74	26.04	18.804	<0.001	***
Comp3(-) - Comp1(-) == 0	21.43	45.59	0.470	0.997	
Comp3(+) - Comp1(-) == 0	506.56	25.98	19.495	<0.001	***
Comp2(-) - Comp1(+) == 0	-288.78	39.85	-7.248	<0.001	***
Comp2(+) - Comp1(+) == 0	44.57	26.94	1.654	0.545	
Comp3(-) - Comp1(+) == 0	-423.73	46.11	-9.189	<0.001	***
Comp3(+) - Comp1(+) == 0	61.39	26.88	2.284	0.189	
Comp2(+) - Comp2(-) == 0	333.36	37.58	8.870	<0.001	***
Comp3(-) - Comp2(-) == 0	-134.95	53.04	-2.544	0.104	
Comp3(+) - Comp2(-) == 0	350.18	37.54	9.328	<0.001	***
Comp3(-) - Comp2(+) == 0	-468.31	44.17	-10.602	<0.001	***
Comp3(+) - Comp2(+) == 0	16.82	23.40	0.719	0.978	
Comp3(+) - Comp3(-) == 0	485.13	44.13	10.992	<0.001	***

Summer precipitation

	Estimate	Std. Error	t value	Pr(>|t|)	
Comp1(+) - Comp1(-) == 0	577.37	29.37	19.661	<0.001	***
Comp2(-) - Comp1(-) == 0	412.40	39.45	10.455	<0.001	***
Comp2(+) - Comp1(-) == 0	487.21	26.18	18.611	<0.001	***
Comp3(-) - Comp1(-) == 0	195.99	45.83	4.277	<0.001	***
Comp3(+) - Comp1(-) == 0	516.18	26.12	19.764	<0.001	***
Comp2(-) - Comp1(+) == 0	-164.98	40.05	-4.119	<0.001	***
Comp2(+) - Comp1(+) == 0	-90.17	27.08	-3.330	0.0105	*
Comp3(-) - Comp1(+) == 0	-381.38	46.35	-8.228	<0.001	***
Comp3(+) - Comp1(+) == 0	-61.19	27.02	-2.265	0.1969	
Comp2(+) - Comp2(-) == 0	74.81	37.77	1.980	0.3373	
Comp3(-) - Comp2(-) == 0	-216.40	53.31	-4.059	<0.001	***
Comp3(+) - Comp2(-) == 0	103.78	37.73	2.751	0.0609	.
Comp3(-) - Comp2(+) == 0	-291.21	44.40	-6.559	<0.001	***
Comp3(+) - Comp2(+) == 0	28.98	23.52	1.232	0.8102	
Comp3(+) - Comp3(-) == 0	320.19	44.36	7.218	<0.001	***

Autumn precipitation

	Estimate	Std. Error	t value	Pr(>|t|)	
Comp1(+) - Comp1(-) == 0	215.46	32.85	6.559	< 0.001	***
Comp2(-) - Comp1(-) == 0	-44.70	44.13	-1.013	0.90759	
Comp2(+) - Comp1(-) == 0	268.39	29.28	9.165	< 0.001	***
Comp3(-) - Comp1(-) == 0	377.96	51.27	7.373	< 0.001	***
Comp3(+) - Comp1(-) == 0	323.81	29.22	11.083	< 0.001	***
Comp2(-) - Comp1(+) == 0	-260.16	44.80	-5.807	< 0.001	***
Comp2(+) - Comp1(+) == 0	52.93	30.29	1.747	0.48272	
Comp3(-) - Comp1(+) == 0	162.50	51.85	3.134	0.01991	*
Comp3(+) - Comp1(+) == 0	108.36	30.23	3.585	0.00428	**
Comp2(+) - Comp2(-) == 0	313.08	42.26	7.409	< 0.001	***
Comp3(-) - Comp2(-) == 0	422.66	59.63	7.087	< 0.001	***
Comp3(+) - Comp2(-) == 0	368.51	42.21	8.731	< 0.001	***
Comp3(-) - Comp2(+) == 0	109.57	49.67	2.206	0.22171	
Comp3(+) - Comp2(+) == 0	55.43	26.31	2.107	0.26872	
Comp3(+) - Comp3(-) == 0	-54.14	49.63	-1.091	0.87733	

Annual mean temperature

	Estimate	Std. Error	t value	Pr(>|t|)	
Comp1(+) - Comp1(-) == 0	-25.19	34.36	-0.733	0.97601	
Comp2(-) - Comp1(-) == 0	-100.36	46.15	-2.175	0.23587	
Comp2(+) - Comp1(-) == 0	87.04	30.63	2.842	0.04734	*
Comp3(-) - Comp1(-) == 0	246.66	53.62	4.600	< 0.001	***
Comp3(+) - Comp1(-) == 0	-68.59	30.56	-2.245	0.20494	
Comp2(-) - Comp1(+) == 0	-75.18	46.86	-1.604	0.57870	
Comp2(+) - Comp1(+) == 0	112.23	31.68	3.542	0.00495	**
Comp3(-) - Comp1(+) == 0	271.85	54.23	5.013	< 0.001	***
Comp3(+) - Comp1(+) == 0	-43.40	31.62	-1.373	0.72968	
Comp2(+) - Comp2(-) == 0	187.40	44.20	4.240	< 0.001	***
Comp3(-) - Comp2(-) == 0	347.02	62.37	5.564	< 0.001	***
Comp3(+) - Comp2(-) == 0	31.77	44.15	0.720	0.97788	
Comp3(-) - Comp2(+) == 0	159.62	51.95	3.073	0.02406	*
Comp3(+) - Comp2(+) == 0	-155.63	27.52	-5.656	< 0.001	***
Comp3(+) - Comp3(-) == 0	-315.25	51.90	-6.074	< 0.001	***

Winter mean temperature

	Estimate	Std. Error	t value	Pr(>|t|)	
Comp1(+) - Comp1(-) == 0	-91.03	34.06	-2.673	0.0751	.

Comp2(-) - Comp1(-) == 0 -221.72 45.75 -4.847 <0.001 ***
Comp2(+) - Comp1(-) == 0 36.33 30.36 1.197 0.8285
Comp3(-) - Comp1(-) == 0 -240.93 53.15 -4.533 <0.001 ***
Comp3(+) - Comp1(-) == 0 -161.28 30.29 -5.325 <0.001 ***
Comp2(-) - Comp1(+) == 0 -130.69 46.45 -2.814 0.0513 .
Comp2(+) - Comp1(+) == 0 127.36 31.40 4.055 <0.001 ***
Comp3(-) - Comp1(+) == 0 -149.90 53.75 -2.789 0.0548 .
Comp3(+) - Comp1(+) == 0 -70.25 31.34 -2.242 0.2064
Comp2(+) - Comp2(-) == 0 258.05 43.81 5.891 <0.001 ***
Comp3(-) - Comp2(-) == 0 -19.21 61.82 -0.311 0.9996
Comp3(+) - Comp2(-) == 0 60.44 43.76 1.381 0.7244
Comp3(-) - Comp2(+) == 0 -277.26 51.49 -5.385 <0.001 ***
Comp3(+) - Comp2(+) == 0 -197.61 27.27 -7.246 <0.001 ***
Comp3(+) - Comp3(-) == 0 79.65 51.45 1.548 0.6164

Spring mean temperature

Estimate Std. Error t value Pr(>|t|)
Comp1(+) - Comp1(-) == 0 74.52 34.16 2.182 0.23289
Comp2(-) - Comp1(-) == 0 -76.74 45.88 -1.673 0.53255
Comp2(+) - Comp1(-) == 0 96.29 30.45 3.162 0.01826 *
Comp3(-) - Comp1(-) == 0 329.84 53.31 6.188 < 0.001 ***
Comp3(+) - Comp1(-) == 0 -53.45 30.38 -1.759 0.47481
Comp2(-) - Comp1(+) == 0 -151.26 46.59 -3.247 0.01395 *
Comp2(+) - Comp1(+) == 0 21.77 31.50 0.691 0.98154
Comp3(-) - Comp1(+) == 0 255.32 53.91 4.736 < 0.001 ***
Comp3(+) - Comp1(+) == 0 -127.97 31.43 -4.071 < 0.001 ***
Comp2(+) - Comp2(-) == 0 173.03 43.94 3.938 0.00105 **
Comp3(-) - Comp2(-) == 0 406.58 62.01 6.557 < 0.001 ***
Comp3(+) - Comp2(-) == 0 23.30 43.89 0.531 0.99448
Comp3(-) - Comp2(+) == 0 233.55 51.64 4.522 < 0.001 ***
Comp3(+) - Comp2(+) == 0 -149.73 27.35 -5.474 < 0.001 ***
Comp3(+) - Comp3(-) == 0 -383.28 51.60 -7.428 < 0.001 ***

Summer mean temperature

Estimate Std. Error t value Pr(>|t|)
Comp1(+) - Comp1(-) == 0 -282.4555 33.3954 -8.458 <0.001 ***
Comp2(-) - Comp1(-) == 0 -282.0756 44.8585 -6.288 <0.001 ***
Comp2(+) - Comp1(-) == 0 -211.6171 29.7696 -7.108 <0.001 ***
Comp3(-) - Comp1(-) == 0 -536.6358 52.1156 -10.297 <0.001 ***
Comp3(+) - Comp1(-) == 0 -217.1980 29.7007 -7.313 <0.001 ***
Comp2(-) - Comp1(+) == 0 0.3798 45.5454 0.008 1.000
Comp2(+) - Comp1(+) == 0 70.8384 30.7949 2.300 0.182
Comp3(-) - Comp1(+) == 0 -254.1803 52.7080 -4.822 <0.001 ***
Comp3(+) - Comp1(+) == 0 65.2575 30.7283 2.124 0.261
Comp2(+) - Comp2(-) == 0 70.4586 42.9576 1.640 0.554
Comp3(-) - Comp2(-) == 0 -254.5602 60.6232 -4.199 <0.001 ***
Comp3(+) - Comp2(-) == 0 64.8777 42.9099 1.512 0.640
Comp3(-) - Comp2(+) == 0 -325.0187 50.4887 -6.437 <0.001 ***
Comp3(+) - Comp2(+) == 0 -5.5809 26.7433 -0.209 1.000
Comp3(+) - Comp3(-) == 0 319.4378 50.4481 6.332 <0.001 ***

Autumn mean temperature

Comp2(-) - Comp1(-) == 0 -230.07 46.45 -4.953 < 0.001 ***
Comp2(+) - Comp1(-) == 0 -52.62 30.83 -1.707 0.50948
Comp3(-) - Comp1(-) == 0 127.78 53.96 2.368 0.15737
Comp3(+) - Comp1(-) == 0 -116.53 30.75 -3.789 0.00192 **
Comp2(-) - Comp1(+) == 0 -190.55 47.16 -4.040 < 0.001 ***

Comp2(+) - Comp1(+) == 0	-13.10	31.89	-0.411	0.99837
Comp3(-) - Comp1(+) == 0	167.31	54.58	3.065	0.02475 *
Comp3(+) - Comp1(+) == 0	-77.01	31.82	-2.420	0.13970
Comp2(+) - Comp2(-) == 0	177.45	44.48	3.989	< 0.001 ***
Comp3(-) - Comp2(-) == 0	357.86	62.77	5.701	< 0.001 ***
Comp3(+) - Comp2(-) == 0	113.54	44.43	2.555	0.10109
Comp3(-) - Comp2(+) == 0	180.40	52.28	3.451	0.00693 **
Comp3(+) - Comp2(+) == 0	-63.91	27.69	-2.308	0.17929
Comp3(+) - Comp3(-) == 0	-244.31	52.24	-4.677	< 0.001 ***

Annual ETo

	Estimate	Std. Error	t value	Pr(>|t|)
Comp1(+) - Comp1(-) == 0	-255.24	33.18	-7.694	< 0.001 ***
Comp2(-) - Comp1(-) == 0	-412.58	44.56	-9.258	< 0.001 ***
Comp2(+) - Comp1(-) == 0	-121.51	29.57	-4.109	< 0.001 ***
Comp3(-) - Comp1(-) == 0	-335.28	51.77	-6.476	< 0.001 ***
Comp3(+) - Comp1(-) == 0	-293.58	29.51	-9.950	< 0.001 ***
Comp2(-) - Comp1(+) == 0	-157.34	45.25	-3.477	0.00631 **
Comp2(+) - Comp1(+) == 0	133.74	30.59	4.371	< 0.001 ***
Comp3(-) - Comp1(+) == 0	-80.04	52.36	-1.529	0.62948
Comp3(+) - Comp1(+) == 0	-38.34	30.53	-1.256	0.79745
Comp2(+) - Comp2(-) == 0	291.07	42.68	6.821	< 0.001 ***
Comp3(-) - Comp2(-) == 0	77.30	60.23	1.284	0.78212
Comp3(+) - Comp2(-) == 0	119.00	42.63	2.792	0.05461 .
Comp3(-) - Comp2(+) == 0	-213.77	50.16	-4.262	< 0.001 ***
Comp3(+) - Comp2(+) == 0	-172.07	26.57	-6.477	< 0.001 ***
Comp3(+) - Comp3(-) == 0	41.70	50.12	0.832	0.95854

Winter ETo

	Estimate	Std. Error	t value	Pr(>|t|)
Comp1(+) - Comp1(-) == 0	80.07	33.95	2.359	0.16048
Comp2(-) - Comp1(-) == 0	303.41	45.60	6.654	< 0.001 ***
Comp2(+) - Comp1(-) == 0	18.79	30.26	0.621	0.98863
Comp3(-) - Comp1(-) == 0	236.12	52.98	4.457	< 0.001 ***
Comp3(+) - Comp1(-) == 0	199.33	30.19	6.602	< 0.001 ***
Comp2(-) - Comp1(+) == 0	223.33	46.30	4.824	< 0.001 ***
Comp2(+) - Comp1(+) == 0	-61.29	31.30	-1.958	0.35048
Comp3(-) - Comp1(+) == 0	156.05	53.58	2.912	0.03879 *
Comp3(+) - Comp1(+) == 0	119.26	31.24	3.818	0.00182 **
Comp2(+) - Comp2(-) == 0	-284.62	43.67	-6.518	< 0.001 ***
Comp3(-) - Comp2(-) == 0	-67.28	61.63	-1.092	0.87691
Comp3(+) - Comp2(-) == 0	-104.07	43.62	-2.386	0.15089
Comp3(-) - Comp2(+) == 0	217.34	51.32	4.235	< 0.001 ***
Comp3(+) - Comp2(+) == 0	180.55	27.19	6.641	< 0.001 ***
Comp3(+) - Comp3(-) == 0	-36.79	51.28	-0.717	0.97819

Spring ETo

	Estimate	Std. Error	t value	Pr(>|t|)
Comp1(+) - Comp1(-) == 0	-347.443	32.736	-10.614	< 0.001 ***
Comp2(-) - Comp1(-) == 0	-399.861	43.973	-9.093	< 0.001 ***
Comp2(+) - Comp1(-) == 0	-264.567	29.182	-9.066	< 0.001 ***
Comp3(-) - Comp1(-) == 0	-454.325	51.086	-8.893	< 0.001 ***
Comp3(+) - Comp1(-) == 0	-352.920	29.114	-12.122	< 0.001 ***
Comp2(-) - Comp1(+) == 0	-52.418	44.646	-1.174	0.83966
Comp2(+) - Comp1(+) == 0	82.876	30.187	2.745	0.06203 .
Comp3(-) - Comp1(+) == 0	-106.882	51.667	-2.069	0.28874
Comp3(+) - Comp1(+) == 0	-5.478	30.121	-0.182	0.99997

Comp2(+) - Comp2(-) == 0 135.294 42.109 3.213 0.01540 *
Comp3(-) - Comp2(-) == 0 -54.464 59.426 -0.917 0.93801
Comp3(+) - Comp2(-) == 0 46.940 42.062 1.116 0.86654
Comp3(-) - Comp2(+) == 0 -189.758 49.492 -3.834 0.00174 **
Comp3(+) - Comp2(+) == 0 -88.353 26.215 -3.370 0.00927 **
Comp3(+) - Comp3(-) == 0 101.405 49.452 2.051 0.29824

Summer ETo

	Estimate	Std. Error	t value	Pr(>|t|)	
Comp1(+) - Comp1(-) == 0	-655.36	27.87	-23.513	< 0.001	***
Comp2(-) - Comp1(-) == 0	-442.26	37.44	-11.813	< 0.001	***
Comp2(+) - Comp1(-) == 0	-540.11	24.85	-21.739	< 0.001	***
Comp3(-) - Comp1(-) == 0	-234.49	43.50	-5.391	< 0.001	***
Comp3(+) - Comp1(-) == 0	-559.91	24.79	-22.588	< 0.001	***
Comp2(-) - Comp1(+) == 0	213.10	38.01	5.606	< 0.001	***
Comp2(+) - Comp1(+) == 0	115.25	25.70	4.484	< 0.001	***
Comp3(-) - Comp1(+) == 0	420.87	43.99	9.567	< 0.001	***
Comp3(+) - Comp1(+) == 0	95.45	25.65	3.722	0.00269	**
Comp2(+) - Comp2(-) == 0	-97.86	35.85	-2.729	0.06471	.
Comp3(-) - Comp2(-) == 0	207.76	50.60	4.106	< 0.001	***
Comp3(+) - Comp2(-) == 0	-117.65	35.81	-3.285	0.01201	*
Comp3(-) - Comp2(+) == 0	305.62	42.14	7.253	< 0.001	***
Comp3(+) - Comp2(+) == 0	-19.80	22.32	-0.887	0.94581	
Comp3(+) - Comp3(-) == 0	-325.42	42.10	-7.729	< 0.001	***

Autumn ETo

	Estimate	Std. Error	t value	Pr(>|t|)	
Comp1(+) - Comp1(-) == 0	-336.659	32.907	-10.230	< 0.001	***
Comp2(-) - Comp1(-) == 0	-414.251	44.203	-9.372	< 0.001	***
Comp2(+) - Comp1(-) == 0	-260.277	29.335	-8.873	< 0.001	***
Comp3(-) - Comp1(-) == 0	-423.950	51.354	-8.255	< 0.001	***
Comp3(+) - Comp1(-) == 0	-333.918	29.267	-11.409	< 0.001	***
Comp2(-) - Comp1(+) == 0	-77.591	44.880	-1.729	0.49488	
Comp2(+) - Comp1(+) == 0	76.382	30.345	2.517	0.11121	
Comp3(-) - Comp1(+) == 0	-87.291	51.938	-1.681	0.52714	
Comp3(+) - Comp1(+) == 0	2.741	30.279	0.091	1.00000	
Comp2(+) - Comp2(-) == 0	153.974	42.330	3.637	0.00353	**
Comp3(-) - Comp2(-) == 0	-9.700	59.737	-0.162	0.99998	
Comp3(+) - Comp2(-) == 0	80.332	42.283	1.900	0.38518	
Comp3(-) - Comp2(+) == 0	-163.673	49.751	-3.290	0.01208	*
Comp3(+) - Comp2(+) == 0	-73.641	26.353	-2.794	0.05438	.
Comp3(+) - Comp3(-) == 0	90.032	49.711	1.811	0.44091	

Annual climate balance

	Estimate	Std. Error	t value	Pr(>|t|)
Comp1(+) - Comp1(-) == 0	-79.377	34.988	-2.269	0.19516
Comp2(-) - Comp1(-) == 0	-124.022	46.998	-2.639	0.08220 .
Comp2(+) - Comp1(-) == 0	-102.665	31.189	-3.292	0.01187 *
Comp3(-) - Comp1(-) == 0	-73.914	54.601	-1.354	0.74117
Comp3(+) - Comp1(-) == 0	-122.049	31.117	-3.922	0.00117 **
Comp2(-) - Comp1(+) == 0	-44.646	47.717	-0.936	0.93260
Comp2(+) - Comp1(+) == 0	-23.288	32.263	-0.722	0.97759
Comp3(-) - Comp1(+) == 0	5.463	55.222	0.099	1.00000
Comp3(+) - Comp1(+) == 0	-42.672	32.194	-1.325	0.75802
Comp2(+) - Comp2(-) == 0	21.357	45.006	0.475	0.99675
Comp3(-) - Comp2(-) == 0	50.108	63.514	0.789	0.96697
Comp3(+) - Comp2(-) == 0	1.973	44.956	0.044	1.00000

Comp3(-) - Comp2(+) == 0 28.751 52.896 0.544 0.99384
Comp3(+) - Comp2(+) == 0 -19.384 28.019 -0.692 0.98143
Comp3(+) - Comp3(-) == 0 -48.135 52.854 -0.911 0.93962

Winter climate balance

	Estimate	Std. Error	t value	Pr(>|t|)	
Comp1(+) - Comp1(-) == 0	457.23	27.35	16.718	<0.001	***
Comp2(-) - Comp1(-) == 0	149.80	36.74	4.078	<0.001	***
Comp2(+) - Comp1(-) == 0	511.04	24.38	20.961	<0.001	***
Comp3(-) - Comp1(-) == 0	198.12	42.68	4.642	<0.001	***
Comp3(+) - Comp1(-) == 0	640.65	24.32	26.338	<0.001	***
Comp2(-) - Comp1(+) == 0	-307.43	37.30	-8.242	<0.001	***
Comp2(+) - Comp1(+) == 0	53.81	25.22	2.134	0.256	
Comp3(-) - Comp1(+) == 0	-259.11	43.17	-6.003	<0.001	***
Comp3(+) - Comp1(+) == 0	183.42	25.17	7.288	<0.001	***
Comp2(+) - Comp2(-) == 0	361.24	35.18	10.268	<0.001	***
Comp3(-) - Comp2(-) == 0	48.32	49.65	0.973	0.921	
Comp3(+) - Comp2(-) == 0	490.85	35.14	13.968	<0.001	***
Comp3(-) - Comp2(+) == 0	-312.92	41.35	-7.568	<0.001	***
Comp3(+) - Comp2(+) == 0	129.61	21.90	5.918	<0.001	***
Comp3(+) - Comp3(-) == 0	442.52	41.31	10.711	<0.001	***

Spring climate balance

	Estimate	Std. Error	t value	Pr(>|t|)	
Comp1(+) - Comp1(-) == 0	244.654	33.033	7.406	< 0.001	***
Comp2(-) - Comp1(-) == 0	238.248	44.372	5.369	< 0.001	***
Comp2(+) - Comp1(-) == 0	362.153	29.447	12.299	< 0.001	***
Comp3(-) - Comp1(-) == 0	37.035	51.550	0.718	0.97805	
Comp3(+) - Comp1(-) == 0	276.162	29.379	9.400	< 0.001	***
Comp2(-) - Comp1(+) == 0	-6.406	45.051	-0.142	0.99999	
Comp2(+) - Comp1(+) == 0	117.498	30.461	3.857	0.00154	**
Comp3(-) - Comp1(+) == 0	-207.619	52.136	-3.982	0.00108	**
Comp3(+) - Comp1(+) == 0	31.508	30.395	1.037	0.89896	
Comp2(+) - Comp2(-) == 0	123.904	42.492	2.916	0.03861	*
Comp3(-) - Comp2(-) == 0	-201.213	59.966	-3.355	0.00968	**
Comp3(+) - Comp2(-) == 0	37.914	42.444	0.893	0.94422	
Comp3(-) - Comp2(+) == 0	-325.117	49.941	-6.510	< 0.001	***
Comp3(+) - Comp2(+) == 0	-85.990	26.453	-3.251	0.01360	*
Comp3(+) - Comp3(-) == 0	239.127	49.901	4.792	< 0.001	***

Summer climate balance

	Estimate	Std. Error	t value	Pr(>|t|)	
Comp1(+) - Comp1(-) == 0	-613.17	27.97	-21.926	< 0.001	***
Comp2(-) - Comp1(-) == 0	-355.43	37.57	-9.462	< 0.001	***
Comp2(+) - Comp1(-) == 0	-516.83	24.93	-20.732	< 0.001	***
Comp3(-) - Comp1(-) == 0	-44.07	43.64	-1.010	0.90869	
Comp3(+) - Comp1(-) == 0	-534.37	24.87	-21.485	< 0.001	***
Comp2(-) - Comp1(+) == 0	257.74	38.14	6.758	< 0.001	***
Comp2(+) - Comp1(+) == 0	96.34	25.79	3.736	0.00254	**
Comp3(-) - Comp1(+) == 0	569.10	44.14	12.894	< 0.001	***
Comp3(+) - Comp1(+) == 0	78.80	25.73	3.062	0.02478	*
Comp2(+) - Comp2(-) == 0	-161.40	35.97	-4.487	< 0.001	***
Comp3(-) - Comp2(-) == 0	311.36	50.77	6.133	< 0.001	***
Comp3(+) - Comp2(-) == 0	-178.94	35.93	-4.980	< 0.001	***
Comp3(-) - Comp2(+) == 0	472.76	42.28	11.182	< 0.001	***
Comp3(+) - Comp2(+) == 0	-17.54	22.40	-0.783	0.96800	
Comp3(+) - Comp3(-) == 0	-490.30	42.25	-11.606	< 0.001	***

Autumn climate balance

	Estimate	Std. Error	t value	Pr(>|t|)	
Comp1(+) - Comp1(-) == 0	558.897	27.440	20.368	< 1e-04	***
Comp2(-) - Comp1(-) == 0	265.202	36.859	7.195	< 1e-04	***
Comp2(+) - Comp1(-) == 0	558.522	24.461	22.833	< 1e-04	***
Comp3(-) - Comp1(-) == 0	57.603	42.822	1.345	0.746338	
Comp3(+) - Comp1(-) == 0	570.917	24.404	23.394	< 1e-04	***
Comp2(-) - Comp1(+) == 0	-293.695	37.423	-7.848	< 1e-04	***
Comp2(+) - Comp1(+) == 0	-0.375	25.303	-0.015	1.000000	
Comp3(-) - Comp1(+) == 0	-501.294	43.309	-11.575	< 1e-04	***
Comp3(+) - Comp1(+) == 0	12.020	25.248	0.476	0.996695	
Comp2(+) - Comp2(-) == 0	293.320	35.297	8.310	< 1e-04	***
Comp3(-) - Comp2(-) == 0	-207.599	49.812	-4.168	0.000442	***
Comp3(+) - Comp2(-) == 0	305.715	35.258	8.671	< 1e-04	***
Comp3(-) - Comp2(+) == 0	-500.919	41.485	-12.075	< 1e-04	***
Comp3(+) - Comp2(+) == 0	12.395	21.974	0.564	0.992679	
Comp3(+) - Comp3(-) == 0	513.314	41.452	12.383	< 1e-04	***

Winter NDVI

	Estimate	Std. Error	t value	Pr(>|t|)	
Comp1(+) - Comp1(-) == 0	432.91	30.82	14.048	< 0.001	***
Comp2(-) - Comp1(-) == 0	95.25	41.39	2.301	0.18225	
Comp2(+) - Comp1(-) == 0	417.56	27.47	15.200	< 0.001	***
Comp3(-) - Comp1(-) == 0	-119.33	48.09	-2.481	0.12119	
Comp3(+) - Comp1(-) == 0	293.76	27.41	10.719	< 0.001	***
Comp2(-) - Comp1(+) == 0	-337.66	42.03	-8.034	< 0.001	***
Comp2(+) - Comp1(+) == 0	-15.35	28.42	-0.540	0.99402	
Comp3(-) - Comp1(+) == 0	-552.24	48.64	-11.354	< 0.001	***
Comp3(+) - Comp1(+) == 0	-139.15	28.36	-4.907	< 0.001	***
Comp2(+) - Comp2(-) == 0	322.31	39.64	8.131	< 0.001	***
Comp3(-) - Comp2(-) == 0	-214.57	55.94	-3.836	0.00165	**
Comp3(+) - Comp2(-) == 0	198.51	39.60	5.013	< 0.001	***
Comp3(-) - Comp2(+) == 0	-536.89	46.59	-11.524	< 0.001	***
Comp3(+) - Comp2(+) == 0	-123.80	24.68	-5.017	< 0.001	***
Comp3(+) - Comp3(-) == 0	413.09	46.55	8.874	< 0.001	***

Spring NDVI

	Estimate	Std. Error	t value	Pr(>|t|)	
Comp1(+) - Comp1(-) == 0	335.106	32.109	10.437	< 0.001	***
Comp2(-) - Comp1(-) == 0	40.199	43.130	0.932	0.93364	
Comp2(+) - Comp1(-) == 0	329.622	28.623	11.516	< 0.001	***
Comp3(-) - Comp1(-) == 0	-194.210	50.108	-3.876	0.00159	**
Comp3(+) - Comp1(-) == 0	172.675	28.557	6.047	< 0.001	***
Comp2(-) - Comp1(+) == 0	-294.907	43.791	-6.734	< 0.001	***
Comp2(+) - Comp1(+) == 0	-5.484	29.609	-0.185	0.99997	
Comp3(-) - Comp1(+) == 0	-529.316	50.678	-10.445	< 0.001	***
Comp3(+) - Comp1(+) == 0	-162.430	29.545	-5.498	< 0.001	***
Comp2(+) - Comp2(-) == 0	289.423	41.303	7.007	< 0.001	***
Comp3(-) - Comp2(-) == 0	-234.409	58.288	-4.022	< 0.001	***
Comp3(+) - Comp2(-) == 0	132.476	41.257	3.211	0.01561	*
Comp3(-) - Comp2(+) == 0	-523.832	48.544	-10.791	< 0.001	***
Comp3(+) - Comp2(+) == 0	-156.947	25.713	-6.104	< 0.001	***
Comp3(+) - Comp3(-) == 0	366.885	48.505	7.564	< 0.001	***

Summer NDVI

	Estimate	Std. Error	t value	Pr(>|t|)	
Comp1(+) - Comp1(-) == 0	96.021	34.545	2.780	0.05649	.
Comp2(-) - Comp1(-) == 0	-69.110	46.403	-1.489	0.65534	
Comp2(+) - Comp1(-) == 0	99.489	30.795	3.231	0.01458	*
Comp3(-) - Comp1(-) == 0	-131.934	53.910	-2.447	0.13130	
Comp3(+) - Comp1(-) == 0	-42.340	30.723	-1.378	0.72628	
Comp2(-) - Comp1(+) == 0	-165.131	47.114	-3.505	0.00561	**
Comp2(+) - Comp1(+) == 0	3.468	31.855	0.109	1.00000	
Comp3(-) - Comp1(+) == 0	-227.955	54.523	-4.181	< 0.001	***
Comp3(+) - Comp1(+) == 0	-138.361	31.786	-4.353	< 0.001	***
Comp2(+) - Comp2(-) == 0	168.598	44.437	3.794	0.00192	**
Comp3(-) - Comp2(-) == 0	-62.825	62.711	-1.002	0.91148	
Comp3(+) - Comp2(-) == 0	26.769	44.388	0.603	0.99003	
Comp3(-) - Comp2(+) == 0	-231.423	52.227	-4.431	< 0.001	***
Comp3(+) - Comp2(+) == 0	-141.829	27.664	-5.127	< 0.001	***
Comp3(+) - Comp3(-) == 0	89.594	52.185	1.717	0.50322	

Autumn NDVI

	Estimate	Std. Error	t value	Pr(>|t|)	
Comp1(+) - Comp1(-) == 0	336.1088	32.1476	10.455	< 0.001	***
Comp2(-) - Comp1(-) == 0	37.9673	43.1823	0.879	0.94777	
Comp2(+) - Comp1(-) == 0	336.4464	28.6573	11.740	< 0.001	***
Comp3(-) - Comp1(-) == 0	-166.3353	50.1683	-3.316	0.01122	*
Comp3(+) - Comp1(-) == 0	172.9737	28.5909	6.050	< 0.001	***
Comp2(-) - Comp1(+) == 0	-298.1415	43.8436	-6.800	< 0.001	***
Comp2(+) - Comp1(+) == 0	0.3376	29.6443	0.011	1.00000	
Comp3(-) - Comp1(+) == 0	-502.4441	50.7386	-9.903	< 0.001	***
Comp3(+) - Comp1(+) == 0	-163.1351	29.5801	-5.515	< 0.001	***
Comp2(+) - Comp2(-) == 0	298.4791	41.3525	7.218	< 0.001	***
Comp3(-) - Comp2(-) == 0	-204.3026	58.3580	-3.501	0.00586	**
Comp3(+) - Comp2(-) == 0	135.0064	41.3066	3.268	0.01282	*
Comp3(-) - Comp2(+) == 0	-502.7817	48.6022	-10.345	< 0.001	***
Comp3(+) - Comp2(+) == 0	-163.4727	25.7441	-6.350	< 0.001	***
Comp3(+) - Comp3(-) == 0	339.3090	48.5631	6.987	< 0.001	***

Average day of the year recording the maximum NDVI

	Estimate	Std. Error	t value	Pr(>|t|)	
Comp1(+) - Comp1(-) == 0	2.2663	0.4383	5.171	< 0.001	***
Comp2(-) - Comp1(-) == 0	0.1933	0.5888	0.328	0.99945	
Comp2(+) - Comp1(-) == 0	1.9048	0.3907	4.875	< 0.001	***
Comp3(-) - Comp1(-) == 0	0.4972	0.6840	0.727	0.97688	
Comp3(+) - Comp1(-) == 0	1.4834	0.3898	3.805	0.00187	**
Comp2(-) - Comp1(+) == 0	-2.0730	0.5978	-3.468	0.00652	**
Comp2(+) - Comp1(+) == 0	-0.3616	0.4042	-0.895	0.94388	
Comp3(-) - Comp1(+) == 0	-1.7691	0.6918	-2.557	0.10076	
Comp3(+) - Comp1(+) == 0	-0.7829	0.4033	-1.941	0.36006	
Comp2(+) - Comp2(-) == 0	1.7114	0.5638	3.035	0.02681	*
Comp3(-) - Comp2(-) == 0	0.3039	0.7957	0.382	0.99885	
Comp3(+) - Comp2(-) == 0	1.2901	0.5632	2.291	0.18604	
Comp3(-) - Comp2(+) == 0	-1.4076	0.6627	-2.124	0.26041	
Comp3(+) - Comp2(+) == 0	-0.4213	0.3510	-1.200	0.82661	
Comp3(+) - Comp3(-) == 0	0.9862	0.6621	1.489	0.65538	

Average day of the year recording the green up

	Estimate	Std. Error	t value	Pr(>|t|)	
Comp1(+) - Comp1(-) == 0	5.7118	2.0853	2.739	0.0631	.
Comp2(-) - Comp1(-) == 0	0.6447	2.8010	0.230	0.9999	

Comp2(+) - Comp1(-) == 0	1.0980	1.8589	0.591	0.9909
Comp3(-) - Comp1(-) == 0	10.1321	3.2542	3.114	0.0211 *
Comp3(+) - Comp1(-) == 0	5.3079	1.8546	2.862	0.0447 *
Comp2(-) - Comp1(+) == 0	-5.0672	2.8439	-1.782	0.4600
Comp2(+) - Comp1(+) == 0	-4.6138	1.9229	-2.399	0.1468
Comp3(-) - Comp1(+) == 0	4.4203	3.2912	1.343	0.7475
Comp3(+) - Comp1(+) == 0	-0.4040	1.9187	-0.211	0.9999
Comp2(+) - Comp2(-) == 0	0.4533	2.6823	0.169	1.0000
Comp3(-) - Comp2(-) == 0	9.4875	3.7854	2.506	0.1143
Comp3(+) - Comp2(-) == 0	4.6632	2.6794	1.740	0.4871
Comp3(-) - Comp2(+) == 0	9.0341	3.1526	2.866	0.0442 *
Comp3(+) - Comp2(+) == 0	4.2099	1.6699	2.521	0.1101
Comp3(+) - Comp3(-) == 0	-4.8243	3.1501	-1.531	0.6276

Soil water capacity

	Estimate	Std. Error	t value	Pr(>|t|)
Comp1(+) - Comp1(-) == 0	170.510	34.516	4.940	< 0.001 ***
Comp2(-) - Comp1(-) == 0	60.380	46.364	1.302	0.77147
Comp2(+) - Comp1(-) == 0	127.987	30.769	4.160	< 0.001 ***
Comp3(-) - Comp1(-) == 0	-57.831	53.865	-1.074	0.88450
Comp3(+) - Comp1(-) == 0	177.195	30.698	5.772	< 0.001 ***
Comp2(-) - Comp1(+) == 0	-110.131	47.074	-2.340	0.16737
Comp2(+) - Comp1(+) == 0	-42.523	31.829	-1.336	0.75173
Comp3(-) - Comp1(+) == 0	-228.341	54.477	-4.192	< 0.001 ***
Comp3(+) - Comp1(+) == 0	6.684	31.760	0.210	0.99994
Comp2(+) - Comp2(-) == 0	67.607	44.399	1.523	0.63343
Comp3(-) - Comp2(-) == 0	-118.211	62.658	-1.887	0.39296
Comp3(+) - Comp2(-) == 0	116.815	44.350	2.634	0.08324 .
Comp3(-) - Comp2(+) == 0	-185.818	52.183	-3.561	0.00468 **
Comp3(+) - Comp2(+) == 0	49.208	27.641	1.780	0.46103
Comp3(+) - Comp3(-) == 0	235.025	52.141	4.507	< 0.001 ***

3. SOYBEAN

Annual precipitation

	Estimate	Std. Error	t value	Pr(>|t|)	
Comp1(+) - Comp1(-) == 0	-53.08	70.13	-0.757	0.9654	
Comp2(-) - Comp1(-) == 0	-157.84	186.02	-0.848	0.9441	
Comp2(+) - Comp1(-) == 0	222.20	71.84	3.093	0.0176	*
Comp3(-) - Comp1(-) == 0	114.16	186.02	0.614	0.9863	
Comp3(+) - Comp1(-) == 0	-108.64	77.09	-1.409	0.6633	
Comp2(-) - Comp1(+) == 0	-104.76	173.14	-0.605	0.9871	
Comp2(+) - Comp1(+) == 0	275.28	23.07	11.930	<0.001	***
Comp3(-) - Comp1(+) == 0	167.24	173.14	0.966	0.9063	
Comp3(+) - Comp1(+) == 0	-55.56	36.26	-1.532	0.5789	
Comp2(+) - Comp2(-) == 0	380.04	173.84	2.186	0.1937	
Comp3(-) - Comp2(-) == 0	272.00	244.26	1.114	0.8414	
Comp3(+) - Comp2(-) == 0	49.20	176.07	0.279	0.9997	
Comp3(-) - Comp2(+) == 0	-108.04	173.84	-0.622	0.9854	
Comp3(+) - Comp2(+) == 0	-330.85	39.46	-8.384	<0.001	***
Comp3(+) - Comp3(-) == 0	-222.80	176.07	-1.265	0.7563	

Winter precipitation

	Estimate	Std. Error	t value	Pr(>|t|)	
Comp1(+) - Comp1(-) == 0	-238.215	73.797	-3.228	0.0114	*
Comp2(-) - Comp1(-) == 0	-193.650	195.753	-0.989	0.8974	
Comp2(+) - Comp1(-) == 0	-167.231	75.594	-2.212	0.1840	
Comp3(-) - Comp1(-) == 0	39.100	195.753	0.200	0.9999	
Comp3(+) - Comp1(-) == 0	-234.184	81.123	-2.887	0.0326	*
Comp2(-) - Comp1(+) == 0	44.565	182.194	0.245	0.9998	
Comp2(+) - Comp1(+) == 0	70.984	24.281	2.923	0.0292	*
Comp3(-) - Comp1(+) == 0	277.315	182.194	1.522	0.5858	
Comp3(+) - Comp1(+) == 0	4.031	38.158	0.106	1.0000	
Comp2(+) - Comp2(-) == 0	26.419	182.929	0.144	1.0000	
Comp3(-) - Comp2(-) == 0	232.750	257.037	0.906	0.9274	
Comp3(+) - Comp2(-) == 0	-40.534	185.282	-0.219	0.9999	
Comp3(-) - Comp2(+) == 0	206.331	182.929	1.128	0.8341	
Comp3(+) - Comp2(+) == 0	-66.953	41.527	-1.612	0.5235	
Comp3(+) - Comp3(-) == 0	-273.284	185.282	-1.475	0.6186	

Spring precipitation

	Estimate	Std. Error	t value	Pr(>|t|)	
Comp1(+) - Comp1(-) == 0	308.06	68.27	4.513	< 0.001	***
Comp2(-) - Comp1(-) == 0	422.94	181.08	2.336	0.13995	
Comp2(+) - Comp1(-) == 0	5.20	69.93	0.074	1.00000	
Comp3(-) - Comp1(-) == 0	-309.31	181.08	-1.708	0.45838	
Comp3(+) - Comp1(-) == 0	25.48	75.04	0.340	0.99916	
Comp2(-) - Comp1(+) == 0	114.88	168.54	0.682	0.97805	
Comp2(+) - Comp1(+) == 0	-302.86	22.46	-13.484	< 0.001	***
Comp3(-) - Comp1(+) == 0	-617.37	168.54	-3.663	0.00244	**
Comp3(+) - Comp1(+) == 0	-282.58	35.30	-8.006	< 0.001	***
Comp2(+) - Comp2(-) == 0	-417.74	169.22	-2.469	0.10141	
Comp3(-) - Comp2(-) == 0	-732.25	237.77	-3.080	0.01755	*
Comp3(+) - Comp2(-) == 0	-397.46	171.40	-2.319	0.14492	
Comp3(-) - Comp2(+) == 0	-314.51	169.22	-1.859	0.36185	
Comp3(+) - Comp2(+) == 0	20.28	38.41	0.528	0.99310	
Comp3(+) - Comp3(-) == 0	334.79	171.40	1.953	0.30662	

Summer precipitation

	Estimate	Std. Error	t value	Pr(>|t|)	
Comp1(+) - Comp1(-) == 0	3.916	73.605	0.053	1.00000	
Comp2(-) - Comp1(-) == 0	425.040	195.245	2.177	0.19837	
Comp2(+) - Comp1(-) == 0	-7.038	75.398	-0.093	1.00000	
Comp3(-) - Comp1(-) == 0	-289.460	195.245	-1.483	0.61265	
Comp3(+) - Comp1(-) == 0	-157.901	80.912	-1.952	0.30768	
Comp2(-) - Comp1(+) == 0	421.124	181.721	2.317	0.14571	
Comp2(+) - Comp1(+) == 0	-10.954	24.218	-0.452	0.99666	
Comp3(-) - Comp1(+) == 0	-293.376	181.721	-1.614	0.52210	
Comp3(+) - Comp1(+) == 0	-161.817	38.059	-4.252	< 0.001	***
Comp2(+) - Comp2(-) == 0	-432.078	182.454	-2.368	0.12901	
Comp3(-) - Comp2(-) == 0	-714.500	256.370	-2.787	0.04427	*
Comp3(+) - Comp2(-) == 0	-582.941	184.801	-3.154	0.01386	*
Comp3(-) - Comp2(+) == 0	-282.422	182.454	-1.548	0.56773	
Comp3(+) - Comp2(+) == 0	-150.863	41.419	-3.642	0.00263	**
Comp3(+) - Comp3(-) == 0	131.559	184.801	0.712	0.97346	

Autumn precipitation

	Estimate	Std. Error	t value	Pr(>|t|)	
Comp1(+) - Comp1(-) == 0	108.07	70.01	1.544	0.5708	
Comp2(-) - Comp1(-) == 0	583.32	185.70	3.141	0.0149	*
Comp2(+) - Comp1(-) == 0	-174.66	71.71	-2.436	0.1103	
Comp3(-) - Comp1(-) == 0	120.57	185.70	0.649	0.9823	
Comp3(+) - Comp1(-) == 0	60.01	76.96	0.780	0.9607	
Comp2(-) - Comp1(+) == 0	475.25	172.84	2.750	0.0483	*
Comp2(+) - Comp1(+) == 0	-282.73	23.03	-12.275	<0.001	***
Comp3(-) - Comp1(+) == 0	12.50	172.84	0.072	1.0000	
Comp3(+) - Comp1(+) == 0	-48.06	36.20	-1.328	0.7173	
Comp2(+) - Comp2(-) == 0	-757.98	173.54	-4.368	<0.001	***
Comp3(-) - Comp2(-) == 0	-462.75	243.84	-1.898	0.3387	
Comp3(+) - Comp2(-) == 0	-523.31	175.77	-2.977	0.0249	*
Comp3(-) - Comp2(+) == 0	295.23	173.54	1.701	0.4629	
Comp3(+) - Comp2(+) == 0	234.67	39.39	5.957	<0.001	***
Comp3(+) - Comp3(-) == 0	-60.56	175.77	-0.345	0.9991	

Annual mean temperature

	Estimate	Std. Error	t value	Pr(>|t|)	
Comp1(+) - Comp1(-) == 0	-255.652	73.749	-3.467	0.00496	**
Comp2(-) - Comp1(-) == 0	-42.370	195.626	-0.217	0.99991	
Comp2(+) - Comp1(-) == 0	-178.915	75.545	-2.368	0.12881	
Comp3(-) - Comp1(-) == 0	-263.870	195.626	-1.349	0.70365	
Comp3(+) - Comp1(-) == 0	-222.551	81.070	-2.745	0.04889	*
Comp2(-) - Comp1(+) == 0	213.282	182.075	1.171	0.81094	
Comp2(+) - Comp1(+) == 0	76.737	24.265	3.162	0.01451	*
Comp3(-) - Comp1(+) == 0	-8.218	182.075	-0.045	1.00000	
Comp3(+) - Comp1(+) == 0	33.101	38.133	0.868	0.93867	
Comp2(+) - Comp2(-) == 0	-136.545	182.810	-0.747	0.96732	
Comp3(-) - Comp2(-) == 0	-221.500	256.869	-0.862	0.94027	
Comp3(+) - Comp2(-) == 0	-180.181	185.161	-0.973	0.90363	
Comp3(-) - Comp2(+) == 0	-84.955	182.810	-0.465	0.99620	
Comp3(+) - Comp2(+) == 0	-43.636	41.500	-1.051	0.87104	
Comp3(+) - Comp3(-) == 0	41.319	185.161	0.223	0.99989	

Winter mean temperature

	Estimate	Std. Error	t value	Pr(>|t|)
Comp1(+) - Comp1(-) == 0	89.83	69.45	1.294	0.7391

Comp2(-) - Comp1(-) == 0 343.92 184.21 1.867 0.3570
Comp2(+) - Comp1(-) == 0 -192.85 71.14 -2.711 0.0540 .
Comp3(-) - Comp1(-) == 0 -43.58 184.21 -0.237 0.9999
Comp3(+) - Comp1(-) == 0 -173.84 76.34 -2.277 0.1593
Comp2(-) - Comp1(+) == 0 254.09 171.45 1.482 0.6131
Comp2(+) - Comp1(+) == 0 -282.68 22.85 -12.371 <0.001 ***
Comp3(-) - Comp1(+) == 0 -133.41 171.45 -0.778 0.9610
Comp3(+) - Comp1(+) == 0 -263.67 35.91 -7.343 <0.001 ***
Comp2(+) - Comp2(-) == 0 -536.77 172.14 -3.118 0.0159 *
Comp3(-) - Comp2(-) == 0 -387.50 241.88 -1.602 0.5305
Comp3(+) - Comp2(-) == 0 -517.76 174.36 -2.970 0.0255 *
Comp3(-) - Comp2(+) == 0 149.27 172.14 0.867 0.9389
Comp3(+) - Comp2(+) == 0 19.00 39.08 0.486 0.9953
Comp3(+) - Comp3(-) == 0 -130.26 174.36 -0.747 0.9672

Spring mean temperature

	Estimate	Std. Error	t value	Pr(>|t|)	
Comp1(+) - Comp1(-) == 0	-225.9965	72.1857	-3.131	0.0151	*
Comp2(-) - Comp1(-) == 0	-39.6900	191.4794	-0.207	0.9999	
Comp2(+) - Comp1(-) == 0	-39.4822	73.9435	-0.534	0.9927	
Comp3(-) - Comp1(-) == 0	42.3100	191.4794	0.221	0.9999	
Comp3(+) - Comp1(-) == 0	-67.3616	79.3514	-0.849	0.9440	
Comp2(-) - Comp1(+) == 0	186.3065	178.2157	1.045	0.8738	
Comp2(+) - Comp1(+) == 0	186.5143	23.7508	7.853	<0.001	***
Comp3(-) - Comp1(+) == 0	268.3065	178.2157	1.506	0.5969	
Comp3(+) - Comp1(+) == 0	158.6349	37.3245	4.250	<0.001	***
Comp2(+) - Comp2(-) == 0	0.2078	178.9349	0.001	1.0000	
Comp3(-) - Comp2(-) == 0	82.0000	251.4247	0.326	0.9993	
Comp3(+) - Comp2(-) == 0	-27.6716	181.2366	-0.153	1.0000	
Comp3(-) - Comp2(+) == 0	81.7922	178.9349	0.457	0.9965	
Comp3(+) - Comp2(+) == 0	-27.8794	40.6200	-0.686	0.9774	
Comp3(+) - Comp3(-) == 0	-109.6716	181.2366	-0.605	0.9871	

Summer mean temperature

	Estimate	Std. Error	t value	Pr(>|t|)	
Comp1(+) - Comp1(-) == 0	203.04	64.25	3.160	0.01388	*
Comp2(-) - Comp1(-) == 0	646.93	170.44	3.796	0.00156	**
Comp2(+) - Comp1(-) == 0	-200.41	65.82	-3.045	0.02015	*
Comp3(-) - Comp1(-) == 0	-99.07	170.44	-0.581	0.98925	
Comp3(+) - Comp1(-) == 0	-133.86	70.63	-1.895	0.34015	
Comp2(-) - Comp1(+) == 0	443.89	158.63	2.798	0.04199	*
Comp2(+) - Comp1(+) == 0	-403.45	21.14	-19.084	< 0.001	***
Comp3(-) - Comp1(+) == 0	-302.11	158.63	-1.904	0.33434	
Comp3(+) - Comp1(+) == 0	-336.90	33.22	-10.140	< 0.001	***
Comp2(+) - Comp2(-) == 0	-847.34	159.27	-5.320	< 0.001	***
Comp3(-) - Comp2(-) == 0	-746.00	223.80	-3.333	0.00766	**
Comp3(+) - Comp2(-) == 0	-780.79	161.32	-4.840	< 0.001	***
Comp3(-) - Comp2(+) == 0	101.34	159.27	0.636	0.98381	
Comp3(+) - Comp2(+) == 0	66.55	36.16	1.841	0.37300	
Comp3(+) - Comp3(-) == 0	-34.79	161.32	-0.216	0.99991	

Autumn mean temperature

	Estimate	Std. Error	t value	Pr(>|t|)	
Comp1(+) - Comp1(-) == 0	-402.8697	73.1359	-5.509	<0.001	***
Comp2(-) - Comp1(-) == 0	-40.6200	193.9999	-0.209	1.000	
Comp2(+) - Comp1(-) == 0	-452.5226	74.9168	-6.040	<0.001	***
Comp3(-) - Comp1(-) == 0	-318.3700	193.9999	-1.641	0.503	

```
Comp3(+) - Comp1(-) == 0 -452.9827    80.3960  -5.634   <0.001 ***
Comp2(-) - Comp1(+) == 0  362.2497   180.5616   2.006    0.278
Comp2(+) - Comp1(+) == 0  -49.6529    24.0635  -2.063    0.249
Comp3(-) - Comp1(+) == 0   84.4997   180.5616   0.468    0.996
Comp3(+) - Comp1(+) == 0  -50.1130    37.8158  -1.325    0.719
Comp2(+) - Comp2(-) == 0 -411.9026   181.2903  -2.272    0.161
Comp3(-) - Comp2(-) == 0 -277.7500   254.7344  -1.090    0.853
Comp3(+) - Comp2(-) == 0 -412.3627   183.6223  -2.246    0.170
Comp3(-) - Comp2(+) == 0  134.1526   181.2903   0.740    0.969
Comp3(+) - Comp2(+) == 0   -0.4601    41.1547  -0.011    1.000
Comp3(+) - Comp3(-) == 0 -134.6127   183.6223  -0.733    0.970
```

Annual ETo

```
                    Estimate Std. Error t value Pr(>|t|)
Comp1(+) - Comp1(-) == 0  -179.04      74.01  -2.419   0.1144
Comp2(-) - Comp1(-) == 0    47.12     196.31   0.240   0.9998
Comp2(+) - Comp1(-) == 0  -182.38      75.81  -2.406   0.1182
Comp3(-) - Comp1(-) == 0    94.87     196.31   0.483   0.9954
Comp3(+) - Comp1(-) == 0  -236.63      81.35  -2.909   0.0311 *
Comp2(-) - Comp1(+) == 0   226.16     182.71   1.238   0.7730
Comp2(+) - Comp1(+) == 0    -3.34      24.35  -0.137   1.0000
Comp3(-) - Comp1(+) == 0   273.91     182.71   1.499   0.6019
Comp3(+) - Comp1(+) == 0   -57.59      38.27  -1.505   0.5977
Comp2(+) - Comp2(-) == 0  -229.50     183.45  -1.251   0.7651
Comp3(-) - Comp2(-) == 0    47.75     257.77   0.185   1.0000
Comp3(+) - Comp2(-) == 0  -283.75     185.81  -1.527   0.5825
Comp3(-) - Comp2(+) == 0   277.25     183.45   1.511   0.5931
Comp3(+) - Comp2(+) == 0   -54.25      41.65  -1.303   0.7329
Comp3(+) - Comp3(-) == 0  -331.50     185.81  -1.784   0.4085
```

Winter ETo

```
                    Estimate Std. Error t value Pr(>|t|)
Comp1(+) - Comp1(-) == 0   284.75      73.69   3.864  0.00106 **
Comp2(-) - Comp1(-) == 0    -0.54     195.48  -0.003  1.00000
Comp2(+) - Comp1(-) == 0   323.15      75.49   4.281  < 0.001 ***
Comp3(-) - Comp1(-) == 0   190.96     195.48   0.977  0.90219
Comp3(+) - Comp1(-) == 0   336.70      81.01   4.156  < 0.001 ***
Comp2(-) - Comp1(+) == 0  -285.29     181.94  -1.568  0.55377
Comp2(+) - Comp1(+) == 0    38.40      24.25   1.584  0.54336
Comp3(-) - Comp1(+) == 0   -93.79     181.94  -0.516  0.99382
Comp3(+) - Comp1(+) == 0    51.94      38.10   1.363  0.69430
Comp2(+) - Comp2(-) == 0   323.69     182.68   1.772  0.41675
Comp3(-) - Comp2(-) == 0   191.50     256.68   0.746  0.96748
Comp3(+) - Comp2(-) == 0   337.24     185.03   1.823  0.38402
Comp3(-) - Comp2(+) == 0  -132.19     182.68  -0.724  0.97146
Comp3(+) - Comp2(+) == 0    13.54      41.47   0.327  0.99930
Comp3(+) - Comp3(-) == 0   145.74     185.03   0.788  0.95900
```

Spring ETo

```
                    Estimate Std. Error t value Pr(>|t|)
Comp1(+) - Comp1(-) == 0   266.93      63.63   4.195  < 0.001 ***
Comp2(-) - Comp1(-) == 0   645.80     168.77   3.826  0.00124 **
Comp2(+) - Comp1(-) == 0  -158.53      65.17  -2.432  0.11121
Comp3(-) - Comp1(-) == 0    17.05     168.77   0.101  1.00000
Comp3(+) - Comp1(-) == 0   -34.11      69.94  -0.488  0.99523
Comp2(-) - Comp1(+) == 0   378.87     157.08   2.412  0.11654
Comp2(+) - Comp1(+) == 0  -425.46      20.93 -20.324  < 0.001 ***
```

Comp3(-) - Comp1(+) == 0	-249.88	157.08	-1.591	0.53817
Comp3(+) - Comp1(+) == 0	-301.04	32.90	-9.151	< 0.001 ***
Comp2(+) - Comp2(-) == 0	-804.33	157.71	-5.100	< 0.001 ***
Comp3(-) - Comp2(-) == 0	-628.75	221.61	-2.837	0.03818 *
Comp3(+) - Comp2(-) == 0	-679.91	159.74	-4.256	< 0.001 ***
Comp3(-) - Comp2(+) == 0	175.58	157.71	1.113	0.84149
Comp3(+) - Comp2(+) == 0	124.42	35.80	3.475	0.00452 **
Comp3(+) - Comp3(-) == 0	-51.16	159.74	-0.320	0.99936

Summer ETo

	Estimate	Std. Error	t value	Pr(>|t|)
Comp1(+) - Comp1(-) == 0	453.84	64.98	6.984	<0.01 ***
Comp2(-) - Comp1(-) == 0	335.38	172.37	1.946	0.310
Comp2(+) - Comp1(-) == 0	58.84	66.56	0.884	0.934
Comp3(-) - Comp1(-) == 0	379.88	172.37	2.204	0.187
Comp3(+) - Comp1(-) == 0	197.83	71.43	2.769	0.046 *
Comp2(-) - Comp1(+) == 0	-118.46	160.43	-0.738	0.969
Comp2(+) - Comp1(+) == 0	-395.00	21.38	-18.474	<0.01 ***
Comp3(-) - Comp1(+) == 0	-73.96	160.43	-0.461	0.996
Comp3(+) - Comp1(+) == 0	-256.01	33.60	-7.619	<0.01 ***
Comp2(+) - Comp2(-) == 0	-276.54	161.08	-1.717	0.452
Comp3(-) - Comp2(-) == 0	44.50	226.34	0.197	1.000
Comp3(+) - Comp2(-) == 0	-137.55	163.15	-0.843	0.946
Comp3(-) - Comp2(+) == 0	321.04	161.08	1.993	0.285
Comp3(+) - Comp2(+) == 0	138.99	36.57	3.801	<0.01 **
Comp3(+) - Comp3(-) == 0	-182.05	163.15	-1.116	0.840

Autumn ETo

	Estimate	Std. Error	t value	Pr(>|t|)
Comp1(+) - Comp1(-) == 0	261.38	63.90	4.091	<0.001 ***
Comp2(-) - Comp1(-) == 0	669.13	169.49	3.948	<0.001 ***
Comp2(+) - Comp1(-) == 0	-156.80	65.45	-2.396	0.1210
Comp3(-) - Comp1(-) == 0	24.13	169.49	0.142	1.0000
Comp3(+) - Comp1(-) == 0	-44.41	70.24	-0.632	0.9843
Comp2(-) - Comp1(+) == 0	407.75	157.75	2.585	0.0755 .
Comp2(+) - Comp1(+) == 0	-418.18	21.02	-19.891	<0.001 ***
Comp3(-) - Comp1(+) == 0	-237.25	157.75	-1.504	0.5983
Comp3(+) - Comp1(+) == 0	-305.79	33.04	-9.255	<0.001 ***
Comp2(+) - Comp2(-) == 0	-825.93	158.39	-5.215	<0.001 ***
Comp3(-) - Comp2(-) == 0	-645.00	222.56	-2.898	0.0318 *
Comp3(+) - Comp2(-) == 0	-713.54	160.43	-4.448	<0.001 ***
Comp3(-) - Comp2(+) == 0	180.93	158.39	1.142	0.8264
Comp3(+) - Comp2(+) == 0	112.39	35.96	3.126	0.0154 *
Comp3(+) - Comp3(-) == 0	-68.54	160.43	-0.427	0.9974

Annual climate balance

	Estimate	Std. Error	t value	Pr(>|t|)
Comp1(+) - Comp1(-) == 0	-98.66	72.51	-1.361	0.69591
Comp2(-) - Comp1(-) == 0	211.20	192.35	1.098	0.84918
Comp2(+) - Comp1(-) == 0	-240.58	74.28	-3.239	0.01091 *
Comp3(-) - Comp1(-) == 0	-202.55	192.35	-1.053	0.87035
Comp3(+) - Comp1(-) == 0	41.45	79.71	0.520	0.99357
Comp2(-) - Comp1(+) == 0	309.86	179.03	1.731	0.44276
Comp2(+) - Comp1(+) == 0	-141.92	23.86	-5.948	< 0.001 ***
Comp3(-) - Comp1(+) == 0	-103.89	179.03	-0.580	0.98933
Comp3(+) - Comp1(+) == 0	140.10	37.49	3.737	0.00187 **
Comp2(+) - Comp2(-) == 0	-451.78	179.75	-2.513	0.09047 .

Comp3(-) - Comp2(-) == 0 -413.75 252.57 -1.638 0.50559
Comp3(+) - Comp2(-) == 0 -169.75 182.06 -0.932 0.91850
Comp3(-) - Comp2(+) == 0 38.03 179.75 0.212 0.99992
Comp3(+) - Comp2(+) == 0 282.03 40.80 6.912 < 0.001 ***
Comp3(+) - Comp3(-) == 0 244.00 182.06 1.340 0.70878

Winter climate balance

	Estimate	Std. Error	t value	Pr(>|t|)	
Comp1(+) - Comp1(-) == 0	-36.08	73.38	-0.492	0.99504	
Comp2(-) - Comp1(-) == 0	-30.85	194.66	-0.158	0.99998	
Comp2(+) - Comp1(-) == 0	48.67	75.17	0.647	0.98251	
Comp3(-) - Comp1(-) == 0	-152.35	194.66	-0.783	0.96007	
Comp3(+) - Comp1(-) == 0	-185.02	80.67	-2.294	0.15337	
Comp2(-) - Comp1(+) == 0	5.23	181.17	0.029	1.00000	
Comp2(+) - Comp1(+) == 0	84.75	24.14	3.510	0.00453	**
Comp3(-) - Comp1(+) == 0	-116.27	181.17	-0.642	0.98321	
Comp3(+) - Comp1(+) == 0	-148.94	37.94	-3.925	< 0.001	***
Comp2(+) - Comp2(-) == 0	79.52	181.90	0.437	0.99715	
Comp3(-) - Comp2(-) == 0	-121.50	255.60	-0.475	0.99577	
Comp3(+) - Comp2(-) == 0	-154.17	184.24	-0.837	0.94724	
Comp3(-) - Comp2(+) == 0	-201.02	181.90	-1.105	0.84564	
Comp3(+) - Comp2(+) == 0	-233.69	41.29	-5.659	< 0.001	***
Comp3(+) - Comp3(-) == 0	-32.67	184.24	-0.177	0.99997	

Spring climate balance

	Estimate	Std. Error	t value	Pr(>|t|)	
Comp1(+) - Comp1(-) == 0	171.460	72.457	2.366	0.130	
Comp2(-) - Comp1(-) == 0	-52.650	192.200	-0.274	1.000	
Comp2(+) - Comp1(-) == 0	27.165	74.222	0.366	0.999	
Comp3(-) - Comp1(-) == 0	-55.650	192.200	-0.290	1.000	
Comp3(+) - Comp1(-) == 0	-57.459	79.650	-0.721	0.972	
Comp2(-) - Comp1(+) == 0	-224.110	178.887	-1.253	0.764	
Comp2(+) - Comp1(+) == 0	-144.295	23.840	-6.053	<0.001	***
Comp3(-) - Comp1(+) == 0	-227.110	178.887	-1.270	0.754	
Comp3(+) - Comp1(+) == 0	-228.919	37.465	-6.110	<0.001	***
Comp2(+) - Comp2(-) == 0	79.815	179.609	0.444	0.997	
Comp3(-) - Comp2(-) == 0	-3.000	252.371	-0.012	1.000	
Comp3(+) - Comp2(-) == 0	-4.809	181.919	-0.026	1.000	
Comp3(-) - Comp2(+) == 0	-82.815	179.609	-0.461	0.996	
Comp3(+) - Comp2(+) == 0	-84.624	40.773	-2.075	0.244	
Comp3(+) - Comp3(-) == 0	-1.809	181.919	-0.010	1.000	

Summer climate balance

	Estimate	Std. Error	t value	Pr(>|t|)	
Comp1(+) - Comp1(-) == 0	-177.393	70.809	-2.505	0.0924	.
Comp2(-) - Comp1(-) == 0	352.760	187.828	1.878	0.3500	
Comp2(+) - Comp1(-) == 0	-402.928	72.534	-5.555	<0.001	***
Comp3(-) - Comp1(-) == 0	-100.990	187.828	-0.538	0.9925	
Comp3(+) - Comp1(-) == 0	-101.642	77.838	-1.306	0.7310	
Comp2(-) - Comp1(+) == 0	530.153	174.817	3.033	0.0210	*
Comp2(+) - Comp1(+) == 0	-225.535	23.298	-9.680	<0.001	***
Comp3(-) - Comp1(+) == 0	76.403	174.817	0.437	0.9972	
Comp3(+) - Comp1(+) == 0	75.751	36.613	2.069	0.2468	
Comp2(+) - Comp2(-) == 0	-755.688	175.523	-4.305	<0.001	***
Comp3(-) - Comp2(-) == 0	-453.750	246.631	-1.840	0.3734	
Comp3(+) - Comp2(-) == 0	-454.402	177.781	-2.556	0.0811	.
Comp3(-) - Comp2(+) == 0	301.938	175.523	1.720	0.4498	

Comp3(+) - Comp2(+) == 0 301.286   39.845   7.561   <0.001 ***
Comp3(+) - Comp3(-) == 0   -0.652   177.781 -0.004   1.0000

Autumn climate balance

	Estimate	Std. Error	t value	Pr(>|t|)	
Comp1(+) - Comp1(-) == 0	70.811	73.859	0.959	0.9090	
Comp2(-) - Comp1(-) == 0	395.210	195.917	2.017	0.2729	
Comp2(+) - Comp1(-) == 0	8.022	75.657	0.106	1.0000	
Comp3(-) - Comp1(-) == 0	-420.540	195.917	-2.147	0.2107	
Comp3(+) - Comp1(-) == 0	56.548	81.191	0.696	0.9759	
Comp2(-) - Comp1(+) == 0	324.399	182.346	1.779	0.4113	
Comp2(+) - Comp1(+) == 0	-62.789	24.301	-2.584	0.0758	.
Comp3(-) - Comp1(+) == 0	-491.351	182.346	-2.695	0.0564	.
Comp3(+) - Comp1(+) == 0	-14.262	38.190	-0.373	0.9987	
Comp2(+) - Comp2(-) == 0	-387.188	183.082	-2.115	0.2249	
Comp3(-) - Comp2(-) == 0	-815.750	257.252	-3.171	0.0132	*
Comp3(+) - Comp2(-) == 0	-338.662	185.437	-1.826	0.3815	
Comp3(-) - Comp2(+) == 0	-428.562	183.082	-2.341	0.1382	
Comp3(+) - Comp2(+) == 0	48.527	41.561	1.168	0.8131	
Comp3(+) - Comp3(-) == 0	477.088	185.437	2.573	0.0785	.

Winter NDVI

	Estimate	Std. Error	t value	Pr(>|t|)	
Comp1(+) - Comp1(-) == 0	111.492	73.852	1.510	0.59447	
Comp2(-) - Comp1(-) == 0	180.900	195.899	0.923	0.92140	
Comp2(+) - Comp1(-) == 0	45.582	75.650	0.603	0.98735	
Comp3(-) - Comp1(-) == 0	-149.100	195.899	-0.761	0.96456	
Comp3(+) - Comp1(-) == 0	189.047	81.183	2.329	0.14165	
Comp2(-) - Comp1(+) == 0	69.408	182.329	0.381	0.99853	
Comp2(+) - Comp1(+) == 0	-65.911	24.299	-2.712	0.05370	.
Comp3(-) - Comp1(+) == 0	-260.592	182.329	-1.429	0.64930	
Comp3(+) - Comp1(+) == 0	77.555	38.186	2.031	0.26544	
Comp2(+) - Comp2(-) == 0	-135.318	183.065	-0.739	0.96872	
Comp3(-) - Comp2(-) == 0	-330.000	257.227	-1.283	0.74546	
Comp3(+) - Comp2(-) == 0	8.147	185.419	0.044	1.00000	
Comp3(-) - Comp2(+) == 0	-194.682	183.065	-1.063	0.86546	
Comp3(+) - Comp2(+) == 0	143.465	41.557	3.452	0.00563	**
Comp3(+) - Comp3(-) == 0	338.147	185.419	1.824	0.38343	

Spring NDVI

	Estimate	Std. Error	t value	Pr(>|t|)	
Comp1(+) - Comp1(-) == 0	68.465	73.697	0.929	0.9196	
Comp2(-) - Comp1(-) == 0	146.370	195.487	0.749	0.9670	
Comp2(+) - Comp1(-) == 0	-9.227	75.491	-0.122	1.0000	
Comp3(-) - Comp1(-) == 0	-187.380	195.487	-0.959	0.9090	
Comp3(+) - Comp1(-) == 0	167.395	81.012	2.066	0.2476	
Comp2(-) - Comp1(+) == 0	77.905	181.946	0.428	0.9974	
Comp2(+) - Comp1(+) == 0	-77.692	24.248	-3.204	0.0121	*
Comp3(-) - Comp1(+) == 0	-255.845	181.946	-1.406	0.6653	
Comp3(+) - Comp1(+) == 0	98.929	38.106	2.596	0.0729	.
Comp2(+) - Comp2(-) == 0	-155.597	182.680	-0.852	0.9433	
Comp3(-) - Comp2(-) == 0	-333.750	256.687	-1.300	0.7346	
Comp3(+) - Comp2(-) == 0	21.025	185.030	0.114	1.0000	
Comp3(-) - Comp2(+) == 0	-178.153	182.680	-0.975	0.9029	
Comp3(+) - Comp2(+) == 0	176.622	41.470	4.259	<0.001	***
Comp3(+) - Comp3(-) == 0	354.775	185.030	1.917	0.3270	

Summer NDVI

	Estimate	Std. Error	t value	Pr(>|t|)
Comp1(+) - Comp1(-) == 0	48.348	74.269	0.651	0.982
Comp2(-) - Comp1(-) == 0	-69.640	197.005	-0.353	0.999
Comp2(+) - Comp1(-) == 0	8.321	76.077	0.109	1.000
Comp3(-) - Comp1(-) == 0	-43.640	197.005	-0.222	1.000
Comp3(+) - Comp1(-) == 0	34.301	81.641	0.420	0.998
Comp2(-) - Comp1(+) == 0	-117.988	183.358	-0.643	0.983
Comp2(+) - Comp1(+) == 0	-40.027	24.436	-1.638	0.505
Comp3(-) - Comp1(+) == 0	-91.988	183.358	-0.502	0.995
Comp3(+) - Comp1(+) == 0	-14.047	38.402	-0.366	0.999
Comp2(+) - Comp2(-) == 0	77.961	184.098	0.423	0.998
Comp3(-) - Comp2(-) == 0	26.000	258.680	0.101	1.000
Comp3(+) - Comp2(-) == 0	103.941	186.466	0.557	0.991
Comp3(-) - Comp2(+) == 0	-51.961	184.098	-0.282	1.000
Comp3(+) - Comp2(+) == 0	25.980	41.792	0.622	0.985
Comp3(+) - Comp3(-) == 0	77.941	186.466	0.418	0.998

(Adjusted p values reported -- single-step method)

Autumn NDVI

	Estimate	Std. Error	t value	Pr(>|t|)
Comp1(+) - Comp1(-) == 0	123.783	74.126	1.670	0.484
Comp2(-) - Comp1(-) == 0	69.760	196.626	0.355	0.999
Comp2(+) - Comp1(-) == 0	71.344	75.931	0.940	0.916
Comp3(-) - Comp1(-) == 0	-107.240	196.626	-0.545	0.992
Comp3(+) - Comp1(-) == 0	118.564	81.484	1.455	0.632
Comp2(-) - Comp1(+) == 0	-54.023	183.006	-0.295	1.000
Comp2(+) - Comp1(+) == 0	-52.439	24.389	-2.150	0.210
Comp3(-) - Comp1(+) == 0	-231.023	183.006	-1.262	0.758
Comp3(+) - Comp1(+) == 0	-5.219	38.328	-0.136	1.000
Comp2(+) - Comp2(-) == 0	1.584	183.744	0.009	1.000
Comp3(-) - Comp2(-) == 0	-177.000	258.182	-0.686	0.977
Comp3(+) - Comp2(-) == 0	48.804	186.108	0.262	1.000
Comp3(-) - Comp2(+) == 0	-178.584	183.744	-0.972	0.904
Comp3(+) - Comp2(+) == 0	47.220	41.712	1.132	0.832
Comp3(+) - Comp3(-) == 0	225.804	186.108	1.213	0.787

Average day of the year recording the maximum NDVI

	Estimate	Std. Error	t value	Pr(>|t|)
Comp1(+) - Comp1(-) == 0	-0.04224	0.83213	-0.051	1.000
Comp2(-) - Comp1(-) == 0	-1.12000	2.20730	-0.507	0.994
Comp2(+) - Comp1(-) == 0	-0.56481	0.85239	-0.663	0.981
Comp3(-) - Comp1(-) == 0	-0.37000	2.20730	-0.168	1.000
Comp3(+) - Comp1(-) == 0	0.27216	0.91473	0.298	1.000
Comp2(-) - Comp1(+) == 0	-1.07776	2.05440	-0.525	0.993
Comp2(+) - Comp1(+) == 0	-0.52257	0.27379	-1.909	0.332
Comp3(-) - Comp1(+) == 0	-0.32776	2.05440	-0.160	1.000
Comp3(+) - Comp1(+) == 0	0.31439	0.43026	0.731	0.970
Comp2(+) - Comp2(-) == 0	0.55519	2.06269	0.269	1.000
Comp3(-) - Comp2(-) == 0	0.75000	2.89833	0.259	1.000
Comp3(+) - Comp2(-) == 0	1.39216	2.08923	0.666	0.980
Comp3(-) - Comp2(+) == 0	0.19481	2.06269	0.094	1.000
Comp3(+) - Comp2(+) == 0	0.83696	0.46825	1.787	0.407
Comp3(+) - Comp3(-) == 0	0.64216	2.08923	0.307	0.999

Average day of the year recording the green up

	Estimate	Std. Error	t value	Pr(>|t|)	
Comp1(+) - Comp1(-) == 0	2.19441	4.52129	0.485	0.9953	
Comp2(-) - Comp1(-) == 0	0.50000	11.99314	0.042	1.0000	
Comp2(+) - Comp1(-) == 0	0.40584	4.63138	0.088	1.0000	
Comp3(-) - Comp1(-) == 0	5.50000	11.99314	0.459	0.9964	
Comp3(+) - Comp1(-) == 0	7.55882	4.97011	1.521	0.5865	
Comp2(-) - Comp1(+) == 0	-1.69441	11.16238	-0.152	1.0000	
Comp2(+) - Comp1(+) == 0	-1.78857	1.48761	-1.202	0.7937	
Comp3(-) - Comp1(+) == 0	3.30559	11.16238	0.296	0.9996	
Comp3(+) - Comp1(+) == 0	5.36441	2.33779	2.295	0.1531	
Comp2(+) - Comp2(-) == 0	-0.09416	11.20743	-0.008	1.0000	
Comp3(-) - Comp2(-) == 0	5.00000	15.74777	0.318	0.9994	
Comp3(+) - Comp2(-) == 0	7.05882	11.35159	0.622	0.9854	
Comp3(-) - Comp2(+) == 0	5.09416	11.20743	0.455	0.9966	
Comp3(+) - Comp2(+) == 0	7.15298	2.54420	2.811	0.0407	*
Comp3(+) - Comp3(-) == 0	2.05882	11.35159	0.181	1.0000	

Soil water capacity

	Estimate	Std. Error	t value	Pr(>|t|)	
Comp1(+) - Comp1(-) == 0	340.68	72.71	4.685	<0.001	***
Comp2(-) - Comp1(-) == 0	42.52	192.87	0.220	0.9999	
Comp2(+) - Comp1(-) == 0	198.30	74.48	2.662	0.0615	.
Comp3(-) - Comp1(-) == 0	302.27	192.87	1.567	0.5546	
Comp3(+) - Comp1(-) == 0	226.14	79.93	2.829	0.0391	*
Comp2(-) - Comp1(+) == 0	-298.16	179.51	-1.661	0.4899	
Comp2(+) - Comp1(+) == 0	-142.38	23.92	-5.951	<0.001	***
Comp3(-) - Comp1(+) == 0	-38.41	179.51	-0.214	0.9999	
Comp3(+) - Comp1(+) == 0	-114.54	37.60	-3.047	0.0197	*
Comp2(+) - Comp2(-) == 0	155.78	180.24	0.864	0.9397	
Comp3(-) - Comp2(-) == 0	259.75	253.25	1.026	0.8823	
Comp3(+) - Comp2(-) == 0	183.62	182.55	1.006	0.8907	
Comp3(-) - Comp2(+) == 0	103.97	180.24	0.577	0.9896	
Comp3(+) - Comp2(+) == 0	27.84	40.92	0.680	0.9782	
Comp3(+) - Comp3(-) == 0	-76.13	182.55	-0.417	0.9977	

4. CORN

Annual precipitation

	Estimate	Std. Error	t value	Pr(>|t|)	
Comp1(+) - Comp1(-) == 0	-43.698	84.758	-0.516	0.999	
Comp2(-) - Comp1(-) == 0	38.708	99.310	0.390	1.000	
Comp2(+) - Comp1(-) == 0	189.519	88.484	2.142	0.339	
Comp3(-) - Comp1(-) == 0	87.137	130.634	0.667	0.997	
Comp3(+) - Comp1(-) == 0	197.711	90.087	2.195	0.308	
Comp4(-) - Comp1(-) == 0	65.049	141.232	0.461	1.000	
Comp4(+) - Comp1(-) == 0	-95.132	91.833	-1.036	0.960	
Comp2(-) - Comp1(+) == 0	82.406	55.531	1.484	0.780	
Comp2(+) - Comp1(+) == 0	233.218	32.416	7.195	<0.001	***
Comp3(-) - Comp1(+) == 0	130.835	101.423	1.290	0.879	
Comp3(+) - Comp1(+) == 0	241.409	36.565	6.602	<0.001	***
Comp4(-) - Comp1(+) == 0	108.748	114.751	0.948	0.975	
Comp4(+) - Comp1(+) == 0	-51.433	40.678	-1.264	0.890	
Comp2(+) - Comp2(-) == 0	150.811	61.068	2.470	0.176	
Comp3(-) - Comp2(-) == 0	48.429	113.865	0.425	1.000	
Comp3(+) - Comp2(-) == 0	159.003	63.369	2.509	0.160	
Comp4(-) - Comp2(-) == 0	26.341	125.882	0.209	1.000	
Comp4(+) - Comp2(-) == 0	-133.840	65.827	-2.033	0.408	
Comp3(-) - Comp2(+) == 0	-102.383	104.557	-0.979	0.970	
Comp3(+) - Comp2(+) == 0	8.192	44.527	0.184	1.000	
Comp4(-) - Comp2(+) == 0	-124.470	117.530	-1.059	0.955	
Comp4(+) - Comp2(+) == 0	-284.651	47.961	-5.935	<0.001	***
Comp3(+) - Comp3(-) == 0	110.574	105.917	1.044	0.958	
Comp4(-) - Comp3(-) == 0	-22.087	151.820	-0.145	1.000	
Comp4(+) - Comp3(-) == 0	-182.268	107.406	-1.697	0.641	
Comp4(-) - Comp3(+) == 0	-132.662	118.742	-1.117	0.940	
Comp4(+) - Comp3(+) == 0	-292.843	50.858	-5.758	<0.001	***
Comp4(+) - Comp4(-) == 0	-160.181	120.072	-1.334	0.860	

Winter precipitation

	Estimate	Std. Error	t value	Pr(>|t|)	
Comp1(+) - Comp1(-) == 0	-139.163	79.260	-1.756	0.60015	
Comp2(-) - Comp1(-) == 0	-124.143	92.868	-1.337	0.85856	
Comp2(+) - Comp1(-) == 0	241.846	82.745	2.923	0.05464	.
Comp3(-) - Comp1(-) == 0	303.778	122.161	2.487	0.16837	
Comp3(+) - Comp1(-) == 0	325.256	84.244	3.861	0.00243	**
Comp4(-) - Comp1(-) == 0	332.786	132.071	2.520	0.15685	
Comp4(+) - Comp1(-) == 0	33.488	85.877	0.390	0.99991	
Comp2(-) - Comp1(+) == 0	15.020	51.930	0.289	0.99999	
Comp2(+) - Comp1(+) == 0	381.009	30.313	12.569	< 0.001	***
Comp3(-) - Comp1(+) == 0	442.941	94.845	4.670	< 0.001	***
Comp3(+) - Comp1(+) == 0	464.419	34.194	13.582	< 0.001	***
Comp4(-) - Comp1(+) == 0	471.949	107.308	4.398	< 0.001	***
Comp4(+) - Comp1(+) == 0	172.651	38.039	4.539	< 0.001	***
Comp2(+) - Comp2(-) == 0	365.989	57.107	6.409	< 0.001	***
Comp3(-) - Comp2(-) == 0	427.921	106.479	4.019	0.00123	**
Comp3(+) - Comp2(-) == 0	449.399	59.259	7.584	< 0.001	***
Comp4(-) - Comp2(-) == 0	456.929	117.717	3.882	0.00218	**
Comp4(+) - Comp2(-) == 0	157.631	61.558	2.561	0.14167	
Comp3(-) - Comp2(+) == 0	61.932	97.776	0.633	0.99783	
Comp3(+) - Comp2(+) == 0	83.410	41.639	2.003	0.42746	
Comp4(-) - Comp2(+) == 0	90.940	109.907	0.827	0.98873	
Comp4(+) - Comp2(+) == 0	-208.358	44.851	-4.646	< 0.001	***
Comp3(+) - Comp3(-) == 0	21.478	99.047	0.217	1.00000	

Comp4(-) - Comp3(-) == 0 29.008 141.972 0.204 1.00000
Comp4(+) - Comp3(-) == 0 -270.290 100.440 -2.691 0.10268
Comp4(-) - Comp3(+) == 0 7.529 111.040 0.068 1.00000
Comp4(+) - Comp3(+) == 0 -291.768 47.559 -6.135 < 0.001 ***
Comp4(+) - Comp4(-) == 0 -299.298 112.284 -2.666 0.10980

Spring precipitation

	Estimate	Std. Error	t value	Pr(>|t|)
Comp1(+) - Comp1(-) == 0	652.45	74.26	8.786	< 0.001 ***
Comp2(-) - Comp1(-) == 0	280.46	87.01	3.223	0.02197 *
Comp2(+) - Comp1(-) == 0	185.69	77.52	2.395	0.20650
Comp3(-) - Comp1(-) == 0	461.20	114.45	4.030	0.00116 **
Comp3(+) - Comp1(-) == 0	88.08	78.93	1.116	0.94060
Comp4(-) - Comp1(-) == 0	595.59	123.74	4.813	< 0.001 ***
Comp4(+) - Comp1(-) == 0	358.44	80.46	4.455	< 0.001 ***
Comp2(-) - Comp1(+) == 0	-371.99	48.65	-7.646	< 0.001 ***
Comp2(+) - Comp1(+) == 0	-466.76	28.40	-16.435	< 0.001 ***
Comp3(-) - Comp1(+) == 0	-191.25	88.86	-2.152	0.33291
Comp3(+) - Comp1(+) == 0	-564.37	32.04	-17.616	< 0.001 ***
Comp4(-) - Comp1(+) == 0	-56.85	100.54	-0.565	0.99895
Comp4(+) - Comp1(+) == 0	-294.01	35.64	-8.249	< 0.001 ***
Comp2(+) - Comp2(-) == 0	-94.77	53.50	-1.771	0.58872
Comp3(-) - Comp2(-) == 0	180.74	99.76	1.812	0.56056
Comp3(+) - Comp2(-) == 0	-192.38	55.52	-3.465	0.00985 **
Comp4(-) - Comp2(-) == 0	315.13	110.29	2.857	0.06645 .
Comp4(+) - Comp2(-) == 0	77.98	57.67	1.352	0.85113
Comp3(-) - Comp2(+) == 0	275.51	91.61	3.008	0.04308 *
Comp3(+) - Comp2(+) == 0	-97.61	39.01	-2.502	0.16227
Comp4(-) - Comp2(+) == 0	409.91	102.97	3.981	0.00174 **
Comp4(+) - Comp2(+) == 0	172.75	42.02	4.111	< 0.001 ***
Comp3(+) - Comp3(-) == 0	-373.12	92.80	-4.021	0.00128 **
Comp4(-) - Comp3(-) == 0	134.40	133.02	1.010	0.96487
Comp4(+) - Comp3(-) == 0	-102.76	94.10	-1.092	0.94695
Comp4(-) - Comp3(+) == 0	507.52	104.04	4.878	< 0.001 ***
Comp4(+) - Comp3(+) == 0	270.36	44.56	6.068	< 0.001 ***
Comp4(+) - Comp4(-) == 0	-237.15	105.20	-2.254	0.27539

Summer precipitation

	Estimate	Std. Error	t value	Pr(>|t|)
Comp1(+) - Comp1(-) == 0	252.75	83.05	3.043	0.03879 *
Comp2(-) - Comp1(-) == 0	-148.37	97.31	-1.525	0.75514
Comp2(+) - Comp1(-) == 0	183.52	86.70	2.117	0.35461
Comp3(-) - Comp1(-) == 0	554.72	128.01	4.334	< 0.001 ***
Comp3(+) - Comp1(-) == 0	-88.97	88.28	-1.008	0.96533
Comp4(-) - Comp1(-) == 0	160.00	138.39	1.156	0.92889
Comp4(+) - Comp1(-) == 0	87.36	89.99	0.971	0.97181
Comp2(-) - Comp1(+) == 0	-401.12	54.41	-7.372	< 0.001 ***
Comp2(+) - Comp1(+) == 0	-69.23	31.76	-2.180	0.31660
Comp3(-) - Comp1(+) == 0	301.97	99.38	3.038	0.03919 *
Comp3(+) - Comp1(+) == 0	-341.72	35.83	-9.537	< 0.001 ***
Comp4(-) - Comp1(+) == 0	-92.75	112.44	-0.825	0.98896
Comp4(+) - Comp1(+) == 0	-165.39	39.86	-4.149	< 0.001 ***
Comp2(+) - Comp2(-) == 0	331.89	59.84	5.546	< 0.001 ***
Comp3(-) - Comp2(-) == 0	703.10	111.57	6.302	< 0.001 ***
Comp3(+) - Comp2(-) == 0	59.40	62.09	0.957	0.97400
Comp4(-) - Comp2(-) == 0	308.37	123.35	2.500	0.16341
Comp4(+) - Comp2(-) == 0	235.74	64.50	3.655	0.00509 **
Comp3(-) - Comp2(+) == 0	371.20	102.45	3.623	0.00604 **

Comp3(+) - Comp2(+) == 0 -272.49 43.63 -6.245 < 0.001 ***
Comp4(-) - Comp2(+) == 0 -23.52 115.17 -0.204 1.00000
Comp4(+) - Comp2(+) == 0 -96.15 47.00 -2.046 0.39961
Comp3(+) - Comp3(-) == 0 -643.69 103.79 -6.202 < 0.001 ***
Comp4(-) - Comp3(-) == 0 -394.72 148.77 -2.653 0.11289
Comp4(+) - Comp3(-) == 0 -467.36 105.25 -4.441 < 0.001 ***
Comp4(-) - Comp3(+) == 0 248.97 116.35 2.140 0.34074
Comp4(+) - Comp3(+) == 0 176.33 49.84 3.538 0.00786 **
Comp4(+) - Comp4(-) == 0 -72.64 117.66 -0.617 0.99815

Autumn precipitation

	Estimate	Std. Error	t value	Pr(>|t|)	
Comp1(+) - Comp1(-) == 0	-102.853	79.844	-1.288	0.8803	
Comp2(-) - Comp1(-) == 0	-27.891	93.553	-0.298	1.0000	
Comp2(+) - Comp1(-) == 0	-430.760	83.355	-5.168	<0.001	***
Comp3(-) - Comp1(-) == 0	-218.923	123.062	-1.779	0.5838	
Comp3(+) - Comp1(-) == 0	-564.336	84.865	-6.650	<0.001	***
Comp4(-) - Comp1(-) == 0	-294.352	133.045	-2.212	0.2978	
Comp4(+) - Comp1(-) == 0	-33.843	86.510	-0.391	0.9999	
Comp2(-) - Comp1(+) == 0	74.961	52.312	1.433	0.8090	
Comp2(+) - Comp1(+) == 0	-327.907	30.537	-10.738	<0.001	***
Comp3(-) - Comp1(+) == 0	-116.070	95.544	-1.215	0.9093	
Comp3(+) - Comp1(+) == 0	-461.483	34.446	-13.397	<0.001	***
Comp4(-) - Comp1(+) == 0	-191.499	108.099	-1.772	0.5890	
Comp4(+) - Comp1(+) == 0	69.010	38.320	1.801	0.5691	
Comp2(+) - Comp2(-) == 0	-402.868	57.528	-7.003	<0.001	***
Comp3(-) - Comp2(-) == 0	-191.032	107.264	-1.781	0.5822	
Comp3(+) - Comp2(-) == 0	-536.444	59.695	-8.986	<0.001	***
Comp4(-) - Comp2(-) == 0	-266.460	118.585	-2.247	0.2792	
Comp4(+) - Comp2(-) == 0	-5.952	62.012	-0.096	1.0000	
Comp3(-) - Comp2(+) == 0	211.836	98.496	2.151	0.3339	
Comp3(+) - Comp2(+) == 0	-133.576	41.946	-3.184	0.0251	*
Comp4(-) - Comp2(+) == 0	136.408	110.717	1.232	0.9027	
Comp4(+) - Comp2(+) == 0	396.916	45.181	8.785	<0.001	***
Comp3(+) - Comp3(-) == 0	-345.413	99.778	-3.462	0.0102	*
Comp4(-) - Comp3(-) == 0	-75.429	143.019	-0.527	0.9993	
Comp4(+) - Comp3(-) == 0	185.080	101.180	1.829	0.5486	
Comp4(-) - Comp3(+) == 0	269.984	111.859	2.414	0.1983	
Comp4(+) - Comp3(+) == 0	530.493	47.910	11.073	<0.001	***
Comp4(+) - Comp4(-) == 0	260.509	113.112	2.303	0.2497	

Annual mean temperature

	Estimate	Std. Error	t value	Pr(>|t|)	
Comp1(+) - Comp1(-) == 0	-331.0045	82.7174	-4.002	0.00127	**
Comp2(-) - Comp1(-) == 0	-222.0000	96.9192	-2.291	0.25618	
Comp2(+) - Comp1(-) == 0	62.0701	86.3543	0.719	0.99520	
Comp3(-) - Comp1(-) == 0	-58.1111	127.4897	-0.456	0.99975	
Comp3(+) - Comp1(-) == 0	-222.5813	87.9188	-2.532	0.15192	
Comp4(-) - Comp1(-) == 0	-175.7143	137.8323	-1.275	0.88590	
Comp4(+) - Comp1(-) == 0	-177.0560	89.6228	-1.976	0.44696	
Comp2(-) - Comp1(+) == 0	109.0045	54.1947	2.011	0.42141	
Comp2(+) - Comp1(+) == 0	393.0746	31.6353	12.425	< 0.001	***
Comp3(-) - Comp1(+) == 0	272.8934	98.9816	2.757	0.08668	.
Comp3(+) - Comp1(+) == 0	108.4232	35.6853	3.038	0.03897	*
Comp4(-) - Comp1(+) == 0	155.2902	111.9888	1.387	0.83349	
Comp4(+) - Comp1(+) == 0	153.9485	39.6986	3.878	0.00220	**
Comp2(+) - Comp2(-) == 0	284.0701	59.5984	4.766	< 0.001	***
Comp3(-) - Comp2(-) == 0	163.8889	111.1240	1.475	0.78519	

Comp3(+) - Comp2(-) == 0 -0.5813 61.8435 -0.009 1.00000
Comp4(-) - Comp2(-) == 0 46.2857 122.8522 0.377 0.99993
Comp4(+) - Comp2(-) == 0 44.9440 64.2430 0.700 0.99594
Comp3(-) - Comp2(+) == 0 -120.1812 102.0405 -1.178 0.92183
Comp3(+) - Comp2(+) == 0 -284.6513 43.4551 -6.550 < 0.001 ***
Comp4(-) - Comp2(+) == 0 -237.7844 114.7013 -2.073 0.38212
Comp4(+) - Comp2(+) == 0 -239.1261 46.8069 -5.109 < 0.001 ***
Comp3(+) - Comp3(-) == 0 -164.4701 103.3679 -1.591 0.71295
Comp4(-) - Comp3(-) == 0 -117.6032 148.1653 -0.794 0.99122
Comp4(+) - Comp3(-) == 0 -118.9449 104.8211 -1.135 0.93531
Comp4(-) - Comp3(+) == 0 46.8670 115.8837 0.404 0.99989
Comp4(+) - Comp3(+) == 0 45.5253 49.6340 0.917 0.97948
Comp4(+) - Comp4(-) == 0 -1.3417 117.1818 -0.011 1.00000

Winter mean temperature

Estimate Std. Error t value Pr(>|t|)
Comp1(+) - Comp1(-) == 0 171.406 83.807 2.045 0.39958
Comp2(-) - Comp1(-) == 0 372.778 98.196 3.796 0.00305 **
Comp2(+) - Comp1(-) == 0 6.846 87.492 0.078 1.00000
Comp3(-) - Comp1(-) == 0 336.278 129.169 2.603 0.12833
Comp3(+) - Comp1(-) == 0 -155.694 89.077 -1.748 0.60576
Comp4(-) - Comp1(-) == 0 215.857 139.648 1.546 0.74191
Comp4(+) - Comp1(-) == 0 87.104 90.804 0.959 0.97365
Comp2(-) - Comp1(+) == 0 201.372 54.909 3.667 0.00492 **
Comp2(+) - Comp1(+) == 0 -164.560 32.052 -5.134 < 0.001 ***
Comp3(-) - Comp1(+) == 0 164.872 100.286 1.644 0.67774
Comp3(+) - Comp1(+) == 0 -327.100 36.156 -9.047 < 0.001 ***
Comp4(-) - Comp1(+) == 0 44.451 113.464 0.392 0.99991
Comp4(+) - Comp1(+) == 0 -84.302 40.222 -2.096 0.36721
Comp2(+) - Comp2(-) == 0 -365.932 60.384 -6.060 < 0.001 ***
Comp3(-) - Comp2(-) == 0 -36.500 112.588 -0.324 0.99997
Comp3(+) - Comp2(-) == 0 -528.472 62.658 -8.434 < 0.001 ***
Comp4(-) - Comp2(-) == 0 -156.921 124.471 -1.261 0.89170
Comp4(+) - Comp2(-) == 0 -285.674 65.089 -4.389 < 0.001 ***
Comp3(-) - Comp2(+) == 0 329.432 103.385 3.186 0.02498 *
Comp3(+) - Comp2(+) == 0 -162.540 44.028 -3.692 0.00418 **
Comp4(-) - Comp2(+) == 0 209.011 116.213 1.799 0.57035
Comp4(+) - Comp2(+) == 0 80.258 47.424 1.692 0.64422
Comp3(+) - Comp3(-) == 0 -491.972 104.730 -4.698 < 0.001 ***
Comp4(-) - Comp3(-) == 0 -120.421 150.117 -0.802 0.99064
Comp4(+) - Comp3(-) == 0 -249.174 106.202 -2.346 0.22901
Comp4(-) - Comp3(+) == 0 371.551 117.411 3.165 0.02741 *
Comp4(+) - Comp3(+) == 0 242.798 50.288 4.828 < 0.001 ***
Comp4(+) - Comp4(-) == 0 -128.753 118.726 -1.084 0.94870

Spring mean temperature

Estimate Std. Error t value Pr(>|t|)
Comp1(+) - Comp1(-) == 0 -210.7281 83.7376 -2.517 0.15724
Comp2(-) - Comp1(-) == 0 -187.6947 98.1146 -1.913 0.48889
Comp2(+) - Comp1(-) == 0 140.1229 87.4194 1.603 0.70496
Comp3(-) - Comp1(-) == 0 -17.0043 129.0622 -0.132 1.00000
Comp3(+) - Comp1(-) == 0 -75.7466 89.0032 -0.851 0.98669
Comp4(-) - Comp1(-) == 0 -123.8297 139.5324 -0.887 0.98303
Comp4(+) - Comp1(-) == 0 -75.3034 90.7282 -0.830 0.98855
Comp2(-) - Comp1(+) == 0 23.0334 54.8632 0.420 0.99985
Comp2(+) - Comp1(+) == 0 350.8510 32.0255 10.955 < 0.001 ***
Comp3(-) - Comp1(+) == 0 193.7238 100.2025 1.933 0.47506
Comp3(+) - Comp1(+) == 0 134.9815 36.1255 3.736 0.00369 **

Comp4(-) - Comp1(+) == 0 86.8984 113.3701 0.767 0.99289
Comp4(+) - Comp1(+) == 0 135.4247 40.1883 3.370 0.01349 *
Comp2(+) - Comp2(-) == 0 327.8177 60.3335 5.433 < 0.001 ***
Comp3(-) - Comp2(-) == 0 170.6905 112.4946 1.517 0.75957
Comp3(+) - Comp2(-) == 0 111.9481 62.6063 1.788 0.57735
Comp4(-) - Comp2(-) == 0 63.8651 124.3675 0.514 0.99944
Comp4(+) - Comp2(-) == 0 112.3914 65.0353 1.728 0.61947
Comp3(-) - Comp2(+) == 0 -157.1272 103.2991 -1.521 0.75736
Comp3(+) - Comp2(+) == 0 -215.8696 43.9911 -4.907 < 0.001 ***
Comp4(-) - Comp2(+) == 0 -263.9526 116.1161 -2.273 0.26537
Comp4(+) - Comp2(+) == 0 -215.4263 47.3842 -4.546 < 0.001 ***
Comp3(+) - Comp3(-) == 0 -58.7424 104.6428 -0.561 0.99900
Comp4(-) - Comp3(-) == 0 -106.8254 149.9928 -0.712 0.99547
Comp4(+) - Comp3(-) == 0 -58.2991 106.1140 -0.549 0.99913
Comp4(-) - Comp3(+) == 0 -48.0830 117.3131 -0.410 0.99988
Comp4(+) - Comp3(+) == 0 0.4433 50.2462 0.009 1.00000
Comp4(+) - Comp4(-) == 0 48.5263 118.6272 0.409 0.99988

Summer mean temperature

Estimate Std. Error t value Pr(>|t|)
Comp1(+) - Comp1(-) == 0 293.589 78.041 3.762 0.00354 **
Comp2(-) - Comp1(-) == 0 642.628 91.440 7.028 < 0.001 ***
Comp2(+) - Comp1(-) == 0 -180.092 81.473 -2.210 0.29889
Comp3(-) - Comp1(-) == 0 94.786 120.283 0.788 0.99159
Comp3(+) - Comp1(-) == 0 199.906 82.949 2.410 0.19951
Comp4(-) - Comp1(-) == 0 433.016 130.040 3.330 0.01605 *
Comp4(+) - Comp1(-) == 0 -3.577 84.556 -0.042 1.00000
Comp2(-) - Comp1(+) == 0 349.039 51.131 6.826 < 0.001 ***
Comp2(+) - Comp1(+) == 0 -473.681 29.847 -15.870 < 0.001 ***
Comp3(-) - Comp1(+) == 0 -198.803 93.386 -2.129 0.34688
Comp3(+) - Comp1(+) == 0 -93.683 33.668 -2.783 0.08062 .
Comp4(-) - Comp1(+) == 0 139.427 105.658 1.320 0.86626
Comp4(+) - Comp1(+) == 0 -297.166 37.454 -7.934 < 0.001 ***
Comp2(+) - Comp2(-) == 0 -822.719 56.229 -14.632 < 0.001 ***
Comp3(-) - Comp2(-) == 0 -547.841 104.842 -5.225 < 0.001 ***
Comp3(+) - Comp2(-) == 0 -442.722 58.347 -7.588 < 0.001 ***
Comp4(-) - Comp2(-) == 0 -209.611 115.907 -1.808 0.56297
Comp4(+) - Comp2(-) == 0 -646.205 60.611 -10.661 < 0.001 ***
Comp3(-) - Comp2(+) == 0 274.878 96.272 2.855 0.06651 .
Comp3(+) - Comp2(+) == 0 379.997 40.999 9.269 < 0.001 ***
Comp4(-) - Comp2(+) == 0 613.108 108.217 5.666 < 0.001 ***
Comp4(+) - Comp2(+) == 0 176.514 44.161 3.997 0.00129 **
Comp3(+) - Comp3(-) == 0 105.119 97.524 1.078 0.95035
Comp4(-) - Comp3(-) == 0 338.230 139.789 2.420 0.19575
Comp4(+) - Comp3(-) == 0 -98.364 98.895 -0.995 0.96772
Comp4(-) - Comp3(+) == 0 233.111 109.333 2.132 0.34519
Comp4(+) - Comp3(+) == 0 -203.483 46.828 -4.345 < 0.001 ***
Comp4(+) - Comp4(-) == 0 -436.594 110.557 -3.949 0.00168 **

Autumn mean temperature

Estimate Std. Error t value Pr(>|t|)
Comp1(+) - Comp1(-) == 0 -287.61 82.69 -3.478 0.00944 **
Comp2(-) - Comp1(-) == 0 -22.43 96.89 -0.232 1.00000
Comp2(+) - Comp1(-) == 0 -10.55 86.33 -0.122 1.00000
Comp3(-) - Comp1(-) == 0 149.69 127.45 1.174 0.92306
Comp3(+) - Comp1(-) == 0 -468.93 87.89 -5.335 < 0.001 ***
Comp4(-) - Comp1(-) == 0 -105.02 137.79 -0.762 0.99312
Comp4(+) - Comp1(-) == 0 -166.36 89.60 -1.857 0.52904

Comp2(-) - Comp1(+) == 0 265.18 54.18 4.894 < 0.001 ***
Comp2(+) - Comp1(+) == 0 277.07 31.63 8.761 < 0.001 ***
Comp3(-) - Comp1(+) == 0 437.30 98.95 4.419 < 0.001 ***
Comp3(+) - Comp1(+) == 0 -181.32 35.68 -5.082 < 0.001 ***
Comp4(-) - Comp1(+) == 0 182.59 111.96 1.631 0.68670
Comp4(+) - Comp1(+) == 0 121.26 39.69 3.055 0.03729 *
Comp2(+) - Comp2(-) == 0 11.89 59.58 0.200 1.00000
Comp3(-) - Comp2(-) == 0 172.13 111.09 1.549 0.73970
Comp3(+) - Comp2(-) == 0 -446.49 61.83 -7.222 < 0.001 ***
Comp4(-) - Comp2(-) == 0 -82.59 122.82 -0.672 0.99683
Comp4(+) - Comp2(-) == 0 -143.92 64.23 -2.241 0.28270
Comp3(-) - Comp2(+) == 0 160.24 102.01 1.571 0.72616
Comp3(+) - Comp2(+) == 0 -458.38 43.44 -10.551 < 0.001 ***
Comp4(-) - Comp2(+) == 0 -94.48 114.67 -0.824 0.98900
Comp4(+) - Comp2(+) == 0 -155.81 46.79 -3.330 0.01603 *
Comp3(+) - Comp3(-) == 0 -618.62 103.34 -5.986 < 0.001 ***
Comp4(-) - Comp3(-) == 0 -254.71 148.12 -1.720 0.62565
Comp4(+) - Comp3(-) == 0 -316.05 104.79 -3.016 0.04242 *
Comp4(-) - Comp3(+) == 0 363.90 115.85 3.141 0.02889 *
Comp4(+) - Comp3(+) == 0 302.57 49.62 6.098 < 0.001 ***
Comp4(+) - Comp4(-) == 0 -61.33 117.15 -0.524 0.99936

Annual ETo

Estimate Std. Error t value Pr(>|t|)
Comp1(+) - Comp1(-) == 0 -140.25 80.99 -1.732 0.61739
Comp2(-) - Comp1(-) == 0 90.65 94.89 0.955 0.97424
Comp2(+) - Comp1(-) == 0 237.16 84.55 2.805 0.07672 .
Comp3(-) - Comp1(-) == 0 212.82 124.82 1.705 0.63582
Comp3(+) - Comp1(-) == 0 -323.03 86.08 -3.753 0.00339 **
Comp4(-) - Comp1(-) == 0 -85.63 134.95 -0.635 0.99780
Comp4(+) - Comp1(-) == 0 68.59 87.75 0.782 0.99198
Comp2(-) - Comp1(+) == 0 230.89 53.06 4.352 < 0.001 ***
Comp2(+) - Comp1(+) == 0 377.41 30.97 12.185 < 0.001 ***
Comp3(-) - Comp1(+) == 0 353.07 96.91 3.643 0.00519 **
Comp3(+) - Comp1(+) == 0 -182.79 34.94 -5.232 < 0.001 ***
Comp4(-) - Comp1(+) == 0 54.61 109.64 0.498 0.99954
Comp4(+) - Comp1(+) == 0 208.84 38.87 5.373 < 0.001 ***
Comp2(+) - Comp2(-) == 0 146.52 58.35 2.511 0.15982
Comp3(-) - Comp2(-) == 0 122.17 108.80 1.123 0.93857
Comp3(+) - Comp2(-) == 0 -413.68 60.55 -6.832 < 0.001 ***
Comp4(-) - Comp2(-) == 0 -176.28 120.28 -1.466 0.79034
Comp4(+) - Comp2(-) == 0 -22.05 62.90 -0.351 0.99996
Comp3(-) - Comp2(+) == 0 -24.34 99.90 -0.244 1.00000
Comp3(+) - Comp2(+) == 0 -560.20 42.55 -13.167 < 0.001 ***
Comp4(-) - Comp2(+) == 0 -322.80 112.30 -2.874 0.06304 .
Comp4(+) - Comp2(+) == 0 -168.57 45.83 -3.678 0.00475 **
Comp3(+) - Comp3(-) == 0 -535.85 101.20 -5.295 < 0.001 ***
Comp4(-) - Comp3(-) == 0 -298.45 145.06 -2.057 0.39177
Comp4(+) - Comp3(-) == 0 -144.23 102.63 -1.405 0.82384
Comp4(-) - Comp3(+) == 0 237.40 113.46 2.092 0.36978
Comp4(+) - Comp3(+) == 0 391.63 48.59 8.059 < 0.001 ***
Comp4(+) - Comp4(-) == 0 154.23 114.73 1.344 0.85483

Winter ETo

Estimate Std. Error t value Pr(>|t|)
Comp1(+) - Comp1(-) == 0 65.233 84.518 0.772 0.99258
Comp2(-) - Comp1(-) == 0 -58.190 99.029 -0.588 0.99865
Comp2(+) - Comp1(-) == 0 -9.860 88.234 -0.112 1.00000

Comp3(-) - Comp1(-) == 0 -259.667 130.265 -1.993 0.43436
Comp3(+) - Comp1(-) == 0 336.406 89.833 3.745 0.00363 **
Comp4(-) - Comp1(-) == 0 -41.929 140.833 -0.298 0.99999
Comp4(+) - Comp1(-) == 0 -64.024 91.574 -0.699 0.99595
Comp2(-) - Comp1(+) == 0 -123.424 55.374 -2.229 0.28925
Comp2(+) - Comp1(+) == 0 -75.093 32.324 -2.323 0.24006
Comp3(-) - Comp1(+) == 0 -324.900 101.136 -3.212 0.02359 *
Comp3(+) - Comp1(+) == 0 271.173 36.462 7.437 < 0.001 ***
Comp4(-) - Comp1(+) == 0 -107.162 114.426 -0.937 0.97695
Comp4(+) - Comp1(+) == 0 -129.257 40.563 -3.187 0.02493 *
Comp2(+) - Comp2(-) == 0 48.331 60.896 0.794 0.99122
Comp3(-) - Comp2(-) == 0 -201.476 113.543 -1.774 0.58658
Comp3(+) - Comp2(-) == 0 394.597 63.190 6.245 < 0.001 ***
Comp4(-) - Comp2(-) == 0 16.262 125.526 0.130 1.00000
Comp4(+) - Comp2(-) == 0 -5.834 65.641 -0.089 1.00000
Comp3(-) - Comp2(+) == 0 -249.807 104.262 -2.396 0.20553
Comp3(+) - Comp2(+) == 0 346.266 44.401 7.799 < 0.001 ***
Comp4(-) - Comp2(+) == 0 -32.069 117.198 -0.274 0.99999
Comp4(+) - Comp2(+) == 0 -54.164 47.826 -1.133 0.93586
Comp3(+) - Comp3(-) == 0 596.073 105.618 5.644 < 0.001 ***
Comp4(-) - Comp3(-) == 0 217.738 151.390 1.438 0.80584
Comp4(+) - Comp3(-) == 0 195.643 107.103 1.827 0.54989
Comp4(-) - Comp3(+) == 0 -378.335 118.406 -3.195 0.02452 *
Comp4(+) - Comp3(+) == 0 -400.430 50.714 -7.896 < 0.001 ***
Comp4(+) - Comp4(-) == 0 -22.095 119.733 -0.185 1.00000

Spring ETo

	Estimate	Std. Error	t value	Pr(>|t|)	
Comp1(+) - Comp1(-) == 0	190.29	77.33	2.461	0.17850	
Comp2(-) - Comp1(-) == 0	508.19	90.61	5.609	< 0.001	***
Comp2(+) - Comp1(-) == 0	-329.52	80.73	-4.082	0.00102	**
Comp3(-) - Comp1(-) == 0	27.13	119.19	0.228	1.00000	
Comp3(+) - Comp1(-) == 0	54.86	82.19	0.667	0.99697	
Comp4(-) - Comp1(-) == 0	318.72	128.86	2.473	0.17359	
Comp4(+) - Comp1(-) == 0	-79.44	83.79	-0.948	0.97526	
Comp2(-) - Comp1(+) == 0	317.90	50.67	6.274	< 0.001	***
Comp2(+) - Comp1(+) == 0	-519.81	29.58	-17.576	< 0.001	***
Comp3(-) - Comp1(+) == 0	-163.16	92.54	-1.763	0.59495	
Comp3(+) - Comp1(+) == 0	-135.43	33.36	-4.060	0.00121	**
Comp4(-) - Comp1(+) == 0	128.43	104.70	1.227	0.90478	
Comp4(+) - Comp1(+) == 0	-269.73	37.11	-7.268	< 0.001	***
Comp2(+) - Comp2(-) == 0	-837.71	55.72	-15.035	< 0.001	***
Comp3(-) - Comp2(-) == 0	-481.06	103.89	-4.631	< 0.001	***
Comp3(+) - Comp2(-) == 0	-453.33	57.82	-7.841	< 0.001	***
Comp4(-) - Comp2(-) == 0	-189.47	114.85	-1.650	0.67418	
Comp4(+) - Comp2(-) == 0	-587.62	60.06	-9.784	< 0.001	***
Comp3(-) - Comp2(+) == 0	356.65	95.40	3.739	0.00352	**
Comp3(+) - Comp2(+) == 0	384.38	40.63	9.462	< 0.001	***
Comp4(-) - Comp2(+) == 0	648.24	107.23	6.045	< 0.001	***
Comp4(+) - Comp2(+) == 0	250.09	43.76	5.715	< 0.001	***
Comp3(+) - Comp3(-) == 0	27.73	96.64	0.287	0.99999	
Comp4(-) - Comp3(-) == 0	291.59	138.52	2.105	0.36144	
Comp4(+) - Comp3(-) == 0	-106.57	97.99	-1.087	0.94795	
Comp4(-) - Comp3(+) == 0	263.86	108.34	2.436	0.18875	
Comp4(+) - Comp3(+) == 0	-134.29	46.40	-2.894	0.05947	.
Comp4(+) - Comp4(-) == 0	-398.15	109.55	-3.634	0.00546	**

Summer ETo

	Estimate	Std. Error	t value	Pr(>|t|)	
Comp1(+) - Comp1(-) == 0	-45.25	78.25	-0.578	0.99879	
Comp2(-) - Comp1(-) == 0	313.97	91.69	3.424	0.01164	*
Comp2(+) - Comp1(-) == 0	-453.98	81.69	-5.557	< 0.001	***
Comp3(-) - Comp1(-) == 0	-391.50	120.61	-3.246	0.02077	*
Comp3(+) - Comp1(-) == 0	178.26	83.17	2.143	0.33824	
Comp4(-) - Comp1(-) == 0	213.88	130.39	1.640	0.68030	
Comp4(+) - Comp1(-) == 0	-209.71	84.79	-2.473	0.17422	
Comp2(-) - Comp1(+) == 0	359.23	51.27	7.007	< 0.001	***
Comp2(+) - Comp1(+) == 0	-408.73	29.93	-13.657	< 0.001	***
Comp3(-) - Comp1(+) == 0	-346.25	93.64	-3.698	0.00449	**
Comp3(+) - Comp1(+) == 0	223.51	33.76	6.621	< 0.001	***
Comp4(-) - Comp1(+) == 0	259.14	105.94	2.446	0.18407	
Comp4(+) - Comp1(+) == 0	-164.46	37.56	-4.379	< 0.001	***
Comp2(+) - Comp2(-) == 0	-767.95	56.38	-13.621	< 0.001	***
Comp3(-) - Comp2(-) == 0	-705.48	105.13	-6.711	< 0.001	***
Comp3(+) - Comp2(-) == 0	-135.71	58.51	-2.320	0.24134	
Comp4(-) - Comp2(-) == 0	-100.09	116.22	-0.861	0.98576	
Comp4(+) - Comp2(-) == 0	-523.68	60.78	-8.617	< 0.001	***
Comp3(-) - Comp2(+) == 0	62.48	96.53	0.647	0.99751	
Comp3(+) - Comp2(+) == 0	632.24	41.11	15.379	< 0.001	***
Comp4(-) - Comp2(+) == 0	667.86	108.51	6.155	< 0.001	***
Comp4(+) - Comp2(+) == 0	244.27	44.28	5.516	< 0.001	***
Comp3(+) - Comp3(-) == 0	569.76	97.79	5.826	< 0.001	***
Comp4(-) - Comp3(-) == 0	605.39	140.17	4.319	< 0.001	***
Comp4(+) - Comp3(-) == 0	181.79	99.16	1.833	0.54548	
Comp4(-) - Comp3(+) == 0	35.62	109.63	0.325	0.99997	
Comp4(+) - Comp3(+) == 0	-387.97	46.96	-8.263	< 0.001	***
Comp4(+) - Comp4(-) == 0	-423.60	110.86	-3.821	0.00260	**

Autumn ETo

	Estimate	Std. Error	t value	Pr(>|t|)	
Comp1(+) - Comp1(-) == 0	170.78	76.96	2.219	0.29528	
Comp2(-) - Comp1(-) == 0	521.49	90.18	5.783	< 0.001	***
Comp2(+) - Comp1(-) == 0	-344.12	80.35	-4.283	< 0.001	***
Comp3(-) - Comp1(-) == 0	-21.69	118.62	-0.183	1.00000	
Comp3(+) - Comp1(-) == 0	16.22	81.80	0.198	1.00000	
Comp4(-) - Comp1(-) == 0	304.42	128.25	2.374	0.21561	
Comp4(+) - Comp1(-) == 0	-119.74	83.39	-1.436	0.80734	
Comp2(-) - Comp1(+) == 0	350.72	50.43	6.955	< 0.001	***
Comp2(+) - Comp1(+) == 0	-514.90	29.43	-17.493	< 0.001	***
Comp3(-) - Comp1(+) == 0	-192.47	92.10	-2.090	0.37085	
Comp3(+) - Comp1(+) == 0	-154.55	33.20	-4.655	< 0.001	***
Comp4(-) - Comp1(+) == 0	133.65	104.20	1.283	0.88268	
Comp4(+) - Comp1(+) == 0	-290.52	36.94	-7.865	< 0.001	***
Comp2(+) - Comp2(-) == 0	-865.61	55.45	-15.610	< 0.001	***
Comp3(-) - Comp2(-) == 0	-543.18	103.39	-5.253	< 0.001	***
Comp3(+) - Comp2(-) == 0	-505.27	57.54	-8.781	< 0.001	***
Comp4(-) - Comp2(-) == 0	-217.07	114.31	-1.899	0.49912	
Comp4(+) - Comp2(-) == 0	-641.24	59.77	-10.728	< 0.001	***
Comp3(-) - Comp2(+) == 0	322.43	94.94	3.396	0.01251	*
Comp3(+) - Comp2(+) == 0	360.34	40.43	8.912	< 0.001	***
Comp4(-) - Comp2(+) == 0	648.54	106.72	6.077	< 0.001	***
Comp4(+) - Comp2(+) == 0	224.38	43.55	5.152	< 0.001	***
Comp3(+) - Comp3(-) == 0	37.91	96.18	0.394	0.99990	
Comp4(-) - Comp3(-) == 0	326.11	137.86	2.366	0.21953	
Comp4(+) - Comp3(-) == 0	-98.05	97.53	-1.005	0.96581	
Comp4(-) - Comp3(+) == 0	288.20	107.82	2.673	0.10682	
Comp4(+) - Comp3(+) == 0	-135.96	46.18	-2.944	0.05159	.

Comp4(+) - Comp4(-) == 0 -424.16   109.03 -3.890 0.00197 **

Annual climate balance

	Estimate	Std. Error	t value	Pr(>|t|)	
Comp1(+) - Comp1(-) == 0	-70.375	85.994	-0.818	0.9894	
Comp2(-) - Comp1(-) == 0	60.625	100.758	0.602	0.9984	
Comp2(+) - Comp1(-) == 0	-237.370	89.775	-2.644	0.1160	
Comp3(-) - Comp1(-) == 0	-13.415	132.540	-0.101	1.0000	
Comp3(+) - Comp1(-) == 0	-168.374	91.401	-1.842	0.5393	
Comp4(-) - Comp1(-) == 0	-226.478	143.292	-1.581	0.7199	
Comp4(+) - Comp1(-) == 0	-19.276	93.173	-0.207	1.0000	
Comp2(-) - Comp1(+) == 0	131.000	56.342	2.325	0.2392	
Comp2(+) - Comp1(+) == 0	-166.995	32.889	-5.078	<0.001	***
Comp3(-) - Comp1(+) == 0	56.961	102.903	0.554	0.9991	
Comp3(+) - Comp1(+) == 0	-97.998	37.099	-2.642	0.1164	
Comp4(-) - Comp1(+) == 0	-156.103	116.425	-1.341	0.8563	
Comp4(+) - Comp1(+) == 0	51.099	41.271	1.238	0.9005	
Comp2(+) - Comp2(-) == 0	-297.995	61.959	-4.810	<0.001	***
Comp3(-) - Comp2(-) == 0	-74.040	115.526	-0.641	0.9977	
Comp3(+) - Comp2(-) == 0	-228.999	64.293	-3.562	0.0070	**
Comp4(-) - Comp2(-) == 0	-287.103	127.719	-2.248	0.2788	
Comp4(+) - Comp2(-) == 0	-79.901	66.788	-1.196	0.9157	
Comp3(-) - Comp2(+) == 0	223.955	106.083	2.111	0.3579	
Comp3(+) - Comp2(+) == 0	68.996	45.176	1.527	0.7535	
Comp4(-) - Comp2(+) == 0	10.892	119.245	0.091	1.0000	
Comp4(+) - Comp2(+) == 0	218.094	48.661	4.482	<0.001	***
Comp3(+) - Comp3(-) == 0	-154.959	107.463	-1.442	0.8039	
Comp4(-) - Comp3(-) == 0	-213.063	154.035	-1.383	0.8356	
Comp4(+) - Comp3(-) == 0	-5.862	108.973	-0.054	1.0000	
Comp4(-) - Comp3(+) == 0	-58.104	120.474	-0.482	0.9996	
Comp4(+) - Comp3(+) == 0	149.097	51.600	2.889	0.0613	.
Comp4(+) - Comp4(-) == 0	207.202	121.824	1.701	0.6386	

Winter climate balance

	Estimate	Std. Error	t value	Pr(>|t|)	
Comp1(+) - Comp1(-) == 0	272.866	80.567	3.387	0.0129	*
Comp2(-) - Comp1(-) == 0	-8.349	94.400	-0.088	1.0000	
Comp2(+) - Comp1(-) == 0	419.184	84.110	4.984	<0.01	***
Comp3(-) - Comp1(-) == 0	459.953	124.176	3.704	<0.01	**
Comp3(+) - Comp1(-) == 0	-184.232	85.634	-2.151	0.3328	
Comp4(-) - Comp1(-) == 0	126.945	134.250	0.946	0.9757	
Comp4(+) - Comp1(-) == 0	181.243	87.293	2.076	0.3804	
Comp2(-) - Comp1(+) == 0	-281.214	52.786	-5.327	<0.01	***
Comp2(+) - Comp1(+) == 0	146.318	30.813	4.749	<0.01	***
Comp3(-) - Comp1(+) == 0	187.087	96.409	1.941	0.4701	
Comp3(+) - Comp1(+) == 0	-457.098	34.758	-13.151	<0.01	***
Comp4(-) - Comp1(+) == 0	-145.921	109.078	-1.338	0.8578	
Comp4(+) - Comp1(+) == 0	-91.623	38.667	-2.370	0.2176	
Comp2(+) - Comp2(-) == 0	427.533	58.049	7.365	<0.01	***
Comp3(-) - Comp2(-) == 0	468.302	108.236	4.327	<0.01	***
Comp3(+) - Comp2(-) == 0	-175.883	60.236	-2.920	0.0550	.
Comp4(-) - Comp2(-) == 0	135.294	119.659	1.131	0.9365	
Comp4(+) - Comp2(-) == 0	189.591	62.573	3.030	0.0402	*
Comp3(-) - Comp2(+) == 0	40.769	99.388	0.410	0.9999	
Comp3(+) - Comp2(+) == 0	-603.416	42.326	-14.257	<0.01	***
Comp4(-) - Comp2(+) == 0	-292.239	111.720	-2.616	0.1242	
Comp4(+) - Comp2(+) == 0	-237.941	45.590	-5.219	<0.01	***
Comp3(+) - Comp3(-) == 0	-644.185	100.681	-6.398	<0.01	***

Comp4(-) - Comp3(-) == 0 -333.008 144.314 -2.308 0.2478
Comp4(+) - Comp3(-) == 0 -278.710 102.097 -2.730 0.0928 .
Comp4(-) - Comp3(+) == 0 311.177 112.872 2.757 0.0865 .
Comp4(+) - Comp3(+) == 0 365.475 48.344 7.560 <0.01 ***
Comp4(+) - Comp4(-) == 0 54.298 114.136 0.476 0.9997

Spring climate balance

	Estimate	Std. Error	t value	Pr(>|t|)	
Comp1(+) - Comp1(-) == 0	194.008	85.168	2.278	0.2621	
Comp2(-) - Comp1(-) == 0	-194.650	99.791	-1.951	0.4632	
Comp2(+) - Comp1(-) == 0	162.807	88.913	1.831	0.5471	
Comp3(-) - Comp1(-) == 0	107.406	131.267	0.818	0.9895	
Comp3(+) - Comp1(-) == 0	49.930	90.524	0.552	0.9991	
Comp4(-) - Comp1(-) == 0	7.819	141.916	0.055	1.0000	
Comp4(+) - Comp1(-) == 0	9.542	92.278	0.103	1.0000	
Comp2(-) - Comp1(+) == 0	-388.658	55.801	-6.965	<0.01	***
Comp2(+) - Comp1(+) == 0	-31.201	32.573	-0.958	0.9738	
Comp3(-) - Comp1(+) == 0	-86.602	101.915	-0.850	0.9868	
Comp3(+) - Comp1(+) == 0	-144.078	36.743	-3.921	<0.01	**
Comp4(-) - Comp1(+) == 0	-186.190	115.307	-1.615	0.6975	
Comp4(+) - Comp1(+) == 0	-184.467	40.875	-4.513	<0.01	***
Comp2(+) - Comp2(-) == 0	357.457	61.364	5.825	<0.01	***
Comp3(-) - Comp2(-) == 0	302.056	114.417	2.640	0.1172	
Comp3(+) - Comp2(-) == 0	244.580	63.676	3.841	<0.01	**
Comp4(-) - Comp2(-) == 0	202.468	126.492	1.601	0.7065	
Comp4(+) - Comp2(-) == 0	204.191	66.147	3.087	0.0345	*
Comp3(-) - Comp2(+) == 0	-55.401	105.064	-0.527	0.9993	
Comp3(+) - Comp2(+) == 0	-112.877	44.743	-2.523	0.1552	
Comp4(-) - Comp2(+) == 0	-154.989	118.100	-1.312	0.8696	
Comp4(+) - Comp2(+) == 0	-153.266	48.194	-3.180	0.0254	*
Comp3(+) - Comp3(-) == 0	-57.476	106.431	-0.540	0.9992	
Comp4(-) - Comp3(-) == 0	-99.587	152.556	-0.653	0.9974	
Comp4(+) - Comp3(-) == 0	-97.864	107.927	-0.907	0.9808	
Comp4(-) - Comp3(+) == 0	-42.112	119.318	-0.353	1.0000	
Comp4(+) - Comp3(+) == 0	-40.389	51.105	-0.790	0.9914	
Comp4(+) - Comp4(-) == 0	1.723	120.654	0.014	1.0000	

Summer climate balance

	Estimate	Std. Error	t value	Pr(>|t|)	
Comp1(+) - Comp1(-) == 0	-317.32	81.38	-3.899	0.00232	**
Comp2(-) - Comp1(-) == 0	81.97	95.35	0.860	0.98588	
Comp2(+) - Comp1(-) == 0	-512.14	84.96	-6.028	< 0.001	***
Comp3(-) - Comp1(-) == 0	-404.77	125.43	-3.227	0.02183	*
Comp3(+) - Comp1(-) == 0	20.58	86.50	0.238	1.00000	
Comp4(-) - Comp1(-) == 0	-267.53	135.61	-1.973	0.44790	
Comp4(+) - Comp1(-) == 0	-240.73	88.17	-2.730	0.09313	.
Comp2(-) - Comp1(+) == 0	399.29	53.32	7.489	< 0.001	***
Comp2(+) - Comp1(+) == 0	-194.82	31.12	-6.259	< 0.001	***
Comp3(-) - Comp1(+) == 0	-87.46	97.38	-0.898	0.98186	
Comp3(+) - Comp1(+) == 0	337.89	35.11	9.624	< 0.001	***
Comp4(-) - Comp1(+) == 0	49.79	110.18	0.452	0.99976	
Comp4(+) - Comp1(+) == 0	76.58	39.06	1.961	0.45612	
Comp2(+) - Comp2(-) == 0	-594.11	58.64	-10.132	< 0.001	***
Comp3(-) - Comp2(-) == 0	-486.75	109.33	-4.452	< 0.001	***
Comp3(+) - Comp2(-) == 0	-61.39	60.84	-1.009	0.96512	
Comp4(-) - Comp2(-) == 0	-349.50	120.87	-2.892	0.06068	.
Comp4(+) - Comp2(-) == 0	-322.71	63.20	-5.106	< 0.001	***
Comp3(-) - Comp2(+) == 0	107.36	100.39	1.069	0.95229	

Comp3(+) - Comp2(+) == 0 532.71 42.75 12.460 < 0.001 ***
Comp4(-) - Comp2(+) == 0 244.61 112.85 2.168 0.32399
Comp4(+) - Comp2(+) == 0 271.40 46.05 5.894 < 0.001 ***
Comp3(+) - Comp3(-) == 0 425.35 101.70 4.183 < 0.001 ***
Comp4(-) - Comp3(-) == 0 137.25 145.77 0.942 0.97623
Comp4(+) - Comp3(-) == 0 164.04 103.13 1.591 0.71321
Comp4(-) - Comp3(+) == 0 -288.11 114.01 -2.527 0.15334
Comp4(+) - Comp3(+) == 0 -261.31 48.83 -5.351 < 0.001 ***
Comp4(+) - Comp4(-) == 0 26.79 115.29 0.232 1.00000

Autumn climate balance

	Estimate	Std. Error	t value	Pr(>|t|)
Comp1(+) - Comp1(-) == 0	386.10	79.88	4.834	< 0.001 ***
Comp2(-) - Comp1(-) == 0	-18.82	93.59	-0.201	1.00000
Comp2(+) - Comp1(-) == 0	183.59	83.39	2.202	0.30345
Comp3(-) - Comp1(-) == 0	507.34	123.11	4.121	< 0.001 ***
Comp3(+) - Comp1(-) == 0	-119.94	84.90	-1.413	0.82003
Comp4(-) - Comp1(-) == 0	72.23	133.10	0.543	0.99920
Comp4(+) - Comp1(-) == 0	338.03	86.54	3.906	0.00208 **
Comp2(-) - Comp1(+) == 0	-404.92	52.33	-7.737	< 0.001 ***
Comp2(+) - Comp1(+) == 0	-202.51	30.55	-6.629	< 0.001 ***
Comp3(-) - Comp1(+) == 0	121.25	95.58	1.269	0.88851
Comp3(+) - Comp1(+) == 0	-506.03	34.46	-14.685	< 0.001 ***
Comp4(-) - Comp1(+) == 0	-313.86	108.14	-2.902	0.05840 .
Comp4(+) - Comp1(+) == 0	-48.07	38.33	-1.254	0.89429
Comp2(+) - Comp2(-) == 0	202.41	57.55	3.517	0.00827 **
Comp3(-) - Comp2(-) == 0	526.17	107.31	4.903	< 0.001 ***
Comp3(+) - Comp2(-) == 0	-101.11	59.72	-1.693	0.64353
Comp4(-) - Comp2(-) == 0	91.06	118.63	0.768	0.99283
Comp4(+) - Comp2(-) == 0	356.85	62.04	5.752	< 0.001 ***
Comp3(-) - Comp2(+) == 0	323.76	98.53	3.286	0.01869 *
Comp3(+) - Comp2(+) == 0	-303.52	41.96	-7.233	< 0.001 ***
Comp4(-) - Comp2(+) == 0	-111.36	110.76	-1.005	0.96580
Comp4(+) - Comp2(+) == 0	154.44	45.20	3.417	0.01151 *
Comp3(+) - Comp3(-) == 0	-627.28	99.82	-6.284	< 0.001 ***
Comp4(-) - Comp3(-) == 0	-435.11	143.07	-3.041	0.03908 *
Comp4(+) - Comp3(-) == 0	-169.32	101.22	-1.673	0.65827
Comp4(-) - Comp3(+) == 0	192.17	111.90	1.717	0.62745
Comp4(+) - Comp3(+) == 0	457.96	47.93	9.555	< 0.001 ***
Comp4(+) - Comp4(-) == 0	265.80	113.16	2.349	0.22746

Winter NDVI

	Estimate	Std. Error	t value	Pr(>|t|)
Comp1(+) - Comp1(-) == 0	299.607	81.918	3.657	<0.01 **
Comp2(-) - Comp1(-) == 0	9.009	95.983	0.094	1.0000
Comp2(+) - Comp1(-) == 0	105.633	85.520	1.235	0.9016
Comp3(-) - Comp1(-) == 0	383.675	126.258	3.039	0.0395 *
Comp3(+) - Comp1(-) == 0	-145.032	87.069	-1.666	0.6629
Comp4(-) - Comp1(-) == 0	36.159	136.500	0.265	1.0000
Comp4(+) - Comp1(-) == 0	264.223	88.757	2.977	0.0471 *
Comp2(-) - Comp1(+) == 0	-290.598	53.671	-5.414	<0.01 ***
Comp2(+) - Comp1(+) == 0	-193.974	31.330	-6.191	<0.01 ***
Comp3(-) - Comp1(+) == 0	84.068	98.025	0.858	0.9861
Comp3(+) - Comp1(+) == 0	-444.639	35.340	-12.582	<0.01 ***
Comp4(-) - Comp1(+) == 0	-263.448	110.906	-2.375	0.2152
Comp4(+) - Comp1(+) == 0	-35.384	39.315	-0.900	0.9816
Comp2(+) - Comp2(-) == 0	96.624	59.022	1.637	0.6823
Comp3(-) - Comp2(-) == 0	374.667	110.050	3.405	0.0120 *

Comp3(+) - Comp2(-) == 0 -154.040 61.246 -2.515 0.1575
Comp4(-) - Comp2(-) == 0 27.151 121.665 0.223 1.0000
Comp4(+) - Comp2(-) == 0 255.214 63.622 4.011 <0.01 **
Comp3(-) - Comp2(+) == 0 278.043 101.054 2.751 0.0884 .
Comp3(+) - Comp2(+) == 0 -250.664 43.035 -5.825 <0.01 ***
Comp4(-) - Comp2(+) == 0 -69.473 113.593 -0.612 0.9983
Comp4(+) - Comp2(+) == 0 158.590 46.355 3.421 0.0115 *
Comp3(+) - Comp3(-) == 0 -528.707 102.369 -5.165 <0.01 ***
Comp4(-) - Comp3(-) == 0 -347.516 146.733 -2.368 0.2182
Comp4(+) - Comp3(-) == 0 -119.452 103.808 -1.151 0.9305
Comp4(-) - Comp3(+) == 0 181.191 114.764 1.579 0.7211
Comp4(+) - Comp3(+) == 0 409.255 49.154 8.326 <0.01 ***
Comp4(+) - Comp4(-) == 0 228.063 116.049 1.965 0.4538

Spring NDVI

Estimate Std. Error t value Pr(>|t|)
Comp1(+) - Comp1(-) == 0 284.563 83.327 3.415 0.01207 *
Comp2(-) - Comp1(-) == 0 83.613 97.634 0.856 0.98623
Comp2(+) - Comp1(-) == 0 47.851 86.991 0.550 0.99912
Comp3(-) - Comp1(-) == 0 401.415 128.430 3.126 0.03044 *
Comp3(+) - Comp1(-) == 0 -56.864 88.567 -0.642 0.99763
Comp4(-) - Comp1(-) == 0 12.978 138.849 0.093 1.00000
Comp4(+) - Comp1(-) == 0 277.652 90.284 3.075 0.03532 *
Comp2(-) - Comp1(+) == 0 -200.950 54.594 -3.681 0.00439 **
Comp2(+) - Comp1(+) == 0 -236.712 31.869 -7.428 < 0.001 ***
Comp3(-) - Comp1(+) == 0 116.852 99.712 1.172 0.92390
Comp3(+) - Comp1(+) == 0 -341.427 35.948 -9.498 < 0.001 ***
Comp4(-) - Comp1(+) == 0 -271.585 112.815 -2.407 0.20061
Comp4(+) - Comp1(+) == 0 -6.911 39.991 -0.173 1.00000
Comp2(+) - Comp2(-) == 0 -35.762 60.038 -0.596 0.99853
Comp3(-) - Comp2(-) == 0 317.802 111.943 2.839 0.06946 .
Comp3(+) - Comp2(-) == 0 -140.477 62.300 -2.255 0.27529
Comp4(-) - Comp2(-) == 0 -70.635 123.758 -0.571 0.99889
Comp4(+) - Comp2(-) == 0 194.039 64.717 2.998 0.04366 *
Comp3(-) - Comp2(+) == 0 353.563 102.793 3.440 0.01067 *
Comp3(+) - Comp2(+) == 0 -104.715 43.776 -2.392 0.20737
Comp4(-) - Comp2(+) == 0 -34.873 115.547 -0.302 0.99998
Comp4(+) - Comp2(+) == 0 229.801 47.152 4.874 < 0.001 ***
Comp3(+) - Comp3(-) == 0 -458.278 104.130 -4.401 < 0.001 ***
Comp4(-) - Comp3(-) == 0 -388.437 149.258 -2.602 0.12813
Comp4(+) - Comp3(-) == 0 -123.762 105.594 -1.172 0.92388
Comp4(-) - Comp3(+) == 0 69.842 116.738 0.598 0.99849
Comp4(+) - Comp3(+) == 0 334.516 50.000 6.690 < 0.001 ***
Comp4(+) - Comp4(-) == 0 264.674 118.046 2.242 0.28180

Summer NDVI

Estimate Std. Error t value Pr(>|t|)
Comp1(+) - Comp1(-) == 0 148.84 84.98 1.752 0.60321
Comp2(-) - Comp1(-) == 0 -1.18 99.57 -0.012 1.00000
Comp2(+) - Comp1(-) == 0 -103.36 88.72 -1.165 0.92604
Comp3(-) - Comp1(-) == 0 291.09 130.97 2.222 0.29190
Comp3(+) - Comp1(-) == 0 -30.78 90.32 -0.341 0.99996
Comp4(-) - Comp1(-) == 0 -89.00 141.60 -0.629 0.99793
Comp4(+) - Comp1(-) == 0 87.42 92.07 0.949 0.97507
Comp2(-) - Comp1(+) == 0 -150.02 55.68 -2.695 0.10174
Comp2(+) - Comp1(+) == 0 -252.20 32.50 -7.760 < 0.001 ***
Comp3(-) - Comp1(+) == 0 142.25 101.69 1.399 0.82731
Comp3(+) - Comp1(+) == 0 -179.62 36.66 -4.900 < 0.001 ***

Comp4(-) - Comp1(+) == 0 -237.85 115.05 -2.067 0.38535
Comp4(+) - Comp1(+) == 0 -61.42 40.78 -1.506 0.76693
Comp2(+) - Comp2(-) == 0 -102.18 61.23 -1.669 0.66042
Comp3(-) - Comp2(-) == 0 292.27 114.16 2.560 0.14176
Comp3(+) - Comp2(-) == 0 -29.60 63.53 -0.466 0.99971
Comp4(-) - Comp2(-) == 0 -87.83 126.21 -0.696 0.99607
Comp4(+) - Comp2(-) == 0 88.60 66.00 1.342 0.85565
Comp3(-) - Comp2(+) == 0 394.45 104.83 3.763 0.00338 **
Comp3(+) - Comp2(+) == 0 72.58 44.64 1.626 0.68990
Comp4(-) - Comp2(+) == 0 14.36 117.84 0.122 1.00000
Comp4(+) - Comp2(+) == 0 190.78 48.09 3.968 0.00154 **
Comp3(+) - Comp3(-) == 0 -321.87 106.19 -3.031 0.03983 *
Comp4(-) - Comp3(-) == 0 -380.10 152.22 -2.497 0.16482
Comp4(+) - Comp3(-) == 0 -203.67 107.69 -1.891 0.50429
Comp4(-) - Comp3(+) == 0 -58.22 119.05 -0.489 0.99960
Comp4(+) - Comp3(+) == 0 118.21 50.99 2.318 0.24263
Comp4(+) - Comp4(-) == 0 176.43 120.39 1.466 0.79046

Autumn NDVI

Estimate Std. Error t value Pr(>|t|)
Comp1(+) - Comp1(-) == 0 289.630 82.254 3.521 0.00842 **
Comp2(-) - Comp1(-) == 0 10.412 96.376 0.108 1.00000
Comp2(+) - Comp1(-) == 0 20.124 85.870 0.234 1.00000
Comp3(-) - Comp1(-) == 0 373.158 126.775 2.943 0.05190 .
Comp3(+) - Comp1(-) == 0 -96.943 87.426 -1.109 0.94244
Comp4(-) - Comp1(-) == 0 -44.374 137.060 -0.324 0.99997
Comp4(+) - Comp1(-) == 0 200.437 89.120 2.249 0.27842
Comp2(-) - Comp1(+) == 0 -279.218 53.891 -5.181 < 0.001 ***
Comp2(+) - Comp1(+) == 0 -269.505 31.458 -8.567 < 0.001 ***
Comp3(-) - Comp1(+) == 0 83.528 98.427 0.849 0.98694
Comp3(+) - Comp1(+) == 0 -386.573 35.485 -10.894 < 0.001 ***
Comp4(-) - Comp1(+) == 0 -334.003 111.361 -2.999 0.04371 *
Comp4(+) - Comp1(+) == 0 -89.192 39.476 -2.259 0.27237
Comp2(+) - Comp2(-) == 0 9.712 59.264 0.164 1.00000
Comp3(-) - Comp2(-) == 0 362.746 110.501 3.283 0.01905 *
Comp3(+) - Comp2(-) == 0 -107.355 61.497 -1.746 0.60703
Comp4(-) - Comp2(-) == 0 -54.786 122.163 -0.448 0.99977
Comp4(+) - Comp2(-) == 0 190.025 63.883 2.975 0.04676 *
Comp3(-) - Comp2(+) == 0 353.034 101.468 3.479 0.00965 **
Comp3(+) - Comp2(+) == 0 -117.068 43.211 -2.709 0.09813 .
Comp4(-) - Comp2(+) == 0 -64.498 114.058 -0.565 0.99895
Comp4(+) - Comp2(+) == 0 180.313 46.544 3.874 0.00233 **
Comp3(+) - Comp3(-) == 0 -470.101 102.788 -4.573 < 0.001 ***
Comp4(-) - Comp3(-) == 0 -417.532 147.335 -2.834 0.07057 .
Comp4(+) - Comp3(-) == 0 -172.721 104.233 -1.657 0.66862
Comp4(-) - Comp3(+) == 0 52.570 115.234 0.456 0.99974
Comp4(+) - Comp3(+) == 0 297.381 49.356 6.025 < 0.001 ***
Comp4(+) - Comp4(-) == 0 244.811 116.525 2.101 0.36426

Average day of the year recording the maximum NDVI

Estimate Std. Error t value Pr(>|t|)
Comp1(+) - Comp1(-) == 0 0.224330 0.841587 0.267 0.99999
Comp2(-) - Comp1(-) == 0 -0.063492 0.986080 -0.064 1.00000
Comp2(+) - Comp1(-) == 0 -0.598131 0.878590 -0.681 0.99658
Comp3(-) - Comp1(-) == 0 0.222222 1.297113 0.171 1.00000
Comp3(+) - Comp1(-) == 0 -1.162500 0.894508 -1.300 0.87524
Comp4(-) - Comp1(-) == 0 0.785714 1.402341 0.560 0.99901
Comp4(+) - Comp1(-) == 0 0.416000 0.911845 0.456 0.99974

Comp2(-) - Comp1(+) == 0 -0.287822 0.551391 -0.522 0.99938
Comp2(+) - Comp1(+) == 0 -0.822461 0.321866 -2.555 0.14356
Comp3(-) - Comp1(+) == 0 -0.002108 1.007064 -0.002 1.00000
Comp3(+) - Comp1(+) == 0 -1.386830 0.363072 -3.820 0.00275 **
Comp4(-) - Comp1(+) == 0 0.561384 1.139402 0.493 0.99957
Comp4(+) - Comp1(+) == 0 0.191670 0.403904 0.475 0.99967
Comp2(+) - Comp2(-) == 0 -0.534639 0.606369 -0.882 0.98366
Comp3(-) - Comp2(-) == 0 0.285714 1.130603 0.253 1.00000
Comp3(+) - Comp2(-) == 0 -1.099008 0.629211 -1.747 0.60653
Comp4(-) - Comp2(-) == 0 0.849206 1.249929 0.679 0.99662
Comp4(+) - Comp2(-) == 0 0.479492 0.653624 0.734 0.99456
Comp3(-) - Comp2(+) == 0 0.820353 1.038186 0.790 0.99146
Comp3(+) - Comp2(+) == 0 -0.564369 0.442123 -1.276 0.88515
Comp4(-) - Comp2(+) == 0 1.383845 1.167000 1.186 0.91931
Comp4(+) - Comp2(+) == 0 1.014131 0.476225 2.130 0.34607
Comp3(+) - Comp3(-) == 0 -1.384722 1.051691 -1.317 0.86772
Comp4(-) - Comp3(-) == 0 0.563492 1.507471 0.374 0.99993
Comp4(+) - Comp3(-) == 0 0.193778 1.066476 0.182 1.00000
Comp4(-) - Comp3(+) == 0 1.948214 1.179030 1.652 0.67207
Comp4(+) - Comp3(+) == 0 1.578500 0.504989 3.126 0.02981 *
Comp4(+) - Comp4(-) == 0 -0.369714 1.192237 -0.310 0.99998

Average day of the year recording the green up

Estimate Std. Error t value Pr(>|t|)
Comp1(+) - Comp1(-) == 0 -3.4176 4.4996 -0.760 0.99328
Comp2(-) - Comp1(-) == 0 -5.9176 5.2721 -1.122 0.93887
Comp2(+) - Comp1(-) == 0 -1.4209 4.6974 -0.302 0.99998
Comp3(-) - Comp1(-) == 0 -4.6795 6.9351 -0.675 0.99677
Comp3(+) - Comp1(-) == 0 -9.7212 4.7825 -2.033 0.40815
Comp4(-) - Comp1(-) == 0 7.6538 7.4977 1.021 0.96282
Comp4(+) - Comp1(-) == 0 -1.0022 4.8752 -0.206 1.00000
Comp2(-) - Comp1(+) == 0 -2.5000 2.9480 -0.848 0.98700
Comp2(+) - Comp1(+) == 0 1.9967 1.7209 1.160 0.92750
Comp3(-) - Comp1(+) == 0 -1.2619 5.3843 -0.234 1.00000
Comp3(+) - Comp1(+) == 0 -6.3036 1.9412 -3.247 0.02071 *
Comp4(-) - Comp1(+) == 0 11.0714 6.0918 1.817 0.55640
Comp4(+) - Comp1(+) == 0 2.4154 2.1595 1.119 0.93984
Comp2(+) - Comp2(-) == 0 4.4967 3.2420 1.387 0.83357
Comp3(-) - Comp2(-) == 0 1.2381 6.0448 0.205 1.00000
Comp3(+) - Comp2(-) == 0 -3.8036 3.3641 -1.131 0.93642
Comp4(-) - Comp2(-) == 0 13.5714 6.6828 2.031 0.40957
Comp4(+) - Comp2(-) == 0 4.9154 3.4946 1.407 0.82341
Comp3(-) - Comp2(+) == 0 -3.2586 5.5507 -0.587 0.99867
Comp3(+) - Comp2(+) == 0 -8.3002 2.3638 -3.511 0.00838 **
Comp4(-) - Comp2(+) == 0 9.0748 6.2394 1.454 0.79702
Comp4(+) - Comp2(+) == 0 0.4188 2.5462 0.164 1.00000
Comp3(+) - Comp3(-) == 0 -5.0417 5.6229 -0.897 0.98199
Comp4(-) - Comp3(-) == 0 12.3333 8.0597 1.530 0.75195
Comp4(+) - Comp3(-) == 0 3.6773 5.7019 0.645 0.99756
Comp4(-) - Comp3(+) == 0 17.3750 6.3037 2.756 0.08742 .
Comp4(+) - Comp3(+) == 0 8.7190 2.6999 3.229 0.02220 *
Comp4(+) - Comp4(-) == 0 -8.6560 6.3743 -1.358 0.84799

Soil water capacity

Estimate Std. Error t value Pr(>|t|)
Comp1(+) - Comp1(-) == 0 269.5638 84.1712 3.203 0.0239 *
Comp2(-) - Comp1(-) == 0 32.5922 98.6227 0.330 1.0000
Comp2(+) - Comp1(-) == 0 -25.8081 87.8721 -0.294 1.0000

Comp3(-) - Comp1(-) == 0	131.5684	129.7305	1.014	0.9642	
Comp3(+) - Comp1(-) == 0	91.9399	89.4641	1.028	0.9615	
Comp4(-) - Comp1(-) == 0	18.6319	140.2549	0.133	1.0000	
Comp4(+) - Comp1(-) == 0	131.9182	91.1981	1.447	0.8012	
Comp2(-) - Comp1(+) == 0	-236.9716	55.1472	-4.297	<0.001	***
Comp2(+) - Comp1(+) == 0	-295.3718	32.1914	-9.175	<0.001	***
Comp3(-) - Comp1(+) == 0	-137.9954	100.7214	-1.370	0.8421	
Comp3(+) - Comp1(+) == 0	-177.6239	36.3125	-4.892	<0.001	***
Comp4(-) - Comp1(+) == 0	-250.9319	113.9571	-2.202	0.3041	
Comp4(+) - Comp1(+) == 0	-137.6456	40.3964	-3.407	0.0119	*
Comp2(+) - Comp2(-) == 0	-58.4002	60.6459	-0.963	0.9730	
Comp3(-) - Comp2(-) == 0	98.9762	113.0771	0.875	0.9843	
Comp3(+) - Comp2(-) == 0	59.3477	62.9305	0.943	0.9760	
Comp4(-) - Comp2(-) == 0	-13.9603	125.0115	-0.112	1.0000	
Comp4(+) - Comp2(-) == 0	99.3260	65.3721	1.519	0.7585	
Comp3(-) - Comp2(+) == 0	157.3764	103.8340	1.516	0.7608	
Comp3(+) - Comp2(+) == 0	117.7480	44.2189	2.663	0.1114	
Comp4(-) - Comp2(+) == 0	44.4399	116.7173	0.381	0.9999	
Comp4(+) - Comp2(+) == 0	157.7262	47.6296	3.312	0.0166	*
Comp3(+) - Comp3(-) == 0	-39.6285	105.1847	-0.377	0.9999	
Comp4(-) - Comp3(-) == 0	-112.9365	150.7695	-0.749	0.9938	
Comp4(+) - Comp3(-) == 0	0.3498	106.6634	0.003	1.0000	
Comp4(-) - Comp3(+) == 0	-73.3080	117.9205	-0.622	0.9981	
Comp4(+) - Comp3(+) == 0	39.9782	50.5064	0.792	0.9914	
Comp4(+) - Comp4(-) == 0	113.2863	119.2414	0.950	0.9750	

5. COTTON

Annual precipitation

	Estimate	Std. Error	t value	Pr(>|t|)	
Comp1(+) - Comp1(-) == 0	-12.069	18.755	-0.643	0.9997	
Comp2(-) - Comp1(-) == 0	5.688	34.745	0.164	1.0000	
Comp2(+) - Comp1(-) == 0	44.893	18.380	2.443	0.2718	
Comp3(-) - Comp1(-) == 0	8.988	32.310	0.278	1.0000	
Comp3(+) - Comp1(-) == 0	15.381	20.067	0.767	0.9987	
Comp4(-) - Comp1(-) == 0	60.943	33.439	1.823	0.6874	
Comp4(+) - Comp1(-) == 0	-13.012	24.586	-0.529	0.9999	
Comp5(-) - Comp1(-) == 0	-72.512	46.761	-1.551	0.8496	
Comp5(+) - Comp1(-) == 0	-41.607	26.347	-1.579	0.8351	
Comp2(-) - Comp1(+) == 0	17.757	33.217	0.535	0.9999	
Comp2(+) - Comp1(+) == 0	56.962	15.298	3.723	<0.01	**
Comp3(-) - Comp1(+) == 0	21.057	30.662	0.687	0.9995	
Comp3(+) - Comp1(+) == 0	27.450	17.288	1.588	0.8309	
Comp4(-) - Comp1(+) == 0	73.011	31.849	2.292	0.3611	
Comp4(+) - Comp1(+) == 0	-0.943	22.376	-0.042	1.0000	
Comp5(-) - Comp1(+) == 0	-60.443	45.638	-1.324	0.9373	
Comp5(+) - Comp1(+) == 0	-29.538	24.297	-1.216	0.9631	
Comp2(+) - Comp2(-) == 0	39.205	33.007	1.188	0.9682	
Comp3(-) - Comp2(-) == 0	3.300	42.374	0.078	1.0000	
Comp3(+) - Comp2(-) == 0	9.693	33.975	0.285	1.0000	
Comp4(-) - Comp2(-) == 0	55.255	43.241	1.278	0.9494	
Comp4(+) - Comp2(-) == 0	-18.700	36.825	-0.508	1.0000	
Comp5(-) - Comp2(-) == 0	-78.200	54.206	-1.443	0.8974	
Comp5(+) - Comp2(-) == 0	-47.295	38.024	-1.244	0.9573	
Comp3(-) - Comp2(+) == 0	-35.904	30.434	-1.180	0.9695	
Comp3(+) - Comp2(+) == 0	-29.512	16.880	-1.748	0.7365	
Comp4(-) - Comp2(+) == 0	16.050	31.630	0.507	1.0000	
Comp4(+) - Comp2(+) == 0	-57.904	22.062	-2.625	0.1849	
Comp5(-) - Comp2(+) == 0	-117.404	45.485	-2.581	0.2036	
Comp5(+) - Comp2(+) == 0	-86.500	24.009	-3.603	0.0107	*
Comp3(+) - Comp3(-) == 0	6.393	31.481	0.203	1.0000	
Comp4(-) - Comp3(-) == 0	51.955	41.311	1.258	0.9541	
Comp4(+) - Comp3(-) == 0	-22.000	34.538	-0.637	0.9997	
Comp5(-) - Comp3(-) == 0	-81.500	52.678	-1.547	0.8514	
Comp5(+) - Comp3(-) == 0	-50.595	35.813	-1.413	0.9087	
Comp4(-) - Comp3(+) == 0	45.562	32.639	1.396	0.9146	
Comp4(+) - Comp3(+) == 0	-28.393	23.486	-1.209	0.9643	
Comp5(-) - Comp3(+) == 0	-87.893	46.192	-1.903	0.6316	
Comp5(+) - Comp3(+) == 0	-56.988	25.324	-2.250	0.3874	
Comp4(+) - Comp4(-) == 0	-73.954	35.596	-2.078	0.5060	
Comp5(-) - Comp4(-) == 0	-133.454	53.378	-2.500	0.2420	
Comp5(+) - Comp4(-) == 0	-102.550	36.834	-2.784	0.1269	
Comp5(-) - Comp4(+) == 0	-59.500	48.327	-1.231	0.9598	
Comp5(+) - Comp4(+) == 0	-28.595	29.036	-0.985	0.9912	
Comp5(+) - Comp5(-) == 0	30.905	49.247	0.628	0.9997	

Winter precipitation

	Estimate	Std. Error	t value	Pr(>|t|)
Comp1(+) - Comp1(-) == 0	-10.542	18.774	-0.562	0.9999
Comp2(-) - Comp1(-) == 0	20.616	34.779	0.593	0.9998
Comp2(+) - Comp1(-) == 0	36.285	18.398	1.972	0.5817
Comp3(-) - Comp1(-) == 0	-26.300	32.342	-0.813	0.9979
Comp3(+) - Comp1(-) == 0	49.581	20.086	2.468	0.2585
Comp4(-) - Comp1(-) == 0	47.207	33.472	1.410	0.9094

```
Comp4(+) - Comp1(-) == 0  -32.038     24.610  -1.302   0.9434
Comp5(-) - Comp1(-) == 0   10.916     46.808   0.233   1.0000
Comp5(+) - Comp1(-) == 0  -17.312     26.373  -0.656   0.9996
Comp2(-) - Comp1(+) == 0   31.158     33.250   0.937   0.9939
Comp2(+) - Comp1(+) == 0   46.827     15.313   3.058   0.0615 .
Comp3(-) - Comp1(+) == 0  -15.758     30.692  -0.513   1.0000
Comp3(+) - Comp1(+) == 0   60.123     17.305   3.474   0.0170 *
Comp4(-) - Comp1(+) == 0   57.749     31.881   1.811   0.6948
Comp4(+) - Comp1(+) == 0  -21.496     22.398  -0.960   0.9927
Comp5(-) - Comp1(+) == 0   21.458     45.683   0.470   1.0000
Comp5(+) - Comp1(+) == 0   -6.770     24.322  -0.278   1.0000
Comp2(+) - Comp2(-) == 0   15.669     33.040   0.474   1.0000
Comp3(-) - Comp2(-) == 0  -46.917     42.417  -1.106   0.9802
Comp3(+) - Comp2(-) == 0   28.964     34.009   0.852   0.9970
Comp4(-) - Comp2(-) == 0   26.591     43.284   0.614   0.9998
Comp4(+) - Comp2(-) == 0  -52.654     36.862  -1.428   0.9029
Comp5(-) - Comp2(-) == 0   -9.700     54.259  -0.179   1.0000
Comp5(+) - Comp2(-) == 0  -37.929     38.061  -0.997   0.9904
Comp3(-) - Comp2(+) == 0  -62.585     30.464  -2.054   0.5226
Comp3(+) - Comp2(+) == 0   13.296     16.897   0.787   0.9984
Comp4(-) - Comp2(+) == 0   10.922     31.661   0.345   1.0000
Comp4(+) - Comp2(+) == 0  -68.322     22.084  -3.094   0.0553 .
Comp5(-) - Comp2(+) == 0  -25.369     45.530  -0.557   0.9999
Comp5(+) - Comp2(+) == 0  -53.597     24.033  -2.230   0.4008
Comp3(+) - Comp3(-) == 0   75.881     31.513   2.408   0.2901
Comp4(-) - Comp3(-) == 0   73.508     41.352   1.778   0.7177
Comp4(+) - Comp3(-) == 0   -5.737     34.572  -0.166   1.0000
Comp5(-) - Comp3(-) == 0   37.217     52.731   0.706   0.9993
Comp5(+) - Comp3(-) == 0    8.988     35.849   0.251   1.0000
Comp4(-) - Comp3(+) == 0   -2.373     32.671  -0.073   1.0000
Comp4(+) - Comp3(+) == 0  -81.618     23.509  -3.472   0.0168 *
Comp5(-) - Comp3(+) == 0  -38.664     46.238  -0.836   0.9974
Comp5(+) - Comp3(+) == 0  -66.893     25.349  -2.639   0.1788
Comp4(+) - Comp4(-) == 0  -79.245     35.631  -2.224   0.4042
Comp5(-) - Comp4(-) == 0  -36.291     53.431  -0.679   0.9995
Comp5(+) - Comp4(-) == 0  -64.519     36.871  -1.750   0.7351
Comp5(-) - Comp4(+) == 0   42.954     48.375   0.888   0.9959
Comp5(+) - Comp4(+) == 0   14.725     29.065   0.507   1.0000
Comp5(+) - Comp5(-) == 0  -28.229     49.295  -0.573   0.9999
```

Spring precipitation

```
                    Estimate Std. Error t value Pr(>|t|)
Comp1(+) - Comp1(-) == 0    8.562     17.483   0.490    1.000
Comp2(-) - Comp1(-) == 0   36.672     32.388   1.132    0.977
Comp2(+) - Comp1(-) == 0  -48.336     17.133  -2.821    0.115
Comp3(-) - Comp1(-) == 0  -20.961     30.119  -0.696    0.999
Comp3(+) - Comp1(-) == 0   92.961     18.705   4.970    <0.01 ***
Comp4(-) - Comp1(-) == 0  -29.628     31.171  -0.951    0.993
Comp4(+) - Comp1(-) == 0    5.487     22.918   0.239    1.000
Comp5(-) - Comp1(-) == 0  -17.028     43.589  -0.391    1.000
Comp5(+) - Comp1(-) == 0   13.705     24.560   0.558    1.000
Comp2(-) - Comp1(+) == 0   28.110     30.964   0.908    0.995
Comp2(+) - Comp1(+) == 0  -56.898     14.260  -3.990    <0.01 **
Comp3(-) - Comp1(+) == 0  -29.523     28.582  -1.033    0.988
Comp3(+) - Comp1(+) == 0   84.399     16.115   5.237    <0.01 ***
Comp4(-) - Comp1(+) == 0  -38.190     29.689  -1.286    0.947
Comp4(+) - Comp1(+) == 0   -3.074     20.858  -0.147    1.000
Comp5(-) - Comp1(+) == 0  -25.590     42.542  -0.602    1.000
Comp5(+) - Comp1(+) == 0    5.143     22.649   0.227    1.000
```

Comp2(+) - Comp2(-) == 0 -85.008 30.768 -2.763 0.133
Comp3(-) - Comp2(-) == 0 -57.633 39.500 -1.459 0.891
Comp3(+) - Comp2(-) == 0 56.289 31.671 1.777 0.718
Comp4(-) - Comp2(-) == 0 -66.300 40.308 -1.645 0.799
Comp4(+) - Comp2(-) == 0 -31.185 34.328 -0.908 0.995
Comp5(-) - Comp2(-) == 0 -53.700 50.529 -1.063 0.985
Comp5(+) - Comp2(-) == 0 -22.967 35.445 -0.648 1.000
Comp3(-) - Comp2(+) == 0 27.375 28.370 0.965 0.992
Comp3(+) - Comp2(+) == 0 141.297 15.735 8.980 <0.01 ***
Comp4(-) - Comp2(+) == 0 18.708 29.484 0.635 1.000
Comp4(+) - Comp2(+) == 0 53.823 20.566 2.617 0.187
Comp5(-) - Comp2(+) == 0 31.308 42.400 0.738 0.999
Comp5(+) - Comp2(+) == 0 62.041 22.381 2.772 0.130
Comp3(+) - Comp3(-) == 0 113.923 29.346 3.882 <0.01 **
Comp4(-) - Comp3(-) == 0 -8.667 38.509 -0.225 1.000
Comp4(+) - Comp3(-) == 0 26.449 32.195 0.822 0.998
Comp5(-) - Comp3(-) == 0 3.933 49.105 0.080 1.000
Comp5(+) - Comp3(-) == 0 34.667 33.384 1.038 0.987
Comp4(-) - Comp3(+) == 0 -122.589 30.425 -4.029 <0.01 **
Comp4(+) - Comp3(+) == 0 -87.474 21.893 -3.996 <0.01 **
Comp5(-) - Comp3(+) == 0 -109.989 43.059 -2.554 0.216
Comp5(+) - Comp3(+) == 0 -79.256 23.606 -3.357 0.025 *
Comp4(+) - Comp4(-) == 0 35.115 33.182 1.058 0.985
Comp5(-) - Comp4(-) == 0 12.600 49.757 0.253 1.000
Comp5(+) - Comp4(-) == 0 43.333 34.336 1.262 0.953
Comp5(-) - Comp4(+) == 0 -22.515 45.049 -0.500 1.000
Comp5(+) - Comp4(+) == 0 8.218 27.067 0.304 1.000
Comp5(+) - Comp5(-) == 0 30.733 45.906 0.669 1.000

Summer precipitation

Estimate Std. Error t value Pr(>|t|)
Comp1(+) - Comp1(-) == 0 -35.534 18.097 -1.963 0.5879
Comp2(-) - Comp1(-) == 0 -63.177 33.527 -1.884 0.6444
Comp2(+) - Comp1(-) == 0 -83.348 17.735 -4.699 <0.01 ***
Comp3(-) - Comp1(-) == 0 -15.060 31.178 -0.483 1.0000
Comp3(+) - Comp1(-) == 0 -67.387 19.363 -3.480 0.0166 *
Comp4(-) - Comp1(-) == 0 -119.613 32.267 -3.707 <0.01 **
Comp4(+) - Comp1(-) == 0 8.562 23.724 0.361 1.0000
Comp5(-) - Comp1(-) == 0 -65.977 45.122 -1.462 0.8895
Comp5(+) - Comp1(-) == 0 27.547 25.423 1.084 0.9828
Comp2(-) - Comp1(+) == 0 -27.643 32.053 -0.862 0.9967
Comp2(+) - Comp1(+) == 0 -47.814 14.762 -3.239 0.0359 *
Comp3(-) - Comp1(+) == 0 20.474 29.587 0.692 0.9994
Comp3(+) - Comp1(+) == 0 -31.854 16.682 -1.909 0.6268
Comp4(-) - Comp1(+) == 0 -84.079 30.732 -2.736 0.1428
Comp4(+) - Comp1(+) == 0 44.095 21.591 2.042 0.5319
Comp5(-) - Comp1(+) == 0 -30.443 44.038 -0.691 0.9994
Comp5(+) - Comp1(+) == 0 63.081 23.446 2.691 0.1580
Comp2(+) - Comp2(-) == 0 -20.171 31.850 -0.633 0.9997
Comp3(-) - Comp2(-) == 0 48.117 40.889 1.177 0.9700
Comp3(+) - Comp2(-) == 0 -4.211 32.784 -0.128 1.0000
Comp4(-) - Comp2(-) == 0 -56.436 41.725 -1.353 0.9290
Comp4(+) - Comp2(-) == 0 71.738 35.535 2.019 0.5482
Comp5(-) - Comp2(-) == 0 -2.800 52.305 -0.054 1.0000
Comp5(+) - Comp2(-) == 0 90.724 36.691 2.473 0.2570
Comp3(-) - Comp2(+) == 0 68.287 29.367 2.325 0.3406
Comp3(+) - Comp2(+) == 0 15.960 16.288 0.980 0.9915
Comp4(-) - Comp2(+) == 0 -36.266 30.521 -1.188 0.9681
Comp4(+) - Comp2(+) == 0 91.909 21.289 4.317 <0.01 ***

```
Comp5(-) - Comp2(+) == 0   17.371     43.890   0.396   1.0000
Comp5(+) - Comp2(+) == 0  110.895     23.167   4.787    <0.01 ***
Comp3(+) - Comp3(-) == 0  -52.327     30.378  -1.723   0.7526
Comp4(-) - Comp3(-) == 0 -104.553     39.862  -2.623   0.1860
Comp4(+) - Comp3(-) == 0   23.622     33.327   0.709   0.9993
Comp5(-) - Comp3(-) == 0  -50.917     50.832  -1.002   0.9901
Comp5(+) - Comp3(-) == 0   42.607     34.558   1.233   0.9596
Comp4(-) - Comp3(+) == 0  -52.226     31.494  -1.658   0.7917
Comp4(+) - Comp3(+) == 0   75.949     22.663   3.351   0.0253 *
Comp5(-) - Comp3(+) == 0    1.411     44.573   0.032   1.0000
Comp5(+) - Comp3(+) == 0   94.935     24.436   3.885    <0.01 **
Comp4(+) - Comp4(-) == 0  128.175     34.348   3.732    <0.01 **
Comp5(-) - Comp4(-) == 0   53.636     51.507   1.041   0.9869
Comp5(+) - Comp4(-) == 0  147.160     35.543   4.140    <0.01 **
Comp5(-) - Comp4(+) == 0  -74.538     46.633  -1.598   0.8252
Comp5(+) - Comp4(+) == 0   18.985     28.018   0.678   0.9995
Comp5(+) - Comp5(-) == 0   93.524     47.520   1.968   0.5847
```

Autumn precipitation

```
                    Estimate Std. Error t value Pr(>|t|)
Comp1(+) - Comp1(-) == 0  -46.0492    16.8197  -2.738   0.1422
Comp2(-) - Comp1(-) == 0   44.5977    31.1594   1.431   0.9018
Comp2(+) - Comp1(-) == 0 -105.8304    16.4832  -6.420    <0.01 ***
Comp3(-) - Comp1(-) == 0   -0.6357    28.9762  -0.022   1.0000
Comp3(+) - Comp1(-) == 0   32.7334    17.9959   1.819   0.6895
Comp4(-) - Comp1(-) == 0  -85.8478    29.9883  -2.863   0.1037
Comp4(+) - Comp1(-) == 0   -3.4177    22.0490  -0.155   1.0000
Comp5(-) - Comp1(-) == 0   49.0977    41.9359   1.171   0.9710
Comp5(+) - Comp1(-) == 0  -15.4928    23.6282  -0.656   0.9996
Comp2(-) - Comp1(+) == 0   90.6468    29.7897   3.043   0.0639 .
Comp2(+) - Comp1(+) == 0  -59.7813    13.7193  -4.357    <0.01 ***
Comp3(-) - Comp1(+) == 0   45.4135    27.4980   1.652   0.7958
Comp3(+) - Comp1(+) == 0   78.7825    15.5040   5.081    <0.01 ***
Comp4(-) - Comp1(+) == 0  -39.7986    28.5625  -1.393   0.9154
Comp4(+) - Comp1(+) == 0   42.6315    20.0669   2.124   0.4723
Comp5(-) - Comp1(+) == 0   95.1468    40.9285   2.325   0.3396
Comp5(+) - Comp1(+) == 0   30.5564    21.7902   1.402   0.9124
Comp2(+) - Comp2(-) == 0 -150.4281    29.6011  -5.082    <0.01 ***
Comp3(-) - Comp2(-) == 0  -45.2333    38.0019  -1.190   0.9678
Comp3(+) - Comp2(-) == 0  -11.8643    30.4693  -0.389   1.0000
Comp4(-) - Comp2(-) == 0 -130.4455    38.7792  -3.364   0.0249 *
Comp4(+) - Comp2(-) == 0  -48.0154    33.0255  -1.454   0.8930
Comp5(-) - Comp2(-) == 0    4.5000    48.6122   0.093   1.0000
Comp5(+) - Comp2(-) == 0  -60.0905    34.1001  -1.762   0.7277
Comp3(-) - Comp2(+) == 0  105.1948    27.2936   3.854    <0.01 **
Comp3(+) - Comp2(+) == 0  138.5638    15.1384   9.153    <0.01 ***
Comp4(-) - Comp2(+) == 0   19.9826    28.3657   0.704   0.9993
Comp4(+) - Comp2(+) == 0  102.4127    19.7857   5.176    <0.01 ***
Comp5(-) - Comp2(+) == 0  154.9281    40.7914   3.798    <0.01 **
Comp5(+) - Comp2(+) == 0   90.3376    21.5316   4.196    <0.01 **
Comp3(+) - Comp3(-) == 0   33.3690    28.2329   1.182   0.9691
Comp4(-) - Comp3(-) == 0  -85.2121    37.0478  -2.300   0.3551
Comp4(+) - Comp3(-) == 0   -2.7821    30.9742  -0.090   1.0000
Comp5(-) - Comp3(-) == 0   49.7333    47.2426   1.053   0.9860
Comp5(+) - Comp3(-) == 0  -14.8571    32.1175  -0.463   1.0000
Comp4(-) - Comp3(+) == 0 -118.5812    29.2706  -4.051    <0.01 **
Comp4(+) - Comp3(+) == 0  -36.1511    21.0626  -1.716   0.7568
Comp5(-) - Comp3(+) == 0   16.3643    41.4258   0.395   1.0000
Comp5(+) - Comp3(+) == 0  -48.2262    22.7105  -2.124   0.4736
```

Comp4(+) - Comp4(-) == 0 82.4301 31.9229 2.582 0.2037
Comp5(-) - Comp4(-) == 0 134.9455 47.8700 2.819 0.1167
Comp5(+) - Comp4(-) == 0 70.3550 33.0335 2.130 0.4690
Comp5(-) - Comp4(+) == 0 52.5154 43.3405 1.212 0.9637
Comp5(+) - Comp4(+) == 0 -12.0751 26.0398 -0.464 1.0000
Comp5(+) - Comp5(-) == 0 -64.5905 44.1649 -1.462 0.8892

Annual mean temperature

	Estimate	Std. Error	t value	Pr(>|t|)	
Comp1(+) - Comp1(-) == 0	9.4036	18.1472	0.518	0.9999	
Comp2(-) - Comp1(-) == 0	20.5023	33.6187	0.610	0.9998	
Comp2(+) - Comp1(-) == 0	-9.2482	17.7842	-0.520	0.9999	
Comp3(-) - Comp1(-) == 0	64.2190	31.2632	2.054	0.5226	
Comp3(+) - Comp1(-) == 0	-71.5727	19.4163	-3.686	<0.01	**
Comp4(-) - Comp1(-) == 0	-86.1522	32.3551	-2.663	0.1693	
Comp4(+) - Comp1(-) == 0	10.1869	23.7892	0.428	1.0000	
Comp5(-) - Comp1(-) == 0	99.3023	45.2458	2.195	0.4249	
Comp5(+) - Comp1(-) == 0	36.4452	25.4931	1.430	0.9025	
Comp2(-) - Comp1(+) == 0	11.0987	32.1409	0.345	1.0000	
Comp2(+) - Comp1(+) == 0	-18.6518	14.8021	-1.260	0.9536	
Comp3(-) - Comp1(+) == 0	54.8154	29.6683	1.848	0.6701	
Comp3(+) - Comp1(+) == 0	-80.9763	16.7277	-4.841	<0.01	***
Comp4(-) - Comp1(+) == 0	-95.5558	30.8168	-3.101	0.0538	.
Comp4(+) - Comp1(+) == 0	0.7833	21.6507	0.036	1.0000	
Comp5(-) - Comp1(+) == 0	89.8987	44.1589	2.036	0.5361	
Comp5(+) - Comp1(+) == 0	27.0416	23.5100	1.150	0.9742	
Comp2(+) - Comp2(-) == 0	-29.7506	31.9374	-0.932	0.9942	
Comp3(-) - Comp2(-) == 0	43.7167	41.0013	1.066	0.9846	
Comp3(+) - Comp2(-) == 0	-92.0750	32.8742	-2.801	0.1213	
Comp4(-) - Comp2(-) == 0	-106.6545	41.8398	-2.549	0.2183	
Comp4(+) - Comp2(-) == 0	-10.3154	35.6321	-0.289	1.0000	
Comp5(-) - Comp2(-) == 0	78.8000	52.4490	1.502	0.8724	
Comp5(+) - Comp2(-) == 0	15.9429	36.7915	0.433	1.0000	
Comp3(-) - Comp2(+) == 0	73.4672	29.4477	2.495	0.2449	
Comp3(+) - Comp2(+) == 0	-62.3244	16.3332	-3.816	<0.01	**
Comp4(-) - Comp2(+) == 0	-76.9040	30.6045	-2.513	0.2363	
Comp4(+) - Comp2(+) == 0	19.4352	21.3473	0.910	0.9951	
Comp5(-) - Comp2(+) == 0	108.5506	44.0109	2.466	0.2584	
Comp5(+) - Comp2(+) == 0	45.6934	23.2310	1.967	0.5857	
Comp3(+) - Comp3(-) == 0	-135.7917	30.4612	-4.458	<0.01	***
Comp4(-) - Comp3(-) == 0	-150.3712	39.9718	-3.762	<0.01	**
Comp4(+) - Comp3(-) == 0	-54.0321	33.4188	-1.617	0.8151	
Comp5(-) - Comp3(-) == 0	35.0833	50.9713	0.688	0.9994	
Comp5(+) - Comp3(-) == 0	-27.7738	34.6524	-0.801	0.9981	
Comp4(-) - Comp3(+) == 0	-14.5795	31.5808	-0.462	1.0000	
Comp4(+) - Comp3(+) == 0	81.7596	22.7249	3.598	0.0112	*
Comp5(-) - Comp3(+) == 0	170.8750	44.6954	3.823	<0.01	**
Comp5(+) - Comp3(+) == 0	108.0179	24.5030	4.408	<0.01	***
Comp4(+) - Comp4(-) == 0	96.3392	34.4425	2.797	0.1221	
Comp5(-) - Comp4(-) == 0	185.4545	51.6482	3.591	0.0117	*
Comp5(+) - Comp4(-) == 0	122.5974	35.6407	3.440	0.0193	*
Comp5(-) - Comp4(+) == 0	89.1154	46.7612	1.906	0.6296	
Comp5(+) - Comp4(+) == 0	26.2582	28.0950	0.935	0.9940	
Comp5(+) - Comp5(-) == 0	-62.8571	47.6506	-1.319	0.9385	

Winter mean temperature

	Estimate	Std. Error	t value	Pr(>|t|)	
Comp1(+) - Comp1(-) == 0	58.663	18.672	3.142	0.0477	*

Comp2(-) - Comp1(-) == 0 -14.067 34.591 -0.407 1.0000
Comp2(+) - Comp1(-) == 0 35.727 18.298 1.952 0.5954
Comp3(-) - Comp1(-) == 0 -23.767 32.167 -0.739 0.9990
Comp3(+) - Comp1(-) == 0 20.322 19.978 1.017 0.9889
Comp4(-) - Comp1(-) == 0 18.414 33.291 0.553 0.9999
Comp4(+) - Comp1(-) == 0 -21.306 24.477 -0.870 0.9965
Comp5(-) - Comp1(-) == 0 -10.567 46.554 -0.227 1.0000
Comp5(+) - Comp1(-) == 0 -39.244 26.230 -1.496 0.8750
Comp2(-) - Comp1(+) == 0 -72.730 33.070 -2.199 0.4214
Comp2(+) - Comp1(+) == 0 -22.936 15.230 -1.506 0.8711
Comp3(-) - Comp1(+) == 0 -82.430 30.526 -2.700 0.1545
Comp3(+) - Comp1(+) == 0 -38.341 17.211 -2.228 0.4024
Comp4(-) - Comp1(+) == 0 -40.249 31.708 -1.269 0.9515
Comp4(+) - Comp1(+) == 0 -79.969 22.277 -3.590 0.0112 *
Comp5(-) - Comp1(+) == 0 -69.230 45.436 -1.524 0.8624
Comp5(+) - Comp1(+) == 0 -97.907 24.190 -4.047 <0.01 **
Comp2(+) - Comp2(-) == 0 49.794 32.861 1.515 0.8667
Comp3(-) - Comp2(-) == 0 -9.700 42.187 -0.230 1.0000
Comp3(+) - Comp2(-) == 0 34.389 33.825 1.017 0.9890
Comp4(-) - Comp2(-) == 0 32.482 43.050 0.755 0.9988
Comp4(+) - Comp2(-) == 0 -7.238 36.662 -0.197 1.0000
Comp5(-) - Comp2(-) == 0 3.500 53.966 0.065 1.0000
Comp5(+) - Comp2(-) == 0 -25.176 37.855 -0.665 0.9996
Comp3(-) - Comp2(+) == 0 -59.494 30.299 -1.964 0.5879
Comp3(+) - Comp2(+) == 0 -15.405 16.806 -0.917 0.9948
Comp4(-) - Comp2(+) == 0 -17.313 31.489 -0.550 0.9999
Comp4(+) - Comp2(+) == 0 -57.033 21.965 -2.597 0.1967
Comp5(-) - Comp2(+) == 0 -46.294 45.284 -1.022 0.9885
Comp5(+) - Comp2(+) == 0 -74.971 23.903 -3.136 0.0480 *
Comp3(+) - Comp3(-) == 0 44.089 31.342 1.407 0.9110
Comp4(-) - Comp3(-) == 0 42.182 41.128 1.026 0.9883
Comp4(+) - Comp3(-) == 0 2.462 34.385 0.072 1.0000
Comp5(-) - Comp3(-) == 0 13.200 52.445 0.252 1.0000
Comp5(+) - Comp3(-) == 0 -15.476 35.654 -0.434 1.0000
Comp4(-) - Comp3(+) == 0 -1.907 32.494 -0.059 1.0000
Comp4(+) - Comp3(+) == 0 -41.628 23.382 -1.780 0.7155
Comp5(-) - Comp3(+) == 0 -30.889 45.988 -0.672 0.9995
Comp5(+) - Comp3(+) == 0 -59.565 25.211 -2.363 0.3177
Comp4(+) - Comp4(-) == 0 -39.720 35.438 -1.121 0.9783
Comp5(-) - Comp4(-) == 0 -28.982 53.142 -0.545 0.9999
Comp5(+) - Comp4(-) == 0 -57.658 36.671 -1.572 0.8388
Comp5(-) - Comp4(+) == 0 10.738 48.113 0.223 1.0000
Comp5(+) - Comp4(+) == 0 -17.938 28.907 -0.621 0.9998
Comp5(+) - Comp5(-) == 0 -28.676 49.028 -0.585 0.9999

Spring mean temperature

Estimate Std. Error t value Pr(>|t|)
Comp1(+) - Comp1(-) == 0 13.167 18.395 0.716 0.9992
Comp2(-) - Comp1(-) == 0 24.356 34.077 0.715 0.9992
Comp2(+) - Comp1(-) == 0 -2.306 18.027 -0.128 1.0000
Comp3(-) - Comp1(-) == 0 61.589 31.689 1.944 0.6027
Comp3(+) - Comp1(-) == 0 -60.333 19.681 -3.066 0.0600 .
Comp4(-) - Comp1(-) == 0 -80.017 32.796 -2.440 0.2733
Comp4(+) - Comp1(-) == 0 14.640 24.114 0.607 0.9998
Comp5(-) - Comp1(-) == 0 81.456 45.863 1.776 0.7183
Comp5(+) - Comp1(-) == 0 41.113 25.841 1.591 0.8289
Comp2(-) - Comp1(+) == 0 11.189 32.579 0.343 1.0000
Comp2(+) - Comp1(+) == 0 -15.473 15.004 -1.031 0.9878
Comp3(-) - Comp1(+) == 0 48.422 30.073 1.610 0.8186

Comp3(+) - Comp1(+) == 0	-73.501	16.956	-4.335	<0.01 ***
Comp4(-) - Comp1(+) == 0	-93.184	31.237	-2.983	0.0752 .
Comp4(+) - Comp1(+) == 0	1.473	21.946	0.067	1.0000
Comp5(-) - Comp1(+) == 0	68.289	44.761	1.526	0.8618
Comp5(+) - Comp1(+) == 0	27.946	23.831	1.173	0.9707
Comp2(+) - Comp2(-) == 0	-26.662	32.373	-0.824	0.9977
Comp3(-) - Comp2(-) == 0	37.233	41.560	0.896	0.9956
Comp3(+) - Comp2(-) == 0	-84.689	33.322	-2.542	0.2210
Comp4(-) - Comp2(-) == 0	-104.373	42.410	-2.461	0.2622
Comp4(+) - Comp2(-) == 0	-9.715	36.118	-0.269	1.0000
Comp5(-) - Comp2(-) == 0	57.100	53.164	1.074	0.9838
Comp5(+) - Comp2(-) == 0	16.757	37.293	0.449	1.0000
Comp3(-) - Comp2(+) == 0	63.895	29.849	2.141	0.4616
Comp3(+) - Comp2(+) == 0	-58.027	16.556	-3.505	0.0155 *
Comp4(-) - Comp2(+) == 0	-77.711	31.022	-2.505	0.2395
Comp4(+) - Comp2(+) == 0	16.946	21.638	0.783	0.9984
Comp5(-) - Comp2(+) == 0	83.762	44.611	1.878	0.6486
Comp5(+) - Comp2(+) == 0	43.419	23.548	1.844	0.6725
Comp3(+) - Comp3(-) == 0	-121.923	30.876	-3.949	<0.01 **
Comp4(-) - Comp3(-) == 0	-141.606	40.517	-3.495	0.0153 *
Comp4(+) - Comp3(-) == 0	-46.949	33.874	-1.386	0.9180
Comp5(-) - Comp3(-) == 0	19.867	51.666	0.385	1.0000
Comp5(+) - Comp3(-) == 0	-20.476	35.125	-0.583	0.9999
Comp4(-) - Comp3(+) == 0	-19.683	32.011	-0.615	0.9998
Comp4(+) - Comp3(+) == 0	74.974	23.035	3.255	0.0350 *
Comp5(-) - Comp3(+) == 0	141.789	45.305	3.130	0.0495 *
Comp5(+) - Comp3(+) == 0	101.446	24.837	4.084	<0.01 **
Comp4(+) - Comp4(-) == 0	94.657	34.912	2.711	0.1509
Comp5(-) - Comp4(-) == 0	161.473	52.352	3.084	0.0566 .
Comp5(+) - Comp4(-) == 0	121.130	36.127	3.353	0.0249 *
Comp5(-) - Comp4(+) == 0	66.815	47.399	1.410	0.9097
Comp5(+) - Comp4(+) == 0	26.473	28.478	0.930	0.9942
Comp5(+) - Comp5(-) == 0	-40.343	48.300	-0.835	0.9974

Summer mean temperature

	Estimate	Std. Error	t value	Pr(>|t|)
Comp1(+) - Comp1(-) == 0	14.315	18.960	0.755	0.9988
Comp2(-) - Comp1(-) == 0	35.863	35.125	1.021	0.9887
Comp2(+) - Comp1(-) == 0	17.365	18.581	0.935	0.9940
Comp3(-) - Comp1(-) == 0	35.163	32.664	1.077	0.9836
Comp3(+) - Comp1(-) == 0	-31.641	20.286	-1.560	0.8451
Comp4(-) - Comp1(-) == 0	-50.110	33.804	-1.482	0.8812
Comp4(+) - Comp1(-) == 0	-13.645	24.855	-0.549	0.9999
Comp5(-) - Comp1(-) == 0	103.963	47.273	2.199	0.4218
Comp5(+) - Comp1(-) == 0	16.306	26.635	0.612	0.9998
Comp2(-) - Comp1(+) == 0	21.548	33.581	0.642	0.9997
Comp2(+) - Comp1(+) == 0	3.050	15.465	0.197	1.0000
Comp3(-) - Comp1(+) == 0	20.848	30.997	0.673	0.9995
Comp3(+) - Comp1(+) == 0	-45.956	17.477	-2.629	0.1822
Comp4(-) - Comp1(+) == 0	-64.425	32.197	-2.001	0.5618
Comp4(+) - Comp1(+) == 0	-27.960	22.620	-1.236	0.9590
Comp5(-) - Comp1(+) == 0	89.648	46.137	1.943	0.6032
Comp5(+) - Comp1(+) == 0	1.991	24.563	0.081	1.0000
Comp2(+) - Comp2(-) == 0	-18.498	33.368	-0.554	0.9999
Comp3(-) - Comp2(-) == 0	-0.700	42.838	-0.016	1.0000
Comp3(+) - Comp2(-) == 0	-67.504	34.347	-1.965	0.5860
Comp4(-) - Comp2(-) == 0	-85.973	43.714	-1.967	0.5861
Comp4(+) - Comp2(-) == 0	-49.508	37.228	-1.330	0.9357
Comp5(-) - Comp2(-) == 0	68.100	54.798	1.243	0.9575

Comp5(+) - Comp2(-) == 0 -19.557 38.440 -0.509 1.0000
Comp3(-) - Comp2(+) == 0 17.798 30.767 0.578 0.9999
Comp3(+) - Comp2(+) == 0 -49.006 17.065 -2.872 0.1017
Comp4(-) - Comp2(+) == 0 -67.475 31.975 -2.110 0.4834
Comp4(+) - Comp2(+) == 0 -31.010 22.304 -1.390 0.9165
Comp5(-) - Comp2(+) == 0 86.598 45.982 1.883 0.6450
Comp5(+) - Comp2(+) == 0 -1.059 24.272 -0.044 1.0000
Comp3(+) - Comp3(-) == 0 -66.804 31.826 -2.099 0.4911
Comp4(-) - Comp3(-) == 0 -85.273 41.762 -2.042 0.5319
Comp4(+) - Comp3(-) == 0 -48.808 34.916 -1.398 0.9139
Comp5(-) - Comp3(-) == 0 68.800 53.255 1.292 0.9459
Comp5(+) - Comp3(-) == 0 -18.857 36.205 -0.521 0.9999
Comp4(-) - Comp3(+) == 0 -18.469 32.995 -0.560 0.9999
Comp4(+) - Comp3(+) == 0 17.996 23.743 0.758 0.9988
Comp5(-) - Comp3(+) == 0 135.604 46.697 2.904 0.0932 .
Comp5(+) - Comp3(+) == 0 47.946 25.601 1.873 0.6526
Comp4(+) - Comp4(-) == 0 36.465 35.985 1.013 0.9892
Comp5(-) - Comp4(-) == 0 154.073 53.962 2.855 0.1060
Comp5(+) - Comp4(-) == 0 66.416 37.237 1.784 0.7135
Comp5(-) - Comp4(+) == 0 117.608 48.856 2.407 0.2912
Comp5(+) - Comp4(+) == 0 29.951 29.354 1.020 0.9887
Comp5(+) - Comp5(-) == 0 -87.657 49.785 -1.761 0.7284

Autumn mean temperature

Estimate Std. Error t value Pr(>|t|)
Comp1(+) - Comp1(-) == 0 4.8493 18.0576 0.269 1.0000
Comp2(-) - Comp1(-) == 0 16.9581 33.4527 0.507 1.0000
Comp2(+) - Comp1(-) == 0 -20.1722 17.6964 -1.140 0.9757
Comp3(-) - Comp1(-) == 0 62.7248 31.1088 2.016 0.5498
Comp3(+) - Comp1(-) == 0 -75.6026 19.3204 -3.913 <0.01 **
Comp4(-) - Comp1(-) == 0 -100.8964 32.1954 -3.134 0.0489 *
Comp4(+) - Comp1(-) == 0 4.1351 23.6718 0.175 1.0000
Comp5(-) - Comp1(-) == 0 94.1581 45.0224 2.091 0.4957
Comp5(+) - Comp1(-) == 0 33.3200 25.3672 1.314 0.9403
Comp2(-) - Comp1(+) == 0 12.1089 31.9822 0.379 1.0000
Comp2(+) - Comp1(+) == 0 -25.0215 14.7290 -1.699 0.7673
Comp3(-) - Comp1(+) == 0 57.8755 29.5218 1.960 0.5902
Comp3(+) - Comp1(+) == 0 -80.4519 16.6451 -4.833 <0.01 ***
Comp4(-) - Comp1(+) == 0 -105.7457 30.6647 -3.448 0.0185 *
Comp4(+) - Comp1(+) == 0 -0.7142 21.5438 -0.033 1.0000
Comp5(-) - Comp1(+) == 0 89.3089 43.9408 2.032 0.5387
Comp5(+) - Comp1(+) == 0 28.4708 23.3940 1.217 0.9628
Comp2(+) - Comp2(-) == 0 -37.1303 31.7797 -1.168 0.9713
Comp3(-) - Comp2(-) == 0 45.7667 40.7988 1.122 0.9782
Comp3(+) - Comp2(-) == 0 -92.5607 32.7118 -2.830 0.1131
Comp4(-) - Comp2(-) == 0 -117.8545 41.6332 -2.831 0.1121
Comp4(+) - Comp2(-) == 0 -12.8231 35.4561 -0.362 1.0000
Comp5(-) - Comp2(-) == 0 77.2000 52.1900 1.479 0.8826
Comp5(+) - Comp2(-) == 0 16.3619 36.6099 0.447 1.0000
Comp3(-) - Comp2(+) == 0 82.8970 29.3023 2.829 0.1130
Comp3(+) - Comp2(+) == 0 -55.4304 16.2526 -3.411 0.0211 *
Comp4(-) - Comp2(+) == 0 -80.7242 30.4534 -2.651 0.1753
Comp4(+) - Comp2(+) == 0 24.3073 21.2419 1.144 0.9752
Comp5(-) - Comp2(+) == 0 114.3303 43.7936 2.611 0.1904
Comp5(+) - Comp2(+) == 0 53.4922 23.1163 2.314 0.3463
Comp3(+) - Comp3(-) == 0 -138.3274 30.3108 -4.564 <0.01 ***
Comp4(-) - Comp3(-) == 0 -163.6212 39.7744 -4.114 <0.01 **
Comp4(+) - Comp3(-) == 0 -58.5897 33.2538 -1.762 0.7279
Comp5(-) - Comp3(-) == 0 31.4333 50.7196 0.620 0.9998

Comp5(+) - Comp3(-) == 0 -29.4048 34.4813 -0.853 0.9970
Comp4(-) - Comp3(+) == 0 -25.2938 31.4249 -0.805 0.9981
Comp4(+) - Comp3(+) == 0 79.7376 22.6127 3.526 0.0144 *
Comp5(-) - Comp3(+) == 0 169.7607 44.4747 3.817 <0.01 **
Comp5(+) - Comp3(+) == 0 108.9226 24.3820 4.467 <0.01 ***
Comp4(+) - Comp4(-) == 0 105.0315 34.2724 3.065 0.0596 .
Comp5(-) - Comp4(-) == 0 195.0545 51.3932 3.795 <0.01 **
Comp5(+) - Comp4(-) == 0 134.2165 35.4647 3.785 <0.01 **
Comp5(-) - Comp4(+) == 0 90.0231 46.5303 1.935 0.6088
Comp5(+) - Comp4(+) == 0 29.1850 27.9563 1.044 0.9867
Comp5(+) - Comp5(-) == 0 -60.8381 47.4154 -1.283 0.9481

Annual ETo

Estimate Std. Error t value Pr(>|t|)
Comp1(+) - Comp1(-) == 0 35.232 17.578 2.004 0.5582
Comp2(-) - Comp1(-) == 0 41.593 32.564 1.277 0.9496
Comp2(+) - Comp1(-) == 0 81.846 17.226 4.751 <0.01 ***
Comp3(-) - Comp1(-) == 0 77.510 30.282 2.560 0.2140
Comp3(+) - Comp1(-) == 0 -46.675 18.807 -2.482 0.2514
Comp4(-) - Comp1(-) == 0 50.457 31.340 1.610 0.8187
Comp4(+) - Comp1(-) == 0 22.016 23.043 0.955 0.9930
Comp5(-) - Comp1(-) == 0 128.693 43.826 2.936 0.0855 .
Comp5(+) - Comp1(-) == 0 26.188 24.693 1.061 0.9851
Comp2(-) - Comp1(+) == 0 6.361 31.133 0.204 1.0000
Comp2(+) - Comp1(+) == 0 46.614 14.338 3.251 0.0351 *
Comp3(-) - Comp1(+) == 0 42.277 28.738 1.471 0.8858
Comp3(+) - Comp1(+) == 0 -81.907 16.203 -5.055 <0.01 ***
Comp4(-) - Comp1(+) == 0 15.224 29.850 0.510 1.0000
Comp4(+) - Comp1(+) == 0 -13.216 20.972 -0.630 0.9997
Comp5(-) - Comp1(+) == 0 93.461 42.774 2.185 0.4308
Comp5(+) - Comp1(+) == 0 -9.044 22.773 -0.397 1.0000
Comp2(+) - Comp2(-) == 0 40.253 30.936 1.301 0.9436
Comp3(-) - Comp2(-) == 0 35.917 39.715 0.904 0.9953
Comp3(+) - Comp2(-) == 0 -88.268 31.843 -2.772 0.1301
Comp4(-) - Comp2(-) == 0 8.864 40.527 0.219 1.0000
Comp4(+) - Comp2(-) == 0 -19.577 34.514 -0.567 0.9999
Comp5(-) - Comp2(-) == 0 87.100 50.804 1.714 0.7579
Comp5(+) - Comp2(-) == 0 -15.405 35.637 -0.432 1.0000
Comp3(-) - Comp2(+) == 0 -4.336 28.524 -0.152 1.0000
Comp3(+) - Comp2(+) == 0 -128.521 15.821 -8.123 <0.01 ***
Comp4(-) - Comp2(+) == 0 -31.389 29.644 -1.059 0.9854
Comp4(+) - Comp2(+) == 0 -59.830 20.678 -2.893 0.0957 .
Comp5(-) - Comp2(+) == 0 46.847 42.630 1.099 0.9810
Comp5(+) - Comp2(+) == 0 -55.658 22.502 -2.473 0.2556
Comp3(+) - Comp3(-) == 0 -124.185 29.506 -4.209 <0.01 **
Comp4(-) - Comp3(-) == 0 -27.053 38.718 -0.699 0.9994
Comp4(+) - Comp3(-) == 0 -55.494 32.371 -1.714 0.7576
Comp5(-) - Comp3(-) == 0 51.183 49.372 1.037 0.9873
Comp5(+) - Comp3(-) == 0 -51.321 33.565 -1.529 0.8601
Comp4(-) - Comp3(+) == 0 97.131 30.590 3.175 0.0433 *
Comp4(+) - Comp3(+) == 0 68.691 22.012 3.121 0.0509 .
Comp5(-) - Comp3(+) == 0 175.368 43.293 4.051 <0.01 **
Comp5(+) - Comp3(+) == 0 72.863 23.734 3.070 0.0586 .
Comp4(+) - Comp4(-) == 0 -28.441 33.362 -0.852 0.9970
Comp5(-) - Comp4(-) == 0 78.236 50.028 1.564 0.8431
Comp5(+) - Comp4(-) == 0 -24.268 34.523 -0.703 0.9993
Comp5(-) - Comp4(+) == 0 106.677 45.294 2.355 0.3217
Comp5(+) - Comp4(+) == 0 4.172 27.214 0.153 1.0000
Comp5(+) - Comp5(-) == 0 -102.505 46.156 -2.221 0.4067

Winter ETo

	Estimate	Std. Error	t value	Pr(>|t|)	
Comp1(+) - Comp1(-) == 0	21.895	17.676	1.239	0.958	
Comp2(-) - Comp1(-) == 0	64.447	32.746	1.968	0.585	
Comp2(+) - Comp1(-) == 0	30.271	17.323	1.748	0.737	
Comp3(-) - Comp1(-) == 0	66.213	30.452	2.174	0.439	
Comp3(+) - Comp1(-) == 0	-80.757	18.912	-4.270	<0.01	***
Comp4(-) - Comp1(-) == 0	-14.226	31.515	-0.451	1.000	
Comp4(+) - Comp1(-) == 0	32.316	23.172	1.395	0.915	
Comp5(-) - Comp1(-) == 0	99.647	44.071	2.261	0.380	
Comp5(+) - Comp1(-) == 0	39.904	24.831	1.607	0.821	
Comp2(-) - Comp1(+) == 0	42.552	31.307	1.359	0.927	
Comp2(+) - Comp1(+) == 0	8.377	14.418	0.581	1.000	
Comp3(-) - Comp1(+) == 0	44.319	28.898	1.534	0.858	
Comp3(+) - Comp1(+) == 0	-102.652	16.293	-6.300	<0.01	***
Comp4(-) - Comp1(+) == 0	-36.121	30.017	-1.203	0.965	
Comp4(+) - Comp1(+) == 0	10.421	21.089	0.494	1.000	
Comp5(-) - Comp1(+) == 0	77.752	43.013	1.808	0.697	
Comp5(+) - Comp1(+) == 0	18.009	22.900	0.786	0.998	
Comp2(+) - Comp2(-) == 0	-34.175	31.108	-1.099	0.981	
Comp3(-) - Comp2(-) == 0	1.767	39.937	0.044	1.000	
Comp3(+) - Comp2(-) == 0	-145.204	32.021	-4.535	<0.01	***
Comp4(-) - Comp2(-) == 0	-78.673	40.754	-1.930	0.612	
Comp4(+) - Comp2(-) == 0	-32.131	34.707	-0.926	0.994	
Comp5(-) - Comp2(-) == 0	35.200	51.087	0.689	0.999	
Comp5(+) - Comp2(-) == 0	-24.543	35.836	-0.685	0.999	
Comp3(-) - Comp2(+) == 0	35.942	28.683	1.253	0.955	
Comp3(+) - Comp2(+) == 0	-111.028	15.909	-6.979	<0.01	***
Comp4(-) - Comp2(+) == 0	-44.497	29.810	-1.493	0.876	
Comp4(+) - Comp2(+) == 0	2.045	20.793	0.098	1.000	
Comp5(-) - Comp2(+) == 0	69.375	42.868	1.618	0.814	
Comp5(+) - Comp2(+) == 0	9.632	22.628	0.426	1.000	
Comp3(+) - Comp3(-) == 0	-146.970	29.670	-4.953	<0.01	***
Comp4(-) - Comp3(-) == 0	-80.439	38.934	-2.066	0.514	
Comp4(+) - Comp3(-) == 0	-33.897	32.551	-1.041	0.987	
Comp5(-) - Comp3(-) == 0	33.433	49.648	0.673	1.000	
Comp5(+) - Comp3(-) == 0	-26.310	33.753	-0.779	0.998	
Comp4(-) - Comp3(+) == 0	66.531	30.761	2.163	0.446	
Comp4(+) - Comp3(+) == 0	113.073	22.135	5.108	<0.01	***
Comp5(-) - Comp3(+) == 0	180.404	43.535	4.144	<0.01	**
Comp5(+) - Comp3(+) == 0	120.661	23.867	5.056	<0.01	***
Comp4(+) - Comp4(-) == 0	46.542	33.548	1.387	0.918	
Comp5(-) - Comp4(-) == 0	113.873	50.307	2.264	0.378	
Comp5(+) - Comp4(-) == 0	54.130	34.715	1.559	0.845	
Comp5(-) - Comp4(+) == 0	67.331	45.547	1.478	0.883	
Comp5(+) - Comp4(+) == 0	7.588	27.366	0.277	1.000	
Comp5(+) - Comp5(-) == 0	-59.743	46.414	-1.287	0.947	

Spring ETo

	Estimate	Std. Error	t value	Pr(>|t|)	
Comp1(+) - Comp1(-) == 0	40.0954	17.4753	2.294	0.3588	
Comp2(-) - Comp1(-) == 0	29.0093	32.3739	0.896	0.9956	
Comp2(+) - Comp1(-) == 0	81.6026	17.1258	4.765	<0.01	***
Comp3(-) - Comp1(-) == 0	60.8760	30.1057	2.022	0.5447	
Comp3(+) - Comp1(-) == 0	-52.3443	18.6974	-2.800	0.1218	
Comp4(-) - Comp1(-) == 0	61.6638	31.1572	1.979	0.5771	
Comp4(+) - Comp1(-) == 0	23.5170	22.9084	1.027	0.9882	

Comp5(-) - Comp1(-) == 0 119.0093 43.5706 2.731 0.1442
Comp5(+) - Comp1(-) == 0 36.0664 24.5492 1.469 0.8868
Comp2(-) - Comp1(+) == 0 -11.0861 30.9509 -0.358 1.0000
Comp2(+) - Comp1(+) == 0 41.5072 14.2540 2.912 0.0912 .
Comp3(-) - Comp1(+) == 0 20.7806 28.5699 0.727 0.9991
Comp3(+) - Comp1(+) == 0 -92.4396 16.1084 -5.739 <0.01 ***
Comp4(-) - Comp1(+) == 0 21.5685 29.6759 0.727 0.9991
Comp4(+) - Comp1(+) == 0 -16.5784 20.8491 -0.795 0.9982
Comp5(-) - Comp1(+) == 0 78.9139 42.5239 1.856 0.6640
Comp5(+) - Comp1(+) == 0 -4.0289 22.6396 -0.178 1.0000
Comp2(+) - Comp2(-) == 0 52.5933 30.7549 1.710 0.7604
Comp3(-) - Comp2(-) == 0 31.8667 39.4832 0.807 0.9980
Comp3(+) - Comp2(-) == 0 -81.3536 31.6570 -2.570 0.2086
Comp4(-) - Comp2(-) == 0 32.6545 40.2907 0.810 0.9980
Comp4(+) - Comp2(-) == 0 -5.4923 34.3128 -0.160 1.0000
Comp5(-) - Comp2(-) == 0 90.0000 50.5071 1.782 0.7145
Comp5(+) - Comp2(-) == 0 7.0571 35.4293 0.199 1.0000
Comp3(-) - Comp2(+) == 0 -20.7266 28.3574 -0.731 0.9991
Comp3(+) - Comp2(+) == 0 -133.9468 15.7285 -8.516 <0.01 ***
Comp4(-) - Comp2(+) == 0 -19.9387 29.4714 -0.677 0.9995
Comp4(+) - Comp2(+) == 0 -58.0856 20.5570 -2.826 0.1131
Comp5(-) - Comp2(+) == 0 37.4067 42.3815 0.883 0.9961
Comp5(+) - Comp2(+) == 0 -45.5361 22.3709 -2.036 0.5369
Comp3(+) - Comp3(-) == 0 -113.2202 29.3334 -3.860 <0.01 **
Comp4(-) - Comp3(-) == 0 0.7879 38.4919 0.020 1.0000
Comp4(+) - Comp3(-) == 0 -37.3590 32.1815 -1.161 0.9726
Comp5(-) - Comp3(-) == 0 58.1333 49.0841 1.184 0.9688
Comp5(+) - Comp3(-) == 0 -24.8095 33.3694 -0.743 0.9990
Comp4(-) - Comp3(+) == 0 114.0081 30.4116 3.749 <0.01 **
Comp4(+) - Comp3(+) == 0 75.8613 21.8836 3.467 0.0179 *
Comp5(-) - Comp3(+) == 0 171.3536 43.0406 3.981 <0.01 **
Comp5(+) - Comp3(+) == 0 88.4107 23.5957 3.747 <0.01 **
Comp4(+) - Comp4(-) == 0 -38.1469 33.1673 -1.150 0.9742
Comp5(-) - Comp4(-) == 0 57.3455 49.7360 1.153 0.9738
Comp5(+) - Comp4(-) == 0 -25.5974 34.3211 -0.746 0.9989
Comp5(-) - Comp4(+) == 0 95.4923 45.0299 2.121 0.4759
Comp5(+) - Comp4(+) == 0 12.5495 27.0548 0.464 1.0000
Comp5(+) - Comp5(-) == 0 -82.9429 45.8864 -1.808 0.6975

Summer ETo

	Estimate	Std. Error	t value	Pr(>|t|)
Comp1(+) - Comp1(-) == 0	61.667	17.931	3.439	0.0193 *
Comp2(-) - Comp1(-) == 0	57.526	33.219	1.732	0.7470
Comp2(+) - Comp1(-) == 0	93.820	17.573	5.339	<0.01 ***
Comp3(-) - Comp1(-) == 0	52.826	30.892	1.710	0.7611
Comp3(+) - Comp1(-) == 0	24.218	19.185	1.262	0.9531
Comp4(-) - Comp1(-) == 0	116.689	31.971	3.650	<0.01 **
Comp4(+) - Comp1(-) == 0	-3.751	23.506	-0.160	1.0000
Comp5(-) - Comp1(-) == 0	149.326	44.708	3.340	0.0258 *
Comp5(+) - Comp1(-) == 0	-8.627	25.190	-0.342	1.0000
Comp2(-) - Comp1(+) == 0	-4.142	31.759	-0.130	1.0000
Comp2(+) - Comp1(+) == 0	32.153	14.626	2.198	0.4217
Comp3(-) - Comp1(+) == 0	-8.842	29.316	-0.302	1.0000
Comp3(+) - Comp1(+) == 0	-37.449	16.529	-2.266	0.3773
Comp4(-) - Comp1(+) == 0	55.022	30.451	1.807	0.6978
Comp4(+) - Comp1(+) == 0	-65.419	21.393	-3.058	0.0610 .
Comp5(-) - Comp1(+) == 0	87.658	43.634	2.009	0.5553
Comp5(+) - Comp1(+) == 0	-70.294	23.231	-3.026	0.0669 .
Comp2(+) - Comp2(-) == 0	36.294	31.558	1.150	0.9742

Comp3(-) - Comp2(-) == 0 -4.700 40.514 -0.116 1.0000
Comp3(+) - Comp2(-) == 0 -33.307 32.483 -1.025 0.9883
Comp4(-) - Comp2(-) == 0 59.164 41.343 1.431 0.9021
Comp4(+) - Comp2(-) == 0 -61.277 35.209 -1.740 0.7417
Comp5(-) - Comp2(-) == 0 91.800 51.826 1.771 0.7219
Comp5(+) - Comp2(-) == 0 -66.152 36.354 -1.820 0.6894
Comp3(-) - Comp2(+) == 0 -40.994 29.098 -1.409 0.9099
Comp3(+) - Comp2(+) == 0 -69.602 16.139 -4.313 <0.01 ***
Comp4(-) - Comp2(+) == 0 22.869 30.241 0.756 0.9988
Comp4(+) - Comp2(+) == 0 -97.571 21.094 -4.626 <0.01 ***
Comp5(-) - Comp2(+) == 0 55.506 43.488 1.276 0.9498
Comp5(+) - Comp2(+) == 0 -102.447 22.955 -4.463 <0.01 ***
Comp3(+) - Comp3(-) == 0 -28.607 30.099 -0.950 0.9932
Comp4(-) - Comp3(-) == 0 63.864 39.497 1.617 0.8153
Comp4(+) - Comp3(-) == 0 -56.577 33.022 -1.713 0.7589
Comp5(-) - Comp3(-) == 0 96.500 50.365 1.916 0.6220
Comp5(+) - Comp3(-) == 0 -61.452 34.241 -1.795 0.7059
Comp4(-) - Comp3(+) == 0 92.471 31.205 2.963 0.0797 .
Comp4(+) - Comp3(+) == 0 -27.970 22.455 -1.246 0.9569
Comp5(-) - Comp3(+) == 0 125.107 44.164 2.833 0.1121
Comp5(+) - Comp3(+) == 0 -32.845 24.212 -1.357 0.9275
Comp4(+) - Comp4(-) == 0 -120.441 34.033 -3.539 0.0135 *
Comp5(-) - Comp4(-) == 0 32.636 51.034 0.639 0.9997
Comp5(+) - Comp4(-) == 0 -125.316 35.217 -3.558 0.0127 *
Comp5(-) - Comp4(+) == 0 153.077 46.205 3.313 0.0282 *
Comp5(+) - Comp4(+) == 0 -4.875 27.761 -0.176 1.0000
Comp5(+) - Comp5(-) == 0 -157.952 47.084 -3.355 0.0250 *

Autumn ETo

Estimate Std. Error t value Pr(>|t|)
Comp1(+) - Comp1(-) == 0 26.6903 18.3876 1.452 0.8938
Comp2(-) - Comp1(-) == 0 56.1093 34.0640 1.647 0.7983
Comp2(+) - Comp1(-) == 0 42.6026 18.0198 2.364 0.3165
Comp3(-) - Comp1(-) == 0 77.2093 31.6773 2.437 0.2744
Comp3(+) - Comp1(-) == 0 -45.8086 19.6735 -2.328 0.3376
Comp4(-) - Comp1(-) == 0 8.0275 32.7837 0.245 1.0000
Comp4(+) - Comp1(-) == 0 27.3631 24.1044 1.135 0.9763
Comp5(-) - Comp1(-) == 0 116.0093 45.8452 2.530 0.2268
Comp5(+) - Comp1(-) == 0 35.0188 25.8308 1.356 0.9278
Comp2(-) - Comp1(+) == 0 29.4190 32.5667 0.903 0.9953
Comp2(+) - Comp1(+) == 0 15.9122 14.9982 1.061 0.9851
Comp3(-) - Comp1(+) == 0 50.5190 30.0614 1.681 0.7790
Comp3(+) - Comp1(+) == 0 -72.4989 16.9493 -4.277 <0.01 ***
Comp4(-) - Comp1(+) == 0 -18.6628 31.2251 -0.598 0.9998
Comp4(+) - Comp1(+) == 0 0.6728 21.9375 0.031 1.0000
Comp5(-) - Comp1(+) == 0 89.3190 44.7439 1.996 0.5646
Comp5(+) - Comp1(+) == 0 8.3285 23.8215 0.350 1.0000
Comp2(+) - Comp2(-) == 0 -13.5067 32.3605 -0.417 1.0000
Comp3(-) - Comp2(-) == 0 21.1000 41.5444 0.508 1.0000
Comp3(+) - Comp2(-) == 0 -101.9179 33.3097 -3.060 0.0608 .
Comp4(-) - Comp2(-) == 0 -48.0818 42.3941 -1.134 0.9765
Comp4(+) - Comp2(-) == 0 -28.7462 36.1041 -0.796 0.9982
Comp5(-) - Comp2(-) == 0 59.9000 53.1438 1.127 0.9775
Comp5(+) - Comp2(-) == 0 -21.0905 37.2789 -0.566 0.9999
Comp3(-) - Comp2(+) == 0 34.6067 29.8378 1.160 0.9727
Comp3(+) - Comp2(+) == 0 -88.4111 16.5496 -5.342 <0.01 ***
Comp4(-) - Comp2(+) == 0 -34.5751 31.0099 -1.115 0.9791
Comp4(+) - Comp2(+) == 0 -15.2394 21.6302 -0.705 0.9993
Comp5(-) - Comp2(+) == 0 73.4067 44.5940 1.646 0.7983

Comp5(+) - Comp2(+) == 0 -7.5837 23.5388 -0.322 1.0000
Comp3(+) - Comp3(-) == 0 -123.0179 30.8647 -3.986 <0.01 **
Comp4(-) - Comp3(-) == 0 -69.1818 40.5013 -1.708 0.7621
Comp4(+) - Comp3(-) == 0 -49.8462 33.8615 -1.472 0.8854
Comp5(-) - Comp3(-) == 0 38.8000 51.6465 0.751 0.9989
Comp5(+) - Comp3(-) == 0 -42.1905 35.1115 -1.202 0.9658
Comp4(-) - Comp3(+) == 0 53.8360 31.9992 1.682 0.7773
Comp4(+) - Comp3(+) == 0 73.1717 23.0260 3.178 0.0438 *
Comp5(-) - Comp3(+) == 0 161.8179 45.2875 3.573 0.0122 *
Comp5(+) - Comp3(+) == 0 80.8274 24.8276 3.256 0.0348 *
Comp4(+) - Comp4(-) == 0 19.3357 34.8988 0.554 0.9999
Comp5(-) - Comp4(-) == 0 107.9818 52.3324 2.063 0.5161
Comp5(+) - Comp4(-) == 0 26.9913 36.1128 0.747 0.9989
Comp5(-) - Comp4(+) == 0 88.6462 47.3807 1.871 0.6538
Comp5(+) - Comp4(+) == 0 7.6557 28.4672 0.269 1.0000
Comp5(+) - Comp5(-) == 0 -80.9905 48.2819 -1.677 0.7804

Annual climate balance

Estimate Std. Error t value Pr(>|t|)
Comp1(+) - Comp1(-) == 0 -55.4133 17.5807 -3.152 0.0462 *
Comp2(-) - Comp1(-) == 0 -58.1070 32.5693 -1.784 0.7131
Comp2(+) - Comp1(-) == 0 -67.1654 17.2291 -3.898 <0.01 **
Comp3(-) - Comp1(-) == 0 -60.8236 30.2873 -2.008 0.5559
Comp3(+) - Comp1(-) == 0 52.2359 18.8102 2.777 0.1291
Comp4(-) - Comp1(-) == 0 -70.0888 31.3452 -2.236 0.3967
Comp4(+) - Comp1(-) == 0 -55.8685 23.0467 -2.424 0.2832
Comp5(-) - Comp1(-) == 0 -121.7070 43.8335 -2.777 0.1289
Comp5(+) - Comp1(-) == 0 -59.1451 24.6974 -2.395 0.2992
Comp2(-) - Comp1(+) == 0 -2.6937 31.1377 -0.087 1.0000
Comp2(+) - Comp1(+) == 0 -11.7521 14.3400 -0.820 0.9978
Comp3(-) - Comp1(+) == 0 -5.4103 28.7423 -0.188 1.0000
Comp3(+) - Comp1(+) == 0 107.6492 16.2055 6.643 <0.01 ***
Comp4(-) - Comp1(+) == 0 -14.6755 29.8549 -0.492 1.0000
Comp4(+) - Comp1(+) == 0 -0.4552 20.9749 -0.022 1.0000
Comp5(-) - Comp1(+) == 0 -66.2937 42.7805 -1.550 0.8504
Comp5(+) - Comp1(+) == 0 -3.7318 22.7762 -0.164 1.0000
Comp2(+) - Comp2(-) == 0 -9.0584 30.9405 -0.293 1.0000
Comp3(-) - Comp2(-) == 0 -2.7167 39.7215 -0.068 1.0000
Comp3(+) - Comp2(-) == 0 110.3429 31.8480 3.465 0.0172 *
Comp4(-) - Comp2(-) == 0 -11.9818 40.5338 -0.296 1.0000
Comp4(+) - Comp2(-) == 0 2.2385 34.5199 0.065 1.0000
Comp5(-) - Comp2(-) == 0 -63.6000 50.8119 -1.252 0.9555
Comp5(+) - Comp2(-) == 0 -1.0381 35.6431 -0.029 1.0000
Comp3(-) - Comp2(+) == 0 6.3418 28.5285 0.222 1.0000
Comp3(+) - Comp2(+) == 0 119.4013 15.8234 7.546 <0.01 ***
Comp4(-) - Comp2(+) == 0 -2.9234 29.6492 -0.099 1.0000
Comp4(+) - Comp2(+) == 0 11.2969 20.6810 0.546 0.9999
Comp5(-) - Comp2(+) == 0 -54.5416 42.6372 -1.279 0.9491
Comp5(+) - Comp2(+) == 0 8.0203 22.5059 0.356 1.0000
Comp3(+) - Comp3(-) == 0 113.0595 29.5103 3.831 <0.01 **
Comp4(-) - Comp3(-) == 0 -9.2652 38.7241 -0.239 1.0000
Comp4(+) - Comp3(-) == 0 4.9551 32.3757 0.153 1.0000
Comp5(-) - Comp3(-) == 0 -60.8833 49.3802 -1.233 0.9596
Comp5(+) - Comp3(-) == 0 1.6786 33.5708 0.050 1.0000
Comp4(-) - Comp3(+) == 0 -122.3247 30.5951 -3.998 <0.01 **
Comp4(+) - Comp3(+) == 0 -108.1044 22.0156 -4.910 <0.01 ***
Comp5(-) - Comp3(+) == 0 -173.9429 43.3002 -4.017 <0.01 **
Comp5(+) - Comp3(+) == 0 -111.3810 23.7381 -4.692 <0.01 ***
Comp4(+) - Comp4(-) == 0 14.2203 33.3674 0.426 1.0000

Comp5(-) - Comp4(-) == 0 -51.6182   50.0361 -1.032   0.9878
Comp5(+) - Comp4(-) == 0   10.9437   34.5282   0.317   1.0000
Comp5(-) - Comp4(+) == 0 -65.8385   45.3016 -1.453   0.8930
Comp5(+) - Comp4(+) == 0   -3.2766   27.2181 -0.120   1.0000
Comp5(+) - Comp5(-) == 0   62.5619   46.1633   1.355   0.9280

Winter climate balance

	Estimate	Std. Error	t value	Pr(>|t|)	
Comp1(+) - Comp1(-) == 0	-9.711	16.575	-0.586	0.99985	
Comp2(-) - Comp1(-) == 0	2.663	30.706	0.087	1.00000	
Comp2(+) - Comp1(-) == 0	-96.084	16.243	-5.915	< 0.001	***
Comp3(-) - Comp1(-) == 0	-4.421	28.555	-0.155	1.00000	
Comp3(+) - Comp1(-) == 0	60.449	17.734	3.409	0.02131	*
Comp4(-) - Comp1(-) == 0	-111.474	29.552	-3.772	0.00616	**
Comp4(+) - Comp1(-) == 0	-1.530	21.728	-0.070	1.00000	
Comp5(-) - Comp1(-) == 0	-59.437	41.326	-1.438	0.89898	
Comp5(+) - Comp1(-) == 0	-16.171	23.284	-0.694	0.99940	
Comp2(-) - Comp1(+) == 0	12.373	29.356	0.421	0.99999	
Comp2(+) - Comp1(+) == 0	-86.374	13.520	-6.389	< 0.001	***
Comp3(-) - Comp1(+) == 0	5.290	27.098	0.195	1.00000	
Comp3(+) - Comp1(+) == 0	70.159	15.278	4.592	< 0.001	***
Comp4(-) - Comp1(+) == 0	-101.763	28.147	-3.615	0.01059	*
Comp4(+) - Comp1(+) == 0	8.181	19.775	0.414	0.99999	
Comp5(-) - Comp1(+) == 0	-49.727	40.333	-1.233	0.95955	
Comp5(+) - Comp1(+) == 0	-6.460	21.473	-0.301	1.00000	
Comp2(+) - Comp2(-) == 0	-98.747	29.170	-3.385	0.02312	*
Comp3(-) - Comp2(-) == 0	-7.083	37.449	-0.189	1.00000	
Comp3(+) - Comp2(-) == 0	57.786	30.026	1.925	0.61608	
Comp4(-) - Comp2(-) == 0	-114.136	38.215	-2.987	0.07527	.
Comp4(+) - Comp2(-) == 0	-4.192	32.545	-0.129	1.00000	
Comp5(-) - Comp2(-) == 0	-62.100	47.905	-1.296	0.94481	
Comp5(+) - Comp2(-) == 0	-18.833	33.604	-0.560	0.99990	
Comp3(-) - Comp2(+) == 0	91.664	26.896	3.408	0.02114	*
Comp3(+) - Comp2(+) == 0	156.533	14.918	10.493	< 0.001	***
Comp4(-) - Comp2(+) == 0	-15.389	27.953	-0.551	0.99991	
Comp4(+) - Comp2(+) == 0	94.555	19.498	4.850	< 0.001	***
Comp5(-) - Comp2(+) == 0	36.647	40.198	0.912	0.99502	
Comp5(+) - Comp2(+) == 0	79.914	21.218	3.766	0.00602	**
Comp3(+) - Comp3(-) == 0	64.869	27.822	2.332	0.33539	
Comp4(-) - Comp3(-) == 0	-107.053	36.509	-2.932	0.08625	.
Comp4(+) - Comp3(-) == 0	2.891	30.523	0.095	1.00000	
Comp5(-) - Comp3(-) == 0	-55.017	46.555	-1.182	0.96916	
Comp5(+) - Comp3(-) == 0	-11.750	31.650	-0.371	1.00000	
Comp4(-) - Comp3(+) == 0	-171.922	28.845	-5.960	< 0.001	***
Comp4(+) - Comp3(+) == 0	-61.978	20.756	-2.986	0.07465	.
Comp5(-) - Comp3(+) == 0	-119.886	40.823	-2.937	0.08520	.
Comp5(+) - Comp3(+) == 0	-76.619	22.380	-3.424	0.02015	*
Comp4(+) - Comp4(-) == 0	109.944	31.458	3.495	0.01575	*
Comp5(-) - Comp4(-) == 0	52.036	47.174	1.103	0.98049	
Comp5(+) - Comp4(-) == 0	95.303	32.553	2.928	0.08711	.
Comp5(-) - Comp4(+) == 0	-57.908	42.710	-1.356	0.92760	
Comp5(+) - Comp4(+) == 0	-14.641	25.661	-0.571	0.99988	
Comp5(+) - Comp5(-) == 0	43.267	43.522	0.994	0.99060	

Spring climate balance

	Estimate	Std. Error	t value	Pr(>|t|)
Comp1(+) - Comp1(-) == 0	-25.316	17.662	-1.433	0.901
Comp2(-) - Comp1(-) == 0	14.540	32.719	0.444	1.000

Comp2(+) - Comp1(-) == 0 -20.535 17.308 -1.186 0.968
Comp3(-) - Comp1(-) == 0 -48.527 30.427 -1.595 0.827
Comp3(+) - Comp1(-) == 0 94.640 18.897 5.008 <0.01 ***
Comp4(-) - Comp1(-) == 0 10.049 31.490 0.319 1.000
Comp4(+) - Comp1(-) == 0 -13.860 23.153 -0.599 1.000
Comp5(-) - Comp1(-) == 0 -4.460 44.036 -0.101 1.000
Comp5(+) - Comp1(-) == 0 -42.384 24.811 -1.708 0.762
Comp2(-) - Comp1(+) == 0 39.856 31.281 1.274 0.950
Comp2(+) - Comp1(+) == 0 4.782 14.406 0.332 1.000
Comp3(-) - Comp1(+) == 0 -23.211 28.875 -0.804 0.998
Comp3(+) - Comp1(+) == 0 119.956 16.280 7.368 <0.01 ***
Comp4(-) - Comp1(+) == 0 35.365 29.993 1.179 0.970
Comp4(+) - Comp1(+) == 0 11.456 21.072 0.544 1.000
Comp5(-) - Comp1(+) == 0 20.856 42.978 0.485 1.000
Comp5(+) - Comp1(+) == 0 -17.068 22.881 -0.746 0.999
Comp2(+) - Comp2(-) == 0 -35.074 31.083 -1.128 0.977
Comp3(-) - Comp2(-) == 0 -63.067 39.905 -1.580 0.835
Comp3(+) - Comp2(-) == 0 80.100 31.995 2.504 0.240
Comp4(-) - Comp2(-) == 0 -4.491 40.721 -0.110 1.000
Comp4(+) - Comp2(-) == 0 -28.400 34.679 -0.819 0.998
Comp5(-) - Comp2(-) == 0 -19.000 51.046 -0.372 1.000
Comp5(+) - Comp2(-) == 0 -56.924 35.807 -1.590 0.830
Comp3(-) - Comp2(+) == 0 -27.993 28.660 -0.977 0.992
Comp3(+) - Comp2(+) == 0 115.174 15.896 7.245 <0.01 ***
Comp4(-) - Comp2(+) == 0 30.583 29.786 1.027 0.988
Comp4(+) - Comp2(+) == 0 6.674 20.776 0.321 1.000
Comp5(-) - Comp2(+) == 0 16.074 42.834 0.375 1.000
Comp5(+) - Comp2(+) == 0 -21.850 22.610 -0.966 0.992
Comp3(+) - Comp3(-) == 0 143.167 29.646 4.829 <0.01 ***
Comp4(-) - Comp3(-) == 0 58.576 38.903 1.506 0.871
Comp4(+) - Comp3(-) == 0 34.667 32.525 1.066 0.985
Comp5(-) - Comp3(-) == 0 44.067 49.608 0.888 0.996
Comp5(+) - Comp3(-) == 0 6.143 33.725 0.182 1.000
Comp4(-) - Comp3(+) == 0 -84.591 30.736 -2.752 0.136
Comp4(+) - Comp3(+) == 0 -108.500 22.117 -4.906 <0.01 ***
Comp5(-) - Comp3(+) == 0 -99.100 43.500 -2.278 0.369
Comp5(+) - Comp3(+) == 0 -137.024 23.848 -5.746 <0.01 ***
Comp4(+) - Comp4(-) == 0 -23.909 33.521 -0.713 0.999
Comp5(-) - Comp4(-) == 0 -14.509 50.267 -0.289 1.000
Comp5(+) - Comp4(-) == 0 -52.433 34.687 -1.512 0.868
Comp5(-) - Comp4(+) == 0 9.400 45.510 0.207 1.000
Comp5(+) - Comp4(+) == 0 -28.524 27.344 -1.043 0.987
Comp5(+) - Comp5(-) == 0 -37.924 46.376 -0.818 0.998

Summer climate balance

Estimate Std. Error t value Pr(>|t|)
Comp1(+) - Comp1(-) == 0 -22.994 18.929 -1.215 0.9632
Comp2(-) - Comp1(-) == 0 17.351 35.067 0.495 1.0000
Comp2(+) - Comp1(-) == 0 25.089 18.551 1.352 0.9289
Comp3(-) - Comp1(-) == 0 27.318 32.610 0.838 0.9974
Comp3(+) - Comp1(-) == 0 -1.956 20.253 -0.097 1.0000
Comp4(-) - Comp1(-) == 0 80.015 33.749 2.371 0.3120
Comp4(+) - Comp1(-) == 0 -32.772 24.814 -1.321 0.9384
Comp5(-) - Comp1(-) == 0 46.851 47.196 0.993 0.9907
Comp5(+) - Comp1(-) == 0 -14.920 26.592 -0.561 0.9999
Comp2(-) - Comp1(+) == 0 40.346 33.526 1.203 0.9654
Comp2(+) - Comp1(+) == 0 48.084 15.440 3.114 0.0524 .
Comp3(-) - Comp1(+) == 0 50.312 30.947 1.626 0.8102
Comp3(+) - Comp1(+) == 0 21.038 17.449 1.206 0.9650

Comp4(-) - Comp1(+) == 0 103.009 32.145 3.205 0.0388 *
Comp4(+) - Comp1(+) == 0 -9.778 22.584 -0.433 1.0000
Comp5(-) - Comp1(+) == 0 69.846 46.062 1.516 0.8659
Comp5(+) - Comp1(+) == 0 8.074 24.523 0.329 1.0000
Comp2(+) - Comp2(-) == 0 7.738 33.314 0.232 1.0000
Comp3(-) - Comp2(-) == 0 9.967 42.768 0.233 1.0000
Comp3(+) - Comp2(-) == 0 -19.307 34.291 -0.563 0.9999
Comp4(-) - Comp2(-) == 0 62.664 43.643 1.436 0.9000
Comp4(+) - Comp2(-) == 0 -50.123 37.168 -1.349 0.9301
Comp5(-) - Comp2(-) == 0 29.500 54.709 0.539 0.9999
Comp5(+) - Comp2(-) == 0 -32.271 38.377 -0.841 0.9973
Comp3(-) - Comp2(+) == 0 2.228 30.717 0.073 1.0000
Comp3(+) - Comp2(+) == 0 -27.045 17.037 -1.587 0.8310
Comp4(-) - Comp2(+) == 0 54.925 31.923 1.721 0.7537
Comp4(+) - Comp2(+) == 0 -57.861 22.267 -2.598 0.1963
Comp5(-) - Comp2(+) == 0 21.762 45.908 0.474 1.0000
Comp5(+) - Comp2(+) == 0 -40.010 24.232 -1.651 0.7963
Comp3(+) - Comp3(-) == 0 -29.274 31.774 -0.921 0.9946
Comp4(-) - Comp3(-) == 0 52.697 41.694 1.264 0.9528
Comp4(+) - Comp3(-) == 0 -60.090 34.859 -1.724 0.7519
Comp5(-) - Comp3(-) == 0 19.533 53.168 0.367 1.0000
Comp5(+) - Comp3(-) == 0 -42.238 36.146 -1.169 0.9714
Comp4(-) - Comp3(+) == 0 81.971 32.942 2.488 0.2466
Comp4(+) - Comp3(+) == 0 -30.816 23.704 -1.300 0.9436
Comp5(-) - Comp3(+) == 0 48.807 46.622 1.047 0.9864
Comp5(+) - Comp3(+) == 0 -12.964 25.559 -0.507 1.0000
Comp4(+) - Comp4(-) == 0 -112.787 35.927 -3.139 0.0486 *
Comp5(-) - Comp4(-) == 0 -33.164 53.874 -0.616 0.9998
Comp5(+) - Comp4(-) == 0 -94.935 37.177 -2.554 0.2168
Comp5(-) - Comp4(+) == 0 79.623 48.776 1.632 0.8067
Comp5(+) - Comp4(+) == 0 17.852 29.306 0.609 0.9998
Comp5(+) - Comp5(-) == 0 -61.771 49.704 -1.243 0.9574

Autumn climate balance

	Estimate	Std. Error	t value	Pr(>|t|)	
Comp1(+) - Comp1(-) == 0	-40.3441	17.2915	-2.333	0.3352	
Comp2(-) - Comp1(-) == 0	7.9837	32.0335	0.249	1.0000	
Comp2(+) - Comp1(-) == 0	-103.2736	16.9457	-6.094	<0.01	***
Comp3(-) - Comp1(-) == 0	-48.7829	29.7891	-1.638	0.8035	
Comp3(+) - Comp1(-) == 0	21.1694	18.5008	1.144	0.9751	
Comp4(-) - Comp1(-) == 0	-129.2981	30.8296	-4.194	<0.01	**
Comp4(+) - Comp1(-) == 0	-31.6547	22.6675	-1.396	0.9145	
Comp5(-) - Comp1(-) == 0	-71.9163	43.1124	-1.668	0.7860	
Comp5(+) - Comp1(-) == 0	0.3123	24.2911	0.013	1.0000	
Comp2(-) - Comp1(+) == 0	48.3278	30.6254	1.578	0.8359	
Comp2(+) - Comp1(+) == 0	-62.9295	14.1042	-4.462	<0.01	***
Comp3(-) - Comp1(+) == 0	-8.4388	28.2695	-0.299	1.0000	
Comp3(+) - Comp1(+) == 0	61.5136	15.9390	3.859	<0.01	**
Comp4(-) - Comp1(+) == 0	-88.9540	29.3638	-3.029	0.0660	.
Comp4(+) - Comp1(+) == 0	8.6894	20.6298	0.421	1.0000	
Comp5(-) - Comp1(+) == 0	-31.5722	42.0767	-0.750	0.9989	
Comp5(+) - Comp1(+) == 0	40.6564	22.4015	1.815	0.6919	
Comp2(+) - Comp2(-) == 0	-111.2573	30.4315	-3.656	<0.01	**
Comp3(-) - Comp2(-) == 0	-56.7667	39.0680	-1.453	0.8933	
Comp3(+) - Comp2(-) == 0	13.1857	31.3241	0.421	1.0000	
Comp4(-) - Comp2(-) == 0	-137.2818	39.8671	-3.443	0.0191	*
Comp4(+) - Comp2(-) == 0	-39.6385	33.9520	-1.167	0.9716	
Comp5(-) - Comp2(-) == 0	-79.9000	49.9760	-1.599	0.8253	
Comp5(+) - Comp2(-) == 0	-7.6714	35.0568	-0.219	1.0000	

Comp3(-) - Comp2(+) == 0 54.4906 28.0592 1.942 0.6034
Comp3(+) - Comp2(+) == 0 124.4430 15.5631 7.996 <0.01 ***
Comp4(-) - Comp2(+) == 0 -26.0245 29.1615 -0.892 0.9957
Comp4(+) - Comp2(+) == 0 71.6188 20.3408 3.521 0.0146 *
Comp5(-) - Comp2(+) == 0 31.3573 41.9358 0.748 0.9989
Comp5(+) - Comp2(+) == 0 103.5859 22.1357 4.680 <0.01 ***
Comp3(+) - Comp3(-) == 0 69.9524 29.0249 2.410 0.2895
Comp4(-) - Comp3(-) == 0 -80.5152 38.0871 -2.114 0.4807
Comp4(+) - Comp3(-) == 0 17.1282 31.8431 0.538 0.9999
Comp5(-) - Comp3(-) == 0 -23.1333 48.5679 -0.476 1.0000
Comp5(+) - Comp3(-) == 0 49.0952 33.0185 1.487 0.8793
Comp4(-) - Comp3(+) == 0 -150.4675 30.0918 -5.000 <0.01 ***
Comp4(+) - Comp3(+) == 0 -52.8242 21.6535 -2.440 0.2738
Comp5(-) - Comp3(+) == 0 -93.0857 42.5880 -2.186 0.4310
Comp5(+) - Comp3(+) == 0 -20.8571 23.3476 -0.893 0.9957
Comp4(+) - Comp4(-) == 0 97.6434 32.8185 2.975 0.0772 .
Comp5(-) - Comp4(-) == 0 57.3818 49.2130 1.166 0.9718
Comp5(+) - Comp4(-) == 0 129.6104 33.9602 3.817 <0.01 **
Comp5(-) - Comp4(+) == 0 -40.2615 44.5564 -0.904 0.9953
Comp5(+) - Comp4(+) == 0 31.9670 26.7703 1.194 0.9670
Comp5(+) - Comp5(-) == 0 72.2286 45.4039 1.591 0.8289

Winter NDVI

Estimate Std. Error t value Pr(>|t|)
Comp1(+) - Comp1(-) == 0 -3.726 18.829 -0.198 1.0000
Comp2(-) - Comp1(-) == 0 -59.753 34.882 -1.713 0.7587
Comp2(+) - Comp1(-) == 0 -39.223 18.453 -2.126 0.4718
Comp3(-) - Comp1(-) == 0 -15.870 32.438 -0.489 1.0000
Comp3(+) - Comp1(-) == 0 -41.078 20.146 -2.039 0.5336
Comp4(-) - Comp1(-) == 0 -62.135 33.571 -1.851 0.6675
Comp4(+) - Comp1(-) == 0 6.354 24.683 0.257 1.0000
Comp5(-) - Comp1(-) == 0 -112.753 46.946 -2.402 0.2952
Comp5(+) - Comp1(-) == 0 35.999 26.451 1.361 0.9263
Comp2(-) - Comp1(+) == 0 -56.028 33.349 -1.680 0.7788
Comp2(+) - Comp1(+) == 0 -35.498 15.358 -2.311 0.3484
Comp3(-) - Comp1(+) == 0 -12.145 30.783 -0.395 1.0000
Comp3(+) - Comp1(+) == 0 -37.353 17.356 -2.152 0.4541
Comp4(-) - Comp1(+) == 0 -58.410 31.975 -1.827 0.6845
Comp4(+) - Comp1(+) == 0 10.080 22.464 0.449 1.0000
Comp5(-) - Comp1(+) == 0 -109.028 45.819 -2.380 0.3074
Comp5(+) - Comp1(+) == 0 39.725 24.394 1.628 0.8087
Comp2(+) - Comp2(-) == 0 20.530 33.138 0.620 0.9998
Comp3(-) - Comp2(-) == 0 43.883 42.542 1.032 0.9878
Comp3(+) - Comp2(-) == 0 18.675 34.110 0.547 0.9999
Comp4(-) - Comp2(-) == 0 -2.382 43.412 -0.055 1.0000
Comp4(+) - Comp2(-) == 0 66.108 36.971 1.788 0.7105
Comp5(-) - Comp2(-) == 0 -53.000 54.420 -0.974 0.9919
Comp5(+) - Comp2(-) == 0 95.752 38.174 2.508 0.2375
Comp3(-) - Comp2(+) == 0 23.353 30.555 0.764 0.9987
Comp3(+) - Comp2(+) == 0 -1.855 16.947 -0.109 1.0000
Comp4(-) - Comp2(+) == 0 -22.912 31.755 -0.722 0.9992
Comp4(+) - Comp2(+) == 0 45.577 22.150 2.058 0.5198
Comp5(-) - Comp2(+) == 0 -73.530 45.665 -1.610 0.8191
Comp5(+) - Comp2(+) == 0 75.222 24.104 3.121 0.0514 .
Comp3(+) - Comp3(-) == 0 -25.208 31.606 -0.798 0.9982
Comp4(-) - Comp3(-) == 0 -46.265 41.474 -1.116 0.9790
Comp4(+) - Comp3(-) == 0 22.224 34.675 0.641 0.9997
Comp5(-) - Comp3(-) == 0 -96.883 52.887 -1.832 0.6805
Comp5(+) - Comp3(-) == 0 51.869 35.955 1.443 0.8973

Comp4(-) - Comp3(+) == 0 -21.057 32.768 -0.643 0.9997
Comp4(+) - Comp3(+) == 0 47.433 23.579 2.012 0.5536
Comp5(-) - Comp3(+) == 0 -71.675 46.375 -1.546 0.8519
Comp5(+) - Comp3(+) == 0 77.077 25.424 3.032 0.0663 .
Comp4(+) - Comp4(-) == 0 68.490 35.737 1.916 0.6215
Comp5(-) - Comp4(-) == 0 -50.618 53.590 -0.945 0.9935
Comp5(+) - Comp4(-) == 0 98.134 36.980 2.654 0.1728
Comp5(-) - Comp4(+) == 0 -119.108 48.519 -2.455 0.2652
Comp5(+) - Comp4(+) == 0 29.645 29.151 1.017 0.9889
Comp5(+) - Comp5(-) == 0 148.752 49.442 3.009 0.0698 .

Spring NDVI

Estimate Std. Error t value Pr(>|t|)
Comp1(+) - Comp1(-) == 0 1.638e+01 1.900e+01 0.862 0.9967
Comp2(-) - Comp1(-) == 0 -3.098e+01 3.520e+01 -0.880 0.9962
Comp2(+) - Comp1(-) == 0 -1.688e+01 1.862e+01 -0.907 0.9952
Comp3(-) - Comp1(-) == 0 -3.165e+00 3.274e+01 -0.097 1.0000
Comp3(+) - Comp1(-) == 0 -1.017e+01 2.033e+01 -0.500 1.0000
Comp4(-) - Comp1(-) == 0 -4.595e+01 3.388e+01 -1.356 0.9278
Comp4(+) - Comp1(-) == 0 1.638e+01 2.491e+01 0.658 0.9996
Comp5(-) - Comp1(-) == 0 -1.066e+02 4.738e+01 -2.250 0.3880
Comp5(+) - Comp1(-) == 0 4.789e+01 2.670e+01 1.794 0.7064
Comp2(-) - Comp1(+) == 0 -4.736e+01 3.366e+01 -1.407 0.9106
Comp2(+) - Comp1(+) == 0 -3.327e+01 1.550e+01 -2.146 0.4572
Comp3(-) - Comp1(+) == 0 -1.955e+01 3.107e+01 -0.629 0.9997
Comp3(+) - Comp1(+) == 0 -2.655e+01 1.752e+01 -1.516 0.8662
Comp4(-) - Comp1(+) == 0 -6.233e+01 3.227e+01 -1.931 0.6108
Comp4(+) - Comp1(+) == 0 -4.869e-04 2.267e+01 0.000 1.0000
Comp5(-) - Comp1(+) == 0 -1.230e+02 4.624e+01 -2.659 0.1708
Comp5(+) - Comp1(+) == 0 3.151e+01 2.462e+01 1.280 0.9488
Comp2(+) - Comp2(-) == 0 1.410e+01 3.344e+01 0.422 1.0000
Comp3(-) - Comp2(-) == 0 2.782e+01 4.293e+01 0.648 0.9997
Comp3(+) - Comp2(-) == 0 2.081e+01 3.442e+01 0.605 0.9998
Comp4(-) - Comp2(-) == 0 -1.496e+01 4.381e+01 -0.342 1.0000
Comp4(+) - Comp2(-) == 0 4.736e+01 3.731e+01 1.269 0.9514
Comp5(-) - Comp2(-) == 0 -7.560e+01 5.492e+01 -1.376 0.9212
Comp5(+) - Comp2(-) == 0 7.888e+01 3.853e+01 2.047 0.5289
Comp3(-) - Comp2(+) == 0 1.372e+01 3.084e+01 0.445 1.0000
Comp3(+) - Comp2(+) == 0 6.714e+00 1.710e+01 0.393 1.0000
Comp4(-) - Comp2(+) == 0 -2.906e+01 3.205e+01 -0.907 0.9952
Comp4(+) - Comp2(+) == 0 3.326e+01 2.235e+01 1.488 0.8786
Comp5(-) - Comp2(+) == 0 -8.970e+01 4.609e+01 -1.946 0.6003
Comp5(+) - Comp2(+) == 0 6.478e+01 2.433e+01 2.663 0.1700
Comp3(+) - Comp3(-) == 0 -7.006e+00 3.190e+01 -0.220 1.0000
Comp4(-) - Comp3(-) == 0 -4.278e+01 4.186e+01 -1.022 0.9885
Comp4(+) - Comp3(-) == 0 1.954e+01 3.499e+01 0.559 0.9999
Comp5(-) - Comp3(-) == 0 -1.034e+02 5.337e+01 -1.938 0.6067
Comp5(+) - Comp3(-) == 0 5.106e+01 3.629e+01 1.407 0.9106
Comp4(-) - Comp3(+) == 0 -3.577e+01 3.307e+01 -1.082 0.9829
Comp4(+) - Comp3(+) == 0 2.655e+01 2.380e+01 1.116 0.9789
Comp5(-) - Comp3(+) == 0 -9.641e+01 4.680e+01 -2.060 0.5188
Comp5(+) - Comp3(+) == 0 5.807e+01 2.566e+01 2.263 0.3796
Comp4(+) - Comp4(-) == 0 6.233e+01 3.607e+01 1.728 0.7494
Comp5(-) - Comp4(-) == 0 -6.064e+01 5.408e+01 -1.121 0.9783
Comp5(+) - Comp4(-) == 0 9.384e+01 3.732e+01 2.514 0.2346
Comp5(-) - Comp4(+) == 0 -1.230e+02 4.897e+01 -2.511 0.2356
Comp5(+) - Comp4(+) == 0 3.151e+01 2.942e+01 1.071 0.9840
Comp5(+) - Comp5(-) == 0 1.545e+02 4.990e+01 3.096 0.0546 .

Summer NDVI

	Estimate	Std. Error	t value	Pr(>|t|)	
Comp1(+) - Comp1(-) == 0	49.5602	19.1081	2.594	0.199	
Comp2(-) - Comp1(-) == 0	55.7349	35.3989	1.574	0.838	
Comp2(+) - Comp1(-) == 0	49.9506	18.7260	2.667	0.168	
Comp3(-) - Comp1(-) == 0	16.2849	32.9187	0.495	1.000	
Comp3(+) - Comp1(-) == 0	73.8385	20.4445	3.612	0.011	*
Comp4(-) - Comp1(-) == 0	53.4440	34.0685	1.569	0.840	
Comp4(+) - Comp1(-) == 0	52.1118	25.0490	2.080	0.504	
Comp5(-) - Comp1(-) == 0	6.9349	47.6417	0.146	1.000	
Comp5(+) - Comp1(-) == 0	46.5825	26.8431	1.735	0.745	
Comp2(-) - Comp1(+) == 0	6.1747	33.8429	0.182	1.000	
Comp2(+) - Comp1(+) == 0	0.3904	15.5859	0.025	1.000	
Comp3(-) - Comp1(+) == 0	-33.2753	31.2394	-1.065	0.985	
Comp3(+) - Comp1(+) == 0	24.2783	17.6135	1.378	0.921	
Comp4(-) - Comp1(+) == 0	3.8838	32.4487	0.120	1.000	
Comp4(+) - Comp1(+) == 0	2.5516	22.7972	0.112	1.000	
Comp5(-) - Comp1(+) == 0	-42.6253	46.4972	-0.917	0.995	
Comp5(+) - Comp1(+) == 0	-2.9777	24.7550	-0.120	1.000	
Comp2(+) - Comp2(-) == 0	-5.7843	33.6286	-0.172	1.000	
Comp3(-) - Comp2(-) == 0	-39.4500	43.1725	-0.914	0.995	
Comp3(+) - Comp2(-) == 0	18.1036	34.6150	0.523	1.000	
Comp4(-) - Comp2(-) == 0	-2.2909	44.0554	-0.052	1.000	
Comp4(+) - Comp2(-) == 0	-3.6231	37.5190	-0.097	1.000	
Comp5(-) - Comp2(-) == 0	-48.8000	55.2264	-0.884	0.996	
Comp5(+) - Comp2(-) == 0	-9.1524	38.7398	-0.236	1.000	
Comp3(-) - Comp2(+) == 0	-33.6657	31.0071	-1.086	0.983	
Comp3(+) - Comp2(+) == 0	23.8878	17.1981	1.389	0.917	
Comp4(-) - Comp2(+) == 0	3.4934	32.2251	0.108	1.000	
Comp4(+) - Comp2(+) == 0	2.1612	22.4778	0.096	1.000	
Comp5(-) - Comp2(+) == 0	-43.0157	46.3415	-0.928	0.994	
Comp5(+) - Comp2(+) == 0	-3.3681	24.4612	-0.138	1.000	
Comp3(+) - Comp3(-) == 0	57.5536	32.0742	1.794	0.707	
Comp4(-) - Comp3(-) == 0	37.1591	42.0885	0.883	0.996	
Comp4(+) - Comp3(-) == 0	35.8269	35.1885	1.018	0.989	
Comp5(-) - Comp3(-) == 0	-9.3500	53.6704	-0.174	1.000	
Comp5(+) - Comp3(-) == 0	30.2976	36.4874	0.830	0.998	
Comp4(-) - Comp3(+) == 0	-20.3945	33.2532	-0.613	1.000	
Comp4(+) - Comp3(+) == 0	-21.7266	23.9283	-0.908	0.995	
Comp5(-) - Comp3(+) == 0	-66.9036	47.0622	-1.422	0.906	
Comp5(+) - Comp3(+) == 0	-27.2560	25.8005	-1.056	0.986	
Comp4(+) - Comp4(-) == 0	-1.3322	36.2664	-0.037	1.000	
Comp5(-) - Comp4(-) == 0	-46.5091	54.3832	-0.855	0.997	
Comp5(+) - Comp4(-) == 0	-6.8615	37.5280	-0.183	1.000	
Comp5(-) - Comp4(+) == 0	-45.1769	49.2374	-0.918	0.995	
Comp5(+) - Comp4(+) == 0	-5.5293	29.5828	-0.187	1.000	
Comp5(+) - Comp5(-) == 0	39.6476	50.1739	0.790	0.998	

Autumn NDVI

	Estimate	Std. Error	t value	Pr(>|t|)
Comp1(+) - Comp1(-) == 0	37.42685	19.12369	1.957	0.594
Comp2(-) - Comp1(-) == 0	10.12558	35.42772	0.286	1.000
Comp2(+) - Comp1(-) == 0	10.10086	18.74119	0.539	1.000
Comp3(-) - Comp1(-) == 0	11.32558	32.94549	0.344	1.000
Comp3(+) - Comp1(-) == 0	39.84344	20.46109	1.947	0.600
Comp4(-) - Comp1(-) == 0	-5.03805	34.09619	-0.148	1.000
Comp4(+) - Comp1(-) == 0	44.09481	25.06935	1.759	0.730
Comp5(-) - Comp1(-) == 0	-55.47442	47.68051	-1.163	0.972

Comp5(+) - Comp1(-) == 0 59.46844 26.86492 2.214 0.411
Comp2(-) - Comp1(+) == 0 -27.30127 33.87045 -0.806 0.998
Comp2(+) - Comp1(+) == 0 -27.32598 15.59860 -1.752 0.735
Comp3(-) - Comp1(+) == 0 -26.10127 31.26483 -0.835 0.997
Comp3(+) - Comp1(+) == 0 2.41659 17.62783 0.137 1.000
Comp4(-) - Comp1(+) == 0 -42.46490 32.47513 -1.308 0.942
Comp4(+) - Comp1(+) == 0 6.66796 22.81571 0.292 1.000
Comp5(-) - Comp1(+) == 0 -92.90127 46.53509 -1.996 0.564
Comp5(+) - Comp1(+) == 0 22.04159 24.77515 0.890 0.996
Comp2(+) - Comp2(-) == 0 -0.02472 33.65597 -0.001 1.000
Comp3(-) - Comp2(-) == 0 1.20000 43.20761 0.028 1.000
Comp3(+) - Comp2(-) == 0 29.71786 34.64316 0.858 0.997
Comp4(-) - Comp2(-) == 0 -15.16364 44.09129 -0.344 1.000
Comp4(+) - Comp2(-) == 0 33.96923 37.54949 0.905 0.995
Comp5(-) - Comp2(-) == 0 -65.60000 55.27136 -1.187 0.968
Comp5(+) - Comp2(-) == 0 49.34286 38.77133 1.273 0.951
Comp3(-) - Comp2(+) == 0 1.22472 31.03234 0.039 1.000
Comp3(+) - Comp2(+) == 0 29.74258 17.21213 1.728 0.750
Comp4(-) - Comp2(+) == 0 -15.13892 32.25137 -0.469 1.000
Comp4(+) - Comp2(+) == 0 33.99395 22.49608 1.511 0.868
Comp5(-) - Comp2(+) == 0 -65.57528 46.37922 -1.414 0.908
Comp5(+) - Comp2(+) == 0 49.36758 24.48112 2.017 0.549
Comp3(+) - Comp3(-) == 0 28.51786 32.10032 0.888 0.996
Comp4(-) - Comp3(-) == 0 -16.36364 42.12273 -0.388 1.000
Comp4(+) - Comp3(-) == 0 32.76923 35.21713 0.930 0.994
Comp5(-) - Comp3(-) == 0 -66.80000 53.71411 -1.244 0.957
Comp5(+) - Comp3(-) == 0 48.14286 36.51709 1.318 0.939
Comp4(-) - Comp3(+) == 0 -44.88149 33.28025 -1.349 0.930
Comp4(+) - Comp3(+) == 0 4.25137 23.94781 0.178 1.000
Comp5(-) - Comp3(+) == 0 -95.31786 47.10049 -2.024 0.544
Comp5(+) - Comp3(+) == 0 19.62500 25.82148 0.760 0.999
Comp4(+) - Comp4(-) == 0 49.13287 36.29588 1.354 0.929
Comp5(-) - Comp4(-) == 0 -50.43636 54.42747 -0.927 0.994
Comp5(+) - Comp4(-) == 0 64.50649 37.55852 1.717 0.756
Comp5(-) - Comp4(+) == 0 -99.56923 49.27750 -2.021 0.547
Comp5(+) - Comp4(+) == 0 15.37363 29.60684 0.519 1.000
Comp5(+) - Comp5(-) == 0 114.94286 50.21478 2.289 0.362

Average day of the year recording the maximum NDVI

	Estimate	Std. Error	t value	Pr(>|t|)
Comp1(+) - Comp1(-) == 0	-0.21666	0.46668	-0.464	1.0000
Comp2(-) - Comp1(-) == 0	-1.39767	0.86455	-1.617	0.8151
Comp2(+) - Comp1(-) == 0	-0.56284	0.45735	-1.231	0.9600
Comp3(-) - Comp1(-) == 0	-0.94767	0.80398	-1.179	0.9697
Comp3(+) - Comp1(-) == 0	-0.41196	0.49932	-0.825	0.9977
Comp4(-) - Comp1(-) == 0	-0.06131	0.83206	-0.074	1.0000
Comp4(+) - Comp1(-) == 0	-0.15921	0.61177	-0.260	1.0000
Comp5(-) - Comp1(-) == 0	-0.69767	1.16356	-0.600	0.9998
Comp5(+) - Comp1(-) == 0	1.30233	0.65559	1.986	0.5715
Comp2(-) - Comp1(+) == 0	-1.18101	0.82655	-1.429	0.9027
Comp2(+) - Comp1(+) == 0	-0.34618	0.38066	-0.909	0.9951
Comp3(-) - Comp1(+) == 0	-0.73101	0.76296	-0.958	0.9928
Comp3(+) - Comp1(+) == 0	-0.19530	0.43018	-0.454	1.0000
Comp4(-) - Comp1(+) == 0	0.15535	0.79250	0.196	1.0000
Comp4(+) - Comp1(+) == 0	0.05745	0.55678	0.103	1.0000
Comp5(-) - Comp1(+) == 0	-0.48101	1.13561	-0.424	1.0000
Comp5(+) - Comp1(+) == 0	1.51899	0.60459	2.512	0.2356
Comp2(+) - Comp2(-) == 0	0.83483	0.82131	1.016	0.9890
Comp3(-) - Comp2(-) == 0	0.45000	1.05441	0.427	1.0000

Comp3(+) - Comp2(-) == 0	0.98571	0.84541	1.166	0.9717
Comp4(-) - Comp2(-) == 0	1.33636	1.07597	1.242	0.9576
Comp4(+) - Comp2(-) == 0	1.23846	0.91633	1.352	0.9292
Comp5(-) - Comp2(-) == 0	0.70000	1.34880	0.519	0.9999
Comp5(+) - Comp2(-) == 0	2.70000	0.94615	2.854	0.1060
Comp3(-) - Comp2(+) == 0	-0.38483	0.75729	-0.508	1.0000
Comp3(+) - Comp2(+) == 0	0.15088	0.42003	0.359	1.0000
Comp4(-) - Comp2(+) == 0	0.50153	0.78704	0.637	0.9997
Comp4(+) - Comp2(+) == 0	0.40363	0.54898	0.735	0.9991
Comp5(-) - Comp2(+) == 0	-0.13483	1.13180	-0.119	1.0000
Comp5(+) - Comp2(+) == 0	1.86517	0.59742	3.122	0.0506 .
Comp3(+) - Comp3(-) == 0	0.53571	0.78335	0.684	0.9995
Comp4(-) - Comp3(-) == 0	0.88636	1.02793	0.862	0.9967
Comp4(+) - Comp3(-) == 0	0.78846	0.85941	0.917	0.9948
Comp5(-) - Comp3(-) == 0	0.25000	1.31080	0.191	1.0000
Comp5(+) - Comp3(-) == 0	2.25000	0.89114	2.525	0.2292
Comp4(-) - Comp3(+) == 0	0.35065	0.81215	0.432	1.0000
Comp4(+) - Comp3(+) == 0	0.25275	0.58440	0.432	1.0000
Comp5(-) - Comp3(+) == 0	-0.28571	1.14940	-0.249	1.0000
Comp5(+) - Comp3(+) == 0	1.71429	0.63013	2.721	0.1476
Comp4(+) - Comp4(-) == 0	-0.09790	0.88574	-0.111	1.0000
Comp5(-) - Comp4(-) == 0	-0.63636	1.32821	-0.479	1.0000
Comp5(+) - Comp4(-) == 0	1.36364	0.91655	1.488	0.8788
Comp5(-) - Comp4(+) == 0	-0.53846	1.20253	-0.448	1.0000
Comp5(+) - Comp4(+) == 0	1.46154	0.72250	2.023	0.5455
Comp5(+) - Comp5(-) == 0	2.00000	1.22540	1.632	0.8064

Average day of the year recording the green up

	Estimate	Std. Error	t value	Pr(>|t|)
Comp1(+) - Comp1(-) == 0	-2.3156	2.9959	-0.773	0.999
Comp2(-) - Comp1(-) == 0	-5.8814	5.5502	-1.060	0.985
Comp2(+) - Comp1(-) == 0	-1.7275	2.9360	-0.588	1.000
Comp3(-) - Comp1(-) == 0	0.8353	5.1613	0.162	1.000
Comp3(+) - Comp1(-) == 0	-0.8850	3.2055	-0.276	1.000
Comp4(-) - Comp1(-) == 0	1.9641	5.3416	0.368	1.000
Comp4(+) - Comp1(-) == 0	-5.4660	3.9274	-1.392	0.916
Comp5(-) - Comp1(-) == 0	-0.1814	7.4697	-0.024	1.000
Comp5(+) - Comp1(-) == 0	0.5615	4.2087	0.133	1.000
Comp2(-) - Comp1(+) == 0	-3.5658	5.3062	-0.672	1.000
Comp2(+) - Comp1(+) == 0	0.5881	2.4437	0.241	1.000
Comp3(-) - Comp1(+) == 0	3.1508	4.8980	0.643	1.000
Comp3(+) - Comp1(+) == 0	1.4306	2.7616	0.518	1.000
Comp4(-) - Comp1(+) == 0	4.2796	5.0876	0.841	0.997
Comp4(+) - Comp1(+) == 0	-3.1504	3.5743	-0.881	0.996
Comp5(-) - Comp1(+) == 0	2.1342	7.2903	0.293	1.000
Comp5(+) - Comp1(+) == 0	2.8770	3.8813	0.741	0.999
Comp2(+) - Comp2(-) == 0	4.1539	5.2726	0.788	0.998
Comp3(-) - Comp2(-) == 0	6.7167	6.7690	0.992	0.991
Comp3(+) - Comp2(-) == 0	4.9964	5.4272	0.921	0.995
Comp4(-) - Comp2(-) == 0	7.8455	6.9074	1.136	0.976
Comp4(+) - Comp2(-) == 0	0.4154	5.8826	0.071	1.000
Comp5(-) - Comp2(-) == 0	5.7000	8.6589	0.658	1.000
Comp5(+) - Comp2(-) == 0	6.4429	6.0740	1.061	0.985
Comp3(-) - Comp2(+) == 0	2.5627	4.8616	0.527	1.000
Comp3(+) - Comp2(+) == 0	0.8425	2.6965	0.312	1.000
Comp4(-) - Comp2(+) == 0	3.6915	5.0525	0.731	0.999
Comp4(+) - Comp2(+) == 0	-3.7385	3.5243	-1.061	0.985
Comp5(-) - Comp2(+) == 0	1.5461	7.2658	0.213	1.000
Comp5(+) - Comp2(+) == 0	2.2889	3.8352	0.597	1.000

Comp3(+) - Comp3(-) == 0	-1.7202	5.0289	-0.342	1.000
Comp4(-) - Comp3(-) == 0	1.1288	6.5990	0.171	1.000
Comp4(+) - Comp3(-) == 0	-6.3013	5.5172	-1.142	0.975
Comp5(-) - Comp3(-) == 0	-1.0167	8.4149	-0.121	1.000
Comp5(+) - Comp3(-) == 0	-0.2738	5.7208	-0.048	1.000
Comp4(-) - Comp3(+) == 0	2.8490	5.2137	0.546	1.000
Comp4(+) - Comp3(+) == 0	-4.5810	3.7517	-1.221	0.962
Comp5(-) - Comp3(+) == 0	0.7036	7.3788	0.095	1.000
Comp5(+) - Comp3(+) == 0	1.4464	4.0452	0.358	1.000
Comp4(+) - Comp4(-) == 0	-7.4301	5.6862	-1.307	0.942
Comp5(-) - Comp4(-) == 0	-2.1455	8.5267	-0.252	1.000
Comp5(+) - Comp4(-) == 0	-1.4026	5.8840	-0.238	1.000
Comp5(-) - Comp4(+) == 0	5.2846	7.7199	0.685	0.999
Comp5(+) - Comp4(+) == 0	6.0275	4.6382	1.300	0.944
Comp5(+) - Comp5(-) == 0	0.7429	7.8667	0.094	1.000

Soil water capacity

	Estimate	Std. Error	t value	Pr(>|t|)
Comp1(+) - Comp1(-) == 0	7.847	19.116	0.410	1.000
Comp2(-) - Comp1(-) == 0	-9.098	35.414	-0.257	1.000
Comp2(+) - Comp1(-) == 0	-13.316	18.734	-0.711	0.999
Comp3(-) - Comp1(-) == 0	-11.114	32.932	-0.337	1.000
Comp3(+) - Comp1(-) == 0	34.409	20.453	1.682	0.778
Comp4(-) - Comp1(-) == 0	-46.334	34.083	-1.359	0.927
Comp4(+) - Comp1(-) == 0	21.841	25.059	0.872	0.996
Comp5(-) - Comp1(-) == 0	62.102	47.661	1.303	0.943
Comp5(+) - Comp1(-) == 0	-24.745	26.854	-0.921	0.995
Comp2(-) - Comp1(+) == 0	-16.944	33.857	-0.500	1.000
Comp2(+) - Comp1(+) == 0	-21.162	15.592	-1.357	0.927
Comp3(-) - Comp1(+) == 0	-18.961	31.252	-0.607	1.000
Comp3(+) - Comp1(+) == 0	26.563	17.621	1.507	0.870
Comp4(-) - Comp1(+) == 0	-54.181	32.462	-1.669	0.785
Comp4(+) - Comp1(+) == 0	13.994	22.807	0.614	1.000
Comp5(-) - Comp1(+) == 0	54.256	46.517	1.166	0.972
Comp5(+) - Comp1(+) == 0	-32.592	24.765	-1.316	0.940
Comp2(+) - Comp2(-) == 0	-4.218	33.643	-0.125	1.000
Comp3(-) - Comp2(-) == 0	-2.017	43.190	-0.047	1.000
Comp3(+) - Comp2(-) == 0	43.507	34.629	1.256	0.954
Comp4(-) - Comp2(-) == 0	-37.236	44.074	-0.845	0.997
Comp4(+) - Comp2(-) == 0	30.938	37.535	0.824	0.998
Comp5(-) - Comp2(-) == 0	71.200	55.249	1.289	0.947
Comp5(+) - Comp2(-) == 0	-15.648	38.756	-0.404	1.000
Comp3(-) - Comp2(+) == 0	2.201	31.020	0.071	1.000
Comp3(+) - Comp2(+) == 0	47.725	17.205	2.774	0.130
Comp4(-) - Comp2(+) == 0	-33.018	32.238	-1.024	0.988
Comp4(+) - Comp2(+) == 0	35.156	22.487	1.563	0.843
Comp5(-) - Comp2(+) == 0	75.418	46.361	1.627	0.809
Comp5(+) - Comp2(+) == 0	-11.430	24.471	-0.467	1.000
Comp3(+) - Comp3(-) == 0	45.524	32.088	1.419	0.906
Comp4(-) - Comp3(-) == 0	-35.220	42.106	-0.836	0.997
Comp4(+) - Comp3(-) == 0	32.955	35.203	0.936	0.994
Comp5(-) - Comp3(-) == 0	73.217	53.693	1.364	0.925
Comp5(+) - Comp3(-) == 0	-13.631	36.503	-0.373	1.000
Comp4(-) - Comp3(+) == 0	-80.744	33.267	-2.427	0.280
Comp4(+) - Comp3(+) == 0	-12.569	23.938	-0.525	1.000
Comp5(-) - Comp3(+) == 0	27.693	47.082	0.588	1.000
Comp5(+) - Comp3(+) == 0	-59.155	25.811	-2.292	0.360
Comp4(+) - Comp4(-) == 0	68.175	36.281	1.879	0.648
Comp5(-) - Comp4(-) == 0	108.436	54.406	1.993	0.567

Comp5(+) - Comp4(-) == 0	21.589	37.544	0.575	1.000
Comp5(-) - Comp4(+) == 0	40.262	49.258	0.817	0.998
Comp5(+) - Comp4(+) == 0	-46.586	29.595	-1.574	0.838
Comp5(+) - Comp5(-) == 0	-86.848	50.195	-1.730	0.748

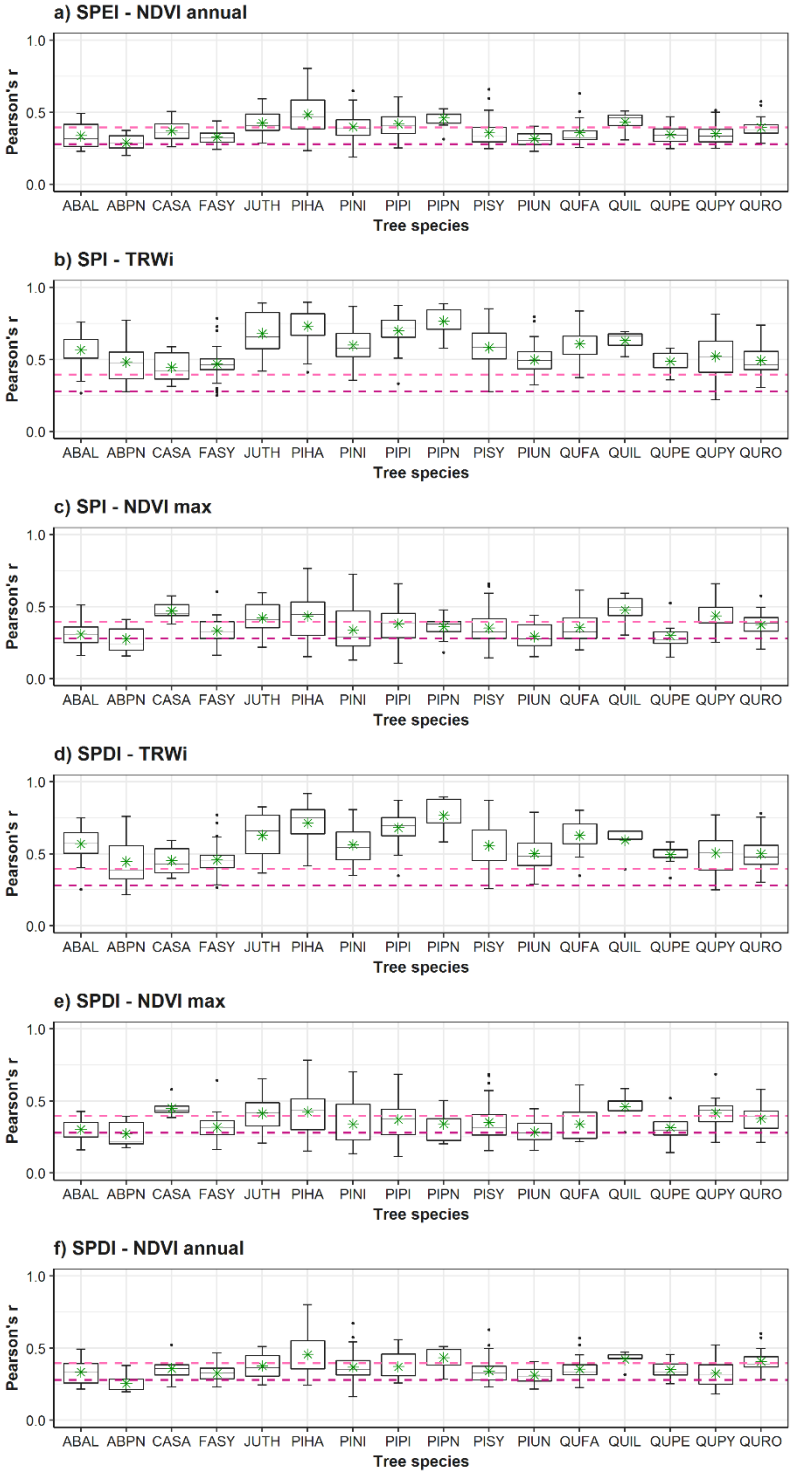

Supplementary Figure 1. Box plots showing the maximum Pearson correlation coefficients computed between NDVIannual (a,f), ring-width indices (TRWi (b,d), and NDVImax (c,e) and the multi-scalar drought indices (SPEI, SPI and SPDI). The solid black line corresponds to the median, green asterisks mark the mean and dashed lines show the significance level at $p < 0.05$ (light pink) and $p < 0.01$ (dark pink). Species' codes correspond to those listed in Table 1.

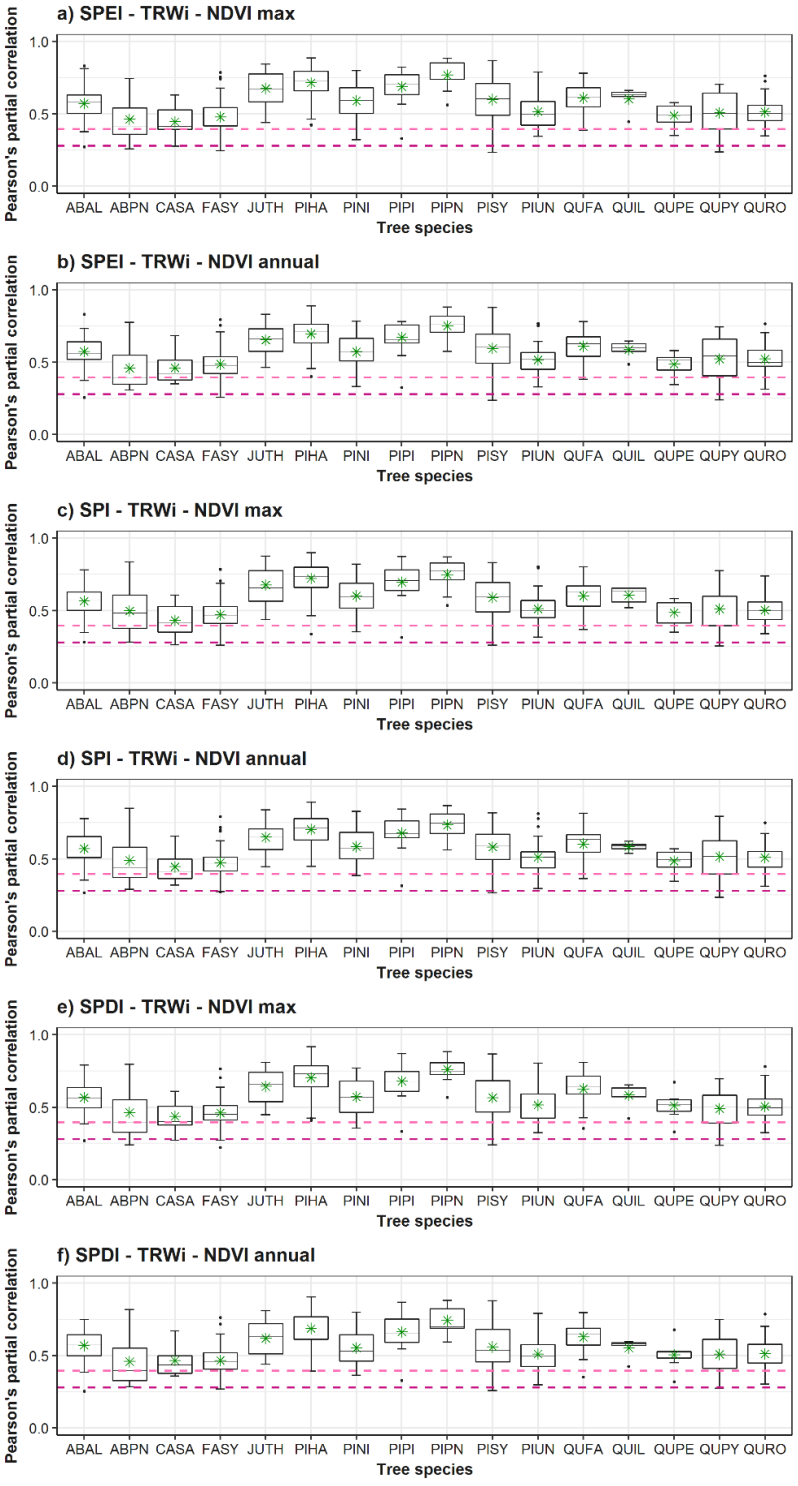

Supplementary Figure 2. Box plots showing the maximum partial Pearson Correlation Coefficients found between TRWi (b,d), NDVImax (c,e), NDVIannual (a,f) and the multi-scalar drought indices. The solid black line corresponds to the median, green asterisks mark the mean and dashed lines show the significance level at $p < 0.05$ (light pink) and $p < 0.01$ (dark pink). Species' codes correspond to those listed in Table 1.

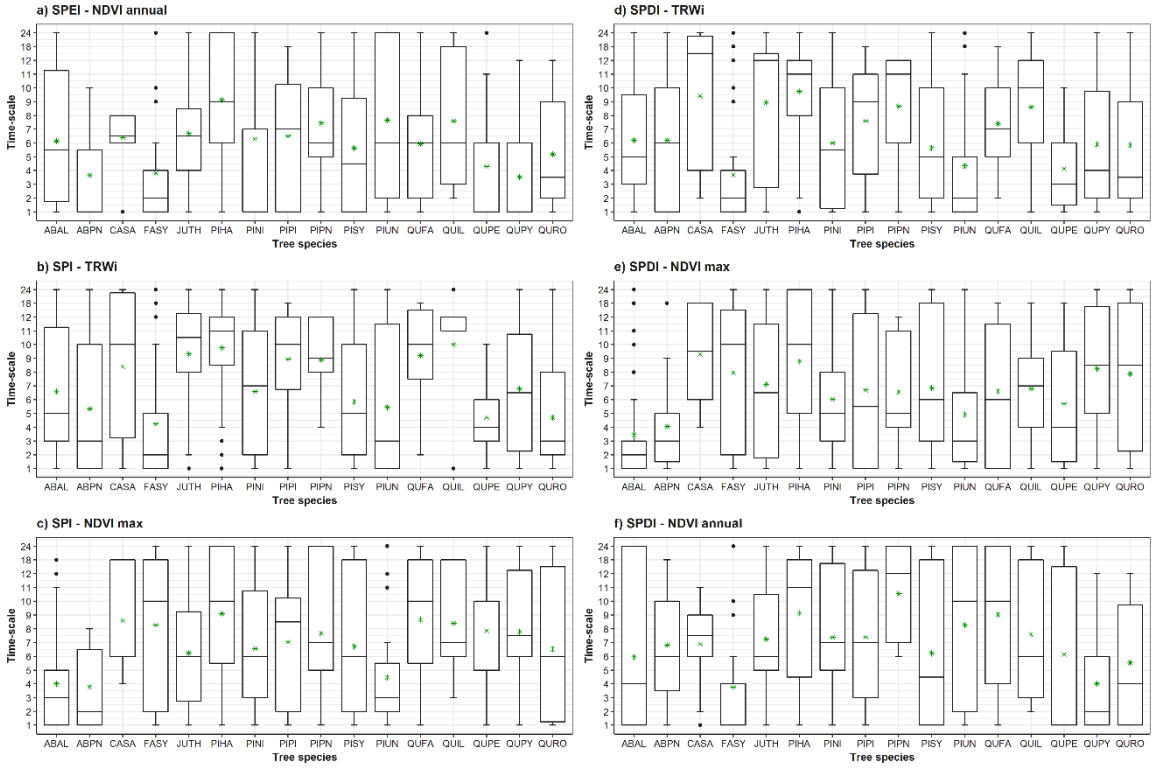

Supplementary Figure 3. Box plots showing the most correlated time-scale found for TRWi (b,d), NDVI max (c,e), NDVI annual (a,f) and the multi-scalar drought indices. The solid black line corresponds to the median, while green asterisks mark the mean. Species' codes correspond to those listed in Table 1.

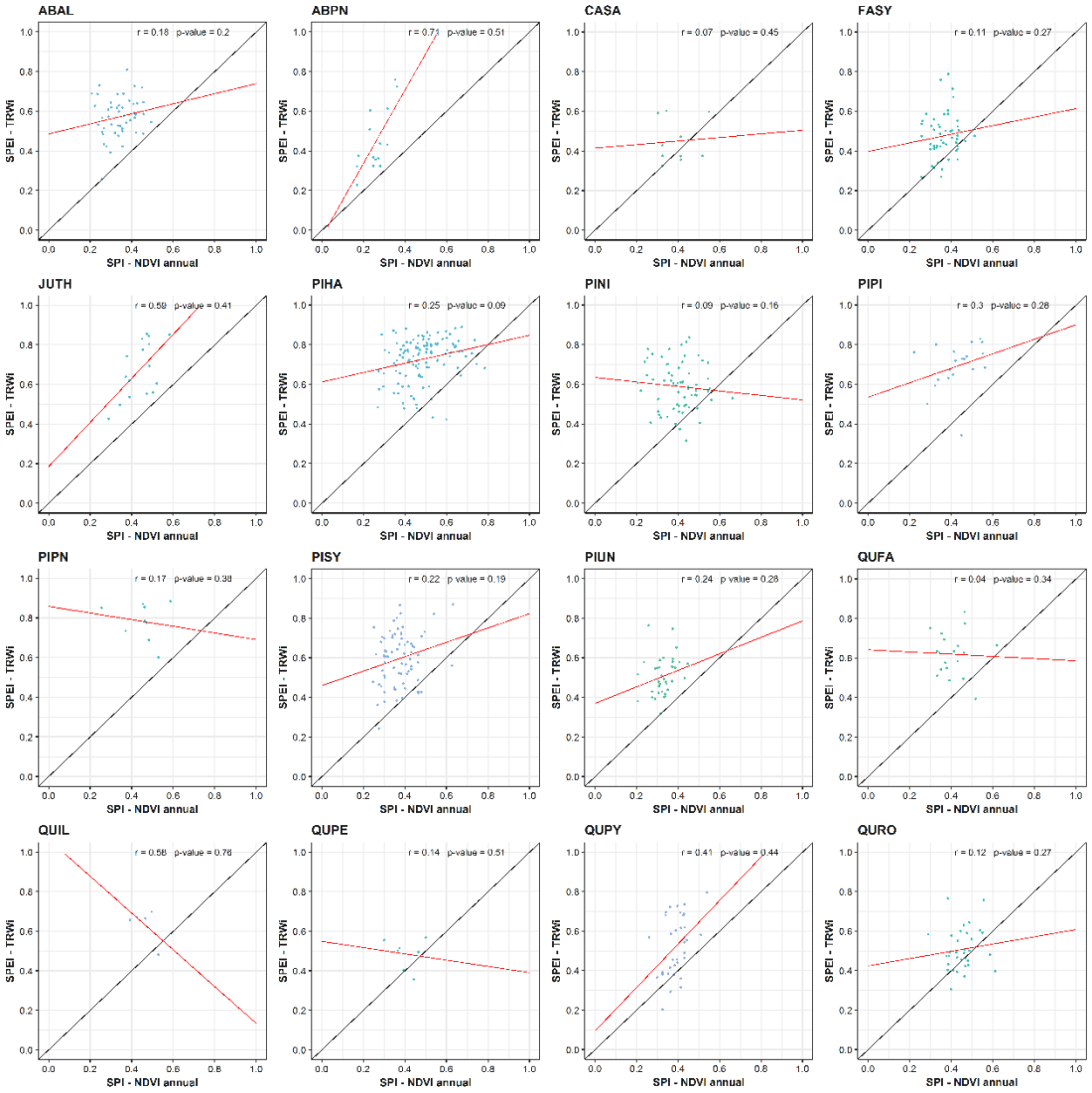

Supplementary Figure 4. Scatterplots showing the maximum Pearson correlation coefficients found for SPEI-TRWi and SPI-NDVI annual by specie. Dashed red line corresponds to the fitted line of regression model and black line 1:1. Species' codes correspond to those listed in Table 1.

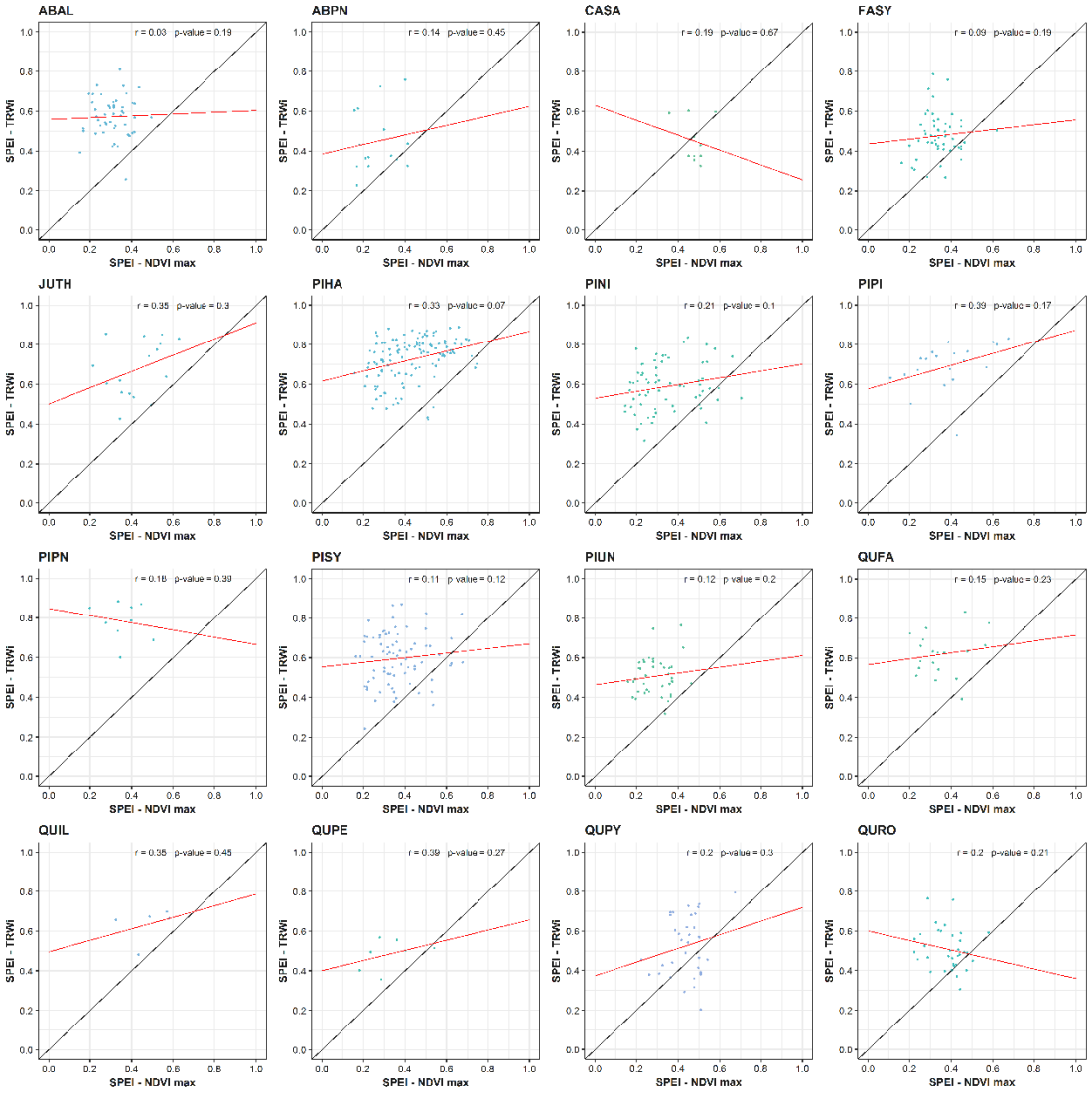

Supplementary Figure 5. Scatterplots showing the maximum Pearson correlation coefficients found for SPEI-TRWi and SPEI-NDVImax by specie. Dashed red line corresponds to the fitted line of regression model and black line 1:1. Species' codes correspond to those listed in Table 1.

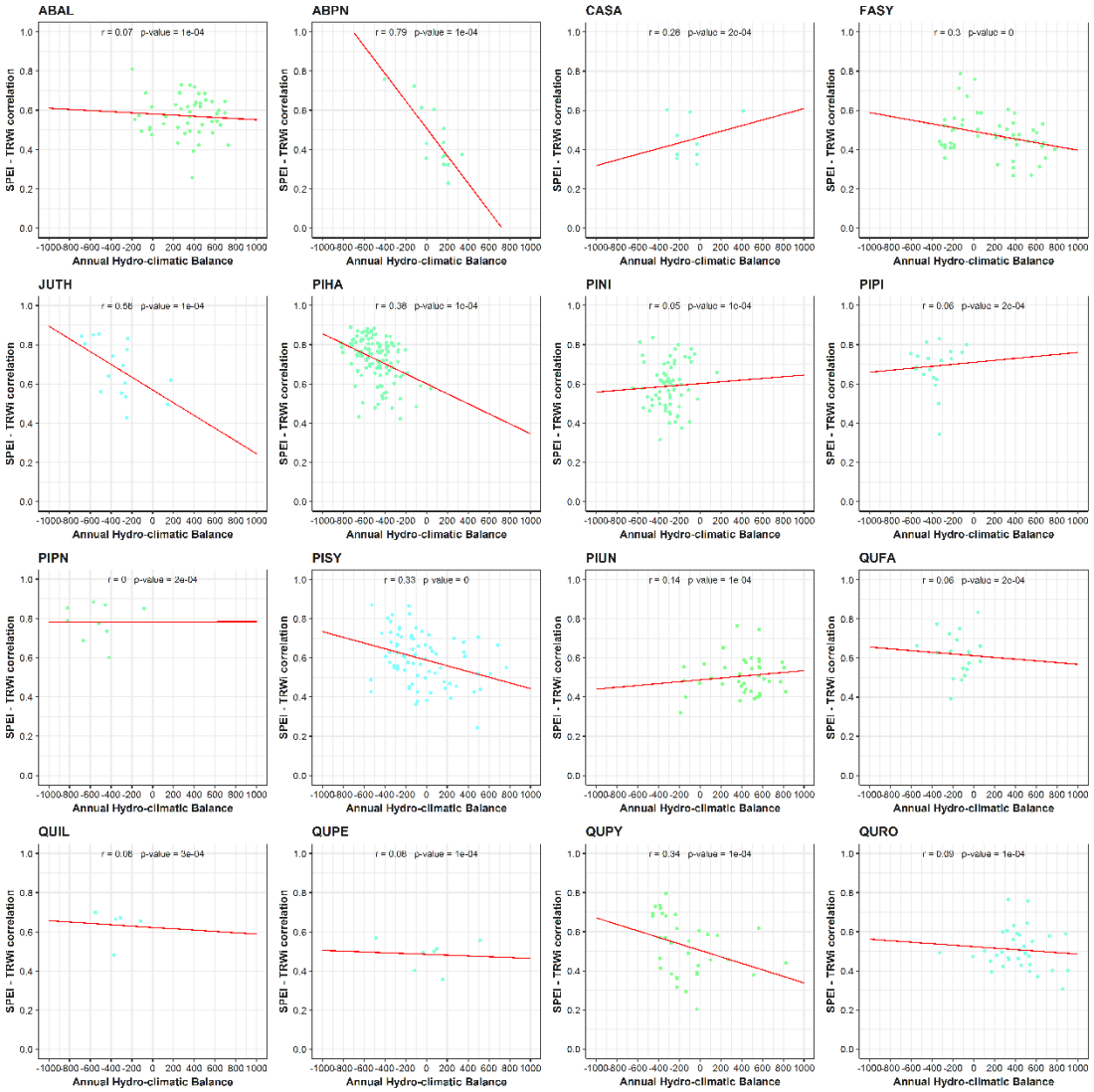

Supplementary Figure 6. Scatterplots showing the maximum Pearson correlation coefficients found for SPEI-TRWi and the average annual hydro-climatic balance by specie. Dashed red line corresponds to the fitted lines of regression models. Species' codes correspond to those listed in Table 1.

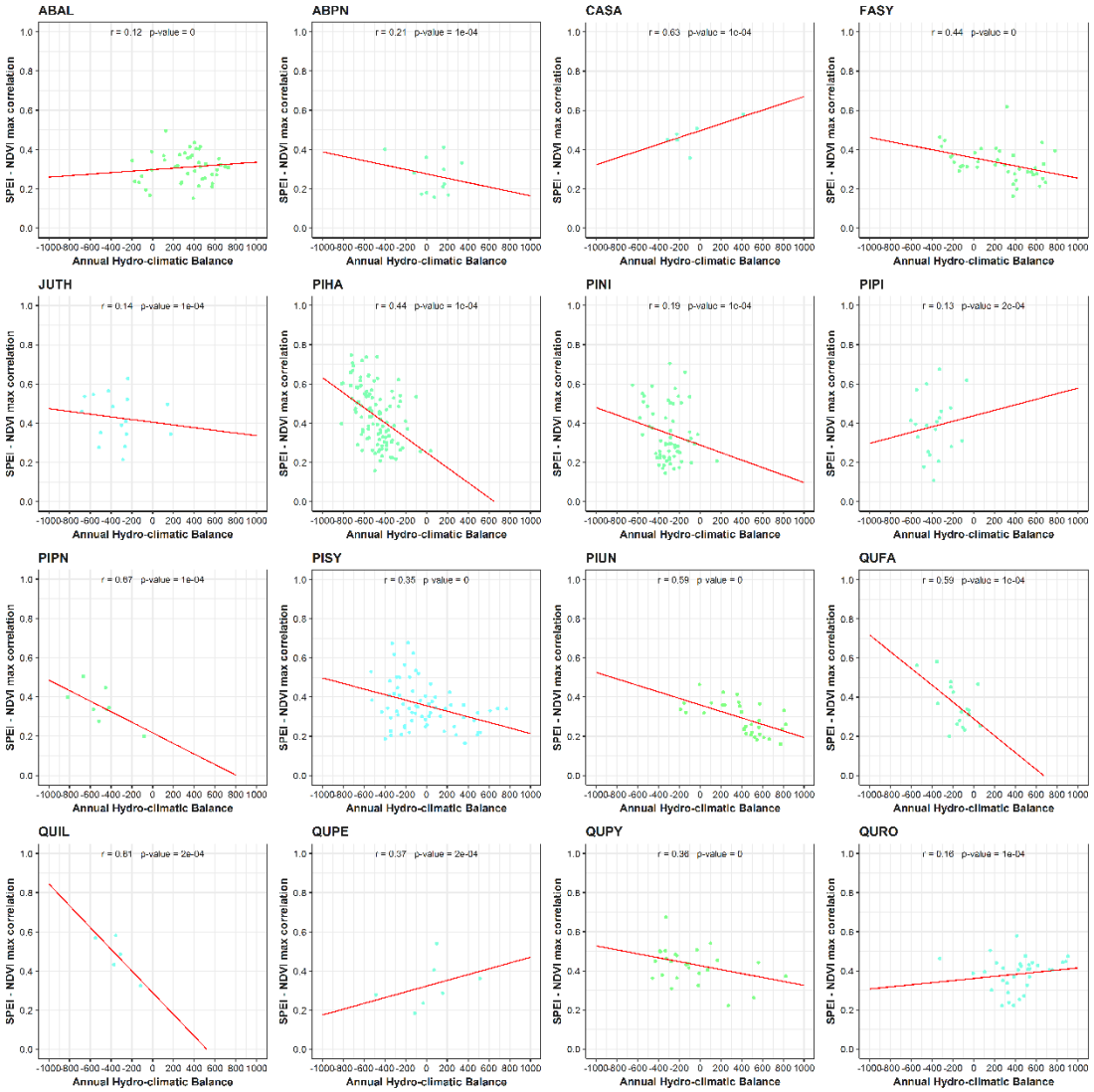

Supplementary Figure 7. Same as Supplementary Figure 6, but for SPEI-NDVImax. Species' codes correspond to those listed in Table 1.

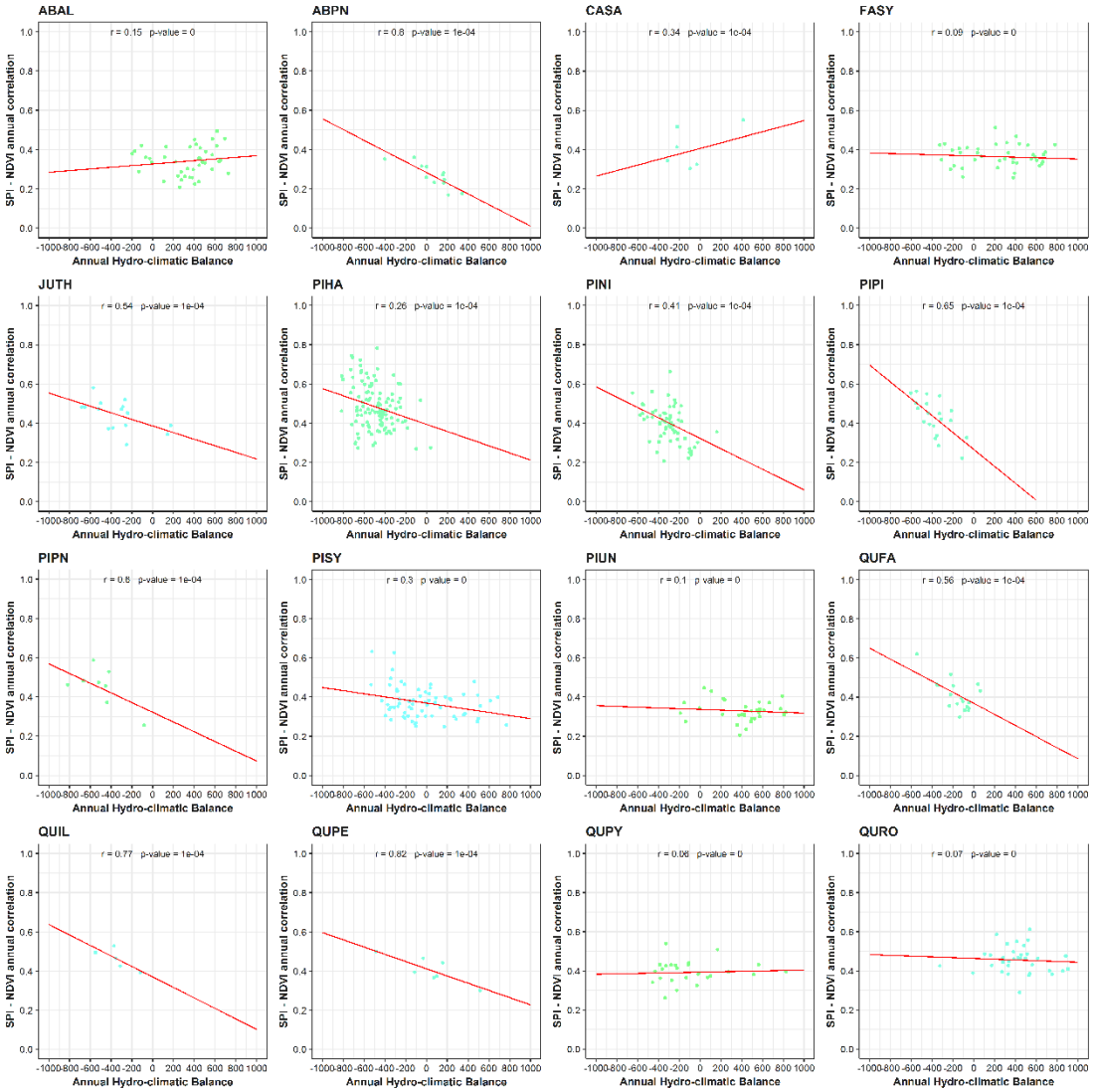

Supplementary Figure 8. Same as Supplementary Figure 6, but for SPEI-NDVIannual. Species' codes correspond to those listed in Table 1.

		January	February	March	April	May	June	July	August	September	October	November	December
TRWi	**SPEI**	6.15	3.76	4.27	8.89	7.52	11.79	17.09	12.14	9.06	9.40	5.30	4.62
	SPI	6.50	3.93	3.93	7.52	8.38	12.31	14.02	15.90	9.91	8.38	4.27	4.96
	SPDI	6.84	4.44	5.30	6.84	7.52	9.06	11.97	12.65	10.43	12.65	5.47	6.84
	Total	19.49	12.13	13.5	23.25	23.42	33.16	43.08	40.69	29.4	30.43	15.04	16.42
NDVImax	**SPEI**	5.21	6.84	8.38	21.28	10.94	10.94	3.76	2.39	8.38	7.35	6.32	8.21
	SPI	4.19	10.09	8.38	21.11	10.60	8.38	3.25	3.08	9.40	6.67	6.67	8.21
	SPDI	4.19	8.21	8.21	20.77	11.45	10.09	3.93	2.56	8.03	8.03	7.01	7.52
	Total	13.59	25.14	24.97	63.16	32.99	29.41	10.94	8.03	25.81	22.05	20	23.94
NDVIannual	**SPEI**	3.42	12.48	5.30	3.25	37.61	2.22	7.18	3.59	2.56	3.76	12.65	5.98
	SPI	2.91	11.45	3.42	2.74	32.48	1.03	3.08	3.93	3.59	4.27	25.13	5.98
	SPDI	5.98	15.21	5.30	3.42	20.85	1.20	5.81	7.69	3.08	5.81	17.26	8.38
	Total	12.31	39.14	14.02	9.41	90.94	4.45	16.07	15.21	9.23	13.84	55.04	20.34

Supplementary Table 1. Percentage of sampled forests per drought index and time-scale (number of months) in which the maximum correlation value was found with ring-width indices (TRWi, a), NDVImax (b) and NDVI annual (c). Bold values indicate the maximum percentage for each drought index.

Supplementary information for: Complex influences of climatic drought time-scales on hydrological droughts in natural basins of the contiguous Unites States

Marina Peña-Gallardo[1], Sergio M. Vicente-Serrano[1], Jamie Hannaford[2], Jorge Lorenzo-Lacruz[3], Mark Sbovoda[4], Fernando Domínguez-Castro[1], Marco Maneta[5], Miquel Tomas-Burguera[6], Ahmed El Kenawy[1,7]

[1]Instituto Pirenaico de Ecología, Consejo Superior de Investigaciones Científicas (IPE–CSIC), Spain
[2]Centre for Ecology and Hydrology, UK.
[3]University of the Balearic Islands, Spain
[4]National Drought Mitigation Centre, University of Nebraska-Lincoln, U.S.
[5]University of Montana, U.S.
[6]Estación Experimental de Aula Dei, Consejo Superior de Investigaciones Científicas (EEAD-CSIC), Spain.
[7]Department of Geography, Mansoura University, Mansoura, Egypt.

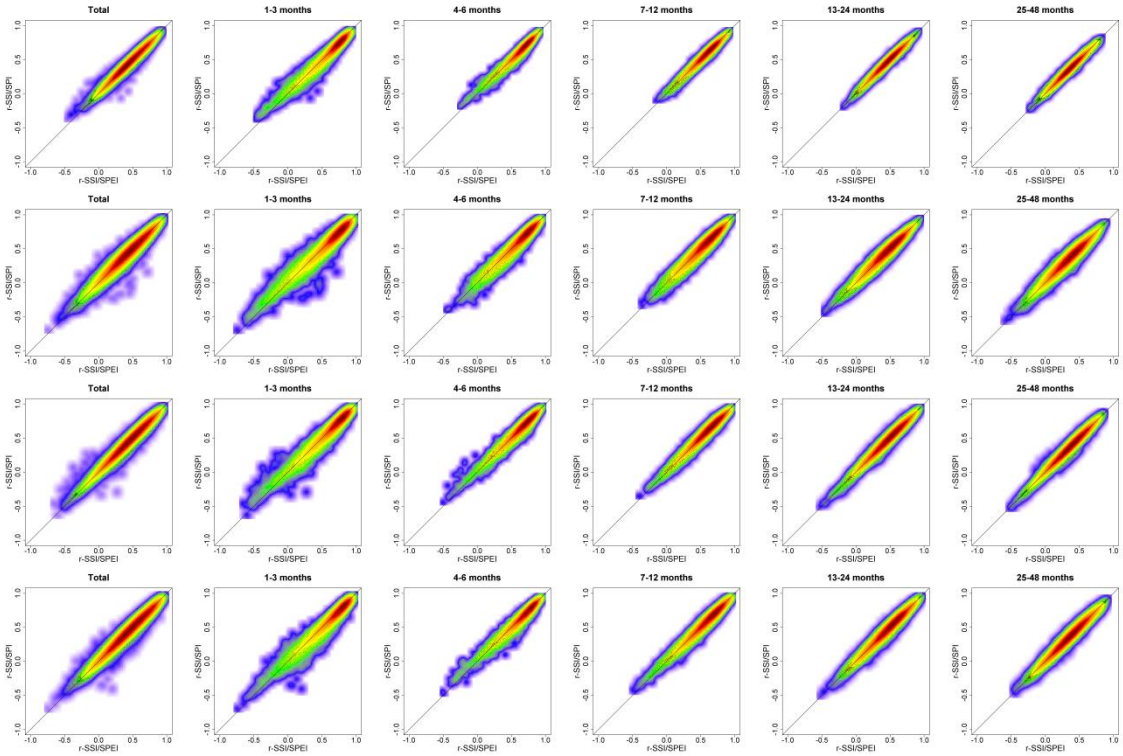

Supplementary Fig 1: Scatter plots showing the relationships between the correlations between SPEI and SSI and between SPI and SSI considering the entire period (1940-2013; first row) and the three subperiods (1940-1964, 1965-1989, 1990-2013). The relationship is shown for the entire set of time-scales as well as for different ranges of time-scales.

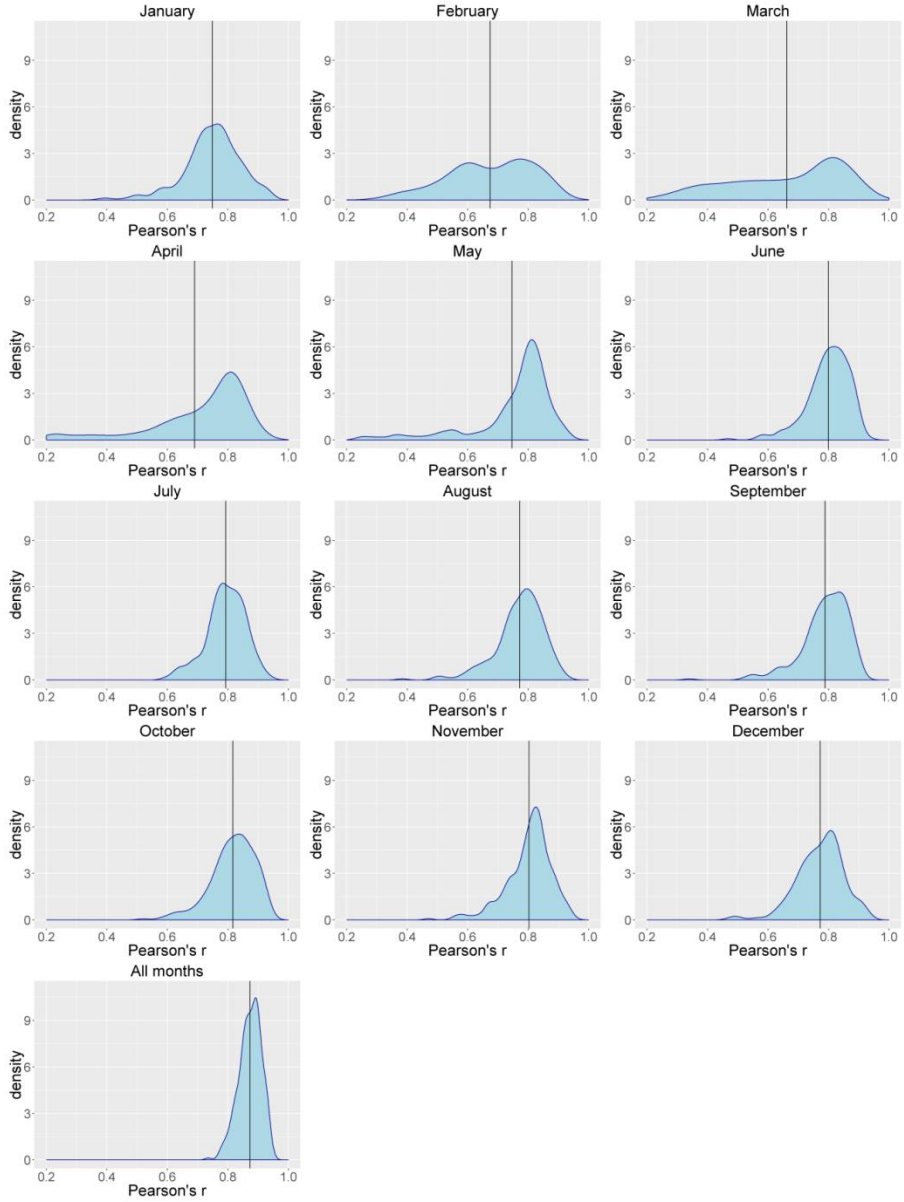

Supplementary Figure 2. Density plots with maximum Pearson's r correlations between the SPEI time-scales and the SSI for each month independently and for all months series. Vertical black line depicts the median.

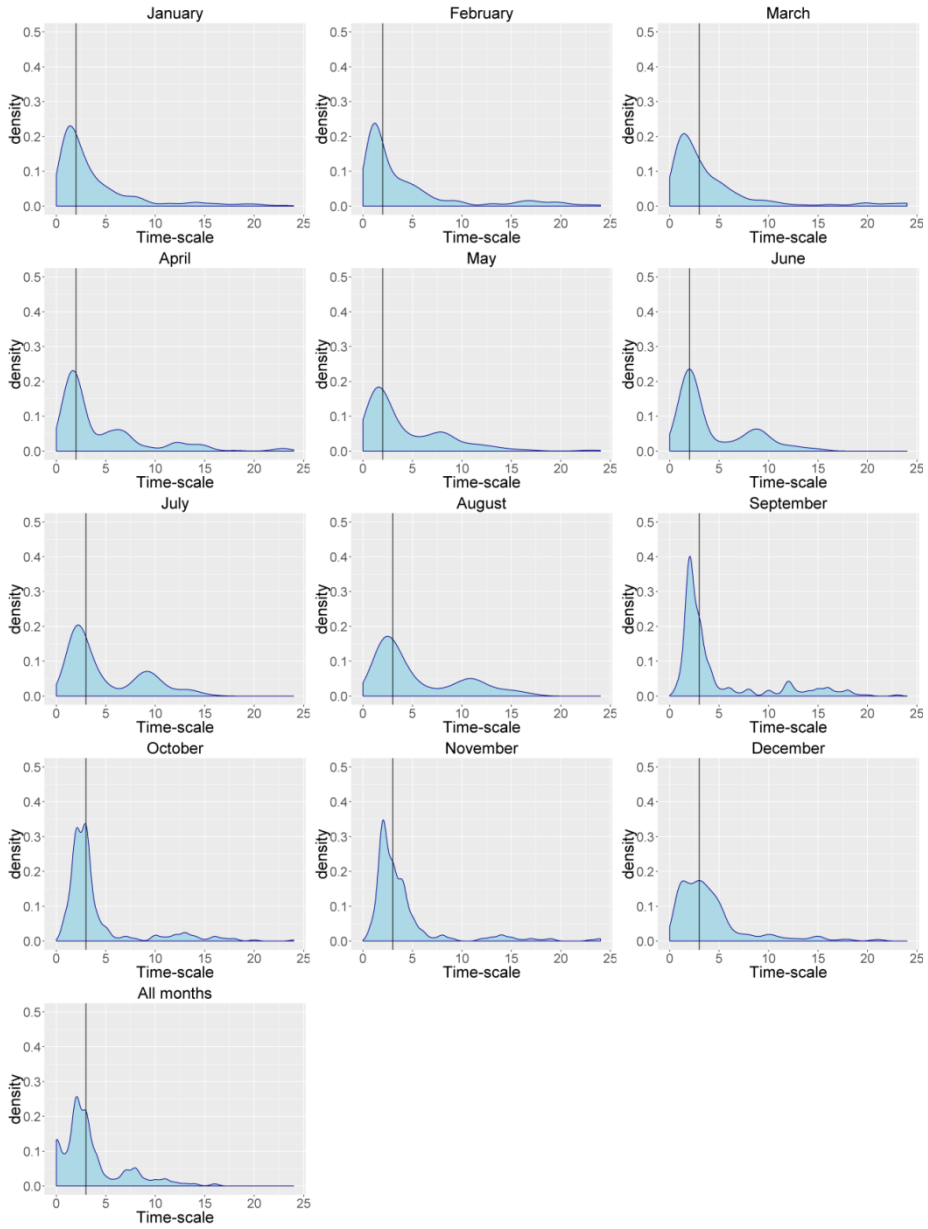

Supplementary Figure 3. Density plots with SPEI time-scale at which maximum Pearson's r correlations between SPEI time-scales and the SSI is found (Monthly series and series of all months). Vertical black line depicts the median.

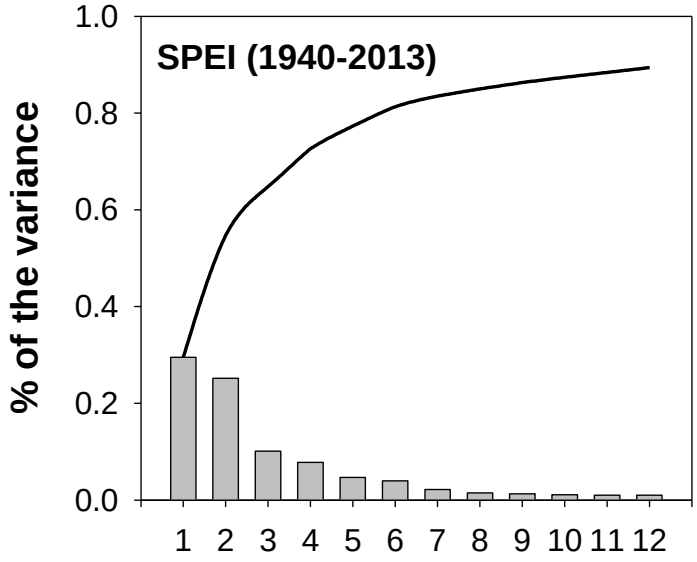

Supplementary Figure 4. Explained variance of the PCs obtained from patterns of correlation between SPEI and SSI over the entire period (1940-2013).

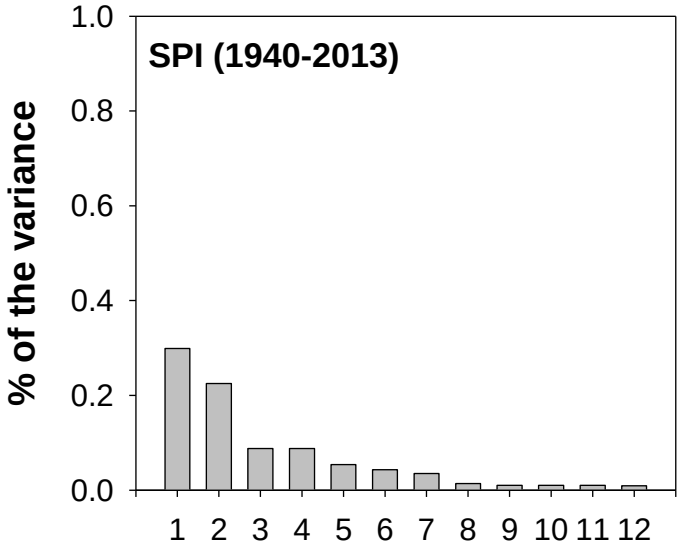

Supplementary Figure 5. Explained variance of the PCs obtained from patterns of correlation between SPI and SSI over the entire period (1940-2013).

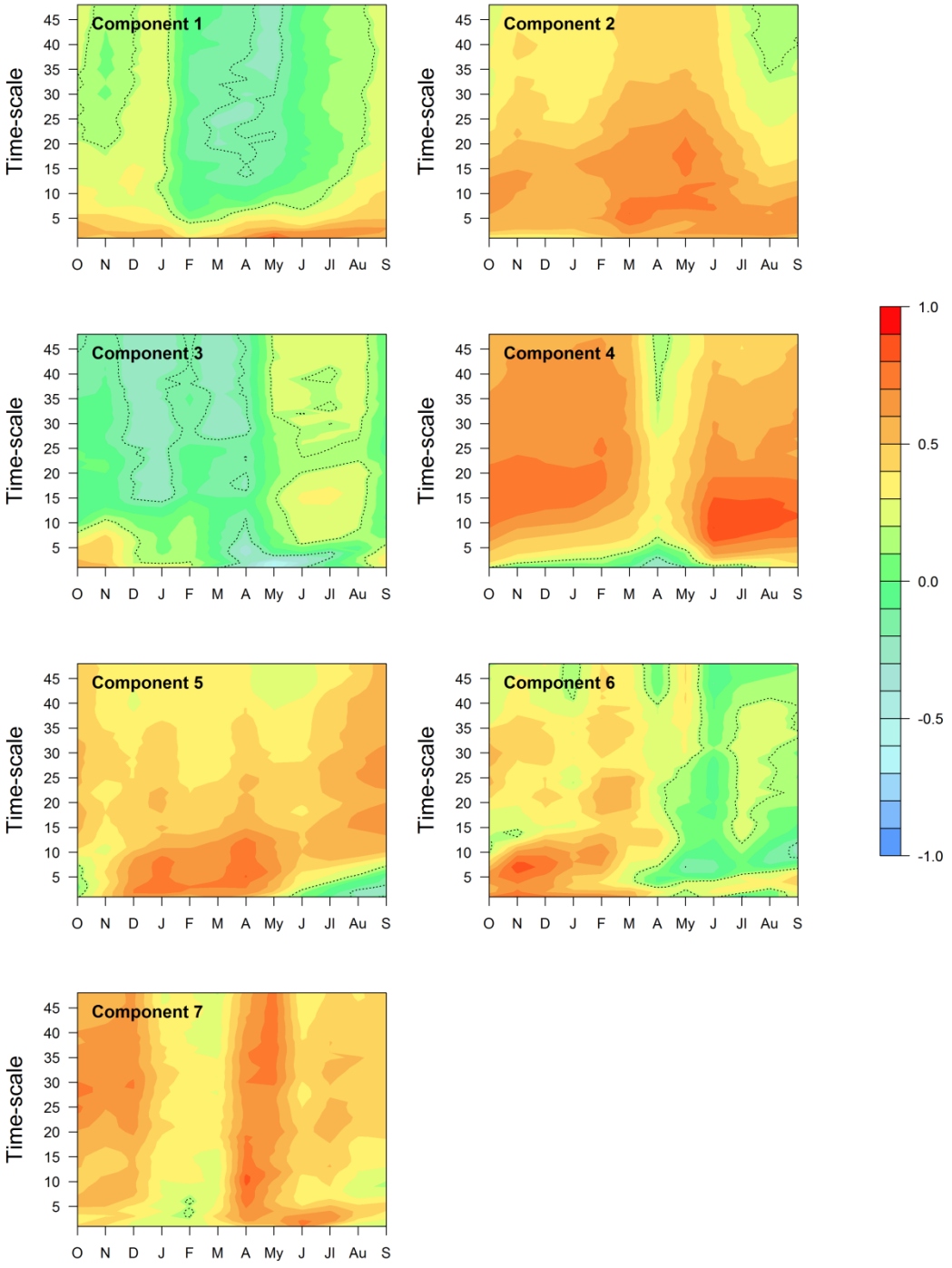

Supplementary Figure 6. Principal component scores obtained from correlations between SPI time-scales and SSI (1940-2013). Dotted lines outline depicts significant correlations at $p < 0.05$.

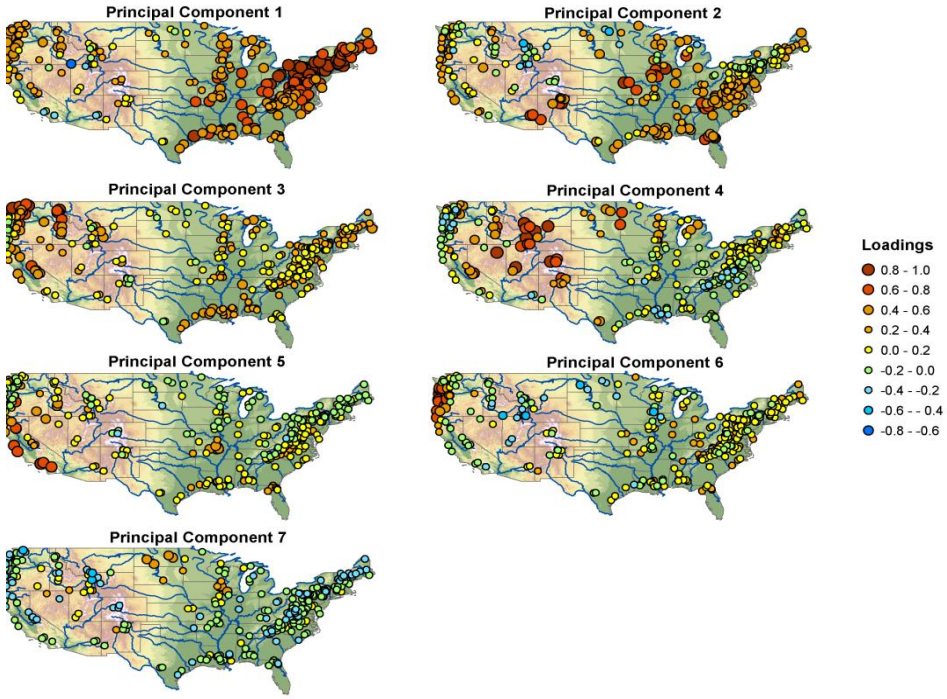

Supplementary Figure 7: Spatial distribution of the loadings of the extracted PCs , summarizing the patterns of correlation between SPI time-scales and SSI. The coefficient of contingency between patterns of SPEI/SSI correlations and SPI/SSI correlations 0.89.

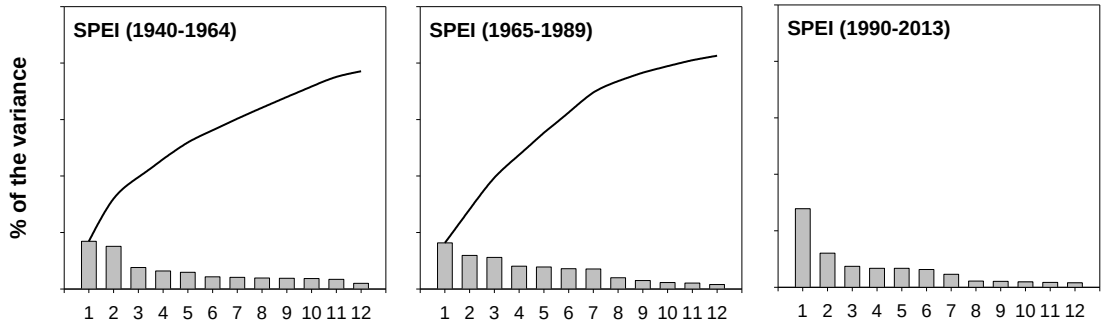

Supplementary Figure 8. Explained variance of the PCs obtained using correlations between SPEI and SSI for the sub-periods 1940-1964, 1965-1989, and 1990-2013.

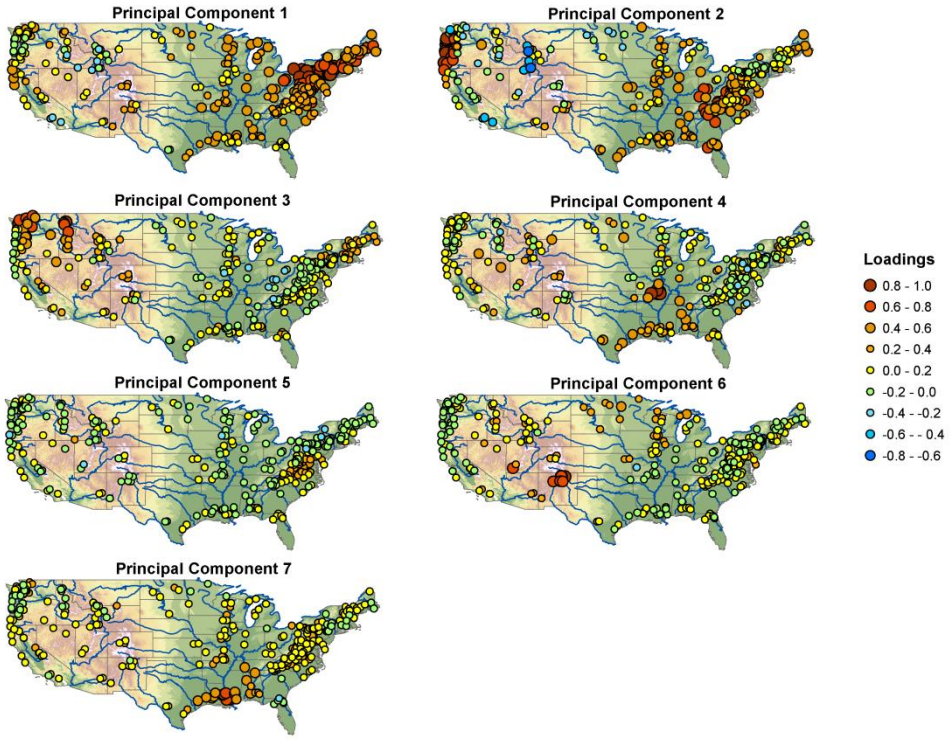

Supplementary Figure 9: Spatial distribution of the loadings of the extracted PCs, which summarize the patterns of monthly correlations between SPEI time-scales and the SSI for the sub-period 1940-1964.

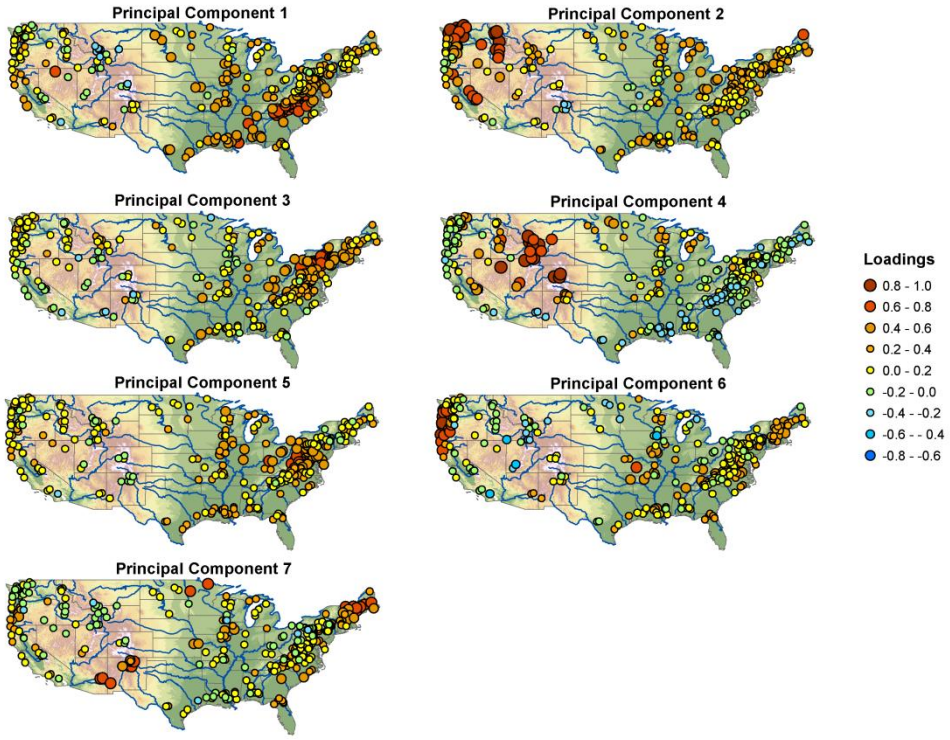

Supplementary Figure 10: Spatial distribution of the loadings of the extracted PCs, which summarize from the patterns of monthly correlation between SPEI time-scales and the SSI for the sub-period 1965-1989.

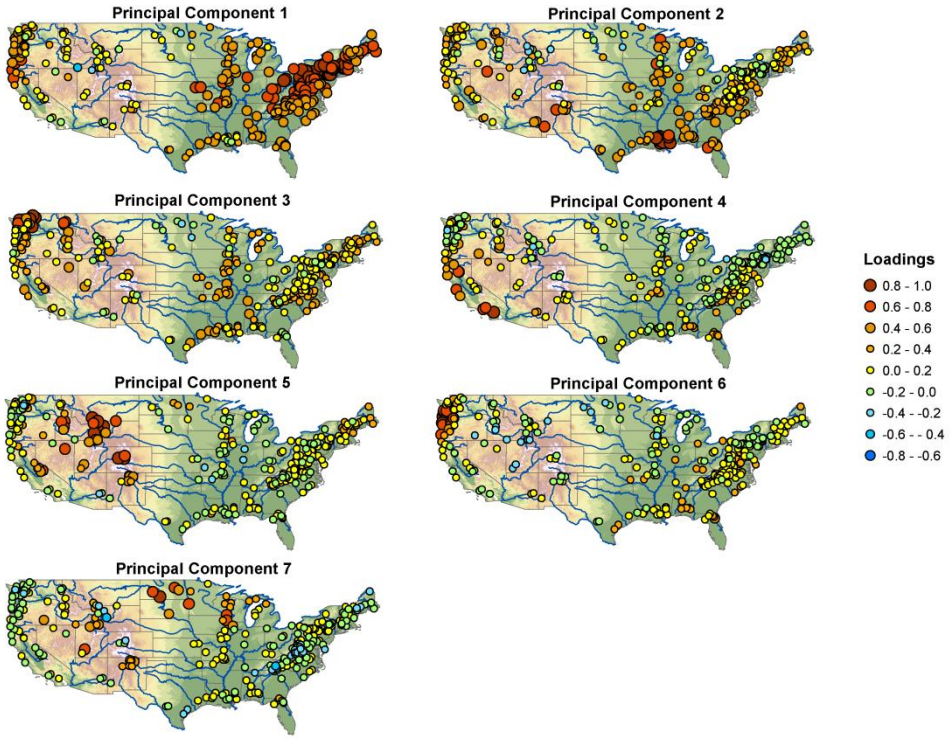

Supplementary Figure 11: Spatial distribution of the loadings of the extracted PCs, which summarize the patterns of monthly correlation between SPEI time-scales and the SSI for the sub-period 1990-2013.

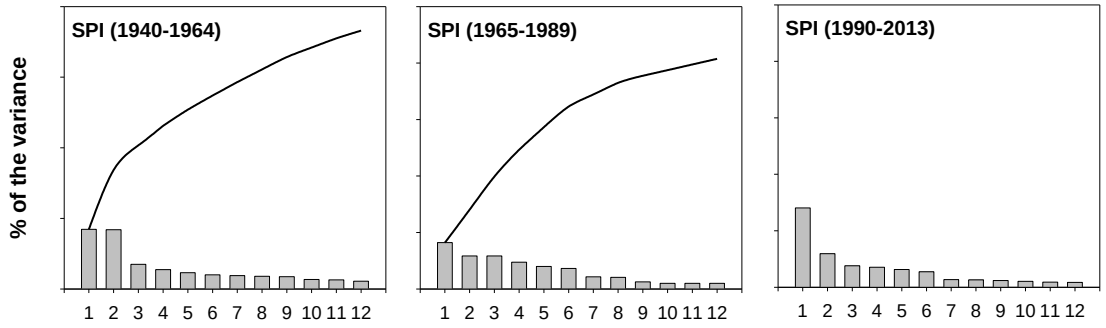

Supplementary Figure 12. Explained variance of the PCs, summarizing from the patterns of correlation between SPI and SSI for the sub-periods 1940-1964, 1965-1989, and 1990-2013.

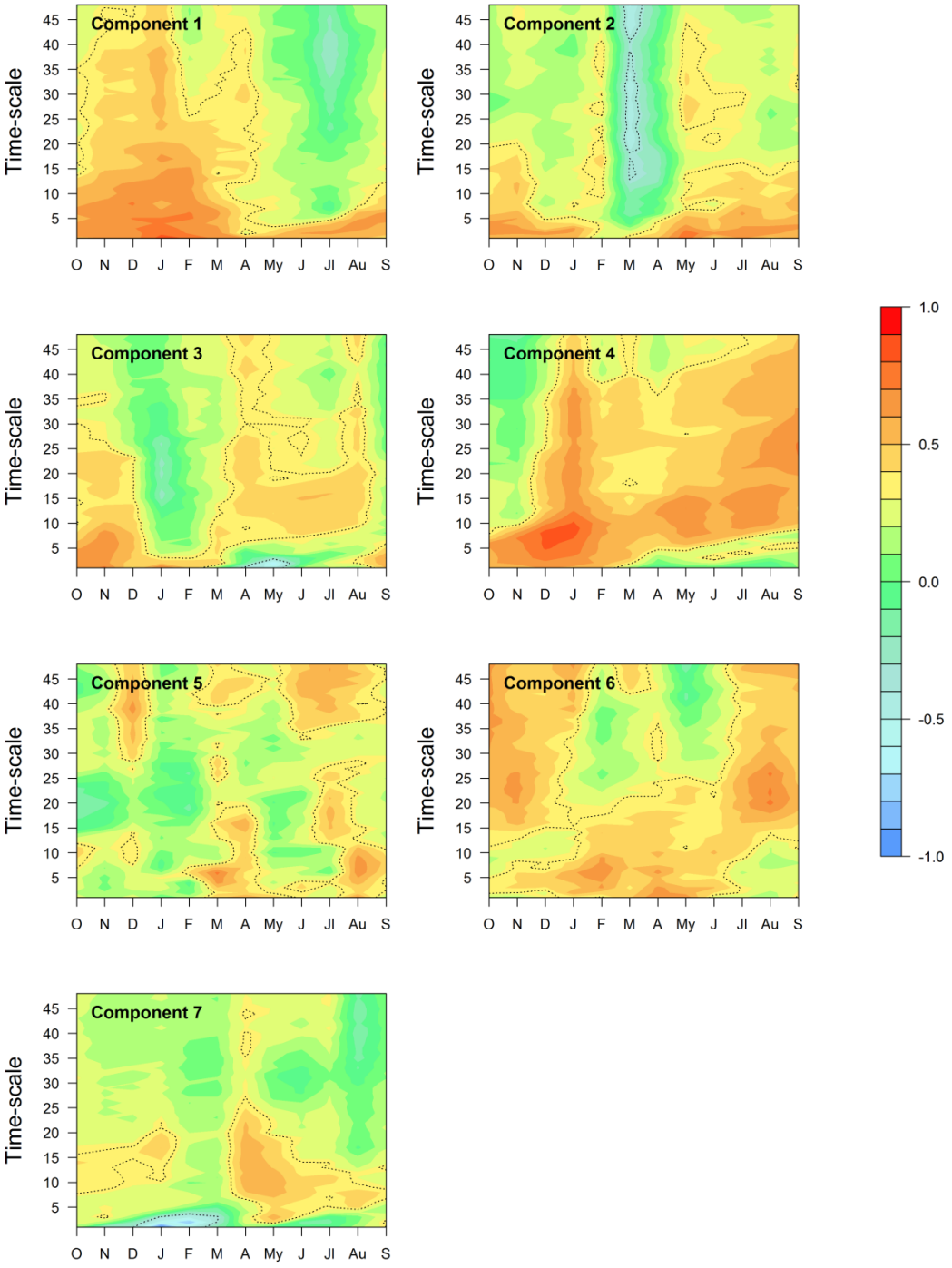

Supplementary Figure 13. Principal component scores obtained from monthly correlations between SPI time-scales and SSI (1940-1964). Dotted lines outline significant correlations at $p < 0.05$.

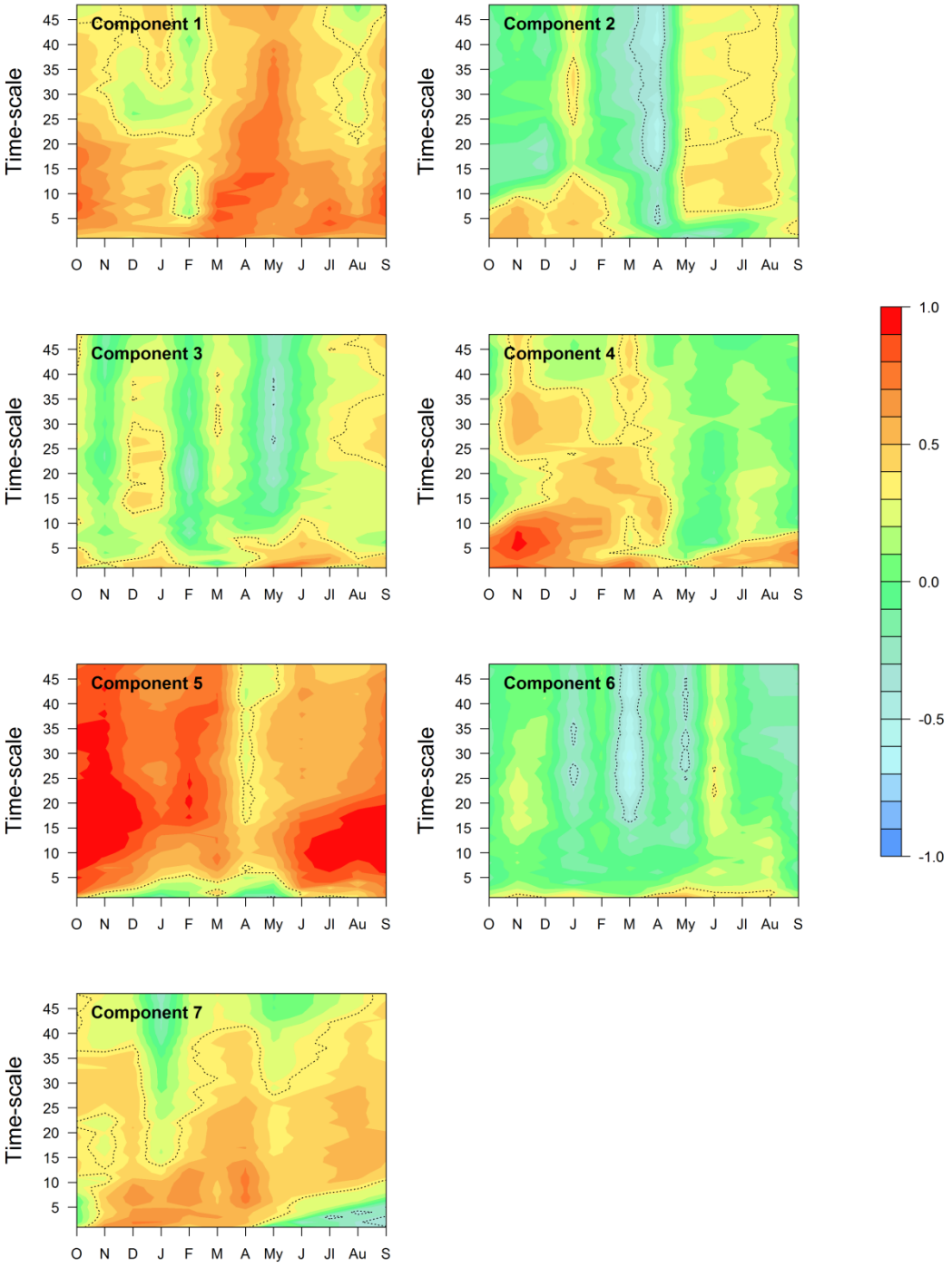

Supplementary Figure 13. Principal component scores obtained from monthly correlations between SPI time-scales and SSI (1965-1989). Dotted lines outline significant correlations at $p < 0.05$.

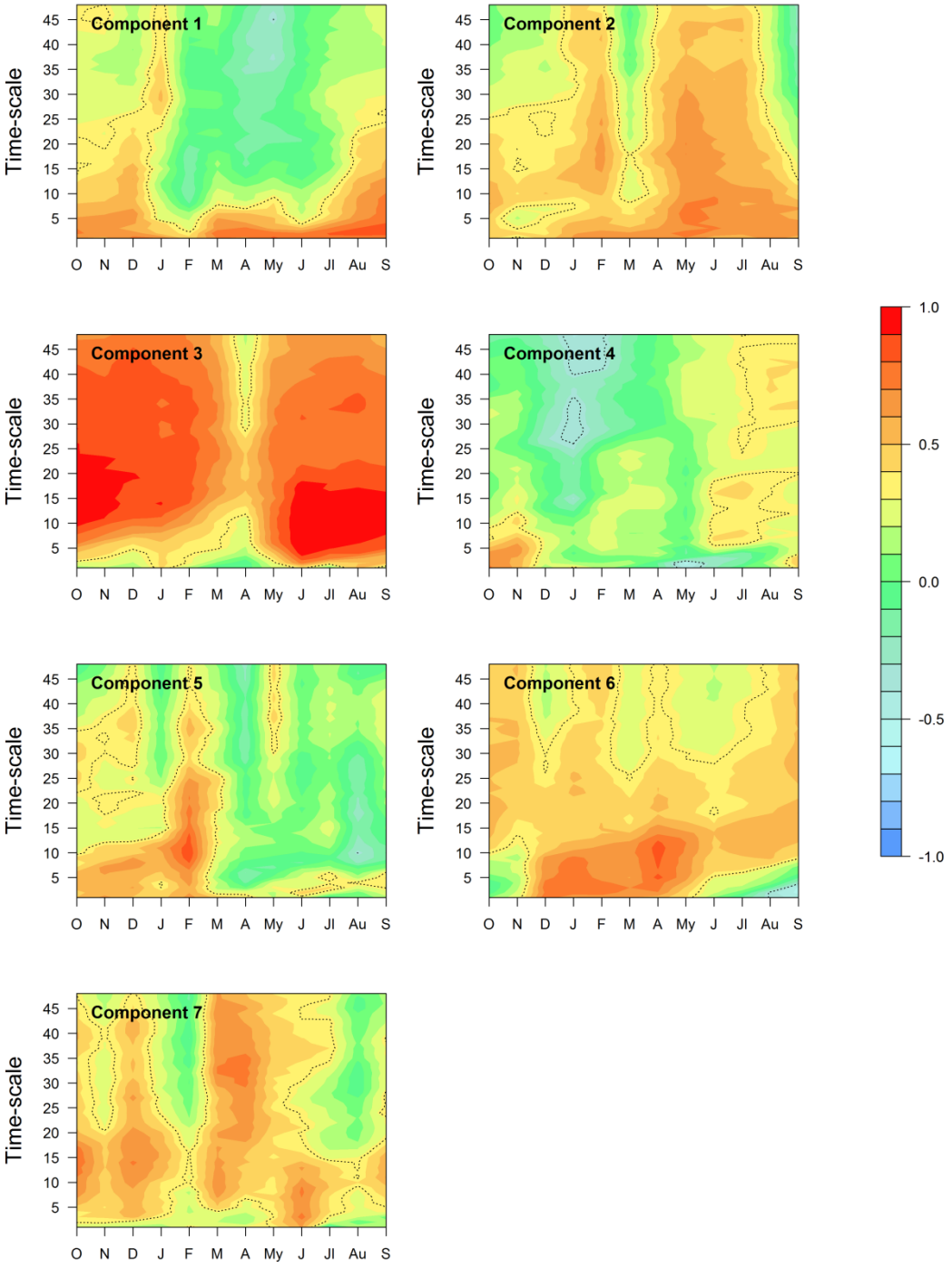

Supplementary Figure 13. Principal component scores obtained from monthly correlations between SPI time-scales and SSI (1990-2013). Dotted lines outline significant correlations at $p < 0.05$.

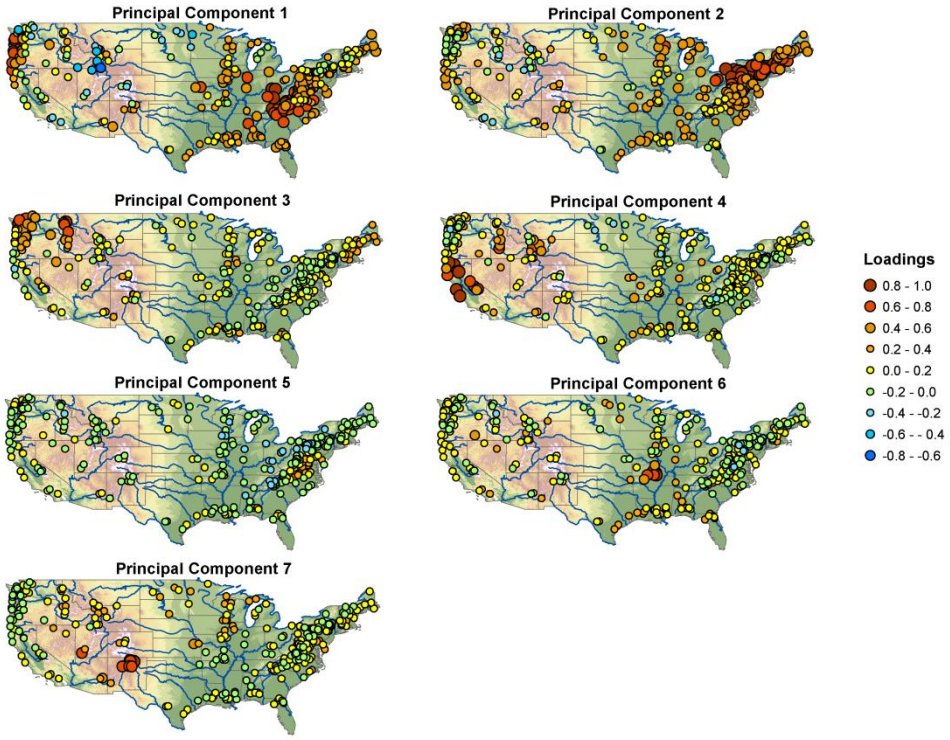

Supplementary Figure 14: Spatial distribution of the loadings of the extracted PCs, summarizing the patterns of correlation between SPI time-scales and SSI for the ssub-period 1940-1964. Coefficient of contingency between patterns of SPEI/SSI correlations and SPI/SSI correlations is 0.87.

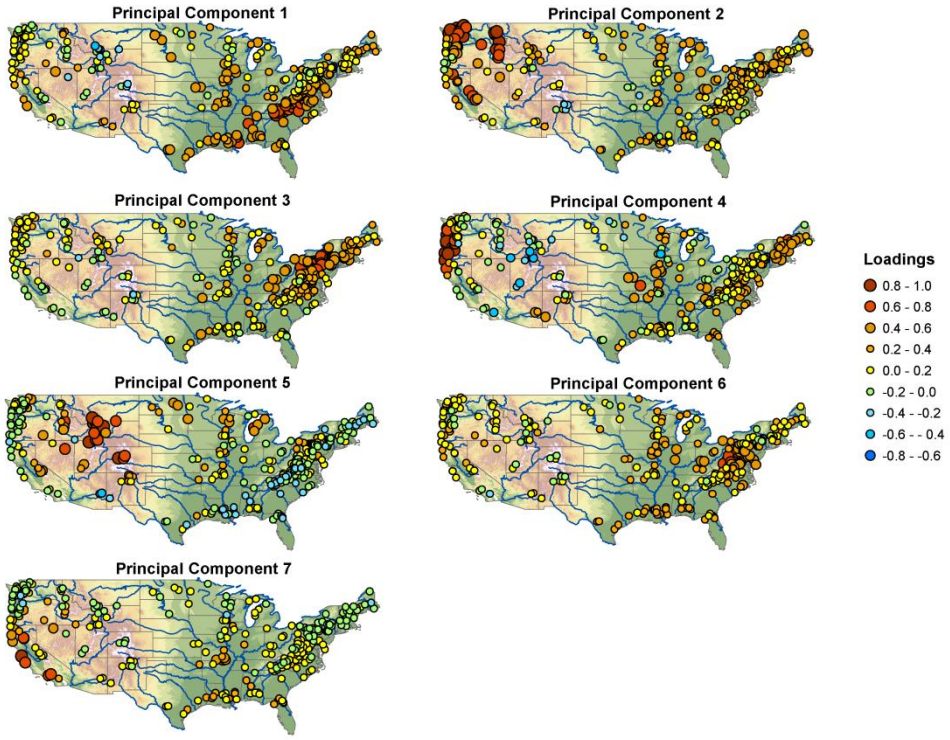

Supplementary Figure 15: Spatial distribution of the loadings of the extracted PCs, summarizing the patterns of correlation between SPI time-scales and SSI for the sub-period 1965-1989. Coefficient of contingency between patterns of SPEI/SSI correlations and SPI/SSI correlations is 0.89.

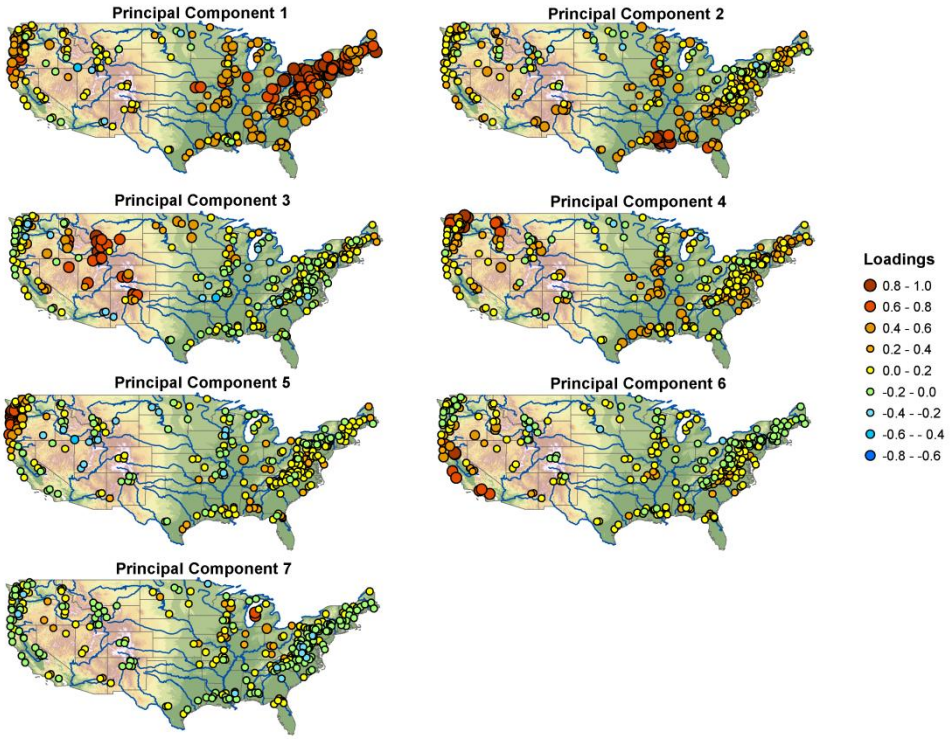

Supplementary Figure 16: Spatial distribution of the loadings of the extracted PCs, summarizing the patterns of correlation between SPI time-scales and SSI for the sub-period 1990-2013. Coefficient of contingency between patterns of SPEI/SSI correlations and SPI/SSI correlations is 0.90.

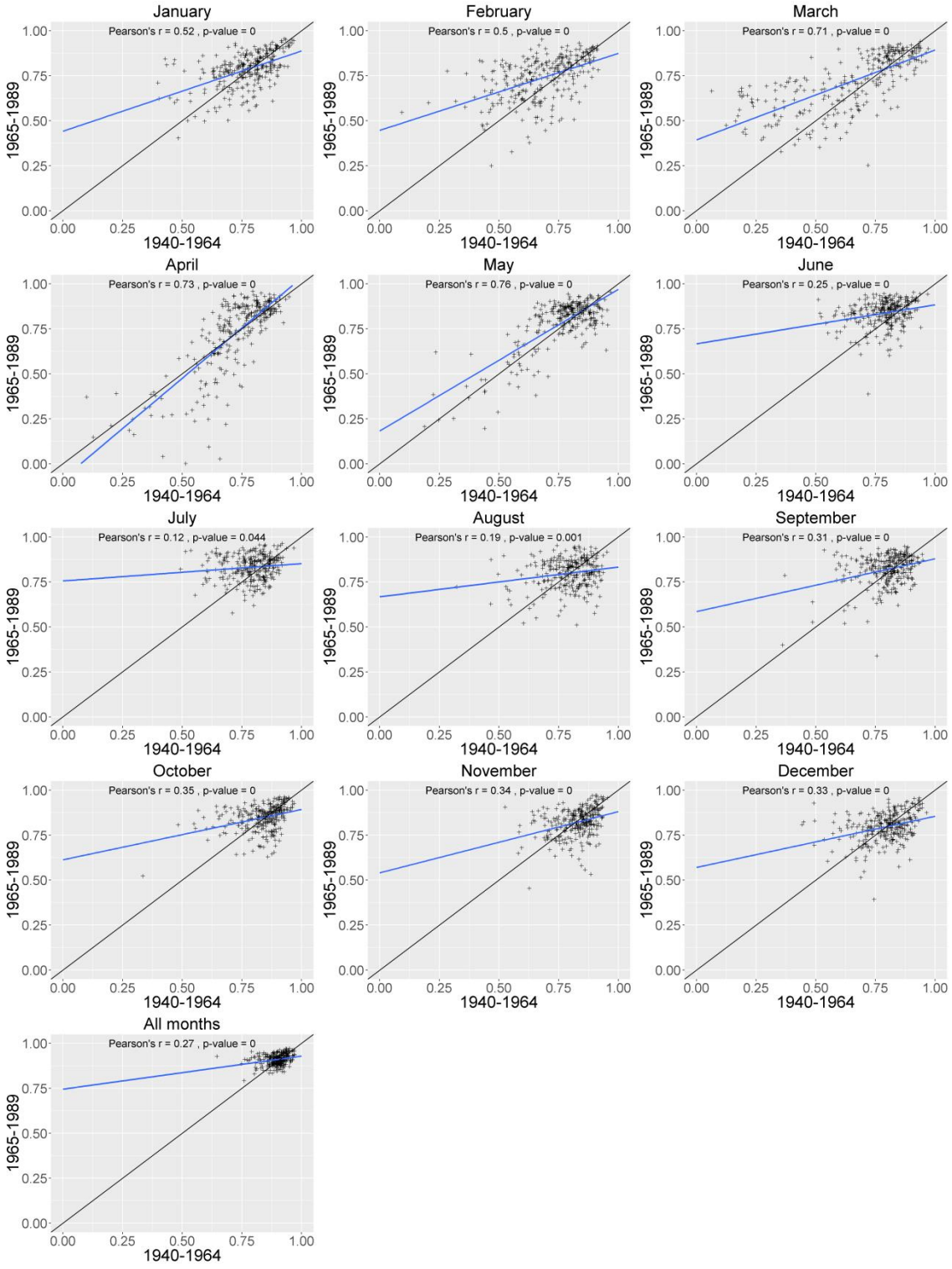

Supplementary Figure 17: Scatterplots with the maximum SPEI/SSI correlation in the different basins between the sub-periods 1940-1964 and 1964-1989.

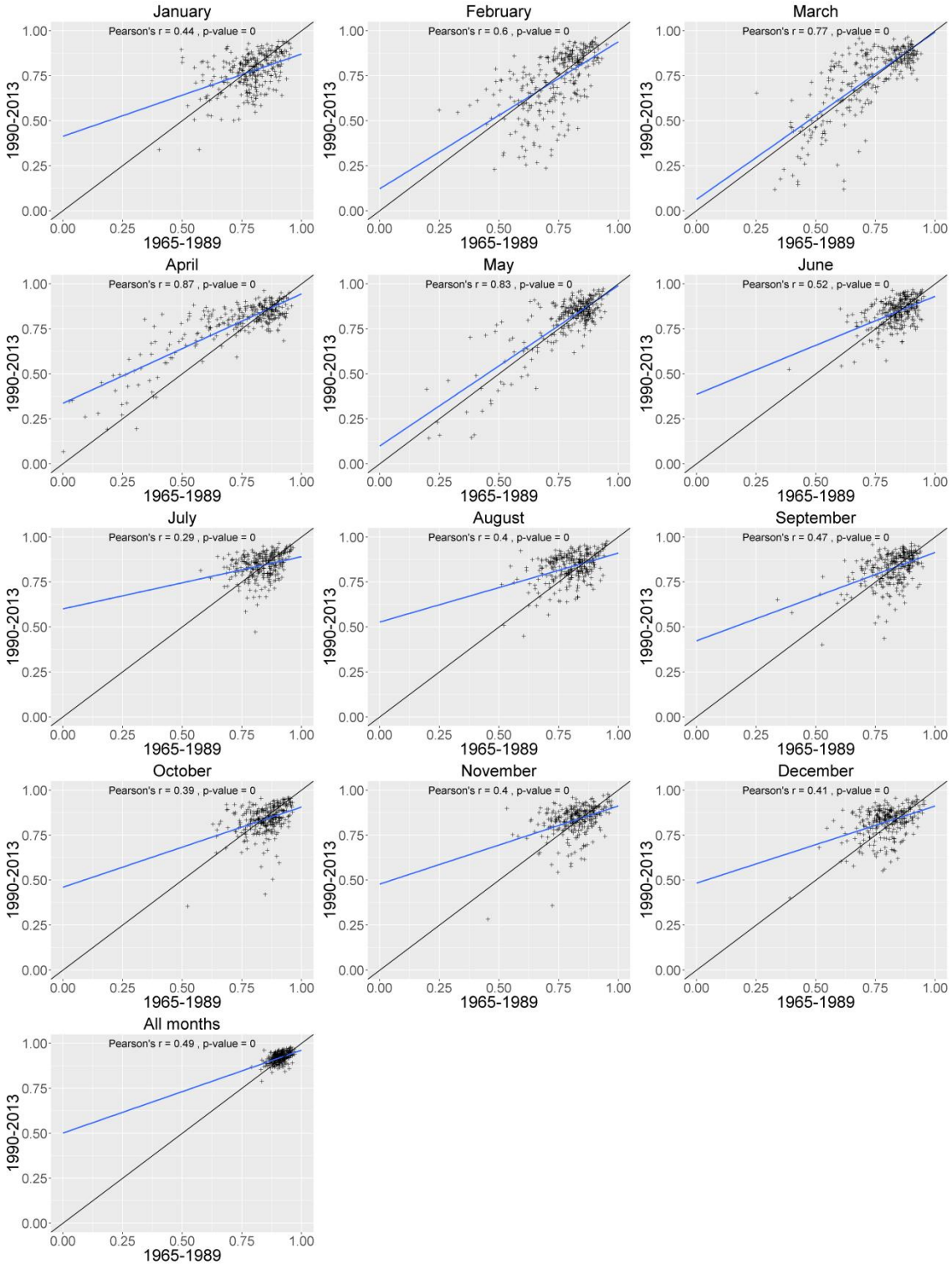

Supplementary Figure 18: Scatterplots showing the maximum SPEI/SSI correlation in the different basins between the sub-periods 1964-1989 and 1990-2013.

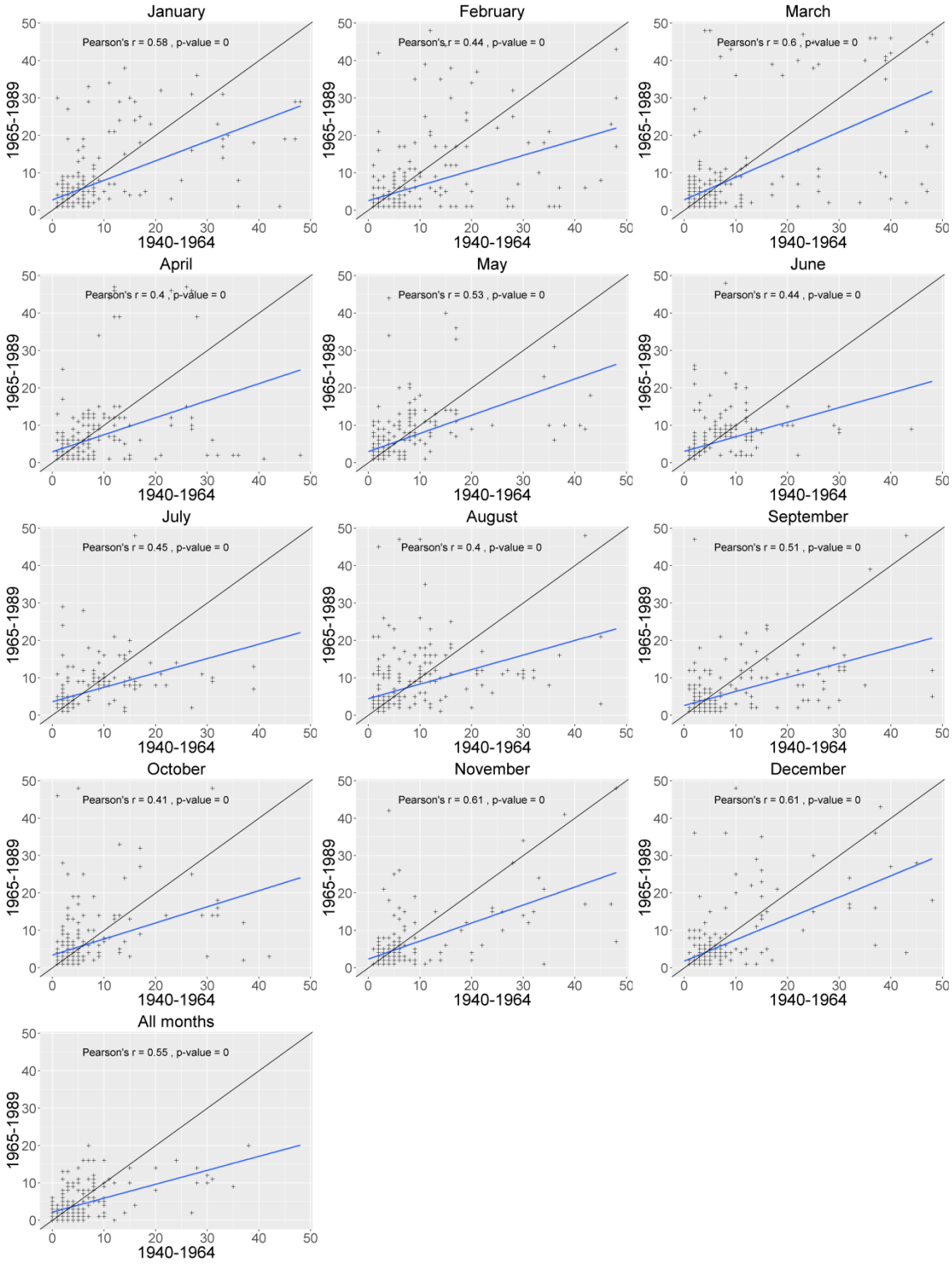

Supplementary Figure 19: Scatterplots showing SPEI time-scale at which the maximum SPEI/SSI correlation is found in the different basins between the sub-periods 1940-1964 and 1964-1989.

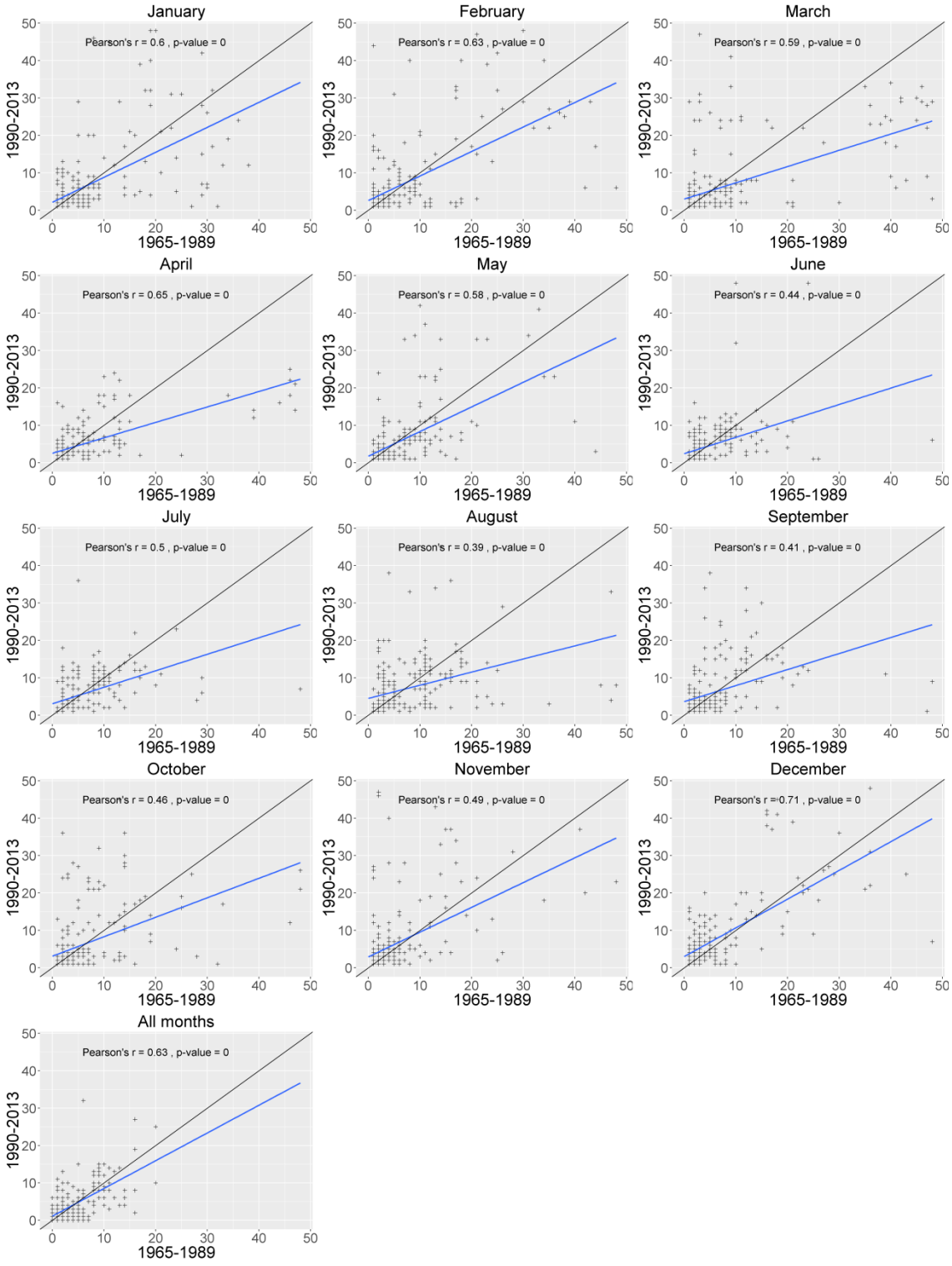

Supplementary Figure 20: Scatterplots showing SPEI time-scale at which the maximum SPEI/SSI correlation is found in the different basins between the sub-periods 1964-1989 and 1990-2013.

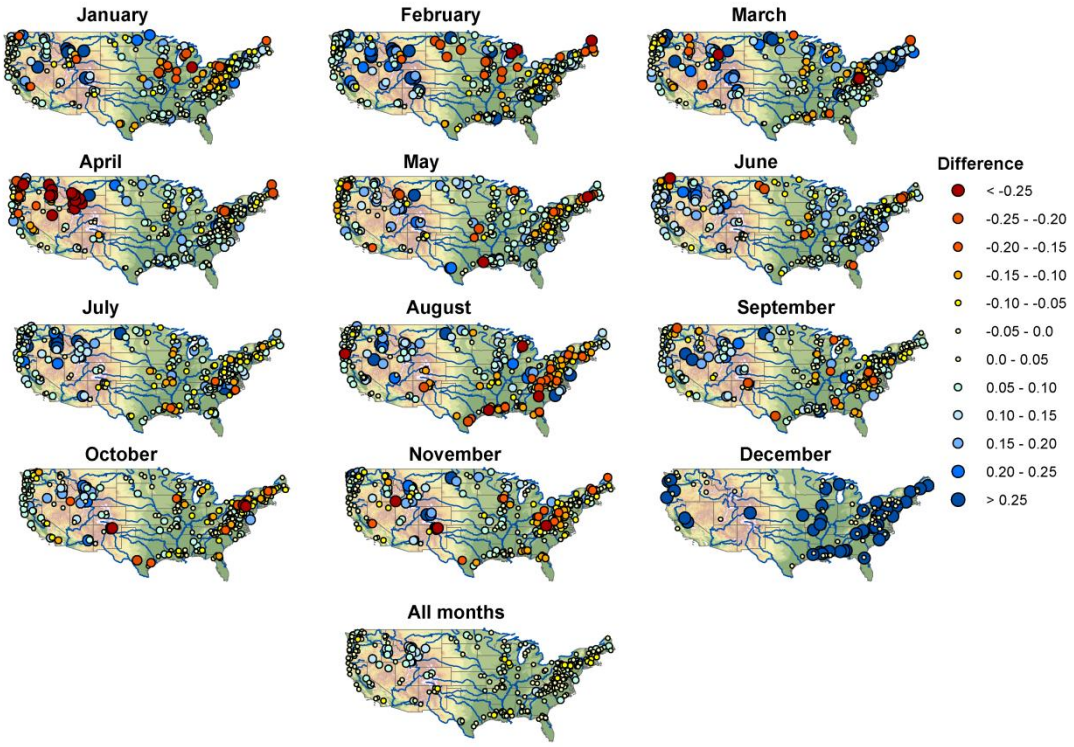

Supplementary Figure 21. Spatial distribution of the differences in the maximum correlation between SPEI time-scales and SSI between the sub-periods 1940-1964 and 1965-1989.

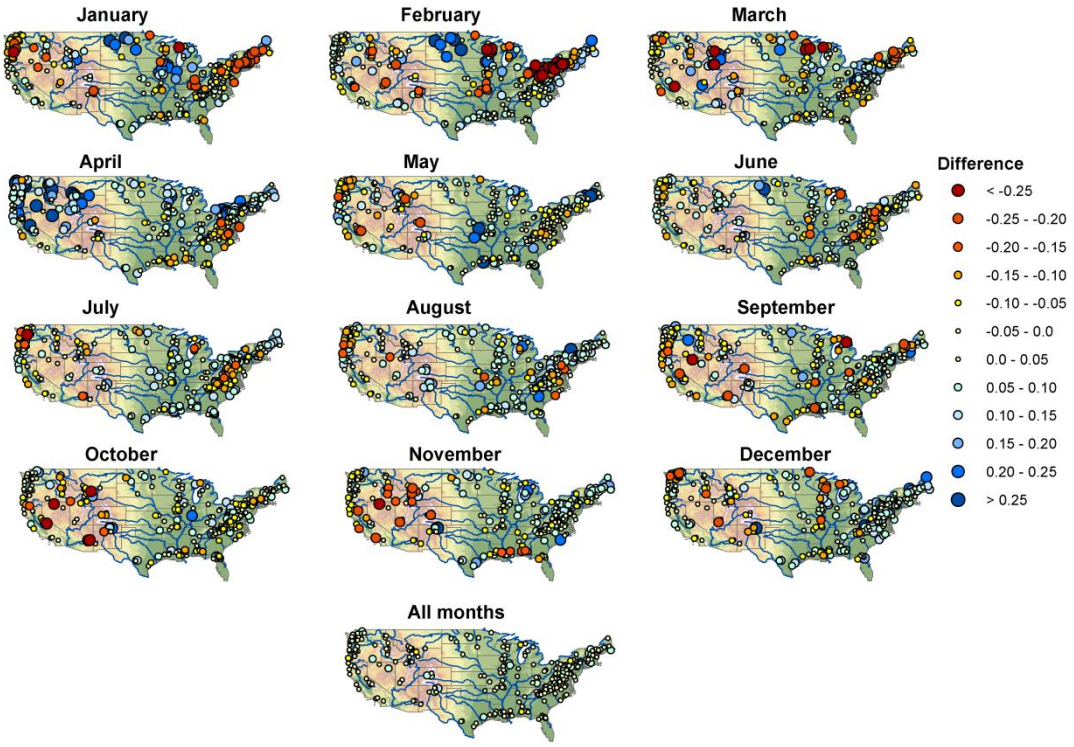

Supplementary Figure 22. Spatial distribution of the differences in the maximum correlation between SPEI time-scales and SSI between the sub-periods 1965-1989 and 1990-2013.

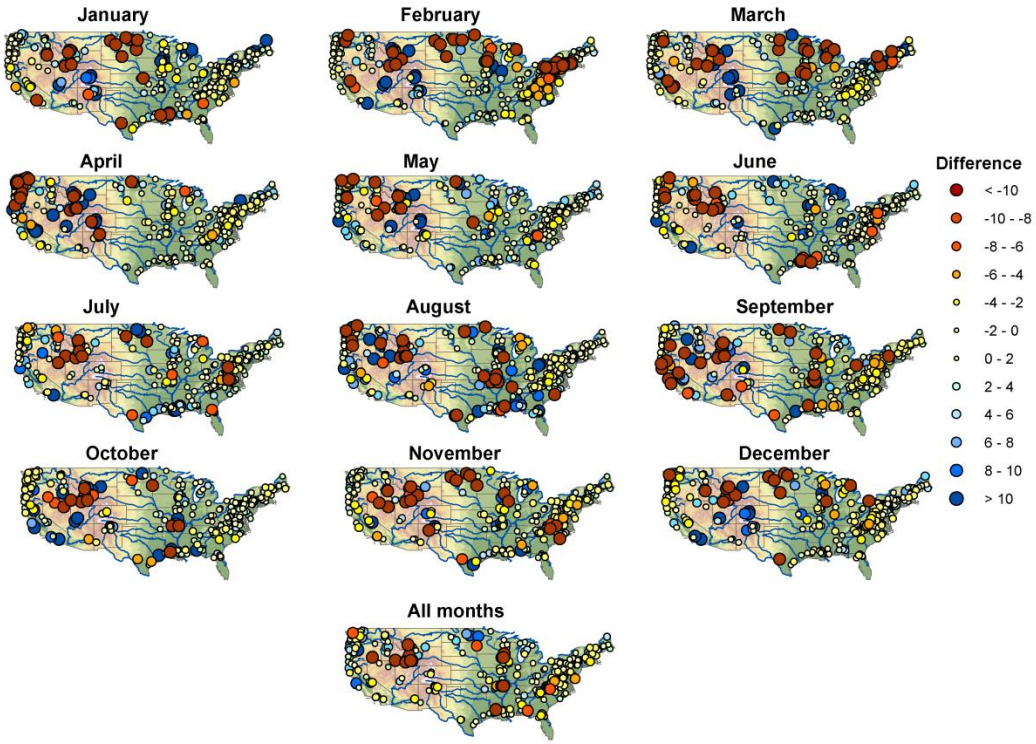

Supplementary Figure 23. Spatial distribution of the differences in the SPEI time-scales at which the maximum correlation between SPEI time-scales and SSI between is found between the sub-periods 1940-1964 and 1965-1989.

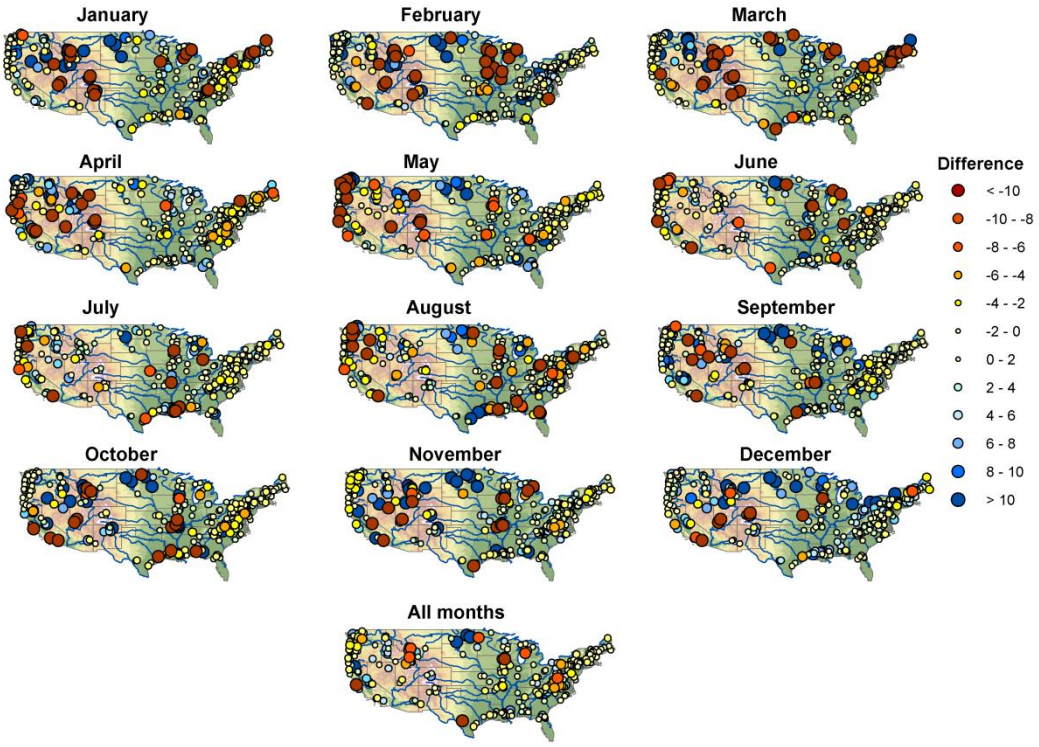

Supplementary Figure 24. Spatial distribution of the differences in the SPEI time-scales at which the maximum correlation between SPEI time-scales and SSI between is found in the sub-periods 1965-1989 and 1990-2013.

	All months	Jan	Feb	Mar	Apr.	May	Jun	Jul	Aug	Sep	Oct	Nov	Dec
NDVI (annual)	-0.41		-0.20		0.47			-0.28	-0.39	-0.20	-0.35	-0.22	-0.22
NDVI (cold season)	-0.35				0.43			-0.23	-0.37	-0.18	-0.31		-0.21
NDVI (warm season)	-0.39	-0.17	-0.20		0.41	-0.20		-0.28	-0.33	-0.20	-0.33	-0.24	-0.24
Soil drainage			-0.22		0.18			-0.25				-0.18	
Soil infiltration cap.								-0.18					
Soil Permeability					-0.18			0.25					
Soil depth layer			-0.19		0.17			-0.18					
Soil wáter capacity	-0.23		-0.26		0.34			-0.27					
Elevation	0.46	0.26	0.38		-0.42			0.34	0.23		0.19	0.29	0.23
Basin Surface													
Average streamflow (annual)				-0.20									
Average streamflow (cold)		0.20			-0.30								
Average streamflow (warm)				-0.18									
Change in anual stream.													
Change in cold stream.		-0.22											
Change in warm stream.		-0.20											
Average ETo (annual)	-0.20		-0.17	-0.23	0.38			-0.21	-0.30				-0.23
Average ETo (cold)	-0.27	-0.17	-0.30	-0.20	0.42			-0.29	-0.28				-0.26
Average ETo (warm)	-0.24		-0.25	-0.22	0.41			-0.26	-0.30				-0.25
Change in anual ETo	0.20		0.23		-0.21			0.31				0.25	
Change in cold ETo												0.18	
Change in warm ETo	0.19											0.23	
Average Tmin (annual)	-0.29		-0.17	-0.29	0.35			-0.18	-0.26				-0.21
Average Tmin (cold)	-0.31	-0.18	-0.19	-0.28	0.37			-0.20	-0.27				-0.22
Average Tmin (warm)	-0.33	-0.19	-0.22	-0.27	0.41			-0.23	-0.29				-0.23
Change in anual Tmin	0.21		0.25		-0.20			0.20	0.23		0.18	0.17	
Change in cold Tmin			0.19						0.19				
Change in warm Tmin									0.17				
Average Tmax (annual)	-0.24		-0.18	-0.26	0.39			-0.21	-0.29				-0.22
Average Tmax (cold)	-0.25		-0.19	-0.26	0.40			-0.22	-0.30				-0.23
Average Tmax (warm)	-0.27		-0.22	-0.25	0.43			-0.24	-0.31				-0.24
Change in anual Tmax	0.22		0.27		-0.28			0.32	0.18			0.19	
Change in cold Tmax								0.20					
Change in warm Tmax													
Average Precip. (annual)													0.18

Average Precip. (cold)	-0.28				0.34			-0.21	-0.25		-0.24	-0.25	
Average Precip. (warm)													
Change in anual Precip.					0.21		-0.24	-0.20		-0.18			
Change in cold Precip.				0.17								-0.19	
Change in warm Precip.				0.17			-0.19	-0.19					

Supplementary Table 1: Significant spatial correlations ($p < 0.005$) between the spatial variability of different environmental and climatic variables and the differences in the maximum correlation obtained between SPEI and SSI among the sub-periods 1940-1964 and 1965-1989 considering the different monthly series and the series of all months.

	All months	Jan	Feb	Mar	Apr.	May	Jun	Jul	Aug	Sep	Oct	Nov	Dec
NDVI (annual)												0.22	
NDVI (cold season)												0.23	
NDVI (warm season)													
Soil drainage													
Soil infiltration cap.													
Soil Permeability													
Soil depth layer													
Soil wáter capacity					-0.17								
Elevation			0.20					-0.18					
Basin Surface		-0.25	-0.17									-0.24	-0.41
Average streamflow (annual)													
Average streamflow (cold)													
Average streamflow (warm)													
Change in anual stream.		-0.24					0.17					-0.27	
Change in cold stream.													
Change in warm stream.													
Average ETo (annual)			0.17					0.20					
Average ETo (cold)		-0.22						0.19					
Average ETo (warm)		-0.20						0.20					
Change in anual ETo													
Change in cold ETo													
Change in warm ETo													
Average Tmin (annual)								0.21					
Average Tmin (cold)								0.21					
Average Tmin (warm)		-0.17						0.21					
Change in anual Tmin													
Change in cold Tmin													
Change in warm Tmin					-0.17								
Average Tmax (annual)		-0.17						0.20					
Average Tmax (cold)		-0.17						0.20					
Average Tmax (warm)		-0.18						0.20					

Change in anual Tmax					-0.20								
Change in cold Tmax					-0.21								
Change in warm Tmax													
Average Precip. (annual)					-0.28		-0.19						
Average Precip. (cold)												0.18	
Average Precip. (warm)					-0.27		-0.19					0.20	
Change in anual Precip.													
Change in cold Precip.													0.24
Change in warm Precip.													0.22

Supplementary Table 2: Significant spatial correlations ($p < 0.005$) between the spatial variability of different environmental and climatic variables and the differences in the time-scales at which the maximum correlation is obtained between SPEI and SSI among the sub-periods 1940-1964 and 1965-1989 considering the different monthly series and the series of all months.

	All months	Jan	Feb	Mar	Apr.	May	Jun	Jul	Aug	Sep	Oct	Nov	Dec
NDVI (annual)		-0.18			-0.37	0.18	-0.21				0.19	0.20	0.22
NDVI (cold season)					-0.40								
NDVI (warm season)					-0.41		-0.22				0.20	0.20	0.22
Soil drainage								0.31					
Soil infiltration cap.							0.19	0.25					
Soil Permeability								-0.18					
Soil depth layer					-0.25			0.18					
Soil wáter capacity					-0.23						0.17		
Elevation					0.29	-0.17	0.18					-0.20	-0.22
Basin Surface													
Average streamflow (annual)													
Average streamflow (cold)													
Average streamflow (warm)													
Change in anual stream.												0.35	
Change in cold stream.		0.18											
Change in warm stream.											0.17	0.27	
Average ETo (annual)			0.17		-0.51			0.17					
Average ETo (cold)					-0.51			0.21					
Average ETo (warm)					-0.53			0.19					
Change in anual ETo							0.20		0.22				
Change in cold ETo		-0.19			0.23								
Change in warm ETo					0.21						-0.18		
Average Tmin (annual)	-0.18				-0.41		-0.18		-0.17				
Average Tmin (cold)	-0.17				-0.43		-0.18						
Average Tmin (warm)					-0.46		-0.18						
Change in anual Tmin					0.20								
Change in cold Tmin					0.23								
Change in warm Tmin					0.25								

Average Tmax (annual)			0.18		-0.50								
Average Tmax (cold)			0.17		-0.51								
Average Tmax (warm)			0.17		-0.53								
Change in anual Tmax									0.18				
Change in cold Tmax			-0.17		0.25				0.18				
Change in warm Tmax			-0.18		0.28				0.19				
Average Precip. (annual)	-0.23	-0.26			0.17			-0.19	-0.23				-0.29
Average Precip. (cold)					-0.27	0.20					0.20	0.23	
Average Precip. (warm)	-0.23	-0.28							-0.19				-0.23
Change in anual Precip.	0.23		-0.17	0.19					0.24		0.21	0.47	0.29
Change in cold Precip.						0.20						0.22	0.31
Change in warm Precip.	0.22							0.18	0.19		0.18	0.45	0.35

Supplementary Table 3: Significant spatial correlations ($p < 0.005$) between the spatial variability of different environmental and climatic variables and the differences in the maximum correlation obtained between SPEI and SSI among the sub-periods 1965-1989 and 1990-2013 considering the different monthly series and the series of all months.

	All months	Jan	Feb	Mar	Apr.	May	Jun	Jul	Aug	Sep	Oct	Nov	Dec
NDVI (annual)					0.20								
NDVI (cold season)													
NDVI (warm season)					0.23								
Soil drainage													
Soil infiltration cap.													
Soil Permeability													
Soil depth layer													
Soil wáter capacity					0.21								
Elevation					-0.26								
Basin Surface		0.24	0.17							0.17			
Average streamflow (annual)													
Average streamflow (cold)													
Average streamflow (warm)													
Change in anual stream.							0.17						
Change in cold stream.							0.28						
Change in warm stream.							0.31						
Average ETo (annual)													
Average ETo (cold)													
Average ETo (warm)													
Change in anual ETo					-0.25								
Change in cold ETo					-0.19								
Change in warm ETo					-0.23								
Average Tmin (annual)											-0.17		
Average Tmin (cold)					0.17								
Average Tmin (warm)					0.18								

Change in anual Tmin													
Change in cold Tmin													
Change in warm Tmin													
Average Tmax (annual)													
Average Tmax (cold)													
Average Tmax (warm)													
Change in anual Tmax					-0.17								
Change in cold Tmax					-0.18								
Change in warm Tmax					-0.21								
Average Precip. (annual)													
Average Precip. (cold)					0.17								
Average Precip. (warm)													
Change in anual Precip.													
Change in cold Precip.							0.18						
Change in warm Precip.													

Supplementary Table 4. Significant spatial correlations ($p < 0.005$) between the spatial variability of different environmental and climatic variables and the differences in the time-scales at which the maximum correlation is obtained between SPEI and SSI among the sub-periods 1965-1989 and 1990-2013 considering the different monthly series and the series of all months.

Supplementary Material

The impact of drought on the productivity of two rainfed crops in Spain

Marina Peña-Gallardo[1], Sergio Martín Vicente-Serrano[1], Fernando Domínguez-Castro[1], Santiago Beguería[2]

[1] Instituto Pirenaico de Ecología, Consejo Superior de Investigaciones Científicas (IPE-CSIC), Zaragoza, Spain.

[2] Estación Experimental de Aula Dei, Consejo Superior de Investigaciones Científicas (EEAD-CSIC), Zaragoza, Spain.

Supplementary Table 1. Relationship between provincial and agricultural district data, aggregated at the provincial scale, for wheat cultivation for the common period 1993–2014.

Codes	Provinces	r	Codes	Provinces	r
1	**Álava**	0.16	**23**	**Jaén**	0.38*
2	**Albacete**	0.41*	**24**	**León**	0.69*
3	**Alicante**	0.1	**25**	**Lleida**	0.52*
4	**Almería**	0.47*	**26**	**La Rioja**	0.35*
5	**Ávila**	0.77*	**28**	**Madrid**	0.81*
6	**Badajoz**	0.49*	**29**	**Málaga**	0.11
7	**Islas Baleares**	-0.22	**30**	**Murcia**	0.13
8	**Barcelona**	0.69*	**31**	**Navarra**	-0.25
9	**Burgos**	0.82*	**32**	**Ourense**	0.37*
10	**Cáceres**	0.34*	**33**	**Asturias**	-0.16
11	**Cádiz**	0.32*	**34**	**Palencia**	0.73*
12	**Castellón**	-0.19	**37**	**Salamanca**	0.87*
13	**Ciudad Real**	0.43*	**40**	**Segovia**	0.94*

14	**Córdoba**	0.46*****	**41**	**Sevilla**	0.25
15	**A Coruña**	0.1	**42**	**Soria**	0.89*****
16	**Cuenca**	0.86*****	**43**	**Tarragona**	0.54*****
17	**Girona**	0.1	**44**	**Teruel**	0.83*****
18	**Granada**	0.3	**45**	**Toledo**	0.48*****
19	**Guadalajara**	0.87*	**46**	**Valencia**	0.2
21	**Huelva**	0.29	**47**	**Valladolid**	0.92*****
22	**Huesca**	0.4*****	**49**	**Zamora**	0.75*****
			50	**Zaragoza**	0.51*****

(*****) correlations are significant at $p < 0.05$

Supplementary Table 2. Relationship between provincial and agricultural district data, aggregated at provincial scale, for barley cultivation for the common period 1993–2014.

Codes	Provinces	r
1	**Álava**	0.11
2	**Albacete**	0.2
10	**Cáceres**	0.48*****
11	**Cádiz**	0.32*****
12	**Castellón**	-0.14
13	**Ciudad Real**	0.28
14	**Córdoba**	0.54*****
15	**A Coruña**	-0.09
16	**Cuenca**	0.88*****
17	**Girona**	0.08

18	**Granada**	0.51*****
19	**Guadalajara**	0.86*****
22	**Huelva**	0.57*****
26	**La Rioja**	0.76*****
31	**Navarra**	0.01
41	**Sevilla**	-0.35*****
43	**Tarragona**	0.88*****

(*****) correlations are significant at $p < 0.05$

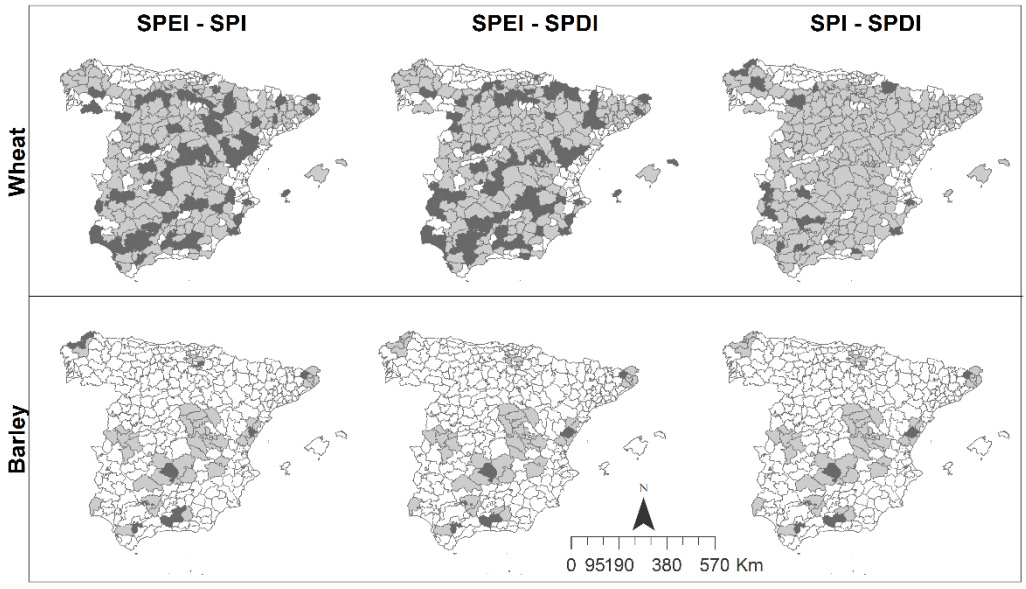

Supplementary Fig. 1. Spatial distribution of regions where significant differences (dark grey) and non significant differences (light grey) were found in the t-tests.

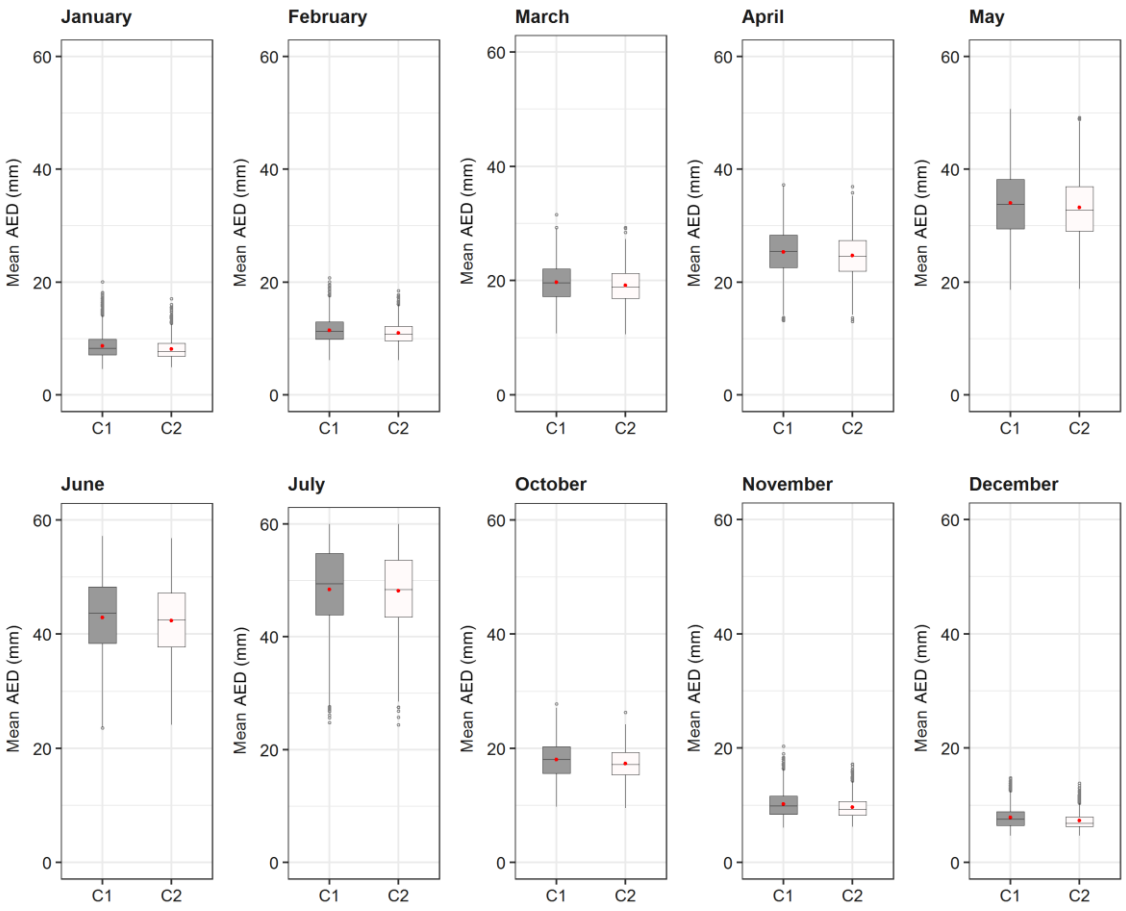

Supplementary Fig. 2. Monthly mean AED conditions in the agricultural districts where wheat was cultivated, classified into principal components (C1 and C2) for the period 1993–2015. The red dot shows the mean, and the black line shows the median.

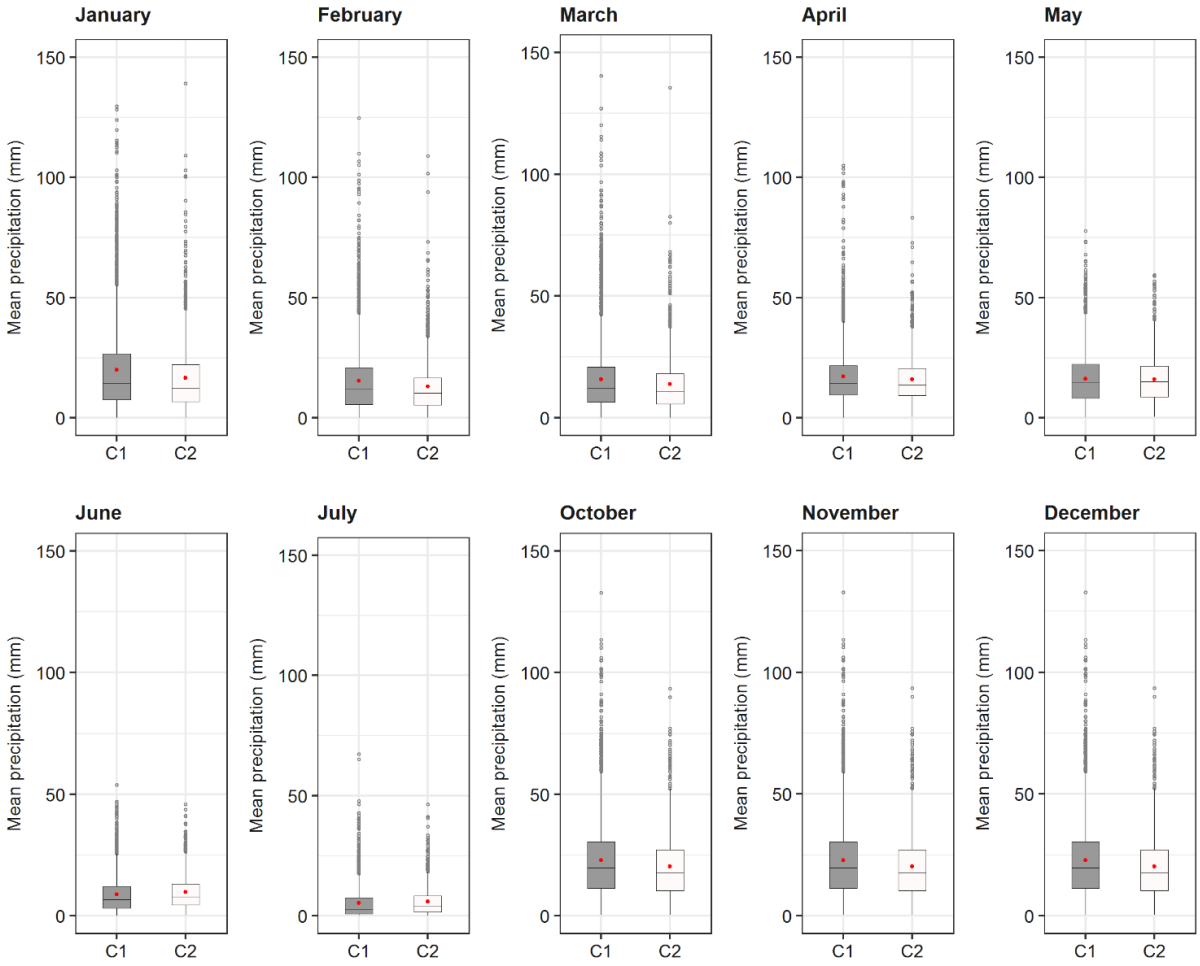

Supplementary Fig. 3. As for Supplementary Fig. 2, but for the monthly mean precipitation.

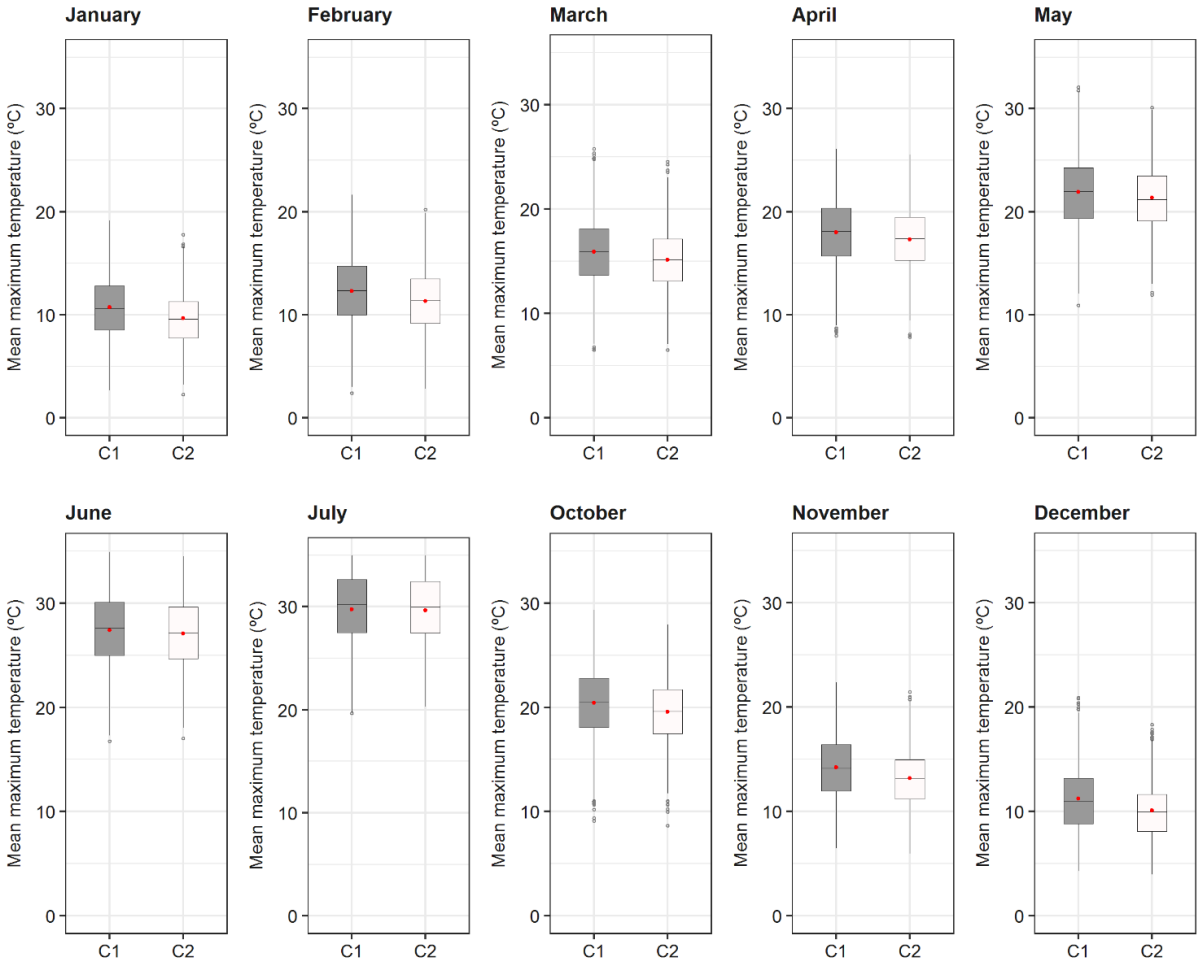

Supplementary Fig. 4. As for Supplementary Fig. 2, but for the monthly mean maximum temperature.

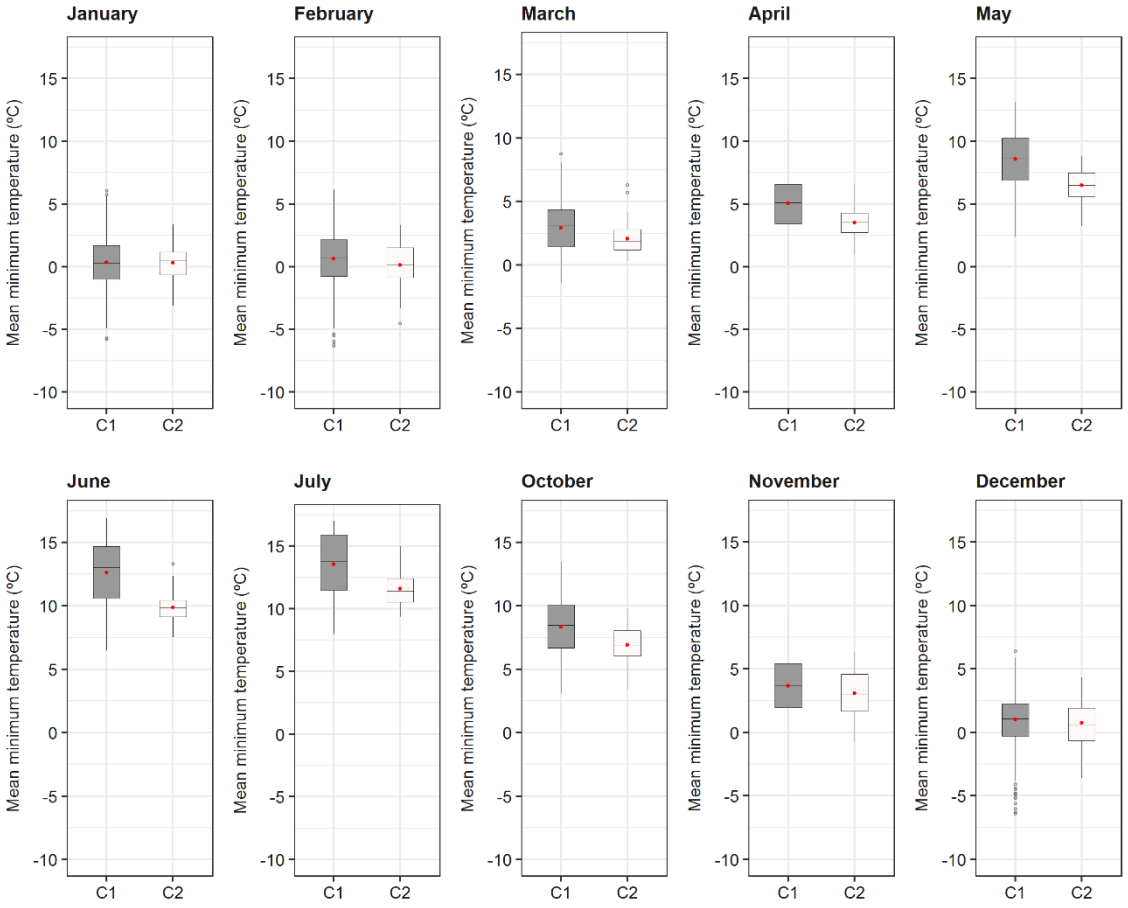

Supplementary Fig. 5. As for Supplementary Fig. 2, but for the monthly mean minimum temperature.

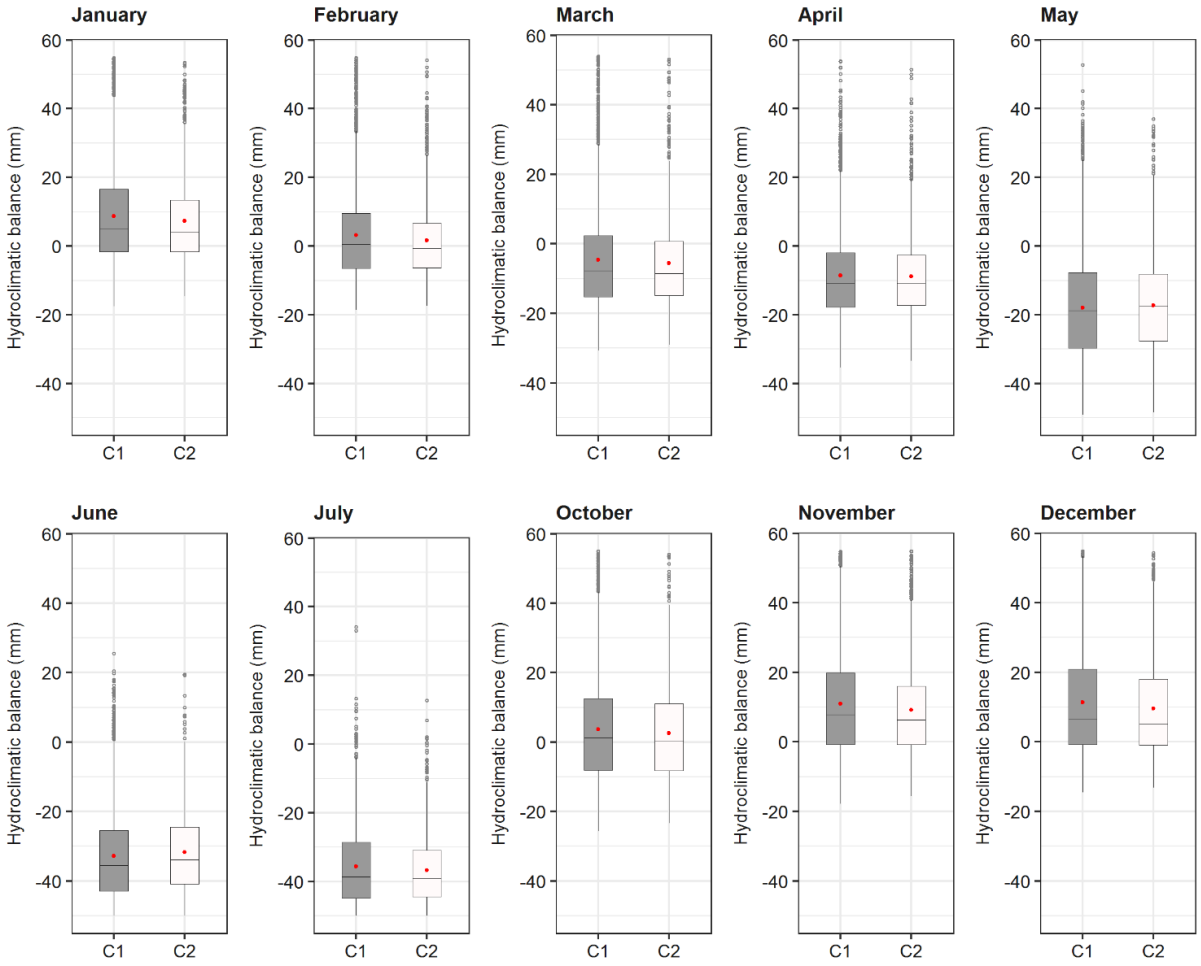

Supplementary Fig. 6. As for Supplementary Fig. 2, but for the monthly mean hydroclimate balance.

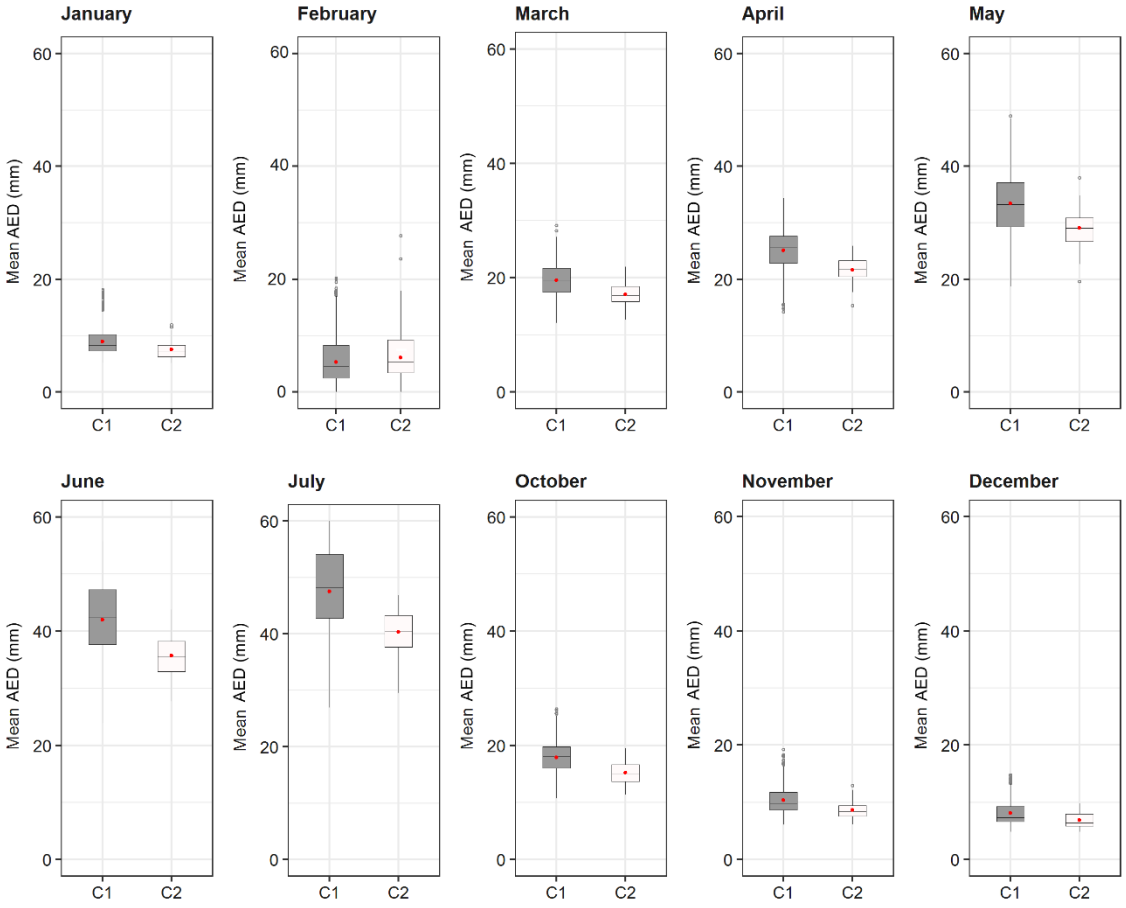

Supplementary Fig. 7. Monthly mean AED conditions in the agricultural districts where barley was cultivated, classified into principal components (C1 and C2) for the period 1993–2015. The red dot show the mean, and black line shows the median.

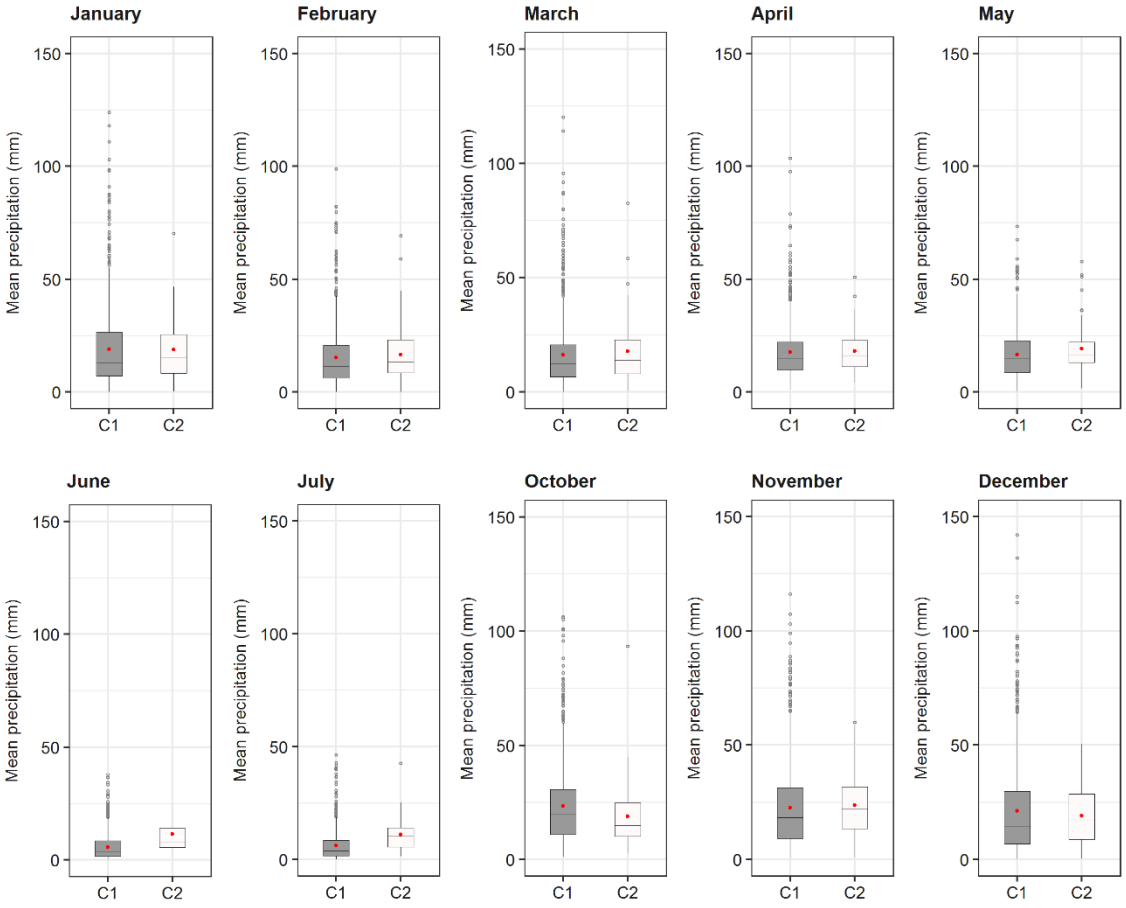

Supplementary Fig. 8. As for Supplementary Fig. 7, but for the monthly mean precipitation.

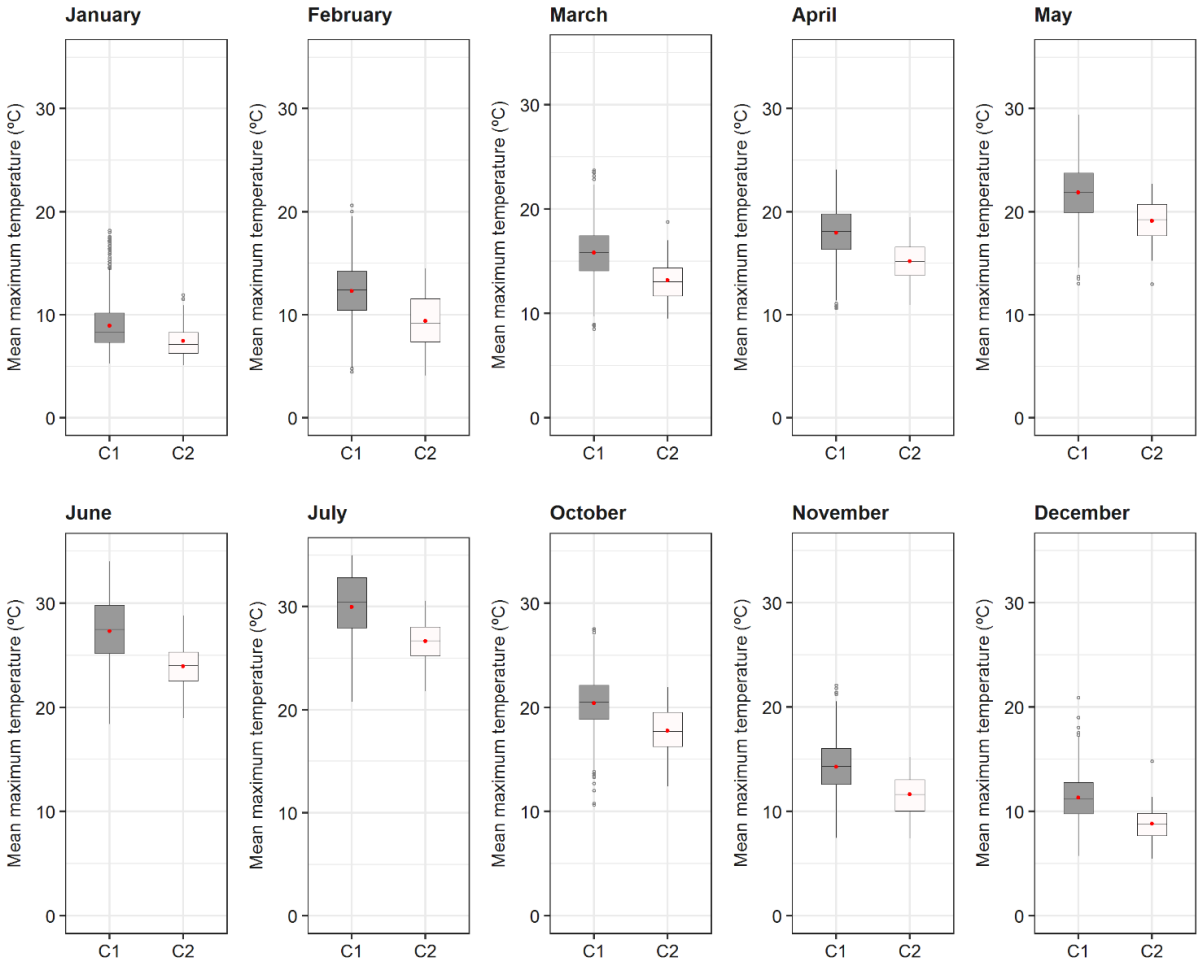

Supplementary Fig. 9. As for Supplementary Fig. 7, but for the monthly mean maximum temperature.

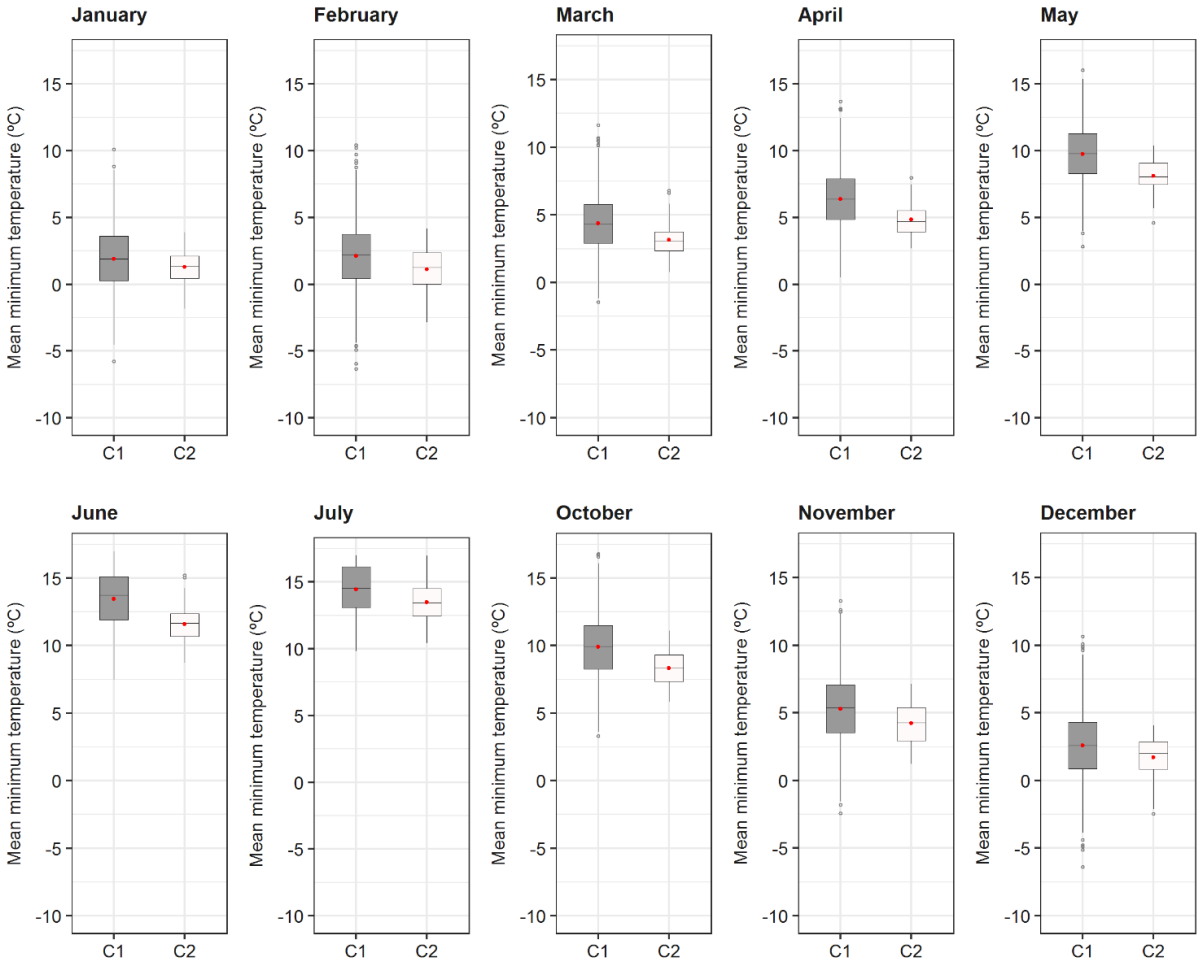

Supplementary Fig. 10. As for Supplementary Fig. 7, but for the monthly mean minimum temperature.

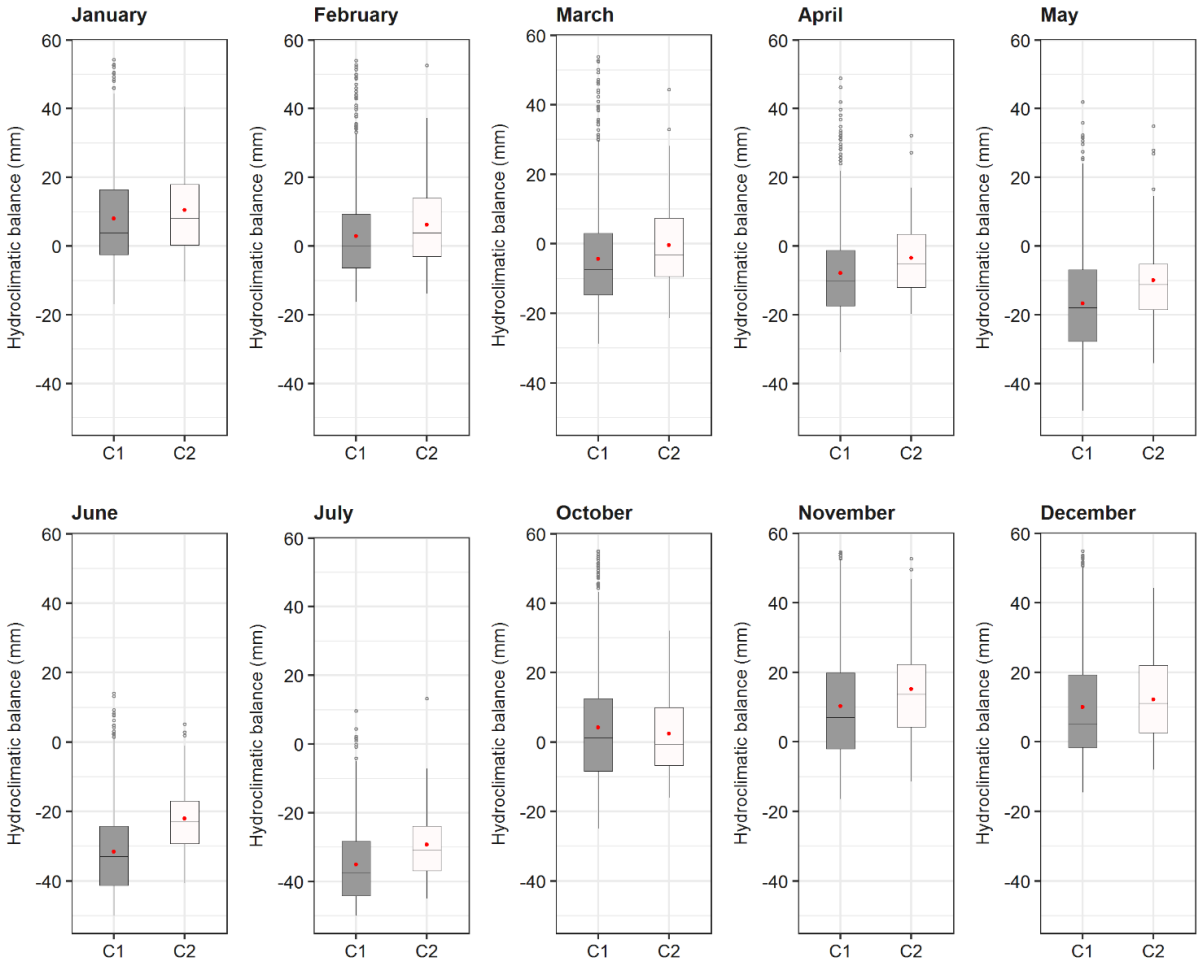

Supplementary Fig. 11. As for Supplementary Fig. 7, but for the monthly mean hydroclimate balance

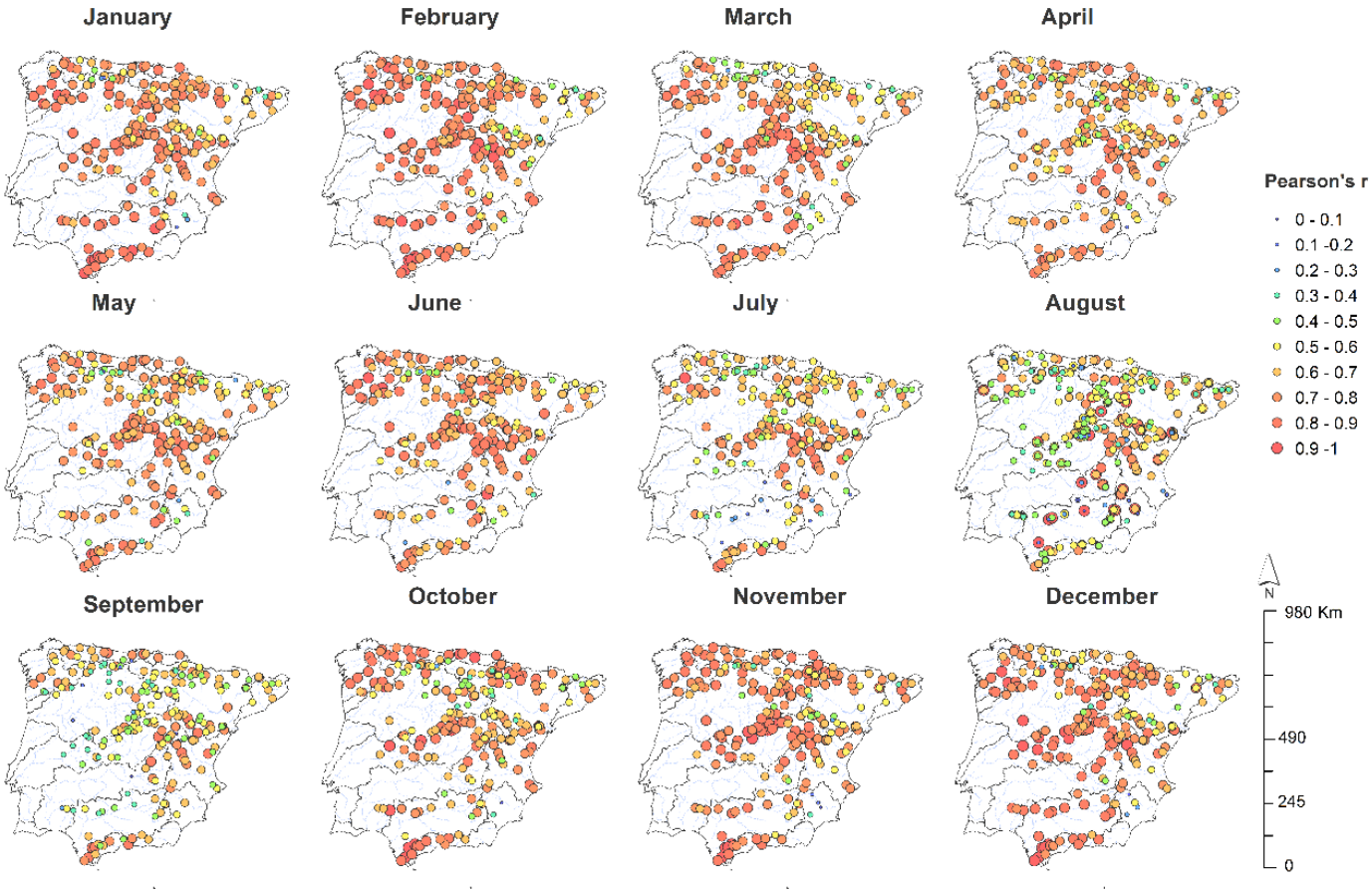

Supplementary figure 1. Spatial distribution of the monthly highest correlation coefficients between the SPEI and the SSI independently of the month and time-scale.

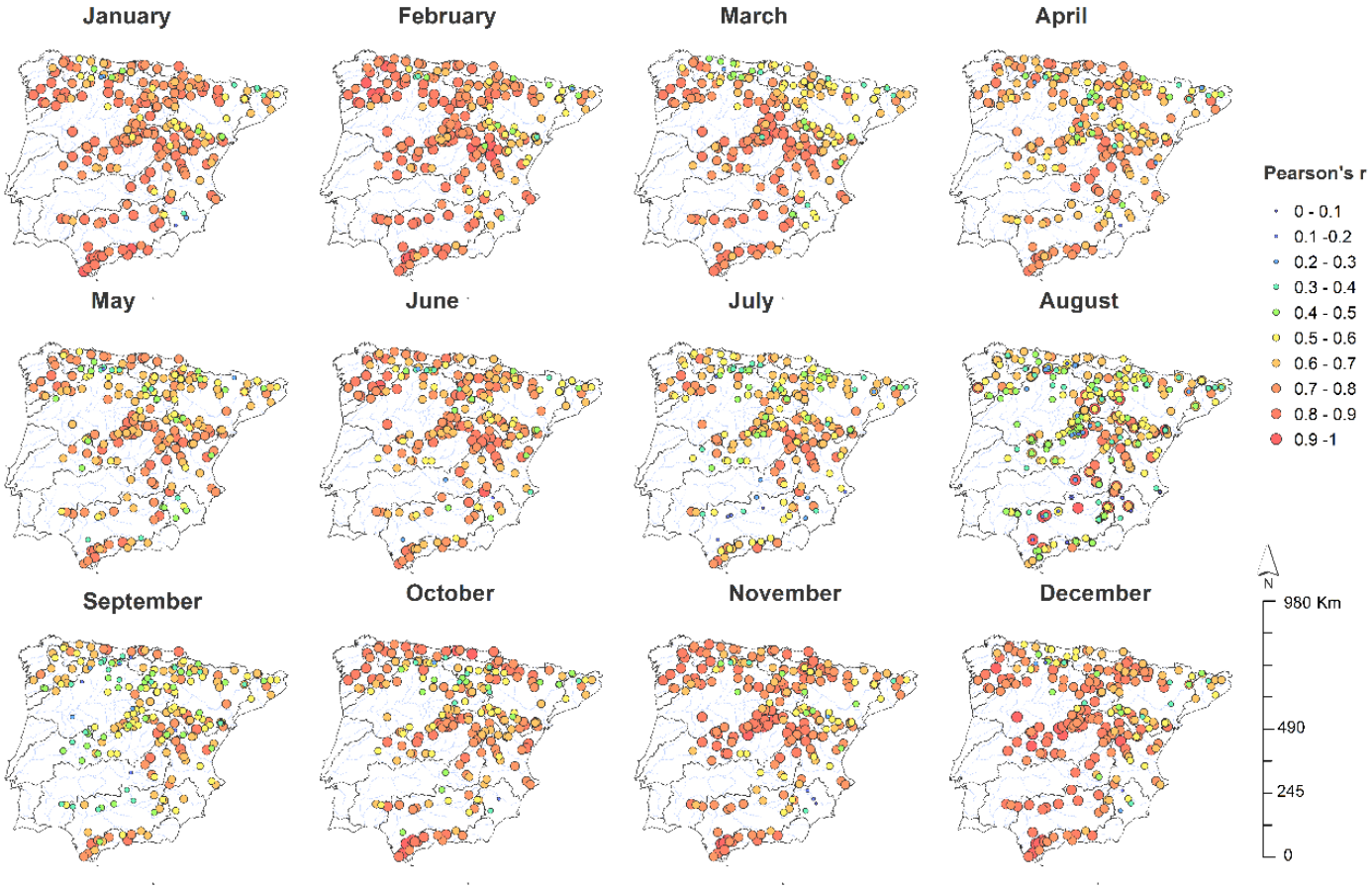

Supplementary figure 2. Spatial distribution of the monthly highest correlation coefficients between the SPI and the SSI independently of the month and time-scale.

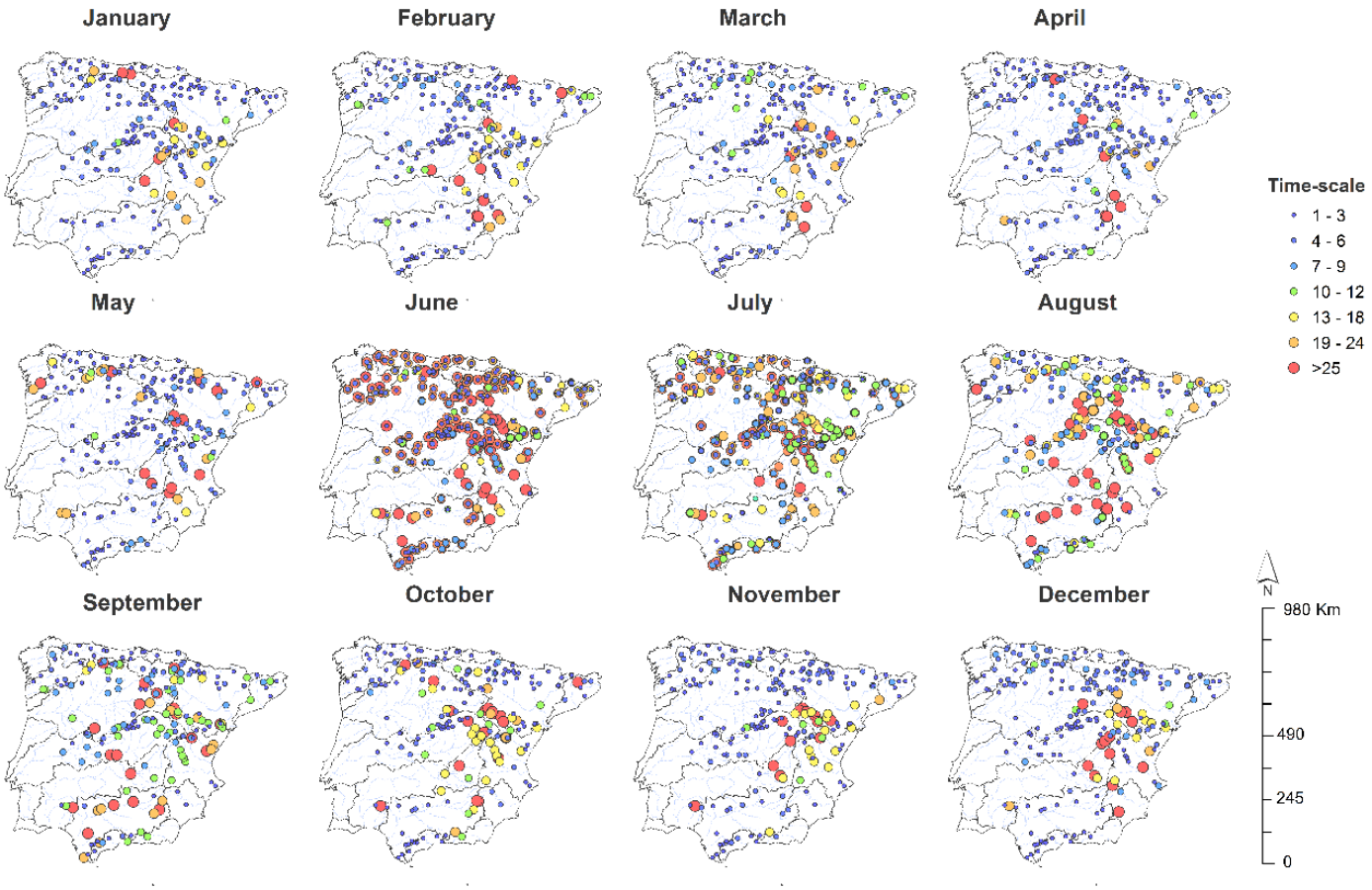

Supplementary figure 3. Spatial distribution of the time-scales at which monthly highest correlation coefficients between the SPEI and the SSI were found.

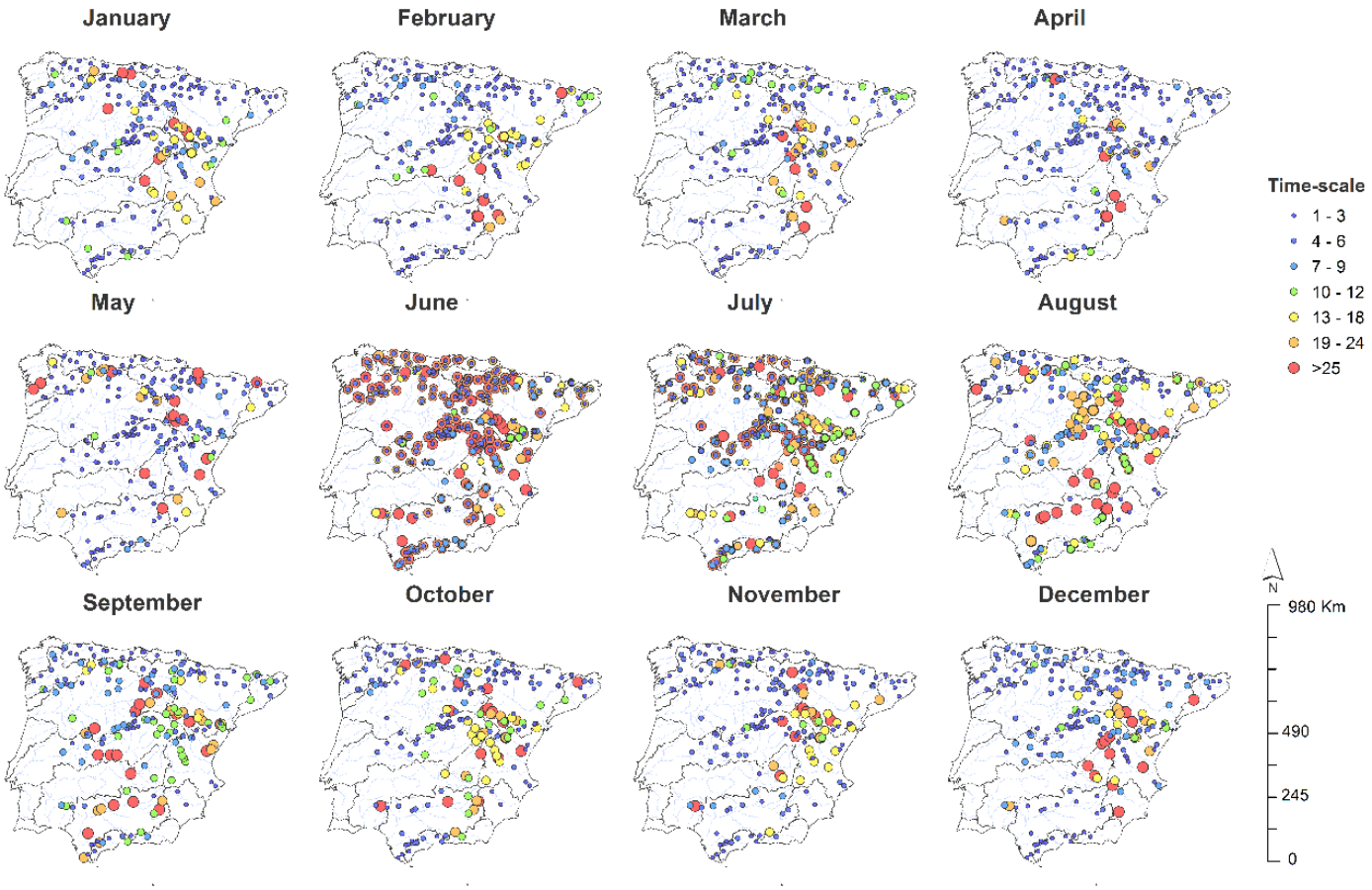

Supplementary figure 4. Spatial distribution of the time-scales at which monthly highest correlation coefficients between the SPI and the SSI were found.

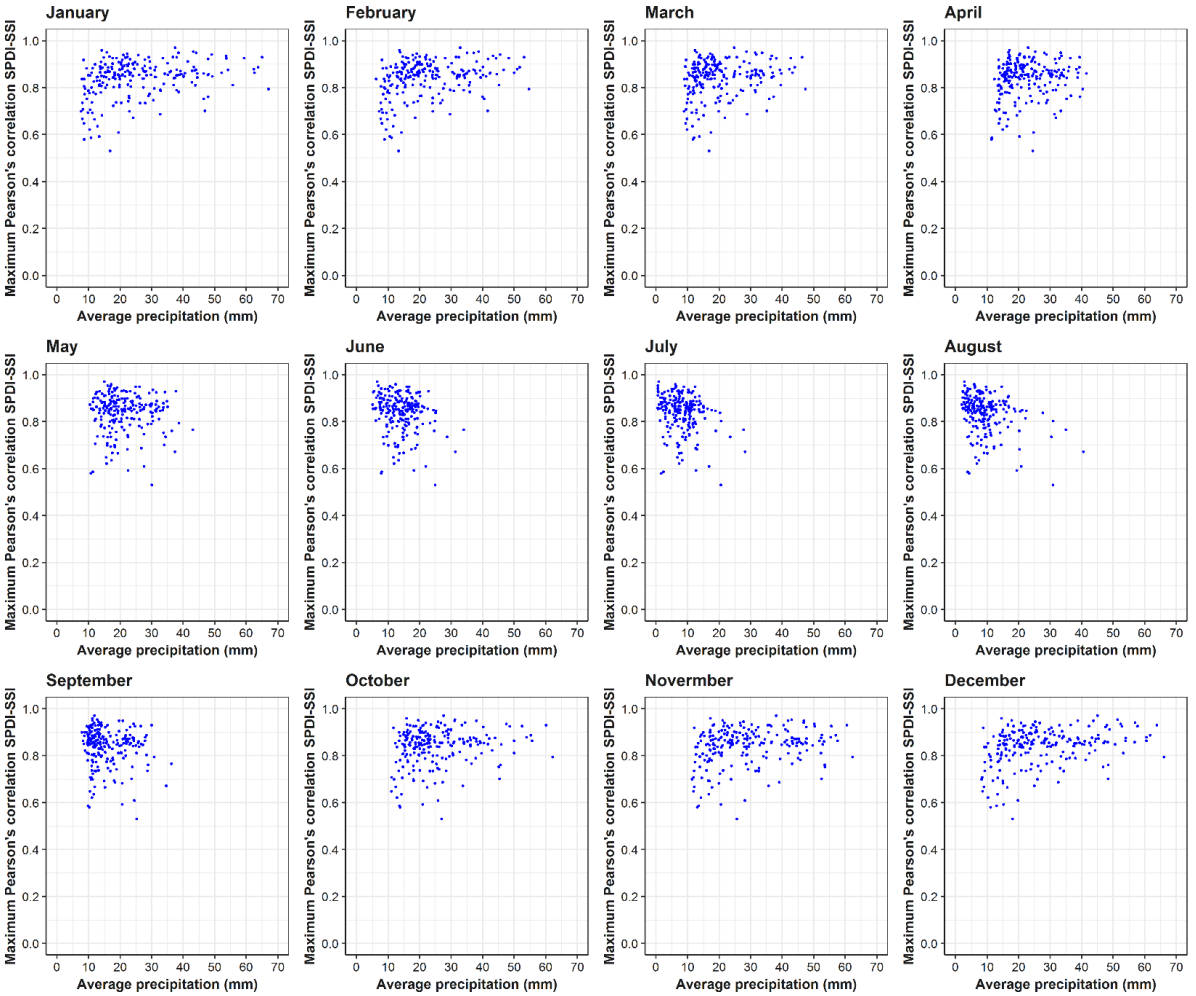

Supplementary figure 5. Temporal relationship between the maximum correlations found between the SSI and the SPDI, and the average precipitation in each basin.

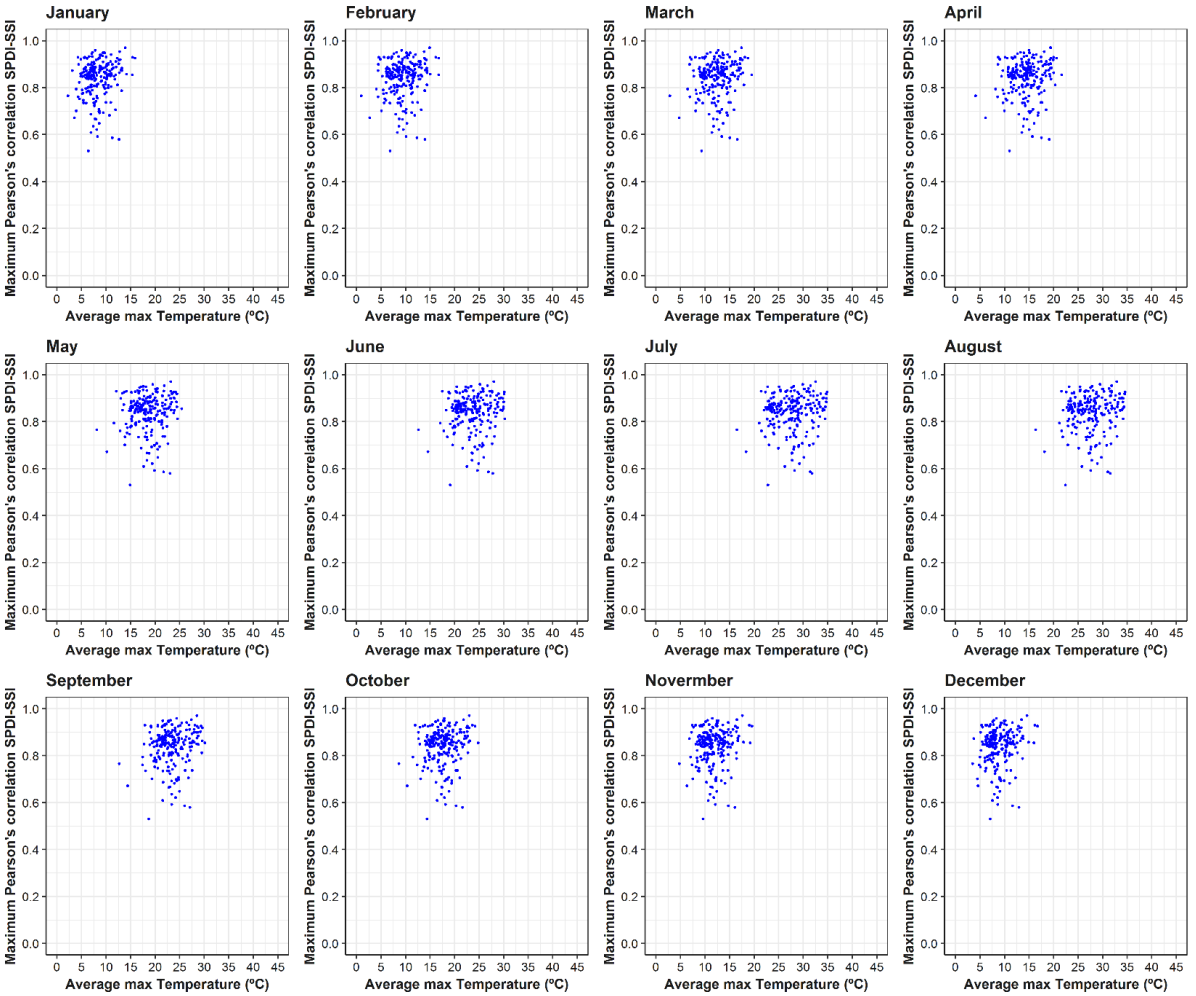

Supplementary figure 6. Temporal relationship between the maximum correlations found between the SSI and the SPDI, and the average maximum temperature in each basin.

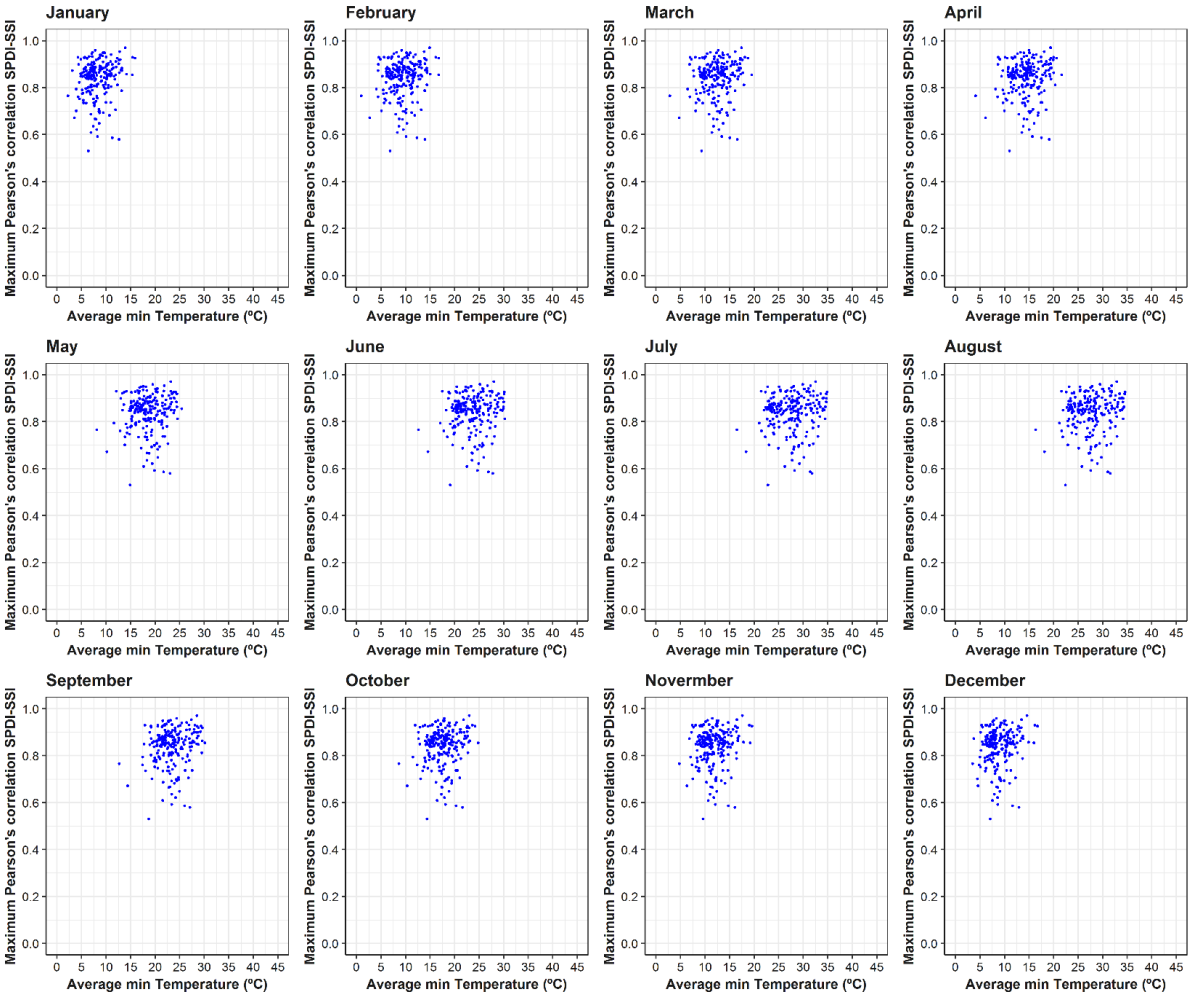

Supplementary figure 7. Temporal relationship between the maximum correlations found between the SSI and the SPDI, and the average minimum temperature in each basin.

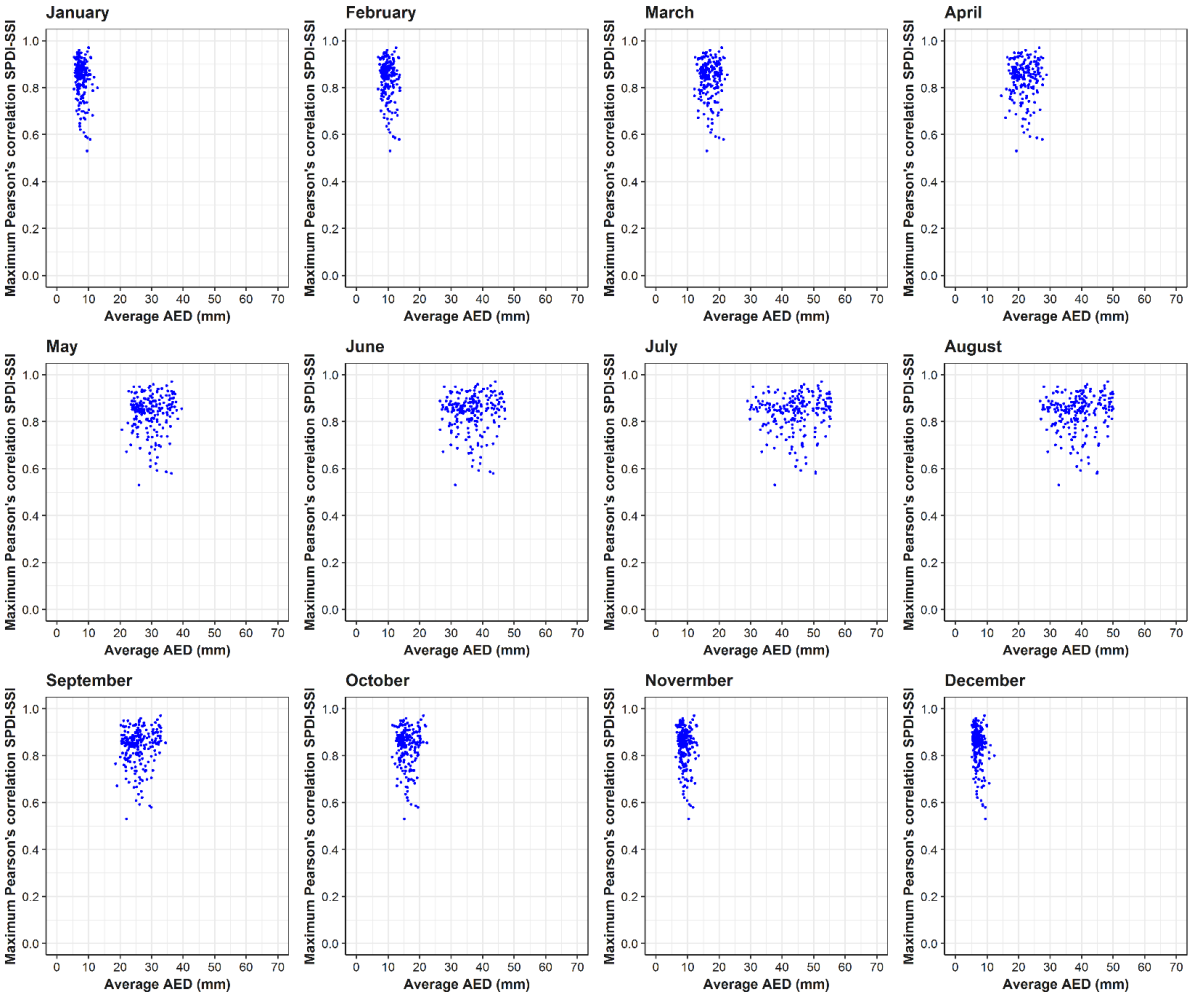

Supplementary figure 8. Temporal relationship between the maximum correlations found between the SSI and the SPDI, and the average AED in each basin.

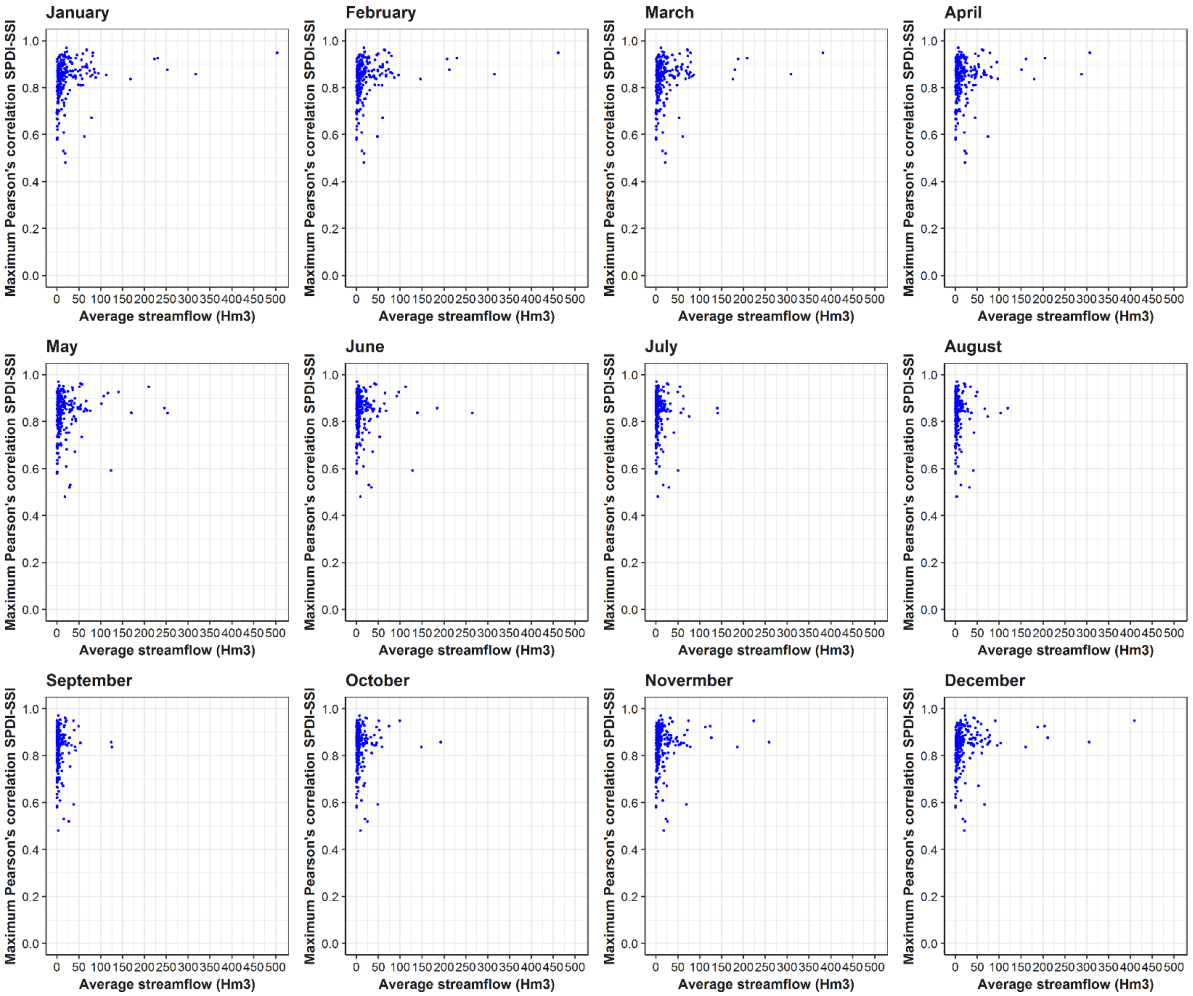

Supplementary figure 9. Temporal relationship between the maximum correlations found between the SSI and the SPDI, and the average streamflow in each basin.

PART **B** – Tesis en **español**

RESUMEN

La presente tesis se centra en la evaluación de distintos índices de sequía en múltiples sistemas, así como en el estudio de la respuesta espacio-temporal de la agricultura, los bosques y los caudales a las condiciones de sequía en dos regiones heterogéneas como son los Estados Unidos y España desde los años 60 a la actualidad. Dada la importancia de seleccionar las correctas herramientas para monitorizar la sequía, aquí se han calculado siete de los índices de sequía más comúnmente utilizados a nivel mundial y validado su capacidad para caracterizar los impactos en sistemas vulnerables. Para ello, se han comparado cuantitativamente tres índices de sequía multi-escalares (el SPI, el SPEI y el SPDI) y cuatro uni-escalares de la familia de los índices de Palmer (el PDSI, el PHDI, el Z-index y el PMDI).

Los Resultados obtenidos de los indiferentes análisis llevados a cabo han demostrado la superioridad del SPEI, el SPI y el SPDI en comparación a los índices de Palmer. Independientemente del tipo de cultivo, la especie arbórea, la cuenca hidrográfica o la escala temporal considerada, los índices de sequía calculados a distintas escalas temporales demuestran una capacidad superior para reflejar los distintos impactos de la sequía en diversos sistemas con un amplio rango de respuestas temporales a las sequías asociada a características específicas propias que dificultan aún más esta identificación.
La variedad de respuestas de los cultivos a las escalas temporales de los índices de sequía observada en las producciones agrarias de EEUU y España estuvo principalmente determinada por la resiliencia de la vegetación y a su capacidad para desarrollar estrategias que le permitan amortiguar los efectos de la falta de humedad en el suelo, así como la resistencia de los distintos tipos de cultivo durante los estados vegetativos más sensibles de crecimiento. De forma simular, los resultados obtenidos de la sensibilidad de los bosques a la sequía en España señalaron la existencia de diferencias entre especies y regiones climáticas, pero también evidenciaron el importante papel de los mecanismos de resiliencia para lidiar con condiciones climáticas extremas. Además, se observó cómo las variaciones estacionales también predeterminaron la respuesta de las distintas especies arbóreas analizadas a las sequías. En general los resultados también mostraron la existencia de un retardo en la respuesta a las sequías en función a la parte del ciclo de decaimiento del árbol afectado, de este modo se observó que el crecimiento secundario fue especialmente sensible a las condiciones de sequía durante los meses de verano mientras que la actividad fotosintética estuvo más correlacionada con las condiciones secas ocurridas en los meses de primavera. De los estudios realizados sobre la propagación de la sequía climática a la hidrológica los resultados sugirieron una respuesta mayoritaria de las cuencas naturales analizadas en EEUU y España a las sequías a escalas temporales cortas. Sin embargo, diferencias locales y patrones espaciales observados en la respuesta de los caudales demostraron la influencia de las propiedades de la cuenca de drenaje (p.ej. cobertura vegetal, usos del suelo, condiciones climáticas y características fisiográficas) en la respuesta hidrológica a las condiciones de sequía climática.

Esta tesis doctoral proporciona evidencias cuantitativas sobre la efectividad de los índices de sequía para una correcta cuantificación y monitorización del riesgo. De igual modo contribuye a ampliar el conocimiento sobre la sensibilidad y la respuesta espacio-temporal de distintos sistemas naturales a uno de los riesgos climáticos más extremos y difíciles de abordar.

1. Introducción

1.1. Definición de sequía. Tipologías y complejidades de un fenómeno natural extremo.

La sequía es reconocida como el fenómeno climático extremo más complejo y recurrente que afecta a prácticamente todas las partes del mundo y a todas las regiones climáticas, desde las húmedas a las áridas. La sequía se inicia cuando durante un periodo prolongado de tiempo, se produce un déficit de las cantidades normales de precipitación, sin embargo, muchos otros elementos se encuentran implicados en el desarrollo de un episodio de sequía. Los mecanismos que condicionan la aparición de una sequía son complejos, la demanda evaporativa por parte de la atmósfera, conocida por sus siglas en inglés como AED, puede favorecer la severidad de una sequía, del mismo modo, otros mecanismos importantes de actúan de retroalimento, también condicionan la intensificación del propio evento (p.ej. Por medio de la relación complementaria entre la evapotranspiración real y la AED) (Seneviratne et al., 2010; Teuling, 2018).
En los episodios de sequía severa, las condiciones de humedad del suelo y el déficit de presión de vapor sufren una reducción considerable, lo que genera unas condiciones sinópticas en las que la estabilidad atmosférica vertical limitan la posibilidad de que se produzcan precipitaciones. Esta circunstancia es reversible únicamente con la llegada de una perturbación húmeda (Mishra and Singh, 2010).

Con frecuencia los conceptos de aridez, ola de calor y sequía son empleados indistintamente sin existir una clara distinción conceptual entre dichos términos. A diferencia de la sequía, la aridez se define, de acuerdo al Glosario de Meteorología de la *Asociación Americana de Meteorología*, como el "grado al cual un tipo de clima carece de los suficientes aportes de humedad como para favorecer el desarrollo efectivo de vida". Es por tanto, una característica propia del clima, principalmente restringida a regiones donde las precipitaciones son muy escasas (Wilhite, 2000). Por su parte, las sequías son ,en general, no se pueden prever, pero tienen con un comienzo y un fin marcado en el tiempo. Constituye un periodo anómalo de baja disponibilidad de recurso hídrico durante el cual no es posible cubrir las demandas hídricas de los diferentes sistemas naturales y/o actividades antrópicas (Wilhite and Pulwarty, 2017). Una ola de calor es por su parte, una condición meteorológica causada por un incremento anormal de las temperaturas, cuya duración aproximada no excede unas pocas semanas. A diferencia de ésta última, la sequía puede extenderse por largos periodos de tiempo, tales como meses o años (Schubert et al., 2014), sin embargo, estudios recientes sugieren la existencia de una fuerte relación entre la severidad de la sequía y la ocurrencia de olas de calor (Hirschi et al., 2011; Miralles et al., 2014).

Entre los peligros naturales, la sequía es a menudo considerada el fenómeno que más riesgos entraña, así como el más insidioso tanto por sus efectos directos e indirectos no sólo en el medio ambiente, sino también en las actividades humanas. La conceptualización de la sequía entraña algunos aspectos a tomar en consideración (Mishra and Singh, 2010). En primer lugar, la sequía es un riesgo climático con un inicio muy lento y progresivo (Gilette, 1950) cuyos efectos son percibidos una vez que el evento ha perdurado en el tiempo o incluso ha finalizado. Por este

motivo, la definición del comienzo y el cese de un episodio de sequía que está ocurriendo a tiempo real, supone una difícil tarea. En segundo lugar, la sequía causa impactos muy diversos. Cuantificar el alcance de los daños causados en los múltiples sistemas afectados supone una dificultad, ya que la sequía impacta indistintamente sobre extensas y pequeñas regiones o sobre recursos hídricos superficiales y subterráneos, además, varía en múltiples escalas temporales. Asimismo, la cuantificación de los impactos de las sequías depende de la vulnerabilidad del sector en el que impacta, y su capacidad de resiliencia a la sequía (Gazol et al., 2018a, 2017). De este modo, la exposición medioambiental a las condiciones de sequía está condicionada a factores inherentes tales como: el régimen climático dominante, las características de los procesos hidrológicos, el tipo de vegetación, la litología (presencia/ausencia de rocas más o menos permeables) o las actividades humanas de la región afectada (Kumar et al., 2016; Leng et al., 2015; Sangüesa-Barreda et al., 2015; Vicente-Serrano et al., 2017b). El tercer y último aspecto a considerar es la influencia antropogénica que juega un importante papel principal en el desencadenamiento de condiciones de sequía (p.ej. la demanda de agua y los cambios en los usos del suelo) al ser causa de la exacerbación o mitigación de situaciones de sequía (Van Loon et al., 2016).

No obstante, aún hoy en día no es posible encontrar un consenso entre la comunidad científica que permita definir universalmente este fenómeno al existir tantos impactos como sectores implicados hay (Wilhite et al., 2007). Las sequías con generalmente clasificadas en cuatro categorías (Dracup and Kendall, 1990; Wilhite and Glantz, 1985) siguiendo el orden de ocurrencia de las mismas como sigue:

i) Las sequías meteorológicas se definen como un decrecimiento anómalo en los aportes de precipitación por debajo de los valores normales en una región, durante un periodo prolongado de tiempo. La sequía meteorológica puede desarrollarse rápidamente y tener una duración corta (días) o muy prolongada (años). La definición de este tipo de sequías es además específica del lugar, ya que cada región se encuentra caracterizada por unas condiciones climáticas propias.

ii) A corto plazo, la ausencia de precipitaciones provoca que la humedad del suelo en las capas más superficiales se agote. Cuando las condiciones secas alcanzan la zona de la raíz, la vegetación se ve afectada, dando lugar a lo que se conoce como sequía agrícola. Este tipo de sequía se desarrolla antes de que los recursos hídricos superficiales y subterráneos se vean amenazados por la falta de precipitación, e incluso suceden cuando las capas más profundas del suelo mantienen condiciones mormales de humedad. No obstante, no únicamente la precipitación condiciona el desarrollo de la sequía en este punto, la temperatura ejerce una influencia sobre los requerimientos de humedad por parte de la atmósfera, y por consiguiente sobre la evapotranspiración como principal elemento demandante de agua por parte de las plantas. Dependiendo de las características fisiológicas y fenológicas de la vegetación y las condiciones climáticas de la zona afectada, la sequía agrícola puede ser responsable en última instancia de la pérdida de las producciones agrarias (Vergni and Todisco, 2011).

iii) Las sequías hidrológicas se caracterizan principalmente por los bajos niveles que presenta el caudal de los ríos y el descenso generalizado de la disponibilidad de agua en el ciclo hidrológico, lo que incluye aguas superficiales (embalses y lagos) y subterráneas (agua en los acuíferos) (Tallaksen et al., 1997). Los niveles de caudal son el indicador más habitual empleado para medir la sequía hidrológica al integrar tanto la señal climática, como la influencia de las prácticas antrópicas en el medio (Lorenzo-Lacruz et al., 2013). Sin embargo, existe una compleja conexión entre las distintas partes del ciclo hidrológico y la sequía al variar sus respuestas en el tiempo. Estudios anteriores han demostrado que no sólo las condiciones climáticas, sino también las características fisiográficas de las cuencas hidrográficas, condicionan la respuesta del sistema hidrológico a las sequías, señalando la existencia de una interacción de todos los mecanismos implicados a distintos niveles (Tijdeman et al., 2016; Van Loon and Laaha, 2015). Cuando persisten condiciones en las que los niveles de caudal se ven reducidos y las recargas que efectúan las aguas subterráneas descienden hasta el punto de empezar a agotarse, se dice que se ha desarrollado una sequía de aguas subterráneas (Bloomfield et al., 2015; Mishra and Singh, 2010).

iv) Las sequías socio-económicas se encuentran asociadas a la incapacidad de los recursos hídricos disponibles a cubrir la demanda de agua por parte de las distintas actividades humanas. El constante incremento generalizado de la demanda de agua debido al aumento de la población, así como la expansión de prácticas agrarias intensivas, entre otros muchos aspectos, suponen un factor de riesgo para la mayoría de los bienes y servicios que dependen directa o indirectamente del agua.

En los últimos años, una nueva tipología de sequías ha despertado el interés entre la comunidad científica, relacionadas con impactos ecológicos y medioambientales en múltiples sistemas naturales entre los que se incluyen la fauna, los bosques y las corrientes de agua (Crausbay et al., 2017).

Además de la clasificación sobre la tipología de las sequías, existe una amplia terminología para caracterizar los eventos. Así, por un lado la descripción conceptual del fenómeno proporciona una definición temática y cualitativa sobre las consecuencias asociadas; por otro lado, una descripción operativa ofrece una caracterización cuantitativa de las características del fenómeno. Siguiendo la terminología más completa enunciada por Salas, (1993) tal como mencionan Zargar et al. (2011), las sequías pueden definirse en base a su:

i) Duración: Las sequías pueden perdurar durante días o años. Una misma región es capaz de alternar entre periodos secos y húmedos a corto y largo plazo.
ii) Magnitud: Referida a la suma positiva del déficit de precipitación producido. Habitualmente se encuentra referida a un umbral determinado.
iii) Intensidad: Definida como el ratio entre la magnitud y la duración del evento.
iv) Severidad: Medida como la magnitud, o nivel de impacto del evento.
v) Extensión geográfica: Cobertura espacial de la sequía en el tiempo. Existen diversas unidades de medida para ella (p.ej. pixeles, regiones, unidades medioambientales).

vi) Frecuencia: Tiempo medio estimado en que se produce otro episodio de sequía de igual o superior intensidad al anterior.

Además, las sequías son un fenómeno multi-escalar, es decir, pueden describirse a diferentes escalas temporales. El concepto de cuantificar las sequías a diversas escalas, fue introducido por Mckee et al. (1993; 1995) con el fin inicial de entender la respuesta de los diferentes sistemas del ciclo hidrológicos (aguas superficiales y subterráneas) a la escasez de precipitación. La sensibilidad de los distintos sistemas naturales a la acumulación de déficits hídricos, varía en el tiempo. Por ejemplo, la respuesta de la vegetación a la sequía varía significativamente en el tiempo dependiendo, entre otros factores, del tipo de especie y de la resistencia que ésta presenta en condiciones secas. Algunos estudios al respecto han confirmado la existencia de respuestas temporales a la sequía opuestas en diferentes especies arbóreas de una misma región (Gazol et al., 2018b; Vicente-Serrano et al., 2013). Del mismo modo, la respuesta de la sequía hidrológica a la sequía climática o meteorológica, depende en gran medida de la temporalidad a la que se observa el propio fenómeno y que varía en cada fase del ciclo hidrológico y la región afectada (Bloomfield et al., 2015; López-Moreno et al., 2013; Lorenzo-Lacruz et al., 2013).

1.2. Los impactos de la sequía en los sistemas naturales.

De acuerdo al Informe Especial sobre Eventos Extremos y Desastres del Quinto Informe del Panel Intergubernamental sobre el Cambio Climático (IPCC, 2014), existe una confianza media en que las sequías tornen más intensas y duraderas en el sur de Europa y el centro de los Estados Unidos (EEUU) durante ciertas estaciones del año en las próximas décadas debido principalmente, a una reducción de las precipitaciones y un aumento de la evapotranspiración.
La mayoría de las regiones semiáridas localizadas en el suroeste de Europa y de EEUU, adeás, son muy probables que experimenten una reducción severa en sus recursos hídricos como consecuencia del incremento de la AED y un cambio en el régimen de distribución de las precipitaciones. Estudios recientes además sugieren que en el futuro, los episodios de sequía podrían afectar zonas cada vez más extensas, llegando a alcanzar niveles de impacto mayores que ningún otro riesgo climático, en especial en actividades relacionadas con el suministro alimenticio (Romm, 2011). En resumen, EEUU y la región mediterránea, son dos escenarios propensos a sufrir los impactos potenciales del cambio climático que se espera, atraiga eventos climáticos extremos cada vez más severos.

Agricultura

La agricultura es el principal sustento de la seguridad alimenticia a nivel mundial, así como un sector altamente dependiente de la disponibilidad de agua. La variabilidad temporal de los rendimientos agrarios puede responder a influencias no climáticas tales como conflictos políticos, crisis sociales o problemas de salud (Ben-Ari and Makowski, 2014; Schauberger et al., 2018) , sin embargo la principal responsable es la variabilidad climática (Lobell et al., 2011). De acuerdo con la FAO (2019), el sector agrícola de los países en vías de desarrollo absorbe el 80% de los impactos directos causados por las sequías, mientras que a nivel mundial, del porcentaje total de pérdidas económicas causadas por estos eventos, el 22% corresponde a pérdidas de producciones.

EEUU es uno de los tres principales productores de cereal en el mundo y el principal de maíz según el USDA (2015). Sin embargo, en las últimas décadas, este país ha sufrido varios episodios de sequías extrema. El más intenso de ellos ocurrido en 1988 tuvo una repercusión muy extendida en el territorio cultivado causando unos costes aproximados de 87 billones de dólares (cifra ajustada a 2019) de los cuales el 40% se debió a pérdidas de cosecha (aproximadamente 38 billones de dólares) (Elliott et al., 2018; Smith and Katz, 2013). Este episodio ha sido catalogado como el segundo más costoso en la historia del país, siendo únicamente superado por el huracán Katrina (Smith and Matthews, 2015). En 2012 otro importante evento de sequía produjo pérdidas por valor de 30 billones de dólares en pérdidas agrícolas (Smith and Matthews, 2015).

En la región mediterránea, diversas sequías severas han causado pérdidas económicas muy importantes que han afectado tanto a cultivos de secano como de regadío (Lopez-Nicolas et al., 2017). Tan solo el episodio de 2003 causó daños en el sector agrario valorados en 13 billones de euros, con gran repercusión en España. Más aún, el evento de sequía acontecido en 2005 supuso el más severo de los últimos 60 años en el país, causando impactos en la agricultura nacional que supusieron una reducción del 10% de la producción de cereal en Europa (Blauhut et al., 2016). En el año 2012, otra sequía severa tuvo lugar, produciéndose nuevamente importantes impactos en la economía y en el medioambiente. Las mayores pérdidas agrarias se produjeron en los campos de cultivo de Aragón y Andalucía, percibiéndose como consecuencia de las condiciones climáticas adversas, un incremento alarmante en la mortalidad abrupta de árboles y en el número de incendios forestales (Navarro-Cerrillo et al., 2018). De acuerdo al Instituto Nacional de Estadística, España es el segundo país de la Unión Europea con mayor proporción de tierras destinadas al cultivo. El cultivo de secano y regadío soporta los impactos acusados por la falta de agua (Tigkas and Tsakiris, 2015), sin embargo, el grado de resiliencia de las especies a dicho estrés, y el momento durante el estado vegetativo de crecimiento del cultivo en el que se produce el impacto, pueden determinar diferentes respuestas a la sequía (Lobell, 2014; Lobell and Field, 2007). En última instancia, si las condiciones climáticas adversas se prolongan durante un tiempo mayor, coincidiendo con los estados vegetativos más sensibles de crecimiento, la sequía tiene la capacidad de producir una pérdida completa de las cosechas (Lobell and Field, 2007).

Las cosechas agrarias son por tanto extremadamente vulnerables a las condiciones de sequía y su amenaza puede traer consigo consecuencias en la seguridad alimentaria global y la economía. En este contexto, múltiples estudios han advertido de la situación de vulnerabilidad de la agricultura a cambios en la frecuencia y severidad de los eventos secos (Asseng et al., 2011; Olesen et al., 2011; Rossi and Niemeyer, 2010) y la variabilidad interanual de la sequía (Capa-Morocho et al., 2016; Loukas and Vasiliades, 2004; Moorhead et al., 2015; Rohli et al., 2016). Sin embargo, muy pocos avances científicos se han producido respecto al estudio de la conexión del carácter multi-temporal de la sequía y diferentes tipologías de cultivo (Páscoa et al., 2016; Tian et al., 2018; Zipper et al., 2016). Además, existen evidencias sobre el aumento de la variabilidad interanual de las producciones agrarias acrecentado por un aumento en la frecuencia y severidad de las sequías, lo cual acentúa la necesidad de adquirir efectivas herramientas de monitorización que proporcionen una cuantificación real de los impactos de la sequía en la agricultura (Asseng et al., 2014; Rossi S and Niemeyer S, 2010; Tack et al., 2015).

Tres de las investigaciones que se presentan en esta tesis abordan los principales mecanismos climáticos y medioambientales que determinan la respuesta de las cosechas a las sequías a distintas escalas temporales; del mismo modo, ofrecen una revisión sobre el desempeño de varios índices de sequía para monitorizar impactos en varios tipos de cultivo en EEUU y España.

Ecología

Los bosques son una parte esencial de los ecosistemas debido a un rol principal en la liberación y absorción de gases de efecto invernadero tales como el dióxido de carbono (CO_2) (Heimann and Reichstein, 2008) así como dentro del ciclo hidrológico (Horton, 1933). El decaimiento y mortalidad de los bosques causados por las sequías ha aumentado en las pasadas décadas a nivel mundial (Greenwood et al., 2017; Young et al., 2017) debido a que el crecimiento primario y secundario de los bosques son procesos especialmente dependientes de la disponibilidad de agua (Pasho et al., 2011).
La península Ibérica, favorecida por su amplio abanico climático, acoge a una gran diversidad de especies. Una vista general al mapa climático de este territorio muestra un abanico que se extiende desde el clima húmedo atlántico, pasando por el clima mediterráneo continental en el centro peninsular hasta el clima mediterráneo semiárido propio del sureste (García-Ruiz et al., 2011). La región mediterránea ha sido objeto de muy frecuentes y severos episodios de sequía que han supuesto a su vez un importante impacto sobre los bosques (Caminero et al., 2018; Granda et al., 2013; Sangüesa-Barreda et al., 2015). No obstante, determinar la incidencia de la sequía en los bosques esconde una serie de limitantes debido a las diferencias que se producen entre regiones y las variaciones estacionales. Estudios al respecto han señalado cómo al producirse condiciones climáticas adversas, tales como la reducción de la humedad del suelo y los altos valores de evapotranspiración inmediatamente antes de la estación de crecimiento de las plantas, la Producción Primaria Neta, conocida por sus siglas en inglés como NPP, se ve limitada, lo que causa la debilitación del crecimiento, una reducción de los valores fotosintéticos y eventualmente la muerte de los bosques (Camarero et al., 2018, 2015; Lloret et al., 2012; Neumann et al., 2017).

La variabilidad interanual característica de las precipitaciones en climas mediterráneos complica además, conocer la respuesta del crecimiento de los árboles a la ausencia de precipitaciones. Pasho et al. (2011) abordaron las distintas respuestas del crecimiento de diversas especies de árboles en Aragón a la escasez de agua. Entre sus resultados, encontraron que el crecimiento de los árboles se veía afectado por la ausencia de humedad a escalas temporales de sequía cortas, mientras que escalar temporales más largas se relacionaron con eventos de sequía menos frecuentes pero más intensos. No obstante, además de las condiciones locales de clima y la propia topografía, la sensibilidad de los bosques a las sequías y la capacidad de recuperación a éstas, difiere ampliamente entre especies e incluso individuos de la misma especia (Forner et al., 2018; Peguero-Pina et al., 2011). Estudios llevados a cabo en España han observado diferencias en los tiempos de recuperación entre especies mediterráneas. Así, algunas especies tienden a alcanzar condiciones 'pre-sequía' más temprano que otras, independientemente del estado de declive de los individuos analizados (Camarero et al., 2018; Carnicer et al., 2011). Recientes avances en la temática además han advertido de un aumento generalizado en la tendencia a la defoliación en la Península Ibérica, que viene observándose desde las pasadas décadas (Carnicer et al., 2011).

En el contexto actual de cambio climático, y las contrastadas evidencias de su impacto en los bosques, es importante llevar a cabo estudios en detalle que permitan entender la relación entre las sequías, la NPP y el crecimiento secundario de los bosques.

En la presente tesis, se ha abordado un estudio al respecto titulado: Drought Sensitiveness on Forest Growth in Peninsular Spain and the Balearic Islands, que pretende proporcionar un conocimiento más en detalle de los impactos de la sequía y las diversas respuestas temporales de diferentes especies arbóreas para una correcta gestión del riesgo.

Hidrología

Entre los muchos impactos causados por la sequía en los ecosistemas, la mayoría de ellos está relacionados con el sistema hidrológico (Van Loon, 2015). Las sequías hidrológicas son un fenómeno muy complejo que implica múltiples interacciones entre las sequías meteorológicas y la propagación de sus efectos a través del completo ciclo hidrológico (Haslinger et al., 2014), desde los caudales (López-Moreno et al., 2013; Lorenzo-Lacruz et al., 2010), lagos and reservas hídricas superficiales (McEvoy et al., 2012) hasta las aguas subterráneas (Lorenzo-Lacruz et al., 2017; Marchant and Bloomfield, 2018). A pesar de que la variabilidad climática está estrechamente conectada con las sequías hidrológicas, existen otros muchos factores que determinan las características de los impactos de éstas, tales como la duración, la extensión espacial y la severidad. Así, la intrincada relación entre el clima y los déficits de agua en los distintos sistemas del ciclo hidrológico, está en ocasiones favorecida por influencias medioambientales y antropogénicas que determinan el desencadenamiento de eventos hidrológicos extremos (Bąk and Kubiak-Wójcicka, 2017; Tijdeman et al., 2018; Vicente-Serrano et al., 2012).

El carácter complejo del proceso de propagación de la sequía supone que sea un reto científico esclarecer las causas originales de las sequías hidrológicas, más aún cuando la propia naturaleza de las variables hidrológicas presenta variaciones significativas en los tiempos de respuesta a condiciones de déficit de humedad. Por ejemplo, la humedad del suelo comienza a acusar los efectos de la falta de agua a escalas temporales cortas (Scaini et al., 2015), mientras que las aguas subterráneas o el agua retenida en depósitos naturales y/o artificiales lo acusan a escalas temporales más largas (Barker et al., 2016; López-Moreno et al., 2013; Lorenzo-Lacruz et al., 2017). La propagación de la sequía es aún más compleja en cuencas de drenaje donde las características fisiográficas y las prácticas de regulación antrópicas tienen una mayor implicación en la respuesta de los caudales a las sequías, determinando el grado de impacto de éstas y la sensibilidad del sistema a las condiciones climáticas a distintas escalas temporales (Sheffield and Wood, 2011; Van Loon, 2015; Van Loon and Laaha, 2015).

Diversos estudios a nivel mundial han demostrado cómo las propiedades fisiográficas de las cuencas de drenaje, así como la cobertura vegetal, son elementos primordiales que ayudan a entender las distintas respuestas temporales de las sequías en los caudales a las sequías climáticas. Barker et al. (2016), por ejemplo, observaron recientemente una gran influencia de las características lito-geológicas en las diversas respuestas temporales que encontraron en un amplio número de caudales en cuencas naturales en el Reino Unido a la sequía climática. De

forma similar, Vicente-Serrano et al. (2011) investigaron la respuesta a la sequía climática a distintas escalas temporales en dos cuencas de cabecera en condiciones naturales en el noreste de España. Estos autores encontraron tiempos de respuestas muy diferentes entre ambas cuencas, atribuibles principalmente a las características litológicas de cada una de ellas. Así, mientras una de las cuencas analizadas tendió a responder a la sequía a escalas de tiempo muy cortas (< 3 meses), la otra cuenca lo hizo a escalas de tiempo mucho más amplias (> 40 meses). En diversas cuencas de Austria, Van Loon and Laaha, (2015) evaluaron los factores que controlan la severidad de las sequías, concluyendo que dichos factores son principalmente una combinación de las particulares características propias de cada cuenca. Igualmente, otros estudios han señalado la influencia producida por las actividades antropogénicas relacionadas con la regulación de los recursos, las prácticas de gestión (López-Moreno et al., 2009; Wu et al., 2017) y los cambios de usos del suelo (Van Loon and Laaha, 2015) en relación las relaciones hidro-climáticas de las sequías, que actúan como agentes paliativos o desencadenadores de episodios de sequía hidrológica (AghaKouchak et al., 2015; Liu et al., 2019; López-Moreno et al., 2009; Terrado et al., 2014).

Estos estudios, a menudo emplean índices de sequía que incluyen información climática y de caudal para abordar la relación entre la sequía climática e hidrológica así como su propagación a través del ciclo hidrológico. Por ejemplo, en el río Tajo Lorenzo-Lacruz et al. (2010) encontraron correlaciones significativas entre índices de sequía climáticos y series de caudal. Sin embargo, en España existe una escasez de estudios que evalúen la idoneidad de las herramientas de monitorización de la sequía en el contexto del sistema hidrológico. Además de ello, la mayoría de las investigaciones a menudo consideran en sus observaciones una variedad de cuencas hidrográficas que por lo general, suelen estar condicionadas por prácticas de regulación antropogénica lo cual sesga la respuesta natural de los caudales a las condiciones de sequía climática. Recientemente, Abatzoglou et al. (2014) llevaron a cabo un estudio en la región pacífica del noroeste de EEUU en el que calcularon diversos índices de sequía para analizar las anomalías de caudal y su relación con la dinámica climática. Por su parte, Tijdeman et al. (2016) analizaron en más de 800 cuencas de EEUU la duración de las sequías hidrológicas, concluyendo que la duración de dichos eventos dependían principalmente del régimen climático y de precipitación de cada región.

No obstante, la influencia de las propiedades de cada cuenca en la propagación de la sequía climática en el sistema hidrológico no ha sido lo suficientemente abordada. En la presente tesis, se presentan dos estudios a este respecto titulados: Complex influences of meteorological drought time-scales on hydrological droughts in natural basins of the contiguous Unites States y Response of natural river basins to drought in Spain: Evaluation of different climatic drought indices. Ambos, pretenden contribuir en la ampliación del conocimiento relativo a la propagación de las sequías y la identificación de apropiados índices de sequía para su monitorización.

1.3. Índices de sequía

Los procesos físicos que conforman el fenómeno de la sequía, así como la intrínseca dinámica no lineal asociada al mismo son muy complejos (Lloyd-Hughes, 2014). Poco puede hacerse para mitigar los efectos de la sequías, el amplio abanico de impactos generados por las mismas en

numerosos sistemas naturales y humanos relacionados con los recursos hídricos, ha llevado a la comunidad científica a desarrollar herramientas y estrategias de gestión tales como planes de acción integral y de mitigación para caracterizas y cuantificar eficientemente los episodios de sequía (Ceglar et al., 2012; Vicente-Serrano et al., 2012).

Los índices de sequía son unas herramientas muy eficientes para dicho propósito. La mayoría están basados en información climática, y son empleados a nivel mundial para cuantificar los impactos de la sequía en diversos sistemas a tiempo real gracias a su capacidad para identificar múltiples características (p.ej. el inicio del evento, la severidad, duración y extensión espacial) con gran precisión (Shukla et al., 2011; WMO, 2012; GWP, 2016). Muchos estudios han demostrado la gran capacidad de los índices de sequía para identificar la variabilidad temporal de los impactos de este fenómeno en múltiples variables medioambientales como las producciones agrarias (Mathieu and Aires, 2018; Sun et al., 2012; Tian et al., 2018), los caudales y aguas subterráneas (Fiorillo and Guadagno, 2010; López-Moreno et al., 2013; Lorenzo-Lacruz et al., 2017; Vasiliades and Loukas, 2009) o el crecimiento de los árboles (Bhuyan et al., 2017; Pasho et al., 2011).

Desde la última década, más de 100 índices de sequía han sido propuestos para caracterizar distintos tipos de sequía (meteorológica, agrícola, hidrológica, etc.) (Heim, 2002) e incluso estudios recientes han realizado una revisión de alguno de estos índices, proporcionando una detallada explicación teórica sobre sus potencialidades y debilidades (Mishra and Singh, 2010; Zargar et al., 2011). Sin embargo, muy pocos trabajos han realizado una comparación estadística entre distintos índices que permitan determinar el correcto empleo de uno u otro en función al sistema objeto de estudio. A este respecto, Trenberth et al. (2014) llevaron a cabo un estudio cuantitativo a nivel global sobre la sensibilidad de los índices de sequía a cambios en la temperatura de superficie que demostró la importancia de incluir la temperatura como variable de referencia en los índices de sequía dado el actual escenario de calentamiento global. Por su parte, Vicente-Serrano et al. (2012) analizaron a escala global la capacidad de algunos de los más utilizados índices de sequía para cuantificar los impactos de las sequías en distintos sistemas naturales.

En esta tesis, se han utilizado siete de los índices de sequía más conocidos a nivel mundial. En las siguientes sub-secciones se presenta una breve descripción de cada uno de ellos.

1.3.1. Los índices de Palmer (PDSI)

El Índice de Severidad de Sequía de Palmer, conocido por sus siglas en inglés como PDSI, supuso un hito en la cuantificación y monitorización de la sequía. Desarrollado por Palmer, (1965), es un índice meteorológico conocido a nivel mundial empleado en la cuantificación de la severidad de los eventos de sequía. Originalmente, el PDSI se basa en cuantificar la magnitud de las condiciones de humedad del suelo en circunstancias definidas por el propio autor como 'Climatically Appropriate for Existing Conditions' (CAFEC por sus siglas en inglés), a partir de un modelo de simulación de humedad superficial en las dos primera capas del suelo. Las mediciones CAFEC son equivalentes al balance de humedad del suelo que tiene en cuenta la relación entre el suministro y la demanda de humedad por parte del suelo (Alley, 1984).

Además del PDSI, otros tres índices relacionados que parten de la formulación original fueron desarrollados al poco tiempo (Heim, 2002):

i. El Índice de Sequía Hidrológica de Palmer (PHDI, por sus siglas en inglés) mide la duración e intensidad a largo plazo de los efectos de la sequía en el sistema hidrológico. Los impactos hidrológicos toman un tiempo mayor en hacerse evidentes, por ello el PHDI tiende a detectar las sequías relativamente más tarde que el PDSI, manteniendo condiciones por debajo del umbral considerado normal durante los meses posteriores en los que niveles del PDSI ya se han recuperado.

ii. El Índice de anomalía de humedad Z de Palmer (Z-index, por sus siglas en inglés) cuantifica los cambios en las condiciones de humedad a corto plazo. Es especialmente sensible en la detección de impactos de las sequías a escalas temporales cortas, identificando cambios en las condiciones de humedad del suelo y variaciones en la magnitud de caudal de los ríos.

iii. El Índice de Sequía Modificado de Palmer (PMDI, por sus siglas en inglés) fue enunciado por Heddinghaus and Sabol, (1991) como una modificación del original PDSI especialmente diseñado para monitorizar la sequía meteorológica y agrícola. Este índice incorpora en la acumulación de anomalías climáticas las condiciones de humedad/sequedad anteriores al tiempo observado.

Los cuatro índices de Palmer (PDSIs) no obstante, presentan ciertas limitaciones que han sido ampliamente discutidas en la literatura científica posterior (Akinremi et al., 1996; Alley, 1984; Heim, 2002; Weber and Kkemdirim, 1998):

i. Carecen de la habilidad para comparar sus valores en el espacio entre distintas regiones. Esto se debe principalmente a que originalmente Palmer concibió el PDSI para monitorizar la sequía en una región muy concreta del oeste de EEUU.

ii. Los PDSIs se calculan a una escala temporal única (son índices uni-escalares), lo cual limita la capacidad de cuantificar y monitorizar distintos tipos de sequía eficazmente. Por lo general, los valores de los PDSIs reflejan las condiciones de humedad/sequía a escalas temporales no menores a 12 meses.

iii. Es necesario un gran número de variables para el cálculo de estos índices (p.ej. Temperatura, evapotranspiración, contenido de agua en el suelo, etc.), hecho que dificultad la posibilidad de computar dichos índices en regiones donde la disponibilidad del dato climático es limitada.

iv. Los índices no tienen en cuenta el desfase de la escorrentía, y asumen que la precipitación potencial es igual al contenido de agua disponible en el suelo.

v. La metodología de cálculo es compleja en comparación a la que presentan otros índices de sequía. En el caso de los PDSIs, el procedimiento de cálculo completo se encuentra descrito en Karl, (1986).

Sin embargo, a pesar de las deficiencias del PDSI, actualmente continua siendo uno de los índices de sequía más empleados gracias a su habilidad para capturar las condiciones de sequía a largo plazo (Lloyd-Hughes and Saunders, 2002). Con el fin de solventar algunas de las deficiencias de los PDSIs, Wells et al. (2004) desarrollaron una versión auto calibrada de los índices que permite obtener valores regionales mucho más fiables y comparables espacialmente.

1.3.2. Índice de precipitación estandarizada (SPI)

El Índice Estandarizado de Precipitación (SPI, por sus siglas en inglés) fue propuesto por Mckee et al. (1993), e introdujo un nuevo concepto en la cuantificación de las sequías a múltiples escalas temporales. Desde su formulación, este índice ha sido utilizado para identificar condiciones de sequía y humedad a diferentes escalas temporales en múltiples estudios a nivel mundial, siendo reconocido por la Organización Meteorológica Mundial como el índice de sequía meteorológica universalmente propuesto para fines de monitorización y alerta temprana (WMO, 2012).

El SPI es un índice basado en la precipitación que transformada a probabilidades a partir del ajuste de una función de distribución determinada, y convertida posteriormente en unidades estandarizadas con media 0 y desviación típica 1. Aunque en sus inicios Mckee et al. (1993) propusieron el ajuste de la precipitación a partir de una distribución Gamma, estudios posteriores notaron que la agregación de las anomalías de precipitación presentaba diferencias dependiendo de las escalas temporales. La distribución Pearson III, de entre las múltiples evaluadas, ha mostrado un mejor ajuste de los datos a cualquier escala de tiempo (López-Moreno et al., 2008; Vicente-Serrano, 2006). En este estudio, el cálculo del SPI se realizó ajustando una función de distribución Pearson III, obteniéndose los parámetros propios de la distribución siguiendo el procedimiento de los L-momentos propuesto por Hosking, (1990).

Las potencialidades que presenta el SPI son múltiples. En primer lugar este índice emplea únicamente la precipitación para caracterizar eventos anormales de sequedad o humedad, posibilitando un cálculo sencillo. En segundo lugar, el SPI permite la comparación espacial de condiciones de sequía entre regiones con condiciones climáticas muy diversas. Por último, permite caracterizar la respuesta variable a la sequía de cualquier variable natural a distintas escalas de tiempo, lo que supone la mayor diferencia conceptual respecto a los PDSIs (Keyantash et al., 2002; Vicente-Serrano et al., 2012).
A pesar de ello, este índice presenta también limitaciones. Por ejemplo, el SPI no considera los efectos de la AED, obviando la importante relación entre las condiciones de humedad de la superficie y la atmósfera. Ello hace que la cuantificación de la severidad de la sequía que realiza este índice, resulte menos exacta que la realizada por otros índices que consideran un balance climático en su formulación.

1.3.3. Índice Estandarizado de precipitación y evapotranspiración (SPEI)

El índice Estandarizado de Precipitación y Evapotranspiración (SPEI por sus siglas en inglés), fue introducido por Vicente-Serrano et al. (2010) supone un paso adelante en la cuantificación y caracterización de las sequías. El SPEI salva las limitaciones de los índices anteriores combinando la sensibilidad del PDSI y el carácter multi-temporal del SPI incorporando además la AED como variable importante en su conceptualización. Al contrario que la asunción principal del SPI que considera que la sequía depende exclusivamente de la variación temporal de la precipitación, el SPEI toma en cuenta el rol de la temperatura en el cálculo de un balance hidroclimático.
Estudios al respecto han informado de la repercusión que supone en los múltiples sistemas naturales el calentamiento, señalando además la importancia de emplear índices de sequía que incluyan la AED como variable primaria (Asseng et al., 2014; Cai and Cowan, 2008; Cheng and Huang, 2016.; García-Ruiz et al., 2011; Vicente-Serrano et al., 2015). Un cambio en los patrones normales de temperatura es capaz de inducir condiciones excepcionalmente secas que impactaría negativamente en el medio dando lugar a un aumento de los incendios forestales (Lindner et al., 2010), plagas (Logan et al., 2003), la reducción de producciones agrarias (Lobell et al., 2011) o la reducción de los recursos hídricos (Barnett et al., 2005).

El PDSI incluye la AED como variable en su formulación, lo que le permite identificar impactos de sequía relacionados con procesos de calentamiento, no obstante carece de la flexibilidad multi-temporal para evaluar los impactos en sistemas que responden a la sequía a muy diversas escalas temporales (Vicente-Serrano et al., 2012). El SPEI considera el efecto de la AED, así como el carácter multi-temporal y la simplicidad de cálculo del SPI. De este modo, el SPEI calcula balances climáticos mensuales (D_i) empleado series mensuales de precipitación y de evapotranspiración de referencia. Los valores mensuales de Di son agregados a diferentes escalas de tiempo y transformados a unidades estándar normalizadas ajustando una distribución log-logística de tres parámetros que posteriormente se convierten en unidades estándar de desviación. Los valores resultantes siguen una distribución normal, siendo comparables a los valores de SPI y permitiendo por tanto la comparación de condiciones secas y húmedas entre regiones con características climáticas específicas.

La descripción completa de la metodología de cálculo del SPEI, así como una detallada comparativa estadística respecto al desempeño del PDSI y el SPI son recogidas por Vicente-Serrano et al. (2010), Vicente-Serrano and Beguería, (2016) y Beguería et al. (2014).

En resumen, el SPEI combina las potencialidades del SPI y del PDSI sin embargo requiere más información climática y es sensible al método seleccionado para la estimación de la AED.

1.3.4. Índice Estandarizado de Sequía de Palmer (SPDI)

El Índice Estandarizado de Sequía de Palmer (SPDI por sus siglas en inglés) es un índice de sequía recientemente desarrollado por Ma et al. (2014) basado en el concepto principal de la relación entre suministro y demanda en las pérdidas de humedad del suelo (CAFEC) del PDSI y el carácter multi-temporal del SPI y el SPEI. Es por tanto un índice que combina las metodologías presentadas por el PDSI y el SPEI.

El SPDI acumula las anomalías de las pérdidas de humedad del suelo siguiendo un procedimiento similar al del PDSI pero acumulando dichas anomalías a distintas escalas temporales. Las anomalías acumuladas son transformadas a una variable estándar con media igual a 0 y desviación típica igual a 1 ajustando para ello la función de distribución de Valores Extremos Generalizada (GEV). Vicente-Serrano et al. (2015) señalaron la idoneidad de emplear la función de distribución log-logística en lugar de la GEV para salvar las limitaciones que esta distribución presenta al ajustar algunos valores extremos. Siguiendo la recomendación de estos autores, en el estudio aquí presentado, se ha empleado la distribución log-logística.

2. Objetivos

En línea con lo expuesto en la sección 1 de Introducción, el análisis que se presenta en esta tesis abarca dos territorios amplios y heterogéneos como son España y los EEUU.

Consciente de la importancia de seleccionar las correctas herramientas para la monitorización de las sequías, el objetivo general de este trabajo ha sido el de proporcionar una validación de la capacidad de siete de los más importantes índices de sequía empleados a nivel mundial para cuantificar los impactos de la sequía en sistemas vulnerables a ella. Para cumplir este propósito, se han comparado tres índices de sequía multi-escalares (el SPI, el SPEI y el SPDI) y cuatro índices de Palmer uni-escalares (El PDSI, el PHDI, el Z-index y el PMDI)

El objetivo general se divide a su vez en objetivos más específicos que se describen a continuación en función al sistema analizado.

En relación al sistema agrario, los objetivos específicos son:

i. Analizar la respuesta temporal de las producciones agrarias anuales de cinco de los principales cultivos de secano en EEUU (trigo, maíz, soja, algodón y cebada) a escala de condado; así como de dos cultivos de cereal de secano en España (trigo y cebada) a dos escalas espaciales, provincial y de comarca agraria.
ii. Desarrollar una nueva base de datos de información agraria con la suficiente cobertura espacial y temporal.
iii. Identificar posibles patrones espaciales en la respuesta de los distintos tipos de cultivo a la sequía y definir lo principales mecanismos medioambientales y climáticos que determinan dichos patrones.

La actividad vegetal fue analizada únicamente en España, y los objetivos específicos al respecto son:

i. Proporcionar una comparación de la respuesta de tres indicadores de actividad vegetal (crecimiento del anillo de los árboles, el valor de verdor máximo y un indicador de la producción primaria neta) a las sequías.
ii. Analizar y comparar la respuesta del crecimiento de los anillos de los árboles y el NDVI a las condiciones de sequía en diferentes especies arbóreas.

Finalmente, los objetivos específicos perseguidos en el análisis del sistema hidrológico son:

i. Determinar las escalas temporales de las sequías climáticas que mejor representan las condiciones de sequía hidrológica caracterizadas por el Índice Normalizado de Caudal (SSI por sus siglas en inglés) en una amplia selección de cuencas naturalizadas en EEUU y España.

ii. Encontrar patrones espaciales de respuesta de los caudales a la sequía climática y su posible relación no estacionaria.

iii. Identificar los factores medioambientales y climáticos que determinan la vulnerabilidad de los caudales a la sequía climática.

3. Resumen breve de los resultados

Los resultados de esta investigación han sido publicados en cuatro revistas internacionales indexadas por el Journal Citation Report (Climate Research, Agricultural and Forest Meteorology, Forests y Journal of Hydrology). Del mismo modo, parte de los resultados aquí presentados pertenecen a dos manuscritos actualmente en revisión en dos revistas indexadas (Natural Hazards and Earth System Sciences y Water Resources Management). Los artículos publicados y sin publicar pueden encontrarse en las secciones 4 y 5 de la Tesis en Inglés respectivamente.

En líneas generales, la relación entre las variables analizadas (producciones agrarias, crecimiento de los árboles y caudales) y los siete índices de sequía evaluados en esta tesis demostró un mejor desempeño de los índices multi-escalares. Así, la magnitud de las correlaciones encontradas entre el SPI, el SPEI, el SPDI y las variables analizadas fue mucho mayor que las encontradas con alguno de los índices de Palmer aquí contemplados.

En las siguientes sub-secciones se presenta un breve resumen de los principales resultados obtenidos en cada uno de los estudios llevados a cabo.

3.1. Artículo de investigación 1 – resumen de los resultados

En EEUU las correlaciones entre las producciones agrarias y los índices de sequía fueron más elevadas en los cultivos de soja que en cualquier otro tipo de cultivo analizado, mientras que las más bajas se encontraron en el algodón. Los PDSIs además mostraron muy diversos rendimientos. Con la excepción del Z-index y el scZ-index, en general los PDSIs no registraron correlaciones estadísticamente significativas con las cosechas independientemente del mes del año observado. Por el contrario, las correlaciones observadas entre el Z-index, el SPI, el SPEI y el SPDI y los rendimientos fueron en su mayoría significativa en la mayoría de los condados analizados. Los PDSIs correlacionaron significativamente con aproximadamente el 50% de los condados, siendo este porcentaje en gran parte debido a la versión auto-calibrada de dichos índices.
Algunas diferencias destacables entre los índices multi-escalares y los distintos tipos de cultivo fueron observadas. De este modo, el SPI presentó el mayor número de condados con correlaciones significativas en el caso de la cebada y la soja mientras que el SPEI correlacionó significativamente más, en la mayoría de los condados donde se cultiva algodón, maíz y trigo. Resultados similares se observaron en el caso del SPDI.

En cuanto a los resultados estacionales y de escala temporal observados en cada tipo de cultivo, escasas diferencias se encontraron entre los índices de sequía multi-escalares.

La correlación de la cebada fue superior en condados localizados en los estados de Montana y Dakota del Norte en el caso de los tres índices multi-escalares. La relación con los índices de sequía fue mayor durante los meses de verano a escalas temporales cortas (de 1 a 3 meses). El SPDI fue el índice que más correlacionó en ~30% de los condados localizados en la frontera con

Canadá. El SPI correlacionó mejor en ~28% de los condados mientras que el SPI lo hizo en ~20% de los condados principalmente localizados en Dakota del Norte y Carolina del Norte.

El maíz mostró las máximas correlaciones en la región oeste del Cinturón del Maíz (Illinois, Indiana y Ohio), sur de Texas, sur de Pensilvania y suroeste de Georgia y Carolina del sur, registrando las máximas correlaciones con los índices multi-escalares durante los meses de julio y agosto a escalas temporales cortas. En los condados del medio oeste (un 51% del total), las máximas correlaciones se encontraron con el SPDI, mientras que con el SPEI y el SPI los condados alcanzaron las máximas correlaciones en el 12.97% y 12.65% de los condados respectivamente.

En el caso del algodón las correlaciones encontradas fueron excepcionalmente bajas en general. Los valores máximos se alcanzaron durante los meses de verano a escalas temporales cortas. El SPEI fue el índice que mejor correlacionó con el mayor porcentaje de condados (29.95%) seguido por el SPDI (26.82%) y el SPI (19.79%).

La soja correlacionó mejor en los estados de Carolina del Norte y del Sur y en las llanuras centrales y del norte de EEUU. Agosto y septiembre fueron los meses en los que este tipo de cultivo resultó ser más sensible a las condiciones de sequía correspondiéndose las máximas correlaciones a unas condiciones secas a escalas temporales de 1 y 2 meses. El SPDI fue el índice con el que se encontró un porcentaje mayor de condados mejor correlacionados.

Por último, el trigo de invierno registró máximas correlaciones en la región de las llanuras del sur, principalmente durante la primavera. Es cultivo presentó una mayor variabilidad en cuanto a la escala temporal a la cual se encontraron las mayores correlaciones. El SPEI fue el índice de sequía con el que se encontró mejor relación en la mayoría de los condados donde se planta este tipo de cultivo.

3.2. Artículo de investigación 2 – resumen de los resultados

Los resultados de esta investigación demostraron la existencia de varios patrones de correlación entre el SPEI y los rendimientos agrarios. El SPEI a distintas escalas temporales presentó una respuesta diferenciada en función al tipo de cultivo, pero también en función a la región, siendo especialmente evidente el caso del trigo de invierno. En algunos condados por ejemplo, la respuesta de las cosechas de trigo al SPEI demostró una relación más fuerte a escalar temporales largas, mientras que en otros lo hizo a escalas temporales cortar. En general, los diversos patrones espaciales de respuesta de las cosechas a la sequía a diferentes escalas de tiempo evidenciaron la necesidad de llevar a cabo un análisis estadístico que permitiera identificar patrones bien definidos. Así, a partir de un Análisis de Componentes Principales (ACP) se obtuvieron distintos patrones de respuesta dependiendo del tipo de cultivo. Además, un análisis predictivo discriminante permitió identificar los factores que explicaban las distintas respuestas al SPEI a diferentes escalas temporales.

Para la cebada, el trigo y la soja se extrajeron tres componentes. La primer componente de la cebada explicó el 78.3% de la varianza y mostró que los rendimientos anuales están

principalmente influenciados por las condiciones de precipitación y AED entre los meses de enero y julio. La segunda y tercera componente representaron un porcentaje menor de varianza explicada. Se observaron además en las tres componentes diferencias significativas en la precipitación anual, principalmente condicionadas por los aportes de primavera.

Las cosechas del trigo de invierno presentaron correlaciones positivas en la primera componente a escalas temporales de 3 a 9 meses en condados principalmente localizados en los estados de Nebraska, Kansas y Oklahoma. La segunda componente no presentó correlaciones significativas mientras que la tercera sí lo hizo a escalas temporales que oscilaron entre cortas y largas, principalmente en condados localizados en las regiones de oeste, Wisconsin e Illinois. Los condados con cargas factoriales positivas se caracterizaron por presentar condiciones de humedad mayores que las componentes que presentaron cargas negativas.

En el caso de la soja el patrón extraído de la primera componente fue coherente presentando altos valores de correlación positiva con el SPEI a escalas temporales entre 1 y 4 meses desde julio a septiembre y entre 4 y 13 meses de julio a diciembre en condados ubicados en la región conocida como cinturón de la soja. La segunda componente mostró correlaciones positivas en el mes de agosto a la escala temporal de 1 mes y valores negativos en el mes de junio a escalas temporales de 2 a 7 meses en los condados situados en los estados de Iowa, Missouri y Nebraska. La tercera componente quedó limitada a determinados condados de la región central atlántica y el noreste, mostrando correlaciones elevadas y positivas con el SPEI a escalas temporales largas desde mediados de los meses de verano hasta el final de la estación. Entre los componentes se evidenciaron diferencias respecto a los valores promedios de temperatura y ETo así como en el promedio anual y estacional de los mismos.

Cuatro componentes se extrajeron en el caso de los rendimientos de maíz. Las dos primeras componentes se focalizaron en la misma región, así la primera de ellas mostró correlaciones elevadas y positivas durante los meses de verano a escalas temporales de 1 a 4 meses, mientras que la segunda presentó correlaciones negativas de enero a julio.
En la tercera y cuarta componente se observaron correlaciones positivas a escalas temporales intermedias durante el final de los meses de invierno y la primavera, principalmente en condados del centro y centro-norte respectivamente. Las diferencias entre las componentes se caracterizaron principalmente por los valores de temperatura y ETo.

Las producciones de algodón se limitan a un área muy específica de EEUU, no obstante presentó un patrón espacial muy disperso que dio lugar a cinco componentes principales de las cuales sólo las dos primeras mostraron correlaciones positivas y significativas a escalas temporales medias y largas en aquellos condados localizados en la región llamada Cinturón del Algodón. En general las diferencias entre estas dos componentes estuvieron controladas por las diferencias en las cantidades promedio de precipitación.

3.3. Artículo de investigación 3 – resumen de los resultados

Los resultados obtenidos de la respuesta espacial y temporal de las tres variables analizadas a la sequía mostraron la existencia de variaciones significativas en la magnitud de los valores de correlación encontrados entre los índices de sequía y el crecimiento del anillo de los árboles (TRW_i), el rango de máximo verdor ($NDVI_{max}$) y la producción primaria neta (NPP, $NDVI_{annual}$). En general, el TRW_i presentó los mayores valores de correlación , tanto con los índices multi-escalares como con los uni-escalares.

Por un lado, la distribución espacial de las correlaciones entre los índices multi-escalares fue muy similar entre los tres índices. Los máximos valores se encontraron principalmente en las regiones más secas del oeste peninsular y en las Islas Baleares. Por el contrario los valores mínimos se observaron en los bosques de frondosas del norte peninsular, región caracterizada por un clima más húmedo. En relación a los resultados obtenidos por cada índice, los valores más altos de correlación en el caso del SPI se hallaron en el noroeste peninsular para la variable $NDVI_{anual}$. Por su parte el SPEI y el SPDI mostraron una correlación con el $NDVI_{anual}$ mayor en el sureste de la península en comparación con la variable $NDVI_{max}$. Resultados similares se obtuvieron con los PDSIs aunque la magnitud de las correlaciones registradas fueron menores que con los índices multi-escalares, no obstante no se encontraron diferencias espaciales entre los índices de Palmer y las variables $NDVI_{max}$ y $NDVI_{annual}$. En general, como se había señalado anteriormente, los resultados demostraron que la variable TRW_i presentó una mayor respuesta a la variación interanual de la sequía que el $NDVI_{max}$ y $NDVI_{annual}$ como se extrae de la magnitud de las correlaciones observadas.

Por otro lado, la respuesta temporal reveló la existencia de distintos patrones temporales dependiendo del parámetro analizado. Mientras que la respuesta del crecimiento secundario alcanzó la máxima correlación en los meses de verano (julio y agosto), el crecimiento anual de la vegetación y la NPP mostraron una respuesta mucho más temprana a la sequía durante la temporada de primavera (abril y mayo). Con frecuencia las especies respondieron a condiciones de sequía a medias (4 a 6 meses) y largas (> 6 meses) escalas de tiempo, lo cual sugirió que la variabilidad anual de los indicadores de crecimiento de los árboles varía no sólo dependiendo de la especie, sino también de las condiciones hidro-climáticas de la región en cuestión.

En cuanto a la relación entre las variables climáticas y las sequías a nivel de especie, no se encontraron patrones claros diferenciales en el desempeño de los índices multi-escalares y los dos indicadores NDVI. Los resultados mostraron que las especies características de regiones húmedas y frías (p.ej. *Abies alba* and *Pinus uncinata*) tendían a mostrar valores de correlación mucho más bajos que aquellas localizadas en climas semi-áridos (p.ej. *Pinus halepensis*). Por el contrario, en el caso del TRWi se observó una mayor variabilidad, especialmente en las especies de coníferas de los bosques de las regiones más secas donde se registraron valores de correlación muy elevados (p.ej. *Pinus halepensis*, *Pinus pinaster* y *Juniperus thurifera*) en contraposición a los valores más bajos encontrados en especies de conífera (p.ej. *Abies pinsapo*) y frondosas (p.ej. *Castanea sativa* y *Fagus sylvatica*) de las regiones templadas y húmedas.

3.4. Artículo de investigación 4 – resumen de los resultados

Los patrones generales de respuesta de las cuencas hidrográficas no perturbadas de EEUU a la sequía mostraron diferencias en la respuesta de los caudales a las sequías climáticas, probablemente debidas a las propiedades fisiográficas de las cuencas. De este modo, correlaciones elevadas y positivas se encontraron en la mayoría de las cuencas analizadas con la excepción de aquellas localizadas en las Montañas Rocosas y la región noreste del país. Estas cuencas a diferencia de la mayoría mostraron valores de correlación más bajos principalmente durante los meses de febrero a abril.

En general, correlaciones positivas y elevadas caracterizaron la relación entre el SPEI y el SSI con valores máximos registrados a escalas temporales cortas salvando las cuencas con régimen nival cuya sensibilidad a las sequías fue mayor a escalas temporales más largas. Del análisis de componentes principales llevado a cabo se extrajeron diversos patrones de respuesta de la sequía hidrológica a la climática. Siete componentes que explicaron el 70% de la varianza fueron extraídos para representar los principales patrones de respuesta espacial de las correlaciones mensuales a distintas escalas temporales entre el SPEI/SPI y el SSI. Las dos primeras componentes representaron el 55% de la varianza total explicada e indicaron el predominio de respuestas del caudal a las condiciones de sequía a escalas temporales cortas en las cuencas del sureste y el medio oeste. Mientras que la primera componente correlacionó fuertemente con escalas temporales menores de 10 meses, la segunda lo hizo a escalas mucho más cortas entre los meses de abril y enero. La tercera componente representaba correlaciones elevadas de SPEI-SSI de la región noroeste del Pacífico a escalas de tiempo cortas de septiembre a febrero, aunque también esta componente mostró correlaciones a escalas temporales largas entre los meses de mayo y agosto. La cuarta componente representativa de las cuencas localizadas en las Montañas Rocosas se caracterizó por mostrar mayor sensibilidad a la sequía entre los meses de enero a febrero a escalas temporales de 8 a 18 meses. El mismo análisis realizado con el SPI mostró modos de variación espacial muy similares a los encontrados con el SPEI.

Entre los factores que explicarían los patrones de correlación entre el SPEI y el SSI, el promedio anual de NDVI mostró fuertes diferencias entre las componentes extraídas. En concreto, las componentes 1,2, 6 y 7 correlacionaron mucho mejor que las componentes 3,4 y 5. Además, las características edáficas observadas variaron entre componentes, en particular la capacidad de retención de agua. A la vez, las componentes 3 y 7 mostraron una elevada variabilidad entre las propias cuencas en cuanto a la magnitud del caudal medio anual. De igual modo la elevación media de las cuencas, la temperatura y la evapotranspiración difirieron entre componentes también. Así, las componentes 3 y 4 estuvieron principalmente caracterizadas por cuencas localizadas a mayor elevación y por poseer temperaturas más bajas que las de cualquier otra componente.

Del análisis llevado a cabo para los diferentes sub-periodos se extrajeron ciertas diferencias en la relación de las sequías climáticas y los caudales en las cuencas estadounidenses, y a la misma vez mostró patrones espaciales similares a los obtenidos por el ACP previamente realizado con el periodo de observación completo, el SPI y el SPEI.

Se demostró que las variaciones del balance hidro-climático y su preponderancia son secundarios en la relación de las sequías climáticas y la hidrológica respecto al importante papel de la variación de las precipitaciones. En general, la magnitud de las correlaciones observadas en ambos sub-periodos fue muy similar a la obtenida para el periodo completo, aunque sí se observaron diferencias en cuanto a la escala temporal a la que las mayores correlaciones se registraron.

3.5. Artículo de investigación 5 – resumen de los resultados

Los resultados de este análisis mostraron una mayor correlación de los índices de sequía con los rendimientos agrarios a escala de región agraria. De igual modo, se observó mayor variabilidad en los datos provinciales debido a la mayor longitud de las series de dato disponible. Entre los rendimientos anuales de trigo y cebada no se observaron grandes diferencias espaciales a nivel provincial. Las correlaciones más fuertes se encontraron con el SPEI y el SPI en las provincias localizadas en Castilla y León, Aragón, Castilla La Mancha y la provincia de Valencia. Por el contrario, las correlaciones más débiles se encontraron en las provincias del sur peninsular.

La distribución espacial de las correlaciones a escala de región agraria mostró un patrón bien definido en el caso del trigo. Las magnitudes de dichas correlaciones fueron muy similares a las observadas a escala provincial en el mismo tipo de cultivo, registrando valores mucho más elevados con los tres índices multi-escalares que con los PDSIs, en especial el PDSI y el PHDI. Las regiones agrarias que más correlacionaron fueron aquellas localizadas en las provincias de Valladolid, Segovia, norte de Ávila y el noreste de Salamanca. Magnitudes de correlación similares se encontraron en las regiones agrarias del noreste peninsular.
Los resultados obtenidos para los rendimientos anuales de cebada mostraron una relación espacial similar con los distintos índices de sequía. Los coeficientes de correlación más elevados se encontraron con los índices multi-escalares, en particular en las regiones agrarias del norte de Cáceres, norte de Galicia y Guadalajara; correlaciones más bajas se encontraron en las regiones agrarias del sur de Córdoba y Jaén. Entre los PDSIs, cupo destacar las correlaciones significativamente altas encontradas en el caso del Z-index y el PMDI.

Estas correlaciones máximas se encontraron principalmente a escalar temporales cortas en el caso de ambos cultivos observándose diferencias insignificantes entre los tres índices multi-escalares. Las escalas variaron de 1 a 3 meses en función al tipo de cultivo. De este modo, más de la mitad de las regiones agrarias donde se cultiva el trigo correlacionaron fuertemente con la escala temporal de 1 mes, mientras que a nivel provincial esta correlación se correspondió con la escala temporal de 3 meses. En el caso de la cebada el patrón temporal observado fue el mismo. Aunque los tres índices multi-escalares respondieron prácticamente sin diferencias estadísticamente significativas, el SPEI fue el índice con el que mayor número de provincias correlacionaron tanto en el caso del trigo como de la cebada, igualmente lo hicieron las regiones agrarias en el caso del trigo. Las regiones agrarias donde se cultiva cebada correlacionaron más con el SPDI.

A partir del ACP se encontraron patrones estacionales definidos en la respuesta de los rendimientos anuales y la sequía a escala de región agraria, con la excepción de los datos regionales de cebada cuya extensión espacial fue muy limitada. A escala provincial por el

contrario se obtuvo un patrón menos definido. Las dos componentes extraídas explicaron el 60% total de la varianza y entre tipos de cultivo y escalas espaciales se encontraron diferencias. De este modo, para los rendimientos de trigo a escala regional la primera componente señaló la sensibilidad de las cosechas a la sequía principalmente durante la primavera y el otoño a escalas temporales cortas, mientras que la segunda componente lo hizo durante los meses de primavera a escalas temporales medias. A nivel provincial los rendimientos de la primera y la segunda componente fueron más sensibles en el mes de mayo a escalas temporales medias y largas respectivamente. En el caso de la cebada a escala regional se encontraron escasas diferencias entre las componentes debido a la limitación de las observaciones, a excepción de la escala temporal de respuesta. Así, la influencia de las condiciones de sequía varió entre las escalas cortas y medias en la primera componente y predominaron las escalas largas en la segunda componente. A escala provincial la variabilidad de las magnitudes de correlación fue mayor, y en general la respuesta a la sequía se observó principalmente a escalar temporales medias y largas, siendo los meses de primavera los más sensibles en ambas escalas de tiempo.

3.6. Artículo de investigación 6 – resumen de los resultados

La relación que presentaron los distintos índices climáticos de sequía analizados y el SSI en cuencas naturales de España fue, en general, muy fuerte. Los índices multi-escalares caracterizaron mejor que los PDSIs dicha relación, reflejando una mayor eficiencia en el momento de monitorizar las sequías hidrológicas. Excepcionalmente el Z-index fue el único índice de los PDSIs cuya magnitud de correlación con el SSI fue muy similar a la encontrada con los índices multi-escalares. La distribución espacial de las correlaciones máximas reveló un rendimiento óptimo de los índices PHDI, PDSI y PMDI en cuencas muy concretas localizadas en las cuencas mayores de los ríos Segura, Guadiana y Ebro, junto a otras con una distribución más dispersa entre las cuencas mayores de los ríos Guadalquivir, Tajo, Duero, Miño y Júcar. Por su parte, los índices multi-escalares y el Z-index (en menor grado) presentaron correlaciones más sólidas que los PDSIs con una distribución más generalizada en el territorio. Las correlaciones más débiles entre estos índices y el SSI se observaron en las sub-cuencas pertenecientes los ríos Segura y Ebro y las cuencas internas localizadas al norte de Cataluña.

Especialmente se encontró una alta variabilidad estacional en la respuesta de los caudales a las sequías climáticas. Los máximos valores de correlación se encontraron, independientemente del índice considerado, en los meses de febrero a septiembre, y los mínimos durante los meses de noviembre y diciembre.
Algunas cuencas (12.24% del total) principalmente localizadas al este de las cuencas principales, presentaron una mayor correlación con el Z-index. El SPDI fue el índice que correlacionó mejor en un mayor porcentaje de cuencas (41.92%) seguido del SPEI (25.33%) y el SPI (20.52%), no obstante los resultados obtenidos del t-test demostraron similitudes estadísticamente significativas entre las correlaciones obtenidas por los tres índices multi-escalares y su capacidad para conectar con las sequías hidrológicas. La respuesta estacional al SSI por parte de los índices climáticos, independientemente de la escala temporal considerada, fue más débil en los meses de verano en la mayoría de las cuencas. Las correlaciones fueron, en general, más bajas en cualquiera de los tres índices multi-escalares. En relación a la escala temporal de respuesta de los caudales, más del 62% de las cuencas estudiadas mostraron magnitudes de correlación elevadas

a escalas temporales cortas (principalmente a 2 meses) sin embargo, se encontraron algunas diferencias entre el SPDI y el SSI a nivel estacional. La diferencia más evidente se encontró en las cuencas ubicadas en sistemas calcáreos donde la máxima correlación encontrada en el mes de junio se correspondió a escalas temporales medias y largas. Esto sugirió la existencia de complejas asociaciones y mecanismos no solamente climáticos que determinan la conexión de las sequías climáticas y las hidrológicas en las cuencas hidrográficas.

4. Discusión general

Esta tesis ha proporcionado un análisis comprensivo de la evaluación de diferentes índices de sequía en múltiples sistemas. A su vez, se ha analizado la respuesta espacio-temporal de la agricultura, los bosques y los caudales a las condiciones de sequía en dos regiones heterogéneas como son los Estados Unidos y España. La relevancia de los resultados obtenidos de los diferentes estudios llevados a cabo tiene como finalidad: (i) mejorar el conocimiento general sobre la correcta y efectiva monitorización y cuantificación del complejo riesgo climático que supone la sequía, y (ii) la creación de nuevos servicios climáticos que permitan abordar eficazmente el riesgo.

4.1. Evaluación de la adecuación de los índices de sequía

En cuatro de los estudios llevados a cabo se ha analizado la idoneidad de diferentes índices de sequía climáticos con fines de monitorización y su capacidad para detectar la respuesta de los distintos sistemas analizados a condiciones de sequía.
Los índices de sequía seleccionados son conocidos a nivel mundial y han sido ampliamente estudiados en la literatura científica y empleados en procesos operacionales de seguimiento de las sequías. En cada uno de los sistemas aquí analizados se observaron resultados similares en relación a la asociación entre los dos grupos de índices (multi-escalares y uni-escalares) y las variables agrícolas, hidrológicas y medioambientales. De este modo, los índices multi-escalares presentaron una mejor respuesta a la variabilidad de los rendimientos agrarios, los indicadores de crecimiento arbóreo y los caudales respecto a los índices uni-escalares. Así, tal como se deriva de las distintas magnitudes de correlaciones obtenidas, la respuesta de estas variables fue diferente en función al tipo de índice.

Los PDSIs mostraron en general magnitudes de correlación bajas independientemente de la variable analizada incluso considerando la versión auto-calibrada de dichos índices, los valores mejoraron respecto a la propuesta original sin calibrar como se desprende de los resultados obtenidos en el *Artículo 1* en cuanto a cuantificar el impacto en pérdidas agrarias. Estos resultados son apoyados por los obtenidos en el trigo de secano en Grecia por Mavromatis, (2007). No obstante, y a pesar de los resultados de estos índices respecto a los multi-escalares, las magnitudes de las correlaciones varían notablemente entre los PDSIS, siendo posible encontrar algunas excepciones. Por ejemplo, el Z-index mostró una mayor sensibilidad reflejando los impactos de la sequía en los rendimientos agrarios, los caudales y los bosques de manera más eficiente que cualquier otro PDSIs al registrar correlaciones más elevadas y significativas. Este índice como ya se ha mencionado, mide las condiciones de humedad a corto plazo, coincidiendo con la respuesta promedio de la vegetación y los caudales de los ríos con regímenes no modificados a condiciones de sequía (Lorenzo-Lacruz et al., 2013; Quiring and Papakryiakou, 2003; Vicente-Serrano et al., 2013). Además, los resultados presentados en el *Artículo sin publicar 2* mostraron que la media de las magnitudes de las correlaciones alcanzadas por los PDSIs con los caudales fue mayor que en cualquiera de los otros dos sistemas analizados en esta tesis. De

hecho, magnitudes similares fueron encontradas en cuencas naturales en la región griega de Thessaly por Vasiliades and Loukas, (2009), quienes también demostraron que, entre los PDSIs, el PHDI fue el índice que peor caracterizó el impacto de las sequías en los caudales. Similares resultados se encontraron en el análisis llevado a cabo en las cuencas no alteradas de España, y en general este mismo índice, seguido por el PDSI y el PMDI presentaron las relaciones menos robustas con cualquiera de las variables analizadas.

A pesar de lo expuesto, numerosos estudios previos han hecho uso de los PDSIs con resultados exitosos, bien para propósitos de monitorización o estudios relacionados con resultados, a menudo, contrarios y/o complementarios a los aquí alcanzados. Es el caso por ejemplo del estudio llevado a cabo por Karl, (1986) que mostró cómo para analizar la variabilidad de los incendios forestales y los rendimientos agrarios en EEUU, el Z-index presentó un mejor rendimiento que el PDSI a la hora de cuantificar la variabilidad de las condiciones de humedad a corto plazo. Conclusiones similares alcanzaron Quiring y Papakryiakou, (2003) en las praderas canadienses, o Hlavinka et al. (2009) en la República Checa. Por su parte, Bhuyan et al. (2017) realizaron un estudio similar sobre nueve especies arbóreas en Europa, comparando el SPEI, el SPI y los PDSIs. Sus resultados mostraron, a diferencia de los aquí alcanzados, que los PDSIs respondían de manera muy similar a los dos índices multi-escalares a escalas temporales largas superiores a los 12 meses.

A pesar de todo, los PDSIs se encuentran limitados por la falta de flexibilidad a la hora de identificar los impactos de la sequía a distintas escalas temporales. Como estudios anteriores han demostrado, y muchos otros posteriores soportan, las diferentes respuestas temporales de la agricultura, la vegetación y la hidrología al déficit hídrico entraña complejidad, evidenciando la necesidad de emplear índices de sequía que permitan conectar las condiciones climáticas del pasado con las condiciones presentes en regiones con una gran variabilidad climática (García-León et al., 2019; Vicente-Serrano et al., 2011).

De acuerdo con esta idea, varios estudios comparativos en diversas regiones como los desarrollados por McEvoy et al. (2012), Wang et al. (2014) o Tian et al. (2018), señalaron la superioridad de los índices multi-escalares a la hora de monitorizar y cuantificar los impactos de las sequías en las tierras cultivadas. De igual modo, Vicente-Serrano et al. (2012) demostraron lo mismo sobre el crecimiento de los árboles a nivel mundial y Liu et al. (2019), Lorenzo-Lacruz et al. (2013) o Dogan et al. (2012) lo hicieron respecto a las cuencas de los ríos.

Las magnitudes de correlación tan similares observadas entre los índices multi-escalares y las diferentes variables mostró además una habilidad análoga para caracterizar impactos de sequía. A este respecto Labudová et al. (2016) también encontró una respuesta muy parecida entre el SPEI (calculado a partir de datos de precipitación y AED) y el SPI (basado únicamente en datos de precipitación) a la hora de analizar los impactos de la sequía en la producción agraria de las tierras bajas del Danubio y el este de Eslovaquia. Sin embargo, se han encontrado ligeras diferencias en la magnitud de las correlaciones observadas entre el SPEI y el SPI y las variables representativas de los tres sistemas analizados, sugiriendo la relevancia de la AED como variable a considerar en el cálculo de la magnitud de las sequías. En general las correlaciones fueron ligeramente superiores en el SPEI, lo cual indica la importancia que tiene la sensibilidad de los cultivos, los caudales y los bosques a variaciones de la AED. Algunos estudios previos también han notado los efectos de la AED en la respuesta de diferentes sistemas a la sequía. Por ejemplo, en relación a

esto, Lobell and Field, (2007) advirtieron el riesgo de las producciones agrarias asociadas a un incremento global de las temperaturas máximas. Bachmair et al. (2018) también notaron similares diferencias entre el SPEI y el SPI como las aquí observadas, asociadas principalmente al rol de la temperatura en los bosques del sur de Europa. No obstante, una de los resultados aquí presentados demostró que incluso cuando las variaciones en la AED afectan a la severidad de las sequías hidrológicas, el rol de esta es menos evidente y difícil de detectar en cuencas naturales. De este modo, las diferencias detectadas en los trabajos que abordan la hidrología no fueron tan evidentes como en otras variables analizadas, siendo difícil encontrar diferencias realmente significativas en las relaciones del SSI/SPI y el SSI/SPEI en las cuencas seleccionadas. En consonancia con ello, los resultados presentados por Vicente-Serrano et al. (2014) también hacen alusión al rol preponderante de la AED en cuencas con algún tipo de intervención humana, que en aquellas menos reguladas. En los diversos análisis hidrológicos llevados a cabo, se ha demostrado la estrecha relación existente entre el clima y los caudales naturales, evidenciando el papel de la precipitación como factor decisivo en el desarrollo de las sequías hidrológicas.

En resumen, los resultados obtenidos con el SPEI, el SPI y el SPDI han demostrado ser superiores que los referidos a los PDSIs. Independientemente del tipo de cultivo, especie arbórea, cuenca de drenaje y escala temporal considerada, los resultados relativos a la capacidad de los índices de sequía demostraron que los índices calculados a diferentes escalas temporales tienen una capacidad superior para reflejar los impactos de las sequías.

4.2. El impacto de las sequías en los cultivos de secano, características temporales y espaciales.

La respuesta global de los cultivos a las sequías presenta una fuerte componente estacional y es altamente dependiente de la escala temporal del índice empleado para cuantificar la severidad de las mismas. Además, algunas de las características que representan la respuesta de los cultivos a las sequías muestran una gran dependencia del nivel de resistencia del tipo de cultivo en cuestión al escenario de escasez de agua (Contreras and Hunink, 2015; Vicente-Serrano et al., 2013). Mientras que estudios previos demostraron que los impactos varían dependiendo de la escala temporal (Wang et al., 2016; Zipper et al., 2016), en este trabajo se ha demostrado que las condiciones de humedad a corto plazo son capaces de favorecer o perjudicar el crecimiento del cultivo del cereal como la cebada, el maíz, la soja, el trigo, y el algodón.

Sin embargo, existen diferencias significativas en el mes del año en el que los rendimientos se encuentran más perjudicados por las condiciones de sequía. En general, se observó que las condiciones de humedad durante los meses de verano fueron determinantes para las cosechas de cebada, maíz, algodón y soja. En EEUU, las cosechas de cebada presentaron un patrón de respuesta al SPEI muy homogéneo, correlacionando sobre todo en el mes de enero a escalas temporales de 3 meses. La principal respuesta de los cultivos de maíz al SPEI en amplias regiones del centro de EEUU se encontró en el mes de agosto a escalas temporales también de 3 meses, mientras que en el caso de la soja el patrón dominante se encontró en el mes de septiembre a una escala temporal de 4 meses. El trigo de invierno por su parte, presentó una mayor sensibilidad a la disponibilidad de agua en los meses de primavera a escalas temporales

cortas y largas. En España los cultivos tanto de trigo como de cebada respondieron mayoritariamente a escalas temporales cortas, aunque el momento más sensible de los cultivos a las condiciones de humedad a escalas temporales medias durante la primavera.

Estudios anteriores ya demostraron cómo las condiciones de vegetación suelen verse afectadas en primer lugar por los cambios producidos en el contenido de agua del suelo (Capa-Morocho et al., 2016; García-León et al., 2019; Moorhead et al., 2015), hecho que explicaría la respuesta generalizada a las escalas temporales cortas encontrada en los resultados de los análisis llevados a cabo. En línea con los resultados encontrados, Zipper et al. (2016) evaluaron el impacto de la sequía sobre los cultivos de maíz y soja en EEUU, y observaron una mayor sensibilidad del maíz a la sequía durante el mes de julio a una escala temporal de 1 mes, mientras que la soja fue más sensible a las sequías ocurridas en el mes de agosto a una escala temporal de 2 meses. Del mismo modo, Moorhead et al. (2015) también encontraron que los impactos negativos de las condiciones de sequía en los cultivos de cereal se produjeron principalmente en el mes de julio en EEUU.

En última instancia, la estacionalidad observada en la respuesta de los cultivos a la sequía estaría relacionada a la fenología. Algunos estudios han sugerido con anterioridad que la respuesta de los cultivos a la disponibilidad de agua en el suelo es mayor durante los periodos más sensibles del estado fenológico de las plantas (Chaves et al., 2003; Poulter et al., 2013; Zipper et al., 2016). El invierno corresponde al primer estado de crecimiento de las plantas, y el verano con la espigazón y los estados reproductivos. Las condiciones de humedad durante el invierno determinan principalmente el correcto desarrollo de los cultivos (Çakir, 2004), de este modo, las respuestas a escalas temporales intermedias durante los meses de verano observadas en algunos cultivos (p.ej. El maíz alcanzó las máximas correlaciones durante la etapa de formación de estigmas y la fase reproductiva) están relacionadas con la respuesta fenológica a las condiciones de humedad o sequedad durante los meses de invierno.

No obstante, no siempre el patrón de respuesta temporal es el mismo. El trigo de invierno mostró en EEUU una estrecha relación con las sequías a escalas temporales medias y largas (a diferencia de los rendimientos de trigo en España que correlacionaron principalmente con la sequía a escalas temporales cortas y medias). Debido a los diferentes tiempos de plantación, el trigo de invierno cultivado principalmente entre septiembre y octubre, es más activo durante la estación fría, momento en el que se produce la recarga de humedad en el suelo y es más sensible a la escasez de agua (Tian et al., 2018; Wang et al., 2016). Además, las características fisiológicas determinan la resiliencia de los cultivos para lidiar con condiciones de sequía incluso durante los estados de crecimiento en los que son más sensibles a las mismas. Este aspecto se ve reflejado en las diferencias encontradas en la magnitud de las correlaciones de las cosechas en España, el trigo mostró correlaciones más altas con los índices de sequía que la cebada. En este caso, la cebada es un cultivo menos dependiente de la disponibilidad de agua para completar con éxito los estados de germinación y formación del grano gracias a mecanismos fisiológicos propios que le permiten desarrollarse bajo condiciones adversas de humedad o incluso en suelos poco propicios (Mamnouie et al., 2006).

Igualmente, se observaron diferencias notables entre tipos de cultivo y regiones en cuanto a las escalas temporales de respuesta más sensibles, acentuando la complejidad del patrón de

respuesta de los cultivos en regiones tan heterogéneas. Además de la explicación lógica que la fenología puede aportar a la respuesta rápida de las condiciones de humedad por parte de la mayoría de los cultivos, las diferentes respuestas temporales observadas en las cosechas de EEUU (p.ej. En los condados del centro norte donde se cultiva el maíz) no estuvieron relacionadas con los periodos vegetativos, sino que fueron evidenciadas por las condiciones medioambientales propias de la región durante el crecimiento de los cultivos, en especial las características climáticas propias (Pasho et al., 2011; Vicente-Serrano et al., 2013).

Una discusión detallada sobre cómo el clima predetermina el impacto de la sequía en los rendimientos agrarios por regiones puede encontrarse en las secciones de discusión en el *Artículo 1*, *Artículo 2* y *Artículo sin Publicar 1*. En general, las diferentes respuestas de los cultivos a las escalas temporales de los índices de sequía están principalmente explicadas, por una parte por la resiliencia de los cultivos y capacidad para desarrollar estrategias que le permitan hacer frente a la reducción de humedad en el suelo, y por otra parte a la resistencia que muestren los distintos tipos de cultivo en los diferentes estados de crecimiento.

4.3. La sensibilidad del crecimiento de los bosques a la escasez de agua

A colación de lo expuesto en el punto anterior, condiciones medioambientales y climáticas adversas causan cambios en el estado de la vegetación, en particular la sequía impacta sobre los ecosistemas degradando la actividad vegetal (Granda et al., 2013). El estudio presentado en el *Artículo 3* ha demostrado una mayor respuesta del TRW_i a las condiciones de sequía en comparación a los indicadores de actividad fotosintética representados por las variables NDVI. Principalmente esto resulta así debido a que la disponibilidad de agua limita la formación de las hojas y la madera, pero también responde a limitaciones técnicas de las medidas de satélite. En ocasiones la información derivada satelital se encuentra distorsionada, bien por la resolución espacial, bien por la influencia de la vegetación circundante (Gazol et al., 2018b). No obstante, la mayor sensibilidad del crecimiento secundario en comparación a la actividad fotosintética no es explicada exclusivamente por las limitaciones técnicas. Algunos estudios científicos al respecto (Aaltonen et al., 2016; Mcdowell et al., 2008) advirtieron el rol de los mecanismos de regulación de los árboles para lidiar con condiciones de estrés hídricos. De este modo, es posible que se observen disminuciones en el ratio de crecimiento pero no en los fotosintéticos durante condiciones de sequía debido a dichos mecanismos de regulación. Sin embargo, si las condiciones de deshidratación de la vegetación se prolongan durante largos periodos de tiempo, la muerte de los árboles inducida por las condiciones de sequía es inevitable (Martínez-Vilalta and Lloret, 2016; McDowell et al. (2013); Sangüesa-Barreda et al. 2015).

Los hallazgos sobre la sensibilidad de los bosques a la sequía mostraron claras variaciones entre especies y regiones climáticas. Como se observó en los estudios sobre cosechas agrarias, los diferentes métodos de resiliencia determinan diferentes formas en que las especies lidian con condiciones climáticas extremas. En climas húmedos, se observó que la respuesta de los árboles a la sequía (p.ej. Especies de frondosa del norte de España) era más débil que la de aquellos árboles que crecen en condiciones propias del clima Mediterráneo (p.ej. Especies de *Quercus*). De igual forma, se observó que la respuesta temporal a las sequías dependía en gran medida de

los mecanismos de adaptación de las distintas especies contempladas. Así, los resultados demostraron que las especies de conífera, características de las regiones húmedas, fueron más sensibles a la sequía a escalas temporales cortas y medias, mientras que la mayoría de las especies de coníferas de hoja perenne características de las regiones mediterráneas, mostraron una respuesta a la sequía a escalas temporales mucho mayores. Estos resultados son apoyados por otros estudios similares al que se presenta y en los que los autores coinciden a la hora de destacar la superioridad de las especies de regiones secas a recuperar las condiciones pre-sequía en situaciones de escasez de agua en comparación a especies propias de ambientes húmedos (Gazol et al., 2018b; Quiring and Ganesh, 2010; Rimkus et al., 2017). Estas últimas especies son más vulnerables a episodios de sequía extremos y prolongados debido a que carecen de los mecanismos de resiliencia para amortiguar los impactos causados por la escasez de agua.

De igual modo, la variación estacional también determina la respuesta de las especies arbóreas a la sequía en España. En general, se observó que el crecimiento secundario fue especialmente sensible a las condiciones de humedad durante los meses de verano, aunque se encontraron ciertas excepciones vinculables a comportamientos fenológicos específicos de cada especie (Camarero et al., 2010). Por su parte, la actividad fotosintética se encontró más afectada por las condiciones de sequía durante los meses de abril y mayo. Este retardo temporal en la respuesta al impacto de la sequía es resultado del ciclo del decaimiento de los árboles que comienza con la reducción de la actividad fotosintética, la captura de carbón y finalmente la formación de madera (Noormets et al., 2008).

4.4. La respuesta de los caudales a la sequía en condiciones naturales

Los caudales de las cuencas no alteradas analizadas estuvieron fuertemente correlacionadas con los índices de sequía climáticos. Las correlaciones medias registradas en cuencas de EEUU y España ($r \sim 0.8$) fueron mucho más elevadas que las correlaciones observadas en estudios previos desarrollados en cuencas reguladas (López-Moreno et al., 2013; Lorenzo-Lacruz et al., 2013; Vicente-Serrano et al., 2017a). De la comparación de la magnitud de las correlaciones entre índices climáticos y cuencas antropizadas, se hace evidente la fuerte influencia de las condiciones climáticas de la región en los caudales no regulados. Este motivo se debe a que las cuencas reguladas se encuentran controladas por factores no climáticos que interrumpen los cambios naturales esperados en un régimen natural debido a condiciones climáticas (Tijdeman et al., 2018). Las alteraciones pueden producirse, bien por la gestión de la capacidad de retención de agua (p.ej. Embalses y balsas, Lorenzo-Lacruz et al., 2013), bien por intervenciones de regulación (p.ej. cortas o canales, Rangecroft et al., 2018).

Un importante hallazgo encontrado mostró que la variabilidad del SSI en la mayoría de las cuencas analizadas en EEUU y España respondían a las sequías a escalas temporales cortas. En general, este resultado demostró que las correlaciones más elevadas ocurrieron a escalas temporales entre 1 y 4 meses, sugiriendo que, bajo condiciones naturales, los caudales de los ríos responden rápidamente a las variaciones climáticas. En concreto, el mayor porcentaje de cuencas españolas correlacionaron mejor con las sequías a 2 meses en los meses de noviembre, abril y julio. En consistencia con los resultados aquí alcanzados, Vicente-Serrano and López-Moreno (2005) demostraron respuestas muy similares en un estudio realizado en cuencas sin perturbar del centro del Pirineo español. No obstante, y a diferencia del patrón de respuesta temporal

encontrado, diferentes estudios realizados en cuencas alteradas probaron que las sequías hidrológicas estaban más influenciadas por las sequías climáticas a escalas temporales largas (Huang et al., 2017; Lorenzo-Lacruz et al., 2013; Lorenzo-Lacruz et al., 2010). Esta diferencia era de esperar dado que estas cuencas de drenaje están caracterizadas por estar influenciadas por prácticas de regulación e infraestructuras humanas que contribuyen a mitigar o reforzar los efectos del clima en los recursos hídricos. De este modo, en ocasiones las influencias no climáticas actúan como amortiguador de los efectos de las sequías incrementando la capacidad de retención de agua en las cuencas y por tanto modulando el caudal aguas abajo (López-Moreno et al., 2009; Lorenzo-Lacruz et al., 2010).

A pesar de que las cuencas reguladas presenten patrones de respuesta muy complejos a las sequías, los resultados concernientes a las cuencas sin regular mostraron una respuesta muy heterogénea en algunos casos a los eventos secos. Por ejemplo, en EEUU alunas cuencas principalmente localizadas en las Montañas Rocosas respondieron en condiciones naturales a escalas de tiempo diferentes. Por lo general las correlaciones encontradas entre el SPEI y el SSI fueron significativamente bajar durante los meses de invierno y verano a escalas temporales cortas, en contraposición a los valores de correlación elevados alcanzados durante la primavera y el otoño a escalas de SPEI mucho más largas. En España también se encontraron algunas excepciones que respondieron a escalas temporales largas, principalmente en aquellas cuencas localizadas en el Sistema Ibérico, la cabecera de la cuenca principal del río Ebro y algunas otras aisladas localizadas en el sur, sureste y norte de España. Por un lado, el comportamiento de las cuencas señaladas en EEUU es atribuible a las características comunes de cuencas montañosas cuyos caudales reciben la influencia de la acumulación de la precipitación en forma de nieve durante la temporada fría, y el deshielo de la misma a partir de primavera más que de la variabilidad interanual de la precipitación. Haslinger et al. (2014) y Rimkus et al. (2013) advirtieron respuestas temporales similares en cuencas hidrográficas con regímenes nivales. Por otro lado, en España las cuencas que respondieron a escalas temporales largas no están sometidas a los procesos de deshielo, sino que se encuentran condicionadas por la litología dominante. Estos resultados apoyan la afirmación del rol predominante de factores locales no climáticos en la conexión entre las sequías hidrológicas y las climáticas, así las condiciones fisiográficas propias de estas cuencas determinaron la respuesta temporal a las sequías (Van Loon and Laaha, 2015). Las cuencas calizas se caracterizan por su alta permeabilidad y transmisividad, actuando como reservorios naturales de agua que retrasan los efectos de la escasez de aportes de precipitación. Resultados encontrados por Lorenzo-Lacruz et al. (2013) también reflejaron distintas respuestas temporales de cuencas hidrográficas españolas con diferentes litologías.

En general, a pesar de que la respuesta temporal dominante a la sequía en caudales naturales se produce mayoritariamente a escalas temporales cortas, patrones estacionales y diferencias en estas respuestas asociadas a las características propias de cada cuenca (p.ej. Cobertura vegetal, usos del suelo, características climáticas y topográficas como la elevación, etc.) son factores a tener presente a la hora de abordar la monitorización de las sequías hidrológicas.